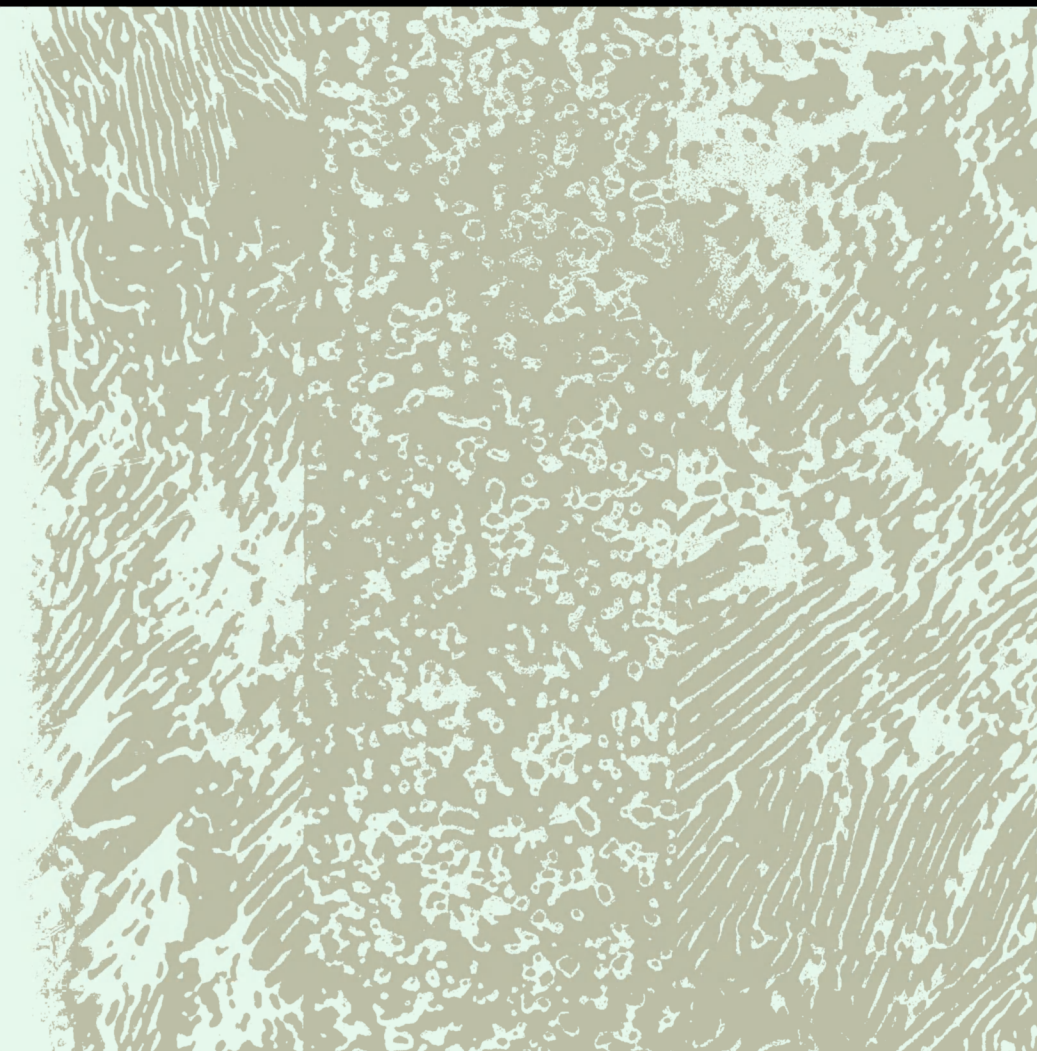


Yu. A. Geller, A. G. Rakhshtadt

SCIENCE OF MATERIALS



MIR PUBLISHERS MOSCOW

Prof. Yu. A. Geller, D. Sc. (Eng.), has been for many years the Head of the Chair of metal science and heat treatment at the Moscow Institute of Machine Tools. For over 40 years he has conducted vast teaching and research work in the field. He is the author of around 280 published works, including 10 textbooks and monographs.

A. G. Rakhshadt, D. Sc. (Eng.), a professor at the Bauman Higher Technical School in Moscow, has been for some 40 years engaged in engineering and research work in the field of metal science. He is the author of more than 220 scientific papers and 10 monographs.



Ю.А.Геллер, А.Г.Рахштадт

МАТЕРИАЛОВЕДЕНИЕ

МЕТОДЫ АНАЛИЗА,
ЛАБОРАТОРНЫЕ РАБОТЫ
И ЗАДАЧИ

ИЗДАТЕЛЬСТВО «МЕТАЛЛУРГИЯ»
МОСКВА

Yu. A. Geller, A. G. Rakhshtadt

SCIENCE OF MATERIALS

METHODS OF ANALYSIS,
LABORATORY EXERCISES
AND PROBLEMS

Translated from the Russian
by
V. AFANASYEV

MIR PUBLISHERS
MOSCOW

First published 1977

Revised from the 1975 (fourth) Russian edition

The Russian Alphabet and Transliteration

Аа	a	Кк	k	Хх	kh
Бб	b	Лл	l	Цц	ts
Вв	v	Мм	m	Чч	ch
Гг	g	Нн	n	Шш	sh
Дд	d	Оо	o	Щщ	shch
Ее	e	Пп	p	Ъ	''
Еѐ	ě	Рр	r	Ы	y
Жж	zh	Сс	s	Ь	
Зз	z	Тт	t	Ээ	e
Ии	i	Уу	u	Юю	yu
Йй	y	Фф	f	Яя	ya

The Greek Alphabet

Αα	Alpha	Ιι	Iota	Ρρ	Rho
Ββ	Beta	Κκ	Kappa	Σσ	Sigma
Γγ	Gamma	Λλ	Lambda	Ττ	Tau
Δδ	Delta	Μμ	Mu	Υυ	Upsilon
Εε	Epsilon	Νν	Nu	Φφ	Phi
Ζζ	Zeta	Ξξ	Xi	Χχ	Chi
Ηη	Eta	Οο	Omicron	Ψψ	Psi
Θθ	Theta	Ππ	Pi	Ωω	Omega

На английском языке

© English translation, Mir Publishers, 1977

CONTENTS

Introduction	11
--------------	----

PART ONE. METHODS FOR ANALYSIS OF MATERIALS

Chapter One. General Characteristics of Methods for Analysis of Materials	15
---	----

Chapter Two. Macroscopic Examination of Metal Structures (Macroanalysis)	18
--	----

2.1. Characteristics and Application of Macroanalysis	18
2.2. Macroanalysis of Metal Fractures	18
2.3. Macroanalysis of Metal Sections	20
2.4. Laboratory Exercises	28

Chapter Three. Determination of Structure of Materials by Microscopic Examination (Microanalysis)	33
---	----

3.1. Characteristics of Microanalysis	33
3.2. Methods of Optical Microscopy	33
3.3. Electron Microscopy	85
3.4. X-ray Spectrum Microscopy	98
3.5. Laboratory Exercises	99

Chapter Four. Determination of Transformation Temperatures (Critical Points) of Metals	104
--	-----

4.1. Thermal Analysis	104
4.2. Differential Thermal Analysis	115
4.3. Dilatometric Analysis	117
4.4. Laboratory Exercises on Thermal Analysis	127
4.5. Laboratory Exercises on Dilatometric Analysis	133

Chapter Five. Determination of Phase Composition of Alloys	135
--	-----

5.1. Methods for Determining Electrical Properties (Resistometric Analysis)	135
5.2. Methods for Measuring Magnetic Properties (Magnetic Analysis)	143
5.3. Laboratory Exercises	152

Chapter Six. Determination of Mechanical Properties of Materials	156
--	-----

6.1. General Characteristics of Test Methods	156
6.2. Static Tests	158
6.3. Tests under Variable Loads (Fatigue Tests)	172

6.4. Dynamic Tests	176
6.5. Fracture Toughness Tests	181
6.6. Low-temperature Tests	186
6.7. Tests at High Temperatures. Determinations of Creep Characteristics	187
Chapter Seven. Determination of Hardness of Materials	192
7.1. General Considerations	192
7.2. Ball Indentation Hardness Test (Brinell Hardness Test)	195
7.3. Hardness Measurement by Indenting a Cone or Ball (Rockwell Hardness Test)	199
7.4. Hardness Measurement by Indenting a Diamond Pyramid (Vickers Hardness Test)	204
7.5. Microhardness Measurements	206
7.6. Hot Hardness Testing	209
7.7. Laboratory Exercises	211
Chapter Eight. Determination of Physical and Chemical Properties of Metals	216
8.1. Determination of Physical Properties	216
8.2. Determination of Chemical Properties	218
8.3. Laboratory Tests	222
 PART TWO. CONSTITUTIONAL DIAGRAMS OF ALLOYS	
Chapter Nine. Constitutional Diagrams of Binary Alloys	224
9.1. Diagrams of Binary Alloys and Methodical Instructions on Their Analysis	224
Chapter Ten. Constitutional Diagrams of Ternary Alloys	251
10.1. Diagrams of Ternary Alloys and Methodical Instructions on Their Analysis	251
 PART THREE. PLASTIC DEFORMATION AND RECRYSTALLIZATION	
Chapter Eleven. Plastic Deformation and Recrystallization of Metals and Alloys	280
11.1. Laboratory Exercises	281
 PART FOUR. LABORATORY EXERCISES AND PROBLEMS ON STEELS AND CAST IRONS	
Chapter Twelve. Structure of Steels and Cast Irons in Equilibrium	286
12.1. The Structure of Steel	286
12.2. The Structure of Cast Iron	291
12.3. Laboratory Exercises	295
Chapter Thirteen. Transformations in Steel During Heating. Determination of Critical Points	299
13.1. Determination of Critical Points	299
13.2. Laboratory Exercises	302

Chapter Fourteen. The Structure of Carbon Steel in Non-equilibrium (Caused by Heat Treatment)	306
14.1. The Structure of Hardened Steel	306
14.2. The Structure of Tempered Steel	311
14.3. Laboratory Exercises	312
Chapter Fifteen. Heat Treatment of Structural Steels	315
15.1. Laboratory Exercises on Hardening and Tempering of Steel	315
15.2. Laboratory Exercises on Steel Hardening with Induction Heating	318
Chapter Sixteen. Heat Treatment of Tool Steels	321
16.1. Determination of Properties of Tool Steels	321
16.2. Laboratory Exercises	323
Chapter Seventeen. Determination of Hardenability of Steels	328
17.1. Methods for Determining Hardenability	328
17.2. Laboratory Exercises	334
Chapter Eighteen. Problems on the Analysis of Microstructure of Steels and Cast Irons	341

PART FIVE. LABORATORY EXERCISES AND PROBLEMS ON NON-FERROUS METALS AND ALLOYS

Chapter Nineteen. Laboratory Exercises on Microanalysis of Non-ferrous Alloys	364
19.1. The Structures of Non-ferrous Metals and Alloys	364
19.2. Laboratory Exercises	372
Chapter Twenty. Laboratory Exercises on Heat Treatment of Duralumin	376
20.1. Methodical Instructions	376
20.2. Laboratory Exercises	378
Chapter Twenty-one. Problems on Analysis of Microstructures of Non-ferrous Metals and Alloys	380

PART SIX. PROBLEMS ON SELECTION AND HEAT TREATMENT OF ALLOYS IN ACCORDANCE WITH OPERATING CONDITIONS OF ELEMENTS AND STRUCTURES

Chapter Twenty-two. Methodical Instructions	395
Chapter Twenty-three. Problems on Structural Steels and Cast Irons	397
Chapter Twenty-four. Problems on Special Steels and Alloys and Plastics	411
Chapter Twenty-five. Problems on Tool Steels and Alloys	417
Chapter Twenty-six. Problems on Non-ferrous Metals and Alloys	421

PART SEVEN. CLASSIFICATION AND INDUSTRIAL APPLICATIONS OF MATERIALS

Chapter Twenty-seven. Classification and Applications of Metals and Alloys 434

A. Steels. Principles of Classification and Designation	435
27.1. Constructional Steels	440
27.2. General-purpose Structural Steels (Table 27.4)	442
27.3. Special Structural Steels and Alloys	452
27.4. Tool Steels	470
27.5. Steels and Alloys with Special Chemical Properties (Corrosion-resistant)	475
27.6. Steels and Alloys with Special Physical Properties	479
B. Cast Irons	485
C. Copper Alloys	489
D. Aluminium Alloys	495
E. Magnesium Alloys	499
F. Titanium Alloys	501
G. Bearing Alloys (Babbitts)	502

Chapter Twenty-eight. Hard Materials 505

28.1. Hard Alloys (1500-2000 HV)	505
28.2. Hard Materials (2000-2500 HV)	508
28.3. Extra-hard Materials (8000-10,000 HV)	508

Chapter Twenty-nine. Plastics 510

Appendix I. Brinell Hardness Numbers 513

Appendix II. Brinell, Rockwell and Vickers Equivalent Hardness Numbers 514

Index 516

LIST OF SYMBOLS

Mechanical Parameters

- E = elastic modulus, kgf/mm²
 σ_t = ultimate tensile strength, kgf/mm²
 τ_t = ultimate torsional strength, kgf/mm²
 σ_b = ultimate bending strength, kgf/mm²
 σ_{-1} = endurance limit, kgf/mm²
 S_k = actual fracture resistance, kgf/mm²
 S_s = actual yield limit, kgf/mm²
 $\sigma_y (\sigma_{0.2})$ = yield limit, kgf/mm²
 σ_{pr} = proportionality limit, kgf/mm²
 σ_e = elastic limit, kgf/mm²
 G = shear modulus (in torsion)
 M = torque, mm
 W = moment of resistance, mm³
 HB = Brinell hardness, kgf/mm²
 HRC = Rockwell hardness, scale C
 HRA = Rockwell hardness, scale A ($HRC = 2HRA - 104$)
 HRB = Rockwell hardness, scale B
 HV = Vickers hardness, kgf/mm²
 δ = relative elongation, per cent
 ψ = relative reduction, per cent
 a_n = impact strength, kgf m/cm² (notched specimens)
 a_{un} = ditto (unnotched specimens)

Physical Parameters

- $4\pi G_s$ = saturation magnetization, gauss
 H_c = coercive force, oersted
 ρ = resistivity, ohm mm²/m
 B = magnetic induction, gauss
 H = magnetic field strength, oersted
 $(BH)_{\max}$ = magnetic energy, Mgauss·oersted
 T = absolute temperature, °K
 t = temperature, °C

INTRODUCTION

The course in the science of materials should not only give students knowledge of the principal laws determining the structure and properties of metals, alloys and plastics, it should also teach them how to make the most common industrial tests of these materials and operate testing machines, to work individually with the specialist literature and reference books in order to select the proper materials and their treatment depending on the operating conditions of articles.

Experience in teaching the course has shown that its vast material can be learned better and more firmly if, apart from the usual laboratory work, students are taught to 'read' constitutional diagrams and typical metal structures and acquire skill in characterizing and estimating the properties of numerous and diverse materials.

Accordingly, three forms of study are envisaged in the book: (1) experimental laboratory exercises, some of them being equivalent to a small part of research work; (2) laboratory analysis of alloy microstructures and calculation of their properties; and (3) home work on some subjects.

Laboratory exercises are aimed at acquainting the students with modern methods and apparatus used for studying the structure and properties of metals and other materials employed in machine-building. Such exercises are given in the book directly after discussing the relevant methods of investigation.

Laboratory exercises are compiled so that they can be individual, i.e. can be independently made by a student. Only a few specific exercises (work with dilatometers, hardening and tempering of steel, heat treatment of duralumin) are accomplished collectively by a group of students but each student of a group has to perform his own individual task in part of this exercise. Besides, the experimental results obtained by each student are used to construct a graph or table which shows the principal patterns in variations of the properties of the material.

In the majority of laboratory exercises, at least two specimens or two alloys differing in their properties are simultaneously examined or analysed. This makes comparison possible and gives better understanding of the theoretical and experimental material.

Along with the laboratory work, the book contains some calculation problems.

The introductory explanations given in various chapters before the laboratory exercises contain no detailed data on the techniques of using the appropriate instruments. Such instructions are not always justified, especially at higher technical schools as they often vary depending on the type of laboratory equipment employed.

Equally, in the majority of the laboratory exercises, students are freed from making some auxiliary operations (grinding and polishing of microsections, preliminary heat treatment, for instance, hardening of specimens when studying on tempering, etc.). Such work only wastes the students time without giving them any new skill.

The laboratory work should be distributed between the students in advance, for instance, a week before the lecture, so that they have time to acquaint themselves with the corresponding methods of analysis in literature and thus prepare for making the work.

Problems on reading and analysis of the most typical microstructures of alloys and determination of qualitative relationships between the structure, composition and properties of alloys are given for the most widely used carbon and alloy steels and cast irons (Ch. 18), and copper and aluminium alloys (Ch. 21).

Each student should solve at least two problems: one on steels and cast irons and one on non-ferrous metals. The solution (record) of a problem should be done during the laboratory period, not more than 10-15 minutes being required, provided that the student has attended lectures, read the textbook, and carried out earlier macroscopic and microscopic examination (Ch. 2 and Ch. 3).

Problems on analysis of constitutional diagrams and selection of a grade (composition) of material are for home work, two groups of such problems being given.

The first group includes problems on the constitutional diagrams of metallic alloys: binary (Ch. 9) and ternary (Ch. 10, for those studying an extended course). These problems conform to the real systems of the most typical alloys in order to show the student that knowledge of the general laws of the theory of al-

loys is indispensable for solving many practical problems on the application of metallic alloys in industry.

Each student must construct a constitutional diagram and cooling curves for the three alloys specified. The corresponding constitutional (phase) diagrams are given in the book and characterize the equilibrium state of the alloys considered. To solve the problem, a structural diagram must be constructed in order to characterize the properties of the alloys because these properties are determined more deeply by the structure, rather than by the phase composition. Experience shows that the greatest difficulties are encountered when attempting this portion of the problem, and sometimes when determining the type (nature) of the transformations feasible in an alloy and the need to employ heat treatment. To help the student a typical problem of this type is solved in detail in Sec. 9.1 (Problem No. 87).

These problems can only be given after the lectures on constitutional diagrams.

The solution and record of a problem of this kind require approximately two or three hours of home work.

The second group contains problems on selecting the composition of alloys and their heat treatment as required by the operating conditions of articles, structures and tools made of these alloys.

The long experience of teaching the course has shown that solving these problems is very effective in promoting teaching quality and raising the total qualification level of students; they then become capable of independently solving engineering problems on the selection of alloys by referring to the specialist literature. Thus, solving problems of this group is of extreme importance. Students studying a concise course should each be given one problem from Ch. 23 on steels, cast irons, and non-metallic materials. For an extended course, each student should attempt three problems: one on steels and cast iron (Ch. 23), one on special alloy steels (Ch. 24), and one on either tool steels (Ch. 25) or non-ferrous alloys (Ch. 26).

The book has an additional part (Part Six) to help students methodically solve these problems. This part systematically presents the most typical metallic alloys and plastics, their principal properties and industrial applications. After having selected an alloy by using the tables of this part of the book, the student can more easily find in the textbook or reference books the required data on the structure, heat treatment and properties of the alloy selected.

Finally, an additional methodical aid to the student is provided in Ch. 22 which contains instructions on the solving of problems.

Chapters 23, 25 and 26 give detailed solutions of typical problems on selection of structural steel (Problem No. 315), tool steel (Problem No. 381) and non-ferrous alloy (Problem No. 413), respectively.

Answers to the problems are not given in the book. There is no analogy here with the solution of many problems in mathematics and physics, where the answer does not disclose the method of solution, but only serves to check that the problem has been solved correctly. Besides, in the science of materials the same problem can be solved in a number of ways, especially when selecting metallic alloys and methods for their heat treatment.

Part One

METHODS FOR ANALYSIS OF MATERIALS

Chapter One

GENERAL CHARACTERISTICS OF METHODS FOR ANALYSIS OF MATERIALS

The science of materials uses diverse methods for the testing and analysis of materials to obtain exhaustive and reliable information on the properties of metals and plastics and variations of these properties depending on the composition, structure, and processing of the materials being studied. These numerous methods, which may differ substantially from one another, may be divided into two large groups as follows:

1. Methods for determining the structure and structural transformations in materials. These in turn should be classed into:

(a) direct methods for examining and determining the structure of materials; they are termed structural and include macroscopic examination (macroanalysis), microscopic examination (microanalysis), and X-ray examination;[†]

(b) indirect methods based on certain relationships existing between the structure and properties of materials; they can provide quite reliable data on the structural transformations occurring in metals during their treatment by measuring the variations of their physical properties: enthalpy (thermal analysis), linear and volumetric thermal expansion (dilatometric analysis), electrical resistance, saturation magnetization, and some chemical and mechanical properties.

2. Direct methods for determining the properties of materials as required by certain operational conditions, in the first place their mechanical properties, and also physical and chemical properties.

The structural methods of analysis of metals, in particular the methods of microscopic analysis, are employed very widely in the study of metals. Their main advantage is that the structure of a metal and its properties are usually related by a reliable qualitative relationship. This makes it possible, by using the

[†] X-ray analysis is beyond the scope of this book.

results of microanalysis (and partially of macroanalysis), to predict the variations of mechanical, physical and chemical properties with some or other variation in the structure, and to explain the causes of these variations. Moreover, the results obtained by these methods can be used to suggest the most efficient ways of improving the structure, and, therefore, the properties of a material, and to forecast the operational reliability of articles made of that material.

For instance, the resistance to brittle fracture of structural and tool steels can be increased appreciably by improving their structure, i.e. by forming a finer grain; this can be controlled by microscopic analysis. The strength properties of a steel can be sometimes improved through the formation of certain compounds, such as carbides or intermetallides, in its structure. On the other hand, the formation of a great number of large particles of a new phase (for instance, the same carbides in steel), which are easily detected by microscopic analysis too, can reduce ductility and promote brittle fracture.

The physical and chemical methods, which provide indirect information on the transformations occurring in a metal or alloy, can complement substantially the results of a structural study. They are capable of determining such variations in the state of metals that are undetectable by the structural methods (in particular, when these transformations cause a change in the electronic structure of atoms of a metal). By measuring the electrical resistance of a metal, we can sometimes judge on the nature of a new phase formed in it, etc.¹

Besides, these methods can provide the principal data required for constructing constitutional diagrams of metallic alloys, which are indispensable for characterizing their phase composition and structure. As is well known, many regions of the iron-carbon constitutional diagram were determined by the methods of thermal and microscopic analysis.

Finally, these methods may be used for the automatic continuous recording of variations in the state of materials under conditions of rapid heating (or cooling) or at high or low pressures.

It should be remembered, however, that the structural methods can give only qualitative results and fail to provide quantitative data on the properties as required for engineering calculations or on the pattern of variations of these properties, as is needed for the development of novel alloys possessing better properties (for instance, higher hardenability).

¹ These data are complemented by X-ray examination.

Therefore, direct determinations of the properties of metals and alloys and plastics are needed. These include, in the first place, methods of determining the mechanical properties, and for some materials, also direct determinations of their physical properties (thermal expansion, density, coercive force, magnetic permeability, etc.) and some chemical properties (electrochemical potential, corrosion resistance in various media, etc.).

Determinations of physico-chemical and mechanical properties are advantageous as they provide quantitative data required for the selection of materials. Without the structural studies discussed above, however, these determinations would be quite insufficient for an exhaustive characteristic of the engineering valuability of some or other metals, for predicting the reliability of articles made of those materials, or for developing novel composite materials. These determinations also fail to characterize the methods by which the materials have been manufactured and treated.

That is why the science of materials relies on a complex of methods which provide comprehensive information on the structure, transformations, and properties of materials. All these methods are discussed later in the book.

Finally, for successful utilization of materials in various structures, machine elements, tools, and the like, we have to determine their technological properties, in particular, casting properties which characterize the behaviour of a material during the manufacture of cast articles; deformability (i.e. the capability of a material of being rolled, forged, or die-formed), weldability, machinability, etc. Determinations of these properties depend, in the first place, on the conditions of manufacture of articles and are discussed in the courses on machine-building technology, foundry, forging, die-forming, and so on.

Chapter Two

MACROSCOPIC EXAMINATION OF METAL STRUCTURES (MACROANALYSIS)

2.1. CHARACTERISTICS AND APPLICATION OF MACROANALYSIS

Macroanalysis is the examination of the structure of metals (macrostructure) by the naked eye or through a magnifying glass of a low magnification (up to 30X). This makes it possible to inspect at once a large area of an article and often obtain some data on metal quality, and determine the conditions of preliminary treatment which might affect the continuity of the metal and its structure, solidification, and the nature and quality of the final treatment (casting, plastic working, welding, cutting).

As distinct from microanalysis (see Ch. 3), macroanalysis fails to detect fine detail of the metal structure. For that reason macroanalysis is more often used for the preliminary, rather than for final, investigation of metals. Using the results of macroanalysis, certain portions of an article that require a more detailed microscopic analysis may be selected.

The results of macroanalysis can be fixed, when needed, by taking a photograph of the macrostructure of the portion being studied. This is made by special cameras enabling plane and relief objects to be photographed with a magnification of from 0.5 to 20X.

Macrostructures can be studied either directly on the metal surface (for instance, on the surface of castings or forgings) or on fractures of articles, or after treating the surface, i.e. after grinding and etching it with reagents. A ground and etched specimen prepared for macroanalysis is called *macrosection*; if cut in a cross section of an article, it is sometimes called *templet*. The ground surface of a macrosection should be clean, without any traces of oil, etc.

2.2. MACROANALYSIS OF METAL FRACTURES

Fractures of metals may be diverse in shape, appearance, and light reflectivity, depending on the composition and structure of the metal, the presence of certain defects, the conditions of heat

treatment and the stressed state at which the fracture has taken place. Analysis of a fracture thus makes it possible to establish many peculiarities of the structure of a metal, and in some cases to determine the causes of brittle or plastic fracture.

The most common kinds of fracture of steels and cast irons are now described.

The surface of a fracture may be either (a) smooth and bright or (b) with protruding cup-shaped edges. The first type is characteristic of a brittle state, when fracture occurs without noticeable plastic deformation, and the second type, of a ductile state (see Ch. 6). This description of fractures is only approximate and in some cases inaccurate, since their surfaces vary depending on the conditions causing the fracture. Torsional specimens of ductile metals have a smooth fracture perpendicular to the axis of torsion, whereas brittle metals produce torsional fractures of a complicated (spiral) shape.

The *structure* of a fracture can more deeply characterize the behaviour of the metal during fracturing. According to this feature, the following kinds of fracture are distinguished:

(a) *granular* or *crystalline* (bright with facets), obtained through brittle fracture of steels of a reduced ductility (including those appreciably overheated during hardening) or in steels being tested below their limit of cold brittleness (see Sec. 6.4 and Fig. 6.13);

(b) *lustreless* or *fibrous*; metal grains are invisible; this type of fracture is found in ductile fracturing preceded by appreciable plastic deformation;

(c) *combined type*, i.e. granular (or crystalline) in some places and fibrous in others; this is characteristic of steels fractured within the transition temperature interval between the upper and lower limits of cold brittleness (see Sec. 6.4) and of steels not hardened fully; in such cases the hardened surface zone of the fracture is lustreless (porcelain-like) and the core granular (or crystalline); the combined type of fracture is also observed under conditions of fatigue breakdown (see Sec. 6.3);

(d) *a fracture having characteristic white spots* (see Fig. 2.1) called flakes; this is observed comparatively rarely in steels of definite composition. It is an indication of poor metal quality, especially low ductility (owing to microsegregation of the hydrogen present in the steel).

According to its ability to reflect light, a fracture may be either bright, which is characteristic of steels and white irons (i.e. those in which all the carbon has been combined into cementite) or dark, as in grey, malleable, and high-strength irons which contain much graphite.

2.3. MACROANALYSIS OF METAL SECTIONS

There are a number of methods of macroanalysis depending on the aim.

(a) Investigation of Discontinuities

Macroanalysis can detect: (a) shrinkage porosity, gas blow-holes, cavities and fissures formed in cast metal (ingots or castings) because of improper conditions of melting, casting and solidification; (b) cracks formed in rolled or forged metal during plastic working or heat treatment; and (c) cavities and gas blow-holes formed in weld seams during welding.

Templets cut from cross-sectional planes should be preferred for analysis of such defects in ingots, castings, and rolled and forged stock, and longitudinal macrosections for analysis of defects of weld seams.

The methods of etching macrosections (templets) are selected according to the kind of metal.

(b) Macroanalysis of Steel

Discontinuity defects in steel can be detected by deep etching or surface etching with appropriate reagents.

Deep-etching reagents are preferably used for macroanalysis of ingots (castings) and rolled stock (or forgings). Their compositions are given in Table 2.1.

Table 2.1. Deep-etching Reagents of Steel Ingots and Rolled Steel

Kind of steel to be etched	Composition			
	HCl (density 1.1), ml	HNO ₃ (density 1.4), ml	K ₂ Cr ₂ O ₇ , g	Water, ml
Structural steels, tool steels, chromium stainless steels (up to 18% Cr)	1000	—	—	1000
Chromium stainless steels (over 18% Cr) and austenitic steels	1000	100	250	1000

Etching is done at a temperature of 60-70 °C for 15-25 minutes for carbon and low-alloy steels and 15-40 minutes for high-alloy steels. Macrosections are preliminarily wiped with alcohol to remove dirt from their surface and then immersed (usually the ground surface sideways) into a heated bath with the reagent.

Etching should be performed under a vent hood. The sections are taken from the bath by means of pincers or hands protected by rubber gloves.

Etched macrosections are rinsed with water and then with a 10-15 per cent aqueous solution of nitric acid and dried; this assures a bright surface and makes surface defects more visible. Good results are obtained after rubbing the etched surface with a common eraser. Sections of stainless steel are rinsed in water and then in an aqueous solution of 100 ml H_2SO_4 and 50 g $\text{K}_2\text{Cr}_2\text{O}_7$ in 100 ml water, after which they are dried.

Deep-etching reagents can strongly affect the surface of steel. The action of concentrated acids and their mixtures may vary over the metal surface, being greater in portions with a more developed and active surface, i.e. ones containing pores, cavities, fissures and stress concentrations, and also in portions which are inhomogeneous in their composition and structure owing to segregation. A steel section having such defects is thus etched selectively, so that its fissures and pores may become visible.¹

Besides, certain peculiarities of the metal composition in some regions and the effect of impurities and transformations can cause appreciable stresses, including tensile stresses which are especially dangerous. Such portions possess poor mechanical properties and can form fissures during subsequent processing; this also can be detected by macroanalysis.

Figure 2.1a shows a fracture of chrome-nickel steel before etching; characteristic white spots (flakes) are clearly seen in the photograph. Etching the macrosection (Fig. 2.1b) reveals fine fissures more numerous at the metal core. Such a steel is a reject.

More homogeneous portions of metal having lower concentrations of impurities and carbon are etched less deeply and appear as bright protrusions on the etched background of metal. Etching with the reagents indicated can also reveal segregation zones and in addition, the dendritic structure in cast steel and fibres in rolled steel (if the section was cut in the longitudinal direction).

Surface-etching reagents develop well comparatively large pores, for instance, in welded specimens, and can also reveal the nature of segregation and flow patterns of the metal. They cannot, however, replace deep-etching reagents for the determination of flakes, and fissures and pores not opened at the surface. Surface-etching reagents are advantageous in being less aggressive

¹ Small pores and fissures are often invisible in metal fractures and non-etched macrosections, since they can be clogged with particles of metal as the sections are being prepared (machining and grinding).

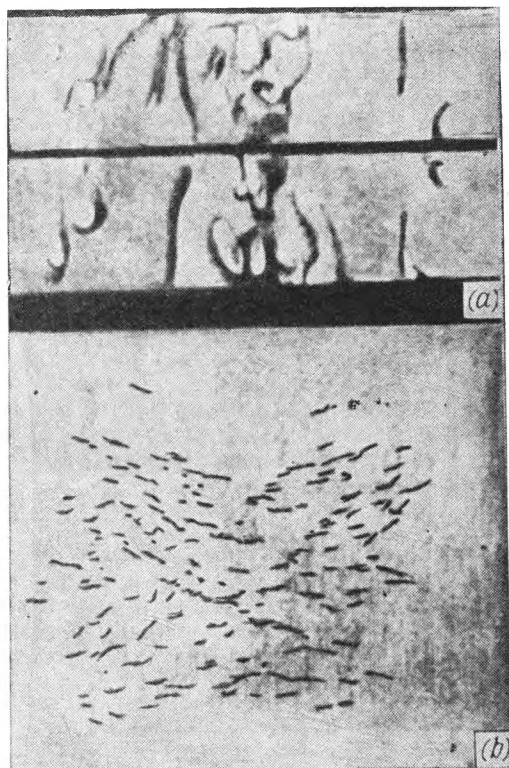


Fig. 2.1. Flakes in Cr-Ni steel (according to V. Doronin)

(a) steel fracture; (b) macrosection of fracture after deep etching (another specimen)

and easier to handle. They are used widely, especially for macro-analysis of low- and medium-carbon steels.

The commonest reagent is that containing copper ions; its composition is 35 g CuCl_2 and 53 g NH_4Cl per 1000 ml water. Microsections are wiped with alcohol and immersed for 30-60 seconds in the reagent, ground surface downwards. An exchange reaction then occurs during which iron substitutes copper in the aqueous solution. Copper settles to the surface of macrosections, except the places where the reaction does not proceed to the end (pores, fissures, non-metallic inclusions); only these places undergo etching. The sections are then taken from the solution, the copper layer is removed by rubbing with cotton wool in running water, and the surface dried. Figure 2.2a shows a macrosection of a weld seam before etching, and Fig. 2.2b, the same section

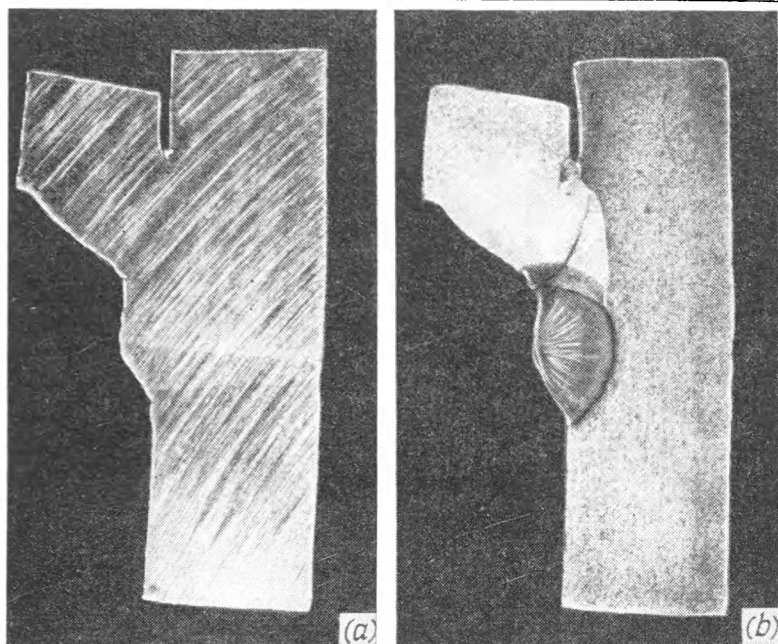


Fig. 22. Macrosection of a weld seam (full scale)
(a) before etching; (b) after etching

after etching. Macroanalysis reveals pores at the point of connection between the main metal and weld seam; dark bands in the main metal represent the regions enriched in carbon, sulphur, and phosphorus.

(c) Macroanalysis of Non-ferrous Metals

Copper alloys can be etched with the following reagents:

- (a) 10-20-percent aqueous solution of ammonium persulphate;
- (b) 10-percent solution of hydrogen peroxide in a saturated aqueous solution of ammonia; or
- (c) solution of 10 g iron chloride and 30 ml hydrochloric acid in 120 ml water.

Discontinuities in aluminium-copper alloys are detected by etching with 10-15-percent aqueous solution of sodium hydroxide. A macrosection is held in the reagent until a dark film forms on its surface; it is then rinsed in water and placed for

1-2 seconds in a 50-percent solution of nitric acid (density 1.50) to remove the film.

Traces of the acid are removed by washing carefully in boiling water.

Duralumins are etched with a reagent composed of a solution of hydrochloric acid of a density of 1.19 g/cm³ (40 ml), nitric acid of density of 1.50 g/cm³ (40 ml), and hydrofluoric acid (10 ml) in water (150 ml). Etching occurs quickly. After etching, the macrosection must be immediately rinsed in water and dried.

Nickel-base alloys are etched with a solution of iron chloride (10 g) and hydrochloric acid (30 ml) in water (120 ml).

(d) Determination of Structure of an Alloy (Dendritic Structure) Formed During Initial Crystallization

The structure of cast steel is revealed by etching in a 15-percent aqueous solution of ammonium persulphate [(NH₄)₂S₂O₈] heated up to 80-90 °C. Macrosections of carbon steel should be kept in the solution for 5-10 minutes, those of alloy steels, a bit longer, depending on their behaviour during etching.

For higher contrast, an etched macrosection is immersed in a 5-percent solution of nitric acid (density 1.4 g/cm³) for 1-2 minutes, after which the film that has formed is removed (mechanically); the section is then dipped in a cold 15-percent solution of ammonium persulphate for 2-3 minutes. Figure 2.3 shows the macrostructure of cast steel after etching with this solution; the macroanalysis has revealed a typical dendritic structure.

The macrostructure of non-ferrous alloys can be revealed by the above-mentioned reagents used to detect discontinuities.

The structure of initial crystallization of aluminium alloys can also be exposed by a reagent prepared from 4 ml nitric acid (density 1.50 g/cm³), 4 ml hydrofluoric acid, 4 ml 10-percent solution of potassium ferrocyanide and 2 ml 30-percent hydrogen peroxide dissolved in 1000 ml of water.

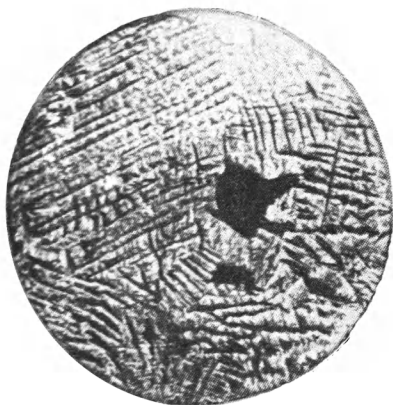


Fig. 2.3. Macrostructure of cast steel after etching (full scale)
The black spot in the centre is a pore (a defect often found in metal castings)

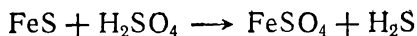
(e) Determination of Chemical Heterogeneity (Segregation) of Alloys

Macroanalysis can reveal the zonal and dendritic segregation of carbon and harmful impurities (sulphur and phosphorus) in steel. The degree and nature of segregation depend not only on the contents of carbon and impurities, but also on the conditions of casting the metal and of solidification of the ingot (casting) and subsequent plastic working.

Macroanalysis provides only a qualitative estimation of a chemical heterogeneity but, as distinct from chemical analysis, cannot determine the content of carbon and impurities. But its advantage over chemical analysis is that it can show the non-uniformity of distribution of impurities (segregation) over the cross section (or volume) of the specimen exposing portions more contaminated with impurities or the less contaminated ones.¹

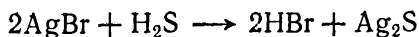
To detect sulphur segregation, the surface of a macrosection is well polished with fine emery paper and then wiped with cotton wool wetted with alcohol to remove abrasive particles, metal dust, and other contaminations. A sheet of photographic (silver bromide) paper is moistened in full light or held for 5-10 minutes in a 5-percent aqueous solution of sulphuric acid and then slightly dried between sheets of filter paper. The photographic paper is then laid onto the prepared macrosection and carefully rolled (without displacement) by a rubber roller or with the hand (in a rubber glove) to remove air bubbles from beneath it, since these may cause white spots on the paper and thus spoil the results of macroanalysis. The paper is held on the macrosection for approximately 30 minutes.

Sulphur can be present in steel as compounds with manganese (MnS) and iron (FeS). In the regions of the metal surface where accumulations of sulphur compounds (sulphides) are present, a reaction occurs between these compounds and the residual acid on the paper:



A similar reaction occurs between the acid and manganese sulphide.

The hydrogen sulphide evolved at the accumulation points acts on crystals of silver bromide of the photographic emulsion by the reaction



¹ More accurate and reliable data on chemical heterogeneity can be obtained by X-ray spectrum examination in apparatus of the MAP type.

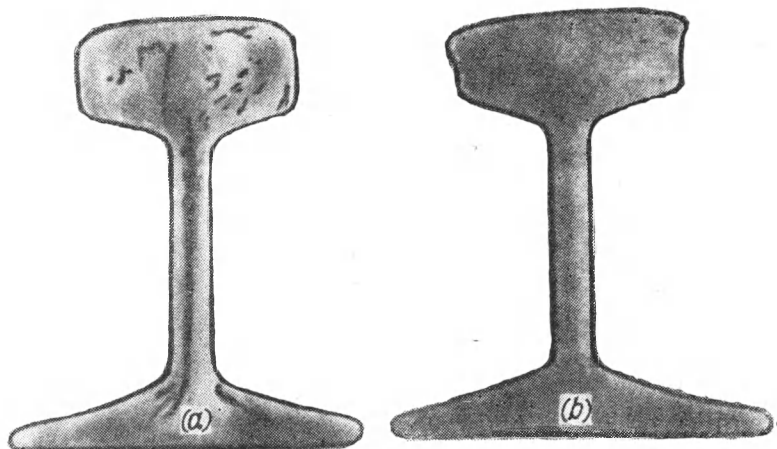


Fig. 2.4. Sulphur segregation in steel ($\frac{2}{5}$ of the full scale)

Silver sulphide is dark and therefore the dark portions of the paper reproduce the form and nature of sulphide distribution in the steel (or cast iron).

The paper is then taken from the macrosection, rinsed in running water, fixed for 20-30 minutes in hyposulphite, washed (for approximately 10 minutes) in water, and dried.

Figure 2.4 shows photographic prints of cross-sectional macrosections of steel rails. The print in Fig. 2.4a shows that the steel has a less uniform distribution of sulphur (owing to segregation) than the steel whose print is shown in Fig. 2.4b.

Phosphorus, if present in increased quantities in some regions of the steel or cast iron owing to segregation, also can react with silver bromide and form dark silver phosphides.

To determine the segregation of carbon and phosphorus, the reagent mentioned above, which contains 85 g CuCl_2 and 53 g NH_4Cl (per 1000 ml water), can be used. When etching a steel macrosection, copper settles less intensively in regions rich in carbon and phosphorus and therefore offers less protection to the metal surface against the etching action of the chloride salt of the reagent. These regions become dark.

This method gives the best results for steels containing up to 0.6 per cent C. Steels with a higher content of carbon have the disadvantage that the copper sediment can only hardly be removed from the surface.

This reagent can simultaneously reveal sulphur segregation, since the distribution of sulphur, phosphorus, and carbon is almost similar.

**(f) Determination of Structural Heterogeneity
Formed Through Plastic Working of Alloys
(Banding)**

Non-metallic inclusions in steel (sulphides, oxides, slag particles) and segregated portions which differ in their composition and structure from the main metal are partially disintegrated and stretched along the direction of deforming during plastic working (rolling, forging or die-forming), thus producing a characteristic longitudinal fibrous pattern (*initial banding*). In addition, the precipitated phase (ferrite) in hypoeutectoid steel is liable to solidify around the stretched non-metallic inclusions and form what is called *secondary banding*.

The impact strength and plasticity of a metal depend on the direction of fibres, being higher in specimens cut along the direction of fibres and lower in those cut across them.

When machining a metal article, fibres in the metal may be cut through. For machine elements operating under high specific loads, especially dynamic ones (crankshafts, engine valves, many types of gear wheel, hammer stamps, etc.) the metal fibres must not be cut through, they should follow the outline of the element or better the lines of highest stresses. This is achieved by properly selecting the methods of forging and die-forming.

Macroanalysis not only reveals the direction of fibres in a deformed metal; it also determines the method of manufacture, in particular whether the element was cast, forged (die-formed) or machined (see Fig. 2.5).

Metal fibres due to their different composition and structure may be etched differently. Banding in a metal can be well revealed by a reagent containing 85 g CuCl_2 and 53 g NH_4Cl per 1000 ml water. Macrosections should be cut out in the longitudinal direction (along the fibres). Since sulphide inclusions also participate in the formation of banding, the method of photographic printing described earlier may be used with success.

**(g) Determination of Compositional and Structural
Heterogeneity Formed Through Heat Treatment or
Chemical-heat Treatment**

Macroanalysis of hardened steel is used to determine:

(a) the thickness of a surface layer which has a higher hardness than its relatively soft core; for instance, articles (or specimens) of carbon steel of diameter or thickness more than 15 mm are not hardened over the whole cross-section, but only in a relatively thin surface layer, sometimes only 2-3 mm thick (see Ch. 17);

(b) the thickness of a cemented (carburized) layer which after hardening acquires a higher hardness and a higher wear resistance than the main metal.

The thickness of a hardened (cemented) layer may be determined by various methods: macroanalysis, microanalysis, and hardness test. Macroscopic examination can be made quickly, with sufficient accuracy under industrial conditions. For this purpose a specimen is hardened and then fractured. The hardened (or cemented and hardened) layer has a finer grain and, if the hardening was accomplished without overheating, a lustreless porcelain-like (silky) fracture differing noticeably from the fracture of the core. The thickness of the layer can be determined by the naked eye or through a magnifying glass. This layer becomes more distinct after a short heating to 300-350 °C, when the core becomes bright-blue and the surface layer, dark-blue (annealing colours).

With specimens of larger cross section (more than 20-25 mm in diameter) this simple method is sometimes inaccurate as it is difficult to break the specimen without substantially distorting its shape at the point of fracture. Such specimens are polished in the plane of fracture (normal to the axis). Polished specimens are etched for 3 minutes in a 50-percent solution of hydrochloric acid at 80 °C. The hardened layer then becomes dark.

Cemented layers can be seen after immersing the specimens for 1-2 minutes in a reagent composed of 2 g $\text{CuCl}_2 \cdot \text{H}_2\text{O}$ and 1 ml HCl dissolved in 100 ml alcohol. The soft non-cemented core becomes covered with a red layer of copper, whereas the cemented layer remains unchanged. The cemented layers can also be revealed by immersing the polished surface in a hyposulphite solution; from this reaction the ferrite grains become covered with a dark film of ferrous sulphide, while the cemented layer, which is rich in carbon, remains bright.

2.4. LABORATORY EXERCISES

Before making laboratory work on a macroscopic examination, students should read Sections 1 and 2 of this Chapter.

Macroanalysis can be done by either (a) a simpler method or (b) a more complicated method which, however, is widely used in industry for quality control.

Macroanalysis should begin from the inspection of a macro-section and its etching with a solution of 85 g CuCl_2 and 53 g NH_4Cl in 1000 ml water. From this treatment it becomes possible to judge (a) the preliminary processing of the metal (casting, forging, rolling, or welding); (b) segregation of phosphorus and

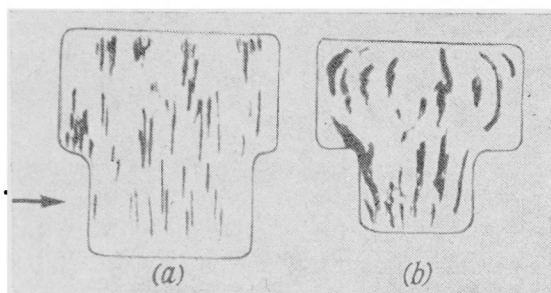


Fig. 2.5. Segregation of sulphur and phosphorus

(a) bolt made by cutting a rolled rod; (b) bolt made by upsetting a rolled blank

carbon; (c) quality and method of welding; and (d) discontinuities in the metal.

The patterns formed by this etching should be sketched. After that, macroanalysis by sulphur printing should be done to determine the degree of segregation. Before using a different reagent, the surface of the macrosection must be prepared anew. Grounding the surface with fine emery paper is sufficient to remove traces of the previous etching. The section must be ground in two perpendicular directions to remove scratches.

The work record must contain.

1. A sketch of the specimen.
2. The aim of the work.
3. Substantiated selection of the method of macroanalysis in accordance with the requirements and aim of the work.
4. Sketches of the etched surface.
5. A photographic sulphur print.
6. Conclusions on the quality of the metal and the method of preliminary processing of the tested specimen.

Figure 2.5 shows, by way of an example, the macrostructure of two bolts. Sulphur prints of these bolts offer the following conclusions:

(a) in both cases, segregation of sulphur and phosphorus in the steel is noticeable, the degree of segregation being lower in the bolt shown in Fig. 2.5a; the second bolt (Fig. 2.5b) was made of a steel containing more sulphur and phosphorus;

(b) the bolt in Fig. 2.5a was cut from a rolled blank; drawing during rolling caused noticeable banding; these bands were later cut through by a cutting tool;

(c) the bolt in Fig. 2.5b was forged and upset from rolled rod; metal fibres were not cut, they followed the direction of flow of the metal during upsetting;

(d) the bolt in Fig. 2.5a has a lower impact strength in the transverse direction (shown by the arrow) than in the longitudinal direction, whereas the bolt in Fig. 2.5b has almost the same impact strength in all directions.

Problems

No. 1. Carry out a macroscopic examination (macroanalysis) of macrosections from two shafts¹ and decide which shaft was made of the higher quality steel (with lower sulphur and phosphorus contents).

Sketch the macrostructure of the specimens and describe the methods of macroanalysis used in the work. Explain why macroanalysis enables the degree of purity of metal to be determined.

No. 2. Specimens of carbon steel were cut from a rolled bar, one along the length of the bar (in longitudinal direction) and the other along the bar diameter (in transverse direction).

Sketch the macrostructure of the specimens.

Determine the specimen that was cut in the longitudinal direction and explain why this problem could be solved by macroanalysis.

No. 3. Carry out macroanalysis of two steel bolts made from rolled blanks by unlike methods.

Determine: (a) which bolt was die-formed and which one was cut; (b) which has the more homogeneous mechanical properties (impact strength) in longitudinal and transverse directions; and (c) why macroanalysis solves these problems.

No. 4. A pipeline was made by welding pipes. Evaluate the quality of weld seams in specimens taken from two sections and sketch their macrostructures.

Explain why macroanalysis solves this problem. Describe the methods of macroanalysis used.

No. 5. Carry out macroanalysis of two specimens and, from this data, decide which was made by welding together two strips of steel and which was cut from a steel blank.

Sketch the macrostructures of the specimens.

Describe the methods of macroanalysis used in the work and explain why these methods are capable of determining the method of manufacture of the specimens.

No. 6. Determine the macrostructure of two gear wheels and, using the data obtained, decide which is more suitable for operation at substantial dynamic loads.

¹ The machine elements recommended in Problems 1-19 are those most convenient for macroanalysis; other elements may also be used.

Sketch the macrostructure of the wheels. What is the basis of the macroanalytical methods for determining the macrostructure of finished articles?

No. 7. Carry out macroanalysis of a weld seam of steel and decide which zones of the seam — either those formed by the electrode or those formed by the main metal — are of better quality.

Sketch the macrostructure of the steel in the specimen and name the method of macroanalysis that must be used to solve this problem.

No. 8. Carry out macroanalysis of two steel specimens and decide which was made from a solid blank and which one by welding.

Sketch the macrostructures of the specimens.

Name the methods of manufacture of each of the elements and assess the quality of the weld.

No. 9. Various types of weld seam (welding connection) are employed in industry. Determine the type of seams of two welded specimens.

Sketch their macrostructures, describe the methods of macroanalysis applied, and explain why they can be employed for this determination.

No. 10. Characterize the type and quality of the weld seam of two welded connections.

Sketch the macrostructure of steel in the specimens studied.

What methods of macroanalysis should be used to solve this problem and why can they characterize the quality of steel, the method of manufacture of articles, and the quality of the weld?

No. 11. Carry out macroanalysis of two specimens cut from steel elements and sketch their macrostructure.

Which element was made from cast steel and which one, from rolled stock?

Explain why macroanalysis can characterize the structure of metal and the method of manufacture of articles.

No. 12. Analyse the macrosections of two brass gear wheels and sketch their macrostructures.

Which wheel was made from a cast blank and which one from rolled brass?

What are the methods of macroanalysis used to study copper alloys?

No. 13. Carry out macroanalysis of two sleeves made of tin bronze and sketch their macrostructures.

Which sleeve was made by casting and which one, from a pressed bronze rod?

Name the method of macroanalysis used to solve this problem.

No. 14. Carry out macroanalysis of two aluminium-alloy (silumin) castings, one of them sand-cast and the other, die-cast.

Using the results of the macroanalysis, name the characteristic features of the initial crystallization in each casting and explain the differences in their structure.

Name the reagent suitable to solve this problem.

No. 15. Carry out macroanalysis of two castings of aluminium alloy (silumin) made by die casting at different temperatures of molten metal, the temperature difference being 100-200 °C.

Describe the specific features of the initial crystallization in the castings and explain the effect of the temperature of molten metal on the macrostructure of the alloy.

No. 16. Carry out macroanalysis of two aluminium-alloy articles.

Decide which article was cast and which one, forged (die-formed).

Name the method of macroanalysis used.

Chapter Three

DETERMINATION OF STRUCTURE OF MATERIALS BY MICROSCOPIC EXAMINATION (MICROANALYSIS)

3.1. CHARACTERISTICS OF MICROANALYSIS

Microscopic examination (microanalysis) is the study of the structure of materials under a microscope at large magnifications. The structure observed is called the *microstructure*. Depending on the magnification required the phases of a structure, their number, shape and distribution may be studied, by using:

(a) visible light and common optical systems, their different magnifications being obtained by changing the combinations of glass lenses and prisms (*optical microscopy*);

(b) electron beams, or more correctly, a flow of electrons in an electron-optical system consisting of electromagnetic and electrostatic lenses (*electron microscopy*).

The preparation of objects ready for observation and the interpretation of the images observed in optical microscopy and electron-optical microscopy are done by different methods depending on the nature of radiation (optical or electron-optical) and the design of microscopes.

3.2. METHODS OF OPTICAL MICROSCOPY

The method of optical microscopy, proposed by P. P. Anosov in 1831, is widely used for studying the structure of metals and for engineering quality control.

As indicated in Ch. 1, a definite though only qualitative, relationship exists between the structure of a metal observed in an optical microscope and certain properties of that metal. In many cases microanalysis shows that the variations in alloy properties are due to variations in the chemical composition and conditions of treatment.

The application of white light in optical microscopy allows the structure of metals to be observed at general magnifications of from a few tens to 2000-3000. The useful magnification, however, cannot exceed 1500 because of light diffraction; this will be discussed later. With such a magnification it is possible to detect



Fig. 3.1. Microstructure of single phase brass after rolling and annealing. 150X

elements of a structure not less than $0.2\text{ }\mu\text{m}$ in size, which is in most cases sufficient for determination of the size of the majority of phases present in an alloy. Thus, the method of optical microscopy can be used with success for observations of the structure of many metallic alloys.

The magnification selected, within the limits allowed by the optical microscope, depends on the structure of alloys. In some cases large magnifications are not needed (and are even inexpedient); in others a large magnification may be required.

Figure 3.1 shows the microstructure of single-phase brass after rolling and annealing with a magnification of 150. Observing the same brass with a magnification of 1500 cannot reveal new characteristic detail, but the general picture of its crystalline structure will be less clear, since only a single grain or, with larger magnifications, a part of a grain, rather than a number of grains, will be seen in the field of vision of the microscope.

Figure 3.2 shows the microstructure of ball-bearing steel after final heat treatment, i.e. in a state when it has a high hardness and a high wear resistance, the properties required for ball and roller bearings.

At *a* and *c* in the Figure, the microstructure of the steel is shown at a magnification of 100, and at *b* and *d*, at 500. In both cases, as seen from the microanalysis, the steel is composed of two phases: the basic component (martensite), which is seen dark and possesses a high hardness and a white component (carbides) possessing even higher hardness and thus increasing the strength of the structure. The operational properties of ball and roller

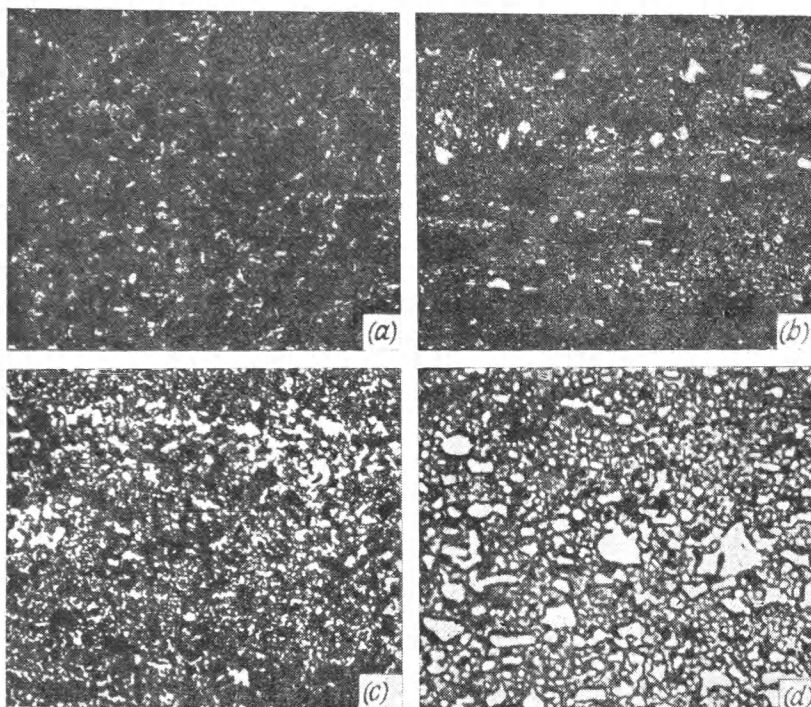


Fig. 3.2. Microstructure of ball-bearing chromium steel (1% C, 1.5% Cr)
(a) slight carbide heterogeneity, 100X; (b) ditto, 500X; (c) appreciable carbide heterogeneity, 100X; (d) ditto, 500X

bearings are better when their structure contains fine carbide grains uniformly distributed through the basic martensite. On the other hand, their properties will be impaired when carbide grains are large and concentrate in certain regions only. Microanalysis clearly determines the distribution of carbides. The study of the structure at a magnification of 100 shows the distribution of carbides better (carbide banding), and the 500-fold magnification reveals clearly the size and shape of individual carbide grains.

In some cases a conception is required of the structure of the metallic matrix of steel, in this case martensite. As established, the structure of the metallic matrix composed of fine martensite crystals gives better mechanical properties to ball-bearing steels, than the matrix with large martensite crystals. With low magnifications, however, (100 to 200) it is impossible to decide whether the structure is composed of fine or coarse martensite grains, since their size is quite small, and therefore, larger magnifica-

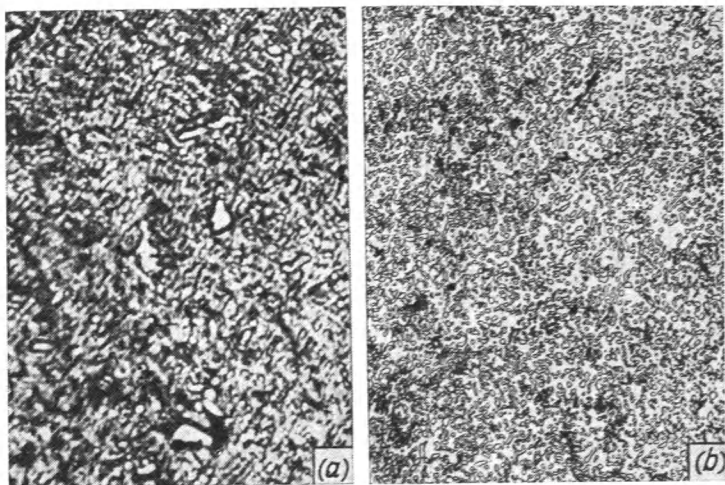


Fig. 3.3. Microstructure of hardened ball-bearing chromium steel (1% C, 1.5% Cr)
(a) 100X; (b) 1000X

tions (up to 1000 or more) are needed. The results of studies of the microstructure of ball-bearing steel at higher magnifications are shown in Figs. 3.2*b* and *d* and 3.3*b*.

At first the microanalysis is usually conducted at a low magnification and then at larger magnifications; this depends on the form of the structure and the object of the study, with a number of regions of a microsection being studied in each case.

(a) Determination of Phase Composition and Structure of Alloys in Equilibrium

Pure metals and single-phase alloys (solid solutions) in cast articles have a characteristic dendritic structure. After plastic deformation and annealing, which brings the metal into the equilibrium state, their structure consists of grains of a like shape (equiaxial polyhedrons). Figure 3.4 shows the microstructure of copper and Fig. 3.1, that of single-phase brass after casting, plastic working and annealing.

In such structures deep etching can reveal what is called etch patterns; these are geometrically regular recesses and projections defined by various crystallographic planes. By measuring the angles between crystal faces or determining the directions of edges on the etch patterns, the orientation of each crystallite, and

therefore, the orientation of the whole totality of crystallites can be determined. Finally, dislocations in single-phase alloys can be detected; they are a special kind of linear crystal defect. Special etch patterns, i.e. groups of etching spots, reveal these dislocations. These spots appear owing to deeper etching of the metal in places where aggregates of dislocations come near to the surface, and also to the accumulation of impurities on dislocations. Etching spots can be revealed by various reagents depending on the nature of the metal. The surface of microsections for such etching must be prepared very carefully without the slightest trace of mechanical processing. From the position of etching spots the specific features of the fine structure of a crystal, i.e. the size of crystal blocks and the degree of their disorientation, may be determined. The number of etching spots may in some cases be used to calculate the dislocation density.¹



Fig. 3.4. Microstructure of copper, 100X

Multi-phase alloys, including two-phase alloys, have a more complicated structure composed of various phase combinations; they may be eutectic, eutectoid, etc.

Figure 3.5 shows the structure typical for eutectics, the Cu-Cu₃P eutectic in the case considered, whose constitutional diagram is shown in Fig. 3.6. For comparison, Fig. 3.7 illustrates the structure of the eutectoid of iron-carbon alloys. Both structures are fine-crystalline, but the eutectoid is more disperse, since it is formed through decomposition of a solid solution when the diffusion processes are slowed down.

In multi-phase alloys whose chemical composition does not correspond exactly to the eutectic concentration a precipitated phase can segregate along with the eutectic, for instance in the alloys whose concentrations are within points *c* and *d* on the diagram (Fig. 3.8). In alloys whose concentrations lie between points *a* and *b* on the diagram the precipitated phase segregates

¹ The spots representing traces of dislocations near the surface retain their places after repeated electropolishing. The spots revealed on the surface of a microsection should rearrange their positions after plastic deformation or heating.

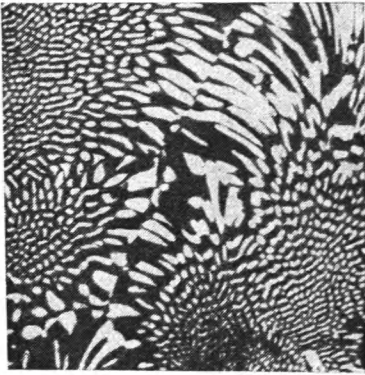


Fig. 3.5. Microstructure of eutectic of the Cu-Cu₃P system, 600X

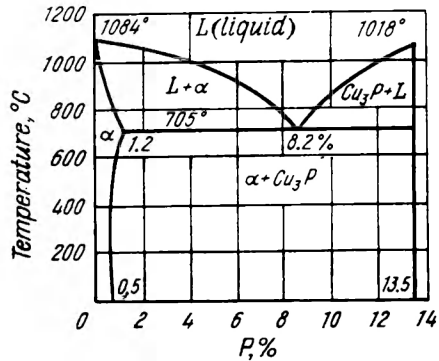


Fig. 3.6. Constitutional diagram of Cu-Cu₃P alloys

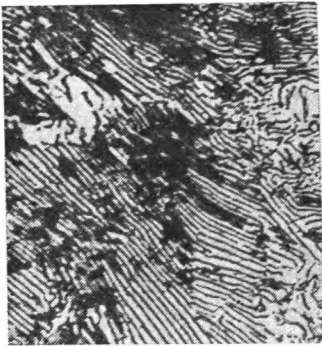


Fig. 3.7. Microstructure of annealed carbon steel of eutectoid composition (0.8% C), 600X

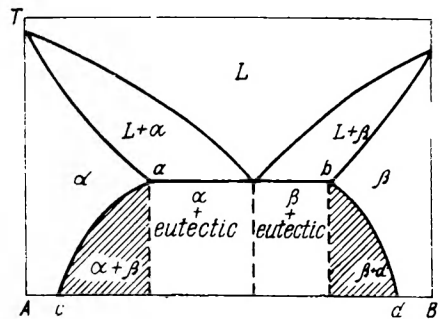


Fig. 3.8. Constitutional diagram of alloys composed of two components having a limited solubility in the solid state which reduces with decreasing temperature

from the liquid, whereas in alloys whose compositions correspond to the hatched areas the precipitated phase segregates from the solid solution only when its solubility decreases.

A precipitated phase usually solidifies in the form of large grains or dendrites, which is linked with the peculiarities of the growth of the precipitated phase as solidification of the alloy proceeds within the temperature interval between the liquidus and solidus (Fig. 3.9).

The precipitated phases, as they segregate from the solid solution, have various forms (Fig. 3.10), needle-like, granular or, very often, the form of a network at grain boundaries. The form and properties of a segregated phase strongly affect the properties of an alloy. When, for instance, a precipitated phase is hard and brittle, its segregation in the form of a network appreciably impairs the plasticity and ductility of the alloy (Fig. 3.10c). A phase in the form of fine granular inclusions uniformly distributed in the matrix usually increases the strength of the alloy without reducing sharply its plasticity.

Figure 3.11 shows a two-phase structure formed through a peritectic reaction. Rounded portions represent the α -phase formed at the beginning of solidification, and regions around these portions, the β -phase formed from the peritectic reaction. Determination of the structure of a peritectic presents more difficulty than the identification of other multi-component structures since peritectic reactions occur only at phase boundaries and cannot proceed to completion under conditions of cooling of alloys used in practice.

Ternary and more complicated alloys also have similar forms of their structural components, i.e. single-phase solid solutions and precipitated phases. A different form is found in alloys containing a eutectic. For instance, when a ternary alloy whose composition does not correspond exactly to the eutectic composition solidifies, its precipitated phase segregates first, then the binary eutectic, and finally at the very end of solidification, the ternary eutectic. In three-component alloys the binary eutectic solidifies within a high temperature range, whereas the ternary eutectic solidifies at a lower constant temperature. This is why segregations of the binary eutectic are larger and more easily discernible by microanalysis than those of the ternary eutectic.

Figure 3.12 shows the microstructure of a ternary alloy of the Pb-Bi-Sn system which corresponds in its composition to the binary eutectic line. Such an alloy has no precipitated phase; the photograph shows the regions with a more differentiated

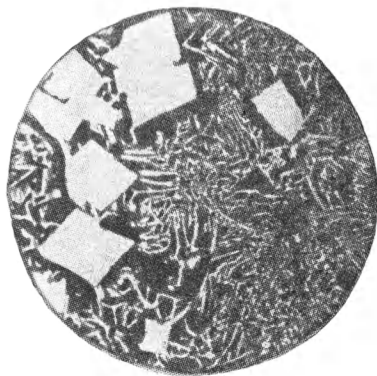


Fig. 3.9. Hypereutectic alloy of the lead-antimony system (20% Sb, 80% Pb)

Large bright grains are crystals of the precipitated phase (antimony), the dark background is eutectic, 100X

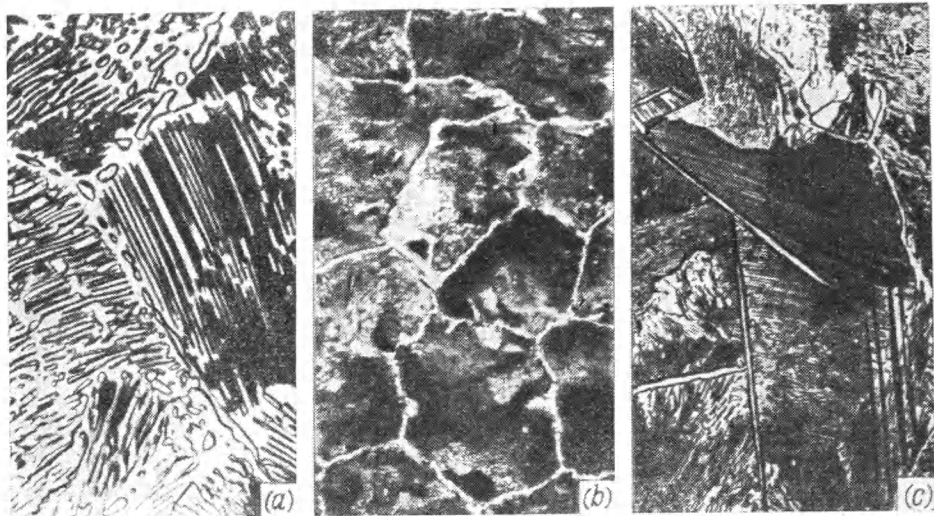


Fig. 3.10. Hypereutectoid steel with precipitated (secondary) cementite
 (a) in granular form, 600X; (b) as a network at grain boundaries, 200X; (c) as needles, 600X



Fig. 3.11 Peritectic structure in an Sn-Sb alloy; precipitation of the secondary phase around initial crystals, 500X

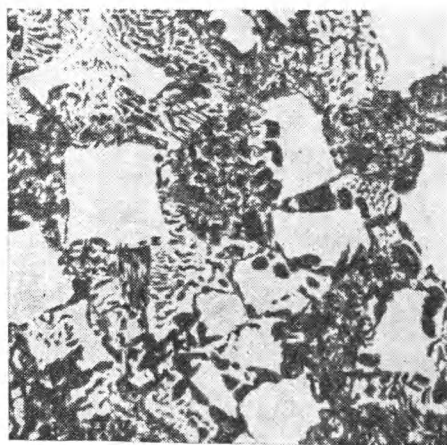


Fig. 3.12. Structure of a Pb-Bi-Sn alloy with binary and ternary eutectic, 100X (according to B. Krimer)

structure (binary eutectic) distributed in the less discernible structure of the matrix, the latter being composed of segregations of the ternary eutectic.

(b) Determination of Non-equilibrium Structures

Microanalysis can also reveal the structures of alloys in non-equilibrium, i.e. in the state in which they are often employed in industry.

Figure 3.13 represents the microstructure of steel with 0.40 per cent C in the equilibrium (after annealing) and non-equilibrium states, i.e. after heating to 750 °C and rapid cooling (incomplete hardening) or after heating to 840 °C and rapid cooling (complete hardening). Rapid cooling makes it possible to form a non-equilibrium structure and, in addition, to characterize the transformations occurring in the steel during heating. Microanalysis clearly establishes that heating to 750 °C, i.e. above the critical point A_{c1} , but still below the point A_{c3} , results in a partial transformation in the steel: instead of the dark (i.e. more etchable) pearlite component and the bright ferrite component a new structure — martensite — forms, with part of the ferrite component (i.e. less etchable component) remaining unchanged. With higher heating (up to 840 °C, i.e. above the critical point A_{c3}), the transformation is complete, the new structure being only martensite.

The formation of martensitic structure in hardened steel sharply changes the steel properties, in particular, it increases strength and hardness but reduces plasticity and ductility appreciably. With a low tempering (at 200-250 °C) of hardened steel its microstructure changes, but microanalysis reveals still larger changes after heating the steel above 300-350 °C; these changes are linked with decomposition of the solid solution (martensite) and coagulation of cementite. Thus, from a microanalysis it is possible to judge important changes of the mechanical and physical properties of steel caused by these transformations.

Microanalysis reveals the characteristic needle-like martensitic structure in hardened steel which differs from other possible structural components but it cannot determine the nature of this phase (see Fig. 3.13).

Microanalysis cannot characterize the structure of a non-equilibrium alloy when the precipitated phases have still not segregated from the matrix phase (i.e. their crystal lattices remain conjugated or coherently linked) or when the particles of the precipitated phase are extremely fine (submicroscopic), i.e. cannot

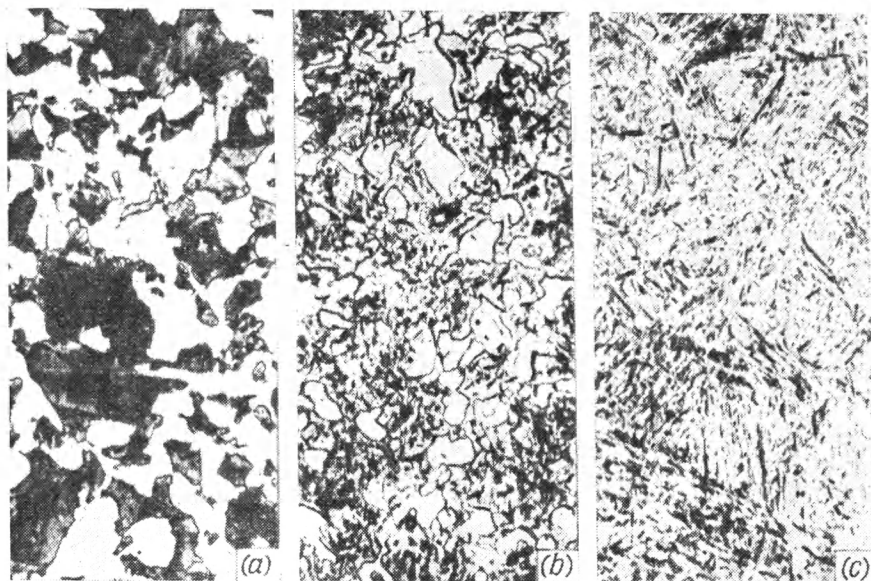


Fig. 3.13. Microstructure of carbon steel (0.40% C)

(a) ferrite + pearlite structure formed through annealing, 200X; (b) ferrite + martensite, structure formed through incomplete hardening from 750 °C with water quenching, 500X; (c) martensite structure after complete hardening from 840 °C with water quenching, 500X

be detected with the given resolution of the microscope. This relates, in particular, to processes occurring during ageing or low tempering of hardened alloys. Data on the structure of such alloys can be obtained by electron microscopy and X-ray examination.

(c) Determination of the Method of Metal Treatment

The method of treatment of an alloy can strongly affect its structure and properties. Microanalysis can disclose the method in which the alloy (or article) being studied has been manufactured and treated. In particular, it shows whether an alloy was cast or subjected to plastic working and how the plastic deformation affected its structure.

Figure 3.14 shows the microstructures of single-phase brass after casting and after plastic working and annealing. As clearly seen, the structure of the solid solution is dendritic after casting and polyhedral after subsequent treatment. The properties of the brass have also changed, in particular, its plasticity for the state shown at *b* is higher than that shown at *a*.

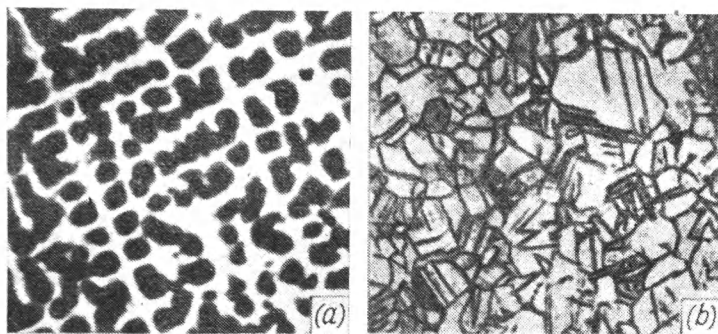


Fig. 3.14. Microstructure of single-phase brass, 100X
(a) after casting; (b) after plastic working and annealing

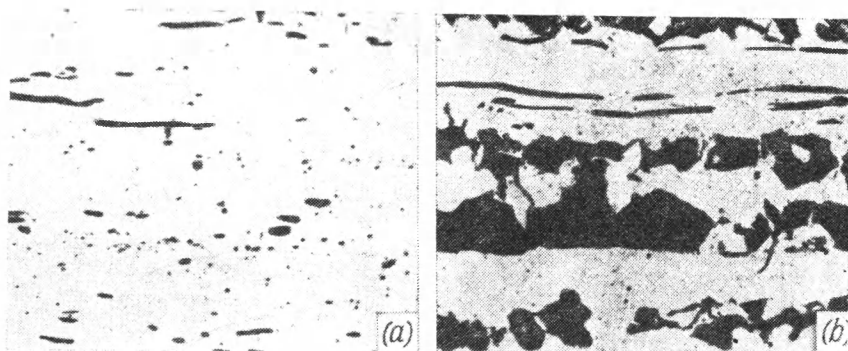


Fig. 3.15. Microstructure of carbon steel
(a) before etching, 100X; (b) after etching, 200X. Dark spots are non-metallic inclusions

In many cases microanalysis is carried out together with macroanalysis. The latter characterizes the structure of a metal over large regions, and the former reveals fine detail of the structure in individual small regions. Figure 3.15a shows the distribution of non-metallic inclusions in rolled carbon steel; as clearly seen, they are stretched along the direction of rolling.

The microstructure of the same steel after etching is illustrated in Fig. 3.15b; here it can be seen, that not only are the non-metallic inclusions stretched, but the pearlite and ferrite portions also, since the non-metallic inclusions have had a nucleation effect on the process of secondary crystallization in the solid state. This kind of banding, termed secondary, cannot be detected by macroanalysis. The impact strength of the steel samples across fibres is higher than that along fibres.

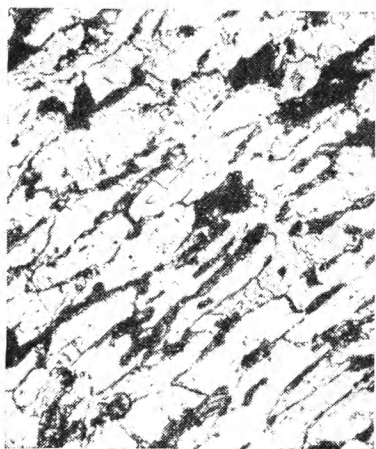


Fig. 3.16. Microstructure of low-carbon steel (0.15% C) after cold deforming, 200X

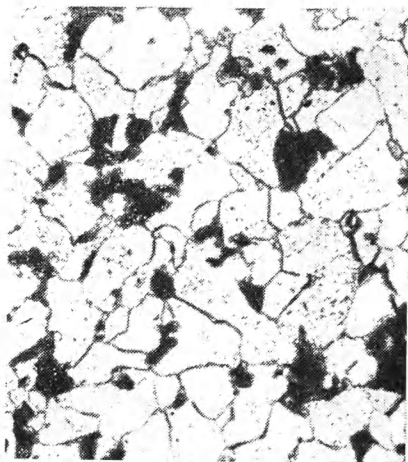


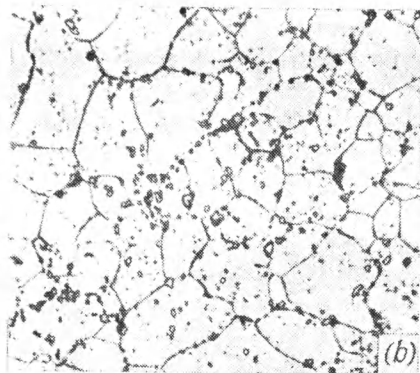
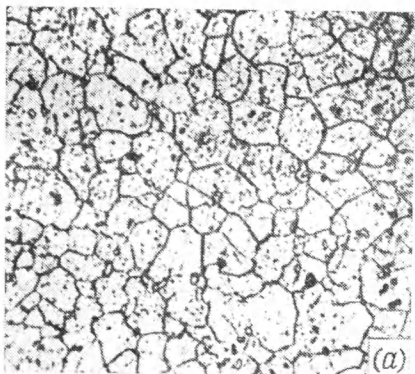
Fig. 3.17. Microstructure of low-carbon steel (0.15% C) after recrystallization, 200X

When some non-metallic inclusions, in particular those of manganese sulphide, have a rounded or even faceted shape, rather than an elongated one, this may indicate that the metal has not been subjected to preliminary deformation, i.e. it is very probably in the cast state.

Further, microanalysis determines with certainty whether an alloy has been subjected to cold deformation and is in a work-hardened state or has been annealed (recrystallized) to eliminate work-hardening. Figure 3.16 shows the microstructure of a low-carbon steel after cold deformation, and Fig. 3.17, the same steel after recrystallization. It is evident that the shape and size of grains have changed through recrystallization.

Microanalysis can determine whether an alloy is in equilibrium or non-equilibrium and in many cases can reveal the kind of heat treatment employed. To do this, the structure observed is compared with that the alloy should possess according to its constitutional diagram, or the alloy is additionally heat treated to transform it to the equilibrium state (for instance, by annealing), and the structure obtained is compared with the initial one. For instance, Fig. 3.13 shows the microstructure of steel after hardening; different structures of the steel may be formed depending on the temperature of heating before hardening either to A_{c1} , but below A_{c3} (incomplete hardening) or above A_{c3} (complete hardening).

The structures of high-speed steel after hardening from different temperatures are shown in Fig. 3.18. An appreciable



g. 3.18. Microstructure of high-speed steel after hardening from various temperatures, 300X
(a) 1250 °C; (b) 1290 °C



Fig. 3.19. Microstructure of carbon steel (0.4% C) overheated when hardening, 500X



Fig. 3.20. Microstructure of carbon steel (0.4% C) after oil quenching from 830 °C; the structure is composed of martensite and troostite (dark places), 200X



Fig. 3.21. Microstructure of low-carbon steel (0.15% C), 200X



Fig. 3.22. Microstructure of the steel shown in Fig. 3.20 after cementation, 200X

increase of temperature causes the formation of larger grains in the alloy, and thus increases the brittleness. By comparing the microphotographs it can be seen that the steel heated to a higher temperature (Fig. 3.18*b*) has coarser grains and therefore a reduced plasticity and strength.

The growth of steel grains during high heating also causes the growth of the martensite crystals formed in the course of cooling. By comparing the microstructures shown in Figs. 3.13*c* and 3.19, it can be found that the structure in Fig. 3.19 has been heated to higher temperatures and has larger martensite crystals, and therefore, greater brittleness.

From the microanalysis, we can also decide whether the rate of cooling of an alloy during hardening was correct. For instance, Figs. 3.13c and 3.19 show the microstructure of carbon steel after water hardening, and Fig. 3.20, the microstructure of the same steel after slower cooling in oil (the latter structure is composed of martensite and troostite).

The processes aimed at varying the composition of the surface layers of steel by saturating the latter with carbon (cementation), nitrogen (nitration) or metals (diffusion coating) are found widely applied in industry. The properties of steel can be thus changed depending on the depth of the saturated layer and the concentration of diffusion elements. The depth of the diffusion layer and the approximate concentration of the saturating element can be determined by microanalysis. Figure 3.21 shows the microstructure of the initial steel with 0.15 per cent C, and Fig. 3.22, the microstructure of the surface layer of the same steel after carbon saturation; the content of carbon determined by the amount of the dark component, pearlite, diminishes from the surface to the core of the sample. From the amount of pearlite we can determine approximately the concentration of carbon in individual portions of the layer and the thickness of the carbon-saturated layer.

(d) Quantitative Metallography

The quantitative methods of metallography are needed to determine the characteristics of many important specific features of the structure, for instance the size of inclusions or grains of the individual phases present in an alloy, especially the size of grains of the matrix phase, or the number of inclusions of various phases in an alloy.

(e) Determination of Grain Size

Alloys having a fine-grained structure usually possess better mechanical properties, i.e. strength, plasticity and ductility. Since grain size depends on the composition of an alloy and the manufacturing process (melting, casting, plastic working and heat treatment), and may be unlike in various melts of the same composition, experimental determination of grain size is often necessary.

The size of actual grains, i.e. of the grains existing in an alloy under actual operating conditions and formed through the

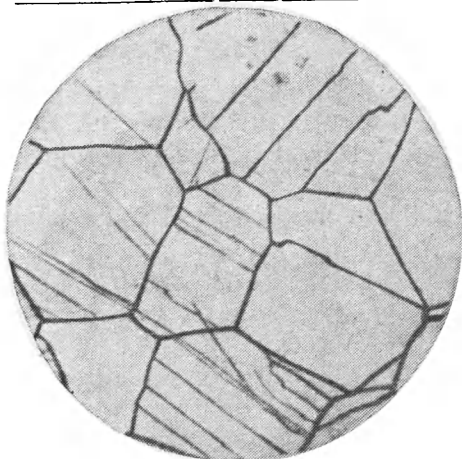


Fig. 3.23. Microstructure of Cr-Ni stain-less steel (etched by aqua regia); grains of austenite, 500X (according to A. Lyapina)

processing technique adopted, is determined by etching¹ of microsections (see Fig. 3.1 and Fig. 3.23).

For some grades of steel, however this method fails to be effective in detecting grains, or more exactly, grain boundaries, with the required clarity. Then special methods of treatment, which are described below, come into use. One has to remember, however, that these methods reveal the grains formed under the selected conditions of heating, i.e. 'inherent' grains rather than actual ones. The inhe-

rent grain characterizes the sensitivity of a metal to grain growth when heated for heat treatment.

The cementation method. Employed for low-carbon steels readily liable to cementation. Specimens of steel are cured in a tightly sealed iron box at $930 \pm 10^\circ\text{C}$ for 8 hours (after they have been heated up through) in a cementing medium, more often in a mixture of 40 per cent BaCO_3 and 60 per cent charcoal (or 30 per cent Na_2CO_3 and 70 per cent charcoal). Specimens are cooled in the box down to 600°C (the rate of cooling is about 100 degrees/hour for carbon steels and 50 degrees/hour for alloy steels and then in air), after which microsections are prepared. The surface layer is removed by grinding to a depth 2 mm at least and microsection is etched in reagents Nos. 1, 2, and 5 (see Table 3.4). The grain size is determined in the hypereutectoid region of the cemented layer from the cementite network formed at the boundaries of the former grains of austenite.

The oxidation method. Used for structural (improved-quality) steels and tool steels (except for high-speed grades). Polished microsections are heated in a dry inert atmosphere of a muffle furnace to a temperature $20\text{-}30^\circ\text{C}$ above the specified hardening temperature and held at that temperature for three hours. Cold air is then admitted to the furnace for 30-60 s, after which the

¹ Grain detection in carbon and alloy steels is made by using reagents Nos. 1 and 2, and etching of austenitic steels, by using reagents Nos. 7 to 10 or 12 (see Table 3.4).

specimens are quenched in water. It is recommended to immerse specimens in molten borax at a temperature of 930-950 °C for 30-40 seconds and only then to quench in water. The microsections are then polished and etched in a 10-percent solution of hydrochloric acid.

The method of etching the boundaries of former austenitic grains. Employed for steels requiring martensitic or bainitic hardening. Specimens are heated at the same temperatures and for the same time as in the previous method, then cooled in oil or water and tempered for 15-30 minutes at 225-250 °C (for carbon and low-alloy steels) or 500-550 °C (for medium- and high-alloy steels). Prepared microsections are etched in a fresh solution of picric acid with addition of surface-active detergents: 0.5-1.0 per cent of some washing powder or 1-4 per cent of washing liquid. The etching is continued for 5-30 min (at 20 °C) or 0.5-6 min (at 50-70 °C).

The method of detection of ferrite (in steels with carbon content of up to 0.6 per cent) **or cementite** (in hypereutectoid steels) **networks formed at the boundaries of former austenitic grains.** Specimens are heated under the same conditions as in the two methods above and then are cooled as follows: (a) carbon steels with 0.3-0.5 per cent C are cooled in air; (b) carbon steels with 0.5-0.6 per cent C are cooled in the furnace at cooling rate of 50-100 degrees/h; (c) alloy steels and hypereutectoid steels are cooled at a rate of 20-30 degrees/h (down to 720-730 °C). The specimens are then cooled in water, and microsections are prepared. The grain is detected by etching with the same reagents as in the cementation method.

The method of detection of troostite network formation. Used for carbon and low-alloy steels of the eutectoid type. Specimens are heated as in the earlier methods (except for cementation) and cooled as follows: one half of a specimen is quenched in water and the other half cooled in air. A structure of martensitic

Table 3.1 Recalculation of Grain Numbers to Standard Magnification (100X) with Actual Magnifications from 25 to 800

Magni- fication 100X	Grain numbers															
	-3	-2	-1	0	1	2	3	4	5	6	7	8	9	10	11	12
25	1	2	3	4	5	6	7	8	9	10						
50			1	2	3	4	5	6	7	8	9	10				
200							1	2	3	4	5	6	7	8	9	10
400									1	2	3	4	5	6	7	8
800											1	2	3	4	5	6

grains fringed with troostite is then formed in the transition region of the specimen. This structure is detected by etching in an alcohol solution of nitric or picric acid.

To determine grain size,¹ the microstructure is compared at a 100-fold magnification to standard scales² (Fig. 3.24), the number of grains per unit area of the microsection is counted, and, finally, the average standard diameter of a grain or the number of grains in 1 mm³ of the metal is calculated. Calculations of these parameters of grain size for standard numbers are given in Table 3.2. The number of grains³ is calculated on the ground glass of the microscope or from a microphotograph within the area of a circle 79.8 mm in diameter.

Table 3.2. Parameters of Steel Structure with Various Grain Numbers

Grain numbers	Average area of grain, mm ²	Average number of grains per mm ² of microsection	Average number of grains per mm ³	Average calculated diameter of grain, mm	Average standard diameter, mm
—3	1.024	1	1	1.00	0.875
—2	0.512	2	2.7	0.694	0.650
—1	0.256	4	8	0.500	0.444
0	0.128	8	21	0.352	0.313
1	0.064	16	64	0.250	0.222
2	0.032	32	179	0.177	0.167
3	0.016	64	512	0.125	0.111
4	0.008	128	1446	0.088	0.0788
5	0.004	256	4096	0.060	0.0553
6	0.002	512	11,417	0.041	0.0391
7	0.001	1024	32,768	0.031	0.0267
8	0.0005	2048	92,160	0.022	0.0196
9	0.00025	4096	262,122	0.015	0.0138
10	0.000125	8192	737,280	0.012	0.0099
11	0.000062	16,384	2,097,152	0.0079	0.0069
12	0.000031	32,768	5,930,808	0.0056	0.0049
13	0.000016	65,536	16,777,216	0.0039	0.0032
14	0.000008	131,072	47,448,064	0.0027	0.0023

¹ The methods for calculation of grain size given here should not be used for work-hardened or partially recrystallized metals.

² The scales (according to the USSR State Standard GOST 5639-65) are 79.8 mm in diameter, i.e. with an area of 5000 mm², which corresponds to the actual area of 0.5 mm² of a microsection. The number of grains (n) per mm² of a microsection is found by the formula $n = 2^{N+3}$, where N is the number of the grain (on the scales). If the grain number is beyond the limits from 1 to 10, a different magnification must be used, and the results then recalculated by Table 3.1.

³ The number of grains in the circle must be not less than 50. With a lower number, a smaller magnification must be used.

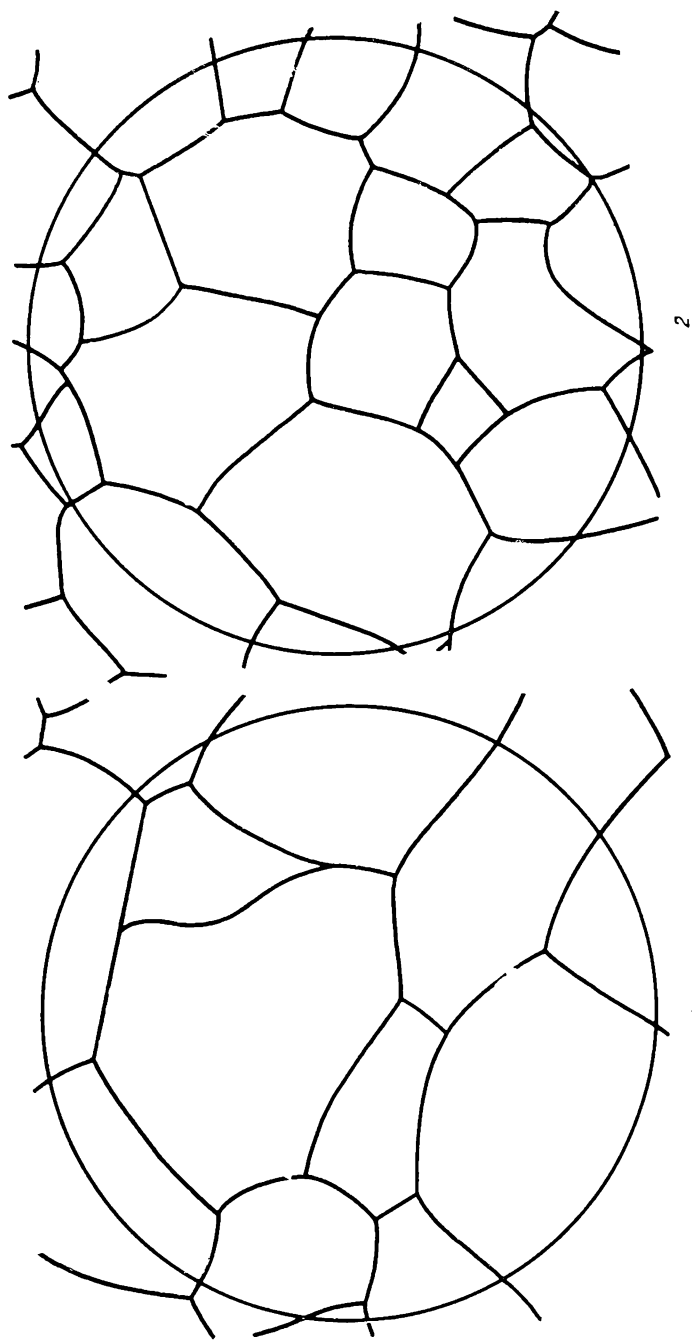
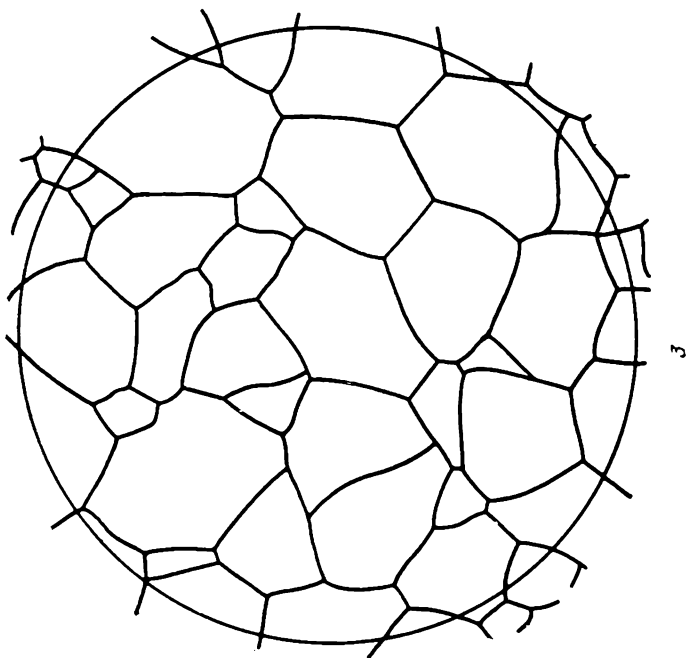
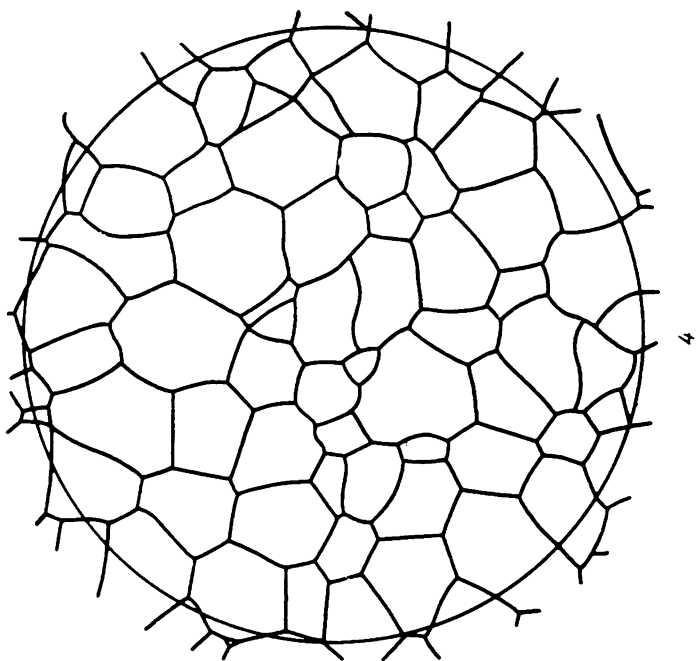
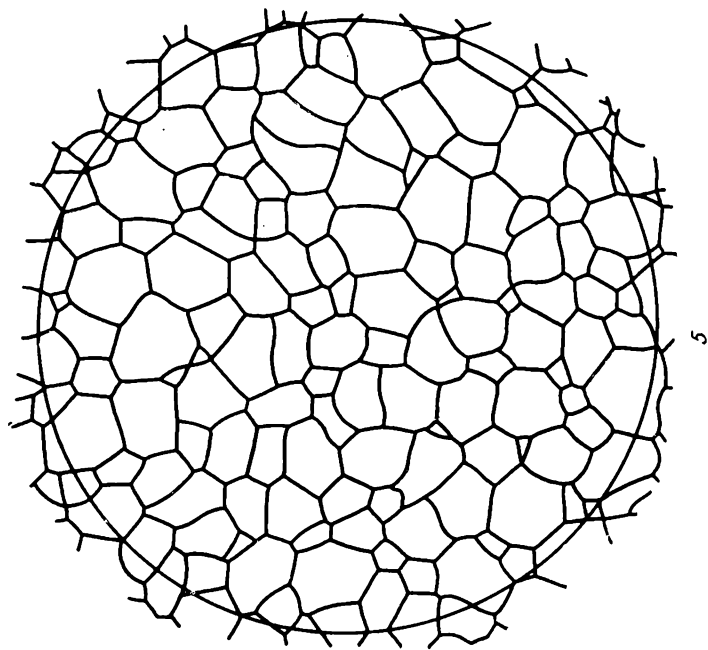
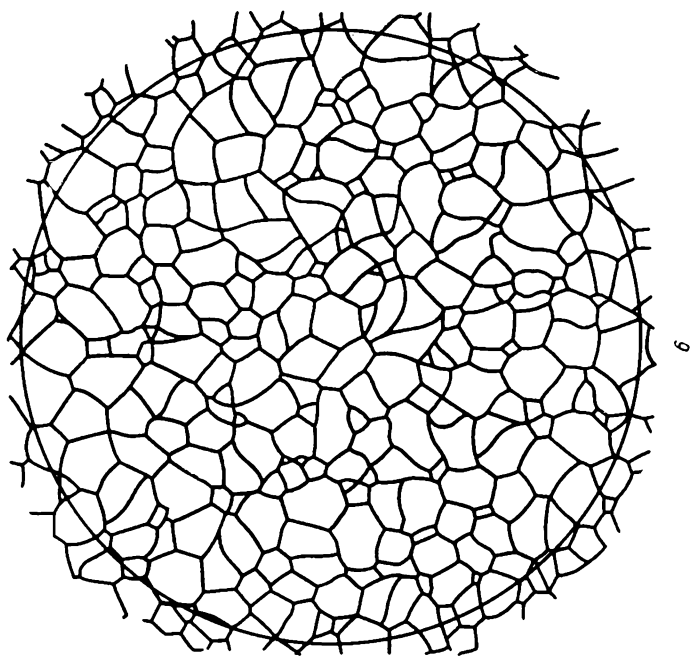


Fig. 3.24. Scale of grain size numbers of structural steels (numbers under drawings are grain numbers), 100X



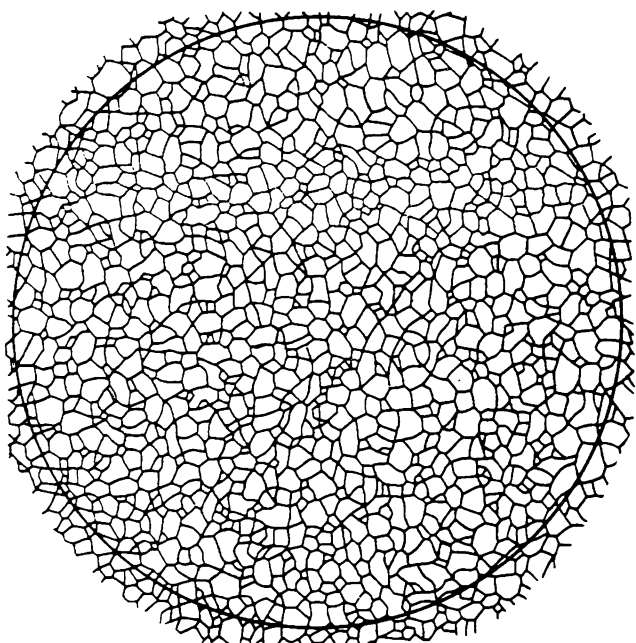
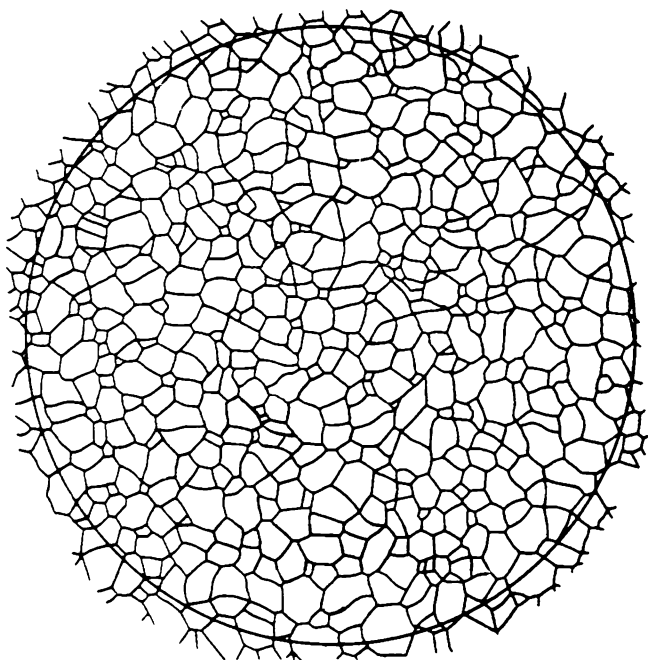


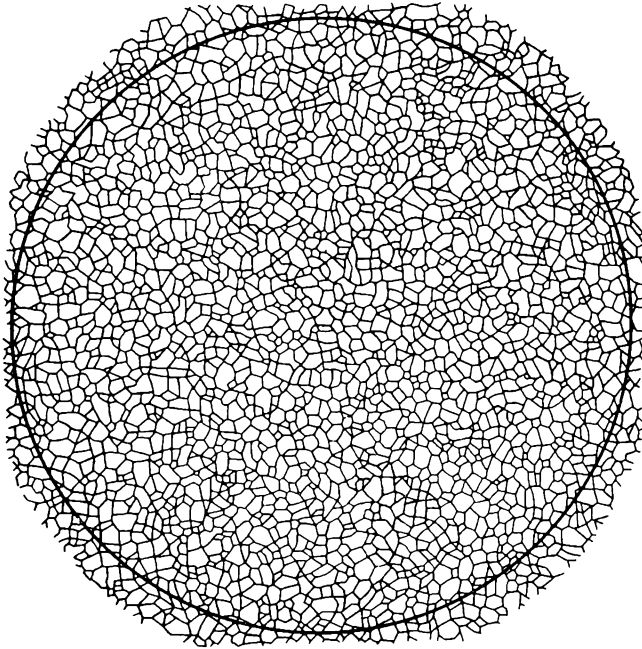
5



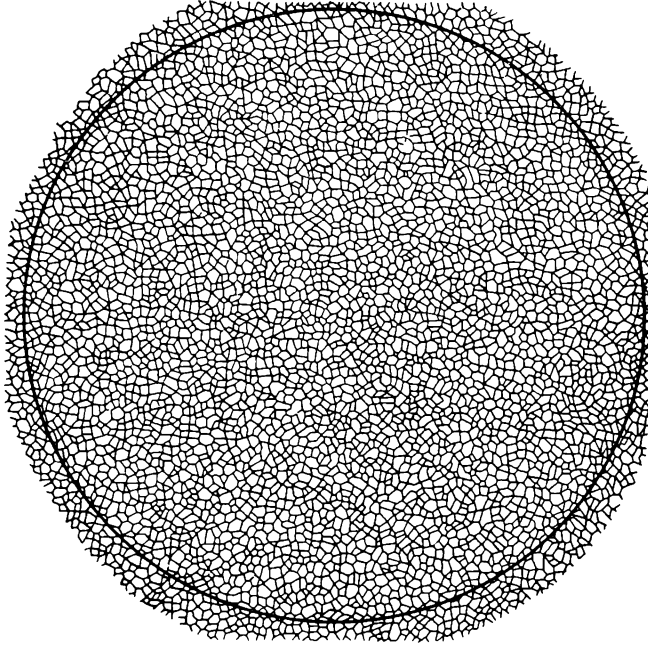
6

Fig. 3.24. Continued





9



10

3.24. Continued

With a 100-fold magnification this corresponds to 0.5 mm^2 of the actual area of a microsection. The total number of grains can be calculated by the formula $m_{100} = m + 0.5 m_1$, where m is the number of grains within the circle and m_1 is the number of grains intersected by the circular line. The number of grains per mm^2 of the surface of a microsection is $M = 2m_{100}$. With a magnification other than 100, $M = 2 \left(\frac{g}{100} \right)^2 m_g$, where g is the actual magnification employed and m_g is the number of grains calculated with this magnification. The average number of grains (M_{av}) is determined from the three most characteristic fields of vision.

The average area of grains (S_{av}) and average grain diameter (d_{av}) are calculated by the formulae

$$S_{av} = 1/M_{av}, \quad d_{av} = 1/\sqrt{M_{av}}$$

The size of equiaxial grains is characterized by their average standard diameter which is determined from the image on the ground glass of the microscope or from a microphotograph. For this purpose a number of straight lines are drawn so that each line can intersect at least ten grains. Then the number of intersections per length of all the lines is counted (including the grains at the line ends not intersected completely). The average standard diameter of grains is found by dividing the total length of all the lines by the number of intersections for the selected magnification.

Quantitative characteristics of the structure, in particular, the grain size, are found by using statistical methods and plotting distribution curves or histograms. To construct a histogram,¹ the number of grains within a given number of divisions of the eyepiece micrometer are counted (for instance, from 0.5 to 1.5 and from 1.5 to 2.5; from 2.5 to 3.5, etc.). If the curve constructed has a number of minima and maxima, an enveloping curve is constructed by counting the number of grains within large size intervals, i.e. larger intervals of grouping are used.

Using the distribution curve thus obtained, the average diameter of grains is calculated by the formula:

$$D_{av} = \frac{k \sum mx}{\sum m} \quad (3.1)$$

where m = group frequency (i.e. the number of grains in the given interval of the scale of the eyepiece micrometer)

¹ Histograms can be obtained quickly by means of scanning microscopes, for instance, the Quantimet type.

x = diameter in scale divisions (i.e. a definite interval of the scale)

k = average scale division, μm

The average grain area (F_{av}) can be calculated using formula (3.1) and assuming that the grains are spherical ($X = \pi D^2/4$):

$$F_{av} = \frac{k^2 \sum \left(\frac{\pi D^2}{4} m \right)}{\sum m} \quad (3.2)$$

Hence the number of grains (N) per mm^2 is found as

$$N = 1/F_{av}$$

(f) Automatic Methods for Determining the Number of Grains and Inclusions

Quantitative characteristics of the structure of alloys, including the size and shape of grains (when grains are not equiaxial), the size and volume distribution of particles or inclusions (existing phases), the density of dislocations (by etching recesses), are obtained by using scanning television microscopes (Fig. 3.25).

Selection of the field to be studied and adjustment of the system are made by using the optical image of the microsection microstructure formed in a microscope or epidiastroscope, this image being projected onto a television screen (monitor). The output signal resulting from the transformation of the light field of the object is sent via a television camera tube to an electronic detector which detects the slightest variations, appearing in this signal as a light spot scans the unevennesses of the surface.

The mode of scanning, i.e. the rate and scanning pitch over the section, is controlled automatically. Variations of the signal are fed to a computer and, after being processed there, can be supplied to a display or printing device which presents the information in the form of graphs or tables.

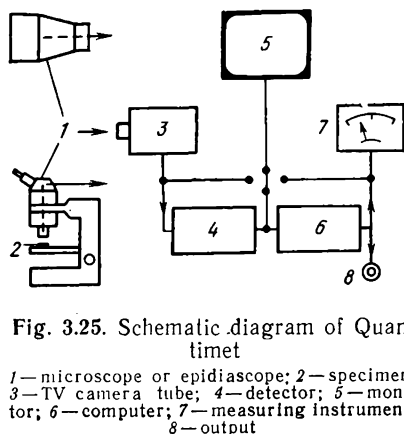


Fig. 3.25. Schematic diagram of Quantimet

1—microscope or epidiastroscope; 2—specimen; 3—TV camera tube; 4—detector; 5—monitor; 6—computer; 7—measuring instrument; 8—output

(g) Preparation of Sections

Investigation of the structure of metals and other non-transparent materials in the microscope is only possible if the light beams are reflected rather intensively from the surface. That is why the surface of a specimen must be specially prepared. A specimen whose surface has been prepared for microanalysis is called a microsection (or simply section). To prepare a section, a specimen must be cut from the metal to be studied and its surface must be made plane and bright.

(h) Cutting Specimens

Small parts and specimens, after their surface has been properly treated, may be placed directly onto the microscope stage. If the size and mass of a part (or specimen) are appreciable or if the part has a complicated shape and it is impossible to find a plane portion on it, a special small-size specimen should be cut and its surface treated as a microsection.

Soft materials can be cut by a saw, milling cutter, cutting tool, etc. Specimens of metals of appreciable hardness can be cut by means of carborundum, diamond or vulcanite discs; care must be taken during cutting to avoid overheating since this can cause changes in the structure. Specimens of hard materials can also be cut by the electro-spark method. If the metal is brittle and a specimen of definite shape and size is not required, a small piece of the metal may be broken off by a hammer and prepared as a microsection.

Of special importance to the results of study is the selection of the place from which a specimen is cut and the surface on which the microsection is prepared. This selection depends on the object of the study and the shape of an article, because of this only general recommendations can be given here.

The microstructure of cast metals and alloys (in castings of complicated shape) should be studied in various sections from the largest to the smallest; the metal in these sections cools at different rates, and the structure of many casting alloys depends on the rate of cooling. It is of great importance to choose correctly the direction in which a microsection must be cut. The plane on which the microstructure will be studied should be selected perpendicular to the peripheral and core layers of the metal so as to obtain data on the structure of the whole casting.

To study the microstructure of an ingot, a number of specimens are cut in such a manner that the variations of structure in a number of cross sections can be determined.

When studying the effect of plastic deformation on the metal structure, it is better practice to select the place for cutting a specimen for microanalysis after the macroanalysis has been done and the direction of the plastic deformation and the most characteristic regions of the article have been determined. In forged and die-formed parts, it is of importance to study the portions subjected to the greatest bending or drawing and also the volumes of the metal not deformed. In such cases it is necessary to study the microstructure mainly in the direction of metal flow and sometimes in perpendicular directions. Here, the microstructure may be studied on two perpendicular planes of a single specimen or two specimens may be cut in two perpendicular directions. With large parts, it is advisable to cut a number of specimens from various places for the uniformity of the structure to be correctly assessed.

The structure of alloys subjected to heat treatment should be studied both in surface layers and in deeper ones. When studying the properties of non-equilibrium alloys the microanalysis should be supported by other methods, in the first place by hardness tests which may be made on the same microsection. The composition of the alloy (i.e. the content of its main components and impurities) must also be known.

Microanalysis is widely used for establishing the causes of failure of machinery parts in operation. In such cases the correct selection of the place for cutting specimens is also important. Specimens are usually cut near the place of failure and at some distance from it, so that possible changes in the structure of the metal can be detected. In addition, the metal structure in the longitudinal and transverse directions must be studied.

(i) Preparation of Specimens

The surface of specimens is subjected to special treatment. It should be approximately plane. With soft metals, the surface is made plane by filing; with harder metals, by grinding with emery discs. Small specimens are held for filing or grinding by clamps made from two plates with screws or set in a matrix of fusible alloys, sulphur, etc.¹

For this purpose a circular or square mandrel (made of steel or brass) with the specimen inserted into it, with the treated face downwards, is placed onto a metallic or ceramic plate after which a fusible melt is poured into the mandrel.

¹ Low-melting alloys should be used for the purpose, since many metals can change their structure even with relatively low heating.

Microsections may also be pressed into polystyrene, bakelite, etc. To do this a specimen is placed into a press mould together with polystyrene or bakelite powder and then subjected to hot pressing which ensures polymerization.

(j) Grinding the Surface of Specimens

After making the surface of a specimen approximately plane, it is ground with emery paper attached to a plane substrate (glass) or clamped by clamping rings or glued to a rotatable disc. Grinding is started with coarse paper and finished with the finest grade.

When changing from one grade of emery paper to another, the direction of motion of the specimen relative to the paper or disc should be periodically varied by 90 degrees to remove scratches. As the paper is changed to a finer grade, scratches become less and less deep.

Particles of abrasive material left on the surface of specimens after grinding are removed by compressed air or by rinsing in water or alcohol.

Soft non-ferrous metals should be carefully ground to prevent their deformation. In addition, abrasive particles and metal chips can be pressed into the surface; to prevent this, wet the emery paper with kerosene; when making aluminium microsections, they must be rubbed with paraffin.

Beryllium and beryllium alloys are ground by using dry or wetted emery discs (with a grain mesh of 120, 240 and 400) rotating at a high speed (1750 rpm); manual grinding is impracticable. With the first (coarse) emery discs grinding can be done with or without wetting. Fine grinding is made by wetting with kerosene. The grinding pressure must be as low as possible to prevent deformation and crumbling.

Specimens of titanium alloys must be cut at low pressures to prevent deformation twins. Their grinding is recommended to be done first by a leather disc coated with 60-mesh emery powder, then with 180- and 320-mesh emery paper and finally with the finest grade.

In all cases care should be taken not to deform the surface of specimens otherwise the results of microanalysis will be distorted.

(k) Polishing the Surface of Specimens

Polishing removes fine surface defects, scratches, etc. remaining after grinding. Mechanical, chemical-mechanical and electro-mechanical methods of polishing can be used.

Mechanical polishing is done by a rotating disc to which a polishing material (felt, velvet or fine cloth) is glued, or fastened by other means, with a very fine abrasive material (aluminium oxide, iron oxide, chromium oxide, etc.) being applied periodically or continuously onto the surface of the material. The polishing substances are suspended in water and then placed on the disc.

The polishing disc must be always wet and exert only a low pressure onto the specimen. When polishing ferrous and non-ferrous metals, the speed of a disc 250 mm in diameter must be 400-600 rpm.

Polishing is finished when the surface of a specimen becomes as bright as a mirror with no scratches or fissures seen on it in the microscope. If scratches cannot be removed even after long polishing, the specimen must be re-ground by a finer paper and then re-polished.

In some cases, when the metals or alloys have a high hardness or when it is required to study the structure of a surface layer whose hardness differs substantially from that of the main metal, polishing by means of a diamond powder may be recommended. The preliminary grinding of a specimen is made in the ordinary manner and finished on a disc with 240-mesh emery paper. The polishing disc is then prepared as follows: 0.025 g of diamond powder with particle size not over 8 μm is rubbed into a fine dry cloth stretched onto a rimless disc approximately 200 mm in diameter; the surface of the disc is then coated with a thin layer of paraffin, and the disc is mounted in a polishing machine; the speed of its rotation must be about 200 rpm.

Chemical-mechanical polishing is done by means of a polishing disc coated with an abrasive material and a substance promoting quicker polishing.

Ferrous metals are polished with polishing pastes (such as the GOI paste manufactured in three grain sizes and consisting of chromium oxide, stearine, kerosene, oleic acid, and soda). The polishing of non-ferrous and some rare metals is done by chemically active reagents (for instance, a solution of potassium ferrocyanide) which accelerate polishing and in some cases reveal the microstructure, so that further etching will become unnecessary.

Electro-chemical polishing is done in an electrolytic bath wherein the anode is the specimen to be polished and the cathode, a strip of stainless steel. The specimen is positioned with its ground surface facing the cathode. The composition of the electrolyte and the anode current density are selected to suit the material of the specimen (Table 3.3).

Table 3.3. Conditions for Electropolishing Selected Metals and Alloys

Metal	Electrolyte composition	Current density, A/cm ²	Temperature, °C
Carbon and alloy steels	Nitric acid (density 1.48)	8-10	≤ 30
Stainless steel	Orthophosphoric acid 38%, glycerine 53%, water 9%	0.2-2	20-115
Copper, brass	Chromium anhydride 7.2%, so- dium bichromate 21.7%, ace- tic acid 7%, sulphuric acid 5.8%, water 58.3%	2-4	60-75
Aluminium alloys	Sulphuric acid (density 1.84) 38%, phosphoric acid 48%, water 14%	7.5	95
Nickel alloys	Sulphuric acid (density 1.84) 60%, water 40%	0.2	30

Under the action of the current, all projections on the surface of the specimen are dissolved (anode dissolution), and the surface gradually becomes mirror-smooth.

This method is the most advanced, ensures quick polishing, causes no deformation (work-hardening) of the surface layer, and sometimes discloses some peculiarities of the microstructure which cannot be revealed by mechanical polishing and common etching.

Irrespective of the method of polishing, the polished microsection must be rinsed with water and alcohol and then dried with filter paper.

(1) Examination of Microstructure

Examination of a microstructure should begin from the 'unetched microsection', i.e. just after polishing, rinsing, and drying. When seen under a microscope, such a microsection has the form of a bright circle with a number of dark (grey or black), or sometimes yellow, etc. regions, the size of these regions usually being small. These regions are traces of non-metallic inclusions, and in some alloys they can represent structural components characteristic of a given alloy.

Non-metallic inclusions can be brought in with the starting charge materials or form during melting owing to the processes of oxidation, deoxidation, desulphurization, etc. Most of them are oxides, sulphides, nitrides, silicates, etc. left in the basic metal

alter melting, casting and solidification. Particles of slag and refractories in the metal are also non-metallic inclusions.

Because of their high brittleness, non-metallic inclusions may crumble out completely during grinding or careless polishing, leaving recesses in the surface of a microsection; these are seen dark as they are shadowed by neighbouring projecting regions. However, in such cases it is difficult to judge on the size and number of inclusions, since particles of the basic metal can also crumble out together with the non-metallic inclusions. With careful polishing the crumbling of non-metallics is insignificant, and they are only polished away a little more noticeably than the basic metal and become easily visible in the microscope owing to a different reflection index. The use of the polarized-light technique gives a clearer determination of non-metallic inclusions (see Sec. 3.2 *n*).

Methods have been developed for revealing the nature of non-metallic inclusions in steel (etching with various reagents and observation of the etchability and colour of the metal)¹ and for determination of the content of inclusions, provided that these did not crumble out during polishing. A scale of numbers (Fig. 3.26) is used for the general characteristic of contamination of steel with non-metallics.

In copper alloys, inclusions of copper oxide have a characteristic greyish-blue colour, and those of sulphides, grey.

In grey irons, dark inclusions seen in unetched sections are indicative of graphite segregation. Determination of graphite inclusions and metallic base in common and grey iron castings is done according to the typical scale established by the USSR State Standard GOST 3443-57. Graphite inclusions are estimated by their content, which is determined by the area occupied by graphite as seen under the microscope, and by the nature of their distribution. The latter can also have a large effect on the properties of iron: the more isolated the graphite inclusions, the better the mechanical properties of the iron.

Microporosity can often be seen in unetched sections; this defect is most frequently found in castings and can affect the properties of the metal. In polished etched sections, micropores form recesses and are seen as dark spots. Micropores can be distinguished from non-metallic inclusions by the following method: by slightly turning the micrometer screw of the eyepiece, the image is brought out of focus and then focused again; the edges

¹ The composition of non-metallic inclusions can be determined by chemical analysis of the precipitate formed after dissolving a steel specimen in weak acids.

Index	Oxides		Sulphides and silicates		Carbides
	<i>fine</i>	<i>coarse</i>	<i>fine</i>	<i>coarse</i>	
1					
2					
3					
4					
5					

Fig. 3.26. Scale of numbers for determining non-metallic inclusions in steel (according to the USSR State Standard GOST 1778-70)

Oxides, sulphides and silicates are examined before etching; carbides, after etching, 100X

of a micropore, due to different depth, then move closer to, or farther from, one another, whereas the edges of an inclusion remain in their places.

Unetched sections after being examined are etched for a deeper study of the metal structure. There are a number of etching methods which differ in the effect exerted on the surface of metal.

Etching by the method of selective dissolution of phases. This method is based on differences in the physico-chemical properties of individual phases and grain boundaries. Because of the different intensities of dissolution of phases, a relief surface is formed on the section. Illumination of such a section by oblique light forms shadow patterns whose shape is indicative of the structure of the metal¹ (see Figs. 3.5 and 3.7). This method is applicable for multi-phase alloys and pure metals. Grains of a pure metal,

¹ Light diffusion is stronger at grains which have been etched more deeply since they reflect less light.

being of the same composition, may differ in their crystallographic orientation. Grains of the metal may be cut along various crystallographic planes in a prepared section, and their properties in these planes are unlike, in particular their etchability by various acids, salts or alkalis. The light directed through the objective of the microscope onto the etched microsection will then be reflected in different ways by these grains (Fig. 3.27); strong diffusion originates at grain boundaries, and the beams reflected from these places pass beyond the field of vision. Therefore the grain boundaries are seen as dark lines reproducing the actual picture of joints between grains. This effect is enhanced as most impurities present in the metal or alloy are concentrated at grain boundaries; the etchability at grain boundaries thus increases owing to the formation of galvanic pairs, so that grain boundaries are clearly seen as dark lines (as, for instance, in Fig. 3.23).

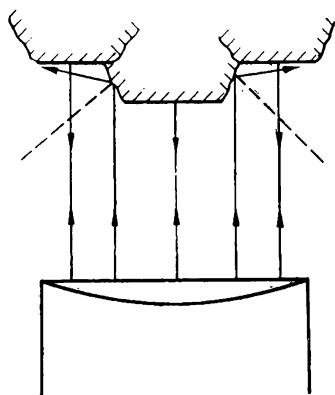


Fig. 3.27. Scheme of reflection of light from polished and etched surface of a microsection

Microsections are etched by immersing their polished surface into a selected etching solution (Table 3.4) and are held there for a definite time depending on the composition of the metal and that of the etching solution. The immersion time can be easily established experimentally. Etching is considered finished when the bright surface of a polished section becomes slightly dull; the section is then removed from the solution, rinsed with water, then with alcohol and dried by means of filter paper.¹

Microsections can also be etched by the electrolytic method. The section acts as the anode, and the cathode is a plate of stainless steel or lead, or, less often, a carbon rod. The reagents used most often for electrolytic etching are given in Table 3.5.

Oxidation etching. A prepared section is heated in an oxidizing atmosphere, giving the metal phases different colours because the oxide films formed on them vary in their composition and thickness.

If heating to the specified temperature in air cannot form an oxide film of a sufficient thickness, the oxidizing effect can be

¹ These operations must be done quickly to prevent oxidation of the etched surface in the air.

Table 3.4. Reagents for Etching Microsections

Name of reagent	Composition	Action
I. REAGENTS FOR ETCHING IRON AND ITS ALLOYS		
<i>(a) For determining the structure of carbon and alloy steels and cast iron</i>		
1. Alcoholic solution of nitric acid (Rzheshotarsky's reagent)	1-5 ml nitric acid ($\gamma = 1.4$), 100 ml ethyl alcohol	Tints pearlite ⁴ dark, reveals grain boundaries of ferrite, structure of martensite and products of tempering.
2. Alcoholic solution of picric acid (Izhevsky's reagent)	4 g picric acid (crystalline), 100 ml ethyl alcohol	Can be also used to reveal the structure of carbon steel and cast iron, and also of nitrated and cemented steel
3. Glycerine solution of nitric and hydrochloric acids	10 ml nitric acid ($\gamma = 1.4$), 20-30 ml hydrochloric acid ($\gamma = 1.19$), 30 ml glycerine	Reveals the structure of high-chromium, high-speed and austenitic manganese steels after hardening. Alternating the etching and polishing is recommended for better results
4. Aqua regia	3 parts hydrochloric acid ($\gamma = 1.19$), one part nitric acid ($\gamma = 1.4$)	Reveals the structure of stainless steels and alloys. Before using the reagent should be cured for 20-30 h
5. Alkaline solution of sodium picrate	2 g picric acid, 25 g sodium hydrate, 100 ml water	Reveals cementite by tinting it dark. Does not tint chromium and tungsten carbides. Used boiling
6. Alkaline solution of potassium ferricyanide	10 g potassium ferricyanide, 10 g potassium hydroxide, 100 ml water	Reveals chromium and tungsten carbides in high-speed and other grades of steel. Used hot. Reveals phosphides in phosphide eutectic by tinting it dark

Table 3.4 (continued)

Name of reagent	Composition	Action
<i>(b) For revealing grain boundaries in steels²</i>		
7. Marble's reagent	20 g CuSO_4 , 100 ml HCl ($\gamma=1.19$), 100 ml ethyl alcohol	Chemically etches austenitic steels. Used for electrolytic etching during 10-15 s with a voltage of 12-15 V across bath terminals if ethyl alcohol is replaced by the same amount of water
8. Oxalic acid solution	10 g oxalic acid, 90 ml water	Electrolytically etches martensitic and austenitic steels. Etching mode: bath terminal voltage 2-10 V, etching time 1-10 s
9. Solution of hydrochloric and nitric acids	10 ml hydrochloric acid ($\gamma=1.19$), 3 ml nitric acid ($\gamma=1.4$), 87 ml ethyl alcohol	Electrolytically etches austenitic, martensitic and martensite-ferritic steels. Etching mode: bath terminal voltage 5-12 V, etching time up to 10 s
10. Concentrated solution of nitric and hydrochloric acids	50 ml hydrochloric acid ($\gamma=1.19$), 8 ml nitric acid ($\gamma=1.4$), 50 ml water	Electrolytically etches austenitic steels. Etching mode: current density 1 A/cm ²
11. Chromic anhydride solution	10-15 g chromic anhydride, 85-90 ml water	Electrolytically etches martensitic steels. Etching mode: current density 1-1.5 A/cm ² at 20°C or with heating up to 50-70°C
12. Picric acid solution	Saturated aqueous solution of picric acid plus 3-4% liquid detergent 'Sintol'	Chemically etches (10-30 min at 20-70°C) martensitic and martensite-ferritic steels.
13. Hydrochloric solution of copper chloride	40 ml hydrochloric acid ($\gamma=1.19$), 5 g copper chloride, water	Reveals nitrides in dispersion hardening of steel. Etching time up to 10 s

Table 3.4 (continued)

Name of reagent	Composition	Action
II. REAGENTS FOR ETCHING COPPER AND COPPER ALLOYS		
14. Hydrochloric solution of ferric chloride	10 g ferric chloride, 25 ml ($\gamma=1.19$) hydrochloric acid, 100 ml water or 5 g ferric chloride, 10 ml hydrochloric acid ($\gamma=1.19$), 100 ml water	Reveals the structure of copper, brass, tin and aluminium bronzes, bismuth-antimony alloys, etc. In brasses, tints β -phase dark. Detects macrostructure
15. Ammonia solution of double salts: copper-ammonia chloride	10 g double salt, 100 ml water, ammonia to make a neutral or alkaline solution	Reveals the structure of copper and copper alloys, in particular two-phase brasses (tints β -phase dark)
16. Ammonium persulphate solution	10 g ammonium persulphate, 90 ml water	Reveals the structure of copper, brass, tin bronze, and monel metal
III. REAGENTS FOR ETCHING NICKEL ALLOYS (see Nos. 7-10)		
IV. REAGENTS FOR ETCHING ALUMINIUM ALLOYS		
17. Hydrofluoric acid	0.5 ml hydrofluoric acid (48%), 99.5 ml water	Reveals the structure of duralumins and aluminium-base casting alloys
18. Sodium hydroxide	1-10 g sodium hydroxide, 90-99 ml water	
19. Solution of acids	1.0 ml concentrated hydrofluoric acid, 1.5 ml hydrochloric acid ($\gamma=1.19$), 2.5 ml nitric acid ($\gamma=1.4$), 95 ml water	Reveals the microstructure of duralumins
V. REAGENTS FOR ETCHING TITANIUM ALLOYS		
20. Bright-etching reagent	25% hydrofluoric acid (48%), 25% nitric acid ($\gamma=1.4$), 50% glycerine	Hydrofluoric acid acts onto the metal; nitric acid makes the latter bright by removing stains and precipitate; glycerine acts as a solvent and stabilizer. When no bright etching is required, the reagent is composed of equal parts of hydrofluoric acid and glycerine

Table 3.4 (continued)

Name of reagent	Composition	Action
21. Hydrofluoric acid solution	5% solution of hydrofluoric acid (48%) in water	

VI. REAGENTS FOR ETCHING BERYLLIUM

22. Alcoholic solution of acids	100 ml ethylene glycol, 2 ml hydrochloric acid ($\gamma = 1.19$), 2 ml sulphuric acid ($\gamma = 1.84$), 10 ml nitric acid ($\gamma = 1.4$)	Etches for 1-3 min at 10-15° C
---------------------------------	---	--------------------------------

¹ At higher magnifications (above 400-500X), it can be clearly seen that pearlite is composed of two phases, i. e. ferrite and cementite.

² Reagents Nos. 1 and 2 are used for revealing the actual or inherent austenitic grain in carbon and alloy steels, structural and tool steels, and also ferritic steels.

Table 3.5 Reagents for Electrolytic Etching Microsections

Reagent	Composition	Application
1. Ferric chloride + hydrochloric acid	0.5% FeCl ₃ , 1% hydrochloric acid ($\gamma = 1.19$); 98.5% methyl alcohol	For etching carbon steels. Current density 0.5 A/cm ²
2. Hydrochloric acid	10% hydrochloric acid ($\gamma = 1.19$), 90% ethyl alcohol	For etching high-alloy steels (high-chromium, high-speed). Current density 0.05 A/cm ²
3. Oxalic acid	2-10 g oxalic acid, 100 ml water	For detecting carbides and the matrix structure of stainless steels and nickel alloys. Voltage 3-6 V
4. Orthophosphoric acid	Solution of orthophosphoric acid ($\gamma = 1.48-1.55$)	For detecting the structure of copper alloys (brasses, bronzes). Current density 0.02-0.05 A/cm ²

intensified by placing crystals of a strong oxidant, such as potassium bichromate (K₂Cr₂O₇), on the surface of the metal.

Oxidation by heating can also be used for determining the size of grains, in particular, of steel.

The method of oxidation with furnace heating, especially when it produces thick oxide films, is unsuitable for studying fine structural changes in metals.

Etching by selective vaporization of phases in a vacuum. Vacuum metallography¹ is based on heating steel in a vacuum to a high temperature at which the rates of vaporization of the substance inside grains and at grain boundaries become noticeably different. Vaporization usually occurs quicker in boundary zones rich in impurities, so that these zones become clearly visible without preliminary etching. The modern apparatus for vacuum vaporization makes it possible to study the structure of metals not only by the different rates of vacuum vaporization, but also by etching with various gases which are supplied into the heating chamber. In the latter case it is possible to study grain size variations and the phase transformation processes occurring during heating.

The magnetic method. A colloid solution of crocus is applied onto a section, and the excess of ferromagnetic particles is removed by means of soap foam. The colloid particles of iron oxides will then be attracted to the regions of the ferromagnetic phase which will be seen dark in the microscope, whereas the paramagnetic regions will remain bright.

(m) Metallurgical Microscopes

The metallurgical microscope enables opaque objects to be seen with a certain magnification in reflected light. In this respect it differs principally from the biological microscope in which transparent objects are seen magnified in transmitted light.

A metallurgical microscope comprises an optical system, illuminating system (including a photographic camera), and mechanical system.

The optical system consists of an objective, eyepiece (or ocular), and a number of auxiliary optical elements: mirrors, prisms, etc. (Fig. 3.28).

The objective forms a magnified inverted real image of an object (microsection) and is a complicated system of lenses mounted in a common body tube positioned fairly close to a microsection. It includes a plane-convex front lens which determines the possible magnification and a number of *correction lenses* that remove undesirable errors, such as chromatic and spherical aber-

¹ For a detailed discussion see: Lozinsky, M. G. *Stroenie i svoistva metallov i splavov pri vysokikh temperaturakh* (The Structure and Properties of Metals and Alloys at High Temperatures). Moscow, Metallurgiya Publishers, 1963.

rations which may form upon passage of light beams through the front lens.

Chromatic aberration is due to unequal refraction of light beams of various colours (i.e. of various wavelengths) by a lens; the refracted beams cannot be brought to a common focus. Chromatic aberration makes an image less sharp and can be fully eliminated only by using monochromatic light. In optical microscopes, chromatic aberration is reduced by fitting correction lenses made of a special material such as fluorspar (fluorite), in the objective.

Microscopic objectives are classed into achromatic and apochromatic depending on the degree of correction of chromatic aberration.¹ Aberration for three monochromatic beams is left uncorrected in achromats, and only for two beams in apochromats, i.e. the latter are better corrected as regards chromatic aberration. Apochromats are mainly used for large magnifications, and achromats, for the medium and small ones.

Spherical aberration is due to the fact that the paths of light beams passing through the centre of a lens and through its outer zones are different, and they cannot be focused into a single point; this also impairs the sharpness of the image.

In order to reduce spherical aberration, an objective may be composed of two lenses, a convex and a concave one, their spherical aberrations being equal in magnitude but opposite in signs. In objectives employed for large magnifications, the front lens

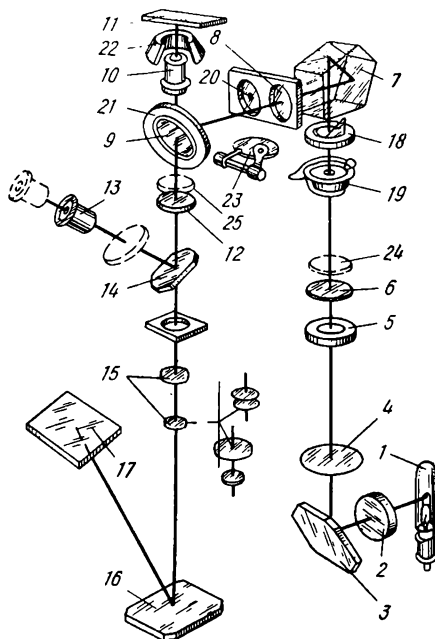


Fig. 3.28 Optical diagram of MIM-7 microscope

1—light source (lamp); 2—collector lens; 3—mirror; 4—lens; 5—aperture stop; 6—lens; 7—prism; 8—lens; 9—semi-transparent mirror plate; 10—objective; 11—microsection; 12—achromatic lens; 13—eyepiece; 14—mirror; 15—photo-ocular; 16—mirror; 17—photographic plate; 18—field aperture; 19—shutter; 20—lens for dark-field technique; 21—annular mirror; 22—parabolic mirror; 23—blind (for dark-field technique); 24—polarizer; 25—analyser

¹ These objectives may have a plane field of vision (planar objectives); they are called planar achromats and planar apochromats.

is hemi-spherical and its spherical aberration is corrected by placing the object at the *aplanatic focus*, i.e. at a singular point on the optical axis of the objective where the spherical aberration is zero. Such objectives are termed aplanats.

Apochromatic objectives are aplanats at the same time. However, because of their design, the image formed by them is not perfectly plane, but slightly curved, which makes it impossible to have the same image sharpness at the centre and outer zones. This defect of apochromatic objectives is corrected by using compensating eyepieces.

Eyepieces (or oculars) form a virtual magnified image (i.e. magnify an intermediate image) and also correct some residual optical errors which cannot be corrected completely even in the most complicated objectives. Metallurgical microscopes use three types of ocular: common (Huygenian), compensating, and projection.

Common oculars are used in combination with achromatic objectives (i.e. for small magnifications). A common ocular is composed of an eye lens and two planar-convex lenses, with their convex sides facing the objective. A diaphragm is mounted between the two planar-convex lenses.

Compensating oculars are combined with apochromatic objectives and have a more complicated optical system comprising two lenses, one is a combination of a planar-concave lens and a biconcave lens glued together, and the second a biconcave lens.

Projection oculars (more commonly called amplifying oculars) are used to photograph microsections.

The magnification of an ocular is less than that of the objective and is selected to enable the observer to see clearly the image formed by the objective. If the magnification of the ocular is too low, some details of the image formed by the objective will not be seen; on the other hand, an ocular with too large a magnification does not detect new details of the image, it only impairs the sharpness of the image and narrows the field of vision.

The magnification provided by common oculars is 2 to 15, that of compensating oculars, up to 25, whereas the magnification of objectives is usually from 9 to 95.

The maximum useful magnification of a microscope is found by the formula

$$M = d_1/d$$

where d_1 = maximum resolving power of the human eye, equal to 0.3 mm

d = maximum resolving power of an optical system

The maximum resolving power of an optical system is determined from the conditions of diffraction by the equation

$$d = \frac{\lambda}{2n \sin \alpha/2}$$

where λ = light wavelength (6000 Å for white light)

n = refractive index

α = subtended angle of the incident light bundle

The maximum useful magnification of a microscope is attained when d is at its maximum and the value $n \sin \alpha/2$, termed the *numerical aperture*, is maximal for the given constant wavelength λ . It is therefore advisable to keep the values of $\alpha/2$ and n at their maxima.

Microscopic examinations are usually done in air ($n = 1$) with the use of common, or dry, objectives. For greater magnifications, a medium having a larger refractive index (usually cedar oil, having its refractive index $n = 1.52$) is placed between the front face of the objective and the object, and examinations are made by using what is called immersion objectives. The resolution of the optical system then may attain

$$d = \frac{6000}{2 \times 1.5 \times 1} = 0.2 \mu\text{m} (0.0002 \text{ mm})$$

and the maximum useful magnification will be

$$M = d_i/d = 0.3/0.0002 = 1500$$

To form a sharp image, the total magnification of the objective must not exceed the useful magnification of the optical system. The useful magnification of a given optical system for visible light can be taken equal to 100 apertures of the objective used. For instance, for an objective having an aperture of 0.65, the useful magnification of the optical system will be 650. Then since the objective has the maximum magnification 40X, the magnification of the ocular must be not more than 15. If, however, the microscopist tries to obtain a larger magnification, for instance 1000X, by using the same objective and an ocular of a greater magnification, the image formed will reveal no details of the structure, but on the contrary, the details that were seen clearly with the magnification of 600 will become blurred, since the useful magnification has been exceeded. To obtain a magnification of 1000X, one has to take an objective of a larger numerical aperture (for instance, 1.25). (The numerical aperture and magnification are always marked on the objective mount.) By using this objective, the useful magnification of the optical system can then be increased up to 1250X.

The total magnification v_m of a microscope can be taken as the product of the magnifications given by the ocular and objective.

The maximum magnification of modern microscopes, for a 25-fold magnification of the ocular (of the compensating type) and the minimum focal distance of the objective of 1.5 mm, may reach $v_m = \frac{250}{1.5} 25 = 4165$, whereas the useful magnification is only one-third of that value.

The total magnification of a microscope can be checked experimentally by means of a 'stage micrometer' which is a scale 1 mm long engraved in 1/100-mm divisions. When the stage micrometer is placed instead of a microsection on the microscope stage, its scale will be distinctly seen in the ocular. By comparing the divisions of the scale with the diameter of the circle of the ocular, one can determine roughly the actual circle diameter. For instance, let the circle diameter be 150 mm and let 15 divisions of the scale be seen within it. Then the actual size of the circle is 0.15 mm and the magnification of the microscope $v_m = 150/0.15 = 1000$. This measurement may be done more accurately by mounting an optical mirror over the eyepiece to reflect the image onto a paper sheet; then it will be possible to measure accurately the circle diameter. The magnification of a microscope for photography can be determined by projecting the image of the stage micrometer onto the ground glass of the photographic camera. By measuring (by means of a scale or, better, a slide gauge) the distance between a certain number of scale divisions on the ground glass and dividing it by the actual (not magnified) distance between these divisions of the stage micrometer, we can find the magnification of the microscope obtained with the given extension of the camera.

Eyepiece micrometers are often used in practical metallurgical studies. This is an eyepiece (ocular) incorporating a glass plate with a scale, usually in 0.1-mm divisions, engraved on it. By simultaneously using a stage micrometer and an eyepiece micrometer, the actual scale spacing of the eyepiece micrometer is determined.

To do this, the eyepiece micrometer is rotated so that its scale can be superimposed over that of the stage micrometer. Then, by turning the screws of the stage, the initial divisions and certain other reference divisions of these two scales are brought into coincidence and the number of scale divisions between the coinciding marks is counted. The spacing of one division of the eyepiece micrometer (D) is then found as

$$D = zT/A$$

where z = spacing of the stage micrometer

T, A = number of divisions of the stage and eyepiece micrometers, respectively, between the coinciding marks

For instance, the number of divisions of the stage micrometer between the coinciding marks is 10, the corresponding number of divisions for the eyepiece micrometer is 50, and the spacing of the stage micrometer is known to be 0.01 mm. Then

$$D = \frac{0.01 \times 10}{50} = 0.002 \text{ mm or } 2\mu\text{m}$$

The magnification of the microscope will then be

$$v = z/D = 0.01 \text{ mm}/0.002 \text{ mm} = 50$$

With the known magnification of the optical system (i.e. the magnification provided by the objective and the eyepiece), one can use the eyepiece micrometer to determine the dimensions of a particular region in the image of a microsection, for instance in studies or control of chemical heat treatment (cementation, nitration, etc.) of steels, or when determining the depth of a saturated surface layer, etc.

(n) Illuminating System of Microscope

Illumination of microsections is usually effected through the objective by means of an illuminating system comprising a light source and a number of lenses, light filters, and diaphragms.

The light source may be a low-voltage incandescent lamp or, less commonly, a d.c. or a.c. lamp for a voltage of 110-120 V, or else an electric arc (an arc lamp). Powerful high-pressure mercury lamps giving a luminance of up to 2500 sb have recently come into use. To reduce light diffusion and increase image sharpness, the illuminating system may incorporate auxiliary lenses and condensers which concentrate the light beam onto a particular region of a microsection.

Diaphragms are used to limit the diameter of the light beam while light filters (which are glass plates made of tinted, opaque or obscured glass) serve to transmit light of a required wavelength only, i.e. of a specified colour, or to control the light intensity so as not to tire the eyes of the observer.

The human eye possesses unequal sensitivity to various colours of the spectrum, being most sensitive to yellow-green light. Therefore, the use of a yellow-green filter, which absorbs all other constituents of white light, makes it possible to see more distinctly

the details of the structure of a microsection. Yellow-green filters diminish chromatic aberration and, besides, increase the resolution of an objective as they transmit only rays of a lower wavelength.

Microscopic examinations may be made by either a *dark-field* or *bright-field technique*.

Dark-field examinations are done by using an epi-objective in which the mount holding the objective lenses is surrounded by a parabolic mirror that receives only the edge beams from the light source. Thus, illumination is effected here by means of the parabolic mirror, rather than through the objective, and only part of the rays diffusely reflected by the microsection will return back into the objective. These rays are reflected by some phases only, which usually protrude above the remaining surface of a microsection and are thus seen bright against a dark background. Thus, the dark-field technique cannot give a complete characteristic of a structure and should only be employed as a supplementary to the main bright-field technique.

The latter is widely used for studies of metals and other opaque materials. It uses vertical illumination,¹ i.e. light beams are directed vertically through the objective onto the microsection.

Since the surface of a microsection becomes rough after etching (owing to the different etchability of various phases), reflection of light will be unequal from various regions, thus forming a pattern representing the structure of an alloy.

The contrast of an image is maximum when oblique beams form a hollow cone; this is achieved by introducing an annular aperture stop. The aperture of the objective is thus utilized fully.

The contrast of relief structures can be additionally increased by using a phase-contrast attachment in the microscope. In this case the beams reflected by the lower (recessed) portions of the etched surface, i.e. passing a longer path, vary the phase of their oscillations as compared with the beams reflected by projecting portions. Owing to the difference in the properties of the metal phases or grain regions (i.e. recessed and projecting regions), a certain phase difference in the reflected light beams occurs. This difference is amplified (up to $\pi/2$ in the limit case) by means of a phase plate placed in the focal plane. This provides a sharp contrast.

¹ Oblique illumination obtained by displacing either the aperture stop or the light source from the optical axis is a variant. With this illumination the projecting portions of a microsection are seen brighter and throw sharp shadows onto adjacent surface of the microsection. The latter, in addition, is less reflective with oblique illumination, and, therefore, the contrast of the image increases even more.

Polarized light, i.e. light whose waves oscillate in a definite plane only, can also be used for visual microscopic studies and microphotography.

Polarized-light microscopes have two polarizing filters; one of them, being the polarizer proper, is mounted near the light source (lamp) in the light path, and the other filter, which is an analyser mounted before the eyepiece or between the objective and eyepiece concentrates the polarized beams reflected by the microsection. If an object is optically isotropic, then full absorption of the light may be achieved by properly positioning the polarizer relative to the analyser (the position of crossed nicols). With optically anisotropic crystallites, however, full absorption of light is impossible, and some of the crystallites are seen bright, while others are dark. The polarized-light technique is employed for studying alloys composed of phases having non-cubic crystal lattices, and also for studying non-metallic inclusions. With a transparent inclusion, the reflected light is partially refracted by its faces and is not polarized. Therefore, with a crossed-nicols position, the inclusion will be seen as a bright or tinted spot (for instance, inclusions of copper oxide in copper alloys are seen red), owing to interference. The nature of the inclusion can then be judged by its transparency, colour, and anisotropy.

For photography, a region of interest is found on a microsection, and its image is projected through an amplifying ocular into a photographic camera.

Photographic cameras employed for microscopic studies may be of diverse designs, those provided with extension bellows being preferable, since they enable photographs to be taken at different magnifications.

The exposure time depends on the brightness of the image, illumination intensity, magnification of the objective, sensitivity of photographic plate or film, etc. It is usually found experimentally for each type of a microscope.¹

Colour-sensitive orthochromatic photographic plates are used mostly for microstructure photography.

Exposed plates are processed in the usual way, i.e. developed, fixed, thoroughly washed in water, and the negatives thus made are used to print positive images on photographic paper.

(o) Mechanical System of Microscope

A metallurgical microscope comprises a stand, tube, and stage (Fig. 3.29). The microsection is placed on the horizontal stage

¹ In modern microscopes, such as 'Neophot-2', exposure time is controlled automatically (see Sec. 3.2 p).

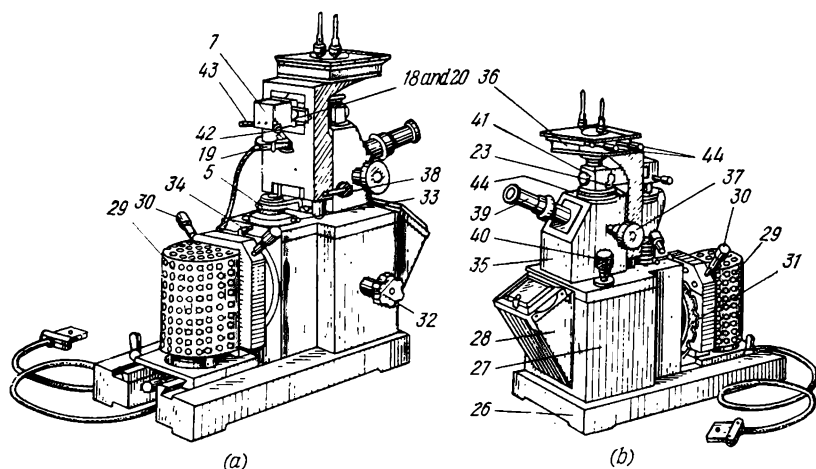


Fig. 3.29. General view of MIM-7 microscope

(a) viewed from the transformer side; (b) viewed from the camera side; 1-25—see Fig. 3.28; 26—plate; 27—camera body; 28—photographic camera; 29—lamp hood; 30—lamp-centring screws; 31—light filter disc; 32—handle for turning turret carrying three photo-oculars; 33—handle for operating iris aperture stop; 34—diaphragm-fixing screw; 35—microscope housing; 36—stage; 37—macrometer screw for moving the stage vertically; 38—macrometer screw stopper; 39—visual tube; 40—micrometer screw; 41—illuminating tube; 42—field aperture handle; 43—centring mechanism; 44—screws for moving the stage in two mutually perpendicular directions

and levelled so that its prepared surface is perpendicular to the optical axis of the objective. Removable inserts with orifices of different diameter are placed in the centre of a stage to pass light rays onto a specimen.

The stage can be moved in the horizontal plane in two mutually perpendicular directions by means of screws 44; this makes it possible to shift the microsection as required (up to 15 mm) and examine its various regions without changing the focal distance.¹

The microsection placed on the stage should be focused to have a clear image. To do this, a macrometer screw 37 (see Fig. 3.29) on the instrument stand is turned to lift or lower the stage, thus ensuring rough focusing. Fine focusing is made by a micrometer screw 40, one turn of which moves the objective, relative to the stage, by a few fractions of a millimetre (in most microscopes, one division of the scale of this screw is 2 μm). The greater the magnification of an objective, the shorter the distance between the stage and objective.

¹ In the MMP-2 microscope, the stage movement is controlled automatically (see Sec. 3.2p).

(p) Types of Metallurgical Microscope

The layout of a microscope, i.e. the position of its optical axis, may be either vertical or horizontal.

The vertical microscope type МИМ-7 (see Figs. 3.28 and 3.29) can be used for dark- and bright-field and polarized-light studies, with either vertical or oblique illumination. Its magnification can be changed within a range of from 60 to 1440.

The light source is a powerful lamp 1 (type K30, 17 V 170 W) connected via a reducing transformer TP-17 of the subdivided type, which makes it possible to control the brightness of the lamp. The light rays from the lamp pass via collector lens 2, mirror 3, and then through aperture stop (diaphragm) 5, lens 6, prism 7, and lens 8 to a plane-parallel semi-transparent mirror plate 9 which reflects about 1/3 of the light flux through objective 10 onto microsection 11 placed in the focal plane of the objective. The light rays reflected by the microsection back to the objective pass as a parallel beam via the plane-parallel plate 9 to an achromatic lens 12 and then, being reflected by mirror 14, enter eyepiece 13.

To take a photograph, the eyepiece with mirror 14 is moved aside so that the light passes to one of three photo-oculars 15 mounted in a turret and is reflected by mirror 16 to a ground glass or photographic plate 17. Exposure is made by means of shutter 19.

For oblique-light examination, the aperture diaphragm and lamp are displaced from the optical axis of the instrument.

With the dark-field technique, lens 8 is replaced with lens 20 having a dark circle in its centre. The light rays passing through the outer zone of this lens are then reflected by an annular mirror 21 (plate 9 being covered by blind 23) to a parabolic mirror 22 surrounding the objective and integral with the latter (epi-objective). The light reflected by mirror 22 onto the microsection is reflected back only from the projecting surfaces of the latter.

With the polarized-light technique, polarizer 24 is placed on the mount of lens 6, and analyser 25, on the mount of lens 12.

The horizontal microscopes types МИМ-8 and МИМ-8М (Fig. 3.30) have a magnification of from 100 to 1350 for visual observation and from 45 to 2000 for photography with high resolution of the image. Dry- and immersion-type achromatic and apochromatic objectives can be used. Achromatic objectives are employed in combination with common coated-glass eyepieces (coating increases light transmissivity and improves contrast of the image); apochromatic objectives are used with compensating eyepieces. Light-yellow filters are used with both achromatic and

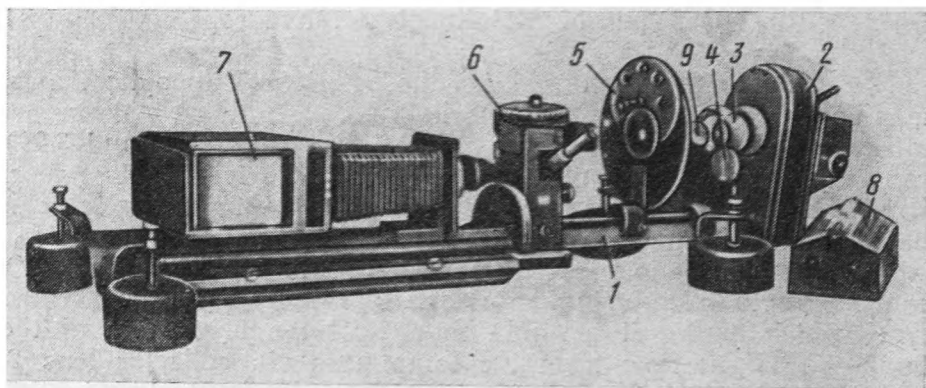


Fig. 3.30. General view of MIM-8 microscope

1—large bench; 2—incandescent lamp; 3—heat filter; 4—swivelling lens; 5—light filter; 6—microscope; 7—photographic camera; 8—rheostat

apochromatic objectives for higher contrast in photography and for reducing light sharpness during visual examinations.

The MIM-8 microscope is suitable for light-field, dark-field and polarized-light techniques. Its light source is a sharp-focus 170-W incandescent lamp.

The design of the MIM-8 microscope is shown in Fig. 3.31. It comprises a swivelling polarizer 1 for the polarized-light technique, which is placed near the light source, an aperture stop 2, an illuminator lens, and field and annular diaphragms 3 mounted on the same plate. For the dark-field technique, the plate is shifted so as to place the annular diaphragm in the path of light rays.

With the polarized-light technique, polarizer 7 (Fig. 3.32) and analyser 18 are shifted into the optical path.

At the front wall of the microscope is handle 8 (see Fig. 3.31), which, being turned away from the observer, shifts the photographic prism in place of the plane-parallel plate. Another handle 12 on the right-hand side of the instrument removes the visual prism before taking photographs.

The microsection is illuminated (Fig. 3.32) through the objective by the beams reflected from the plane-parallel plate or sector prism, the latter being used when it is required to increase the brightness of light for photography. Since the prism reduces the resolving power of the objective, it is only used at relatively low magnifications (500-600). At higher magnifications, the required brightness is ensured by switching on a K30 lamp and using the plane-parallel plate instead of the prism. With the bright-field technique (vertical illumination), light beams pass through the

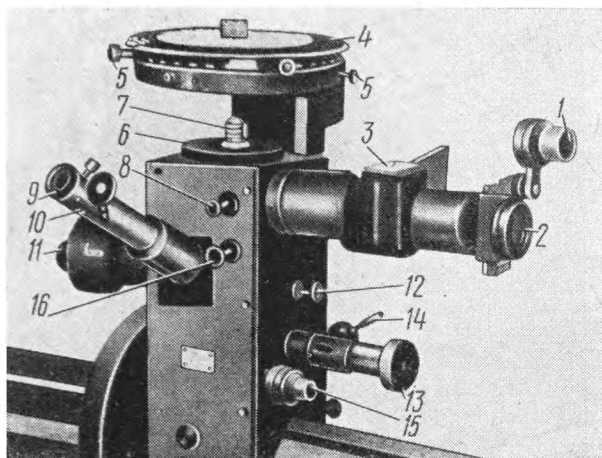


Fig. 3.31. МИМ-8 microscope design

1—polarizer; 2—aperture stop; 3—field and annular diaphragms; 4—stage; 5—stage-moving screws; 6—objective plate; 7—objective; 8—handle for replacing plane-parallel plate with prism; 9—eyepiece; 10—visual tube; 11—phototube; 12—handle for withdrawing visual prism for photography; 13—macrometer screw; 14—stopper; 15—micrometer screw; 16—analyser handle

system of lenses and diaphragms to the plane-parallel plate placed at 45 degrees and are reflected by this through the objective onto the microsection. The light reflected by the microsection passes again through the objective, plane-parallel plate, and achromatic lens.

With visual examination, the light is reflected by prism 18 (Fig. 3.32) into the eyepiece. When taking photographs at low magnifications, the light beams pass through prism 11 and then through the objective onto the microsection; the reflected beams pass through two prisms 19 and photographic eyepiece 20 into the camera.

With the dark-field technique the light beams pass through an additional lens 4 and an annular diaphragm 16, then being reflected from an aluminium-plated mirror embracing the plane-parallel plate, they are further reflected by the parabolic reflecting surface of the condenser and directed at an angle onto microsection 15, thus bypassing the objective. The light reflected from the microsection enters the objective and passes through the plane-parallel plate, achromatic lens and further as in visual examination or bright-field photography.

The photographic camera of the microscope comprises a camera proper, extension bellows (which can be extended between 160 and 660 mm) for controlling the magnification ratio in pho-

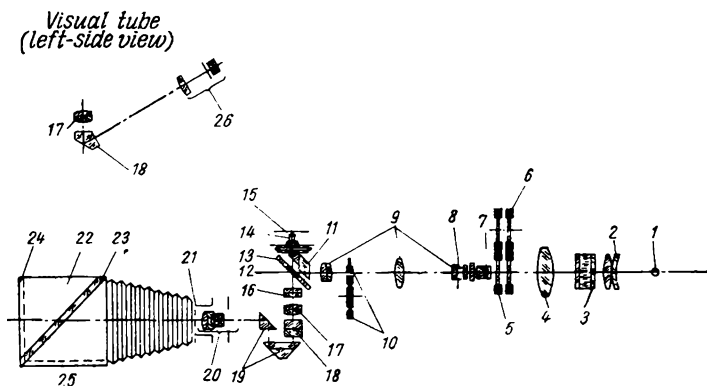


Fig. 3.32. Optical diagram of МИМ-8 microscope

tography, shutter, and adapter sleeve. The image may be formed on either the rear or side wall of the camera by using a tilting mirror placed at 45 degrees to the camera axis. Correspondingly, photographic plate holders can be mounted on either of these walls, the other wall then receiving a ground glass for visual examination and focusing. Double plate holders 13×18 cm and single plate holders 9×12 cm can be used with the camera.

In an advanced model of the МИМ-8М microscope the condenser can be moved in the illuminator to control illumination brightness and adjust the light for either bright-field or dark-field examination.

With the phase-contrast technique, a phase contrast attachment type КФ-3 can be used with the microscopes of both types. It is fastened on the microscope tube in place of the photographic tube, with the annular diaphragm being simultaneously placed onto the aperture stop (Fig. 3.32).

When taking photographs, the visual tube (Fig. 3.32), which carries the 45-degree mirror in its lower portion, is moved back, and the camera is attached to the clamp carrying the photographic eyepiece.

In microscopes of more advanced design, such as type ММР-2 (Fig. 3.33), stage 1 is placed at the top of the instrument. Structures of metals and other opaque materials can be studied here either directly by visual examination 2 or by the image formed on a 9×12 cm screen 4, using the bright-field, dark-field, or polarized-light technique. The light source is an incandescent lamp type ОП12-100. As distinct from МИМ-7 and МИМ-8 microscopes, the objectives (planachromats) are mounted in a revolving turret 5,

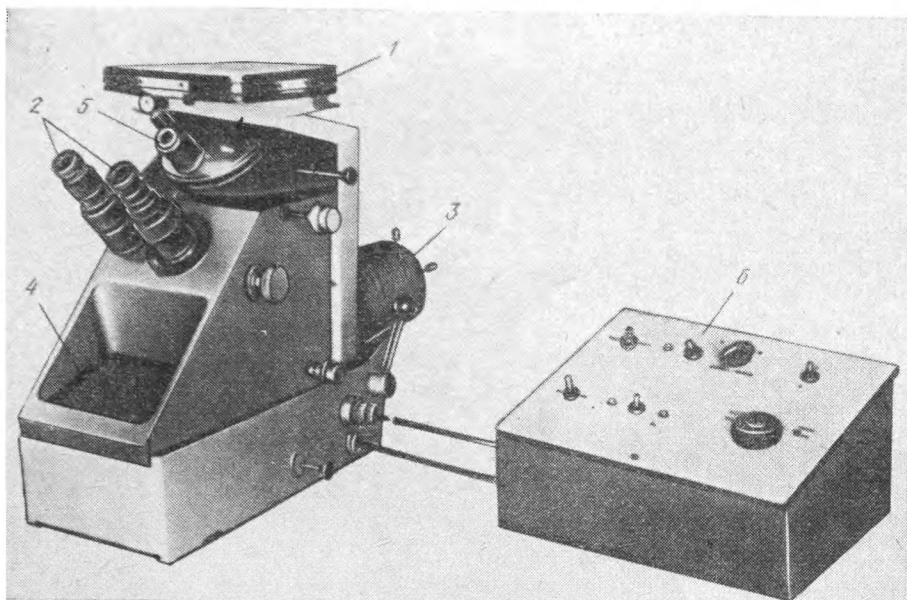


Fig. 3.33 General view of an MMP-2 microscope

The instrument is provided with two stages which can be controlled either manually or automatically by means of a programming device 6. The time of passage of any point of an object through the eyepiece field (in automatic stage control) is 3-4 s, which is very convenient for computation of structure elements. The magnification ratio can be varied from 100X to 1000X.

Photography of objects can be done on 9×12 cm photographic plates or miniature film (by using a miniature camera, such as 'Zorky-4').

The 'Neophot-2' horizontal microscope (C. Zeiss, GDR) is used for examination of the structure of opaque objects in reflected light at magnifications up to 2000 (Fig. 3.34). The instrument is provided with two illuminators: one for the bright- and dark-field technique at low magnifications (10-50), and the other for the dark-field, polarized-light, and phase-contrast technique at large magnifications (50-2000). Besides, there is an additional illuminator for special polarized-light examinations. The light source is a 12-V, 100-W incandescent lamp or high-pressure xenon lamp type XBO-100. Objects are placed on a precision stage which has a lever mechanism to lift it rapidly when interchanging objectives. The objectives are planachromats with magnifications of from 1.25 to 100 (with a numerical aperture of from 0.025 to

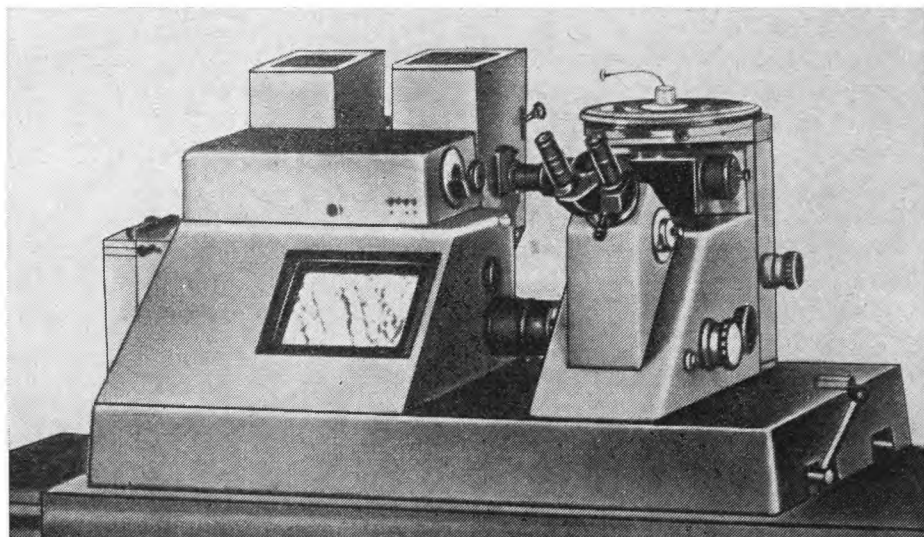


Fig. 3.34. General view of a 'Neophot-2' microscope (GDR)

1.30), planapochromats with magnifications of from 10 to 100 (numerical apertures 0.25-1.35) and planachromats with magnifications of from 6.3 to 100 for the special polarized-light technique. The objectives are matched so that rough focusing is not required when interchanging objectives.

Both monocular and binocular observations are possible, by using the eyepiece type PK12.5 with the virtual diameter of eyepiece field of 200 mm. The magnification ratio of the eyepiece can be controlled from 8 to 20 by rotating a knob.

Photographs can be taken by a large-size camera on photographic plates of a size from 6.5×9 cm to 13×18 cm or by a special microphotographic device MF. As distinct from other microscopes, 'Neophot-2' has an automatic exposure-controlling device which adjusts the optimum exposure for any brightness of illumination, the exposure time being controlled from 0.1 to 30 minutes and more.

The instrument has an attachment for microhardness measurements and another attachment for interference observations and control of the state of surface of specimens.

(q) Infra-red Microscopes

The structures of semiconductors and some minerals are examined in infra-red light ($\lambda = 0.75\text{-}1.2\ \mu\text{m}$) by using infra-red microscopes, such as the МИК-3 and МИК-4 types. A large group

of semiconductor materials, for instance, silicon, gallium arsenide, etc., are transparent to infra-red light. This enables blow-holes and other internal structural defects in these materials to be seen in infra-red light, as the refractive indices between the parent material and a defect are different. It is also possible, by using the polarized-light technique, to obtain data on fine structure—the presence of blocks and the nature of stresses.

The magnification range of the МИК-3 microscope is 25-270 and that of МИК-4, 45-5260 for transmitted light and 95-5625 for reflected light.

3.3. ELECTRON MICROSCOPY

The resolving power of an optical system can be increased essentially if electron beams possessing a low wavelength are used instead of light beams.

The wavelength of electrons is inversely proportional to their momentum, i.e.

$$\lambda = h/mv$$

where h = Planck's constant

m and v = mass and velocity of an electron, respectively

Thus, it is possible to change the wavelength by varying the velocity of electrons, for instance, by passing them through an electric field of high intensity; then

$$v = \sqrt{2meV}/m \quad \text{or} \quad \lambda = h/\sqrt{2meV}$$

where V = voltage applied

e = charge of an electron

Substituting the physical constants and introducing a coefficient for the voltage to be expressed in other units, we find

$$\lambda = \sqrt{\frac{150}{V}} 10^{-8} \text{ cm} = \frac{12.25}{\sqrt{V}} \text{ \AA}$$

or, considering that the mass of an electron varies with velocity,

$$\lambda = \frac{1}{1 + 9.76V \times 10^{-7}} \sqrt{\frac{150}{V}} \text{ \AA}$$

The resolving power feasible in an electron microscope is 100,000 times that attainable in an optical microscope. However, because of various phenomena accompanying the passage of a stream of electrons, i.e. spherical and chromatic aberrations, etc.,

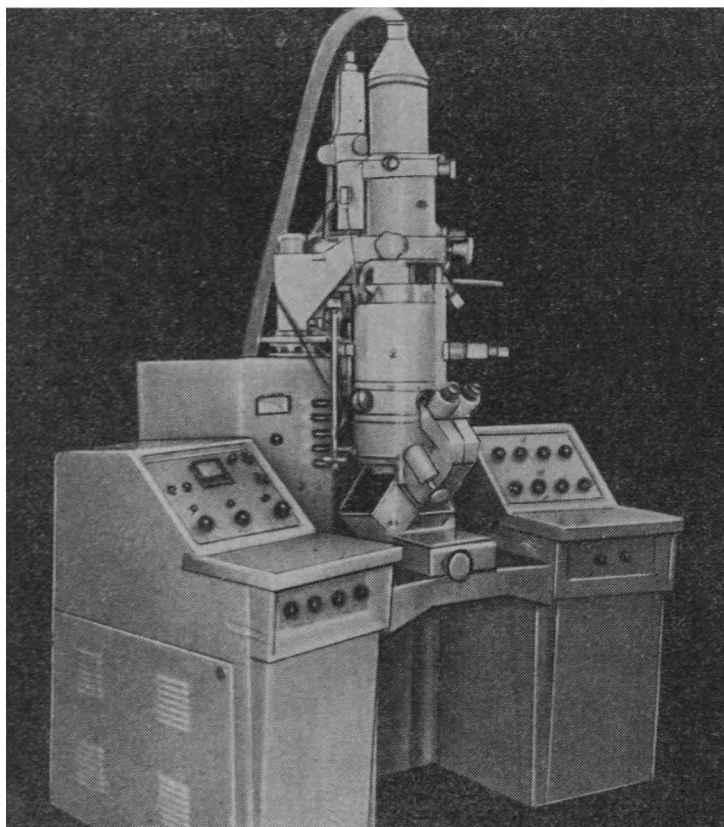


Fig. 3.35. General view of EM-8 microscope

the maximum resolving power of an electron microscope is actually only 100-200 times greater than that of optical microscopes. Thus, the maximum magnification that can be realized in an electron microscope is 100,000 to 200,000.

Design of an electron microscope. The external view of an electron microscope is shown in Fig. 3.35, and its principal diagram, in Fig. 3.36.

A modern electron microscope comprises a source of electrons, i.e. an electron gun (1-3 in Fig. 3.36) which emits electrons and accelerates them owing to the voltage applied. The cathode, which is a heated tungsten coil, emits electrons. The anode, which is a plate with a hole in its centre, is placed quite close to the coil, and a powerful electric field is induced in the gap between them in order to accelerate electrons to the required velocity. The emitted electrons pass through the hole and condenser lenses po-

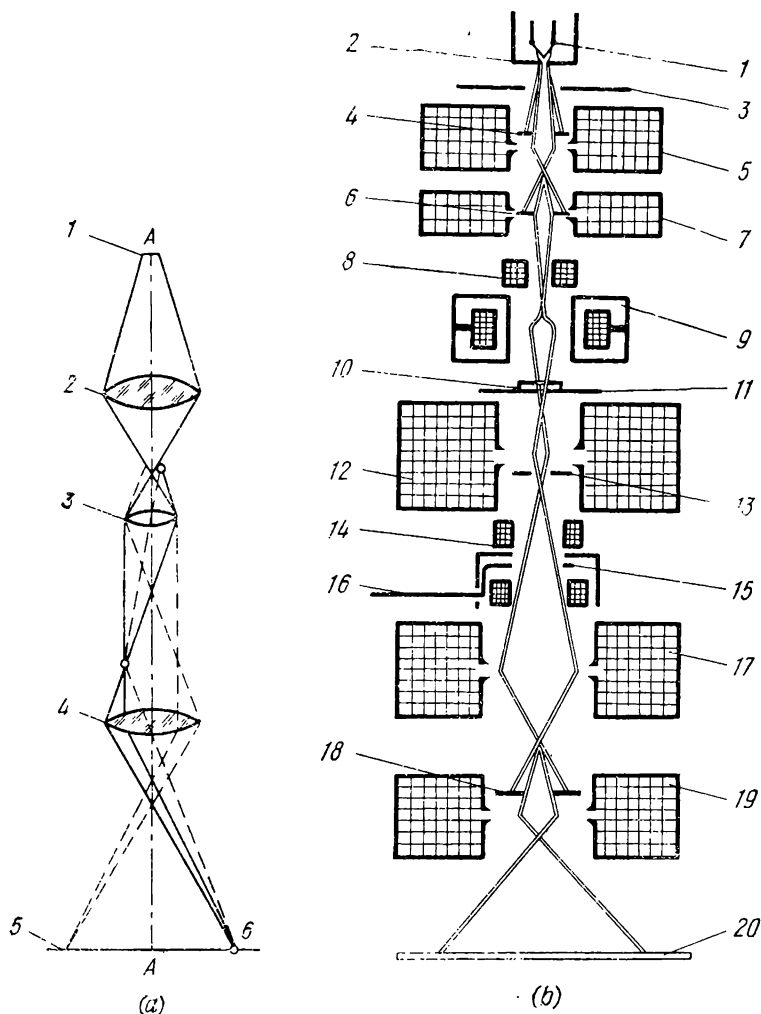


Fig. 3.36. Principal diagrams of (a) optical and (b) electron microscopes
 (a) 1—light source; 2—condenser lens; 3—objective; 4—eyepiece; 5—image; (b) 1—cathode; 2—focusing electrode; 3—anode; 4—first condenser diaphragm; 5—first condenser; 6—second condenser diaphragm; 7—second condenser; 8—second condenser stigmator; 9—adjustment corrector; 10—object; 11—object stage; 12—objective lens; 13—aperture stop; 14—objective lens stigmator; 15—sector diaphragm; 16—intermediate lens stigmator; 17—intermediate lens; 18—field aperture; 19—projector lens; 20—screen

sitioned below that hole.¹ The condenser lens or an intermediate objective lens and projector lens form magnetic or electrostatic field of appreciable intensity. Here, electron microscopes may be either the magnetic or electrostatic type or a combination of both.

Magnetic microscopes can be electromagnetic in which the field in a lens is induced by a solenoid, or magnetostatic wherein the field is formed by powerful permanent magnets made of highly coercive alloys.

Of the two types electromagnetic microscopes have found wider application. The principal diagram of the projector and objective lenses in such microscopes is shown in Fig. 3.36. These lenses play the same part as the objective and eyepiece in the system of an optical microscope. The focusing effect of the lenses in an electron microscope is due to the interaction of electrons with the magnetic (or electric) field whose intensity and the distribution of the lines of force (or equipotential surfaces) may be determined by calculation. An electromagnetic lens comprises a coil encased in an iron shroud, since a very strong field should be formed. Pole pairs are mounted in the coil with very narrow gaps between them, and in the gaps a strong field is induced. This reduces the focal distance, and, therefore, provides a large magnification, and also reduces image distortion.

The stream of electrons then hits the object. According to the method in which the object is examined by means of electron beams, the following types of electron microscope exist:

(a) transmission electron microscope in which the stream of electrons passes through the object, the image formed being the result of different scattering of electrons by the object;

(b) reflection electron microscope wherein the image is formed by the electrons reflected from the surface of the object; the principal diagram of the electron-optical system of such a microscope is very similar to the optical system of a microscope;

(c) field-emission electron microscope in which the image is formed on a surface fluorescing under the action of the electrons;

(d) scanning electron microscope wherein the image is produced from the secondary emission of electrons emitted by the surface being scanned by a stream of primary electrons.

(a) Transmission Microscopes

This type of electron microscope is the one used most widely as it has some advantages over other types. In reflection electron

¹ There is no condenser lens in electrostatic microscopes, while in electromagnetic microscopes of high resolving power a double condenser lens is employed.

microscopes, for instance, reflection of electron beams from the surface of an opaque object, such as metal, causes chromatic aberration and other phenomena which sharply reduce resolution and, therefore, ruin the principal merit of the electron microscope.

There are a number of models of transmission microscope.

The ЭМВ-100Л microscope has an accelerating voltage of up to 100 kV, magnification up to 400,000, and resolution of 3 Å.

Transmission observation of structures in this microscope can be done by the bright-field or dark-field technique. Besides, a special attachment ППОН-3 enables variations of the structure of metallic and other film objects to be studied during tension (maximum elongation is 75 μm) and heating up to 1000 °C. To use this attachment, the pole piece of the objective lens is replaced with another one having a larger orifice, and the power supply unit is connected to the network and the terminals of the objective lens. When using this attachment, however, the resolution of the system reduces to 20 Å in tension studies and to 30 Å in heating.

The microscope can also be employed for determining the crystalline structures of particles of precipitated phases by the microdiffraction method, if the size of particles is not less than 2-3 μm .

The ЭМ150 microscope has an accelerating voltage of up to 150 kV and resolution of 5 Å. The instrument can also be used with the ППОН-3 attachment for studying structures of particles of a size not less than 2 μm by the microdiffraction method. Its magnification is up to 150,000.

The УЭМВ-100К microscope provides a resolution of 8 Å and magnification of up to 200,000.

A family of electron microscopes type ЭМ has also been developed: ЭМ8 (see Fig. 3.35) with the maximum resolution of 5-6 Å and magnification of up to 200,000; ЭМ9 (35 Å, 140,000X); and ЭМ114 (120 Å, 100,000X).

The EM-200A microscope (Japan) has a resolution of 3.4 Å and magnification of up to 200,000 (with the accelerating voltage of up to 200 kV); another model, EM-100B, has a resolution of 2 Å and magnification of up to 500,000.

The objects to be examined in a transmission microscope must be transparent to electrons, i.e. their thickness must be very small. They are usually made in the form of thin metallic films (100-2000 Å) or replicas (moulds) of the surface of a metallic microsection. Replicas can be made of various materials, but their thickness is always so small that the passage of electrons does not interfere with the structure. As the thickness of a replica

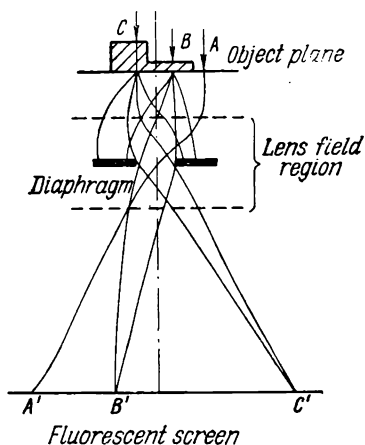


Fig. 3.37. Diagram of contrast formation in electron microscope

varies all over the section, the replica scatters the electrons differently (Fig. 3.37).

The total amount of scattered electrons passing through various portions of a replica is however approximately the same, so that if the objective lens collects and focuses all the electrons, the image formed by it will lack contrast.

To form a high-contrast image, the objective lens is provided with an aperture diaphragm made in the form of a small metallic plate having a very small hole (approx. 0.003 mm in diameter) in its centre, as shown in Fig. 3.37. The diaphragm catches all

the most widely scattered electrons, i.e. ones that have passed through the thickest or most dense portions of the object (replica). The lens will then pass different amounts of electrons from various portions of the object in accordance with the scattering effects, i.e. more electrons will pass from thinner portions and less from thicker ones. This produces contrast of the image, and the intermediate image formed by the objective lens will represent the structure of the object. This intermediate image can be observed on a fluorescent screen through special windows provided in the microscope housing.

The fluorescent screen has an orifice in its centre which passes part of the electron beams to the projector lens; this produces a secondary magnified (final) image and projects it onto another fluorescent screen.

This latter image can be seen through an optical microscope placed opposite the screen or can be photographed; to do this, the screen is moved aside, and the stream of electrons is directed onto a photographic plate; this is developed and fixed, and thus an image representing the structure of the object is obtained.

When the object is a metal film, the image is formed in a somewhat different manner. Strictly speaking, the point is the different regularities in the passage of electron waves through matter. The passage of electron waves through a thin film produces a phase-contrast effect, i.e. a change of the phase of these waves owing to the displacement of atoms from their normal positions

in the lattice in places of structure defects (dislocations, packing defects, etc.).

Two methods are used to detect these defects.

1. The schlieren method which produces a magnified image of a lattice through interference of electron beams. The method is however only applicable for crystals having large interplanar distances (5 Å), i.e. mainly for non-metallic materials.

2. The method of diffraction contrast which is based on the fact that the electron beams diffracted by structural defects cannot reach the aperture diaphragm, whereas straight (non-diffracted) beams pass freely through the latter. A bright-field image can be formed in this way. If, on the contrary, only the diffracted beams reach the image plane, but not straight beams (this is achieved by displacing the aperture diaphragm), a dark-field image is produced. Unlike the first method, atomic planes cannot be resolved in the diffraction-contrast method, and only the effects of displacement of atoms are observed, so that dislocations are usually imaged as dark lines, and packing defects and grain boundaries, as interference bands.¹ The contours of precipitated-phase inclusions in thin films are detected quite clearly owing to a change in the conditions of diffraction, and through the interference effect and accumulation of defects at grain boundaries.

The work with an electron microscope is more intricate than with an optical one. The parameters of the electric circuit which determine the microscope 'optics' must be maintained strictly constant by means of electrical measuring instruments. The procedure of electron-microscopic examination is usually as follows. A specimen is placed into an object chamber, all elements of the apparatus are checked for tightness, and vacuum pumps evacuate the system. When the pressure has been reduced to the specified value, a tungsten-coil anode is fed with current. Then a high-voltage current is supplied to form an electric field for acceleration of electrons and a magnetizing current to feed the electromagnetic lenses. The object being studied is gradually moved to examine or photograph the portions that are of interest to the observer. In some older models of electron microscope, the whole system must be refilled with air and then re-evacuated when it is necessary to replace the object or photographic plate. In many microscopes of more advanced design, the object chamber and

¹ With an edge dislocation, the maximum contrast is formed only at one side of its centre, since the crystal is locally turned in different directions, at its two sides, relative to the position of the maximum reflection. With a screw dislocation, when atoms above and below the dislocation centre are displaced relative to each other, a phase shift is formed between the electron waves scattered by these atoms. A similar picture is observed with packing defects.

photographic camera are isolated from the system, and re-evacuation takes less time.

Preparation of objects. The procedure is more complicated than preparation of microsections for optical microscopy. An object to be examined must be transparent to electrons, i.e. its thickness must be very small. Such objects may be thin metallic films or replicas of the surface of microsections, which reproduce the pattern of their surface, and, therefore, the structure.

Thin films, 100-2000 Å, for transmitted-light examination¹ can be prepared by the methods of deposition, deformation or dissolution. The objects obtained by the methods of deposition and deformation cannot characterize the structure of massive metallic specimens. For this reason the most widely used method is that of dissolution (thinning) of massive machined specimens by means of chemical or electrochemical polishing.

Chemical polishing is only applicable to pure metals and single-phase alloys and cannot be used for alloys having a heterogeneous structure, since their phases usually dissolve at different rates. Electrolytic polishing is employed most often for the purpose. A specimen is usually polished electrolytically (by using pointed cathodes) until holes form in it. The thin portions around holes are quite suitable for electron-microscopic examination.

In cases by properly selecting the electrolyte and the positions of the cathode and specimen, a number of holes are made in a specimen, the spaces (strips) between the holes having a thickness quite suitable for 'transmitted-light' examination. For instance, thin films of copper alloys are produced by using an electrolyte consisting of 33 per cent nitric acid and 67 per cent methyl alcohol (current density 0.5-0.6 A/cm²); iron alloys are polished electrolytically by a mixture of 20 parts glacial acetic acid and 1 part perchloric acid (current density 0.7 A/cm²).

The procedure of making replicas requires much care, since even slight deviations in their shape can result in an incorrect picture of the metal structure.

To begin with, the surface of a microsection must be prepared very carefully. A section is polished electrolytically and etched to form a relief surface. All traces of the etching reagent must be removed from the surface, which is controlled by means of an optical microscope.

Etching may also be done by the gas-discharge method. In this case the section serves as the cathode in a gas-discharge tube, and etching is effected through impacts of ions of a gas (neon) at a pressure of 0.5-0.6 mm Hg.

¹ High-voltage microscopes (for a voltage of approx. 1 MeV) enable thicker objects to be examined with a resolution of 7 Å.

To get a deeper relief, copper, chromium or other metals can be vacuum-deposited onto the surface of a microsection; this is favourable for producing a higher contrast of the image. The surface of a section is set at a small angle to the direction of motion of deposited particles, so that these adhere to surface projections only.

A replica of the surface of the microsection is then made by some or other method. One of such methods is to make a lacquer replica (film). For this, a droplet of 1-percent solution of collodion in amylacetate is applied onto the inclined surface of a section or the latter is immersed in the solution and then dried. The lacquer film must be very thin (not more than $0.1\ \mu\text{m}$); thicker films can strongly absorb electrons, become heated through this, and their structure may change; besides, they may possess their own structure which might obscure the results of microscopic examination. The metallic microsection is then dissolved in an acid, the film floats up and can be picked up for examination. In other cases, the film is incised into pieces which then can be easily detached by slight dissolution of the metal surface. The dissolution may be either chemical or electrochemical; in the latter case the section is connected as an anode in a low-voltage circuit.

The lacquer film is picked up from the solution by means of metallic discs with small holes in their centres ($0.1\ \text{mm}$ in diameter) or metallic nets with meshes $0.05 \times 0.06\ \text{mm}$; these serve as object diaphragms and are mounted in the object chamber of the electron microscope.

A convenient method for detaching lacquer films is to apply gelatine solution. The gelatine film contracts on drying and strips off the lacquer replica. The latter is then placed into hot water to dissolve gelatine, the lacquer replica floats up and may be picked up by a disc or net as mentioned above.

Lacquer replicas produce a negative image in an electron microscope since their ridges correspond to recesses in the microsection copied.

A positive replica may be obtained by making first an intermediate negative replica of polystyrene. To do this, polystyrene is pressed together with a microsection in a mould under a high pressure ($350\ \text{kgf/cm}^2$) and at a temperature of 130°C .

The polystyrene replica is stripped off the microsection and placed into a vacuum chamber where a thin film of quartz is deposited on it by means of a heating tungsten coil. The polystyrene negative is then dissolved in ethyl bromide, and the quartz film is removed by an object diaphragm. The quartz film is transparent to electrons, but these are scattered in different ways on

ridges and recesses and thus produce an image representing the structure of the metal.

This method suits better for revealing fine detail of the structure, i.e. ensures a higher 'resolution' of the replica, than the lacquer-film method wherein the sharpness of the image produced depends on wettability of the microsection surface by the lacquer used; besides, if the section has a shallow relief (after etching), a lacquer replica will not reproduce a clear enough image of the structure.

Quartz replicas and, more often, carbon replicas may be prepared by a one-stage method, with quartz or carbon being deposited directly onto the surface of a microsection. This method has certain advantages over the two-stage method described above, in particular in that it obviates the intermediate stage, i.e. the preparation of a polystyrene replica which may deform during stripping.

To obtain a higher contrast, lacquer, quartz and carbon replicas may be shadowed, i.e. a very fine layer of a heavy metal (chromium, gold, etc.), which possesses no definite structure, is vacuum-deposited at a certain angle. This produces a larger difference in scattering of electrons by the various portions of the replica, increases contrast, and facilitates decoding of images (in particular, ridges can be more easily distinguished from recesses).

Apart from the methods discussed above, which all may be termed indirect, there is a semi-direct method proposed by L. M. Utevsy. The method is used for examination of two-phase structures, for instance, ferrite-carbide structures in iron alloys. The surface of a metallic section is etched electrolytically so that only the matrix is dissolved. Particles of the precipitated phase (carbides) remain undissolved, but some of them become loose owing to the dissolution of the matrix. A quartz or carbon film is applied onto the etched surface and then detached together with the loose carbide particles by means of partial electrolytic dissolution of the metal.

The detached film may be subjected to electronographic study¹ to determine the nature of the phase whose particles are included in the film or replica.

Segregation of precipitated phases may also be fixed in oxide replicas prepared by oxidation of the surface of a microsection or through respective etching and heating. Since various phases possess different oxidizability, they will form oxide films of different

¹ Electronographic study is the examining of the diffraction pattern (electron microdiffraction) formed on the surface of a given phase through the interaction of the atoms of that phase with an electron beam. Microdiffraction is one of the most efficient methods for determining the phase composition of alloys.

thickness and composition. The matrix can then be dissolved by an appropriate reagent so that the oxide film will be detached together with particles of the precipitated phase.

Electron microscopy of the replicas obtained by any of the methods described should be preceded with the examination of the microsection under an optical microscope at various magnifications, up to the maximum ones. This will facilitate decoding of the structure seen in the electron microscope. It is also advisable, when making an electron-microscopy examination, to increase gradually the magnification used from the lowest, as in an optical microscope, to the maximum feasible, so as to obtain a continuous series of images.

If the structure being studied is sufficiently homogeneous or distributed uniformly over the whole volume of a metallic section, it suffices to examine any portion of the film. The problem becomes much more difficult if a particular portion must be studied, i.e. the one selected by optical microscopy, since a large area of the film must then be examined and the field of vision of an electron microscope is very small, only 5-6 μm in diameter. A method of sighting can then be used to speed up the procedure and give reliable results.

(b) Scanning Microscopes

A scanning electron microscope has a lower resolution than the common type, but its advantage is that the structure of the surface of an object can be examined directly, i.e. without making replicas or thin foils.

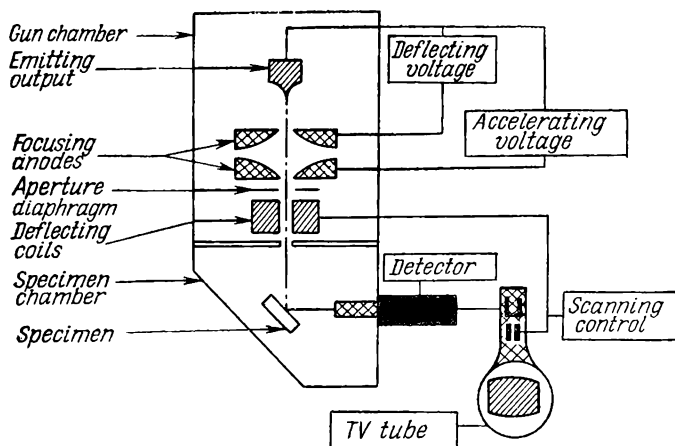


Fig. 338. Principal diagram of scanning electron microscope

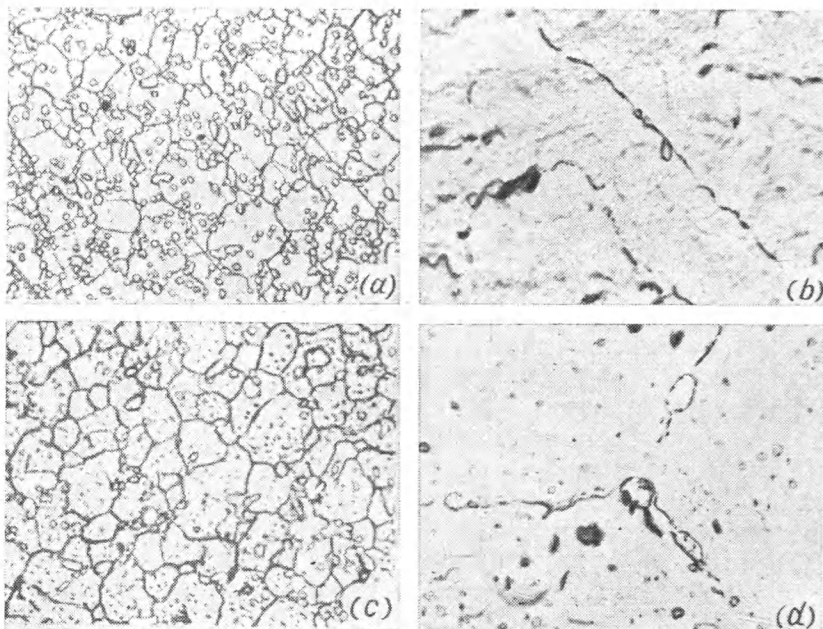


Fig. 3.39. Structure of steel containing 0.5% C, 6% W, 4% Cr, and 0.8% V After hardening; (a) optical microphotograph, 1000X; (b) electron microphotograph, 3500X after hardening and tempering at 400 °C for 10 hours; (c) optical microphotograph, 1000X (d) electronic microphotograph, 17,000X; (according to T. G. Sagadeeva and A. G. Gordeziani)

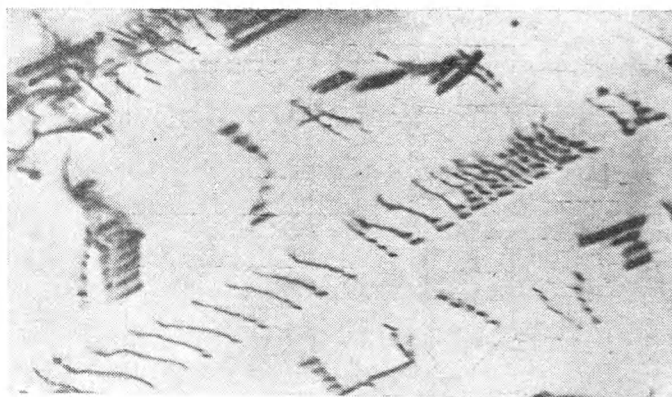


Fig. 3.40. 'Transmitted-light' electron microphotograph of a copper-aluminum alloy (bronze Grade Бр. А7), 40,000X (according to N. P. Gorlenko)

Figure 3.38 shows the principal diagram of a scanning microscope (Quickscan) which uses secondary emission and provides a resolution of 250 Å; the image is formed on the screen of a television tube.

(c) The Structures Seen in an Electron Microscope

Electron microscopy has provided us with many new data and extended our knowledge of the peculiarities of the fine structure of materials, the structure of ageing alloys, and the disperse structures of isothermic transformations in supercooled austenite, etc.

Figure 3.39 shows the structure of high-alloy steel with 0.5 per cent C, 6 per cent W, 4 per cent Cr and 0.8 per cent V¹ after hardening and tempering at 400° C for 10 hours, as seen in an optical microscope and in an electron microscope at a magnification of 17,000. As is seen, electron microscopy is capable of resolving fine detail which cannot be resolved by the optical microscope.

In particular, the electron photograph (17,000X) has revealed boundary segregations of precipitate carbides of the MC type, which affect the properties of this grade of steel.

Figure 3.40 is an electronic microphotograph of a deformed specimen of copper-aluminium alloy, showing microscopic twins, plane accumulations of dislocations, and packing defects. This microphotograph was made by the method of 'transmitted-light' examination of thin foils. It has also been found by electron microscopy that the precipitated phase in ageing beryllium bronze segregates at grain boundaries in the form of small ellipsoids (Fig. 3.41).

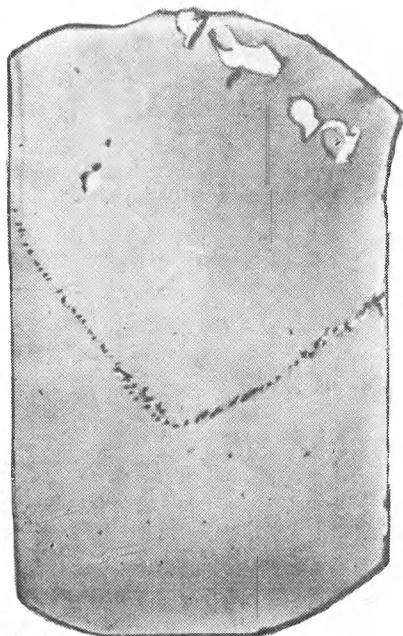


Fig. 3.41. Electron microphotograph of the structure of beryllium bronze after hardening from 800° C and ageing at 300° C during 3 hours, 12,000X

¹ This composition corresponds to the content of alloying elements in the matrix (i.e. α -solid solution) of hardened high-speed steel.

3.4. X-RAY SPECTRUM MICROSCOPY

The properties of various materials, including metals, depend not only on their structure, but also on the homogeneity of their composition.

Chemical analysis of various objects either metallic or non-metallic, in microscopic volumes ($3\text{--}10\text{ }\mu\text{m}^3$) for elements from B to U (except for oxygen and fluorine) can be made by means of an X-ray microanalyser type MAP-2 (Fig. 3.42). The basic operating principle of the apparatus is that a beam of electrons of a definite wavelength, emitted by an electron gun, interacts with microscopic volumes of the surface of an object and produces a characteristic X-ray radiation. Its wavelength is inherent only in a particular element contained in some or other local portion of the object. By measuring the intensity of the characteristic radiation and comparing it with the intensity of radiation of a reference specimen having a known content of the same element, the concentration of that element in the object being studied can be determined.

The results of analysis obtained by means of an MAP-2 microanalyser can be recorded continuously for a scanned area of $200 \times 200\text{ }\mu\text{m}^2$ of the object (the maximum size of an object is $9 \times 15 \times 8\text{ mm}$).

The microanalyser comprises an electron-optical system, object chambers, two X-ray spectrometers (a vacuum spectrometer for $\lambda=12.5\text{--}67\text{ }\text{\AA}$ and a non-vacuum spectrometer for $\lambda=0.7\text{--}1.25\text{ }\text{\AA}$),

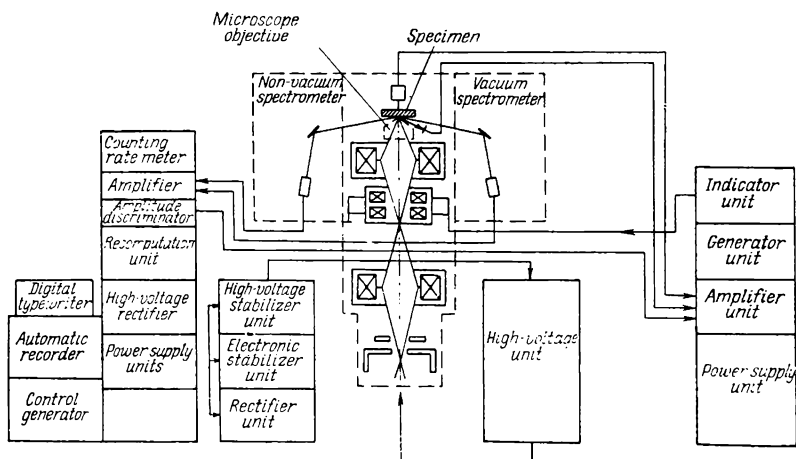


Fig. 3.42. Diagram of X-ray microanalyser type MAP-2

and a recording-counting system including an amplifier, amplitude discriminator, recomputation unit, high-voltage rectifier, power supply units, digital type-writer, automatic recorder, and control generator

Besides, the apparatus has an electron scanning device. The screens of electron-beam tubes form an image of the scanned portion of the object produced by X-rays or absorbed and reflected electrons; a concentration curve along any line of the scanned portion can also be displayed on the screen.

3.5. LABORATORY EXERCISES

In the exercises on microscopic examination (microanalysis), the students should acquaint themselves with the design and operation of the metallurgical microscope and use it to examine the most typical and simple structures of metals. The visual impressions gained by the students in microanalysis must be firmly memorized so that the metallurgical concepts of grain, eutectic, solid solution, cast and deformed structure, etc. can be easily associated with their images as seen in the microscope.

After having obtained this elementary knowledge, the students may proceed to further exercises on microanalysis of more complex alloys: industrial steels, cast irons, and non-ferrous alloys.

(a) Analysis of Typical Microstructures of Pure Metals and Binary (Simple-structure) Alloys

Before making the exercises of this section, the students must study or recall the material of the book on the objects of microanalysis, the structures of simple alloys, preparation of specimens (microsections) for microanalysis (Sec. 3.2 g, h, i), and design of metallurgical microscopes types МИМ-7 and МИМ-8 (Sec. 3.2p).

Each student must make the following five problems in the order.

Prepared microsections are supplied from a laboratory. The student should begin with the examination of microsections under a vertical microscope, such as type МИМ-7, with a relatively small magnification, of an order of 100-200X (except for Problem No. 20); this will facilitate for the beginner the task of adjusting and re-adjusting the microscope.

When making each of the problems below, the student must examine the structure under the microscope, sketch it carefully, and answer the questions.

Problems

No. 17. Examine and sketch the structures of pure antimony and commercially pure iron.

Explain how grain boundaries are revealed by microanalysis. Explain the phenomenon causing the various grains of one and the same metal to be seen differently coloured in the microscope (this phenomenon is in particular observed with pure antimony).

No. 18. Examine and sketch the structures of pure copper and brass with 30 per cent Zn after rolling and annealing.

Explain why the microscopic structure of the pure metal (copper) does not differ principally from that of the two-component alloy (brass).

What method of analysis can reveal differences in the structures of these metals?

No. 19. Examine and sketch the microstructures of two low-carbon steel specimens: after casting and after rolling.

Indicate the difference in the size of crystals between the first and the second steel. Explain how this can affect their plasticity.

No. 20. Examine and sketch the microstructures of alloys of the lead-antimony system: (a) with 13 per cent Sb and (b) with 25 per cent Sb.

The constitutional diagram of the system is shown in Fig. 4.18.

Examine the structure of the alloy with 13 per cent Sb at magnifications of 200X and 600X.¹

Explain what is represented in the microscopic image by (a) the dark structural component which is seen in both specimens; how it is formed and how many phases it is composed of; (b) the bright component seen in the second specimen (with 25 per cent Sb). Indicate the conditions for the formation of crystals of the bright component and the causes why its crystals are larger than the crystals of the dark component.

No. 21. Examine and sketch the microstructure of malleable ferritic iron as seen (a) on a non-etched microsection and (b) on an etched microsection.

Explain why a non-etched microsection suits better for determining the shape, size, and distribution of graphite inclusions.

Indicate why microanalysis of an etched microsection can additionally characterize the structure of the metallic matrix of iron.

(b) Exercises on Determining the Magnification of a Metallurgical Microscope and on Quantitative Metallography ²

Before making Problems Nos. 19-24, the students have to recall the material given in Sec. 3.2 e, f, m, n, o, p.

¹ Etching must be done in a 4-percent alcoholic solution of nitric acid.

² For colleges with an extended programme of the course.

Problems

No. 22. Using an object micrometer, determine the magnifications of the microscope for visual examination with its various objectives and eyepieces. From the results compile a table of the microscope magnifications.

No. 23. Using an object micrometer, determine the magnifications of the microscope for photography with its various objectives and eyepieces and for various extensions of its photographic camera. From the results compile a table of the microscope magnifications.

No. 24. Determine the average grain size of ferrite (α -iron) in two low-carbon steel specimens after heating to various temperatures, in particular, to 900 and 1200 °C.

The average area of grains may be calculated by the formula ¹

$$F_{av} = \frac{k^2 \sum \left(\frac{\pi D^2}{4} m \right)}{\sum m} \text{ sq } \mu\text{m}$$

where m = group frequency, i.e. the number of grains per interval of the eyepiece-micrometer scale

D = grain diameter, μm

k = spacing of one division of the eyepiece-micrometer scale, μm

Explain the causes of the growth of metal grain size during heating and name a reagent suitable for micro-etching low-carbon steel.

No. 25. Determine: (a) the degree of drawing ² of deformed copper; (b) average grain size of copper after deformation and heating to various temperatures for recrystallization. To calculate the average grain size, use the formula given in Problem No. 24.

Indicate a reagent suitable for micro-etching copper and name the factors that can affect the metal grain size during cold deformation and subsequent annealing (recrystallization).

No. 26. Using a scale (see Fig. 3.24), determine the grain size ³ of two specimens of steel specially treated to reveal grains of austenite.

The size of austenitic grains can affect the properties and behaviour of steel during heat treatment. Since austenite can exist in

¹ See Sec. 3.2e.

² Determine the degree of drawing as a ratio between the maximum and the minimum dimensions of a grain.

³ With a 100-fold magnification of the microscope.

steel at high temperatures only, special methods of heat treatment are employed to reveal its grains, such as cementation or oxidation, etc. The network of carbides or oxides formed through this treatment remains in the metal after cooling and characterizes the austenitic grain size.

Describe the conditions of etching and the method for revealing grain size, suitable for this problem, and explain how the mechanical properties of metals depend on grain size.

No. 27. Determine the grain size number of two steel specimens after special heat-treatment to reveal austenitic grains (see Problem No. 26). Use the formula $n = 2^{N+3}$, where n is the average number of grains per mm^2 of the microsection surface.

Note. The grain size number according to the scale (see Fig. 3.24) may be given by using the data presented in Sec. 3.2e.

No. 28. Etch deeply a microsection of commercial iron (low-carbon steel) by a 10-percent solution of ammonium persulphate $[(\text{NH}_4)_2\text{S}_2\text{O}_8]$.

Describe the structure observed and explain why grains of similar structure and composition have different etchability.

No. 29. Carry out microanalysis of two specimens of single-phase brass: after deforming and after recrystallization. Select a reagent for micro-etching and the required magnification which characterizes most fully the structure of the alloy.

Explain the effect of deformation on the structure of the alloy and describe the mechanism of recrystallization and how it affects the properties of the deformed metal.

No. 30. Carry out microanalysis of two specimens of a bismuth-antimony alloy with 50 per cent Bi and 50 per cent Sb (see Fig. 4.19), one of them being examined directly after solidification and the other, after being annealed at 200°C for 10 hours.

Indicate a reagent suitable for etching and select the microscope magnification that characterizes most fully the structure of the alloy.

Explain the differences in the microstructures of the two specimens and describe the nature of crystallization of alloys of this system.

No. 31. Carry out microscopic analysis of two specimens of a copper-nickel alloy with 60 per cent Cu and 40 per cent Ni, one of them being cast and the other, annealed.

Explain the differences in the microstructures of the two specimens and describe the nature of crystallization of alloys of this system. Explain the phenomenon of segregation by considering the copper-nickel constitutional diagram.

No. 32. Carry out microscopic analysis of two alloys of the copper-aluminium system: a hypoeutectoid aluminium bronze and eutectoid bronze in equilibrium (after annealing). Select a reagent suitable for micro-etching and the microscope magnification that characterizes most fully the structure of the alloys.

Using the copper-aluminium diagram (see Fig. 9.24,) describe the structure observed and determine by the amount of the eutectoid the content of aluminium in the hypoeutectoid alloy (assuming conditionally that the densities of the structural components are equal to each other).

Chapter Four

DETERMINATION OF TRANSFORMATION TEMPERATURES (CRITICAL POINTS) OF METALS

The methods used for this purpose are based on measuring the difference in enthalpy (thermal analysis) or in thermal expansion of specimens (dilatometric analysis).

4.1. THERMAL ANALYSIS

(a) Characteristics and Applications of the Method

Thermal analysis is used for determinations of the temperatures of phase transformations (critical points) of metals and other materials by determining the pattern of variation of the temperature in the course of heating and cooling.

A phase transformation, e.g. melting (or solidification), a change of the type of crystal lattice, polymorphous transformations, dissolution (or precipitation) of a phase — all can change the enthalpy (heat content) of a metal.

If a phase transformation occurs quickly at a definite temperature and the temperature derivative of enthalpy (in this case heat capacity) tends to infinity, the transformation will change the number of phases and obey the phase rule (phase transition of the first order).

If the enthalpy varies smoothly and the heat capacity changes sharply, attaining a finite value, then no new phase will be formed (second-order transition), and the phase rule is inapplicable.

As heating or cooling proceeds, the temperature varies non-uniformly owing to liberation or absorption of heat during phase transitions, so that the corresponding heating (cooling) curves will have flex points or horizontal portions.

A flex point on a curve is formed when the transformation occurs within a definite temperature interval, so that the tempe-

rates at the beginning and end of the transformation can be fixed.

Horizontal portions on curves show that the transformation occurs at a constant temperature; examples are polymorphous (eutectic and eutectoid)¹ transformations in pure metals and peritectic and peritectoid transformations in binary alloys.

The accuracy of thermal analysis depends on the thermal effect per unit mass of the substance or phase being transformed, and also on the rate of heating or cooling.

Solidification of melts or melting of solids is usually accompanied with a high thermal effect. Solid-state transformations, even those occurring at a constant temperature, produce lower thermal effects requiring more sensitive instruments and methods for their detection, in particular those based on measuring thermal expansion.

Special methods of analysis are required in cases when the transformation can only occur at high cooling rates, for instance, in the formation of martensite during hardening of steel. The thermal effect of this process is rather high (38.2 J/g), but the rate of heat removal is so large that the temperature of martensite transformation cannot practically be determined by ordinary instruments.

With non-uniform heating or cooling, additional flex points can be formed on the temperature curves; these may be erroneously taken by the metallurgist for those actually representing phase transformations.

(b) Methods of Temperature Measurement

Thermal analysis uses thermoelectric pyrometers comprising a thermocouple and a recording measuring instrument (millivoltmeter or potentiometer).

Thermocouples. In a closed circuit comprising two electrodes made of unlike metals or alloys a thermoelectromotive force E forms, its magnitude being dependent on the composition of electrodes and the difference between the temperatures of the two junctions of the circuit. The greater the temperature difference between the electrode junctions, the greater the thermoelectromotive force: $E = E_2(T_2) - E_1(T_1)$. With a constant temperature of one of the junctions (for instance that connected to the measuring instrument called the cold junction), the resulting thermoelectromotive force depends on the temperature of the second

¹ Only a ternary eutectic or a ternary eutectoid can form at constant temperatures in ternary alloys.

(hot) junction placed in, or very close to, the object being studied.

The temperature relationship for the thermoelectromotive force can be written as

$$E = at + bt^2 + ct^3 + \dots$$

where a , b , and c are coefficients depending on the composition of electrodes.

The appearing thermoelectric current flows through the hot junction from the more electronegative metal electrode to the more electropositive one. This value can be determined from the thermoelectric series of elements: Sb, Fe, Au, Cu, Ag, Zn, Pb, Pt, Bi, etc., wherein each next metal is more electronegative than the previous one.

Metals used for making thermocouple electrodes should meet the following principal requirements:

(a) a pair of unlike metals must produce a thermo-emf of an appreciable magnitude and varying smoothly within the wide temperature range being studied; this is only possible if no phase and interphase transformations occur in the metals;

(b) the thermo-emf formed should remain stable during a sufficiently long time of operation;

(c) the metals must be chemically stable under various operating conditions, in particular in the air and furnace atmospheres.

The following combinations of metals and alloys are most often used in thermocouples: platinorhodium (10 per cent Rh) — platinum (ПП1); platinorhodium (30 per cent Rh) — platinorhodium (6 per cent Rh) (ПП 30/6); chromel — alumel (XA); chromel — Copel (XK). For measuring high temperatures (up to 2400 °C), various tungsten-rhenium alloys are used, in particular, thermocouples with the electrodes made of an alloy of tungsten with 5 per cent Re and tungsten with 20 per cent Re (BP 5/20) or an alloy of tungsten with 10 per cent Re and tungsten with 20 per cent Re (BP 10 20). These thermocouples can only be used in vacuum or inert atmospheres.

Low temperatures (down to -250 °C) are measured by copper-Copel thermocouples.

The values of thermo-emf for the most common types of thermocouple are given in Table 4.1. The highest temperatures indicated in the Table are the maximum allowable under prolonged heating conditions. With short-time heating, higher temperatures (by 200-300 °C on the average) are permissible.

When selecting the type of thermocouple, one should consider the state of the medium where temperatures will be measured and the maximum temperatures possible. Thermocouples having the

Table 4.1 Thermo-emf of Various Thermocouples at Various Temperatures of Heating

Hot junction temperature, °C	Thermo-emf (mV) with the cold junction at 0 °C			
	platinorhodium-platinum (ПП-1)	chromel-alumel (XA)	chromel-Copel (XK)	platinorhodium (30% Rh)-platinorhodium (6% Rh) (ПР-30/6)
0	0	0	0	0
100	0.64	4.10	6.90	—
200	1.42	8.13	14.65	—
300	2.31	12.21	23.16	0.46
400	3.24	16.39	13.53	0.81
500	4.21	20.64	10.15	1.27
600	5.22	24.90	49.00	1.82
700	6.25	29.14	17.75	2.47
800	7.32	33.31	66.40	3.20
900	8.43	37.36	—	4.02
1000	9.57	41.31	—	4.91
1100	10.74	45.14	—	5.88
1200	11.95	—	—	6.90
1300	13.15	—	—	7.98
1400	14.37	—	—	9.11
1500	15.55	—	—	10.27
1600	16.76	—	—	11.47
1700	—	—	—	12.69
1800	—	—	—	13.93

highest and most stable thermo-emf within the given range of temperatures should be chosen.

The accuracy of temperature measurement depends on the method of manufacture of thermocouples. The hot junction should be made by welding (preferably by electro-arc welding) of two twisted wires insulated from each other by porcelain sleeves.¹ A thermocouple made in this way can be directly used for measurements.

Thermocouples for measurements in chemically aggressive media are sheathed by a protective tube made of refractory steel, quartz or porcelain.² The free ends of thermocouples are either connected directly to a measuring instrument or to compensation wires and then to the instrument.

¹ With high rates of temperature variation and small dimensions of heated or cooled specimens, the thermocouple junction must be small and have low inertia.

² Porcelain tubes should be heated and cooled slowly in the temperature interval from 300 to 600 °C.

Compensation wires are required in order to place the cold junction as far as possible from the source of heat, since any heating of this junction reduces the resulting thermo-emf of the hot junction and requires an appreciable correction which cannot be determined accurately.

The composition of compensation (extension) wires is selected (Table 4.2) according to the metal composition of the electrodes.¹

Table 4.2 Metals and Alloys for Compensation Wires

Type of thermocouple	Electrode	Composition of wire
XA	Chromel Alumel	Copper (up to 100 °C); HM alloy (Ni + 17% Cu)—up to 250 °C Constantan (up to 100 °C); MT alloy (Cu + 0.5% Ti)—up to 250 °C
XK	Chromel Copel	The same alloy as in the main electrode * Ditto *
ППП	Platinum Platinorhodium (10% Rh)	Copper ТН alloy (Cu + 0.5% Ni)
BP 5/20	Tungsten + 5% Re Tungsten + 20% Re	Copper MH2.4 alloy (Cu + 2.4% Ni)

* Wires of these alloys serve as extensions of thermocouple electrodes.

The thermo-emf formed by a thermocouple can be measured by millivoltmeters (galvanometers) or potentiometers (Fig. 4.1).

Millivoltmeters are magnetoelectric instruments based on the interaction of a field formed by a thermoelectric current flowing through a measuring winding and the magnetic field of a permanent magnet. This interaction causes the frame and winding of the instrument to turn through an angle proportional to the thermoelectric current against the action of a spring (in needle-type instruments) or the torque of an elastic suspension (in mirror galvanometers), this deviation being sensed by an optical system.

¹ At points of their connection to thermocouple electrodes, compensation wires form equal thermo-emf of opposite signs.

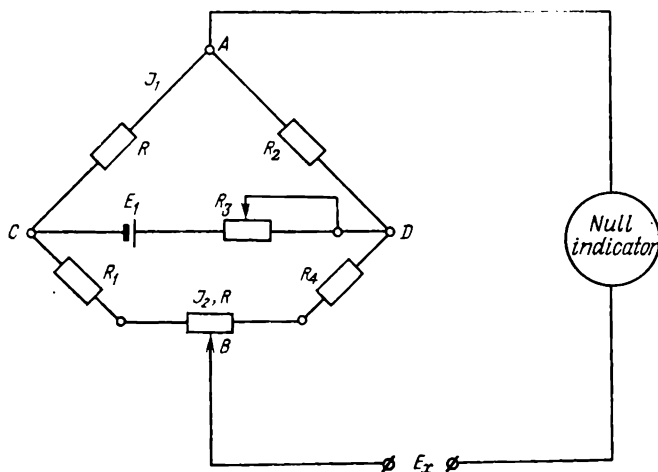


Fig. 4 1. Diagram of potentiometer

A millivoltmeter has a scale graduated in millivolt divisions or a temperature scale (degrees C), or sometimes both. The temperature scale is suitable only for certain types of thermocouple and for a constant temperature of the cold junction (0 or 20 °C). With a higher temperature of the cold junction, a correction is made by shifting correspondingly the needle of the instrument from its zero position. With a millivolt scale, a different temperature of the cold junction can also be corrected. Knowing this temperature, the corresponding variation of the thermo-emf is found from the calibration curve, and the needle (or mirror) is shifted correspondingly from its zero position.

The accuracy of an instrument also depends on variations in the resistance of the external circuit, i.e. the thermocouple and connecting wires. If this resistance changes, for instance, owing to oxidation of the thermocouple, the actual thermo-emf can be found by the formula:

$$E = E_m \frac{R_a}{R_{in}}$$

where E_m = thermo-emf as measured by the instrument
 R_{in} = initial resistance of the instrument for which its millivolt scale has been calibrated
 R_a = actual resistance

The correction for the temperature scale can be found by a similar formula:

$$T = T_m \frac{R_a}{R_{in}}$$

Standard tables for recalculation of thermo-emf values into temperatures have been compiled for the main types of thermocouple. For high-precision experiments, however, the thermocouples must be calibrated, i.e. their relationship between the thermo-emf and temperature must be found, especially for the temperature interval being studied. This is necessary because the thermo-emf of a thermocouple can change during operation owing to structural changes in the metal of the electrodes, oxidation, etc. Finally, the characteristics of the instrument can undergo certain changes.

A calibration curve is constructed from the melting temperature (solidification) of pure substances—metals or salts¹ whose melting or solidification temperatures are constant (Table 4.3).

Table 4.3. Substances Used for Calibration of Thermocouples *

Substance	Melting or solidification point, °C	Material of crucible	Protective coating
Mercury	-38.39	Glass	None
Water	0	Any	None
50.5% KNO ₃ + 49.5% NaNO ₃	218	Stainless steel	None
Tin	231.85	Graphite, porcelain	Graphite, carbon
Lead	327.30	Same	Same
Zinc	419.40	Same	Same
35% BaCl ₂ + 65% CaCl ₂	600	Stainless steel	None
Antimony	630	Graphite, porcelain	Graphite, carbon
NaCl	801	Stainless steel	None
BaCl ₂	940	Same	None
Silver	960	Graphite, porcelain	Graphite, carbon
Gold	1063	Same	Same
CaSO ₄	1360	Platinum	None

* When using salts, calibration is made by their melting points.

A substance is melted in a crucible and the thermocouple to be calibrated is immersed in the melt; the temperature indicated by the thermocouple during cooling of the substance is recorded, and the temperature arrest (horizontal portion) is found on the curve. The thermo-emf measured at this temperature corresponds to the solidification (melting) point of the substance.

¹ The thermal effects of solidification of salts are appreciably lower than those of metals.

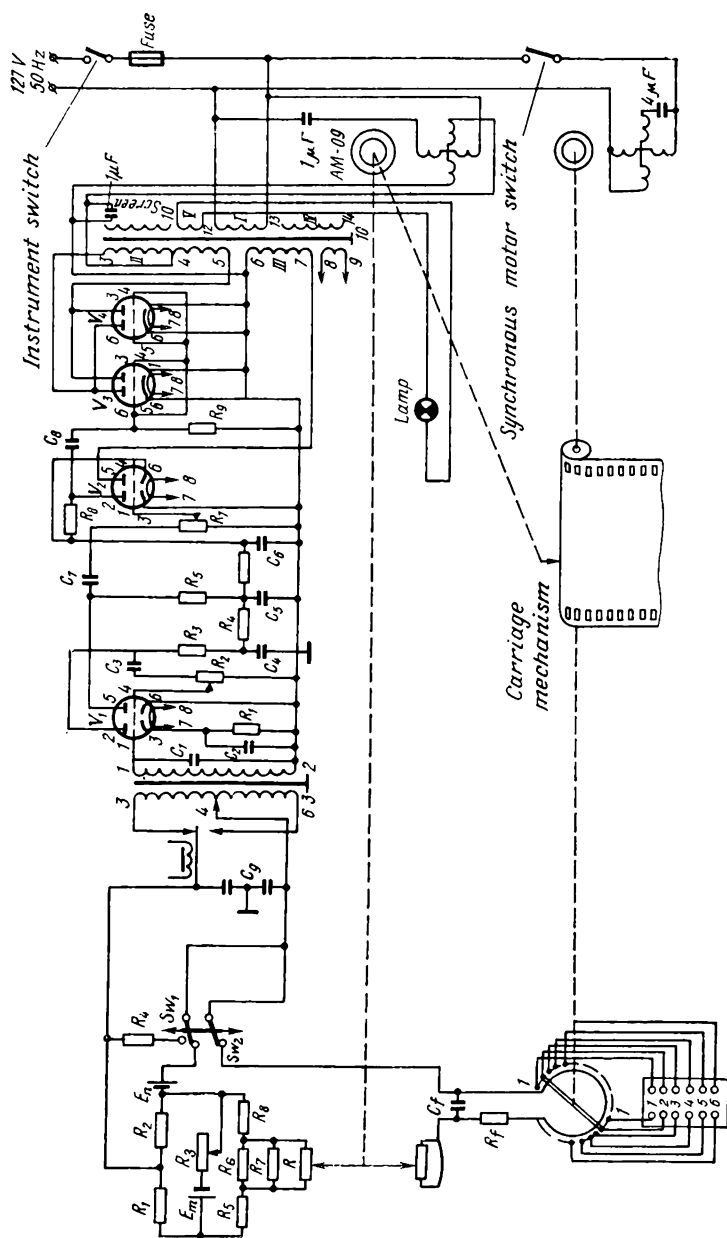


Fig. 4.2. Principal diagram of multi-point potentiometer type ЭИП-09

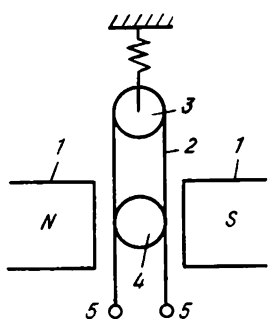


Fig. 4.3. Diagram of the stub of permanent-magnet oscillograph

1—permanent magnet; 2—stub filament; 3—pulley; 4—mirror; 5—terminals

Another calibration method is to use a calibrated standard, i.e. a precisely calibrated thermocouple. For this purpose, the hot junctions of the two thermocouples are placed close to each other into a heated block made of copper, stainless steel or nichrome.

In potentiometers (see Fig. 4.1), the measured thermo-emf is compensated by a known emf produced by a standard or auxiliary current source (E_{st}). The accuracy of potentiometer measurements is quite high, 0.01-0.001 mV. The electrical resistance of the whole circuit of the thermocouple is inessential in this case. Potentiometer measurements, however, require an appreciable time to compensate the thermo-emf being measured. The

time for passing over the whole scale is a few seconds, even with the use of automatic recording potentiometers, such as the type ЭПП09 or ЭПП09М.

An automatic potentiometer (Fig. 4.2) can record simultaneously the measurements of six thermocouples. It comprises three circuits: a measuring circuit, power supply circuit, and signalling circuit. The measuring circuit is a bridge circuit with a thermocouple and an electronic amplifier connected into one of the diagonals. The bridge circuit (see Fig. 4.1) has two arms: the working arm (resistors R , R_1 , R_3 , and R_4) and an auxiliary arm (resistors R and R_2).¹ The free ends of thermocouples and the copper resistor (R) are thermostabilized, so that their temperature is always almost the same. A change in the resistance of resistor R_3 indicates that a variation in the temperature has caused an additional voltage of some or other sign at the apex of the bridge (see AB in Fig. 4.1), which compensates the change in the thermo-emf caused by the change in temperature of the free end of the thermocouple.

The operating principle of an automatic potentiometer is as follows. The thermo-emf of the thermocouple is fed via an electronic amplifier, which serves as a zero galvanometer (see Fig. 4.1), to the apexes of the measuring bridge. When the change in the emf is greater than the sensitivity of the amplifier, the latter is fed with a signal in the form of a certain d.c. voltage which is converted into an a.c. voltage ($f = 50$ Hz). This voltage

¹ Resistor R_2 serves to adjust the current.

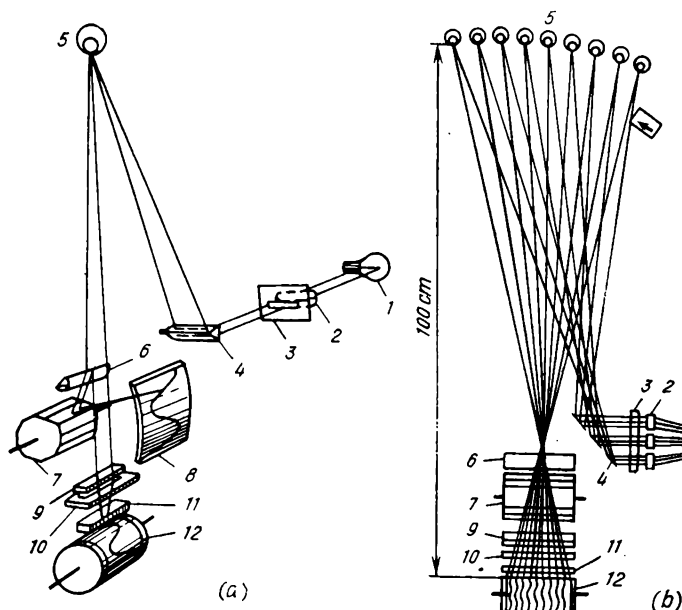


Fig. 4.4. Diagram of nine-channel oscillograph

(a) schematic diagram; (b) paths of light beams in the oscillograph; 1—light source; 2—lens; 3—diaphragm; 4—prism; 5—stub; 6—prism; 7—drum; 8—screen; 9—lens; 10—diaphragm; 11—lens; 12—drum cassette

is then amplified and fed to an asynchronous motor (type ПД-09) which continues to rotate as long as the signal caused by the non-equilibrium of the system is supplied. The direction of rotation of the motor is decided by the sign of the signal. The shaft of the motor is linked with a lever which moves the contact roller of the slide rheostat towards the equilibrium of the system. The motor is connected with a printing carriage carrying an indicator which moves over the temperature scale and indicates the temperature of the hot junction. At the moment of equilibrium, the printing carriage prints the temperature and the number of the thermocouple on the tracing tape.

Mirror- and needle-type millivoltmeters possess appreciable inertia, and, therefore, they cannot be used for measuring quickly varying temperatures, for instance, during high-frequency heating or hardening of metals. In such cases permanent-magnet (vibrator) and electron-beam (cathode) oscillographs are used.

In a permanent-magnet oscillograph, the recording unit is made as an elastically stretched metallic loop (vibrator) fed with the voltage (or emf) to be measured. Owing to the interaction of its

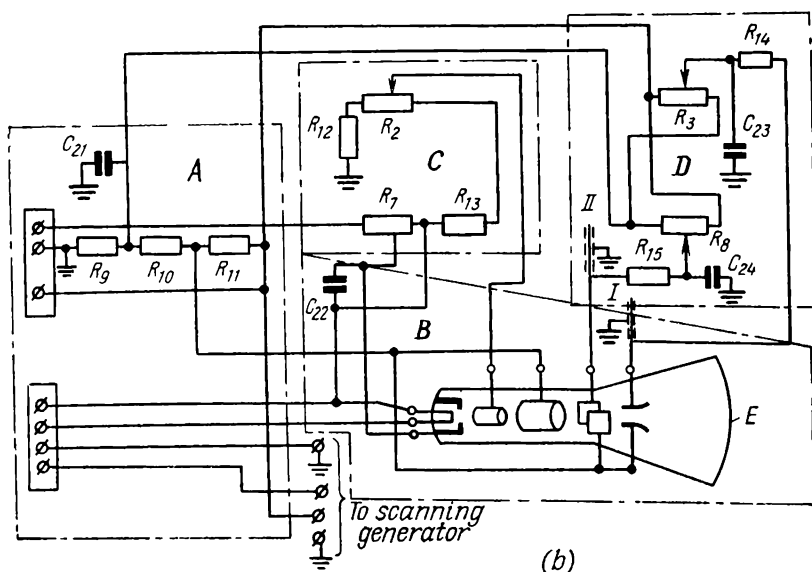
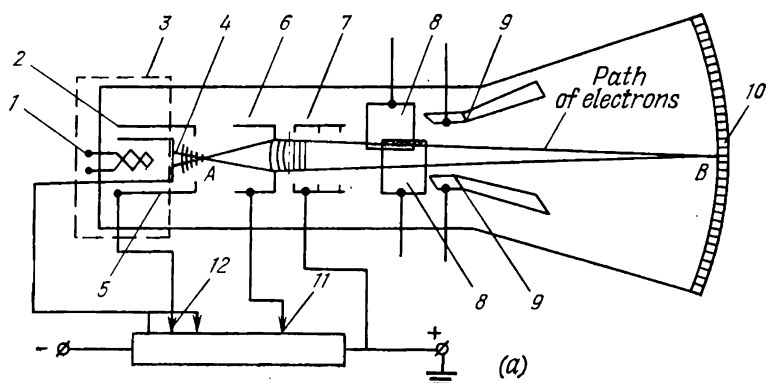


Fig. 4.5. Diagram of electron-beam oscillograph

(a) electron-beam tube; 1—heater; 2—cathode; 3—electron gun (dotted rectangle); 4—imitating surface; 5—focusing cylinder; 6—first (focusing) anode; 7—second anode; 8 and 9—horizontal and vertical deflecting plates supplied with the voltage being measured; 10—fluorescent screen; 11—focus control; 12—brightness control; (b) principal diagram of an oscillograph: A—power supply unit; B—tube unit; C—focus-brightness unit; D—beam-deflecting unit; E—tube; I and II—to scanning generator; R_2 —50-kohm potentiometer; R_3 —50-kohm potentiometer; R_7 —18-kohm potentiometer; R_8 —50-kohm potentiometer; R_9 —15-kohm resistor; R_{10} —30-kohm resistor; R_{11} —30-kohm resistor; R_{12} —220-kohm resistor; R_{13} —100-kohm resistor; R_{14} —1.5-Mohm resistor; R_{15} —10-Mohm resistor; C_2 —10- μ F electrolytic capacitor; C_{22} —1- μ F capacitor; C_{23} —0.5- μ F capacitor; C_{24} —0.5- μ F capacitor

magnetic field with the field formed by a powerful permanent magnet, the loop turns through an angle depending on the magnitude of thermocurrent (or emf). This angle of rotation is fixed by an optical method (Fig. 4.3). The response time of this instrument is only 5 ms. By using vibrators with different electrical and mechanical (natural frequency) parameters, the range of measured currents (or emfs) and their frequencies can be varied.

In some types of oscillograph, a number of vibrators are employed, which makes it possible to record simultaneously several different processes (Fig. 4.4).

Electron-beam (cathode-ray) oscillographs are used to record very quick variations in temperature during heating or cooling and also quick variations of the non-electric parameters of processes; this is done by measuring variations in the electric parameters of various sensors, resistive, inductive or capacitive type, etc. A change in the emf in an oscillograph causes a vertical shift of the electron current on the luminescent screen (Fig. 4.5). These instruments can record processes occurring in a very short time, less than 10^{-8} - 10^{-9} s.

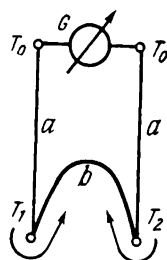


Fig. 4.6. Diagram of differential thermocouple

(a) electrodes of the same material; (b) electrode of a different material; T_1 and T_2 — hot junctions

4.2. DIFFERENTIAL THERMAL ANALYSIS

Differential analysis is used for determining the temperatures of transformations accompanied with the evolution (or absorption) or a small amount of heat, for instance, in studies of the transformations in the solid state or in determining the solidification points of very small amounts of substances. With a low thermal effect of transformation, the accuracy of thermal analysis is low and greatly affected by various non-uniformities of heating and cooling.

Differential thermal analysis can ensure high accuracy and, as will be shown in Figs. 4.6 and 4.7, is capable of distinguishing between random temperature variations and those caused by actual phase transformations.

During the differential thermal analysis the substance being studied and a reference substance are heated simultaneously in both the solid and molten state. A temperature difference forms between the tested specimen and reference substance at the moment of transformation and is measured by a differential thermocouple connected to a sensitive instrument.

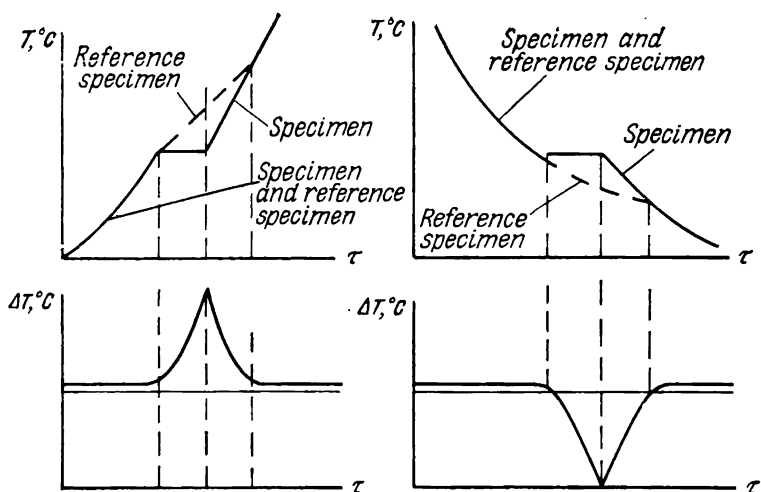


Fig. 4.7 Variations in temperature (T , °C) and temperature difference (ΔT , °C) during heating and cooling of a reference substance and a specimen undergoing a phase transformation

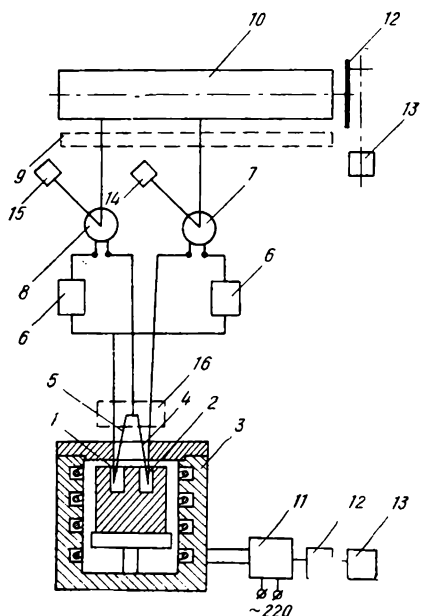


Fig. 4.8. Diagram of Kurnakov's pyrometer

1—specimen; 2—reference specimen; 3—electric furnace; 4—differential thermocouple; 5—ordinary thermocouple; 6—resistor box; 7 and 8—mirror galvanometers; 9—lens; 10—photographic paper drum; 11—auto-transformer; 12—reducer; 13—electric motor; 14 and 15—galvanometer illuminators; 15—thermal stabilization of cold junctions of thermocouples

A differential thermocouple has two hot junctions connected by a common electrode (Fig. 4.6). With an equal temperature of both junctions, the difference of the thermo-emf is zero. At the moment of transformation, the temperatures of the specimen and reference substance become unlike (Fig. 4.7) due to the evolution or absorption of heat, and therefore, the resulting thermo-emf of the differential thermocouple is other than zero. The absolute temperature is measured simultaneously with the temperature difference, either by means of a usual thermocouple or from the corresponding electrodes of the differential thermocouple by using the diagram shown in Fig. 4.8 (Kurnakov's pyrometer).

Figure 4.9 shows the results of differential thermal analysis of the transformations in carbon steel Grade V8A. As is seen, the temperature of the critical point A_1 is determined more distinctly on the differential curve than on the curve of temperature variations; thus the accuracy of the differential thermal analysis is higher than that of the common thermal analysis.

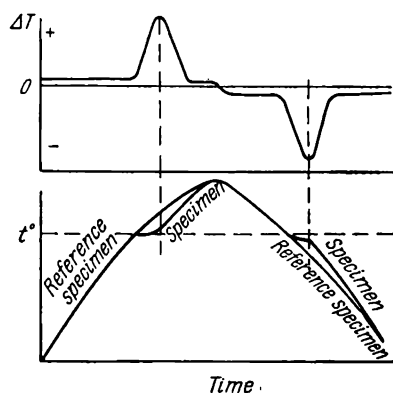


Fig. 4.9. Variations in temperature (T , $^{\circ}\text{C}$) and temperature difference (ΔT , $^{\circ}\text{C}$) measured by a differential thermocouple when determining the critical point of steel V8A by differential thermal method

4.3. DILATOMETRIC ANALYSIS

Dilatometric analysis consists in measuring variations of the length of specimens during heating (cooling) or under isothermal conditions. It is employed for the determination of transformation points in solid substances.

With no phase transformations occurring in a metal or alloy, its length (and volume) varies smoothly; if, however, a phase transformation takes place, the length (or volume) will change stepwise.¹

¹ Length variations characterize volume changes during isotropic expansion or contraction of specimens of either cubic-lattice metals (mono- and polycrystals) or metals (polycrystals) of a different type of lattice but having no texture. In monocrystals of such metals, linear changes cannot characterize volume variations because of the anisotropy of the linear expansion.

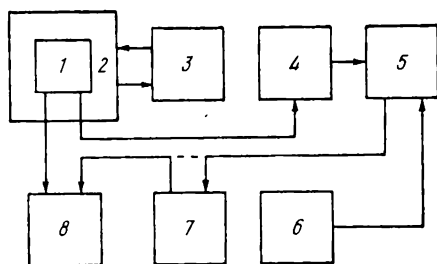


Fig. 4.10. Functional diagram of automatic dilatometer type АД-3

1—specimen; 2—thermostat; 3—heat control unit; 4—displacement-measuring unit with electric converter; 5—summing circuit; 6—correcting unit; 7—functional voltage converter; 8—two-coordinate electron potentiometer

By measuring time variations in the length (or volume) under isothermal conditions the kinetics of transformations can be determined, since the degree of these transformations in time is proportional to the variations in the phase (or volume).

The advantage of dilatometric analysis, as compared with thermal analysis, is that the results obtained are independent

of the rate of cooling or heating (provided that the type of transformation is not changed).

The variations in length can be measured by various methods and instruments of the mechanical, optical or electrical type. In mechanical instruments, the linear displacement is recorded by means of an indicator or pen on recording paper attached to a rotating drum. In optical instruments, measurements are made by various comparators, cathetometers or microscopes or by using an optical lever which transforms the linear motion of an expanding specimen into rotary motion recorded by the movement of a light spot on a scale. There are a number of designs of dilatometers in which the linear motion of the specimen is transformed into an electric signal, for instance, by means of photoelectric or electronic devices and various sensors of the tensometric, inductive or capacitive type. Such transformers are used in programme-controlled automatic dilatometers and special dilatometers used for studying high-speed processes during rapid heating or cooling. Figure 4.10 shows the functional diagram of an automatic dilatometer type АД-3 developed at the Institute of Physics of Metals of the Ukrainian Academy of Sciences.

Dilatometers are usually provided with means for controlling the temperature of specimens and sometimes with devices for programming the conditions of heating (cooling) or isothermal holding.

Temperature measurements in dilatometers are done by thermocouples or often by dilatometric pyrometers, i.e. reference specimens having a smooth curve of linear expansion on heating or

cooling.¹ Therefore, the temperature of a reference specimen can be determined by measuring its expansion (or contraction). The advantages of such dilatometers are their non-inertiality and the more accurate determination of the temperature of the specimen being heated under the same conditions as the reference one, since the temperature averaged along the whole length of the specimen, rather than the temperature fixed at a point, is being measured.

Dilatometric pyrometers (or reference specimens) are indispensable in what are called differential dilatometers which simultaneously determine the expansion of a reference specimen and the difference between the expansions of the reference specimen and the specimen being studied. Differential dilatometers have found wide use.

Ordinary dilatometers which determine only the expansion of a specimen are used more seldom.

(a) Differential Dilatometers

Chevenard's dilatometer. The device comprises a head (dilatometer proper), a heating furnace (or cryostat for cooling) and a recorder (Fig. 4.11).

The head contains two quartz tubes 1 and 2, each of them being closed at one end and welded into spacer 3 attached by screws 4 and 5 to a metal support. Reference specimen 6 is introduced into the upper tube, and specimen 7 to be studied, into the lower one, both specimens being in the form of rods 4-5 mm in diameter and 50 mm long with one end pointed.

The pointed ends of both specimens abut the sealed end of each quartz tube, their other ends abutting the ends of quartz rods 8 and 9. The latter are connected via pistons 10 and 11 with steel rods 18 and 19, and their motion is thus transmitted to optical lever 15 having three sharp projections (supports) 12, 13, and 14 located at the corners of a right triangle. Steel springs are placed over the steel rods, their ends abutting the pistons and the wall of the head. On elongation of the specimens the springs are compressed, while on contraction of the specimens the elastic force of the springs retains a rigid connection between the specimen (or reference specimen) and the quartz and steel rods.

Points 12 and 13 of the optical lever abut the recesses made in the steel rods, and point (support) 14 abuts the recess in

¹ Reference specimens are made of Pyros alloy (82 per cent Ni, 7 per cent Cr, 5 per cent W, 3 per cent Mn, and 3 per cent Fe) whose linear expansion varies smoothly from 12.58×10^{-6} to 21.24×10^{-6} 1/degree C within the temperature range of from 0 to 1000 °C.

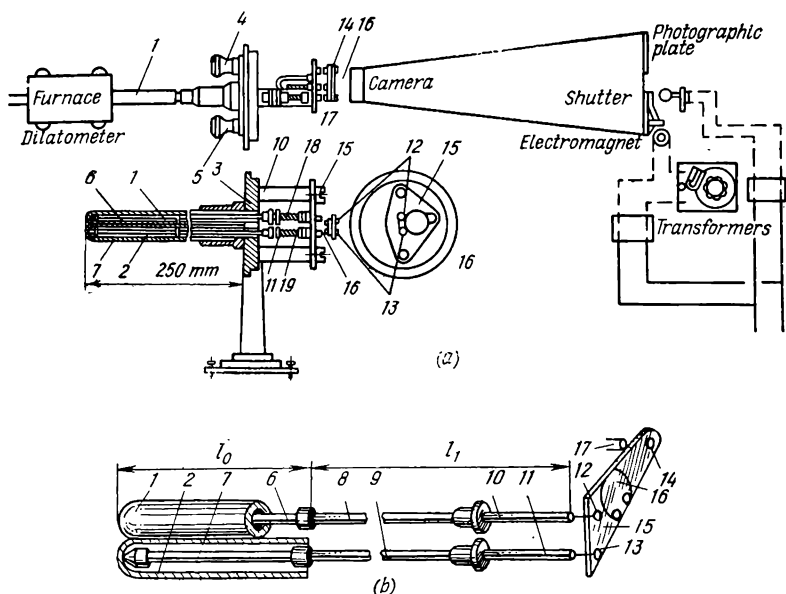


Fig. 4.11. Chevenard's dilatometer
(a) schematic diagram; (b) measuring head

fixed support 17. Before starting the test, a photographic camera is placed near mirror 16. The motion of a specimen causes the optical lever to turn and, therefore, changes the path of a reflected light beam directed by the lamp and either fixed visually on the ground glass of the camera or recorded on a photographic plate.

The following motions of the mirror and respectively of the light spot are possible on the ground glass:

(a) with a simultaneous and equal displacement of the steel rods acting on supports 12 and 13; mirror 16 then turns about axis OY , and the light spot moves along axis OX (Fig. 4.12);

(b) with support 12 being only moved (on expansion of the specimen); optical lever 16 then turns about horizontal axis OX , and the light spot moves along vertical line OB ;

(c) with support 13 being only moved (on expansion of the reference specimen); optical lever 15 then turns about the axis passing through projections 13 and 14, and the light spot moves along line OA ;

(d) when supports 12 and 13 move simultaneously but differently; with the simultaneous motion of the specimen and refe-

Fig. 4.12. Scheme of motion of a light spot on the screen of a differential dilatometer

The motion of the light spot Δx relative to axis OX (see Fig. 4.12) is proportional to the difference in the expansions of the reference specimen and the quartz tube (on the length of the reference specimen), i.e.

$$\Delta x = k_1 l_0 (\Delta_{ref} - \Delta_{qu})$$

$(\Delta_{ref} - \Delta_{qu})$ = difference of relative expansions of the reference specimen and quartz tube (on equal lengths)

$$\Delta y = k_2 l_0 (\Delta_{ref} - \Delta_{qu})$$
$$\tan \varphi = \frac{\Delta y}{\Delta x} = \frac{k_2 l_0 (\Delta_{ref} - \Delta_{qu})}{k_1 l_0 (\Delta_{ref} - \Delta_{qu})} = \frac{k_2}{k_1}$$

Hence, having measured Δy and Δx on the photographic plate or ground glass, we can determine the accuracy of adjustment

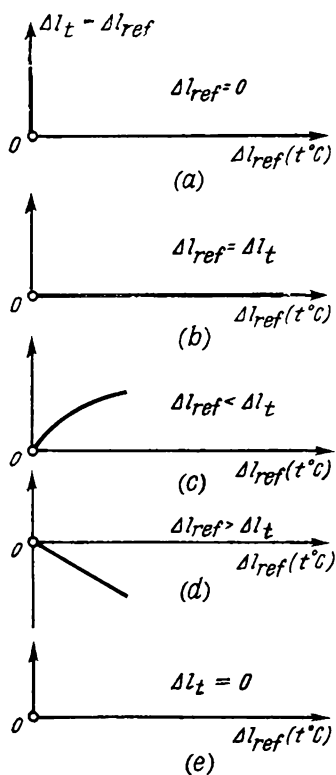


Fig. 4.13. Expansion curves of a reference specimen (Δl_{ref}) and specimen (Δl_t)

of the dilatometer, since the magnitude of $\tan \varphi$ is often given in the instrument certificate.

By decoding the dilatometric curves, we can determine the temperatures corresponding to some or other variations in these curves. The motion of the light spot along axis OY depends on the expansion of the reference specimen, which is usually known for various temperatures, and on the expansion of the specimen being tested, which varies depending on the composition and treatment of the latter, i.e.

$$\Delta y'' = \Delta y - \Delta y'$$

where

$$\Delta y' = k_2 l_0 (\Delta t - \Delta_{qu})$$

Hence

$$\Delta y'' = k_2 l_0 (\Delta_{ref} - \Delta t)$$

The motion of the light spot along axis OY cannot therefore be calibrated in temperatures, since both the specimen and the reference specimen are simultaneously heated in the dilatometer. Only axis OX can be calibrated in temperatures, as the motion of the light spot along this axis is determined only by the expansion of the reference specimen. The OX axis can be calibrated by various techniques. One of them consists in marking a number of points corresponding to heating to a definite temperature on the dilatometric curve, this heating being controlled by a thermocouple whose hot junction is placed in the direct vicinity of the reference specimen. These points are then transferred to axis OX , and by measuring Δx and determining $(\Delta_{ref} - \Delta_{qu})$ by the equation $\Delta_{ref} - \Delta_{qu} = 1.21 \times 10^{-5} t + 0.525 \times 10^{-8} t^2$ or from Table 4.4, the values of k_1 for the selected temperatures are calculated.¹

¹ Knowing k_1 and $\tan \varphi$, we can find k_2 , which is needed in calculations of expansion coefficients.

Table 4.4. Values of Δ_{ref} and Expansion Coefficients for Various Temperatures

Temperature, °C	Δ_{ref}	$\Delta_{ref} - \Delta_{qu}$	Expansion coefficient of reference specimen at the given temperature, $\alpha \times 10^6$
0	0	0	12.57
50	0.644×10^{-3}	0.617×10^{-3}	13.19
100	1.319×10^{-3}	1.264×10^{-3}	13.73
200	2.740×10^{-3}	2.630×10^{-3}	14.69

Knowing k_1 and having measured Δx for any point on the dilatometric curve, we can calculate $(\Delta_{ref} - \Delta_{qu})$ and find the corresponding temperature from a table or graph. The temperature values obtained are used to calibrate axis OX , after which the temperature for any point on the dilatometric curve can be found by projecting it onto axis OX . This calibration becomes unnecessary if the instrument is supplied with a special rule on which its temperature scale is plotted. To determine the temperature, we then only have to project the point of interest on the dilatometric curve onto axis OX , and, by applying the rule, to find the temperature.

In some cases the dilatometer may be provided with a calibration temperature scale constructed for the given instrument and a given reference specimen (pyros) and usually plotted on the ground glass of the instrument. By applying the negative obtained from the study and the dilatometric record onto the ground glass, we can immediately determine the critical points.

When the reference specimen is replaced (owing to its wear or other causes), a new calibration curve should be found experimentally.

A different technique is more often used to determine the heating temperature. A thermocouple is placed in the dilatometer furnace between the quartz tubes. At definite indicated temperatures (for instance, 100, 200, 300, 400 °C, etc.) a narrow slit is opened in the camera shutter, so that the points or strokes corresponding to these temperatures are exposed on a photographic plate.

The universal dilatometer type ДКМ. The apparatus (Fig. 4.14) can operate either by the ordinary method, when the expansion curve of a specimen is fixed in time (including isothermal conditions) or by the differential method, when the difference between the expansions of the specimen and reference specimen as a func-

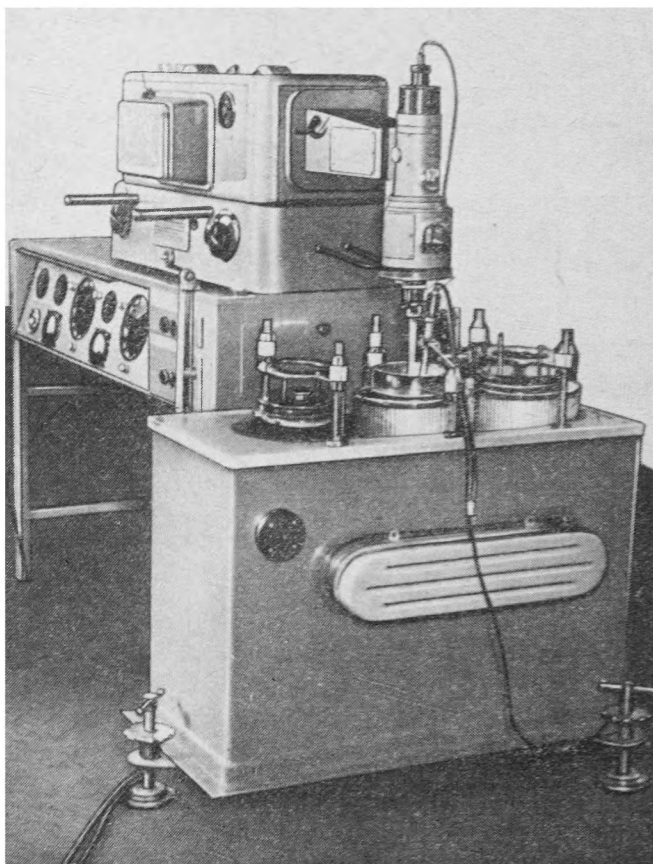


Fig. 4.14. General view of ДКМ dilatometer

tion of temperature is fixed. The optical magnification of the instrument may be 100, 200 or 400.

The apparatus comprises a dilatometer proper, heating furnaces with mechanisms for their moving and a control panel.

When operating by the ordinary method (Fig. 4.15), the expansion (s) of the specimen causes plane mirror a to turn about axis b in the direction of arrow MN from position I to position II .

The light beam directed onto mirror a reflects from concave mirror d which serves as an objective. The reflected light spot (see direction II) moves vertically upwards and traces a curve

on moving photographic paper. Thus the expansion of the specimen is recorded as a function of time.

When operating by the differential method, mirror *a* turns owing to the expansion of both the reference specimen *c* and specimen *s*, and the light beam directed onto this mirror is reflected onto mirror *d* which also turns due to the expansion of the reference specimen. Thus, the light spot is shifted vertically on the photographic paper in accordance with the difference between the expansion of the reference specimen and that of the specimen and is additionally shifted in the horizontal direction owing to the expansion of the reference specimen and proportional to its temperature.

A more detailed diagram of optical recording of the expansion of a specimen is shown in Fig. 4.16. The motion of carriage 15 varies the positions of three contacting rods 14*a*, 14*b*, 14*c* and changes the magnification of the system to 400X, 200X or 100X, respectively.

Figure 4.17 (*a* and *b*) shows dilatograms obtained by the ordinary method, and Fig. 4.17 (*c* and *d*), those obtained by the differential method. As is seen, the differential method is more sensitive and accurately determines the critical points.

For a specimen of steel Grade Y8, the curve shows a smooth initial expansion up to the critical point *A_{c1}*, after which contraction is observed owing to the formation of austenite, and the curve droops. With further increase in temperature, the specimen expands strongly owing to the higher expansion coefficient of austenite, and the curve rises again.

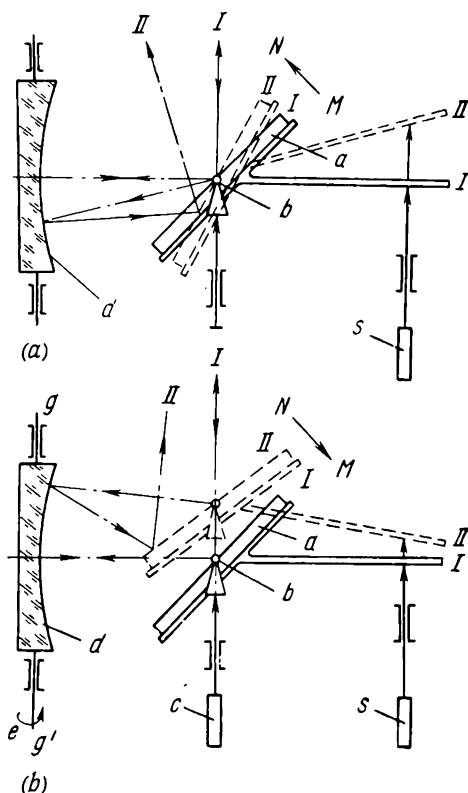


Fig. 4.15. Diagram of movements of mirrors and light spot in the ordinary method (*a*) and differential method (*b*)

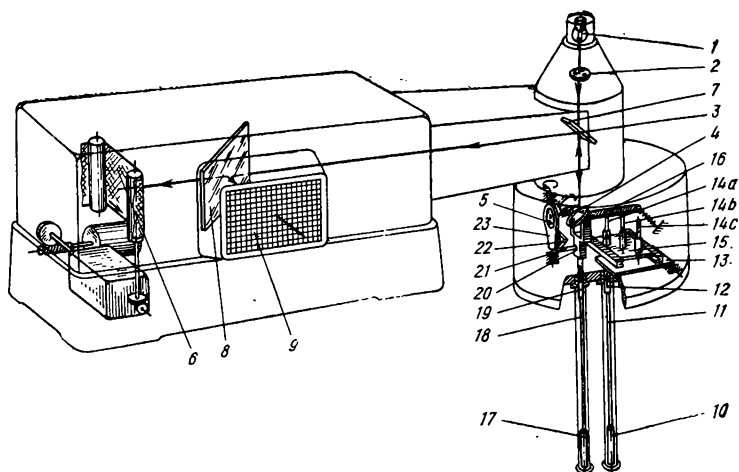


Fig. 4.16. Optical diagram of DKM dilatometer

1—light source; 2—condenser; 3—diaphragm; 4—plane mirror; 5—concave mirror (objective); 6—photographic paper; 7—mirror; 8—semi-transparent mirror; 9—screen; 10—specimen; 11—quartz rod; 12—pusher; 13—plate lever; 14a, b, and c—rods; 15—carriage; 16—lever; 17—reference specimen; 18—quartz rod; 19—pusher; 20—frame; 21—pin; 22—inclined plane; 23—frame

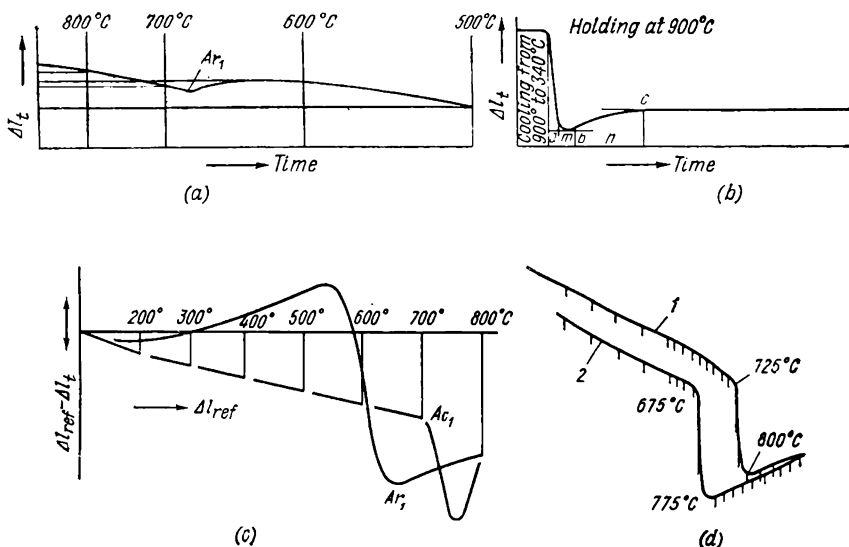


Fig. 4.17. Dilatograms of steel

(a) steel Y8 heated in furnace to 800°C (ordinary method, DKM dilatometer); (b) steel Y8 hardened from 800°C with water quenching (ordinary method, DKM dilatometer); (c) steel Y8 heated in furnace and cooled in air (differential method, DKM dilatometer); (d) steel with 0.5% C heated and cooled in furnace (differential method, Chevenard's dilatometer)

With hypoeutectoid steel, the volume of a specimen continues to decrease after passing through the critical point Ac_1 (notwithstanding the higher expansion of austenite); this occurs up to point Ac_3 after which the curve rises with higher temperatures of heating.

By comparing the critical points obtained on heating and cooling, it can be seen that they have different positions, i.e. temperature hysteresis takes place. For steel Grade V8, the critical point Ac_1 is 710°C , while point Ar_1 obtained through cooling in air is 640°C (Fig. 4.17c). For steel with 0.5 per cent C, points Ac_1 and Ac_3 are respectively 725 and 800°C , and points Ar_3 and Ar_1 obtained when cooling in the furnace are respectively 775 and 675°C (Fig. 4.17d).

When the critical points coincide with the temperature marks on a dilatometric curve, they can be determined directly without additional construction. When, however, there is no coincidence and the critical points are located between temperature marks, these points and marks must be projected onto the horizontal axis. Assuming that the temperature varies uniformly between two neighbouring marks, the temperature corresponding to a critical point is found by measuring the distance between the corresponding neighbouring marks (on the horizontal axis) and the distance between one of the marks and the critical point.

4.4. LABORATORY EXERCISES ON THERMAL ANALYSIS

These exercises include problems on the determination of: (a) crystallization temperatures when cooling molten alloys; (b) temperatures of solid-state transformations of alloys by the differential method (Kurnakov's method).

Determination of crystallization temperatures. To make these exercises, the student should recall the material given in Secs. 4.1 and 4.2. A crucible made of stainless steel, porcelain or quartz is used in the work. 150-200 g of the alloy to be tested is placed in the crucible (with a smaller amount of the metal, the critical points on the cooling curve may be not distinct enough). To avoid metal contamination different crucibles should be employed for each type of alloy. The surface of the molten metal should be covered with charcoal powder to prevent oxidation; the crucible is then to be placed under a draught hood. The metal is melted by heating it somewhat above its melting point. In the problems given below (Nos. 33-43), light-melting alloys possessing an appreciably high thermal effect are used for convenience. After

melting, the melt is to be stirred with a porcelain or graphite stick, and a thermocouple is immersed into it; the hot junction of the thermocouple should be protected against the direct action of the metal by placing it in a porcelain, quartz or stainless-steel tube with a closed end. The thermocouple is connected to a millivoltmeter (before starting the work, the thermocouple and millivoltmeter are calibrated in the laboratory and a calibration curve is constructed if necessary); higher accuracy can be achieved by using a potentiometer.

After that the crucible is closed by a refractory lid or a layer of asbestos, and the furnace is switched off and left to cool. If cooling occurs too rapidly, a lower rate can be established by reducing the current supplied to the furnace, rather than by switching off the latter. The readings of the millivoltmeter are recorded from the very beginning of cooling at intervals of 30 or 60 s up to the end of the crystallization process and for 2-3 minutes until the completely solidified metal cools.

The recorded measurements are used to construct time-temperature curves or time-thermo-emf curves; in the latter case the temperatures are determined for the critical points only on the calibration curves.

The recommended practice in such laboratory work is to share the experiment among three students, one measuring time (by means of a stop watch) and informing the others in the specified intervals (every 30 or 60 s); one observing and saying aloud the millivoltmeter readings, and one recording the millivoltmeter readings and observing the crucible.

Each student then makes his own report on the work, which should include answers to the questions posed in the problem, the cooling curves, and the plotted constitutional diagram (if asked).

Problems

No. 33. Determine the transformation temperatures of the following lead-antimony alloys: (a) 13 per cent Sb and 87 per cent Pb; (b) 20 per cent Sb and 80 per cent Pb; (c) 5 per cent Sb and 95 per cent Pb.

Construct experimental cooling curves of these alloys.

Explain the form of the curves obtained and say which processes occurring in the alloys characterize the individual portions of the curves.

Construct approximately a schematic constitutional diagram of the lead-antimony system by using (a) the cooling curves obtained; (b) the data on the melting points of pure antimony and pure lead.

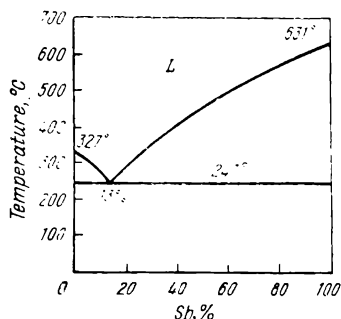


Fig. 4.18. Constitutional diagram of Pb-Sb system

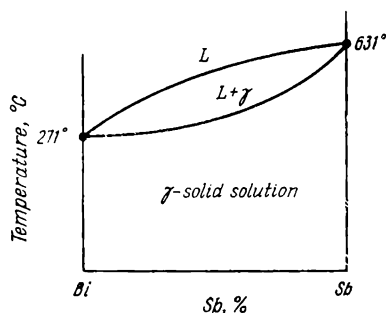


Fig. 4.19. Constitutional diagram of Bi-Sb system

No. 34. Determine the transformation temperatures and compositions of two hypoeutectic alloys of the lead-antimony system.¹

Construct experimental cooling curves of these alloys.

Explain the form of the curves obtained and say which processes occurring in the alloys characterize the individual portions of the curves.

Construct to a definite scale the constitutional diagram of the lead-antimony system (Fig. 4.18) and, using this diagram and the cooling curves obtained, indicate the approximate composition of the alloys tested.

No. 35. Determine the transformation temperatures of three alloys of the lead-antimony system: (a) 13 per cent Sb and 87 per cent Pb; (b) 35 per cent Sb and 65 per cent Pb; (c) 10 per cent Sb and 90 per cent Pb.

Construct experimental cooling curves of these alloys.

Using the constitutional diagram of the lead-antimony system (see Fig. 4.18), explain the transformations occurring at the critical temperatures determined in the work and name the phases and structures of the alloys in the solid state.

No. 36. Determine the transformation temperatures of the following alloys of the antimony-lead and bismuth-antimony systems: (a) 13 per cent Sb and 87 per cent Pb; (b) 20 per cent Sb and 80 per cent Bi.

Construct experimental cooling curves of these alloys.

Indicate: (a) the transformations occurring in these alloys at a constant temperature and the number of phases (according to the phase rule) which must participate in these transformations;

¹ Alloys with different temperatures of the beginning of crystallization are selected for the work.

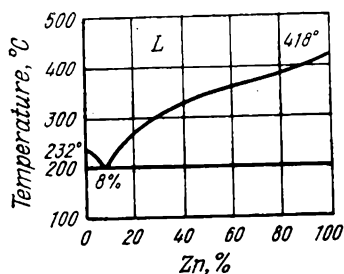


Fig. 4.20. Constitutional diagram of Sn-Zn system

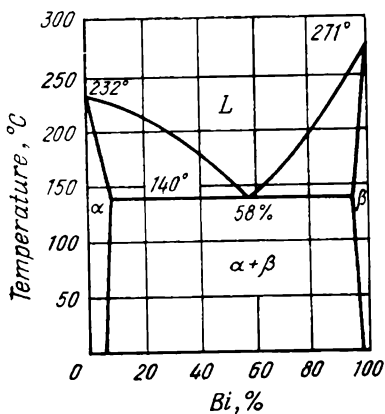


Fig. 4.21. Constitutional diagram of Sn-Bi system

(b) in which alloy the crystallization process occurs within an interval of temperatures.

No. 37. Determine the transformation temperatures and compositions of two hypoeutectic alloys of the bismuth-antimony system. Construct experimental cooling curves of these alloys.

Explain the form of the curves obtained and name the processes occurring in these alloys at the critical points.

No. 38. Determine the transformation temperatures and approximate compositions of two hypereutectic alloys of the bismuth-antimony system.

Construct experimental cooling curves of these alloys and draw to a definite scale the constitutional diagram of the bismuth-antimony system (Fig. 4.19).

No. 39. Determine the temperatures of phase transformations of three alloys of the zinc-tin system: (a) 5 per cent Zn and 95 per cent Sn; (b) 9 per cent Zn and 91 per cent Sn; (c) 20 per cent Zn and 80 per cent Sn.

Construct experimental cooling curves of these alloys.

Explain the form of the curves obtained and name the processes occurring in these alloys, which characterize the individual portions of the curves.

No. 40. Determine the transformation temperatures and approximate compositions of two hypoeutectic alloys of the tin-zinc system.

Construct experimental cooling curves of these alloys and draw to a definite scale the constitutional diagram of the tin-zinc system (Fig. 4.20).

Explain the form of the curves obtained and name the processes occurring in the alloys, which characterize the individual portions of the curves.

No. 41. Determine the transformation temperatures of two alloys of the bismuth-tin system: (a) 42 per cent Sn and 58 per cent Bi; (b) 60 per cent Sn and 40 per cent Bi.

Construct experimental cooling curves of these alloys.

Explain the form of the curves obtained and name the processes occurring in these alloys, which characterize the individual portions of the curves.

Draw to a definite scale the constitutional diagram of the bismuth-tin system (Fig. 4.21) and explain the differences between the cooling curves and crystallization processes of the alloys (a) and (b).

No. 42. Determine the transformations and compositions of two hypoeutectic alloys of the bismuth-tin system.

Construct experimental cooling curves of these alloys. Draw to a definite scale the constitutional diagram of the bismuth-tin system (see Fig. 4.21).

Explain the form of the curves obtained and name the processes occurring in the alloys, which characterize the individual portions of the curves.

No. 43. Determine the temperatures of phase transformations of two hypereutectic alloys of the tin-lead system.

Construct experimental cooling curves of these alloys and draw to a definite scale the constitutional diagram of the tin-lead system (Fig. 4.22).

Explain the form of the curves obtained and name the processes occurring in the alloys, which characterize the individual portions of the curves.

Problems on differential thermal analysis. For the determination of transformation temperatures (Problems Nos. 44-45), a steel specimen and a copper reference specimen are prepared, both in the form of half-cylinders 30 mm high and 25 mm in diameter (recommended dimensions). A blind hole is bored in the end of each specimen for placing a differential thermocouple; this is connected so as to record the absolute temperature of the steel specimen (see Fig. 4.8). An additional absolute thermocouple may also be placed in the end of the steel specimen. The

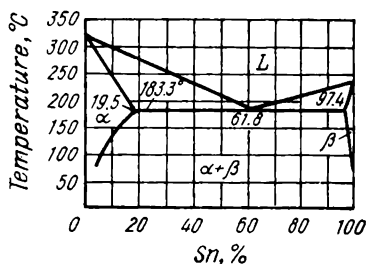


Fig. 4.22. Constitutional diagram of Pb-Sn system

bores for the differential and absolute thermocouples must be 3 mm in diameter and 10 mm deep.

These half-cylinders are insulated from one another by a porcelain or quartz spacer, they are then wrapped up with asbestos cord and placed into the furnace; this ensures their uniform heating.

Cylindrical specimens and reference specimens may also be used. They are placed into a common unit provided with corresponding bores (see Fig. 4.8). Both specimens should be insulated from the walls of the unit by means of asbestos or porcelain.

Irrespective of the shape of specimen and reference specimen and the conditions of their cooling or heating, the electrodes of the thermocouples should be carefully insulated from each other so that no short-circuiting can occur.

The readings of the differential thermocouple can be recorded by a high-sensitive mirror galvanometer (10^{-8} - 10^{-9} A) which should be capable of fixing both positive and negative temperature differences, like a null-galvanometer. The temperature of steel specimens must be registered by high-precision instruments.

The measured results are used for plotting time-temperature difference and time-temperature curves which are then combined into a single graph with a common time axis.

In experiments carried out with the use of Kurnakov's pyrometer (see Fig. 4.8), the results are recorded on photographic paper, after which they must be processed according to the available calibration scales.

The best technique is to carry out heating at a rate of 50 - $80^{\circ}\text{C}/\text{h}$ from a temperature of above 600°C up to a temperature 50 - 60°C above the supposed critical points and to perform cooling in the furnace with the current switched off down to 600°C (for carbon steels) and still lower temperatures for alloy steels (especially for air-hardening grades).

The temperature of recrystallization can only be determined by heating to 700°C (at a rate of 100 degrees/h beginning from 300°C). Rectangular composite specimens made from strips of cold-rolled steel are more suitable for determination of recrystallization temperature; the reference specimen can be made of the same steel, but only after annealing.

No. 44. Determine the phase transformation temperatures (critical points) when heating and cooling hypoeutectoid carbon steel.

What method of analysis must be employed for this problem? Explain the transformations occurring during heating and cooling and the cause of hysteresis of critical points.

No. 45. Determine the recrystallization temperature when heating cold-deformed steel.

Explain why the recrystallization temperature can be determined by thermal analysis and what is the essence of the process of recrystallization and how it affects the properties of steel.

4.5. LABORATORY EXERCISES ON DILATOMETRIC ANALYSIS

Laboratory exercises for determining the critical points are to be made by the differential method, and the kinetics of transformations is studied by the ordinary method using dilatometers of various types (ДКМ, Chevenard's, etc.).

Specimens 5 mm in diameter and 50 mm long are to be used. The end abutting the quartz tube should be pointed and the opposite end abutting the quartz rod, which transmits length variations of the specimen, should be flat.

The dilatogram determining the temperatures of phase transformations can be obtained by the photographic method, for which purpose the shutter of the illumination system of the photographic camera is opened periodically at 50 °C intervals (within the temperature region including the supposed interval of phase transformations) to produce marks on the photographic plate. Similar marks may be drawn manually by the experimenter on the curve traced by the light spot on the instrument screen.

Problems

No. 46. Determine the phase transformation temperatures (critical points) of carbon steel with 0.4 per cent C during heating and cooling.

Construct a dilatogram by the differential method.

Describe the design principle of the dilatometer employed. Explain, what peculiarities of phase transformations in steel, causing a variation in the length of a specimen, make it possible to use dilatometers for determining critical points.

No. 47. Determine the phase transformation temperatures (critical points) of alloy steel with 0.4 per cent C during heating and cooling.

Construct a dilatogram by the differential method.

Describe the design principle of the dilatometer employed. Explain what peculiarities of phase transformations in steel, causing a variation in the length of a specimen, make it possible to use dilatometers for determining critical points.

No. 48. Determine the phase transformation temperature during the tempering (heating to 560 °C and cooling) of hardened high-speed steel.

Construct a dilatogram by the differential method.

Decide when the γ -to- α transformation occurs: during heating, holding at 560 °C, or cooling.

No. 49. Determine the kinetics of transformations during tempering of hardened high-carbon steel at 200 °C.

Construct a dilatogram by the ordinary method in the coordinates: length variation against time of tempering.

Describe the design of the dilatometer employed and explain the processes occurring during low-temperature tempering.

Chapter Five

DETERMINATION OF PHASE COMPOSITION OF ALLOYS

The methods of physical analysis can in many cases be more advantageous than the structural methods discussed earlier.

In the first place, variations of physical properties, and, therefore, the kinetics of variation of phase composition of alloys, can be measured continuously and automatically; this can also be done under conditions of quickly varying external actions, for instance, rapid heating, cooling, etc.

In addition, variations of physical properties of alloys can be used for determining interphase transformations (concentrational segregation, ordering and magnetic transformations), since these properties vary on redistribution of atoms and electrons in the phases.

According to the type of temperature variation of physical properties, in particular of electrical resistance (or electric conductivity), all solids can be classed into metals, semiconductors, and dielectrics. Metals possess high electric conductivity which reduces with increasing temperature. Semiconductors have a substantially lower electric conductivity which increases with temperature. The electric conductivity of dielectrics is negligible.

The phase composition of alloys and the kinetics of its variation can be studied by methods based on determining the electrical and magnetic properties of these alloys.

5.1. METHODS FOR DETERMINING ELECTRICAL PROPERTIES (RESISTOMETRIC ANALYSIS)

The methods used most often¹ are based on determining the resistivity at sub-zero, normal, and high temperatures. Such measurements make it possible to determine:

¹ Some special methods are based on determining the Hall constant which is characterized by the potential difference appearing between two opposite surfaces of a specimen placed into a constant magnetic field and fed with an electric current that flows in a direction perpendicular to the magnetic field

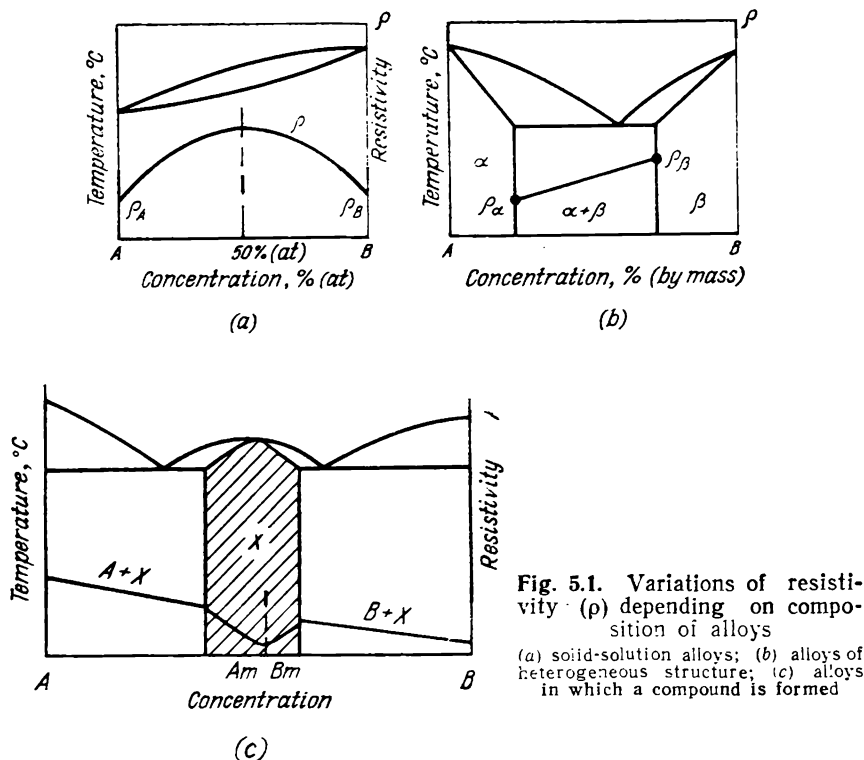


Fig. 5.1. Variations of resistivity (ρ) depending on composition of alloys

(a) solid-solution alloys; (b) alloys of heterogeneous structure; (c) alloys in which a compound is formed

(a) the structural and phase states of alloys according to the regularities of changes in the resistivity depending on the composition of these alloys. The solution of the problem proposed by N. S. Kurnakov is based on the well-known regularities expressed graphically by composition-property (electrical resistance) diagrams for different phase states: solid solutions, heterogeneous systems, intermediate phases, chemical compounds, etc. (Fig. 5.1);

(b) the kinetics of phase transformations — ordering, allotropy, decomposition of supersaturated solid solutions, tempering of hardened steel, etc. Figure 5.2 shows the curve of decomposition of a supersaturated solid solution upon hardening (Fig. 5.3). The

vector. The sign of the Hall constant, for instance, can determine the nature of current carriers in semiconductors, and the magnitude of this constant in metals can determine the number of conduction electrons, and therefore, the number of electrons participating in the formation of a chemical bond.

The properties of dielectrics are characterized by their breakdown voltage.

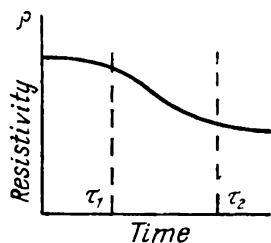


Fig. 5.2. Variations of resistivity (ρ) during tempering of a hardened alloy (supersaturated solid solution) at constant temperature

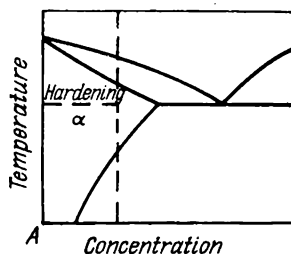


Fig. 5.3. Constitutional diagram of alloys in which the solubility of a second component reduces with decreasing temperature

data in Fig. 5.2 can also be used for determining the kinetics of the decomposition process, since $d\rho/d\tau$ is proportional to the rate of this process;

(c) the density of structural defects, especially of point defects (vacancies), and the energy of their activation.

The formula of resistivity is $\rho = RS/l$, where R is the electrical resistance, ohms; S is the cross-sectional area, mm^2 ; and l is the length of a specimen, m. Therefore, to determine the resistivity, we have to measure carefully the electrical resistance and linear dimensions of a specimen.

The accuracy of determining the electrical resistance depends on the accuracy of the measuring instruments and apparatus being used and on the temperature and its variations in the course of measurements.

The electrical resistance of a metallic conductor (as well as the resistivity) is known to depend on temperature by the relationship

$$R_t = R_0(1 + \alpha t + \beta t^2 + \gamma t^3 + \dots)$$

Since coefficients β , γ , etc. are small, the expression is usually reduced to the binomial form $R_t = R_0(1 + \alpha t)$. Hence the coefficient $\alpha_R = \frac{dR}{dt} \frac{1}{R_0}$. It is equal to $2 \times 10^{-3} \text{ } 1/^\circ\text{C}$ for copper and $4 \times 10^{-3} \text{ } 1/^\circ\text{C}$ for iron, thus a temperature change of one degree C can cause an error of respectively 0.2 or 0.4 per cent in the measured electrical resistance.

The temperature coefficient of electrical resistance (for a given temperature change) is a structure-sensitive property varying depending on composition by the same law as electric conductivity, i.e. proportional to $1/\rho$. It is then essential that the tempera-

ture coefficient α_R can be determined without measuring the linear dimensions of a specimen, and, therefore, no additional error will be introduced.

The following methods are used for measuring electrical resistance.

(a) Contact Methods

In these methods the power source forming an electric field in a specimen and the elements of the measuring circuit are in direct contact with the specimen.

The bridge methods. *The ordinary-bridge method.* This method is fairly accurate when measuring specimens having a relatively large electrical resistance (more than 10 ohms), since the resistances of the contacts and current conductors also can contribute to the value being measured.

The principal diagram of an ordinary bridge is shown in Fig. 5.4. The bridge circuit comprises three known resistances R_1 , R_2 and R_N (the reference specimen) and an unknown resistance X . To determine this resistance, the bridge is balanced by varying resistances R_1 and R_2 or the ratio R_2/R_1 , so that the potentials at points B and D are equalized, and the current through galvanometer G becomes zero. The calculation formula

$$X = R_N \frac{R_2}{R_1}$$

is derived from the theorem on bridge balance. The balance of a bridge is established when opening and closing one of the bridge diagonals cause no current in the other diagonal (the null method).

When measuring small resistances by the ordinary-bridge method, the effect of contacts and current conductors can be reduced by alternatively connecting the unknown resistance into various arms of the bridge.

The double-bridge method. This method (Fig. 5.5) provides high accuracy when measuring small resistances (from 1×10^{-6} to 1 ohm). A simple rearrangement of the double-bridge circuit (which converts it into an ordinary bridge) can make it suitable for measuring rather large resistances.

The double-bridge method is used for determining the phase compositions of alloys whose electrical resistance (in specimens) is small and varies only slightly after various processes of metal treatment.

The application of the double-bridge method for measuring low resistances and their small variations is based on the fact that the series resistances of the contacts and current conductors have

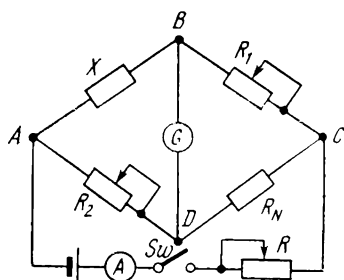


Fig. 5.4. Principal diagram of ordinary bridge

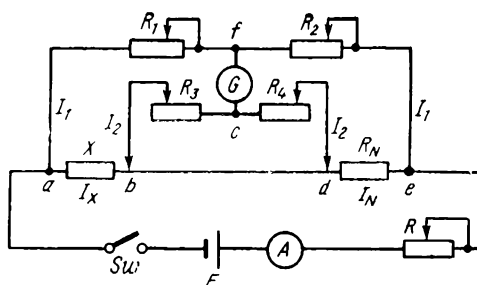


Fig. 5.5. Principal diagram of double bridge
 X —measured resistance; R_1 , R_2 , R_3 and R_4 reference resistances (a decade-type resistor box); R_N —reference resistance

no effect on the potentials at points f and c to which a null-galvanometer is connected, since the arm resistances R_1 , R_2 , R_3 , and R_4 are substantially greater (>100 ohms) than these series resistances.

Measurements are made as follows. By varying the resistance $R_1 - R_2$, $R_3 - R_4$, with a constant reference resistance R_N , the potentials at points f and c are equalized, which corresponds to the zero reading of the galvanometer (see Fig. 5.5). At this moment of balance of the bridge, the voltage drops across sections af and fe are equal respectively to the voltage drops across sections ac and ce . Hence

$$I_x X + I_2 R_3 = I_1 R_1; \quad I_x X = I_1 R_1 - I_2 R_3$$

or

$$I_N R_N + I_2 R_4 = I_1 R_2; \quad I_N R_N = I_1 R_2 - I_2 R_4$$

Since $I_x = I_N$, we divide these equations termwise and obtain

$$X = R_N \frac{I_1 R_1 - I_2 R_3}{I_1 R_2 - I_2 R_4}$$

If $R_1 = R_3$ and $R_2 = R_4$, then

$$X = R_N \frac{R_1}{R_2}$$

The equality of resistances R_2 and R_4 in the apparatus is achieved by using a resistance box in which these resistances are linked together by levers, so that a change of one of them causes an equal change of the other. Resistances R_1 and R_3 in the circuit are always equal to each other.

As follows from the formula given above, the unknown resistance is calculated in the same way as for the ordinary-bridge

circuit. Balancing is achieved by controlling the reference resistance R_N with a constant arm ratio $R_1/R_2 = R_3/R_4$, or, on the contrary, by varying the arm ratio with a constant reference resistance R_N .

Bridge circuits with constant R_N are used more often, the balancing of the circuit being done by varying resistances R_2 and R_4 , while resistances R_1 and R_3 are left unchanged.

The high accuracy of the double-bridge circuit is due to the fact that resistances R_1 , R_2 , R_3 , and R_4 are much greater than X and R_N . Thus, the current through arms afe and bcd is substantially lower than that flowing through X and R_N . This is why, small variations in the resistance of these arms, owing to a varying resistance of the contacts and current conductors, can have only a negligible effect on the potentials at points f and c .

On the contrary, even a small change in the resistance of the specimen will be sensed by the circuit. This causes the potential to change at points b and d , and, therefore, at point c , to which the null-galvanometer is connected. Thus, slight variations in resistance X change the reading of galvanometer G , so that the latter must be zeroed by varying resistances R_1 and R_2 .

To check that the bridge circuit readings are correct, a known reference resistance R_N is connected into the bridge instead of the measured unknown resistance X . The actual value X_{act} of the unknown resistance can then be found from the proportion

$$X_{act}/X' = R_N/R'_N$$

where X' = circuit reading with resistance X connected into it
 R'_N = reading with X replaced by R_N

This checking can reduce substantially the measuring error of the double-bridge circuit (approximately from 0.1-0.2 to 0.001-0.002 per cent).

For higher accuracy of double-bridge circuits, mirror-type galvanometers having the sensitivity of an order of 10^{-8} - 10^{-9} A per one degree are used, recording the deviations on an optical scale. The circuit sensitivity can also be affected by the voltage of the supply source. The current is controlled according to the magnitude of resistance of the specimen to be measured.

The potentiometric method ensures a high accuracy when measuring small resistances. In this case the voltage drop across the specimen is compared with that across the reference specimen which is connected in series with the former. The voltage drops E_D and E_N are measured by a potentiometer (see Sec. 4.1b). The sought-for resistance is then found as

$$X = R_N \frac{E_X}{E_N}$$

where R_N = resistance of the reference specimen
 E_X and E_N = voltage drops across the measured specimen and
 reference specimen, respectively

The ammeter — voltmeter method. The principal measuring circuit of this method is shown in Fig. 5.6.

To find the electrical resistance, the current in the circuit is measured by ammeter A , and the voltage drop along the length of the measured resistance X , by voltmeter V . The resistance is then found by the formula

$$X = V/I$$

where V = voltage drop, V
 I = current, A

The method is not accurate enough, since the ammeter measures both current I_1 flowing in the specimen and current i in the voltmeter. The actual resistance of the specimen is found as

$$X_{act} = \frac{V}{I - i} = \frac{V}{I - V/r_v}$$

where r_v is the resistance of voltmeter windings.

The lower the resistance of the voltmeter and the greater the resistance of the specimen, the greater the error in calculation by the formula $X = V/I$. When the resistance of the voltmeter exceeds more than 100 times that of the measured specimen, the formula $X = V/I$ is applicable, since its error is then below 1 per cent. To make this error smaller, a series resistor should be connected with the voltmeter.

The accuracy of the method depends mainly on the accuracy of the ammeter and voltmeter used in the circuit and on the transition resistances at the points of switching on of these instruments and of the resistance being measured. The latter in turn depends on the nature of the metal and the linear dimensions of the specimen.

Metal specimens are sometimes made in the form of wires or strips of small cross-sectional area and large length, in order to increase the resistance to be measured. Since $R = \rho \frac{l}{s}$, resistance R becomes greater, and the accuracy of measurements becomes higher.

The ammeter — voltmeter method has the advantage of being quite simple. In addition, measurements can be done by mirror-type instruments, with their readings recorded continuously on

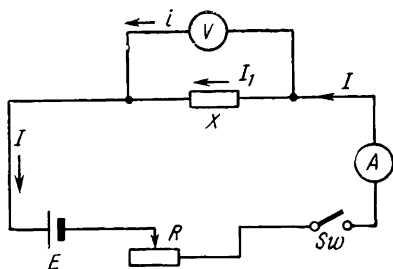


Fig. 5.6. Principal circuit of measurements by the ammeter-voltmeter method

E —current source; R —control rheostat; X —measured resistance; A —ammeter; V —voltmeter

photo-sensitive paper by means of an optical system. Thus, changes occurring in an alloy directly in the course of heat treatment, i.e. during heating or cooling, may be directly observed. The ammeter—voltmeter method with continuous recording is employed for studying the transformations in steel occurring during isothermal decomposition of austenite, tempering of martensite, etc.

In such measurements, the accuracy of the whole experiment depends mainly on the accuracy of measurement of temperature; it must therefore be measured very accurately.

(b) Contactless Methods

These methods are based on inducing an electromotive force in specimens. Their advantage is the possibility of measuring electrical resistance in hermetically sealed vessels, at high temperatures, in melts, etc.

The rotating magnetic field method. The electric conductivity of a specimen is determined by the magnitude of the moment of forces acting on the specimen, this moment being measured by the angle of twist of a suspension. The accuracy of the method is approximately 1 per cent, but this accuracy can only be achieved by introducing certain corrections for the shape, self-induction, and variation in the magnetic state of ferromagnets.

The eddy-current method. A specimen is placed into the variable magnetic field of an inductor. The field excites eddy currents in the specimen, which vary the impedance of the inductor by reducing its inductance and increasing the ohmic resistance. A change in the latter characterizes the electrical resistance of the specimen.

The method based on reflection of high-frequency oscillations. In this method mainly used for semiconductors, the electrical resistance is measured by the reflection coefficient of electromagnetic waves, which depends on the conductivity (the permittivity of the material is assumed to be constant),

5.2. METHODS FOR MEASURING MAGNETIC PROPERTIES (MAGNETIC ANALYSIS)

Phase transformations occurring in alloys cause variations of their magnetic properties: the magnetic susceptibility in paramagnetic and diamagnetic alloys and the saturation magnetization and coercive force in ferromagnetic alloys.

The phase composition of ferromagnetic alloys based on iron, nickel, cobalt or rare-earth metals (Gd, Ho, etc.) and the kinetics of transformations in them can be characterized by the saturation magnetization and coercive force (Fig. 5.7).¹

Measurement of saturation magnetization. The saturation magnetization of pure metals is a constant and cannot be changed in the course of plastic deformation or heat treatment. But the magnetization of metals gradually decreases during their heating and becomes zero at the Curie point.

During subsequent cooling, the magnetization increases, its values at each temperature being constant and independent of the process of heating or cooling.

The saturation magnetization of single-phase alloys depends on their composition, and of heterogeneous alloys (i.e. those containing both a ferromagnetic and a paramagnetic phase), on the composition and the content of the ferromagnetic phase; but it is independent of the dispersity of the existing phases, the level of macro- and microstresses, and variations in the density of dislocations. Thus, the saturation magnetization is not a structurally sensitive property. If only the content and structure of the ferromagnetic phase change during the phase transformations (with its composition and, therefore, the saturation magnetization remaining constant), the content of this phase can be determined with a high accuracy by measuring the change in saturation magnetization. If, however, a number of ferromagnetic phases are present in an alloy (for instance, α -phase and δ -ferrite, in addition to paramagnetic austenite, in semiferritic stainless steels), the content of each of these ferromagnetic phases in the alloy cannot be determined accurately by measuring the saturation magnetization at 20°C.

The calculation of the content of a ferromagnetic phase (present together with a paramagnetic phase) for alloys having a

¹ Magnetic properties vary depending on the alloy composition according to known relationships proposed by N. S. Kurnakov, which are reflected in the composition-property diagrams (see, for instance, Fig. 5.1). Alloys containing transition metals do not, however, obey completely these relationships owing to redistribution of the free electrons which pass to unfilled levels in the transition metals.

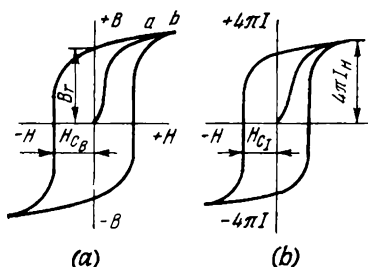


Fig. 5.7. Magnetization of a ferromagnetic metal *versus* field strength
(a) relationship $B = q(H)$; (b) relationship $4\pi I = f(H)$

heterogeneous structure is also very complicated if the composition of that phase varies in the course of the phase transformations being studied. This calculation can only be made when the saturation magnetization for each composition of that phase is known.

Thus, for instance, the content of residual austenite (and respectively of martensite) in hardened steel can be determined accurately if the reference specimen is a specimen containing 100 per

cent of martensite of the same composition as in the initial case, i.e. of the same saturation magnetization.

The composition of a ferromagnetic phase, irrespective of its content, is only characterized by the Curie point which is determined, in particular, to construct constitutional diagrams.

This condition is easily fulfilled in studies of carbon and low-alloy steels if the specimen being tested and the reference specimen are hardened simultaneously under the same conditions and the reference specimen is then immediately cooled to a low temperature (down to approximately -70°C), so that almost the total residual austenite is transformed to martensite.

In this case the content of austenite ($A\%$) is found by the relationship:

$$A\% = \frac{4\pi I_{s(\text{ref})} - 4\pi I_{s(t)}}{4\pi I_{s(\text{ref})}} 100\%$$

It is assumed in the calculation that the phases are distributed uniformly throughout the volume (cross section).

The determination of the residual austenite is more complicated for high-alloy and hypereutectoid carbon steels which are heated to high temperatures before hardening. An appreciable amount of residual austenite is then left in the reference specimen even after cooling to a very low temperature. Technique of calculation for this more complicated case can be found in the specialist literature.¹

The content of residual austenite is often calculated by the relationship given above, with the reference specimen being made of the same steel as the specimen being studied, but additionally

¹ See, for instance: Yu. A. Geller, in: *Zavodskaya laboratoriya*, 1955, No. 3.

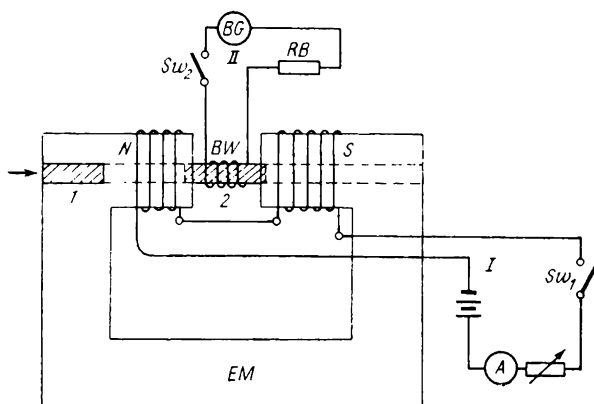


Fig. 5.8. Circuit for determining saturation magnetization

EM—electromagnet; *I*—magnetization circuit; *II*—measuring circuit; *A*—ammeter; *Sw*₁ and *Sw*₂—switches; *BW*—ballistic winding; *RB*—resistor box; *BG*—ballistic galvanometer; 1 and 2—initial and final positions of the specimen

subjected to annealing and tempering. The structure of the reference specimen then differs substantially from that of the specimen, and the calculation is less accurate and can give an appreciable error for some grades of steel. The concentrations of α -solid solution in the specimen and reference specimen are different; therefore, their saturation magnetizations are also different. In addition, they contain different amounts of carbides, and the presence of unequal amounts of the third phase in the specimen and reference specimen distorts the calculation results.

Saturation magnetization is mostly determined by the ballistic method.

The diagram of a ballistic apparatus for determining the saturation magnetization is shown in Fig. 5.8. A magnetic field of an intensity of ≥ 5000 oersteds is formed between the poles of electromagnet *EM*, so that a specimen (usually of circular or square cross section) placed in this field is magnetized to saturation. A rheostat in magnetization circuit *I* controls the current in the windings of the electromagnet, and, therefore, the magnetic field intensity. The measuring (ballistic) circuit *II* is then closed by switch *Sw*₂ and the specimen pushed through the bores in the poles into the interpole space of the magnet. The specimen is thus magnetized to saturation, and its magnetic lines of force intersect the turns of ballistic winding *BW*. An emf is formed in the ballistic circuit owing to magnetic induction, and ballistic galvanometer *BG* is supplied with a definite amount of electricity depending on the magnetic flux of the specimen, the number of

turns of the ballistic winding, and the impedance of the circuit. For a given cross-sectional area of the specimen, the number of turns of winding BW and a constant intensity H of the external field, the electric current flowing through the ballistic galvanometer will be proportional to the magnetic saturation of the specimen.

The ballistic galvanometer has a mirror which turns through an angle proportional to the electric current. The mirror is illuminated by a lamp and reflects a light spot onto a semitransparent scale measuring the deviation of the mirror.

The magnitude of $4\pi I_s$ is found by the formula:

$$4\pi I_s = \frac{c_b r \alpha}{ns} 10^2 \text{ gauss}$$

where c_b = ballistic constant determined by the amount of electricity (microcoulombs) passing through the galvanometer windings, which causes the light spot to deviate through 1 cm on the scale; c_b is determined preliminarily by means of a standard of mutual induction

r = resistance of the ballistic circuit (ohms), which is composed of the resistance of the ballistic winding, resistance of box RB , and internal resistance of the galvanometer

α = deviation of the light spot on the scale, cm

s = cross-sectional area of the specimen, cm^2

n = number of turns of the ballistic winding

The saturation magnetization of specimens of a given alloy is often found by using a reference specimen, for instance, one made of commercially pure iron whose magnetic saturation is known exactly.

If the specimen being tested and reference specimen are tested under the same conditions, i.e. on the same apparatus, with the same ballistic winding, and with the same circuit resistance, then

$$4\pi I_{s(t)} = 4\pi I_{s(ref)} \frac{\alpha_t s_{ref}}{\alpha_{ref} s_t}$$

If the specimen and reference specimen are of the same cross-sectional area, then

$$4\pi I_{s(t)} = 4\pi I_{s(ref)} \frac{\alpha_t}{\alpha_{ref}}$$

In many experimental studies, for instance, of isothermic or continuous transformations of supercooled austenite in steels, of

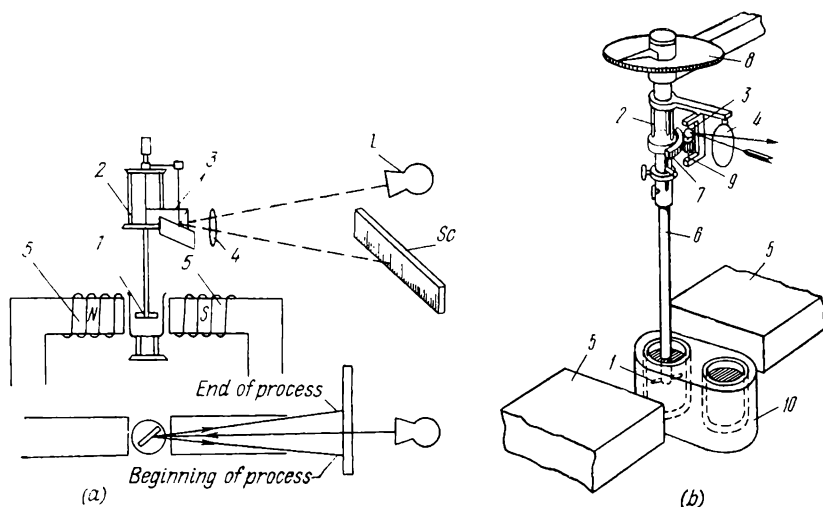


Fig. 5.9. Akulov's anisometer

(a) principal diagram: 1—specimen; 2—tensometer; 3—mirror; 4—lens; 5—electromagnet; L—lamp; Sc—scale; (b) general view: 1—specimen; 2—tensometer (an elastic system to counteract the turning of the specimen caused by the magnetic field); 3—mirror; 4—lens; 5—electromagnet; 6—porcelain tube for placing specimens; 7—friction arrangement; 8—dial (to position the specimen at a definite angle relative to the field direction); 9—mirror axis; 10—heating furnace

transformations of residual austenite in the process of tempering or low-temperature cooling of hardened steel, in determinations of the Curie points of various alloys, it is required to find the variations of the saturation magnetization (or of a property proportional to it) during heating and cooling. This can be most conveniently done by means of a special instrument, an anisometer, developed by N. S. Akulov (Fig. 5.9). The instrument has high sensitivity and makes a continuous record of the variations in the properties of an alloy, occurring in the course of phase transformations. Specimen 1 (3 mm in diameter and 30 mm long) is placed into a powerful magnetic field formed by an electromagnet and is held by a holder at an angle of 10 degrees to the direction of the magnetic field. The holder allows the specimen to move in the horizontal plane under the action of the ponderomotoric forces appearing in it. The turning of the specimen in the direction of the field is counteracted by an elastic system, so that the angle of turning of the specimen is proportional to its magnetization (and, therefore, to the content of the ferromagnetic phase in it). The motion of the specimen is recorded by an optical system comprising an illuminator, lens, mirror system, and scale; records can be made by replacing the scale by a photographic

camera. The amount of residual austenite in the specimen is determined by the displacement of the light spot on the scale or photographic paper.

To do this, displacement α of the specimen being tested is compared with that of a reference specimen made of the same alloy, but containing 100 per cent of the ferromagnetic phase; for steels, such a reference specimen is prepared by subjecting the metal to annealing and high tempering, with account of the remarks made on p. 144 of the book. The calculation is made by the formula

$$A\% = \left(1 - \frac{\alpha_t s_{ref}}{\alpha_{ref} s_t}\right) 100\%$$

where A = content of austenite

α_t and α_{ref} = displacements of the light spot from the zero position produced by the specimen being tested and reference specimen (i.e. $\alpha_{ref} = \alpha_1 - \alpha_0$ and $\alpha_t = \alpha_2 - \alpha_0$, where α_0 is the zero position of the light spot, α_1 and α_2 are the displacements of the light spot produced respectively by the specimen and reference specimen on application of a magnetic field)

s_t and s_{ref} = cross-sectional areas of the specimen and reference specimen, respectively

Measurements by the anisometer may be done during heating, holding at a constant temperature or cooling. The instrument has a special arrangement with two furnaces which can be moved into the interpolar space, with only a few seconds required to transfer the specimen from one furnace to the other having a different temperature.

Since the saturation magnetization reduces gradually with increasing temperature, the angles of turning of the specimen and reference specimen must be measured at the same temperature.

If, however, the temperature at which the measurements are being done is close to the Curie point, displacement α , which is proportional to the ponderomotoric forces, will vary sharply even at small temperature oscillations, thus introducing an appreciable error in the measured results. For this reason the temperature of the experiment for testing steels must not exceed 600-650 °C. The hot junction of the thermocouple should be placed close to the specimen. In addition, the accuracy of measurements should be improved by increasing displacements α_1 and α_2 by rearranging the system of mirrors or by placing the scale (or photographic paper) farther from the mirror, or finally, by increasing the angle

of turning of the specimen relative to the direction of the magnetic field. Besides, the windings of the electromagnet should be fed with a stabilized voltage for better accuracy of measurements.

If it is required by the test to cool the specimen to a low temperature, a thermostat filled with liquid nitrogen may be placed in the interpolar space instead of the furnace; the temperature of the specimen can be controlled within a wide range by varying the distance between the specimen and the level of liquid nitrogen.

Measurements of coercive force. As distinct from the saturation magnetization, the coercive force is a structurally sensitive property. It is numerically equal to the intensity of a magnetic field which, when applied opposite to the direction of the initial saturation magnetization, reduces to zero the intrinsic magnetization of a ferromagnetic alloy.

Pure metals, and solid solutions not subject to ordering, are usually characterized by a low coercive force. The coercive force of these metals and alloys can be increased somewhat by plastic deformation, but it then still remains low in its absolute magnitude.

Alloys with a heterogeneous structure have a higher coercive force; the higher the dispersity of the structure, the greater the coercive force. The growth in the coercive force is especially noticeable with high dispersity of the ferromagnetic phase in which each particle is single-domain and anisotropic in shape and the phase is located in a paramagnetic matrix.

The coercive force also becomes larger with greater microstresses and larger density of dislocations, as for example, in the case of martensite hardening of steel.

The coercive force can be conveniently measured by the ballistic method by means of special apparatus, such as the BY-3 apparatus (Fig. 5.10). The principal elements of such an apparatus are a magnetizing device (a solenoid or electromagnet, see Fig. 5.8) and a measuring instrument, such as a ballistic galvanometer, characterized by a large period of oscillations. When an induced emf appears in the measuring circuit, the movable system of the ballistic galvanometer begins to turn after passage of an impulse in the initial (magnetization) circuit. The angle of this turn (and, therefore, the displacement of the light spot on the scale) is proportional to the amount of electricity conveyed through the winding of the measuring coil of the instrument and through the other current-conducting elements of the measuring circuit.

In measurements of the coercive force, specimens are magnetized to saturation and their magnetization ($4\pi I$) is then de-

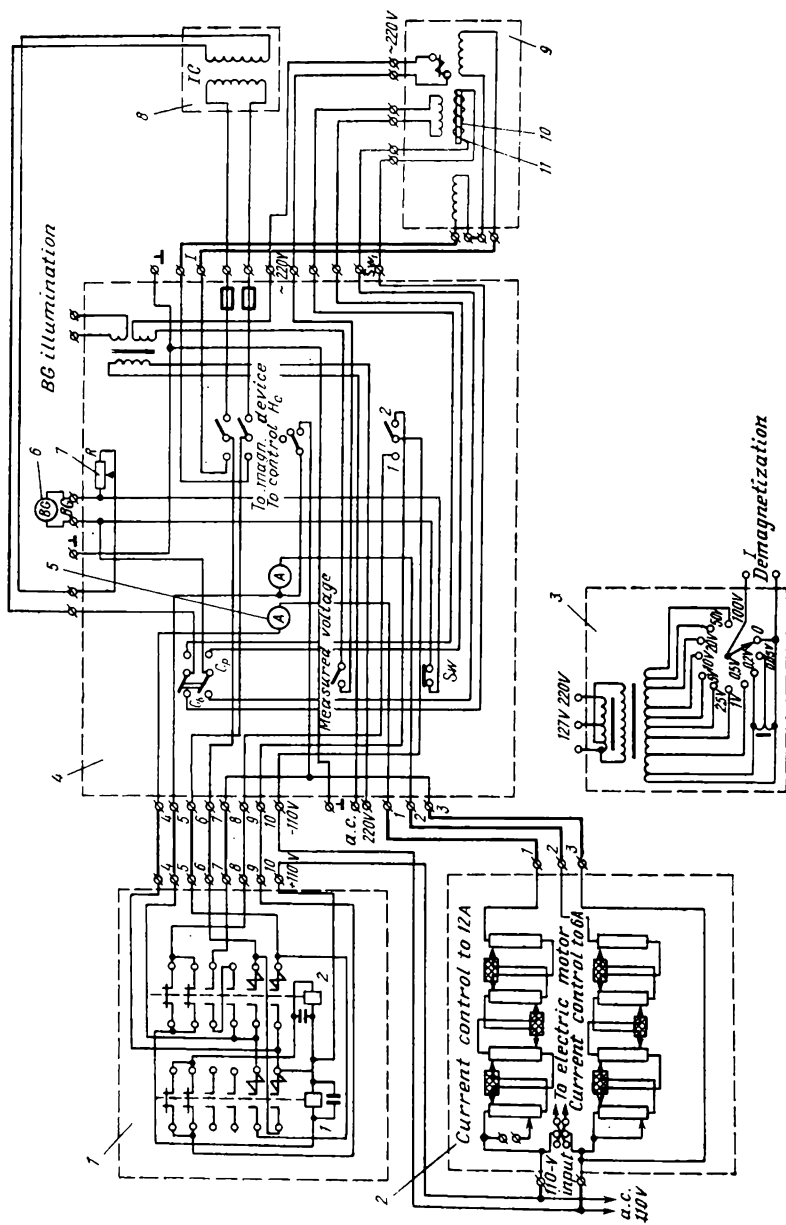


Fig. 5.10. Circuit of ballistic apparatus BY-3

1—contactor unit; 2—demagnetizing unit; 3—demagnetizing unit; 4—control board; 5—ammeter; 6—ballistic galvanometer; 7—variable resistor; 8—mutual induction coil; 9—magnetizing unit; 10—specimen; 11—measuring coil (here used to magnetize a solenoid)

terminated by altering the direction of the magnetic field.¹ The specimens are then again magnetized to saturation, and their magnetization is determined by altering the direction of the magnetic field and increasing the intensity of the latter. The measurements are repeated until the intrinsic magnetization becomes equal to zero or changes its sign. In the latter case the intensity of a demagnetizing field corresponding to the zero intrinsic magnetization is found graphically. The intensity of this field is numerically equal to the coercive force being sought.

The following method (Fig. 5.11) is often used to measure the coercive force, especially that of the so-called magnetically hard alloys. A specimen is magnetized to saturation in a suitable magnetizing device and then placed into a solenoid which can also be used for the preliminary magnetization. A measuring coil is then pulled onto the specimen, this coil being connected to a ballistic galvanometer (or fluxmeter). The field of the coil is applied in the direction opposing the initial magnetization and the coil is withdrawn from the specimen,² after which the deflection is measured by the instrument. This deflection is proportional to the magnetic flux, i.e. $4\pi Is$, where s is the cross-sectional area of the specimen, cm^2 . The coercive force is determined by repeating these operations with ever increasing intensity of the demagnetizing field (as in the ballistic method). It is numerically equal to the field intensity when $4\pi I = 0$.

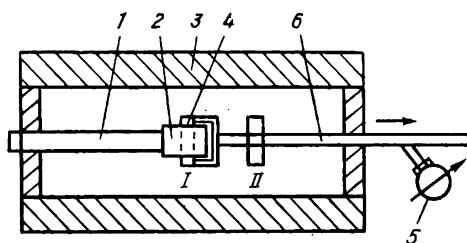


Fig. 5.11. Diagram of apparatus for determining coercive force

1—specimen-clamping arrangement; 2—specimen; 3—solenoid; 4—measuring coil; 5—ballistic galvanometer or fluxmeter; 6—arrangement for mounting and moving the measuring coil from I to II

¹ This magnetization is found by the relationship $4\pi I = B - H$, where B is the induction in a field of the given H . From the readings of a ballistic galvanometer it is possible to determine the induction by the formula

$$B = \frac{c_b r \alpha}{ns} 10^{-2} \text{ gauss.}$$
 The field intensity H of the solenoid is found from the formula $H = 0.4\pi nI/l$, where n is the number of turns, l is the solenoid length, cm, and I is the current, A. When an electromagnet is used, the intensity of the field in the interpolar space is determined by withdrawing the measuring coil connected to a ballistic galvanometer from the space. The formula for calculating H is the same as that for calculating B or $4\pi I$ (see above).

² The coil then remains in a field having the same intensity as that of the specimen.

5.3. LABORATORY EXERCISES ¹

Laboratory determinations of phase composition of alloys by measuring their resistivity and the temperature coefficient of the resistivity can be made by any of the methods discussed in Sec. 5.1a, the selection of the method only depending on the instruments available in the laboratory. Preference should always be given to the double-bridge method. When using the ammeter — voltmeter method or the ordinary-bridge method, it is advisable to employ wire specimens of a small diameter (0.5-1 mm) but a large length (1 to 2 m) so as to make their resistance as high as possible. Wires should be wound into coils for convenience of measurements and heat treatment.

Specimens for the double-bridge method may be round or square, 3 to 10 mm thick and 80-150 mm long (depending on the opening and space of clamping arrangements). Some explanations on the various methods and measuring circuits and measures for increasing the accuracy of measurements are given in this chapter.

Each student must make one of the problems given below.²

Problems

No. 50. Determine whether an increase in the carbon content of steel can change its phase state in equilibrium.

To solve the problem make the following: (a) measure the resistivity of three carbon steel specimens with 0.2, 0.5, and 0.9 per cent C; (b) construct the curve: steel electrical resistance *versus* carbon content; (c) using Kurnakov's relationships (composition-property diagrams), determine the phase state to which the relationship found corresponds.

No. 51. Determine the effect of hardening on the phase state of steel.

To solve the problem, make the following: (a) measure the resistivity of steel specimens with 0.4, 0.7, and 0.9 per cent C after annealing and hardening;³ (b) construct a curve showing the variations of the electrical resistance of annealed and hardened steel depending on its carbon content, and explain the observed dependence.

¹ Exercises on magnetic analysis are not given here; measurements of magnetic properties are included in some laboratory exercises on heat treatment (Problems Nos. 203, 214-216).

² Heat treatment can be preliminarily made in the laboratory.

³ Steel specimens should be hardened from 850, 820, and 800 °C with quenching in water.

No. 52. Determine the effect of hardening on the phase state of steel.

To solve the problem, make the following: (a) measure the resistivity of annealed and hardened steel specimens with 0.2, 0.5, and 0.7 per cent C;¹ (b) construct the curve: the electrical resistance of the annealed and hardened steel *versus* carbon content, and explain the observed dependence.

No. 53. Determine the variations in the phase state of steel caused by hardening from various temperatures.

To solve the problem, make the following: (a) measure the resistivity of steel specimens with 0.4 and 0.9 per cent C after annealing and after hardening² from 700, 750, 800, 850, and 900 °C; (b) construct curves showing the dependence of the resistivity of each specimen on the hardening temperature and determine the temperature interval within which the phase state of the steel can be changed.

No. 54. Determine the variations in the phase state of hardened steel caused by tempering.

To solve the problem, make the following: (a) measure the resistivity of the steel with 0.8 per cent C after hardening from 780 °C with water quenching and after subsequent tempering at 100, 200, 400, and 600 °C for 30 minutes, and also after annealing; (b) construct the curve expressing the variations in the electrical resistance depending on the tempering temperature and establish the temperature interval within which the phase state of the hardened steel varies most sharply, and when this state coincides with that of the annealed steel.

No. 55. Determine the variations of the phase state of hardened steel caused by tempering.

To solve the problem, make the following: (a) measure the resistivity of steel with 0.5 per cent C after hardening from 850 °C and water quenching, and after subsequent tempering at 100, 200, 400, and 600 °C for 30 minutes, and also after annealing; (b) construct the curve showing the variations in the electrical resistance depending on the tempering temperature and establish the temperature interval within which the phase state of the hardened steel varies most sharply and when this state coincides with that of the annealed steel.

No. 56. Determine the effect of alloying elements on the phase state of steel.

To solve the problem, make the following: (a) measure the resistivity of specimens of annealed carbon steel with 0.2, 0.5,

¹ Steel specimens should be hardened from 900, 820, and 800 °C with quenching in water.

² Water quenching.

and 0.7 per cent C and of annealed chromium steel with the same carbon contents; (b) construct curves showing the dependence of the electrical resistance of carbon and alloy steel on their carbon content and explain why these curves differ, taking into account the phase states of the steels.

No. 57. Determine whether an increase in the zinc content in copper alloys can change their phase state in equilibrium.

To solve the problem, make the following: (a) measure the resistivity of four specimens—copper, brass with 10 per cent Zn (Л190), brass with 20 per cent Zn (Л180), and brass with 30 per cent Zn (Л170); (b) construct curves showing the dependence of the resistivity of these alloys on zinc content; (c) using Kurnakov's relationships (composition-property diagrams), find the phase state corresponding to the relationship found.

No. 58. Determine whether an increase in the zinc content in copper alloys can change their phase state in equilibrium.

To solve the problem, make the following: (a) measure the resistivity of five specimens made of copper, brass with 10 per cent zinc (Л190), brass with 30 per cent zinc (Л170), brass with 38 per cent zinc (Л162), and brass with 41 per cent zinc (Л159); (b) construct the curve: resistivity *versus* zinc content; (c) using Kurnakov's relationships, determine at what concentration of zinc and in which direction this state of the alloys can be changed.

No. 59. Determine why and in which direction the temperature coefficient of electrical resistance changes with increase in the alloying degree of alloys.

To solve the problem, make the following: (a) measure the resistivity of copper, brass with 20 per cent zinc (Л180), brass with 30 per cent zinc (Л170), and brass with 41 per cent zinc (Л159) at 20 and 100 °C; (b) calculate the average temperature coefficient of the electrical resistance; (c) construct curves showing the dependences of the resistivity and its average temperature coefficient ($\alpha_{20-100^\circ\text{C}}$) on zinc content and explain the form of the curves obtained.

No. 60. Determine why and in which direction the temperature coefficient of alloys changes on the formation of solid solutions.

To solve the problem, make the following: (a) measure the resistivity of copper, nickel, and constantan alloy (МНМц 40-1.5) at 20 and 100 °C; (b) calculate the average temperature coefficient of the electrical resistance within a temperature interval of 20-100 °C ($\alpha_{20-100^\circ\text{C}}$) and name the branches of industry in which the knowledge of this coefficient is of prime importance.

No. 61. Determine the nature of the variation in the phase state of duralumin in the course of isothermic artificial ageing.

To solve the problem, make the following: (a) measure the resistivity immediately after hardening the duralumin specimens from 500 °C with water quenching and after annealing at 320 °C for one hour; (b) measure the resistivity of the duralumin specimens after hardening and after ageing at 175 °C for 15, 30, 45, and 60 minutes; (c) construct the curve showing the variation of the resistivity against the ageing time and, by comparing its value with those for the hardened and annealed specimens, indicate the direction of variation in the phase state of the alloy during ageing.

No. 62. Determine the nature of variation in the phase state of duralumin in the course of artificial ageing.

To solve the problem, make the following: (a) measure the resistivity of duralumin immediately after hardening from 500 °C with water quenching and after annealing at 320 °C for one hour; (b) measure the resistivity of the hardened duralumin specimens after artificial ageing at 100, 150, 175, and 200 °C for 30 minutes; (c) construct the curve of variation of the resistivity against the ageing time and, by comparing its value with those for the hardened and annealed specimens, indicate the direction of variation in the phase state of the alloy during ageing.

Chapter Six

DETERMINATION OF MECHANICAL PROPERTIES OF MATERIALS

6.1. GENERAL CHARACTERISTICS OF TEST METHODS

Mechanical properties of materials largely depend on the stressed state formed in the course of testing and, therefore, on the nature of the test being made.

According to this, all methods determining the mechanical properties of materials may be divided into two principally different groups: (a) those using specimens and (b) those carried out on manufactured articles.

Tests of the first category use special specimens of standard shape and dimensions, usually specified in national standards. In such tests, therefore, the mechanical properties are always determined under conditions of a specified stressed state. An obvious advantage of such tests is that it is possible to characterize and compare the properties of materials from different melts, with various compositions, manufacturing methods and treatments, and the initial variations in their composition and processing. Another advantage is that the tests are relatively simple and independent of a great number of variable factors that might appear in the course of tests. A valuable feature of tests of this kind is that they have been carried out for many years (there are records of tensile and fatigue tests carried out more than 100 years ago). This is why a vast systematized material on tests of various metals has been accumulated in the specialist literature (reference books and monographs), which can be conveniently used for comparative evaluation of the properties of newly developed or tested materials.

It should be remembered, however, that the results of the tests of standard specimens are only conditional and not universally applicable. In the first place, there is no direct relationship between the properties determined by testing standard specimens and the conduct of the material in machine elements which have a different and often more complicated shape and are subjected to a more complicated stressed state; in some cases this discrepancy can be even larger.

Besides, specimens of a small cross-sectional area are usually employed, whereas most machine elements have larger cross sections and, therefore, more defects (segregation, pores, microfissures, etc.) which impair their mechanical properties.

Tests of the second category, termed natural tests, are carried out on manufactured machine elements and are aimed at determining the behaviour of the material under a stressed state which approximates to the maximum, or even fully simulates the actual operating conditions.

Such tests are widely applied, especially for mass produced mechanisms and elements. They, in particular, include durability tests of ball bearings carried out on special stands, tests of some types of crankshaft for heavy-duty operation, etc. In a broader sense, service tests of engines, in particular test runs of automobiles, can be related to this group.

A disadvantage of this category of test is that it is difficult to apply the data obtained for one article to others operating under different conditions or stressed states. In addition, in such tests it is sometimes difficult to distinguish between the role and properties of the material being tested and the structural factors. Finally, tests of manufactured articles are rather complicated and often require much time and labour.

Another type of mechanical test, an intermediate one between the two types discussed above, is carried out on specimens of a relatively complex shape. The object of such tests is to determine the behaviour of a material under a more complicated stressed state than in the tests of the first group. These tests include tensile tests of specimens fastened eccentrically in testing machines, i.e. subjected simultaneously to tension and bending; tests of notched specimens, carried out to study the behaviour of machine elements having notches in the form of fillets, key-grooves, etc. which can change the distribution of stresses over the cross section and throughout the volume and form local stress concentrations; tests of hollow specimens subjected to the action of internal hydrostatic pressure, etc. The technique of a typical test of this group, namely the fracture toughness test, will be described in Sec. 6.5.

Tests of specimens of a relatively simple shape are most common in industry. Practically one piece out of every material batch used for the manufacture of critical articles is tested. The results obtained serve as starting data to characterize the properties and quality of the material.

Such tests can reduce, to some or other extent, the effect of the drawbacks mentioned above. Materials to be used in heavy-duty or critical elements or mechanisms are subjected to a number of

tests, rather than a single test, and therefore, to various stressed states. Such tests will be discussed below. They may be static or dynamic or else at varying loads.

6.2. STATIC TESTS

There are a number of methods for determining the mechanical properties of materials under conditions of static loading, a particular method being chosen depending on the created stressed state (characterized, in the first place, by the 'rigidity' of the method, i.e. the ratio of the maximum shear stress to the maximum normal stress) and the plasticity of the material.

(a) Tensile Tests

In these tests a uniform stressed state is formed over the cross section of a smooth specimen (either cylindrical or rectangular), and the material is subjected to normal and shear stresses. The proportion of normal stresses is predominant: the maximum shear stress usually constitutes half the maximum normal tensile stress, i.e. $\sigma_{\max}/S_{\max} = 0.5$; such tests are termed 'rigid', which implies that the principal mechanical properties (strength and plasticity in tensile tests) can only be determined for plastic materials with noticeable plastic deformation before destruction. This group of materials includes those widely employed in engineering, such as structural steels, non-ferrous metals, and most of plastics. Tensile tests can be carried out for tool steels¹ if these possess sufficient plasticity (after high tempering or annealing, i.e. with a reduced hardness).

Tensile tests of smooth specimens of plastic materials are the oldest and the most widely used among the methods determining mechanical properties (the sole exception being the hardness measurements discussed in Ch. 7). Data on the mechanical properties of materials in literature are usually based on tensile tests of smooth specimens.

Tensile tests determine the strength characteristics of a material, i.e. the ultimate tensile strength σ_t , yield limit σ_y ($\sigma_{0.2}$) and sometimes the proportionality limit σ_{pr} , and also the plasticity characteristics: relative elongation δ and relative reduction ψ .

¹ Tensile tests are excessively rigid and therefore are not employed for low-plastic materials, such as cast irons, most grades of steel after hardening or low tempering, and some plastics. These materials are very sensitive to even a slight misalignment of specimens and often break at the very beginning of the test.

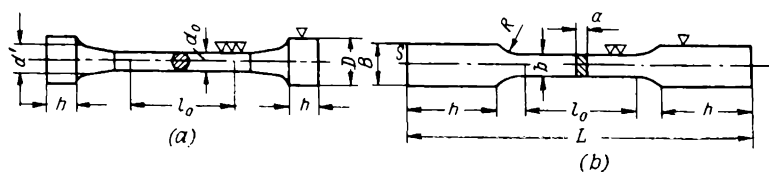


Fig. 6.1. Standard specimens for tensile tests
(a) cylindrical; (b) rectangular

Tensile tests are carried out on standard specimens of cylindrical or rectangular cross section, whose dimensions are specified in the USSR State Standard GOST 1497-61 (Fig. 6.1 and Table 6.1), the specimens being gripped and tested in testing machines of mechanical or hydraulic type, which automatically record, on an enlarged scale, the load applied and the length of the specimen, i.e. a stress-strain diagram is drawn.

Table 6.1. Standard Specimens for Tensile Tests

Specimen	Gauge length l_0 , mm	Cross-sectional area, mm ²	Diameter of cylindrical specimen, d_0 , mm	Symbols to denote relative elongation
Normal:				
long	200	314	20	δ_{10}
short	100	314	20	δ_5
Proportional:				
long	$11.3 \sqrt{F_0}$	Arbitrary	Arbitrary	δ_{10}
short	$5.65 \sqrt{F_0}$	Same	Same	δ_5

The testing load is increased gradually.¹ The elongation of a specimen first increases proportional to the load applied. Then, at a definite load, the proportionality between the load and specimen elongation is disturbed. The conditional stress corresponding to the moment when this proportionality is violated, is termed the *proportionality limit* σ_{pr} and is equal to the ratio of load P_{pr} to the initial cross-sectional area of the specimen:

$$\sigma_{pr} = P_{pr}/F_{in}, \text{ kgf/mm}^2$$

¹ In advanced-design machines, the load can be varied within a wide range (from a few grams to tons) without altering the type of stressed state. Besides, induction sensors make it possible to record specimen elongation on a scale of 1:1000, which appreciably improves the accuracy of measurements.

The magnitude of P_{pr} , from which the proportionality limit is found, can also be determined, with a certain approximation, from the stress-strain diagram.¹

With a specimen loaded to the proportionality limit, the ratio between stress σ and elongation ϵ of the specimen is determined by Hooke's law:

$$\sigma = E\epsilon$$

whence

$$E = \sigma/\epsilon$$

The *modulus of elasticity* E is a constant of the material and characterizes the slope of the deformation curve on the stress-strain diagram. With a higher elastic modulus, the material is less deformed under the same stress and possesses a higher rigidity. Each metal has a definite elastic modulus which depends little on the structure and treatment of the metal. The moduli of elasticity of some metals are as follows:

Steel	20×10^3 kgf/mm ²
Copper	10×10^3 kgf/mm ²
Aluminium	7×10^3 kgf/mm ²
Titanium	11×10^3 kgf/mm ²

With a metal specimen loaded below the proportionality limit, only elastic deformations are formed in it and the elongation is negligible. For a steel whose proportionality limit is 20 kgf/mm², the elastic deformation caused by the load is

$$\epsilon = \sigma/E = 20/20,000 = 0.001$$

i.e. does not exceed 0.1 per cent.

The elastic modulus of copper is only half that of steel, but the elongation at elastic deformations is also insignificant, since the proportionality limit of copper is lower than that of steel.

After removal of the load which does not exceed the proportionality limit, the elongated specimen will contract practically to its initial length.

With an applied load which is close to, or greater than, P_{pr} , a slight plastic deformation is formed in the metal; upon removing the load, the specimen does not restore fully its shape, but acquires a slight residual deformation. The conditional stress corresponding to the formation of a residual deformation after loading is termed the *elastic limit*, or *limit of proportionality*.

¹ The deviation from the linear relationship between the load and elongation must attain a value at which the slope of the deformation curve relative to the load axis will increase by 50 per cent of its value on the linear elastic portion.

The transition from the region of elastic deformations¹ to that of plastic deformations occurs gradually and begins at different loads in various grains of the metal; because of this the position of the elastic limit cannot be easily determined directly on the stress-strain diagram. The elastic limit is usually taken as the maximum stress that the metal being tested can withstand with a definite residual deformation remaining after removal of the load. The technical (conditional) elastic limit is taken as the stress at which the residual deformation is 0.05 of the initial length of the specimen.²

With a further increase in the load, plastic deformation occurs and a curvilinear portion is formed on the stress-strain diagram.

As distinct from other metals, the stress-strain diagrams for low-carbon steel and annealed aluminium and manganese bronzes show a stepwise passage from the elastic to the plastic region. This transition is seen on the curve as a horizontal portion ('yield tooth') which shows that the elongation of the metal increases at a constant load P . The minimum stress at which the deformation continues to proceed without any noticeable increase in the load is termed the (physical) *yield limit*.

For most metals, in particular, medium- and high-carbon steels, no such horizontal portion is formed on the stress-strain diagram. The conditional yield limit for these metals is taken equal to the stress causing a 0.2 per cent residual deformation of the initial length of the specimen:

$$\sigma_{0.2} = P_{0.2}/F_{in}, \text{ kgf/mm}^2$$

The yield limit can be determined with an accuracy sufficient for engineering calculations directly from the stress-strain diagram plotted by the testing machine, whereas the elastic limit must be found by tensometric methods. Since the absolute values of the limits of proportionality, elasticity and yield differ only slightly from each other, the allowable stress calculations in the design of structures and machine elements are often begun from the yield limit of the metal. The yield limit is the most important characteristic of materials. The allowable stresses for machine elements and structures are substantially lower than the yield limit.

¹ Non-elastic effects, i.e. elastic lag, stress, relaxation, elastic hysteresis, and internal friction can be observed in the region of elastic deformations of a real metal.

² In some cases the allowable residual deformation is lower, 10^{-3} to 10^{-4} per cent.

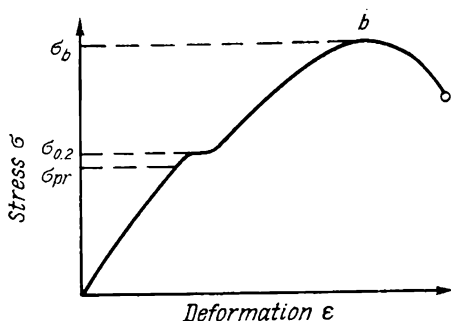


Fig. 6.2. Diagram of tension of specimens made of a plastic material

specimen is called the *ultimate tensile stress*, or *ultimate tensile strength* σ_b :

$$\sigma_b = P_b / F_{in}, \text{ kgf/mm}^2$$

For plastic metals, the maximum tensile load is not the destructive one but a load corresponding to the point of transfer from the uniform plastic deformation to that concentrated in a small definite (usually the weakest) portion along the length of the specimen. Here a more appreciable local contraction of the cross section of the specimen occurs with the formation of a neck.¹ Therefore, the ultimate strength characterizes the resistance of a metal to plastic deformation. Further application of a high load develops the plastic deformation (neck) still more, therefore, the absolute load to break the specimen becomes lower.

In the determinations of the proportionality limit, elastic limit, yield limit, and ultimate strength, the corresponding load P was related to the initial cross-sectional area of the specimen, i.e. the area it had before the tests. With specimens being tested within the region of elastic deformations or near it, i.e. in determinations of the limits of proportionality and elasticity, the change in the cross-sectional area of the specimen is small and can be neglected. In the region of plastic deformations, however, this change is appreciable, so that, when determining the ultimate strength or the yield limit, the corresponding load must be related to the actual cross-sectional area of the specimen at the moment of measurement, rather than to the initial area.

The stresses determined relative to the load applied to the initial cross-sectional area of specimens are termed *conditional*

¹ Austenitic steels capable of appreciable work-hardening deform rather uniformly along their length and break with almost no neck being formed.

Increasing the load above the yield limit causes plastic deformation in all volumes of the metal and its work-hardening. For this reason the load required to tension a specimen gradually increases and attains its maximum at point b in Fig. 6.2. The stress corresponding to the maximum load P_b and immediately preceding the rupture of the specimen

stresses, and those determined for the actual cross-sectional area, *actual stresses*.

Figure 6.3 shows a curve of actual stresses. The yield limit in this case is denoted as S_s , and the ultimate strength, or more precisely, the actual ultimate resistance, as S_k . It is clear that S_s and S_k are greater respectively than σ_y and σ_t , the difference between these values being greater for plastic metals having a large deformation in tension, and lower for brittle metals. On the other hand, the difference between S_k and σ_t is in turn greater than that between S_s and σ_y , since the deformation of a specimen is not high until the yield strength is attained.

For steels, the experimental determination of S_k is rather complicated, the more so as it is difficult to control the load of the testing machine that corresponds to the moment of destruction of the specimen (since the load decreased rapidly), but this method gives a high accuracy and is finding ever wider application.

In practical industrial tests, conditional stresses are usually determined; in the specialist literature, the data on $\sigma_{0.2}$ and σ_t are more common.

Brittle metals undergo almost no plastic deformation in tension, their yield limit being almost equal in magnitude to the ultimate strength; rupture occurs when the latter limit is attained.

The plasticity of a tested metal can be determined by measuring the length and cross-sectional area of specimens before and after rupture.

The *relative elongation* δ is the ratio (percentage) of the increment of the gauge length of a specimen after rupture to its initial length, i.e.

$$\delta = \frac{l_{fin} - l_{in}}{l_{in}} 100\%$$

The absolute elongation $l_{fin} - l_{in}$ formed in tension is the sum of the uniform elongation of the whole specimen Δl_1 and the concentrated (local) elongation of the neck, Δl_2 .

The uniform elongation Δl_1 depends on the properties of the metal and is proportional to the length l of the specimen, whereas the local elongation Δl_2 also depends on the properties of the metal, but is generally independent of the initial length l .

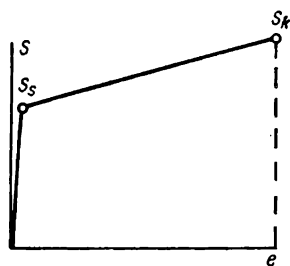


Fig. 6.3. Diagram of actual stresses (in tension)

Thus, the total elongation of a specimen depends on the gauge length of the specimen and the properties of the metal. The dimensions of specimens for tensile tests are standardized so that test results can be compared (see Table 6.1).

Further, the relative elongation depends on the position of rupture: being maximum when the specimen breaks at its middle. Thus, the relative elongation is a conditional characteristic of the properties of a metal and can be used only for qualitative judgements, e.g. to choose a metal that can withstand better the plastic deformation under the given conditions.

The *relative reduction* ψ is the percentage ratio of the maximum reduction of cross-sectional area of a specimen to the initial cross-sectional area F_{in} :

$$\psi = \frac{F_{in} - F_{fin}}{F_{in}} 100\%$$

The cross-sectional area of cylindrical specimens at the place of break can be determined sufficiently accurately, since it generally remains circular. The problem is more complicated with rectangular specimens.

Plasticity also determines the redistribution capability of a metal, and consequently, the lowering of the local peak stresses which appear at the points of structural defects and various stress concentrators. A metal of high plasticity is less probable to break abruptly by brittle fracture, and, therefore, higher stresses can be assigned.

It is essential that there be no proportionality between the plasticity characteristics (δ , ψ) and strength properties of materials. Materials having a high strength (σ_t , $\sigma_{0.2}$), as a rule, have a low relative elongation and a low relative contraction. The plasticity of metals increases as their strength reduces.

For these reasons, the ultimate strength, which can be usually increased by heat treatment, is often restricted to a definite safe limit. For structural steels, for instance, the magnitude of σ_t , as a rule, must not be higher than 110-150 kgf/mm², an exception being maraging steels (see Table 27.6).

Specimens for testing plastics are similar to those for testing metals and are usually tested to determine mainly the ultimate strength (σ_t) and, for more plastic materials, also the yield limit ($\sigma_{0.2}$).

It should be considered, however, that the testing conditions for plastics differ substantially from those for metals. The strength of plastics largely depends on the test duration and reduces with increasing time. Therefore, data on the strength of

plastics should be supplemented with data on the test duration (if longer than the common short-term tests).

In addition, the mechanical properties of many plastics may depend on their ability to absorb moisture, therefore, the moisture content in the place where these materials are kept or tested must be taken into consideration.

(b) Compression Tests

In compression tests the maximum shear stresses exceed appreciably (by a factor of two) the maximum normal compression stresses: $\tau_{\max}/S_{\max} = 2$. For this reason compression, uniaxial or three-dimensional, is the most gentle way of loading.

Compression tests are very suitable for brittle materials which break almost without plastic deformation, and therefore, without expansion (formation of a 'barrel'), in particular for tool steels with a high hardness number (when their yield limit must be determined), for white and low-plastic grey cast irons, and also for mineral rocks and cements.

For the reasons indicated, the compression strength of these materials is 1.5-3 times higher than their tensile strength.

It is essential that compression tests be used to determine the yield limit of low-plastic materials, which is accomplished by applying increasing loads (or unloading) and measuring the residual deformation.

Compression tests are less suitable for plastic materials as they cannot determine sufficiently clearly the effect of the material structure on the mechanical properties; in addition, specimens of these materials strongly deform, become barrel-shaped, and turn out to be under conditions of non-uniform three-dimensional compression, which complicates still more the determination of their mechanical properties. With a further increase in the load, the specimens flatten, which in many cases makes it impossible to break them and determine the ultimate strength and the total plasticity. On the other hand, the strength of plastic materials in compression differs only slightly from that in tension.

The relative shortening (compression deformation) δ and the relative expansion ψ of a specimen in compression tests (in place of the relative elongation and relative contraction respectively in tensile tests)¹ can be found by the formulae:

$$\delta = \frac{l_{in} - l_{fin}}{l_{in}} 100\%$$

¹ For this reason the actual stresses determined in compression tests are lower than the conditional ones (unlike tensile tests).

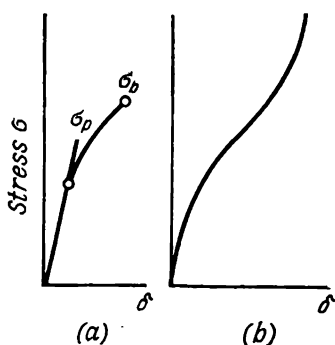


Fig. 6.4. Compression diagram (a) for brittle material; (b) for plastic material

and

$$\psi = \frac{F_{fin} - F_{in}}{F_{in}} 100\%$$

A compression diagram is shown in Fig. 6.4.

The results of compression tests depend on the shape and dimensions of specimens. According to the USSR State Standard GOST 2055-43, compression specimens must be 10 or 25 mm in diameter and of the same height. Fracture of specimens of low-plastic metals usually occurs along planes at angles of 45 degrees to the axis of the specimen.

In tests of short specimens, however, the friction forces between the end surfaces of a specimen and the support planes can become largely effective; they restrict the motion of the metal over the support planes and thus affect substantially the results of the tests. In order to minimize friction, specimens of a different shape or various caps must be used, which makes the tests more complicated. On the other hand, with reduced friction the nature of destruction can be changed: longitudinal fissures form in the specimen and, owing to a change in the conditions of metal flow, destruction can occur under a lower load.

(c) Torsional Tests

In torsional tests the maximum shear stresses are close to the normal ones: $\tau_{\max}/S_{\max} = 0.8$. By their severity, these tests are intermediate between tensile tests and compression tests.

For most metals, the strength properties found by torsional tests differ only slightly from those determined in tensile tests. Nevertheless, torsional tests, though being more complicated, are being used more and more widely for testing both plastic and low-plastic metals because of a number of advances as compared with tensile tests.

During torsional tests, no neck forms in specimens, and the torque increases up to the moment of destruction. Plastic deformation is almost uniform over the whole length of a specimen, which makes it possible to determine deformations and stresses more reliably for very plastic materials, especially pure metals. When subjected to tensile tests, such metals usually form a very

long neck; the deformations then cannot be calculated accurately because of the non-uniform cross-section change.

Low-plastic metals, which are difficult to test in tension, obtain quite a measurable deformation in torsional tests, which enables their mechanical properties to be determined.

In addition, from torsional tests it is possible to determine the nature of destruction by the form of the break. A break perpendicular to the axis of a specimen is indicative of viscous destruction (by shear), which is characteristic of plastic metals. A break along a helical line is characteristic of brittle destruction (by tension).

A torsional testing machine may be provided with a device for plotting on an enlarged scale the deformation curve of a specimen in the coordinates: torque — angle of twist. Measurements of the angles of twist, which are usually insignificant, in particular of the angles corresponding to torques M_{pr} (up to the proportionality limit) and M_e (up to the elasticity limit) are done by means of extensometers, in particular of the mirror-type. The angle of twist is determined as the difference of angles (angular indices) φ_1 , φ_2 of turning of sections f_1 and f_2 positioned at the ends of the gauge length of the specimen.

Specimens for torsional tests are cylindrical (Fig. 6.5), most often 10 mm in diameter (but not less than 5 mm) with a gauge length of 100 mm, having large square-shaped ends. For less plastic materials (for instance, high-hardness steels), the junction between the cylindrical portion and square ends is made more smooth.

Torsional tests determine: the modulus of elasticity in shear G and the following strength characteristics: proportionality limit τ_{pr} , conditional yield limit $\tau_{0.3}$, actual ultimate strength τ_t , and conditional ultimate strength τ_b ; ductility of the metal; and relative shear in torsion γ .

To determine the modulus of elasticity in shear G (or simply, shear modulus), the specimen is loaded with a torque corresponding to the initial shear stress τ_0 . According to the USSR State

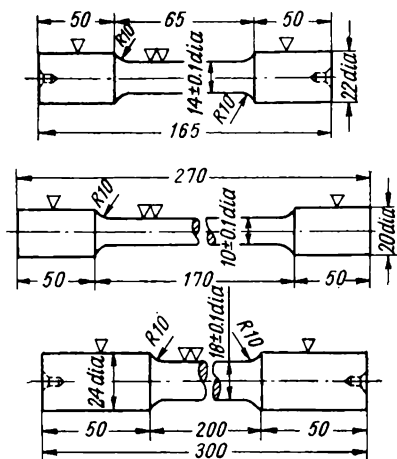


Fig. 6.5. Standard specimens for torsional tests

Standard GOST 3565-58, the recommended value of τ_0 for steels is approximately 3 kgf/mm² and not more than 10 per cent of the expected proportionality limit for other metals. The mirror extensometer is then adjusted, the zero angle of twist is marked, and the specimen is loaded with a torque such as not to exceed the proportionality limit.

The modulus of elasticity is found by the formula:

$$G = \frac{Ml}{(\varphi_1 - \varphi_2) I_p}$$

where M = torque (minus the initial torque), kgf/mm

l = gauge length of the specimen, mm

φ_1 and φ_2 = angular indices (angles of twist) at the ends of the gauge length, radians

I_p = polar moment of inertia, mm⁴ ($I_p = \pi d^4/32$ for a cylindrical cross section)

The proportionality limit τ_{pr} is found from the formula:

$$\tau_{pr} = M/W$$

where W is the moment of resistance, mm³ ($W = \pi d^3/16$ for a cylindrical cross section).

Torque M is determined as follows. After the specimen has been loaded with the torque corresponding to the initial shear stress and the mirror extensometer adjusted, the specimen is additionally loaded, successively, first in large steps (by loads of up to two-thirds of the expected proportionality limit) and then in small steps, the angular deformation being recorded after each application.

Loading in small steps is discontinued when the angular deformation caused by all these small loads exceeds 2 or 3 times the angular deformation formed through the first small load. The results obtained are used to plot the torsional curve. The average angle of twist is determined from the portion of the curve which follows Hooke's law. The value thus found is increased by 50 per cent and torque M_1 corresponding to this point is used to calculate the proportionality limit.

The yield limit $\tau_{0.3}$ can be determined graphically from the torsional curve (Fig. 6.6), if the latter has been plotted to a large deformation scale, or calculated by the formula

$$\tau_{0.3} = M/W$$

Torque M corresponding to the yield limit is calculated according to the USSR State Standard GOST 3565-58.

The conditional ultimate strength τ_b is found from the formula

$$\tau_b = M_t / W$$

where M_t is the maximum torque preceding the rupture of the specimen.

To find the actual ultimate strength τ_t , the specimen is additionally loaded until a noticeable plastic deformation occurs, after which it is loaded in small, preferably equal steps, with torque M and the corresponding angular indices φ_1 and φ_2 being recorded for a number of step loads. For a number of difference $\varphi_1 - \varphi_2$ corresponding to the points on the curve immediately before rupture, the unit angle θ of twist, in radians, is calculated by the formula

$$\theta = \frac{\varphi_1 - \varphi_2}{l'}$$

where l is the gauge length of the specimen.

These data are used to plot the curve of dependence of M on θ , and the magnitude $dM/d\theta$ is found graphically for the point on the curve which corresponds to the maximum torque as the slope of that point.

The actual ultimate strength is found from the formula

$$\tau_t = \frac{4}{\pi d^3} \left(3M_t - \theta \frac{dM}{d\theta} \right)$$

where M_t is the maximum torque before rupture.

The relative torsional shear γ (%) is determined from the formula

$$\gamma = \frac{(\varphi_1 - \varphi_2) d}{2l} 100 \quad \text{or} \quad \gamma = \frac{\theta d}{2} 100$$

where φ_1 and φ_2 are angular indices before rupture and

$$\theta = \frac{\varphi_1 - \varphi_2}{l}$$

For plastic materials in which the elastic deformation is relatively small (compared with the plastic deformation), the total shear found by the above formula may be taken as the residual one.

For low-plastic materials in which the elastic deformation is relatively high (compared with the plastic deformation) the total

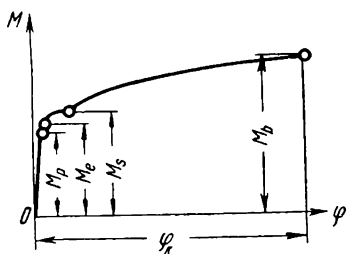


Fig. 6.6. Torsional diagram

shear found by the formula above must be reduced¹ by the elastic shear γ_e :

$$\gamma_e = \frac{\tau}{G} 100$$

where τ = ultimate strength in torsion

G = shear modulus of the material being tested

(d) Bending Tests

In bending, both tensile and compressive stresses are formed in the corresponding zones of a specimen; therefore, bending tests are less severe than tensile tests, but more severe than compressive ones.

This kind of test is employed for low-plastic materials, mainly for grey and white irons, tool steels with a high hardness number, and for studying the effect of corrosion (see Ch. 8). The strength of these materials in bending is higher (owing to the effect of the compressed zone) than in tension, but lower than in compression.

The disadvantage of bending tests (as compared with tensile and compressive tests) is that a non-uniform stressed state forms in the specimen, which makes it difficult to analyse the behaviour of the materials during loading.

Bending tests are not employed for plastic materials, since their specimens can be bent fully (their ends can touch each other) without rupture. As in compressive tests, it becomes impossible to determine the rupture resistance and maximum plasticity.²

Specimens for bending tests may be of either circular or rectangular (preferably square) cross section, their ends being placed onto two supports. Relatively low loads are recommended to prevent crumpling of supports; this is achieved by using long specimens with $l/h \geq 10$.

Bending tests can be carried out:

(a) by applying a concentrated load at the span centre (Fig. 6.7); this method is used most often. The maximum bending moment is then found as

$$M_b = \frac{Pl}{4}$$

¹ The calculation is approximate.

² Such materials are tested by 180° multiple bending in two opposite directions (folding tests); the quality of a material is then determined by the number of foldings the specimen withstands before rupture.

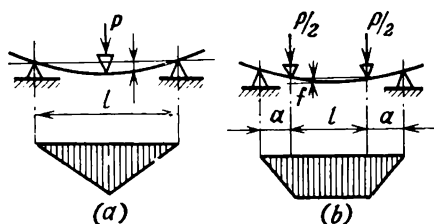


Fig. 6.7. Diagram of bending test
(a) concentrated-load bending; (b) pure bending

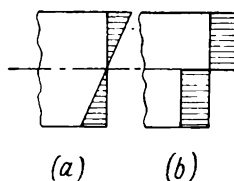


Fig. 6.8. Stress distribution in bending
(a) within the region of elastic deformation;
(b) within the region of plastic deformations

(b) by applying two loads $P/2$ at equal distances from the supports (pure-bending tests); the recommended distance from a support is equal to $1/3$ of the specimen gauge length (see Fig. 6.7). In pure bending

$$M_{\max} = \frac{Pa}{2}$$

Pure-bending tests characterize better the properties of the material being tested. The rupture of a specimen occurs at the most weakened cross section along portion l owing to some specific features of the structure, in particular, macroscopic or microscopic heterogeneity of the material.

The stressed state formed in pure bending is, however, more complicated than in concentrated-load bending.

With concentrated-load bending, rupture occurs generally where load P is applied, i.e. at an arbitrary cross section (relative to the possible defects of the internal structure).

The ultimate strength in bending is found from the relationship

$$\sigma_b = M_{\max}/W$$

where W is the moment of resistance; $W = \pi d^3/32$ for circular specimens and $W = bh^2/6$ for rectangular ones. These moments of resistance correspond to bending within the region of elastic deformations (Fig. 6.8a).

With bending of plastic metals in the zone of appreciable plastic deformations and rupture, the moment of resistance for rectangular specimens is (Fig. 6.8b)

$$W = bh^2/4$$

For brittle materials, whose rupture occurs without noticeable plastic deformation (white and grey irons, high-carbon steels

after hardening without tempering), the moment of resistance is very close to the values given above, i.e. $bh^2/6$ or $\pi d^3/32$.

For low-plastic metals which exhibit a slight plastic deformation before rupture (hardened tool and other grades of steel with a hardness of 52-62 HRC), the moment of resistance may be between $bh^2/6$ and $bh^2/4$ (for rectangular specimens). Accurate calculation of the moment of resistance is difficult but with a certain approximation, it can be taken equal to $bh^2/6 \times 1.2$.

For less plastic materials the tests are more often reduced to the determination of ultimate strength in bending (σ_b).

Deflection in bending cannot be a reliable characteristic of plasticity of these materials. It depends mainly on the strength of the specimen, since the proportion of plastic deformation is insignificant in such cases and, as a rule, is less than that of elastic deformation.

6.3. TESTS UNDER VARIABLE LOADS (FATIGUE TESTS)

These tests are employed to characterize the behaviour of materials (either plastic or brittle) under repeated loads, when most metals exhibit a lower strength compared with that determined in static tests.

Fatigue tests are gaining in importance, since many machine elements operate under conditions of repeated loading (for instance, crankshafts in symmetric-cycle conditions, connecting rods in asymmetric conditions, and the like). The characteristic of fatigue strength, or endurance limit, is often given in reference books and specialist literature along with the properties determined by static tests (ultimate tensile strength and impact strength).

Rupture of a metal subjected to repeated alternating (fatigue) loads occurs abruptly, without any noticeable plastic deformation, i.e. is brittle and caused by normal stresses. The break usually has two portions which are different in their appearance. The smaller portion near the surface layers has a smooth (lapped) surface and is called the *zone of fatigue fracture*; the larger portion has a coarse crystalline structure characteristic of breaks obtained in static tests.

This seemingly abrupt rupture actually develops gradually. Plastic deformation begins first in the most stressed or most weakened section under the action of the repeated loads, this deformation forming a small fissure. Further application of repeated loads causes the fissure to increase in size, and it gradually transforms into a fatigue fracture thus weakening the critical cross section. When the remaining non-ruptured portion of

the cross section (volume) becomes incapable of withstanding the load applied, rapid rupture of the article takes place.

The property of a metal to withstand a large cycle of alternating loads is termed the *endurance*. The highest stress a metal can withstand without rupture upon application of a specified cycle of alternating loads is called the *endurance limit*, or *fatigue strength*.¹

Fatigue strength depends on the number of cycles of varying loads and the nature of the cycle proper, since the loads can be either alternating, i.e. changing signs (tension followed by compression and vice versa), or without sign alternation. A cycle can be:

(a) symmetrical, when the stresses are equal in magnitude and opposite in signs;

(b) asymmetrical, when the stresses are not equal (but may be of the same sign).

The fatigue strength is lower with a symmetrical cycle and is most often determined under these conditions with an appreciably high number of cycles of alternating loading (see p. 175).

An approximate quantitative relationship can be established between the ultimate strength and fatigue strength of a material. For steels, the fatigue strength determined by bending smooth (unnotched) specimens is $0.45\text{--}0.55 \sigma_b$ or, what is more characteristic, approximately $0.25S_h$. The fatigue strength in torsion is $0.5\text{--}0.6$ of the fatigue strength in bending.² These relationships, however, can only be used under the following considerations:

1. If the ultimate strength of a metal is increased by varying its composition or by heat treatment, the fatigue strength increases in an appreciably smaller proportion. For steels, especially high-strength alloy steels with $\sigma_b > 90\text{--}120 \text{ kgf/mm}^2$ and reduced plasticity, the endurance limit (for smooth specimens) corresponds to the lower value of the above-mentioned coefficient and may be even lower for steels having martensitic or troostite-martensitic structure. This reduction of fatigue strength is less noticeable in high-strength maraging steels (see Table 27.4).

2. The surface state of a specimen can have a greater effect on fatigue strength than on ultimate strength. An insufficiently smooth surface obtained after machining (roughness below class 6), corroded places or a decarbonized layer can reduce sharply the fatigue strength. The same effect is produced by various inclusions (non-metallic inclusions and large carbide grains

¹ In some cases the endurance limit is determined at higher stresses and a comparatively small number of cycles (low-cycle endurance).

² Under symmetric-cycle loading for plastic materials.

in steel) and gas blowholes. Such defects in subsurface layers act as stress concentrators in alternating loading and cause quicker fatigue rupture of the specimen.

For these reasons the fatigue strength can be increased by using some machining operations which improve the quality of the surface (honing, polishing, etc.) or some methods which increase the strength of the surface layer and form compressive stresses in it (cementation, nitration, etc.). Shot-blasting and rolling of steel articles, which work-harden the surface layers, are also very effective in increasing the fatigue strength.

3. For the same reasons, the presence of notches and sharp junctions in the cross section of an article, which are made from the design considerations, can also reduce the fatigue strength of materials, especially of steels of a high strength (and, therefore, of low plasticity).

Materials possessing higher plasticity, for instance, duralumin and brass, are less sensitive to notches, and their fatigue strength is reduced less. The same applies to grey irons, in which lamellar inclusions of graphite act as internal notches.

4. The fatigue strength can be largely dependent on the dimensions of an article (or specimen). Increasing the diameter of specimens of structural steel from 7 to 200 mm lowers their fatigue strength by 50-60 per cent. The fatigue strength can decrease even more in steel articles having precipitated carbides whose distribution is less uniform in large sections.

Fatigue strength is measured in various fatigue-testing machines in which specimens can be subjected to alternating stresses in bending, tension, compression, torsion or impact (mainly symmetric cyclic loads). The test conditions depend on the operating conditions of the finished article. Fatigue strength is more often determined in bending tests of rotating specimens and less frequently, in torsion or impact tests. For plastic materials, their fatigue strengths determined in bending and tension are very close to each other.

The diagram of a machine for fatigue tests in rotational bending and the shape and dimensions of specimens are shown in Fig. 6.9.

The fatigue strength in bending is determined¹ by testing a series of specimens (at least six) of the same composition, treatment, shape, and surface state. The first specimen is tested at a constant stress kept at $0.6 \sigma_b$ for steels and $0.4 \sigma_b$ for light-weight alloys. The second and subsequent specimens are tested with the

¹ Test methods for determining fatigue strength are specified in the USSR State Standard GOST 2860-65.

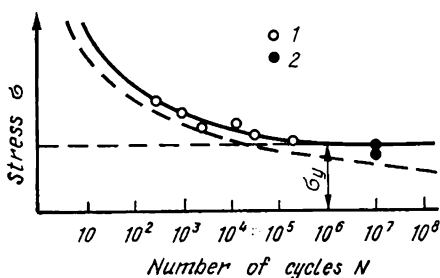


Fig. 6.10. σ - N curve to calculate the endurance limit

1—specimen was fractured; 2—specimen was not fractured

endurance limit of steel. The highest stress corresponding to the asymptotic approach to the horizontal line under such conditions is taken as the fatigue strength.¹

In some cases, such as for duralumin after natural ageing, some other non-ferrous metals, large steel specimens, and specimens tested simultaneously for fatigue and corrosion the experimental curve droops gradually instead of approach-

ing asymptotically a horizontal line (see the dotted line in Fig. 6.10). The fatigue strength is then determined for a specified number of cycles (for instance, 10^8); the fatigue strength determined in this way is a conditional parameter and depends on the duration of operation of an article.

The fatigue strength can also be affected by the testing conditions. A pause in the course of tests or preliminary training of specimens at lower loads, and overloading of specimens to a certain limit, can increase the fatigue strength.

6.4. DYNAMIC TESTS

These tests are employed for metals having a body-centred cubic lattice, i.e. for steels (mainly plastic structural steels), zinc and zinc alloys, and some plastics. Dynamic tests are valuable for the materials not displaying brittleness in tensile tests (which are a relatively gentle way of loading) but becoming brittle under the action of some operational factors, such as high deformation rates, i.e. at impact loads, when notches or fissures are present, in biaxial or three-dimensional stressed states, at low temperatures, etc.

The liability of steel to brittle fracture increases with a higher phosphorus content, larger grain, segregation of carbides at

¹ The fatigue strength determined by symmetric cyclic loading is denoted as σ_{-1} , that found in asymmetric loading, as σ_2 (r being the coefficient of asymmetry of the cycle, i.e. the algebraic ratio of the minimum stress to the maximum one), that found by sign-alternating loading as $\sigma_{\leq 0}$, that found by loading with the same sign, as $\sigma_{> 0}$, that in a tension cycle started from zero, as σ_0 , and that in a compression cycle started from zero, σ_{∞}

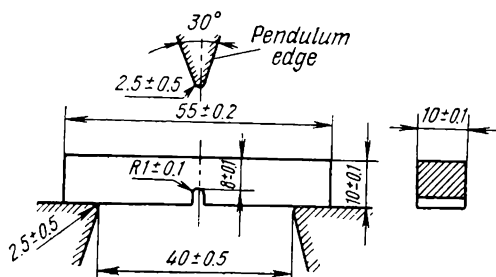


Fig. 6.11. Shape and size of specimen for impact strength tests

grain boundaries, and banding (in the latter case the brittleness increases in definite directions only, see Ch. 2).

Dynamic tests are widely applied to very hard steels, in particular, tool steels.

These tests are needless for steels and alloys having an austenitic structure, duralumins, single-phase brasses, and bronzes as such alloys can only hardly be transformed into a brittle state.

Determination of impact strength. The impact strength, kgf m/cm^2 , (a_n for plastic materials and a_s for brittle ones) determined by the tests discussed below, is the work of impact fracture (through bending) related to the area of the notched cross section of a specimen.¹

Figure 6.11 illustrates a typical specimen. Its dimensions, the shape of the notch, and the method of making the notch can strongly affect the test results. Notches must be made by an emery disc, and in soft materials, by a profile cutter with subsequent grinding or honing of the notch bottom.

Test results may also depend on the orientation of metal fibres in the specimen; therefore, the place of the notch in a specimen relative to the direction of deforming in rolling, forging or deforming is usually specified in particular, along the direction of rolling (longitudinal specimens), or transversely to it (transverse specimens), or radially. Besides, in transverse specimens cut from rolled stock (round, square, etc.), the axis of a notch can be parallel with the direction of banding of the metal. For specimens cut from sheets or strips, the notch must be perpendicular to the surface of rolling. Work-hardening and heating of specimens in the course of their manufacture and their oxidation and decarbonization during heat treatment should be avoided. If heating cannot be done without oxidation or decarbonization, notching should be done after heat treatment.

¹ a_n for notched specimens and a_s for smooth (unnotched) specimens.

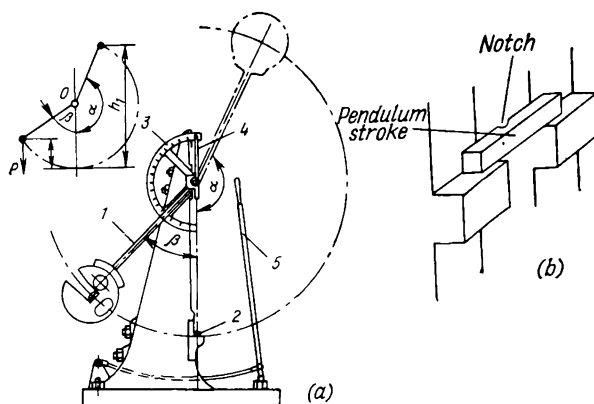


Fig. 6.12. Diagram of pendulum hammer (a); position of specimen during testing (b)
1—pendulum; 2—specimen; 3—scale; 4—pointer; 5—brake

Determination of impact strength is made in impact-testing machines (Fig. 6.12), the specimens being fractured by means of a pendulum freely suspended from supports and provided with a knife of specified shape and size.

The specimen is mounted symmetrically on the lower supports of the machine, its notched side away from the pendulum (as shown in Fig. 6.12).

The pendulum is first lifted into the upper position and held by a catch. In this position the pendulum possesses potential energy Ph_1 , where P is its weight and h_1 , the height of lift. Releasing the catch frees the pendulum. It drops down and breaks the specimen, then lifts to height h_2 where its potential energy equals Ph_2 which is lower than Ph_1 . Their difference determines the work spent to break the specimen.

Pointer 4 mounted on the machine stand is caught by the moving pendulum and indicates on scale 3 the angle of lift of the pendulum after breaking the specimen. The work of fracture A_n is given by the formula

$$A_n = Pl(\cos \beta - \cos \alpha)$$

where l = distance between the axis and the centre of gravity of the pendulum

α and β = angles of lift before and after fracture, respectively

Angle α is kept constant by moving the pointer before a test into the position corresponding to 0° on the scale.

Some impact-testing machines are provided with a chart containing the corresponding values of A_n for each value of the angle, so that the above calculation becomes unnecessary.

The lower the work of fracture A_n , the more accurate must be the measurement; for this reason specimens requiring a lower amount of fracture work should be tested in a less powerful machine. Impact machines in which the height of pendulum lift, and, therefore, the energy of impact can be controlled, are more convenient in operation.

With A_n being known, the impact strength is found from the formula

$$a_n = A_n/F \text{ kgf m/cm}^2$$

where F is the cross-sectional area of a specimen at the place of notch, cm^2 .

In this formula, the work of fracture A_n is related to the area of the notched cross section of the specimen, while the impact of the pendulum is absorbed not by this area, but by a definite volume around the notch in which deformation occurs. The greater the deformed volume, the better the metal disperses deformation, and, therefore, the greater the impact strength.

The impact strength reduces with increase in metal strength (if its plasticity is simultaneously impaired). In engineering calculations, however, the following important peculiarity of variations of toughness must be taken into consideration. A definite cross-sectional volume of an article (or specimen) resists impact fracture, although to different extents. In torsion or bending, however, the highest stresses are formed only in the surface layer, whereas the core remains almost non-loaded. This is why work-hardening by surface treatment, induction heating, cold deforming or, to a smaller extent, by chemical heat treatment, hardly affects toughness (except for articles of a small cross section).

It would be more appropriate to relate the work of fracture to a unit of deformed volume but this volume is very difficult to determine experimentally. Because of this, impact strength is calculated in a simple conditional way by dividing the work of fracture A_n by the cross-sectional area at the place of fracture. The determination can also be reduced to measuring the work of fracture of a standard specimen, without relating it to the cross-sectional area.

The work of fracture of low-plastic materials (in particular of steels with a hardness number higher than 55 HRC) when determined on notched specimens is low in absolute magnitude, and, usually, does not exceed the scatter of results obtained when

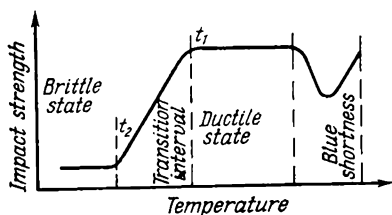


Fig. 6.13. Testing of impact strength as a function of temperature

impact strength tests are used to determine the cold shortness of metals, i.e. the temperature point below which a tough metal becomes brittle (Fig. 6.13).

With decrease in temperature, a gradual reduction in impact strength is first observed, which thus drops to its lowest value and then remains unchanged with further reduction of temperature. Temperatures t_1 and t_2 (see Fig. 6.13) are respectively called the upper and the lower limits of brittleness, or cold shortness limits.

The transition into the brittle state causes a change in the nature of fracture, and, therefore, in the form of break. For annealed structural steel, the break at the upper temperature limit t_1 shows visually (see Ch. 2) ≥ 90 per cent of a tough component (fibrous fracture), whereas a break at the lower limit t_2 shows approximately 90 per cent of the brittle component. A. P. Gulyaev has proposed to use this phenomenon for more accurate determination of the temperature limits t_1 and t_2 . However, this method is inapplicable for structural steels with an increased hardness (above 45-50 HRC) and for steels containing more than 0.6 per cent C; in such steels the zones of the tough and brittle components are poorly discernible, since they often are located together within a single or a few grains.

The upper temperature limit of brittleness of some steels may be above 0°C , because of which tests are often conducted within a temperature range from $+50^\circ\text{C}$ (or even $+100^\circ\text{C}$ for some high-carbon alloy steels) to -60°C , if the metal is to be employed under conditions of atmospheric temperature variations. Specimens are tested at different temperatures at intervals of 20-25 degrees C. When a given temperature is attained, the specimen is immediately subjected to a fracture test. The impact testing machine is provided with a thermostat and a cooler (in the simplest form: a reservoir with a mixture of alcohol or gasoline and solid carbonic acid). The interval between attaining the specified temperature and testing a specimen should not exceed 10-15 s.

testing a series of plastic steel specimens. For this reason unnotched specimens are used when testing brittle metals.

In dynamic tests, impact strength varies with decrease in temperature (i.e. when viscous fracture changes to a brittle one), to a greater extent than the properties determined from static tests. This is why

The dynamic tests discussed above reduce to determination of the total work of impact fracture, i.e. the resistance of a metal to the formation and development of cracks. The work of fracture is, however, defined as the work spent for the formation (A_f) and propagation (A_p) of a crack. These components of the total work of fracture must be known in many cases in order to characterize more reliably the behaviour of the metal under conditions of dynamic loading.

6.5. FRACTURE TOUGHNESS TESTS

Some materials, especially high-strength ones, which are not brittle under relatively moderate conditions of loading, may become brittle through the action of a number of factors: the presence of cracks or notches, a biaxial or three-dimensional stressed state, a reduced temperature, etc.

The impact strength (a_n) and the unit work of propagation of a crack ($a_{c.i}$)¹ do not characterize to a sufficient degree the tendency of a structural material to brittle fracture. This, in the first place, is linked with the fact that a_n and $a_{c.i}$ are the characteristics of fracture resistance of a particular specimen under the given laboratory conditions of loading; secondly, the impact strength a_n is an integral characteristic which includes the energy of crack formation and that of crack propagation, whereas cracks are always present in a real metal, so that no energy is required for their formation; and, thirdly, a_n and $a_{c.i}$ can only be used as control characteristics, rather than the working parameters that guarantee fracture safety.

The toughness of metals can be more fully characterized by fracture toughness tests. The results of the tests are used to construct fracture diagrams showing how the length of a crack increases depending on the stress applied (or the number of load cycles), after which the fracture toughness is calculated. Fracture toughness can be characterized by the coefficient of stress intensity K (kgf/mm^{3/2}) at the end of a crack or by force G (kgf/mm or kgf m/cm²) required to propagate a crack per unit length. Coefficients K and G are related by the relationships $G = K^2/E$ for a plane stressed state, when the stress over the thickness of the specimen is zero and fracture occurs through

¹ $a_{c.i}$ characterizes the work of propagation of a crack. It is determined on specimens $10 \times 10 \times 55$ mm having a V-shaped notch 1.5 mm deep, with a fatigue crack 1-2 mm deep being specially formed in the metal under the notch (by cyclic loading at a frequency of 300-400 cycles per minute). $a_{c.i} = A/F$, where A is the work of fracture, kgf m and F is the net cross-sectional area at the point of the notch and crack, cm².

shear, the plane of break making an angle of approximately 45 degrees with the plane of the specimen, or $G = K^2 (1 - \mu)^2 / E$ for conditions of plane deformation, where μ is Poisson's ratio. In the latter case the plane of break is perpendicular to the surface of the specimen, the deformation over the thickness is zero, and fracture occurs through rupture.

In a stressed cracked specimen, a local increase of tensile stresses forms at the end of the crack (Fig. 6.14):

$$\sigma = \frac{K}{\sqrt{2\pi r}} \cos \frac{\theta}{2} \left(1 + \sin \frac{\theta}{2} - \sin \frac{3}{2} \theta \right)$$

On the X axis, $\theta = 0$, and therefore, $\sigma = K / \sqrt{2\pi r}$.

It can be seen that the field of tensile stresses at the end of the crack is determined only by the magnitude of K which may be termed the coefficient of intensity of the rise of tensile stresses at the end of a crack, or simply, the coefficient of stress intensity. It is independent of r and θ and is a constant of the material. It can be determined experimentally by testing standard specimens.

For specimens of infinite dimensions $K = \sigma \sqrt{\pi l}$ (l is the half-length of the crack) and for specimens of a finite width $K = y \sigma \sqrt{\pi l}$, y being a correction for the finite width, which is found by analysing the stresses for each type of specimen.

Spontaneous fracture occurs as K attains a definite critical magnitude owing to slow growth of the crack, this critical limit being in turn determined by the critical length l_{cr} and by the stress acting in the specimen.

The critical value of K for a plane stressed state is denoted K_c , and that for plane deformation, K_{Ic} .

The tests are made on specimens having a central crack (Fig. 6.15). For this purpose, a notched hole is made in a specimen and after that two fatigue cracks are formed at the sides of the hole by applying load to the specimen. To obtain reliable values of fracture toughness, the length of the plastic zone at the end of a fatigue crack must be less than that formed in subsequent rupture (when K_{Ic} is being determined) and the path covered by a crack before passing into the supercritical stage (when K_c is being determined) must be as small as possible. This is achieved by properly selecting the maximum tensile stress of the cycle, which must not exceed 0.5σ and be such that a crack $0.3W$ long (where W is the width of the specimen) will be formed after 20,000-30,000 loading cycles.

The specimen with a fatigue crack formed in it is subjected to tension with a large electric current being simultaneously pas-

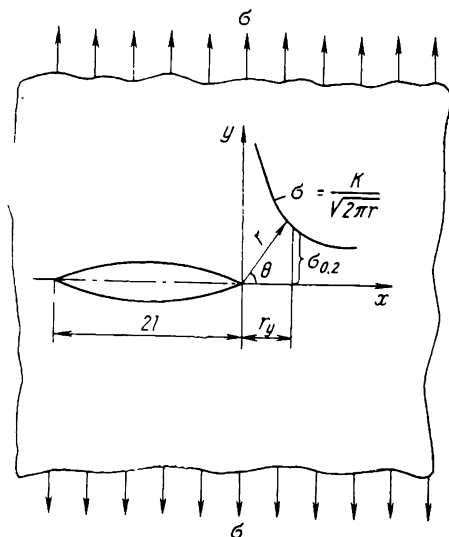


Fig. 6.14. Stress distribution at the end of a crack in an infinite-length plate under the action of tensile stresses

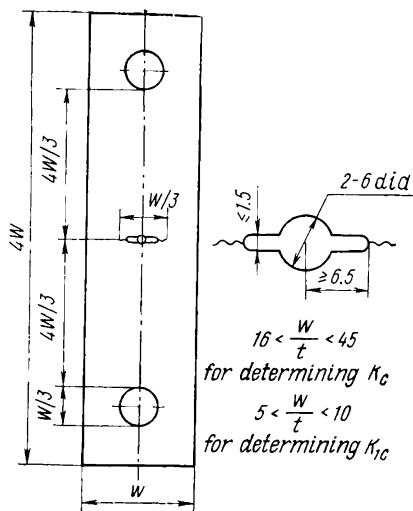


Fig. 6.15. Specimen with a central crack for testing fracture toughness in tension

sed through it. With the load applied, the crack begins to grow, because of which the potential difference between its edges increases.

To record the curve of crack growth as a function of load, measurements are made of the potential difference and the displacement (opening) of the crack between two fixed points positioned on each side of the notch on the axis of the specimen. As the crack grows, the potential difference increases (provided that the current is kept constant). The diagram of a testing apparatus is shown in Fig. 6.16. A current of 40 A is supplied to points A and B from the rectifier.

The signal formed is supplied via a photo-amplifier 116/2 dia to an XY-recorder type ПДС-021; the second input of the instrument is fed via a tensometric amplifier with a signal from a load cell which measures the load on the specimen.

The record is decoded by means of a calibration curve in the coordinates crack length *versus* signal (ΔE). The calibration curve for specimens whose dimensions are proportional to those of the specimen shown in Fig. 6.15 is given in Fig. 6.17, with the potential difference between points A and O being laid off along the axis of ordinates (as a percentage of the voltage across the specimen).

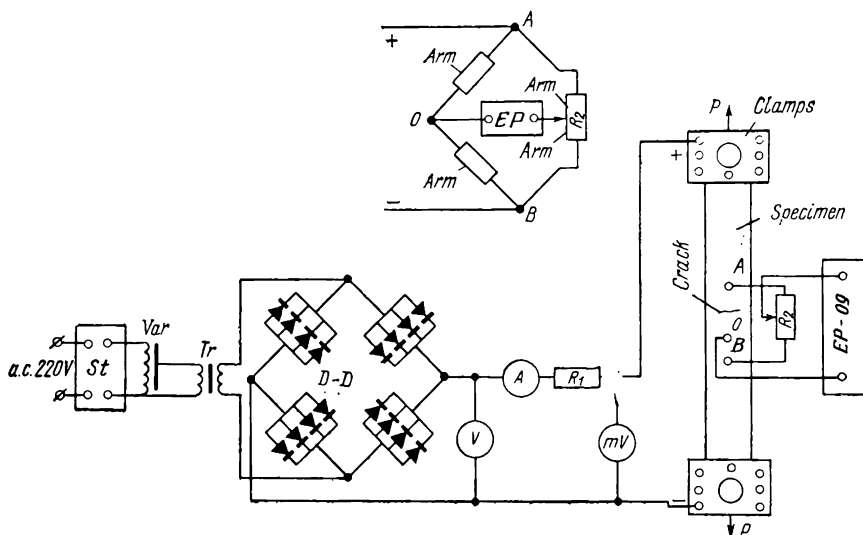


Fig. 6.16. Circuit of apparatus for recording potential difference-load diagram. *St*—voltage stabilizer; *Var*—variator; *Tr*—transformer; *R*₁—constant resistance (0.5 ohm); *R*₂—constant resistance (500 ohms); *D-D*—diodes (type Д242А); *V*—voltmeter (up to 100 V); *A*—ammeter (up to 40 A); *mV*—millivoltmeter (up to 20 mV); *EP*—electronic potentiometer

With this method of recording, the specimen must be insulated from the testing machine which is the 'earth' relative to it. Current-conducting contacts are located at a suitable distance from the edges of the crack, so that small positional variations have no effect on the measurement results. The contacts are placed as close as possible to the end of a crack in order to ensure the maximum sensitivity at the initial moment of crack development.

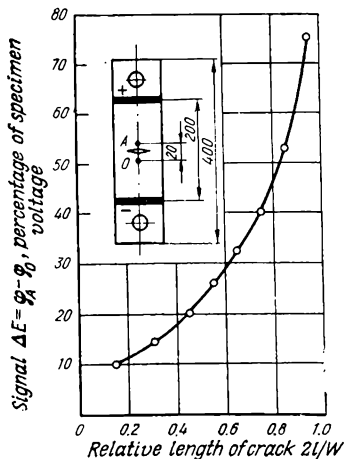


Fig. 6.17. Calibration curve to recalculate potential difference into crack length (for specimens having a through crack)

The displacement is measured by a special sensor made in the form of an elastic bracket which deforms as the notch and crack open. A resistance sensor (Fig. 6.18) is glued onto this sensor and the two are connected into a bridge circuit. The appropriate sensitivity of the sensors must be combined with a high linearity of their output signals

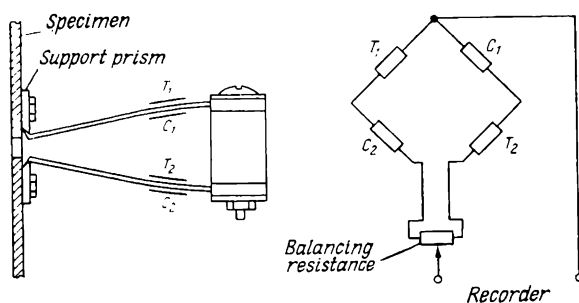


Fig. 6.18. Construction and mounting of sensor to measure displacements

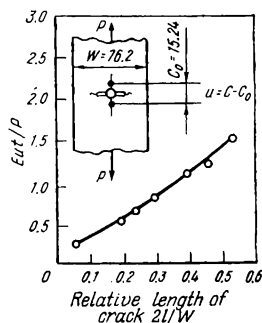


Fig. 6.19. Calibration curve to convert displacement into crack length

caused by displacements of the datum points. The sensor is fixed by means of small support prisms screwed to the surface of the specimen along the axis, on each side of the cracked notch. The length of the crack for the given load is then determined from a calibration curve (Fig. 6.19) constructed with the use of calibrating specimens having slots of different length and subjected to elastic stresses. This calibration curve is applicable to any specimen, provided its dimensions and the base of the sensors are proportional to a standard calibrating specimen.

Fracture toughness can then be calculated by using:

(a) Irwin's correction which ensures an accuracy of 5 to 7 per cent:

for the plane stressed state

$$K_c = \frac{P_c}{Wt} \sqrt{\pi l_c} \sqrt{\frac{W}{\pi l_c} \tan \frac{\pi l_c}{W}} = \frac{P_c}{Wt} \sqrt{W \tan \frac{\pi l_c}{W}}$$

for the plane deformed state

$$K_{lc} = \frac{P_c}{Wt} \sqrt{\frac{W \tan \frac{\pi}{Wt} l_c}{1 - \mu^2}}$$

(b) Forman — Kobayashi correction which makes it possible to calculate fracture toughness for plane stressed and plane deformed states with an accuracy of up to 1 per cent for crack lengths not exceeding $0.6 W$:

$$K = \frac{P_c}{Wt} \sqrt{\pi l_c} \left[1 - 0.1 \left(\frac{2l_c}{W} \right) + \left(\frac{2l_c}{W} \right)^2 \right]$$

where $2l_c$ = critical length of the crack, mm, at the moment the load of the specimen attains its critical value, P_c , kgf
 W and t = width and thickness of specimen, respectively, mm

In calculations of K_c and K_{Ic} , a correction for the zone of plastic deformation at the end of the crack is added to the actual crack length $2l_c$. For the case of plane deformation $r_{1y} = \frac{1}{6\pi} \left(\frac{K_{Ic}}{\sigma_{0.2}} \right)^2$, and for the case of plane stressed state $r_y = \frac{1}{2\pi} \left(\frac{K_c}{\sigma_{0.2}} \right)^2$.

The calculation of K_c is made by the method of successive approximations, i.e. K_c is calculated for the actual half-length of crack l_c . Correction r_y is then found for the value of K_c thus determined, this correction being added to l_c and a new value of K_c calculated for the crack length of $(l_c + r_y)$. To find K_c , three or four successive calculations are usually needed, while K_{Ic} can be found in a single calculation.

The calculations of K_c and K_{Ic} by the formulae of linear mechanics of fracture will be correct when no macroplastic creep occurs in the critical cross section of the specimen, i.e. when the stress in the net cross section $\sigma_{net} = P_c/t(W - 2l_c)$ does not exceed $0.8 \sigma_{0.2}$.

If this condition is not observed, the critical crack length $2l_c$ and the rupture stress $\sigma_c = P_c/Wt$ are determined, which are important characteristic parameters of materials.

The magnitude of K_{Ic} is taken as the coefficient of stress intensity at which the length of a crack increases by 2 per cent against its initial length. The corresponding load, found from the displacement-load or potential difference-load diagram, is substituted into the formulae for calculation of K_{Ic} . The magnitude of K_{Ic} is assumed to be correct when the thickness of the specimen and the initial length of the crack are greater than $2.5 (K_{Ic}/\sigma_{0.2})^2$.

6.6. LOW-TEMPERATURE TESTS

The behaviour and mechanical properties of many metals and alloys at low temperatures differ from those determined at $+20^\circ\text{C}$. The lowered temperature, in the first place, causes an increase in the resistance to the development of plastic deformation, and, therefore, an increase in strength. In addition, an appreciable localization of plastic deformation is observed at low temperatures; the number of the acting crystallographic system of slip may also change, and the mechanism of the development of plastic deformation may change from slipping to twinning. In this connection the adverse effect of large grains and impurities

in metals on their plasticity and toughness increases at low temperatures.

These properties are impaired especially strongly in metals possessing volume-centred cubic lattice (which confirms the existence of a cold-brittleness limit in such metals). In metals having face-centred lattice, these properties either reduce very slowly or even remain at the same level as at 20 °C.

For these reasons, direct measurements of mechanical properties are required for metals used in containers for liquefied gases, shells of rockets and spaceships, elements of refrigerators, and the like.

Low-temperature tests are carried out by the same methods and in similar machines as at 20 °C, but the testing machines are additionally provided with cryostats to cool specimens down to helium temperatures (—269 °C).

Cryostats used for cooling to moderate temperatures (—70 °C) are well insulated chambers containing a mixture of solid carbonic acid and acetone or provided with tube coils in which liquid nitrogen circulates.

In cryostats operating at lower temperatures (down to —196 °C), the specimen is brought into direct contact with liquid nitrogen supplied into the working space; the apparatus has double walls with the space between them being evacuated to provide better thermal insulation.

In tests at still lower temperatures (liquid hydrogen, —253 °C or liquid helium, —269 °C), the specimen is in direct contact with the respective liquefied gas, and liquid nitrogen circulates between the walls for thermal insulation of the cryostat.

In tensile tests, the cryostat is fastened to the fixed traverse of the testing machine, and the working space of the cryostat, in which the specimen is placed, is carefully hermetized.

Specimens used in the tensile tests may be smooth, notched or of special shape (for fracture toughness tests).

In fracture toughness tests, specimens after cooling are quickly placed in the testing machines and immediately subjected to fracture. To prevent their heating, the specimens are placed in paper bags and then into the cryostat and tested without removing these bags.

6.7. TESTS AT HIGH TEMPERATURES. DETERMINATIONS OF CREEP CHARACTERISTICS

Determinations of mechanical properties of metals on heating differ basically from those made at 20 °C. This is linked with the fact that slow plastic deformation is possible within the range

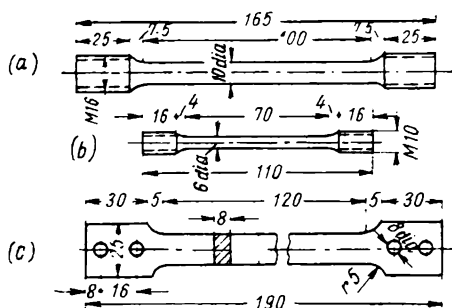


Fig. 6.20. Standard specimens for tensile tests at high temperatures

(a) cylindrical specimen of standard size; (b) cylindrical specimen of reduced size; (c) rectangular cross-section specimen

of temperatures near or just above the point of the recrystallization beginning (the metal 'creeps'). These temperatures are 300-450 °C for steels, approximately 100 °C for aluminium alloys, and roughly 300 °C for titanium alloys.

The strength properties determined under conditions of long-term loading, i.e. on heating under operational conditions, are usually lower than those determined by common

tests of mechanical properties, with short-term loading, this reduction being more pronounced with a long time of loading and a high temperature of testing. Besides, it must be taken into account that a long-term loading and very high stresses can cause a metal to creep even at normal temperature of 20 °C (called cold creep).

The mechanical properties of plastics depend more on the time of loading, even at normal temperatures, than those of metals. In addition, these materials can deform at stresses substantially lower than their yield limit or ultimate strength.

Short-term tests at high temperatures. These tests are usually tensile ones in usual testing machines additionally provided with a heating furnace. The tests are made on structural and tool steels used in machine elements and tools which can be subjected to high temperatures for very short periods during operation.

The test specimens may be round or rectangular (Fig. 6.20); the ends of round specimens are threaded for fastening in the clamping devices of the machine. Specimens are fastened in the furnace of the machine and heated to the required temperature.

The test results can be substantially affected by the rate of load application and the holding time of specimens under load at the test temperature. The effect of these factors becomes greater when heating above the indicated temperatures. Because of this the tests are carried out after a certain holding of a specimen (30 to 60 minutes) at the specified temperature. The rate of unloading (for specimens not subjected to fracture) has only a slight effect on the test results.

The characteristics of strength and plasticity are determined in the same way as in common tensile tests. A stress-elongation diagram is constructed to determine the conditional yield limit, proportionality limit, and elasticity modulus.

Creep tests (long-term tests at high temperatures). The strength properties of a metal in long-term loading are appreciably lower than those determined in short-term tests (Table 6.2).

Table 6.2. Mechanical Properties of Some Steels at High Temperatures

Steel grade	Ultimate strength σ_b determined by short-term tests, kgf/mm ²			Creep limit (for total deformation of 1%) in tests during 10,000 h, kgf/mm ²	
	20 °C	600 °C	700 °C	600 °C	700 °C
4X10C2M	90	30	6	6	1
4X14H14B2M	104	56	37	12	4.5
4X18H25C2	108	56	36	8	3

The development of plastic deformation (creep) in long-term loading can be strongly dependent on testing conditions.

With an increased test time, the process of deformation of a metal can either occur at a low rate or, on the contrary, accelerate rapidly up to fracture, depending on the load, temperature, and the metal properties (Fig. 6.21).

Creep characteristics can be determined in tension, torsion, bending or a complicated stressed state, the tensile tests being used most often.

Test specimens are shown in Fig. 6.20. It is recommended¹ to use cylindrical specimens 10 mm in diameter with a gauge length of 100 or 200 mm or rectangular specimens 15 mm wide with a gauge length of 100 mm.

The tests can be made: (a) at a constant temperature and constant stress (isothermic method); (b) at a variable temperature and constant stress (dilatometric method); (c) at a constant temperature and variable stress (relaxation method), the isothermic method being used more often.

Creep tests can determine the stresses needed to cause: (a) a uniform (stable) creep rate (section *cd* of curve *B* in Fig. 6.21);

¹ Methods of tensile creep tests are specified in the USSR State Standard GOST 3248-60.

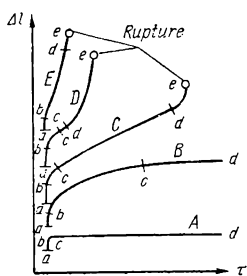


Fig. 6.21. Creep curves

(b) a definite total deformation during a specified time interval; or (c) no deformation (the theoretical creep limit).

Generally, the conditional creep limit is found, i.e. the stress that causes a specified (total or residual) elongation or a specified creep rate on the straight section of the creep curve. For this purpose the test results are often presented in the coordinates: relative elongation against time or stress against average creep rate on the straight section (in logarithmic coordinates). In the

latter case the duration of the tests must be not less than 2000-3000 hours and the linear section, not shorter than 500 hours. The creep limit is usually determined with allowances for elongation of 0.1-1 per cent and the test duration of 100, 300, 500 and 1000 hours; in some tests a different duration and other values of allowance are required. The results obtained in tests of duration of 1000 hours are sometimes extrapolated to obtain a longer duration of operation for an article, but this method is not reliable, since the actual rate of creep in the longer operation can differ from the extrapolated value owing to structural transformations in the metal.

Because of the long duration of tests, the dependence of results on relatively small variations in temperature and the necessity of measuring very small deformations, creep tests are made with the use of special testing machines and high-precision instruments. The accuracy of instrument readings in deformation measurements is ≥ 0.002 mm.

Creep tests are made as follows. A specimen is heated and held at the specified temperature for at least 60 minutes, after which it is loaded gradually with a preliminary load equal to approximately 10 per cent of the total load specified (but so that the stress formed by it can be not higher than 1 kgf/mm^2) and a strain gauge is connected to the specimen. If the instrument readings remain stable for at least 5 minutes, the specimen is gradually loaded up to the specified load. Fracture of specimens is not practised, as a rule, and the deformation diagram plotted by the test results has only two sections: the initial curvilinear section and the subsequent section which is almost linear. After the tests the specimen is unloaded and its residual elongation is measured.

The conditional creep limit is determined as follows:

(a) four or more specimens are tested at different stresses and the specified temperature;

(b) using the initial creep curves thus obtained, diagrams are constructed of the relationship between the stress and total elongation (or between the stress and average uniform rate of elongation on the linear section in logarithmic coordinates);

(c) the sought-for stress is found on the diagram by interpolation.

Such tests are carried out at least for three different temperatures and the results obtained are used to construct a temperature-stress diagram.

For a full characteristic of materials intended for operation at high temperatures, the 'long-term strength' is often determined in addition to the creep limit.

The 'long-term strength' characterizes the fracture resistance of a material under long acting constant load with various (specified) loading modes: tension, bending, or torsion, and usually at a constant temperature (the isothermic method).

Tests of commercial grades of metal are made on cylindrical specimens 5 or 10 mm in diameter with threaded ends; sheets and strips are tested on rectangular specimens 15 or 10 mm wide (and of respective thickness).

The results of isothermic tests are usually represented graphically in the coordinates: $\log \sigma_D$ (σ_D being the stress causing fracture) against $\log \tau_D$ (the time before fracture at the given stress) or σ_D against $\log \tau_D$. The $\log \sigma_D - \log \tau_D$ relationship is linear for relatively short tests, and the $\sigma_D - \log \tau_D$ is linear for longer tests also.

Chapter Seven

DETERMINATION OF HARDNESS OF MATERIALS¹

7.1. GENERAL CONSIDERATIONS

Hardness measurements are widely used in laboratory and industrial tests as a tool characterizing the mechanical properties of metals. As will be shown below, they have a number of advantages over the other methods of determining the mechanical properties of metals, already discussed in Ch. 6.

Hardness is determined by locally stressing the surface of a tested metal by means of a ball, cone, pyramid or needle made of a non-deformable material (hardened steel, hard alloys, diamond, or sapphire).

There are a number of methods for determining hardness, depending on the type of this stressing: by indenting (indentation test), by scratching (scratch hardness test), by impact (dynamic hardness test), or by the rebound of a falling ball (rebound test). The hardness determined by scratching characterizes the resistance of a metal to fracture (which occurs by shear in most metals); the hardness found by the rebound test characterizes the elastic properties of a metal; and the hardness found by the indentation test, the resistance to plastic deformation.

Of these methods, the indentation test is employed the most. It essentially consists in indenting an end-piece into the surface layer of a metal with an appreciably high force, so that the metal under and near the indenter undergoes plastic deformation and an indent is left in the surface on removing the force. A feature characteristic of this deformation is that it occurs only in a small volume surrounded by undeformed metal. Under such conditions, which are similar to non-uniform three-dimensional compression, mainly shear stresses are formed, and the tensile stresses that can be formed are substantially lower than in the other types of mechanical test (tension, bending, torsion or compression). For this reason, indentation test can cause plastic deformation not only in plastic metals, but also in such metals as, cast iron, which

¹ This chapter was written in collaboration with G. I. Pogodin-Alekseev.

in the common mechanical tests (tension, compression, torsion or bending) exhibit brittle fracture without any macroscopically noticeable plastic deformation.

Thus, the hardness of a metal is its resistance to plastic deformation and is its mechanical property which is different from its other mechanical properties in the method of measuring. Ya. B. Fridman proposed to consider hardness measurements as "local mechanical tests of surface layers of a material".

The advantages of hardness measurements are:

1. The hardness of a plastic metal determined by the indentation test is related by definite relationships with its other mechanical properties (in particular, with the ultimate strength).

The value of hardness can characterize the ultimate strength of metals which undergo local plastic deformation (formation of a 'neck') in tensile tests, such as steels (except for those having austenitic or martensitic structure) and many non-ferrous alloys. This plastic deformation is similar to the local deformation in the surface layers of a metal in the indentation test.

This relationship is not observed for brittle materials which show no noticeable plastic deformation in tensile tests (or compression, bending, or torsional tests), but undergo plastic deformation in indentation tests. In some cases, however, a qualitative relationship between the ultimate strength and hardness can be established for such metals too (for instance, for grey irons); a higher hardness is usually linked with a higher value of the ultimate compressive strength.

Hardness numbers may also be used to determine some plastic properties of metals.

A hardness number found by the indentation test can also characterize the endurance limit of some metals, in particular of copper, duralumin and annealed steels.

2. Hardness measurements are substantially simpler than the mechanical tests for determining the strength, plasticity or toughness. They need no specially prepared specimens and can be made directly on articles by simply preparing a smooth flat area on the surface of an article, or sometimes even without such preparation. The articles being tested are not destructed and can be used for their direct purpose.

Hardness measurements can be made quickly; for 30-60 s when using a cone indenter or 1-3 min when using a ball.

3. Hardness tests are usually non-destructive, i.e. are not linked with spoilage of an article being tested, so that the latter can be used for its direct purpose, whereas the determinations of strength, plasticity and toughness are always based on using specially made specimens.

4. Hardness can be measured on articles of small thickness and in very thin layers (a few tenths of a millimetre in some hardness tests) or in microscopic volumes of a metal (microhardness tests). This is why some hardness tests can be used to evaluate the structure and properties of various metal layers in an article, for instance, the hard surface layer of cemented, nitrated or hardened steel. The microhardness test makes it possible to determine the hardness of individual components in alloys.

Hardness tests, as being non-destructive, can be used for complete inspection, i.e. for checking all the articles produced, whereas other mechanical tests can be employed for sampling inspection only.

There are two principal types of indentation hardness test: macrohardness (or simply hardness) test and microhardness test.

The macrohardness (hardness) test is characterized by the fact that an indenter penetrates an appreciable depth into the tested material, depending on the force applied and the properties of the material. In some tests the indenter may be a large one, for instance, a steel ball up to 10 mm in diameter, as a result the deformed volume includes all the phases and structural components of the alloy, their amounts and location being characteristic of the bulk of the metal. The measured hardness number then represents the hardness of the tested material as a whole.

The shape and size of the indenter and the magnitude of the force applied are selected in accordance with the purpose of the test, the structure and supposed properties of the metal being tested, the state of its surface, and the size of the specimen.

With metals having a heterogeneous structure with large inclusions of individual structural components (for instance, grey iron or non-ferrous bearing alloys) hardness tests should be performed with a large-size ball. If, however, the metal has a homogeneous fine structure, then even very small volumes can be sufficiently representative of the bulk of the metal as regards its hardness. In such cases indentation tests may be made with a smaller indenter, for instance, a diamond cone or pyramid, pressed to a lower depth, and therefore, with a lower force.

The last requirement is indispensable for measuring the hardness of hard materials, for instance, hardened or low-tempered steels, since pressing a steel ball or diamond cone with a high force might deform the ball or crush the diamond.

On the other hand, too small a force is undesirable, since this would sharply reduce the volume deformed and might give a hardness value not characterizing the whole bulk of the metal.

Therefore, the magnitude of the force applied and the diameter of the indenter (and hence, the indentation produced) must be properly selected within an optimum range for a given material.

Microhardness tests are made to determine the hardness of individual grains, phases and structural components in alloys (but not an 'averaged' hardness, as is the case with hardness tests). In this case the volume deformed through indenting should be smaller than the volume (or area) of the grain to be tested. For this reason, a light force is applied to the indenter. In addition, microhardness tests may be used to measure the hardness of very small articles.

With plastics, hardness tests give less information on their mechanical properties, since the relationship between their hardness and strength is not so determinate as with metals. The results of hardness tests of plastics can only serve as a supplementary characteristic of their properties.

Hardness measurements can be strongly affected by the state of the surface of the material being tested. With a curvilinear or rough surface, its various portions will participate to a different extent in the resistance to indentation and in deformation, which may result in an error of measurement.¹ The lower the indentation force, the more carefully the surface to be tested must be prepared. Hardness tests are usually made on a ground plane, and microhardness measurements, on a polished plane (in the latter case, work-hardening of the surface layer should be avoided).

The plane for hardness tests should be placed horizontally, i.e. perpendicular to the indenter axis. The opposite face of the specimen should be made parallel with the upper face and freed of scale, since this might be crushed during the test and cause an error in measurement.

7.2. BALL INDENTATION HARDNESS TEST (BRINELL HARDNESS TEST)

This method is used for measuring the hardness of metals and plastics.

The method consists in indenting a steel ball, the hardness number being determined by the area of the indent formed by the ball, and the force of indentation applied by means of a press or controlled hydraulically or by counterweights moved by an electric motor.

¹ For spherical surfaces, a correction can readily be calculated for a given radius of specimen.

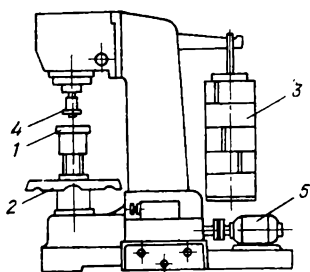


Fig. 7.1. Brinell hardness tester

1—stage for centring a specimen;
2—handwheel; 3—weights;
4—ball indenter; 5—electric motor

The specimen (article) to be tested is placed, its ground face upwards, on stage 1 in the lower portion of the fixed stand of a press (Fig. 7.1). By manually rotating handwheel 2 clockwise, the stage is raised so that the ball can indent the surface being tested. In electrically controlled testers, first, handwheel 2 is rotated manually to bring the ball into contact with the surface, electric motor 5 is then switched on to move a lever with counterweights and thus gradually indent the ball. The load is applied for a specified time, usually 10 to 60 s, depending on the hardness of the material being

tested (see Table 7.1), after which the load is removed by rotating the motor in the opposite direction. After automatically stopping the motor, handwheel 2 is rotated counterclockwise to lower the stage, and the specimen is removed. The time of load application can be varied by controlling the time relays of the motor.

After the test, a spherical imprint (indent) is formed in the specimen. The diameter of the indent is measured by using a magnifying glass having a scale graduated in 0.1-mm divisions. The indent diameter is measured to an accuracy of up to 0.05 mm (for a ball indenter 10 or 5 mm in diameter) in two perpendicular directions, the hardness number being found from the mean of these two values.

In some hardness testers (briviscopes), the indent is projected magnified on a screen, where its diameter may be measured by a scale.

In hardness tests, the distance from the centre of an indent to an edge of a specimen should be not less than two indent diameters, otherwise the results can be distorted owing to the 'bulging' of the specimen edge. Each next indent should be made at a distance not less than two diameters from the previous one. The Brinell hardness number is found as the ratio of the load applied to the area of the indent:

$$HB = \frac{P}{F} = \frac{P}{\frac{\pi D}{2} (D - \sqrt{D^2 - d^2})}$$

where P = load applied to the ball, kgf

F = indent area, mm²

D = ball diameter, mm

d = indent diameter, mm

All other things being equal, the hardness number is determined by the indent diameter d , the latter being smaller for a higher hardness of the tested material.

Certain conditions must be observed, however, in order to obtain a constant relationship between the load and indent diameter, which is needed for accurate determination of the hardness. If the ball is indented to different depths, i.e. with a different force, in one and the same material, there will be no similarity between the indents obtained. The highest deviations are observed when the ball is indented with a small force and makes the indent of small diameter, or on the contrary, with a very large force, so that the diameter of the indent is close to that of the ball. To avoid such deviations Brinell tests are usually made with a constant ratio between load P and the square of ball diameter D^2 , this ratio being different for soft and hard metals. The deformation of the metal in its different portions under the ball is not the same, and the resulting non-uniformity of the stressed state increases with increase in the area of the indent, i.e. with increase in the force.

The indentation process causes both plastic deformation of the metal being tested and elastic deformation of the indenter ball, the latter deformation being rather high when testing hard materials; this can cause an error in the measured results. Therefore, the Brinell hardness tests are limited to the testing metals of low and medium hardness (for steels not higher than 450 HB).

A certain effect can also be produced by the time the force is applied to the ball. Low-melting metals (lead, zinc, babbittes, etc.), which have a low temperature of recrystallization, can undergo plastic deformation not only at the moment of indenting, but also for a certain time after the load has been removed. With increasing the load application time, the plastic deformation of these metals becomes practically stabilized.

For metals having a high melting point, the effect of the load application time is insignificant, thus a test can be accomplished in a shorter time (10-30 s).

Brinell hardness tests are standardized by the USSR State Standard GOST 9012-59 (Table 7.1).

The hardness of plastics and their strength depend to a large extent on the load application time.

When measuring hardness by indenting a ball of a definite diameter and with a specified load being applied, there is no need to make a calculation by the formula given above. In practice, hardness number tables are used (see Appendix I) which give Brinell hardness numbers HB depending on the indent diameter and the ratio between load P and indent area F . Brinell

Table 7.1. Brinell Hardness Test Conditions

Metals /	HB hard- ness number	Specimen thickness, mm	P to D^2 ratio	Ball diameter D , mm	Load P , kgf	Time of load appli- cation, s
Ferrous	140-450	6.3	$P = 30D^2$	10	3000	10
		4.2		5	750	10
		< 2		2.5	187.5	10
Ferrous	≤ 140	> 6	$P = 10D^2$	10	3000	10
		6.3		5	250	10
		< 3		2.5	62.5	10
Non-ferrous	≥ 130	6.3	$P = 30D^2$	10	3000	30
		4.2		5	750	30
		< 2		2.5	187.5	30
Non-ferrous	35-130	9.3	$P = 10D^2$	10	1000	30
		6.3		5	250	30
		2.3		2.5	62.5	30
Non-ferrous	8-35	> 6	$P = 2.5D^2$	10	250	60
		6.3		5	62.5	60
		< 3		2.5	15.6	60

hardness HB is sometimes written with the load and ball diameter being indicated.

The following approximate relationships were found for the ultimate strength and the corresponding HB number of various metals:¹

Steel with Brinell hardness:

120-175 HB $\sigma_b \approx 0.34$ HB

175-450 HB $\sigma_b \approx 0.35$ HB

Copper, brass, bronze:

annealed $\sigma_b \approx 0.55$ HB

work-hardened $\sigma_b \approx 0.40$ HB

Aluminium and aluminium alloys

with Brinell hardness:

20-45 HB $\sigma_b \approx (0.33-0.36)$ HB

annealed duralumin $\sigma_b \approx 0.36$ HB

duralumin after hardening and

ageing $\sigma_b \approx 0.35$ HB

¹ Minkevich, N. A., *Zhurnal Russkogo metallurgicheskogo obshchestva*, 1912.

According to M. P. Markovets, by measuring the area of an indent, F_{ind} , and the area of its projection, F_{pr} , it is possible to characterize the plasticity of a steel by the formula

$$\psi_{ind} = \frac{F_{ind} - F_{pr}}{F_{ind}}$$

The value of ψ_{ind} has definite relationship with relative reduction ψ (per cent).

A less explicit relationship exists between Brinell hardness and endurance limit of metals. A relatively simple relationship was established only for alloys in the equilibrium state (after annealing), for which the endurance limit determined by alternate bending test of a rotating specimen (having no sharp changes of cross section and no decarbonized surface layer) can be characterized as follows:

Copper	0.15 HB
Duralumin	0.12 HB
Steel with 0.2 per cent C . .	0.15 HB
Steel with 0.45 per cent C . .	0.15 HB
Steel with 0.77 per cent C . .	0.12 HB

These results correspond to the relationship according to which the endurance limit is approximately $0.5 \sigma_b$.

The endurance limit cannot be determined with sufficient accuracy by the Brinell hardness numbers for steel after hardening, tempering or normalization, aged duralumin, and metals in a cold-deformed state.

The indentation test with the use of a steel ball has only a limited application. It is unsuitable for (a) materials with HB numbers higher than 450; (b) measuring the hardness of thin surface layers (less than 1-2 mm thick), since the ball breaks through this layer and penetrates into the softer metal. The thickness of the hard surface layer should be at least ten times greater than the depth of indent.

7.3. HARDNESS MEASUREMENT BY INDENTING A CONE OR BALL (ROCKWELL HARDNESS TEST)

This test differs principally from the previous one in the fact that hardness is determined in terms of the depth of an indent produced by a diamond cone or steel ball, rather than by the indent area.

The advantage of this method over the Brinell one is that the force of indentation can be varied within a wide range without

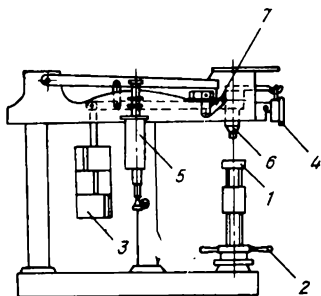


Fig. 7.2. Rockwell hardness tester

1—stage for mounting a specimen; 2—handwheel; 3—weight; 4—dial; 5—oil regulator; 6—rod with a diamond cone (or steel ball); 7—handle

influencing the hardness value, since the indentation of a cone obeys a similarity law, while the deformation conditions under the end of the cone remain constant with increase in pressure.

A Rockwell hardness tester (Fig. 7.2) has stage 1 mounted in the lower portion of its fixed stand, the upper portion carrying dial 4, oil regulator 5, and rod 6. The latter has an end-piece with a diamond cone having an included angle of 120° or with a steel ball 1.59 mm in diameter. Dial 4 has two scales (a black and a red one) and two pointers, the larger pointer indicating hardness numbers and the

smaller one serving to control the preliminary load produced by rotating handwheel 2.

The top surface of a specimen to be tested must be carefully ground, and the opposite surface must be smooth and clean. Rotating the handwheel clockwise raises the stage so that the specimen is brought into contact with the indenter which is pressed into its surface. The wheel is turned until the smaller pointer moves into the vertical position and reaches a red mark on the dial, which shows that the indenter has been pressed into the specimen with a preliminary load of 10 kgf. The preliminary loading is made in order to eliminate the effect of elastic deformation and compensate for the influence of the roughness of the specimen surface on the results.

When the specimen is loaded preliminarily by a load of 10 kgf, the larger pointer moves into the vertical or almost vertical position. For accurate measurement, the larger pointer should be set to the zero of the black scale. To do this, the dial is turned so that its zero mark coincides with the larger pointer, but without rotating the handwheel, i.e. without altering the preliminary load. The allowable deviation of the larger pointer from the vertical is within ± 5 divisions of the scale.

By turning handle 7 smoothly to the stop the specimen is then loaded additionally by means of a lever carrying a weight (or weights). One weight on the lever produces an additional load of 50 kgf, i.e. the total load will be 60 kgf. Two weights provide an additional load of 90 kgf, i.e. a total load of 100 kgf, and three weights, respectively 140 kgf of additional load or 150 kgf of the total load. The pointer indicates the total load on the dial.

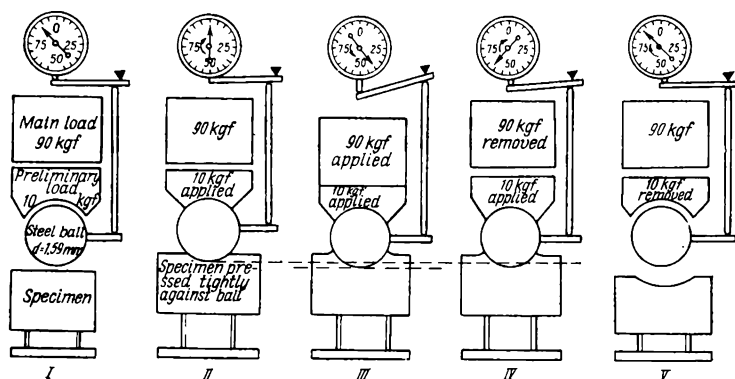


Fig. 7.3. Diagram of loading and releasing a specimen in Rockwell hardness test

With the additional load being applied, the larger pointer moves to the left (counterclockwise) on the dial. The time of application of the additional load is 5 to 7 s. The handle of the tester then returns to its initial position, i.e. the additional load is released, but the specimen remains loaded by the preliminary load. The larger pointer then moves clockwise. The number it indicates on the scale is the Rockwell hardness number. This number is recorded and the handwheel is then turned counterclockwise to lower the stage and release the preliminary load. The diagram of loading and releasing a specimen in the Rockwell hardness test is shown in Fig. 7.3.

The Rockwell tester measures the depth of indent of a diamond cone (or steel ball) or, more precisely, the difference between the depths produced by the preliminary load and the total load. Each division of the scale corresponds to $2\text{-}\mu\text{m}$ of the depth of the indent. The pointer of the instrument indicates, however, not the depth of indent h , but the difference $100 - h$ on the black scale (for diamond testing) or $130 - h$ on the red scale (for ball testing). Therefore, the harder the material being tested, the smaller the value of h and the greater the Rockwell hardness number, and vice versa. Thus, the Rockwell hardness numbers are greater for harder materials, which makes it possible to compare them with the Brinell hardness numbers. On the other hand, the Rockwell hardness numbers lack the dimension and physical sense of the Brinell hardness numbers. Despite this, they can be recalculated into the Brinell hardness numbers by means of a diagram (Fig. 7.4) or a table compiled from numerous experimental results (see Appendix II). As seen from the diagram, there

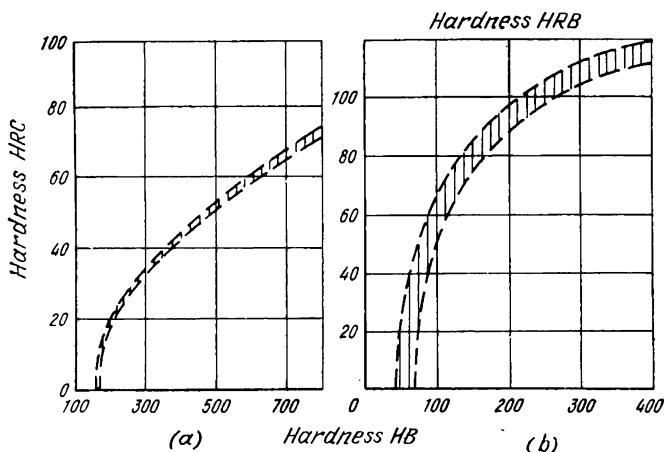


Fig. 7.4. Relationship between Brinell and Rockwell hardness numbers (a) for steel ball indentation (Rockwell B scale); (b) for diamond cone indentation (Rockwell C scale)

is no linear relationship between the Rockwell and Brinell hardness numbers.

A Rockwell hardness tester enables the following measurements to be made:

(a) with a diamond cone and a total load of 150 kgf; the results are read off the black scale (C scale) and designated HRC numbers. For instance, 65 HRC implies that the hardness of a material is 65 units on the Rockwell C scale with a total load of 150 kgf;

(b) with a diamond cone and a total load of 60 kgf; the hardness number is read off the black C scale, but designated HRA; HRA numbers can be recalculated into HRC numbers by the formula $HRC = 2HRA - 104$;

(c) with a steel ball and a total load of 100 kgf; the hardness number is read off the red scale B and designated HRB.

Measurements with a diamond cone and load of 150 kgf (HRC measurements) are made for: (a) hardened or low-tempered steel (with a hardness above 450 HB), i.e. under the conditions where indenting a steel ball (by the Brinell or Rockwell B test) into a hard material would cause deformation of the ball and give erroneous results; (b) for medium-hard materials (>230 HB) as a quicker method of measurement and, besides, leaving a smaller indent in the tested surface than in the Brinell hardness test; (c) for hardness measurements of thin surface layers (but not less than 0.5 mm thick), for instance, of cemented steel.

Measurements with a diamond cone and load of 60 kgf (HRA tests) are employed for very hard metals (>70 HRC), for instance, hard alloys, where indenting the diamond cone with a large force would crush the diamond, and also for measuring the hardness of hard surface layers (0.3-0.5 mm thick) or thin specimens (plates).

Measurements with a steel ball and load of 100 kgf (HRB tests) are applicable for mild (annealed) steel or annealed non-ferrous metals in articles and specimens 0.8-2 mm thick, i.e. under the conditions where the Brinell hardness test with a large-diameter ball would cause the specimen to crumble.

Rockwell hardness tests are standardized by the USSR State Standard GOST 9013-59 (Table 7.2).

Table 7.2. Rockwell Hardness Test Conditions

Approximate Vickers hardness HV	Rockwell scale	Indenter	Load, kgf	Allowable range of measured Rockwell hardness
60-240	B	Steel ball	100	25-100
240-900	C	Diamond cone	150	20-67
390-900	A	Same	60	70-85

The distance from an indent to an edge of a specimen or to the centre of another indent should be not less than 1.5 mm for diamond-cone testing and at least 4 mm for ball indentation. The thickness of a specimen should be at least 10 times the depth of the indent.

Measurements must be made in at least three points (especially in the diamond cone test), i.e. at least three times on a specimen, the first measurement being disregarded and the hardness found as an average between the second and the third tests.

The Rockwell hardness test requires less time (30-60 s) than the Brinell test, the result being immediately seen on the dial. Besides, it leaves a smaller indent in the surface of a specimen.

The hardness of very thin layers of a metal (less than 0.3 mm thick) cannot be measured by the Rockwell test with the loads indicated (60 or 150 kgf), since the diamond cone indents to a greater depth and therefore determines the hardness of the deeper softer layers of the metal. On the other hand, the depth of the indent becomes smaller with increase in hardness, thus reducing the accuracy of a test (especially for metals with a hardness more than 60 HRC). Special testers, such as the Superficial Rockwell machine, are then used for the purpose, using a small-

ler load and therefore, a lower depth of indentation. The preliminary load is only 3 kgf, and each division of the scale is only $1\text{ }\mu\text{m}$ of indent depth; therefore the machine has a higher sensitivity.

7.4. HARDNESS MEASUREMENT BY INDENTING A DIAMOND PYRAMID (VICKERS HARDNESS TEST)

This method is based on indenting a tetrahedral diamond pyramid with an angle between opposite faces of 136° , the hardness being characterized by the area of the indent produced.

With pyramid indentation, the ratio between the diagonals of the indent formed remains constant with a change of the load, which makes it possible to vary the load within a wide range in accordance with the object of the study.

The tests are carried out in a machine (Fig. 7.5) having a fixed stand with stage 1 mounted in its lower portion, the stage

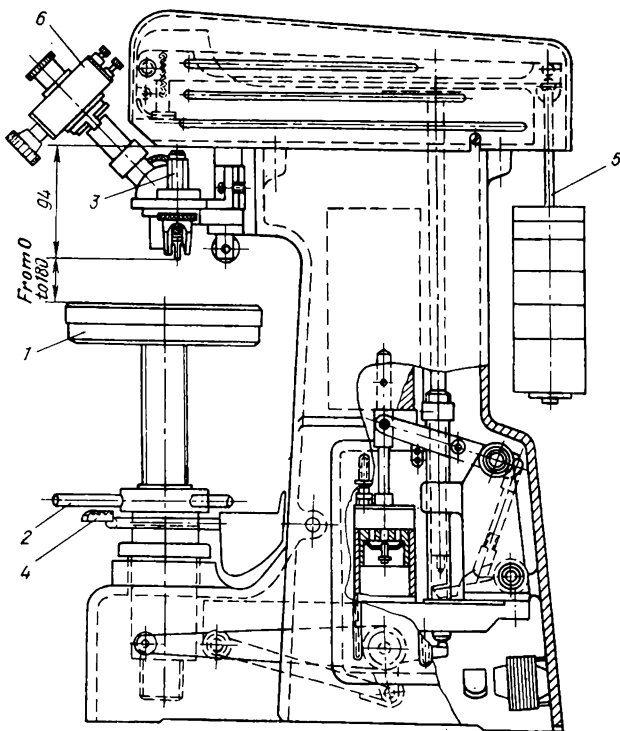


Fig. 7.5. Vickers hardness tester

1—stage for mounting a specimen; 2—handwheel; 3—diamond holder; 4—starting lever pedal; 5—weights; 6—microscope

being moved vertically by rotating handwheel 2. A specimen is placed onto the stage with its prepared surface facing upwards (perpendicular to the pressing force) and the stage is then raised to contact the diamond pyramid fastened in the holder 3. A loading mechanism is actuated by pressing the pedal of starting lever 4, so that the pressure from weights 5 is transferred to the pyramid. Afterwards the stage is lowered and the length of the diagonal of the indent produced is measured by using a microscope. The eyepiece of the microscope has two blinds: a fixed blind and a movable one. The movable blind is moved by means of a micrometer screw so as to align the blind with the right corner of an indent, the screw being connected to a rotating drum scale (Fig. 7.6). The scale reading is taken and the corresponding Vickers number is found from a table. Measurements are taken on both diagonals, and their average calculated.

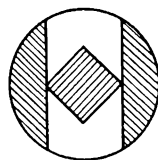


Fig. 7.6. Diagram for measuring an indent of a diamond pyramid in the micrometer eyepiece (Vickers hardness test)

The loads employed are 1, 3, 5, 10, 20, 30, 50, 100 or 120 kgf, greater loads causing a deeper indent. The low load values are employed for measuring the hardness of thin layers.

The machine can be used to measure the hardness of specimens 0.3-0.5 mm thick or surface layers 0.03-0.05 mm thick. A light load, such as 1 kgf, however, can give an undistinct indent, which might result in an error when measuring its diagonal. For this reason the hardness of very thin surface layers, for instance a cyanidized layer 0.04-0.06 mm thick, is measured with a load of 5 kgf; a layer of nitrated steel up to 0.05 mm thick should be measured with a load of 5 or 10 kgf. The designation of the Vickers hardness must include the load employed in the test, for instance, HV₅, HV₁₀, etc.).

The surface of specimens for the pyramid hardness test should be carefully ground with fine emery paper or even polished. The thickness of specimens must be at least 1.5 times the indent diagonal.

The Vickers hardness HV, like the Brinell hardness, is the ratio of the pressing force to the area of the indent,¹ i.e.

$$HV = \frac{2P \sin \alpha/2}{d^2} = 1.854 \frac{P}{d^2} \text{ kgf/mm}^2$$

where P = pyramid load, kgf

α = angle between pyramid faces (136 °C)

¹ The loading time for ferrous metals is 10-15 s, and for non-ferrous metals, 30 ± 2 s.

d = arithmetic mean of the lengths of the two diagonals of the indent after load releasing, mm

The Vickers hardness numbers and Brinell numbers have the same dimension and practically coincide for materials with HB numbers up to 450. On the other hand, pyramid tests provide better accuracy for high-hardness metals than is possible with ball or cone tests. A diamond pyramid has a wider included angle (136°) and the diagonals of the indent produced are approximately seven times larger than the indent depth, which ensures higher measurement accuracy even when the indent penetration depth is small. This makes the Vickers test especially suitable for hardness measurements in thin layers and hard alloys.

The Vickers hardness test is standardized in the USSR State Standard GOST 2999-59. Recalculations from Vickers to Brinell and Rockwell or vice versa may be made by using the table given in Appendix II.

When testing hard and brittle layers (nitrated or cyanidized steel), cracks can sometimes be seen in the corners of an indent, these being an indication of the high brittleness of the layer being tested.

7.5. MICROHARDNESS MEASUREMENTS

When studying the properties and transformations in alloys, it is often required not only to know the 'averaged' hardness which is the result of the total effect of all the phases and structural components present, but it is also necessary to determine the hardness values of these phases and components, i.e. to make microhardness measurements. This is done by indenting a diamond pyramid and the method is standardized in the USSR State Standard GOST 9450-60.

The microhardness tester type ПМТ-3, developed by M. M. Khrushchov and E. S. Berkovich (Fig. 7.7), comprises stand 1 of a vertical microscope with a tube, which can be moved up and down by means of macrometer screw 2 and micrometer screw 3. Micrometer eyepiece 4 is mounted in the upper portion of the tube, the lower portion carrying rod 5 with a diamond pyramid, opaque illuminator 6, and objectives 7. The opaque illuminator comprises a 6-V lamp fed from the mains via a transformer.

The instrument is provided with two objectives for microsection examination at magnifications of 478X and 135X. The magnification of the eyepiece is 15X. The eyepiece has a fixed reticule, a micrometer barrel, and a movable carriage with another reti-

cule. The fixed reticule 5 mm long is calibrated and has two dotted lines forming a right angle. The movable reticule has two marks and another angle facing in the opposite direction.

The diamond pyramid used in the instrument has an edge angle of 136° , i.e. the same as in Vickers testers, which facilitates recalculation to the Vickers hardness numbers. Loading of the pyramid is effected by means of weights 12 on rod 5. Weights from 1 g to 200 g are employed depending on the structure being tested and the object of study.

The surface of specimens for microhardness tests is ground and polished¹ and, when needed, etched by the reagents employed for a microscopic examination of corresponding alloys (see Table 3.3).

A prepared specimen (microsection) is placed onto stage 8, its upper surface being parallel to that of the stage. With specimens of a complicated shape this is achieved by using plasticine and levelling the ground surface by means of a hand press.

The specimen is viewed through the eyepiece and the stage moved by two screws in two perpendicular directions to select the point of the microsection where hardness will be measured and place this point exactly inside the dotted angle of the fixed reticule. Weights are then placed on the rod and the stage is turned through 180° by handle 9 to bring the selected portion of the microsection under the diamond pyramid. Then handle 13 is slowly (for 10-15 s) turned approximately through 180° to lower the pyramid rod onto the specimen. In this position, the

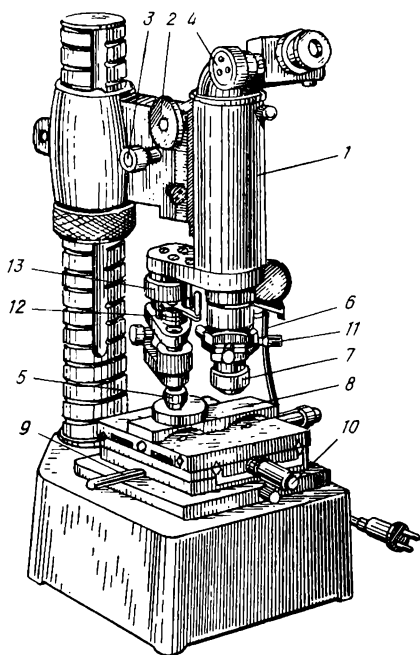


Fig. 7.7. Microhardness tester type ПМТ-3

1—microscope; 2—macrometer screw; 3—micrometer screw; 4—micrometer eyepiece; 5—diamond pyramid rod; 6—opaque illuminator; 7—objective; 8—microsection stage; 9—stage handle; 10—stage screw; 11—adjustment screws; 12—weights; 13—loading handle

¹ Electrolytic polishing is recommended for microhardness specimens to avoid work-hardening of the surface layer.

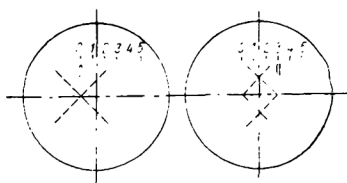


Fig. 7.8. Scheme of measuring the size of indents in a microhardness tester

the indent will be seen in the microscope field very close to the corner of the 'angle' of the fixed reticule, the guaranteed deviation in this instrument being not more than $3\text{ }\mu\text{m}$. By rotating screws 11, the image is then brought into full coincidence with the angle so that its left-hand sides are aligned with the dotted lines of the angle. Then, by turning the micrometer barrel of the eyepiece, the angle of the movable reticule is aligned in the same manner with the right-hand portion of the indent image. The length of the indent diagonal can then be read off the micrometer barrel scale. The eyepiece is then turned through 90° to measure the other diagonal, and the average value is calculated. The corresponding Vickers hardness number is found from the table. These measurements are repeated two or three times for the same indent. The Vickers hardness numbers given in the table are calculated from the formula

$$HV = 1.854P/d^2 \text{ kgf/mm}^2$$

More accurate results are obtained by measuring the hardness of a selected portion of a microsection (for instance, a grain) two or three times. For this, the area of the grain must be large enough to make two or three indents. Bearing this in mind, the load is chosen experimentally. It should be remembered, however, that very small loads (less than 20 gf) may cause errors in measurements.

The instrument makes it possible to take photographs of microstructures of alloys together with the indents.

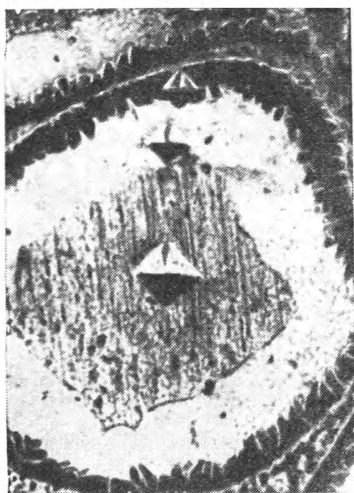


Fig. 7.9. Cast high-speed steel after hardening (with diamond pyramid indents), 500X

Microhardness tests are widely employed for studies of the structures and properties of alloys.

Figure 7.9 shows the microstructure of cast high-speed steel after hardening. It consists of large grains of heterogeneous structure, each grain having three concentric layers: the core (320-350 HV, or 35 HRC), an intermediate layer (700-725 HV or 58 HRC), and the outer layer (940-1000 HV or 65-67 HRC). This nonuniformity of the hardness and structure could not be revealed by common hardness (macrohardness) testing; a Rockwell test of a specimen of this steel showed a uniform hardness of 65 HRC.

7.6. HOT HARDNESS TESTING

Hardness measurements during heating (hot hardness testing) are important when studying various grades of heat-stable and heat-resistant structural and tool steels and alloys.

It should be remembered that the local cooling caused by a colder indenter may vary appreciably the measured hardness and thus affect the accuracy of measurements. Appreciable errors may also be due to the oxidation of the specimen surface, which occurs if heating is done in a furnace without a protective atmosphere, the oxidation being more pronounced with increasing temperature.

These drawbacks are eliminated by heating specimens in vacuum or an inert gas and measuring their hardness by indenting a diamond pyramid (according to Vickers),¹ in particular in a multi-position instrument designed by M. G. Lozinsky and N. A. Bogdanov,² where a number of specimens can be heated simultaneously and therefore, tested under similar conditions. The hardness tester is placed in a hermetized chamber formed by a glass hood and copper housing (Fig. 7.10), which is evacuated to 10^{-4} - 10^{-5} mm Hg; this prevents oxidation of specimens at temperatures up to 800 °C.

Polished specimens are placed into the seats of the tester. After evacuating the chamber, they are heated by molybdenum-coil heaters. At the same time, the indenters are heated too. Temperatures are measured by thermocouples spot-welded to the specimens.

The stage of the instrument carries six detachable weights with indenters to measure hardness of six specimens. The weights are

¹ A pyramid made of artificial sapphire is recommended for temperatures above 800 °C.

² Lozinsky M. G., *Stroenie i svoistva metallov i splavov pri vysokikh temperaturakh* (Structure and Properties of Metals and Alloys at High Temperatures). Moscow, Metallurgiya Publishers, 1963.

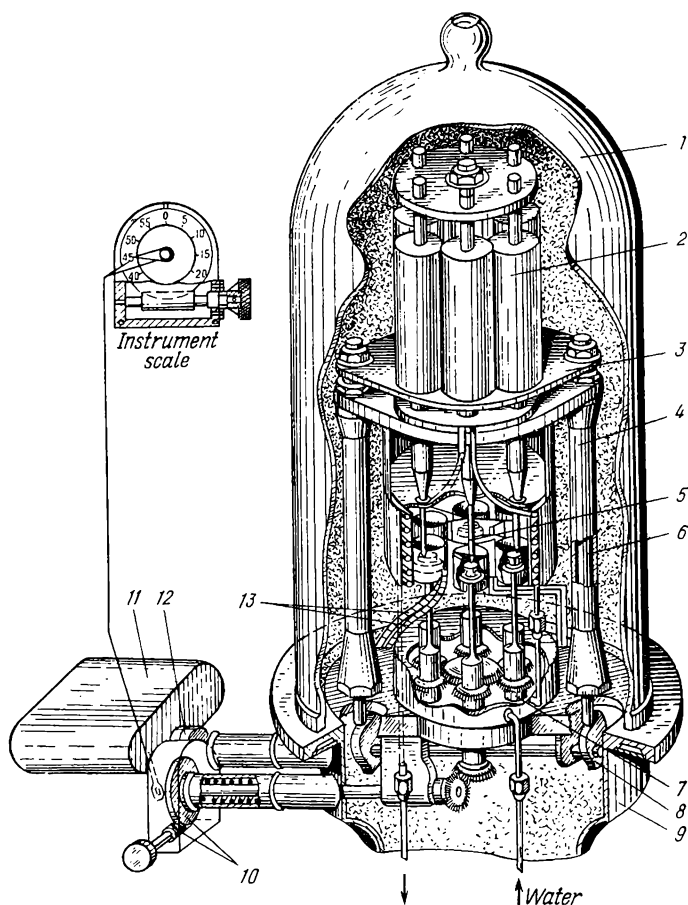


Fig. 7.10. Apparatus for diamond-pyramid hardness testing in vacuum (according to M.G. Lozinsky)

1—glass hood; 2—detachable weights; 3—lifting platform; 4—hollow stands; 5—indicators; 6—tie; 7—scale and pointer for control of indents; 8—cam mechanism; 9—copper housing; 10—reduction gear; 11—actuating mechanism; 12—clutch; 13—thermocouples

lifted by a tie and a cam mechanism. On pressing a knob of the control panel, the motor of an actuating mechanism turns a coupling through 180°, lowering the stage with the weights and indenters onto the specimens. Loads are usually applied for 30 s and controlled by a timer, after which the timer reverses the actuating mechanism motor and thus releases the load.

The specimens are removed from the chamber and cooled, and then the indent diagonals are measured. For more accurate re-

sults, measurements should be repeated four or five times on each specimen.

Hot hardness tests with the use of a ball (made of a hard alloy) or diamond cone are less reliable. They can be made at temperatures up to 300-400 °C.

7.7. LABORATORY EXERCISES¹

Before making the exercises, the students should recall the material of Secs. 1-5 of this chapter.

Each laboratory exercise on hardness measurement consists of two parts.

When making the first part, the students should acquire the skill of hardness measurement. Each student must measure the hardness of one or two steel specimens after various heat treatment (their hardness should be within 220-400 HB). The content of the first part: measure the Brinell hardness (with a 10-mm ball) and Rockwell hardness (C scale) of a steel specimen and give an approximate value of its ultimate strength. Explain the principle of hardness measurement by indenting a ball or diamond cone.

The second part of each exercise includes one of the problems Nos. 63-80 which should be solved by a student. The problems are arranged so that the student must explain how the hardness, which is one of the most important mechanical properties of most metals, is linked with the structure and other strength properties of that metal.

Some problems require knowledge on how heat treatment may affect the structure and properties of a metal. If this part of the course has not been studied up to the moment of making these exercises, the teacher must give additional explanations or point out the corresponding chapters in the textbook.

Problems

No. 63. (a) Select a tester and a load for measuring the hardness of alloys of the Sn-Zn system;

(b) measure the hardness of pure tin, pure zinc and three specimens of alloys of this system with zinc content of 5, 20, and 50 per cent, respectively;

(c) plot the constitutional diagram of the Sn-Zn system (see Fig. 4.20) and use the measured hardness values to draw a line on it showing how the hardness of these alloys depends on zinc

¹ The methods for determining the ultimate tensile strength and impact strength are described in Ch. 6, Secs. 2 and 4.

concentration. Explain the law by which the hardness of these alloys varies and how the variations of hardness are linked with the structure of these alloys.

Note. When casting the specimens (20 mm \times 20 mm \times 100 mm), remember that zinc may burn out during smelting of the charge. Hardness variations are more noticeable in Pb-Sb alloys, but these are less convenient for laboratory tests because of their appreciable density segregation.

No. 64. (a) Measure the hardness of four specimens of annealed carbon steel with the carbon content of 0.1, 0.3, 0.5, and 1.1 per cent, respectively; indicate their approximate values of ultimate tensile strength;

(b) plot a hardness-carbon content diagram (up to 1.1 per cent C) and show on it the variations in the hardness of annealed steel with increasing carbon content, and explain the corresponding changes in the structure (see Figs. 3.10 and 12.2).

No. 65. Measure the hardness of four specimens of annealed carbon steel with 0.4, 0.7, 1.0, and 1.2 per cent carbon.

Indicate the law of hardness variation with increasing carbon content and, using the measured Brinell hardness numbers, determine approximately the steel ultimate strength and yield limit. Indicate the standard grades of steel corresponding to these compositions (by carbon content) and their possible applications in industry.

No. 66. Measure the hardness of four specimens of hardened carbon steel with 0.2, 0.4, 0.6, and 0.75 per cent carbon.

Select the type of tester suitable for measuring their hardness and determine the law of hardness variation of hardened steel with the carbon content being varied within the limits indicated.

Characterize the effect of carbon on the hardening capacity of steel. Assume that the specimens were hardened from the commonly adopted temperatures ($A_{c3} + 30\text{--}50^\circ\text{C}$) and quenched in water. Indicate the standard grades of steel corresponding to these compositions (by carbon content) and their possible applications in industry.

No. 67. Select the type of hardness tester to measure the hardness of annealed steel and grey iron.

Measure the hardness of the specimens: (a) of steel with 0.1 per cent C; (b) of steel with 0.45 per cent C; and (c) of grey iron with 3 per cent C.

Explain how the hardness of annealed steel varies with carbon content and why this relationship is not true of grey iron.

No. 68. (a) Determine experimentally what type of tester and what hardness scale should be used to measure the hardness of alloys of the Cu-Zn system (Fig. 9.16) and measure the hardness of four annealed specimens: of pure copper, brass with 90 per cent

Cu, brass with 68 per cent Cu, and brass with 58 per cent Cu;

(b) plot to a definite scale a portion of the Cu-Zn constitutional diagram (up to 42 per cent Zn) and a hardness-zinc content diagram; plot on the latter the experimental points and draw a curve through them. Explain how the shape of the curve obtained is related with the lines of the constitutional diagram of this system and with the structure of the alloys indicated;

(c) select the standard grades of alloys corresponding to the compositions given above and indicate their applications in industry.

No. 69. (a) Determine experimentally what type of tester and what load should be used to measure the hardness of alloys of the Cu-Sn system. Measure the hardness of three specimens: of pure copper and of pressed tin bronze (after recrystallization) with 4 and 6 per cent Sn;

(b) plot to a scale a portion of the copper-tin diagram (see Fig. 9.17) for copper-base alloys and a hardness-tin content diagram (up to 15 per cent Sn) and plot on the latter the experimental points of hardness numbers and draw a curve through them. Explain how the shape of this curve is related to the structure of tin bronze;

(c) select the standard grades of tin bronze corresponding to the compositions given above and indicate its applications in industry.

No. 70. Indicate which of the hardness tests, either Brinell or Rockwell, should be used to measure the hardness of mild steels.

Measure the hardness of a specimen of low-carbon steel Grade 10 and, using the known relationships between hardness and strength properties, determine approximately the ultimate strength and yield limit of the steel being tested.

No. 71. Measure the hardness of two specimens of brass with 20 per cent Zn; determine the type of hardness tester and load suitable for brass.

Both specimens were cut from a cold-rolled rod, one of them being then subjected to recrystallization.

Indicate the specimen that has been recrystallized and the approximate temperature of heating.

What changes in the structure of the brass during the recrystallization have caused the change of its hardness and how has the plasticity of the brass changed through this? Using the hardness numbers found in the tests, indicate the approximate values of the ultimate strength of these brass specimens.

No. 72. A specimen of carbon steel Grade 10, 20 mm thick, was cemented and then hardened to increase the hardness and wear resistance of the surface layer.

What type of hardness tester and what scale should be used for testing this specimen?

Measure the hardness of the surface layer of the specimen, remove 1 mm of surface layer with an emery disc, measure the hardness, again remove another 1 mm from the surface and then measure the hardness again.

Explain how the hardness of this specimen varies in the direction from its surface to the core and what structural and constitutional changes have caused this.

No. 73. A specimen of carbon steel (0.5 per cent C) 15 mm thick underwent strong decarbonization of its surface layer owing to long high-temperature heating, after which it was hardened.

Measure the surface hardness, remove a layer of about 1 mm with an emery disc, again measure the hardness, remove another 1-mm layer, and again measure the hardness.

Write down the hardness numbers found and explain:

(a) how the hardness varies in the direction from the surface to the core;

(b) how this defect impairs the properties of the steel.

Measure the hardness of the specimen by indenting a diamond cone with a load of 60 kgf and recalculate the hardness to the Rockwell C scale.

Explain why the Rockwell test (C scale) and Brinell test are less sensitive in this case and what method should be used to determine more accurately the thickness of the decarbonized layer.

No. 74. A cylindrical specimen 25 mm in diameter and 70 mm long, made of carbon steel with 0.45 per cent C, was hardened from 840 °C with water quenching, broken (cut) in the middle, and the break plane was ground.

Name the type of tester and the scale to measure the hardness of the specimen and then, the hardness of its ground surface along a diameter at 2-mm intervals.

Using the results of measurement, plot a hardness-distance from the surface diagram and draw a curve through the experimental points. Explain the transformations during hardening and the structural changes in the steel from the shape of the curve obtained.

No. 75. A cylindrical specimen 35 mm in diameter and 90 mm long, made of carbon steel with 0.5 per cent C, was hardened (heating to $A_{c3} + 30$ °C, water quenching) and then broken (cut) in the middle, and the break was ground.

Name the type of tester and the scale to measure the hardness of the specimen and then the hardness of its ground surface along a diameter at 2-mm intervals.

Using the results of measurement, plot a hardness-distance diagram from the surface and draw a curve through the experimental points. Explain the transformations during hardening and the structural changes in the steel from the shape of the curve obtained.

No. 76. Two cylindrical specimens 15 mm in diameter, made of carbon steel (0.45 per cent C), were hardened and then tempered, one of them by heating to 450 °C (to form the structure of troostite) and the other, to 580 °C (to form the structure of sorbite).

Measure the hardness of both specimens by Rockwell test (C scale) and recalculate to Brinell hardness numbers. Determine approximately the ultimate strength of the steel in these states.

Determine which of the two specimens has higher toughness.

No. 77. Measure the hardness of two specimens of steel with 0.45 per cent C; both specimens were made from an annealed blank, the second specimen being then hardened and tempered by heating to 550 °C (to form the structure of sorbite).

Select the type of hardness tester most suitable for both specimens.

Using the measured hardness number, determine approximately the values of the ultimate strength.

No. 78. Measure the hardness of two cylindrical milling cutters made of high-speed steel (on the end faces of the cutters).

Using the results, decide which of the two cutters was subjected to a final heat treatment and suitable for its purpose and which one should still be heat treated (hardened and tempered) to provide high cutting properties.

Hardness measurements should be made by the diamond-cone method.

Explain why the hardness test by indenting a steel ball is inadmissible in this case.

No. 79. Measure the hardness of two circular screw dies made of tool steel (Grade 9XC or Y11).

Say which of the dies has been hardened and tempered and which one still must be heat treated.

Hardness measurements should be made by indenting a diamond cone.

Explain why the ball indentation test is inadmissible in this case.

No. 80. Measure the hardness of two duralumin specimens: (a) after annealing and (b) after hardening and ageing.

Select a method most suitable for measuring the hardness of aluminium alloys and, using the measured results and the relationships given in Sec. 7.2, indicate approximately the ultimate strength of duralumin in these two structural states.

Chapter Eight

DETERMINATION OF PHYSICAL AND CHEMICAL PROPERTIES OF METALS

8.1. DETERMINATION OF PHYSICAL PROPERTIES

The role of physical properties of metals in various machine parts and elements may be different, and the following cases should be distinguished:

1. The physical properties are the principal ones determining the service life of machine elements. The mechanical properties are then of secondary importance. In this case one or two of the physical characteristics of an alloy must be high, for instance a high coercive force and a high remanence (see Table 27.24). These conditions are required, in the first place, for alloys intended for making permanent magnets; the high magnetic permeability and low coercive force with high ohmic resistance then ensure low hysteresis and eddy-current losses, which is required for the magnetic circuits of transformers and the like (see Table 27.21); the high ohmic resistance with a low temperature coefficient of resistance is required for rheostats, heating elements of electric furnaces, etc. (see Table 27.25); a low constant coefficient of thermal expansion is required for many elements of instruments, special-purpose springs, etc. (see Table 27.20); a low constant temperature coefficient of modulus of elasticity is needed for special-purpose springs.

2. The physical properties are of high importance, but with other properties, especially the mechanical ones, being at a high level too. This combination of properties is required for steels used in steam pipelines and other elements of thermal power plants; these steels must have a high thermal resistance with a low thermal expansion. Another example are alloys for combustion chambers of internal combustion engines, which along with the specified heat resistance must possess the highest possible thermal conductivity.

3. The high physical properties are desirable, but they should be complementary to a combination of other properties which are indispensable for a high durability of an article. Examples are cutting tools and dies for hot die-forming; these must have

a high thermal stability to retain the high hardness and wear resistance of their working edges on heating. If the steels used for this purpose can at the same time retain their high thermal conductivity, this will ensure a better and quicker removal of heat from the working edge and thus additionally increase the durability of such tools.

4. The physical properties are selected to characterize the phase composition and the transformations occurring in alloys. Tests related to this category were discussed in Chapters 5 and 6.

5. The physical properties are the parameters checked in control tests. When a physical parameter of metal remains at a definite level in a group of articles, this may be an indirect indication that other principal parameters of the metal are satisfactory, and therefore, the quality of the metal and heat treatment are as specified. This role of physical properties is of extreme importance, provided that the physical parameter selected can be easily tested on a specimen or an article by one or another non-destructive method.

These conditions are easily realizable in practice and can be widely used for automatic quality control in mass production. The following methods of testing characterizing these possibilities may be named:

(a) magnetic flaw detection used for the detection of surface cracks and poor penetration of welds. The method is based on the fact that the dissipation fields are formed in the vicinity of such defects, these fields being detected by various instruments (inductive, ponderomotoric, etc.) or by the pattern formed by magnetic powder on the surface of an article being tested (during or after the application of a magnetic field);

(b) ultrasonic methods; these are based on differences in the intensity of a directed ultrasonic beam after reflection (or dissipation) by discontinuities in the metal of an article, including those deep below the surface;

(c) methods based on variations in magnetic properties, principally in magnetic permeability. These are used for testing of cutting tools made of high-speed steels. After the final heat treatment (hardening and tempering), the structure of these steels should contain no soft component — residual austenite. The degree of transformation of austenite depends on the number of tempering stages and on how accurately the temperature of heating is maintained. The quality of tempering, and therefore, the quality of the steel, is checked by a special instrument — austenometer. The specified level of magnetic permeability in the steel specimen is a reliable indication that the austenite has un-

dergone full transformation. With a low value of magnetic permeability, the metal must be additionally tempered.

The methods for determining resistivity, saturation magnetization and coefficient of expansion were discussed in Chapters 4 and 5. The methods for determining other parameters may be found in specialist literature [see, for instance: *Metody ispytaniya, kontrolya i issledovaniya mashinostroitelnykh materialov* (Methods for Testing, Checking and Investigation of Machine-building Materials). Volume 1. Moscow. Mashinostroenie Publishers, 1971.]

8.2. DETERMINATION OF CHEMICAL PROPERTIES

The chemical properties of metals depending on their composition, structure and treatment are mainly characterized by their resistance to total corrosion, intercrystalline corrosion and corrosion cracking.

(a) Tests for Total Corrosion

A number of methods are in use: (1) in a liquid with the full immersion of a specimen; (2) in a liquid with a variable multiple immersion of specimens; (3) in vapours; (4) in a boiling salt solution; and (5) in a surrounding atmosphere under laboratory conditions.

The compositions of liquids, vapours and solutions are selected according to the actual conditions in which the metal will operate. Specimens having a large area-to-volume ratio are used in these tests.

The results obtained are processed quantitatively, most often in terms of the corrosion rate characterized by the loss of mass (after corrosion products have been removed from the surface of specimens) during a specified time per unit area. The rate of corrosion is also used to determine the depth of corrosion

$$P = \frac{K}{\gamma} 10^{-3} \text{ mm/year}$$

where K = corrosion rate, g/m² year
 γ = density of metal, g/cm³

This estimation is only suitable for a uniform corrosion action and becomes unreliable with local disturbances.

Apart from determination of the mass loss, visual observation of the surface of specimens may be carried out (either by the naked eye or under the microscope). This makes it possible to estimate the resistance to point corrosion. For this purpose, the

density of corrosion points (i.e. the number of points per unit area) and their depth are measured. Microscopic examination can detect the appearance of very small points and the beginning of corrosion.

Another parameter of the development of corrosion is variations in the mechanical properties of specimens. Total corrosion reduces the cross-sectional area of an article and is thus accompanied by a lowered ultimate load. Point corrosion can also lessen plasticity (relative elongation).

Corrosion resistance of metals is evaluated according to the scale given in Table 8.1; lower indices in the table relate to the more stable metals.

Table 8.1. Evaluation of Corrosion Resistance of Metals

Stability group	Corrosion rate, mm/year *	Index	Stability group	Corrosion rate, mm/year *	Index
Perfectly stable	$0.001 > P$	1	Of reduced stability	$0.1 < P < 0.5$	6
Rather stable	$0.001 < P < 0.005$	2	Poorly stable	$0.5 < P < 1.0$	7
Stable	$0.005 < P < 0.001$	3		$1.0 < P < 5.0$	8
	$0.001 < P < 0.05$	4		$5.0 < P < 10.0$	9
	$0.05 < P < 0.1$	5	Unstable	$10 < P$	10

* Corrosion medium and method of testing must be indicated.

(b) Tests for Intercrystalline Corrosion (according to GOST 6032-58)

These tests are made for austenitic-structure stainless steels (see Table 27.19) used in relatively strong aggressive media, mainly acids. Under such conditions, corrosion can occur along grain boundaries and penetrate deep into the metal. Tests are made on steel plates of specified thickness (appr. 3 mm). The following methods of testing in solutions can be used:

(a) in a solution of sulphuric acid with an addition of copper sulphate. The solution only slightly affects steels hardened from usual temperatures (950° - 1150° °C) and quenched in water, which acquire a single-phase austenitic structure, but on the contrary, causes strong intercrystalline corrosion of steels after their heating to 500° - 800° °C, which results in segregation of part of the carbides at grain boundaries and impoverishment of the solid solution (anode etching of individual portions of the surface of

articles is made by the same solution with an addition of copper chips);

(b) in boiling concentrated (65 per cent) nitric acid, which provides an advantage of a more intense corrosion and the possibility of expressing the test results as a loss in mass;

(c) in a mixture of nitric acid (10- or 65-per cent) and hydrofluoric acid (3- or 50-per cent) at a test temperature of 70°C. This is quite a quick test, with intercrystalline corrosion noticeable after five immersions (of one hour each). The results are evaluated by the loss of mass and by the strength of specimens in bending tests.

The degree of the development of intercrystalline corrosion is determined either qualitatively or quantitatively.

The qualitative methods include: (a) sounding (noise) tests; intercrystalline corrosion strongly reduces the duration of sounding of an article; (b) bending tests; appearance of intercrystalline corrosion causes fine cracks and even brittle fracture in tension zones; (c) metallographic investigation which can detect the initial formation of microfissures; this method is used for more accurate determination of the appearance of intercrystalline corrosion.

The quantitative methods include: (a) determination of the loss of mass; (b) determination of ohmic resistance (which increases owing to intercrystalline corrosion); and (c) determination of the sensitivity to corrosion cracking.

(c) Tests for Corrosion Cracking

Corrosion cracking is a complex process of destruction of a metal under the simultaneous action of static stresses and electrochemical process, resulting in the formation of surface cracks in the metal, which develop perpendicular to the direction of tensile stresses; these cracks may be of intercrystalline (i.e. along grain boundaries), crystalline or combined nature.

The stability of metals against corrosion cracking may be characterized as follows:

(a) by the value inverse of the time elapsed before cracking begins; this is termed the rate or sensitivity to corrosion cracking;

(b) by the percentage of specimens cracked during a test (of the total number of tested specimens);

(c) by the relative change in the ultimate strength of the metal during the specified time of holding in a corrosion medium with the specimen held in a stressed state formed by external or internal forces.

The methods for forming static stresses, in turn, can be different and are selected according to the objects of the tests and the properties of the metal being tested. The test stresses are usually equal to the operating stresses or the yield limit of the metal and are formed by subjecting the specimens to a constant load (force) or constant deformation.

With uniaxial tensioning of specimens, the stresses are distributed uniformly and can be calculated for the initial state with sufficient accuracy. Such a stress may be formed directly by loading the specimen with a weight, spring or by means of lever testing machines (such as the ИHK-I machine designed at the USSR Central Research Institute of Heavy Machine-building). It is possible with this machine to study the development of corrosion in hot solutions or in fully hermetized vessels.

A feature characteristic of the stressed state formed under such conditions is that the actual stresses in the specimen increase continuously during the process of corrosion cracking (owing to the reduction of the actual cross-sectional area of the specimen) though the initial stresses are formed by application of a constant load.

On the contrary, when a specimen is subjected to constant deformation, the reduction of its cross-sectional area results in a continuous reduction of the actual stresses.

A coarser method for forming stresses is to bend a plane specimen into a loop; such specimens can be tested for corrosion cracking in a relatively shorter time.

(d) Aggressive Media for Corrosion Tests

Either natural or artificial corrosive media can be selected depending on the object of tests.

Artificial media. These have the advantage that the composition and aggressive action of a medium are fully reproducible and controllable. It is also possible to change the temperature of the medium and control the pH index and oxygen content of the solution.

The ideal artificial medium for laboratory tests should develop corrosion cracking in an appreciably shorter time than under actual operating conditions. Such a medium should also contain the same ions that interact with the metal under actual conditions. On the other hand, the corrosion medium formed in the laboratory should not cause total corrosion, i.e. it should be harmless to non-load materials. These conditions are fulfilled, for instance, in the medium used for corrosion cracking tests of austenitic stainless steels; its composition is the boiling solution

of 42 per cent MgCl_2 , 0.5N solution of NaCl , and 0.1N solution of NaNO_2 , with addition of chlorides and oxygen.

Natural media. These provide conditions more resembling the actual operating conditions of materials. The aggressiveness of a natural medium selected for tests must be not less than that observed in real conditions. Such media may contain traces of impurities which play an important part in the development of corrosion. The materials being tested may then be subjected to cyclic wetting and drying by wind or sun. The following tests in natural media are most common:

(a) in sea water, including at special sea stations; these tests are made on materials and structures in which corrosion cracking under loads is inadmissible even after long immersion in sea water;

(b) in industrial atmospheres which may contain chlorine, sulphur compounds, nitrogen oxides, ammonia, carbon dioxide, water vapours, and thin layers of moisture condensed on the surface of specimens;

(c) in moist tropical conditions at special stations set up in various parts of the world.

The tests may be carried out under loads; then the aggressive action of these media can result in total corrosion and destruction of specimens.

8.3. LABORATORY TESTS

The laboratory tests below determine the stability of steel against gaseous corrosion (depending on the steel composition and heating conditions). These tests can be made under relatively simple conditions and in a relatively short time (30 to 60 minutes). At the same time they may characterize the scale resistance of steel (which is of great importance for steels subjected to high-temperature heating) and the effect of the principal alloying elements on it. Suitable materials for the tests are scale-resistant steels such as those given in Table 27.7, with common carbon or alloy steel taken as reference specimens.

To increase the sensitivity of tests, specimens having a large surface area should be used, for instance, 2-3 mm thick, 5-8 mm wide, and 60-80 mm long. Their surface must be polished or etched.

The simplest method to evaluate corrosion resistance is to measure the weight increase of a specimen (caused by its oxidation). A test is made in the following sequence. The surface area of a specimen is measured, after which the specimen is laid into a heated porcelain boat and weighed on analytical scales. The two specimens being compared are then heated in an electric

furnace in air to the temperature given in a problem and held at that temperature for the specified time. It is advisable to open the door of the furnace two or three times (for 1-2 minutes) to ensure stronger oxidation. After the specified time, the specimens in the boats are carefully placed onto the scales (in order not to lose scale) and weighed again. The accuracy of weighing must be 0.1 mg. The relative scale resistance is expressed as a weight increase, in $\text{g/cm}^2 \text{ h}$.

No. 81. Compare the scale resistance at 800°C (for 60 minutes) of two steels: carbon steel Grade 10 and an alloy steel of the same carbon content but with addition of 6 per cent Cr (steel Grade 15X6C10).

Explain why chromium makes steel scale-resistant.

No. 82. Compare the scale resistance at 850°C (for 60 minutes) of structural alloy steel with 1.5 per cent Cr (Grade 40X) and steel with 9 per cent Cr (Grade 40X9C2).

Explain: (a) why chromium increases scale resistance and (b) why the chromium content for the purpose should be not less than 9 per cent.

No. 83. Determine the temperature of the beginning of intense oxidation of scale-resistant steel 15X6C10 and explain the mechanism of the protective effect of chromium and silicon with which the steel is alloyed.

The first specimen should be heated to 800°C , and the second, to 900°C , both held for 30 minutes at the temperature specified.

No. 84. Compare the oxidation resistance of two scale-resistant steels: with 5 per cent Cr (Grade 15X5) and 17 per cent Cr (Grade 12X17); explain which of these steels can be recommended for use in heat exchangers subjected to prolonged heating to 850°C in operation.

The specimens must be heated to 900°C .

No. 85. Exhaust valves of automobile and tractor engines are heated up to 850°C in operation. Decide which of two steels (with either 6 or 9 per cent Cr) is more suitable for the purpose.

The materials to be tested: steel Grade 15X5 and Grade 40X9C2. The specimens are to be heated to 850°C (for 30 minutes).

No. 86. Compare the scale resistance of two grades of steel at 850°C (for 60 minutes): carbon steel Grade 45 and alloy steel with the same carbon content but with 9 per cent Cr (Grade 40X9C2).

Explain why chromium increases the resistance of steel to gaseous corrosion.

Part Two

CONSTITUTIONAL DIAGRAMS OF ALLOYS

Chapter Nine

CONSTITUTIONAL DIAGRAMS OF BINARY ALLOYS

Constitutional diagrams of alloys show their phase composition under conditions of equilibrium, depending on the temperature and the concentration of the constituents. They can be used for the qualitative estimation of many physicochemical, mechanical, and technological properties of alloys.

In addition, by analysing constitutional diagrams it is possible to solve some engineering problems of importance. For instance, such diagrams enable one to determine which particular alloys undergo changes in their structure and many properties, the direction of these changes as well, as they pass into a non-equilibrium state depending on the actual conditions of casting, plastic working and heat treatment.

The exercises given below show the methods and possibilities for solving such problems by analysing the transformations occurring in alloys as indicated in their constitutional diagrams. In this connection the constitutional diagrams used in the exercises characterize the phase composition of the alloys that are very close to those employed in engineering.

9.1. DIAGRAMS OF BINARY ALLOYS AND METHODICAL INSTRUCTIONS ON THEIR ANALYSIS

To solve the problems given below, the student should fulfil the following:

1. Draw the given constitutional diagram (as indicated in Fig. 9.4).
2. For each region of the diagram, show the structures formed in the alloys of the given system under conditions of equilibrium.

The diagrams given in the exercises show the phase composition corresponding to the state of equilibrium. One, however, cannot judge of the transformations and properties of an alloy knowing only its phase composition.

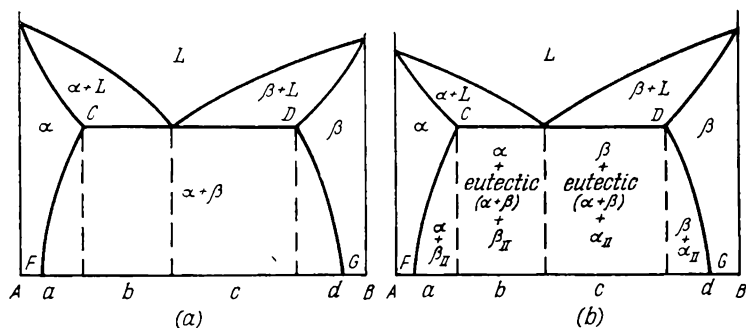


Fig. 9.1 Constitutional diagram of alloys having limited solubility of their components in the solid state

(a) phase diagram; (b) structural diagram

Figure 9.1 shows, as an example, the constitutional diagram of alloys having the same phase composition (Fig. 9.1a) in regions *a*, *b*, *c* and *d* and composed of a mixture of two solid solutions α and β , where α is a solid solution based on component A, and β , a solid solution based on B. The structural composition (Fig. 9.1b) for each of the regions will, however, be different.

In the *a* region the alloys are composed of crystals of α -solid solution and some β_{II} crystals (secondary β -crystals) that have precipitated as small particles from the α -solid solution.

The structural composition in the *b* region (hypoeutectic alloys) is α -solid solution + eutectic + β -solid solution (secondary crystals).

The structural composition in the *c* region (hypereutectic alloys) is β -solid solution + eutectic + α -solid solution (secondary crystals).

When solving the problems, the regions of different structural compositions should be separated by vertical dotted lines, with the corresponding structural constituents being indicated in each region.

3. Show the specified alloys on the constitutional diagram, and draw the corresponding vertical lines (see Fig. 9.4).

4. Plot the cooling curves of the alloys in the temperature-time coordinates.

Constitutional diagrams characterize transformations occurring on slow cooling (or heating). These transformations may proceed in different ways depending on the composition of the alloy, and therefore, the cooling (or heating) curves of alloys may be of different forms.

The primary crystallization, i.e. crystallization from the liquid state, in pure metals occurs at a constant temperature and with a definite thermal effect, because of which their cooling curves always have a horizontal portion corresponding to the solidification point (or to the melting point on the heating curves).

The primary crystallization of binary (two-component) alloys occurs in the way indicated, i.e. at a constant temperature, only for eutectic alloys, for alloys forming chemical compounds, and for solid solutions whose composition corresponds to the minima or maxima on the diagram.

Alloys of other types solidify within a certain temperature range. Since crystallization in a liquid occurs with the evolution of heat, the cooling of an alloy is thus slowed down, and the slope of its cooling curve changes. For this reason a flex point corresponding to the beginning of crystallization is characteristic of the cooling curves of such alloys.

The end of the solidification process may be characterized by either a flex point or a horizontal portion on the cooling curve, depending on the number of phases.

If a melt solidifies into a single-phase alloy (solid solution), then two phases — the liquid and the solid solution crystals — are in equilibrium during the whole solidification time. The end of solidification is characterized by a flex point on the cooling curve (the slope of the curve changes). This case is reflected on the constitutional diagram by an inclined solidus line and by a change of the solidification point with the concentration of the alloy (Fig. 9.2, *Ia* and *Ib*).

In alloys that are mechanical mixtures (heterogeneous systems) forming a eutectic, three phases — the crystals of both components (or crystals of their solutions and compounds) and the liquid — are in equilibrium on the solidus line at the moment the solidification ends. According to the phase rule ($C = K + 1 - P$), this equilibrium is non-variant: $C = 2 + 1 - 3 = 0$. The primary crystallization is therefore finished at a constant temperature and characterized by a horizontal portion on the cooling curve (Fig. 9.2, *I*). This case is reflected on the constitutional diagram by a horizontal solidus line (straight line).

The cooling curve plotted in an exercise must show not only the nature of transformation, but also the relative amount of the alloy being transformed at a constant temperature. This follows from the fact that the length of the horizontal portion of the curve depends on the thermal effect of the transformation and, with the same mass and cooling rate of the alloy, is proportional to the amount of the eutectic being formed.

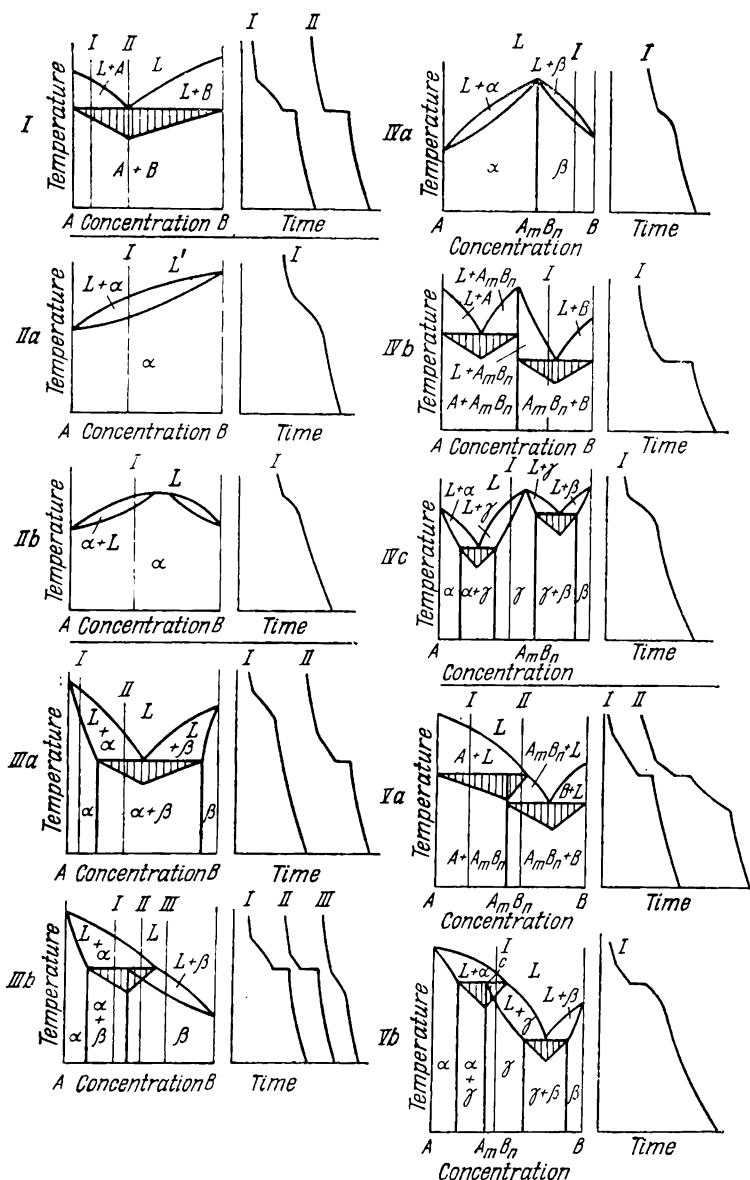


Fig. 9.2. Principal types of constitutional diagrams and cooling curves of binary alloys undergoing no transformations in the solid state

I—complete insolubility; *II*—complete solubility; *III*—limited solubility [(a) with the formation of eutectic; (b) with the formation of peritectic]; *IV*—formation of a compound (a) with complete solubility in the components; (b) with no solubility; (c) with limited solubility; *V*—formation of a compound which is unstable at high temperatures [(a) with no solubility in the components; (b) with limited solubility]

In order to show the length of the horizontal portion on the cooling curve, one should select a scale to depict the solidification of an alloy containing 100 per cent eutectic. When plotting cooling curves in the exercises, it is advisable, for instance, to take the length of the horizontal portion of the curve for the eutectic alloy at 10 mm and then, using the rule of sections, determine the relative amount of the eutectic formed during the solidification of the given alloy and draw a horizontal portion of the corresponding length on the cooling curve of that alloy. For instance, if an alloy contains 50 per cent eutectic, its solidification should be depicted by a curve with a horizontal portion 5 mm long (to the scale chosen).

In alloys of one and the same system both kinds of transformation can often occur, depending on the concentration and number of phases being formed. For instance, in alloys of the system shown in Fig. 9.2, *IIIa*, the solidification of the α -phase (as also of the β -phase) occurs at a varying temperature, while that of the eutectic occurs at a constant temperature.

For alloys with peritectic transformations (Fig. 9.2, *IIIb*), cooling curve *I* shows: (a) a flex point indicating the beginning of solidification (when two phases, the liquid and the separated primary crystals of the phase that is richer in the high-melting component are in equilibrium); (b) a horizontal portion corresponding to the peritectic reaction during which three phases — primary crystals of the phase that is richer in the high-melting component, the liquid, and crystals of the phase that is richer in the low-melting component — are in equilibrium. For alloys retaining the liquid phase after these transformations (curve *II*, Fig. 9.2, *IIIb*), the cooling curve has an additional flex point indicating the end of solidification.

The stop on the cooling curve corresponds to the horizontal line of the constitutional diagram.

A somewhat different process of solidification is observed in alloys forming a chemical compound that is unstable at high temperatures (if the chemical compound formed and the alloy constituents are mutually insoluble). For a number of such alloys, the cooling curve shows first a flex point (the beginning of solidification), then a horizontal portion corresponding to the reaction of the compound formation, and finally, a second horizontal portion corresponding to the formation of eutectic. These two stops (horizontal portions) on the cooling curve accord with the two horizontal lines on the constitutional diagram (Fig. 9.2, *Va*, curve *II*).

If the unstable chemical compound is soluble at high temperatures in the components it is formed from, the constitutional dia-

gram and cooling curve will be of the forms shown in Fig. 9.2, *Vb*.

Secondary crystallization, i.e. transformations in the solid state (polymorphous transformations, full or partial decomposition of solid solution, ordering of solid solutions,¹ formation or decomposition of unstable compounds), also occurs with a thermal effect. But this effect is often insignificant and, therefore, to measure the temperature of these transformations use is made, in addition to the cooling curves, of such analytical methods (dilatometric method, resistivity measurements, etc.) as prove more sensitive for these alloys. In pure metals, transformations in the solid state (polymorphous transformations) occur at a constant temperature, because of which a characteristic horizontal portion corresponding to the transformation is observed on the cooling (heating) curves.

Solid transformations in binary alloys occur at a constant temperature in the following cases.

I. In alloys that are solid solutions:

(a) during eutectoid transformations as a result of full decomposition of the solid solution;

(b) during peritectoid transformations; and

(c) during the formation of intermetallic or ordered phases.

The decomposition of the initially formed solid solution (that is stable at high temperatures) in the course of the subsequent eutectoid or peritectoid transformation occurs at a constant temperature. If the composition of an alloy differs from that corresponding to the eutectoid (or peritectoid), then a partial decomposition first occurs, with the precipitation of a new phase from the initial solid solution, and only then, after the temperature of eutectoid is attained, the transformation proceeds at a constant temperature. The beginning of the decomposition is reflected by a flex point on the cooling curve, and the end of the decomposition with the eutectoid (or peritectoid) transformation, by a horizontal portion (Fig. 9.3, *IIIa* and *IIIb*). For some alloys with peritectoid transformations, the cooling curves have another flex point at a lower temperature corresponding to the end of the transformation process (under the cooling conditions commonly employed in engineering, however, peritectoid transformations never proceed to their end). For alloys in which intermetallic phases can form the cooling curve has a horizontal portion only when the concentration of the alloys exactly corresponds to their stoichiometric composition. This kind of transformation in other

¹ The ordering process, as also other phase transformations of the second kind (magnetic, etc.), cannot be analysed by using the phase rule, since the region of the new phase formed has no boundaries.

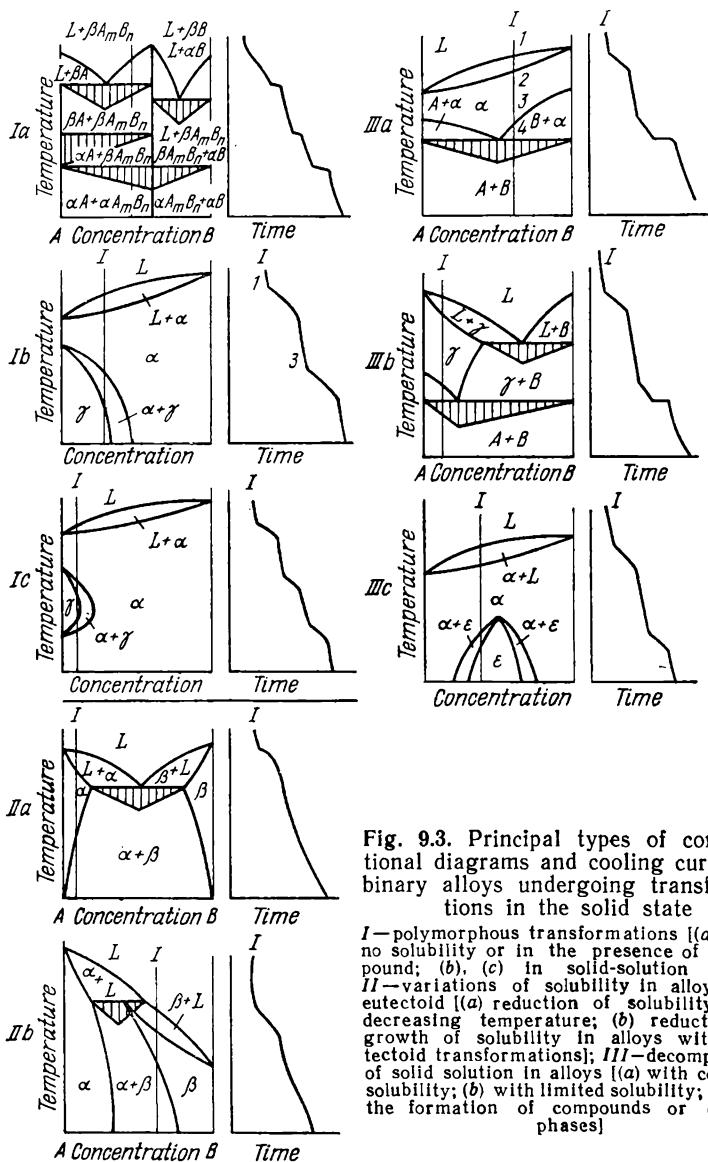


Fig. 9.3. Principal types of constitutional diagrams and cooling curves of binary alloys undergoing transformations in the solid state

I—polymorphous transformations [(a) with no solubility or in the presence of a compound; (b), (c) in solid-solution alloys]; *II*—variations of solubility in alloys with eutectoid [(a) reduction of solubility with decreasing temperature; (b) reduction or growth of solubility in alloys with peritectoid transformations]; *III*—decomposition of solid solution in alloys [(a) with complete solubility; (b) with limited solubility; (c) with the formation of compounds or ordered phases]

types of alloy occurs within a temperature range which may vary depending on the composition of the alloy, and is characterized by two inflexions on the cooling curve (Fig. 9.3, *IIIc*).

II. In alloys that are mechanical mixtures:

during polymorphous transformations of one of the components or of the chemical compound formed by them (Fig. 9.3, *Ia*).

These transformations are reflected as horizontal lines on constitutional diagrams and as horizontal portions (stops) on the cooling (heating) curves.

Since the thermal effect of a solid-state transformation (secondary crystallization) is lower than that in the primary crystallization from the liquid, the horizontal portion of the curve corresponding to the relative amount of the phase being transformed can be plotted to a smaller scale.

In other cases, solid-state transformations occur within a definite temperature interval, beginning at different temperatures in alloys of various concentrations; the corresponding curves on the constitutional diagram are sloped and show either the transformation (Fig. 9.3, *Ib*, *Ic*) or partial decomposition of the solid solution (Fig. 9.3, *IIa*, *IIb*, *IIc*). In such cases, the beginning and end of the transformation are characterized by an inflexion on the curve, after which the slope of the curve changes somewhat.

5. Draw a crystallization diagram of the given alloys: show graphically the structures that are formed in the process of crystallization and also the transformations occurring in the alloys during their cooling.

The crystallization diagram must be drawn to the same scale (for temperatures) as taken earlier. Individual structures (solid solution, mechanical mixture, chemical compound) should be denoted by corresponding symbols.

The symbols used should reproduce as close as possible the real structures observed in the given or similar alloy during metallographic analysis. When seen under a microscope, pure metals and solid solutions under conditions of equilibrium (after annealing) have a granular (polyhedral) structure similar, for instance, to the polyhedral structure of α -iron (ferrite) or to the polyhedrons of the solid solution of zinc in copper (see Fig. 3.21) after plastic working and annealing. If solid solutions of a number of types can be formed in the alloys of the given system, each solid solution then should be denoted by an individual symbol as, for instance, shown in the diagram to the solution to Problem 87 below (Fig. 9.4).

Chemical compounds can exist as crystals of various shape; on the decomposition of solid solutions they often precipitate as a network at grain boundaries or form lamellar or needle-shaped inclusions.

Eutectics and eutectoids crystallize in the form of areas of a heterogeneous mixture of different fineness, i.e. of dotted,

Constitutional Characteristics of Given Alloys at Various Temperatures

Alloy	Temperature, °C	Phase or structural composition of alloy	Calculation of the number of phases and structural components by the rule of sections
I	20	Homogeneous solid solution with α -iron as the base	Amount of liquid (Q_l): $Q_l = \frac{ab \cdot 100}{ac} = \frac{1.1 \times 100}{3.7} = 30\%$
II	135C	Crystals of α -solid solution of a concentration of 0.9 per cent P (point a) and the liquid phase containing 4.6 per cent P (point c)	
II	100	Basic structure of solid solution of a concentration of 1.2 per cent P (point f) and a small amount of secondary crystals of Fe_3P (magnetic)	Amount of α -phase (Q_α): $Q_\alpha = \frac{ln \cdot 100}{jl} = \frac{13.5 \times 100}{14.3} = 94\%$ $Q_{\text{Fe}_3\text{P}} = 100 - 94 = 6\%$
III	1200	Crystals of Fe_2P and liquid phase whose concentration corresponds to point $g = 16$ per cent P	$Q_l = \frac{hi \cdot 100}{gi} = \frac{4 \times 100}{5} = 80\%$
III	20	Mixture of two compounds: Fe_2P and Fe_3P	$Q_{\text{Fe}_3\text{P}} = \frac{jk \cdot 100}{jm} = \frac{4 \times 100}{5.5} = 73\%$ $Q_{\text{Fe}_2\text{P}} = 27\%$

lamellar, or granular form (see, for instance, the eutectic in Fig. 3.5).

When drawing a crystallization diagram, the approximate amount of each constituent should be taken into account. Thus, for instance, when a small amount of secondary crystals of another phase precipitates from a solid solution owing to the reduction of solubility with decreasing temperature, this phase must be depicted as small crystals (located, for instance, at grain boundaries) against the background of the polyhedral structure of the basic solid solution.

6. Characterize the state of the given alloys at the temperatures specified in the problem.

If the alloy is heterogeneous at the specified temperature, one has to determine the phases or structures present in it, indicate the composition of each of the constituents and the percentage of the individual components. To do this, draw a horizontal line through the point defining the given alloy at the specified temperature until it intersects the lines of the diagram (the conode, i.e. the line showing the compositions of the phases in equilibrium); determine the concentration of each of the components by dropping perpendiculars from the ends of the conode onto the axis of abscissae.

Then, using the rule of sections, determine the relative amounts of the individual phases or structures present in the alloy under conditions of equilibrium. The amount of the eutectic or eutectoid present in the alloy should be calculated for the temperature of their formation. The calculation results must be tabulated under the diagram as shown in the solution to Problem 87 (see Fig. 9.4).

7. Having analysed the transformations, answer the principal question of the Problem as to the structure, properties, treatment, and fields of application of the given alloys.

Problems

No. 87. Analyse the Fe-P constitutional diagram in the portion confined to the Fe-Fe₂P region and the transformation processes in the alloys, *I*, *II* and *III* containing 0.05, 2.0, and 17.0 per cent P, respectively.

Determine the phase composition and the phase ratio: for alloy *I* at 20 °C, for alloy *II* at 100 and 1350 °C, and for alloy *III* at 20 and 1200 °C.

Indicate structural deviations that may be expected under accelerated cooling conditions during the primary crystallization of the system.

Solution. The solution to the problem is given in the diagrams and Table in Fig. 9.4, except for the last question which is discussed below.

The constitutional diagram considered is an equilibrium one. However, some transformations in alloys occur so slowly that they do not really come to an end even after very long cooling. Such transformations include, in particular, the formation of solid solutions or unstable compounds by peritectic reactions.

A change in the cooling rate causes certain transformation points and lines on the diagram to shift, the magnitude of the shift depending on the degree of the deviation of the alloy from the state of equilibrium. For this reason the structures observed in industrial alloys can differ from those predicted by the equilibrium diagram.

The given system might be more fully characterized if, instead of a plane equilibrium diagram in the temperature-concentration coordinates we used a spatial diagram in the temperature-concentration-time coordinates, which would show the transition from a non-equilibrium to the equilibrium state, but such a diagram would be very complicated. By considering the equilibrium diagram on the basis of a more detailed analysis of the processes occurring in the alloys and of the regularities governing these processes, it is possible to indicate, with a sufficient degree of probability, the nature of the transformations occurring on rapid cooling (especially during the primary crystallization).

Let us discuss the process of crystallization from this standpoint.

According to the diagram, alloy *I* solidifies with the formation of a homogeneous structure of α -solid solution. Its solidification occurs between 1520 and 1500 °C, with the concentrations of the liquid and the precipitating solid phase varying between a few hundredths of a per cent and 1.8 per cent P. Therefore, this alloy is liable to segregation.

On rapid cooling, the composition of the crystals of solid solution will not be uniform, but their concentration will not exceed the solubility limit of phosphorus in $\alpha(\delta)$ -iron. Therefore, the phase composition of the alloy upon solidifying under the actual cooling conditions will not differ from the equilibrium one, but individual crystals (grains) of the alloy will have a non-uniform chemical composition.

This non-homogeneity of the chemical composition of the crystals of solid solution is termed intracrystalline or dendritic segregation. In accordance with the effect of phosphorus on iron, it additionally reduces the impact strength and ductility of the alloy, especially at low temperatures, this reduction being greater

at higher concentrations of phosphorus. For this reason the phosphorus content in quality steels is limited to 0.04-0.05 per cent, and even to 0.02-0.03 per cent in high-quality steels.

Upon solidification alloy *II* with 2 per cent P in the equilibrium state should have, like alloy *I*, the structure of a homogeneous solid solution. But this alloy is characterized by a large divergence between the liquidus and solidus lines both in temperature and in concentration; therefore, the alloy must be liable to segregation, similar to alloy *I* (with 0.05 per cent P). Alloy *II* begins to solidify at a temperature around 1500°C, the process finishing at approximately 1200°C. Already at 1350°C, as can be seen from the diagram and table (Fig. 9.4) the liquid phase (point *c*) contains approximately 4.6 per cent P, i.e. 50 per cent more than can be dissolved in iron in the solid state at the eutectic temperature. It is clear from the diagram (see Fig. 9.4) that the solubility limit of phosphorus in iron is 2.6 per cent. The composition of the liquid phase at the end of solidification will correspond to point *d*, i.e. to approximately 7.5 per cent P. On rapid cooling, the process of diffusion causing the equalization of the alloy composition does not have time to end, so that the last portion of the liquid phase of the composition corresponding to point *d* solidifies like hypoeutectic alloy of the same concentration, i.e. by forming some crystals of α -solid solution and a eutectic mixture composed of α -crystals and Fe_3P compound.

Thus, on rapid cooling, alloy *II* may have present some eutectic in addition to the crystals of α -solid solution of variable concentration. The presence of the low-melting eutectic improves the fluidity of the alloy. On the other hand, the eutectic is highly brittle and, therefore, impairs mechanical properties.

In the course of solidification alloy *III* forms a compound Fe_2P and additionally a compound Fe_3P which is unstable at high temperatures. Then, as follows from the constitutional diagram, alloy *III* at a normal temperature must be composed of a mixture of crystals of two compounds: $\text{Fe}_3\text{P} + \text{Fe}_2\text{P}$. The amount of each of these compounds in the alloy is determined by the rule of sections and comes to 73 per cent Fe_3P and 27 per cent Fe_2P (see Table in Fig. 9.4).

The compound Fe_3P is formed by the reaction between the liquid phase of the composition corresponding to point *d* and the compound Fe_2P , i.e. by a typical peritectic reaction which, as is known, occurs at interphase surfaces.

On rapid cooling such reactions cannot proceed to their end, and the alloy will contain a lower amount (if any) of Fe_3P than follows from the diagram. Moreover, the last portions of the

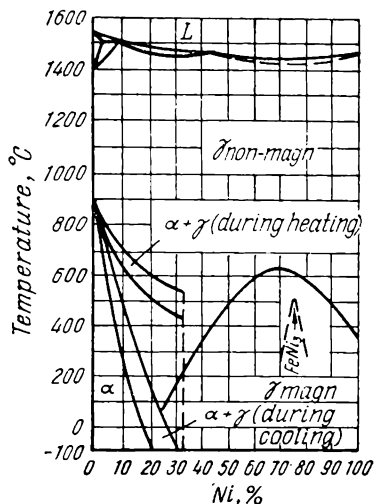


Fig. 9.5. Constitutional diagram of Fe-Ni alloys

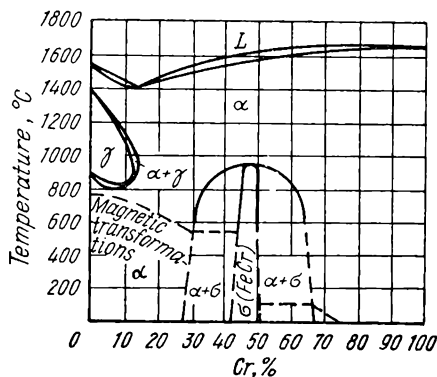


Fig. 9.6. Constitutional diagram of Fe-Cr alloys

liquid phase, which contain iron in an amount greater, than that corresponding to the composition of Fe_3P (for instance, point *f*) may in some cases solidify with the formation of some eutectic composed of a finely disperse mixture of Fe_3P (Fe_2P) and α -solid solution.

Thus, alloy *III* may also have a structure differing substantially from that predicted by the constitutional diagram, if it solidifies under special conditions (for instance, when it is rapidly cooled).

Magnetic transformations of α -solid solution and Fe_3P occurring in these alloys and shown by dotted lines in the diagram (Fig. 9.4) cause no structural changes.

No. 88. Maraging alloys based on the iron-nickel system (see Table 27.6) obtain a martensitic structure upon hardening even with slow cooling, provided the nickel content is within definite limits.

Determine at which nickel concentration — 5, 10 or 20 per cent — the $\gamma \rightarrow \alpha$ transformation occurs as a martensitic rather than diffusion transformation.

To solve the problem, consider the transformation points of Fe-Ni alloys (Fig. 9.5) and analyse the transformation processes in these alloys and their phase ratios at 200 °C.

No. 89. The ductility and plasticity of some high-chromium steels of a low carbon content can be substantially improved by

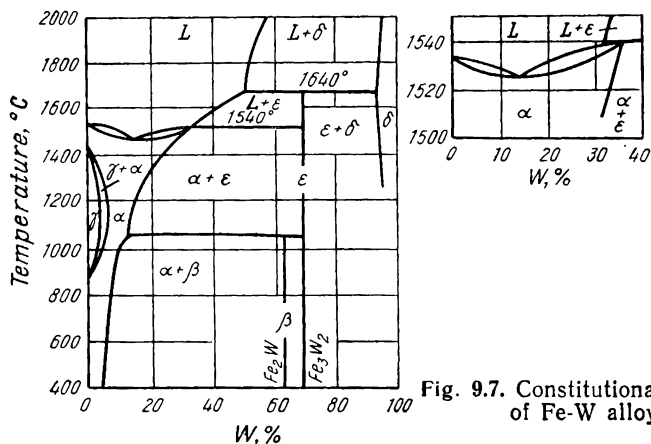


Fig. 9.7. Constitutional diagram of Fe-W alloys

heat treatment. Indicate the alloys of the Fe-Cr system, to which such a treatment is applicable, describe the treatment and its effect on the structure of such a steel.

To solve the problem, analyse the transformation processes in alloys with 10, 20, and 30 per cent Cr (Fig. 9.6); indicate the phase composition and phase ratios: for alloy *I* at 20 and 1000 °C; for alloys with 20 and 30 per cent Cr, at 20 °C.

No. 90. Iron-chromium alloys become corrosion-resistant if their chromium content comes to 12 per cent; with a higher chromium content (25 per cent or more) the corrosion resistance increases even more (see Fig. 9.6), but at the same time the plasticity of the alloys reduces, which in some cases restricts their application.

Explain why chromium has such an effect on the mechanical properties of the alloys. For this purpose, analyse the transformation processes and the structure of alloys with 12, 25, and 35 per cent Cr. Determine the phase composition of alloy *I* at 1000 and 20 °C; and of alloys *II* and *III*, at 20 °C.

No. 91. Alloys of the Fe-W system (Fig. 9.7) of a definite concentration acquire a very high hardness (63-65 HRC) and a high coercive force as a result of precipitation hardening on tempering at 600-650 °C.

Indicate: (a) the approximate tungsten content in such alloys; (b) the recommended heat treatment prior to tempering, and the type of structure it will form in the alloy; (c) the causes of the growth of hardness and coercive force on tempering.

To solve the problem, analyse the transformation processes in alloys with 1, 10, and 45 per cent W and indicate their phase compositions and phase ratios at 400 °C.

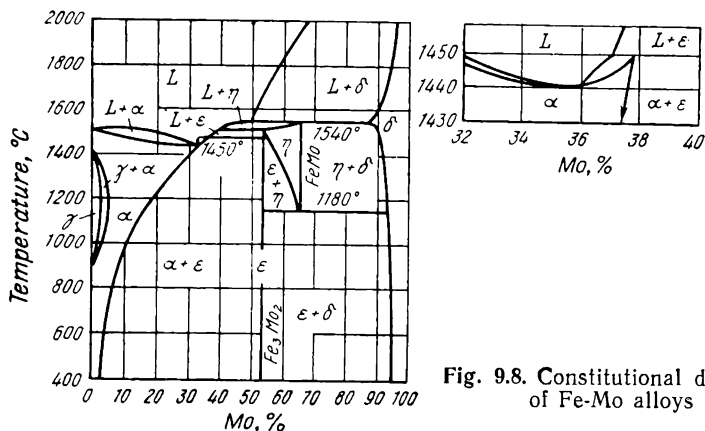


Fig. 9.8. Constitutional diagram of Fe-Mo alloys

No. 92. Solid transformations may occur in some alloys of the Fe-W system, the development of these transformations being dependent on the kind of heat treatment and capable of changing strongly the mechanical properties of the alloys.

Analyse the transformations in alloys with 2, 15, and 75 per cent W (see Fig. 9.7).

Determine the phase compositions and phase ratios: for alloy *I* at 1200 °C; for alloy *II* at 400 °C, and for alloy *III* at 1400 °C. Indicate in which of these alloys the structure and properties can be changed by heat treatment; describe the treatment and its effect (qualitative) on the properties of the alloys.

No. 93. Some alloys of the Fe-Mo system, having a definite composition, are capable of precipitation hardening on tempering subsequent to hardening (which changes the alloy to a supersaturated solid solution).

Analyse the transformations in alloys with 2, 10, and 70 per cent Mo (Fig. 9.8) and determine their phase compositions and phase ratios: for alloy *I* at 1050 °C; for alloy *II* at 400 °C; and for alloy *III* at 1200 °C.

Indicate which of these alloys can be subjected to precipitation hardening; describe its structure after hardening and after tempering, and the effect of this process on its hardness, strength, and ductility.

No. 94. The ductility of some alloys of the Fe-Mo system can be improved by heat treatment.

Analyse the transformations in alloys with 3, 15, and 80 per cent Mo and determine the phase compositions and phase ratios: for alloy *I* at 1100 °C, for alloy *II* at 600 °C, and for alloy *III* at 1000 °C (see Fig. 9.8).

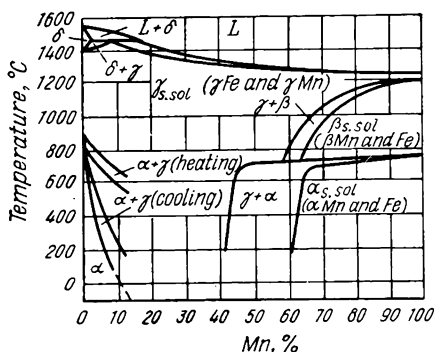


Fig. 9.9. Constitutional diagram of Fe-Mn alloys

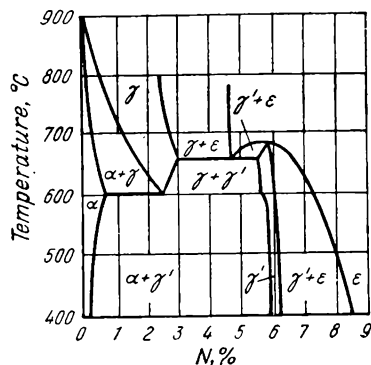


Fig. 9.10. Constitutional diagram of Fe-N alloys

Indicate which of these alloys can be subjected to heat treatment to increase its ductility; describe the treatment and the changes in the structure of the alloy it is responsible for.

No. 95. Iron-manganese alloys employed in industry may obtain: (a) a face-centred lattice and become non-magnetic; or (b) a martensitic structure and high hardness even on slow cooling.

Determine the manganese concentration (5, 12, or 70 per cent) corresponding to the composition of the alloys of each of these two groups.

To solve the problem, consider the transformation processes in the given alloys from the Fe-Mn constitutional diagram (Fig. 9.9); determine the phase composition and phase ratio for each of these alloys at 20 °C.

No. 96. The saturation of the surface layer of steel (especially of that alloyed with chromium and aluminium, or with chromium and titanium) by nitrogen increases its hardness, wear resistance, fatigue strength, and corrosion resistance.

Using the Fe-N constitutional diagram (Fig. 9.10), explain why nitration increases hardness and wear resistance. Recommend the nitrogen concentration to be formed in the thin surface layer.

To solve the problem, analyse the transformations in alloys containing 0.5, 3, and 6 per cent N and determine the phase composition and phase ratio of these alloys at 400 °C.

Take into account that the ϵ -phase in these alloys is excessively brittle and its presence in the nitrated layer is not advisable. The effect of alloying elements on the nitration process may be neglected.

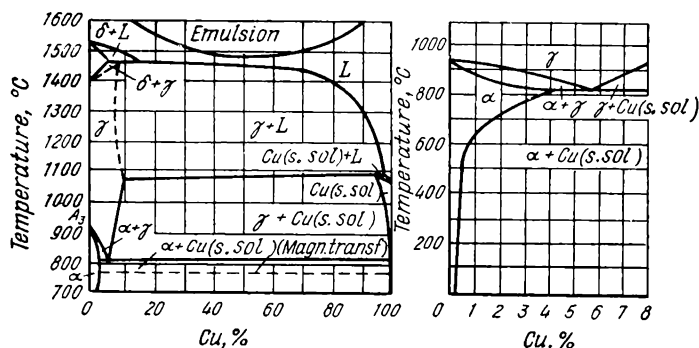


Fig. 9.11. Constitutional diagram of Fe-Cu alloys

No. 97. The corrosion resistance and strength of some stainless and high-strength maraging steels can be improved by additions of copper. But the effect of copper differs depending on its concentration.

Determine copper concentrations that can provide for the following effects: (a) a rise in the strength and hardness through precipitation hardening; describe the heat treatment required for the purpose; (b) a change in grain size, plasticity and ductility owing to the $\alpha \rightarrow \gamma$ transformation; describe the heat treatment suitable for this case.

To solve the problem, consider the transformation processes in alloys with 2, 7, and 20 per cent Cu from the constitutional diagram of the Fe-Cu system (Fig. 9.11); determine their phase composition and phase ratio at 850 °C.

When solving the problem, the effects of the other components in stainless and maraging steels may be disregarded.

No. 98. Introduction of beryllium into certain stainless or maraging steels increases their strength.

Determine the beryllium content (0.1, 3, or 7.5 per cent) that will produce the greatest strengthening effect and describe the heat treatment required for this purpose.

To solve the problem, determine from the Fe-Be constitutional diagram (Fig. 9.12) the transformation processes in the alloys of the given concentrations and indicate the proportions of structural components for the alloys with 0.1 and 3 per cent Be at 1000 °C and for the alloy with 7.5 per cent Be at 600 °C.

When solving the problem, the effects of the other components of the stainless and maraging steels may be disregarded.

No. 99. The strength of many heat-resistant and maraging steels can be increased by additions of titanium.

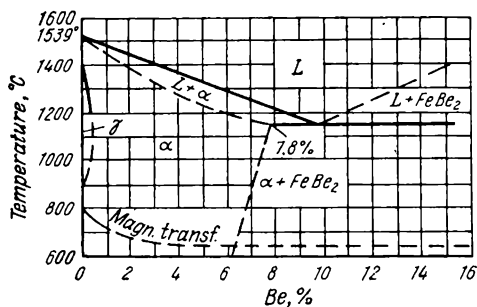


Fig. 9.12. Constitutional diagram of Fe-Be alloys

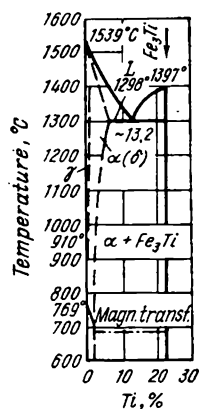


Fig. 9.13. Constitutional diagram of Fe-Ti alloys

Indicate: (a) which titanium content (0.1, 4 or 10 per cent) produces the greatest strengthening effect; (b) the heat treatment which will cause precipitation hardening and thus improve the strength properties; (c) the type of the strengthening phase.

To solve the problem, consider the transformation processes in the Fe-Ti alloys of the above composition from the Fe-Ti constitutional diagram (Fig. 9.13); determine the structures and phase ratios for these alloys at 1100°C, and for the alloy with 10 per cent Ti, additionally at 1300°C.

When solving the problem, the effects of other alloying elements in these steels may be disregarded.

No. 100. Steels made without additions of manganese are unsuitable for plastic working (rolling, forging at 1100-900°C) because of the formation of fissures. This type of defect is called red-shortness. Consider the following diagrams:

(a) Fe-FeS diagram (Fig. 9.14); consider the transformation processes in alloys with 0.03, 2, and 10 per cent S; determine the nature of the phases and the phase ratio for alloys I and II at 1050°C and for alloy III at 1100°C; explain the cause of red-shortness;

(b) Fe-MnS diagram (Fig. 9.15); explain why an addition of manganese eliminates red-shortness and why manganese in an amount of at least 0.4-0.5 per cent is a useful and indispensable addition to steel.

No. 101. Two types of brass are employed in industry: (a) of an increased ductility and (b) of an increased strength.

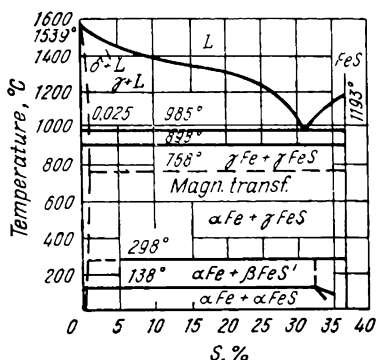


Fig. 9.14. Constitutional diagram of Fe-FeS alloys

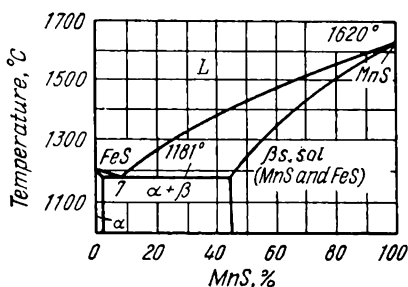


Fig. 9.15. Constitutional diagram of FeS-MnS alloys

Indicate which types of brass (either single- or two-phase) meet these basic requirements and for what reasons, and which of them have better casting properties.

To solve the problem, consider the transformations in alloys with 20, 30, and 41 per cent Zn (Fig. 9.16), determine their phase compositions and phase ratios at 100°C, and indicate the specific features of the structure and properties of these phases.

No. 102. Among Cu-Zn alloys, brass with 32-34 per cent Zn has the highest ductility; it is widely used for cold drawing. With a further increase in the zinc content the brass becomes less ductile, but its strength increases. Alloys with more than 42 per cent Zn are not employed in industry because of their low ductility.

Explain the causes of this effect of zinc.

To solve the problem, consider the transformation processes in alloys with 33, 42, and 45 per cent Zn (Fig. 9.16) and determine their phase compositions and phase ratios at 100°C.

No. 103. Tin bronzes are widely used for the manufacture of sliding

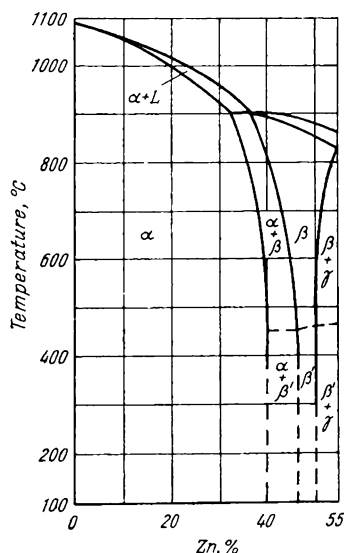


Fig. 9.16. Constitutional diagram of Cu-Zn alloys

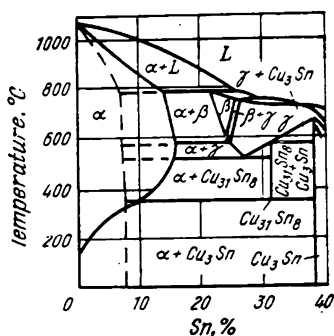


Fig. 9.17. Constitutional diagram of Cu-Sn alloys (the dotted line shows the state after casting into a metallic mould)

bearings as these alloys have a low coefficient of friction.

Determine which types of tin bronze (either single- or two-phase) have, in addition, a higher wear resistance and thus ensure better quality of bearings.

To solve the problem, consider the transformation processes in alloys with 6 and 10 per cent Sn (Fig. 9.17) and determine their phase composition and phase ratio at 20°C. Assume that bearings are to be cast into metallic moulds.

No. 104. Tin-bronze articles are manufactured from either (a) rolled stock (tubes, rods, or strips) or

(b) castings, depending on the ductility of the alloy determined by its tin content.

Decide which types of bronze (either single- or two-phase) are more suitable for these applications and indicate the causes of their having different ductility.

To solve the problem, consider the transformation processes in alloys with 3, 5, and 10 per cent Sn (see Fig. 9.17) and determine their phase composition and phase ratio at 20°C (assume that the castings are cooled in metallic moulds).

No. 105. Lead bronzes for casting sliding bearings must have a uniform distribution of lead particles in the copper matrix.

Determine: (a) which alloy — with 1, 35 or 70 per cent Pb — is most suitable for the purpose; (b) which mode of cooling — either slow or fast — should be recommended for the alloy selected.

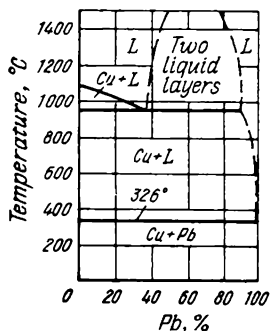


Fig. 9.18. Constitutional diagram of Cu-Pb alloys

To solve the problem, consider the transformation process in the given alloys from the Cu-Pb constitutional diagram (Fig. 9.18), and indicate the phase composition and phase ratio for the alloys with 1 and 35 per cent Pb at 400°C, and for the alloy with 70 per cent Pb at 1200°C.

No. 106. Some alloys of copper and beryllium (beryllium bronzes) are used to make springs for electric machines and instruments, since, as distinct from other copper alloys, the heat treatment of

these alloys can provide a high ultimate strength (up to 100-120 kgf/mm²), high elastic limit (60-70 kgf/mm²) and high electrical conductivity (approx. 0.06 ohm mm²/m).

Indicate the alloys of this system that can be strengthened by heat treatment; describe the treatment. For this purpose consider the transformations in alloys with 2 and 10 per cent Be (Fig. 9.19), determine the structure and phase ratio in these alloys at 20 and 500°C.

No. 107. Resistance elements in many heating devices and furnaces are made from wire or strips of nichrome (alloys of the nickel-chromium system).

Decide which of the alloys (with 5, 20 or 50 per cent Cr, Fig. 9.20) has the highest electrical resistance and can be recommended for the purpose. Note that these alloys must, in addition, have a high ductility at 20°C to be suitable for cold rolling and drawing.

To solve the problem: (a) determine the phase composition and phase ratio in the given alloys at 20 and 1100°C; (b) using Kurnakov's rule, show qualitatively how the electrical resistance of the alloys of this system will change with the nickel content.

No. 108. Aluminium in an amount of approximately 5 per cent is added to titanium alloys to improve their strength and refractory properties, with their ductility remaining at a suitable level.

The addition of aluminium gives a smaller strength rise than the addition of the same amount of chromium ($\sigma_t = 70-90$ kgf/mm² and 100-110 kgf/mm², respectively), but the alloy has a higher ductility. Explain why the same amounts (5 per cent) of chromium and aluminium affect differently the mechanical properties of titanium.

To solve the problem, consider the transformations in titanium alloys

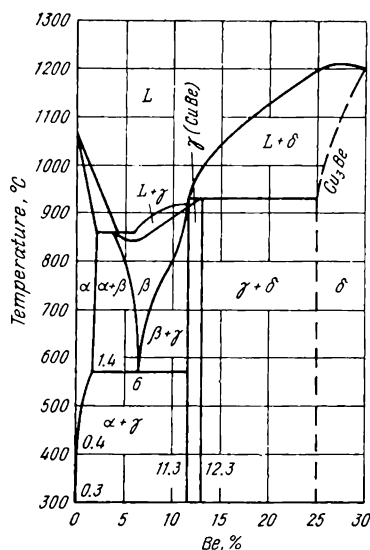


Fig. 9.19. Constitutional diagram of Cu-Be alloys

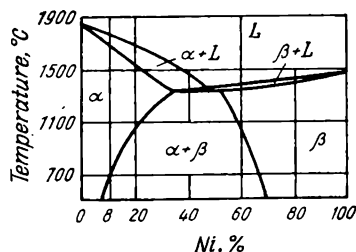


Fig. 9.20. Constitutional diagram of Cr-Ni alloys

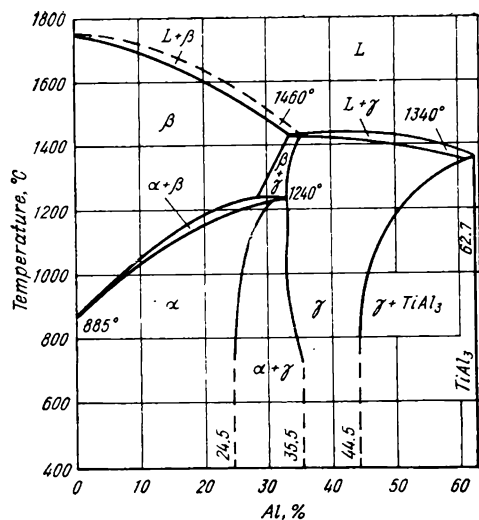


Fig. 9.21. Constitutional diagram of Ti-Al alloys

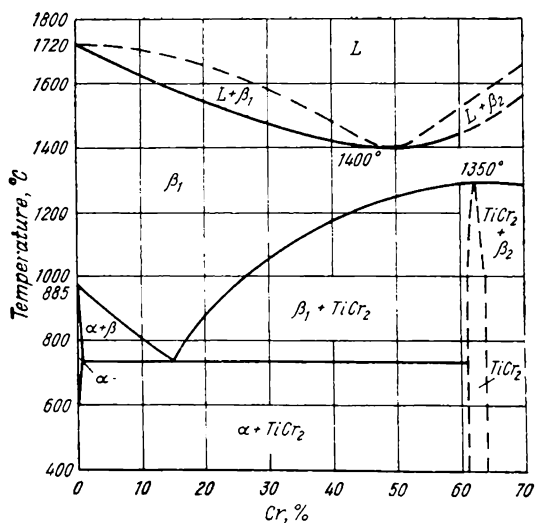


Fig. 9.22. Constitutional diagram of Ti-Cr alloys

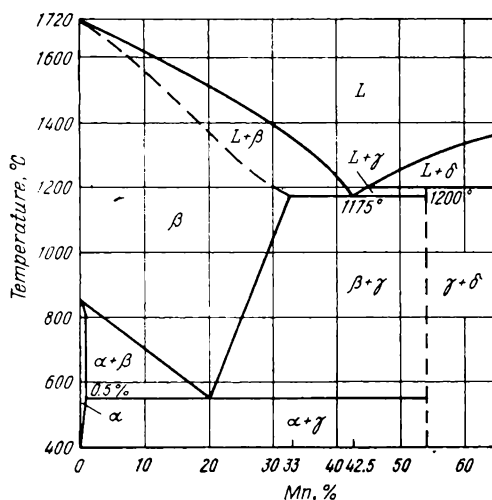


Fig. 9.23. Constitutional diagram of Ti-Mn alloys

with 5 per cent Al and with 5 per cent Cr from the Ti-Al (Fig. 9.21) and Ti-Cr diagrams (Fig. 9.22) and determine their phase composition and phase ratio at 400 °C.

The effect of heat treatment may be disregarded.

No. 109. The formation of a two-phase structure in titanium alloys at 20-400 °C, effected, in particular, through alloying with chromium, makes it possible to improve appreciably their strength properties ($\sigma_t \approx 100$ -110 kgf/mm² approx.), but this effect is not achieved if the second phase is greatly in excess.

Select the optimum chromium content (4, 10 or 15 per cent) and explain your decision.

To solve the problem, consider the transformations in these alloys from the Ti-Cr diagram (see Fig. 9.22) and determine their phase composition and phase ratio at 400 °C.

The effect of heat treatment may be disregarded.

No. 110. Manganese is added to many titanium alloys to improve their mechanical properties, especially hot ductility (malleability).

Indicate the manganese content (2, 22, or 40 per cent) which can ensure this effect.

To solve the problem, consider the transformations in these alloys from the Ti-Mn diagram (Fig. 9.23) and determine their phase composition at 600 °C and phase ratio at 400 °C.

No. 111. Duralumins, i.e. aluminium alloys with 2-5 per cent Cu (and small additions of magnesium, silicon, and manganese)

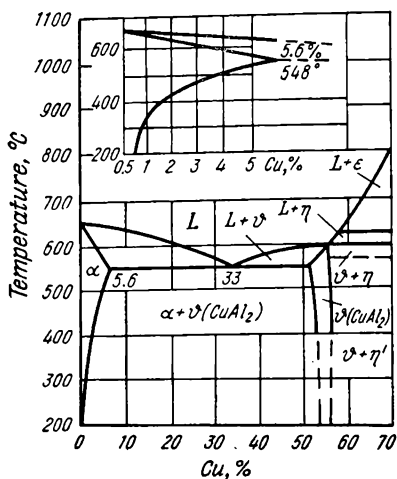


Fig. 9.24. Constitutional diagram of Al-Cu alloys

have a strength of 20-22 kgf/mm² under conditions of equilibrium (after slow cooling) and an appreciably greater strength (40-50 kgf/mm²) after strengthening by heat treatment.

Analyse the transformations in Al-Cu alloys with 0.2, 4, and 40 per cent Cu (Fig. 9.24) and find their structural compositions and phase ratios at 20°C for alloys *I* and *III* and at 400 and 200°C for alloy *II*.

Explain why alloys *I* and *III*, as distinct from alloy *II*, are unsuitable for heat treatment and what kind of heat treatment is suitable for alloy *II* (disregard the effect of small additions of Si, Mg, and Mn in duralumins).

No. 112. Aluminium-silicon alloys of a definite composition, called silumins, possess good casting properties and, because of their low density and satisfactory mechanical properties, are widely employed in industry for casting various articles.

By analysing the Al-Si constitutional diagram (Fig. 9.25) and the dependence between the casting properties of these alloys and the form of the diagram, determine the composition of silumin and decide whether heat treatment of this alloy can be effective.

To solve the problem, consider the transformation processes in alloys with 5, 12, and 20 per cent Si and determine the structure and phase ratio for this alloy at 100°C.

No. 113. The magnesium-aluminium system (Fig. 9.26) includes some magnesium-base alloys which are strongly liable to strengthening by heat treatment because of the presence of aluminium in definite concentrations. These alloys, which have a low density and satisfactory strength, are used in aircraft and other branches of industry.

Recommend the composition for such an alloy and describe the heat treatment and the strengthening phase.

To solve the problem, analyse the transformation processes in alloys with 1, 4, and 30 per cent Mg and determine their structure and phase ratio at 150°C.

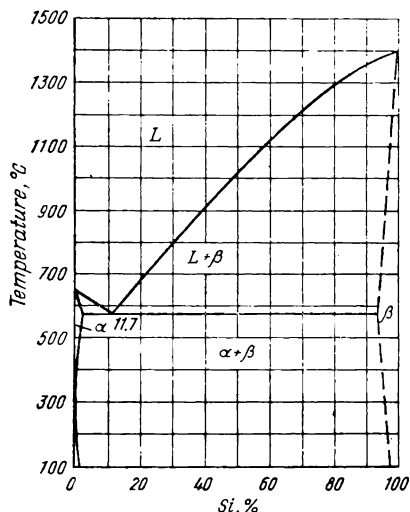


Fig. 9.25. Constitutional diagram of Al-Si alloys

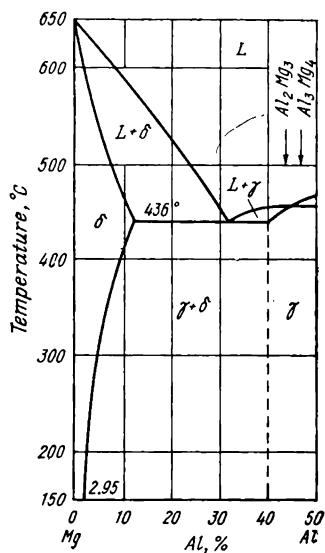


Fig. 9.26. Constitutional diagram of Mg-Al alloys

No. 114. Bearing shells of heavily loaded sliding bearings must have a structure composed of hard particles ensuring a high wear resistance and a softer metallic matrix enveloping these particles and providing for good running-in of the shell against the shaft surface. For this purpose, use is made of bearing alloys (babbitts) based on the Sn-Sb system (Fig. 9.27).

Indicate the region in the diagram (see Fig. 4.22) corresponding to the alloys of this structure and describe the transformations occurring in them during cooling after casting.

To solve the problem, analyse the transformation processes in alloys with 15, 50, and 80 per cent Sb and determine their phase composition and phase ratio at 20°C (note that antimony is harder than tin).

No. 115. Special alloys of the Pb-Sb system (babbitts) are used for making shells of sliding bearings operating at mo-

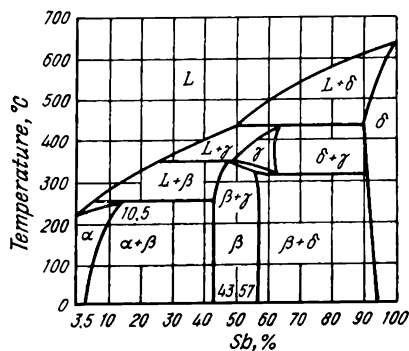


Fig. 9.27. Constitutional diagram of Sn-Sb alloys

derate loads. The structure of such alloys must be composed of a plastic metallic matrix that can be well run-in against the shaft and of hard inclusions of the second phase to ensure a high wear resistance.

Indicate which alloy (with 5, 12 or 14-15 per cent Sb) is most suitable for the purpose (the effects of copper and tin additions in lead babbitts may be disregarded).

To solve the problem, analyse the transformation processes in these alloys (see Fig. 4.18) and determine their structure and phase ratio at 20 °C.

Chapter Ten

CONSTITUTIONAL DIAGRAMS OF TERNARY ALLOYS

10.1. DIAGRAMS OF TERNARY ALLOYS AND METHODOICAL INSTRUCTIONS ON THEIR ANALYSIS

The phase and structural compositions of ternary alloys in equilibrium depending on their temperature and concentration, are determined by using three-dimensional diagrams having the form of a trihedral prism. The base of the prism is usually an equilateral triangle ('concentration triangle'), since the concentrations of all the components can then be conveniently shown in it to the same scale. The components of the alloy are placed at the vertices of the triangle, the concentrations of binary alloys, on its corresponding sides, and those of ternary alloys, inside the triangle. Each point within the triangle will then characterize a ternary alloy of a definite composition.

(a) Determination of Alloy Concentration

The concentration of a ternary alloy can be determined by any one of the three methods discussed below.

1. The first method, called the method of perpendiculars, is based on the geometrical theorem stating that the sum of the perpendiculars dropped from any point within an equilateral triangle onto its sides is equal to the altitude of the triangle.

The altitude of the triangle is taken as 100 per cent, i.e. as the sum of the concentrations of all the three components of the ternary alloy, and the lengths of the perpendiculars, as the percentage concentrations of the components. A perpendicular drawn from any vertex, and therefore, coinciding with the altitude and equal to the latter, will then indicate that all the points at the vertices correspond to pure components, in particular, to 100 per cent of the component placed at that vertex. For instance, perpendicular Cc in Fig. 10.1 shows that vertex C corresponds to 100 per cent of concentration of component C in the alloy, i.e. to pure component C . To determine the concentration of a ternary alloy, i.e. an alloy corresponding to any point within the tri-

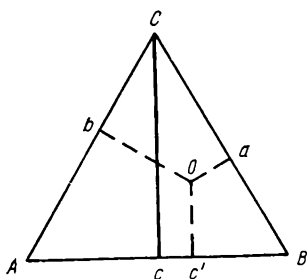


Fig. 10.1. Determining the concentrations of the components of a ternary alloy by the method of perpendiculars

angle, one has to drop perpendiculars from that point onto the sides of the triangle.

The length of a perpendicular shows the concentration of the component at the vertex opposite the side onto which the perpendicular is dropped. For instance, the length of perpendicular Oc' in Fig. 10.1 shows the concentration of component C in the ternary alloy characterized by point O ; the length of perpendicular Oa , the concentration of component A in the same alloy, and the length of perpendicular Ob , the concentration of component B . The

lengths of perpendiculars can be read by using a scale grid plotted within the triangle.

Measurements of the lengths of perpendiculars are somewhat inconvenient, since the concentrations of the components constituting an alloy are laid along the sides of the triangle, and therefore, to a scale proportional to the side (and not to the altitude) of the triangle. Difficulties then arise in solving an inverse problem, i.e. finding the point within the triangle, which corresponds to the composition of an alloy whose concentration is known.

2. By the second method shown as the method of parallels, the concentrations of the components are measured by the lengths of line-segments drawn from the point corresponding to the alloy in question parallel to the sides of the triangle to intersect its other sides. As can be seen from Fig. 10.2a, the composition of a ternary alloy can be expressed not only by the lengths of perpendiculars Oa , Ob and Oc , but also by the lengths of line-segments Oa_1 , Ob_1 and Oc_1 drawn from point O parallel to the sides AB , BC , and AC . These line-segments together with the perpendiculars and the corresponding portions of the sides of the basic triangle form new right triangles in which the perpendiculars drawn from point O are the legs and the line-segments drawn, the hypotenuses, the angles between the legs and hypotenuses being equal to 30 degrees.

All these triangles are similar and, owing to the proportionality between their legs and hypotenuses, the sum of all the three hypotenuses is equal to the side of the basic triangle, just as the sum of the perpendiculars dropped from this point onto the sides of the basic triangle is equal to the altitude of the latter. For this reason, the concentration measurement by the legs (perpendiculars) can be replaced with that by the hypotenuses, which

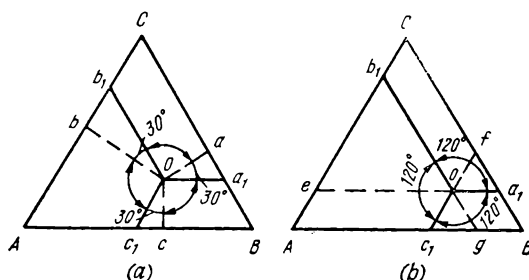


Fig. 10.2. Determining the concentrations of the components of a ternary alloy by the method of parallels

(a) determination by the lengths of line-segments; (b) selection of parallel line-segments

gives the advantage that their lengths can be read directly on the scale plotted for the given concentration on the sides of the basic triangle.

This rule holds true only when the three line-segments drawn from any point within the triangle parallel to its sides form angles of 120 degrees with one another. For instance, the sum of line-segments $Oa_1 + Ob_1 + Oc_1$ (or $Of + Oe + Og$) in Fig. 10.2b is equal to the side of the triangle, whereas the sum $Oa_1 + Og + Oc_1$ (or $Ob_1 + Oe + Oc_1$) is not equal to the side.

Then, to find the concentration of a ternary alloy, draw lines from point O parallel to the sides of the triangle to intersect its other sides (Fig. 10.3). The length of each section cut on the sides of the triangle and confined between the line drawn and the side that is parallel to it will then represent the concentration of the component placed at the opposite vertex.

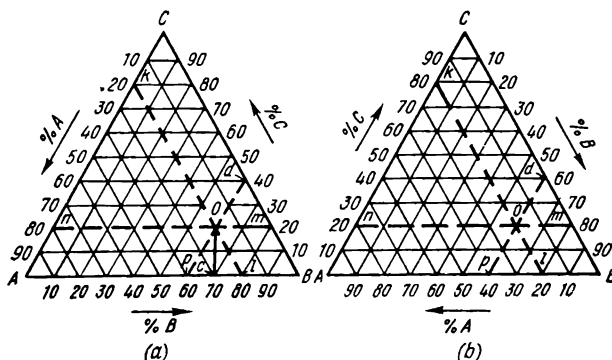


Fig. 10.3. Drawing parallel lines to determine the concentrations of components in a ternary alloy

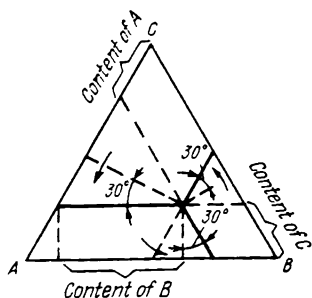


Fig. 10.4. Determining the concentrations of ternary alloys by the lengths of parallel sections (with the perpendiculars being turned through 30 degrees)

For instance, the line drawn parallel to side AB of the triangle in Fig. 10.3a cuts sections B_m and A_n on the two other sides; these sections are equal to the hypotenuse Op of the right triangle Ocp and their lengths represent the concentration of component C in the ternary alloy.

Similarly, the length of section Ck or Bl (see Fig. 10.3) represents the concentration of component A , while the length of section Ap or Cd (or Ok), the concentration of component B in the same alloy.

The application of this method sometimes presents difficulties, since there is no established rule for indicating the concentration of components on the sides of the triangle; in the diagrams found in specialist literature this may be done in different ways, as shown, for instance, in Fig. 10.3a and b.

Though the absolute lengths of the sections, which must be measured to determine the concentration of an alloy, are independent of the position of the numerals on the diagram, a quick calculation of the contents of all the three components may encounter difficulties because of the different positioning of these sections, the more so as the three lines drawn cut six sections on the sides of the triangle.

A different technique may be used to determine the concentration of an alloy by this method. We mentally drop perpendiculars from the point in question onto the sides of the triangle and turn each perpendicular counterclockwise through an angle of 30 degrees to make it parallel to the corresponding side and project the line-segment thus obtained onto this side.

The length of this projection will give the concentration of the component placed at the vertex opposite the side onto which the perpendicular has been dropped (Fig. 10.4).

3. The rule of three sections, proposed by Yu. A. Geller, is the simplest one. From the point considered, we draw two lines parallel to two sides of the triangle to intersect the base (Fig. 10.5). The length of section kl cut by these lines on the base will then represent the concentration of component C placed at the opposite vertex; the length of section Bl on the right will represent the concentration of component A placed at the left vertex of the triangle, and that of section Ak will give the concentration of the component at the right vertex (i.e. of component B in Fig. 10.5a);

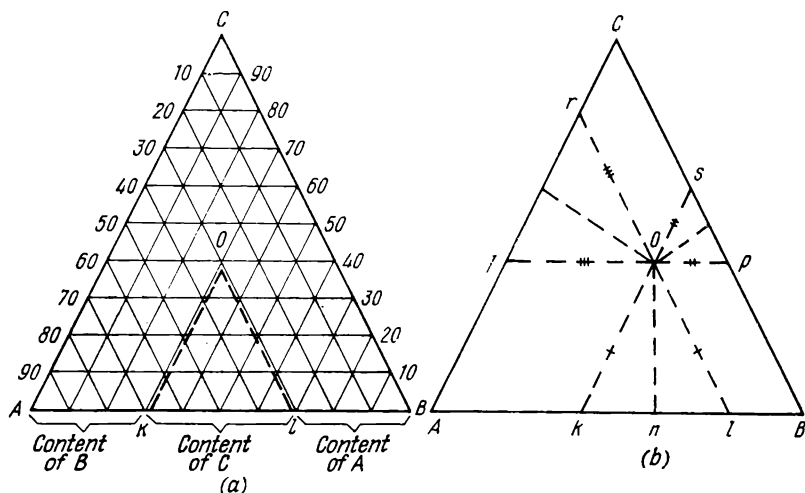


Fig. 10.5. Determining the concentrations of ternary alloy by the rule of three sections

(a) determination of concentrations; (b) demonstration of the rule

This rule can be deduced from the following. The triangle kOl formed by the lines drawn from point O parallel to the sides of the equilateral triangle ABC is similar to the latter (Fig. 10.5b), and is, therefore, also equilateral. The sides Ol and Ok of triangle kOl are the hypotenuses of right triangles kOn and lOn . As has been shown, the length of these hypotenuses represents the concentration of component C ; therefore, side kl , which is equal to kO and Ol (in equilateral triangle OkI) also represents the concentration of component C .

Similarly, as shown in Fig. 10.5b, the length of side Op of triangle pOs represents the concentration of component A . But line-segments Op and lB are equal to one another (as two parallel line-segments cut by two parallel lines). It may be shown in a similar way that the length of section Ak determines the concentration of component B .

This rule is only applicable to determining the concentrations of alloys. It should not be concluded that a side of the triangle, while characterizing the structure of a two-component alloy, can characterize the structure of a ternary alloy.

(b) Three-dimensional Diagrams

A three-dimensional constitutional diagram (spatial model) is a trihedral prism with an equilateral triangle as its base; temperatures are laid along the altitude of the prism.

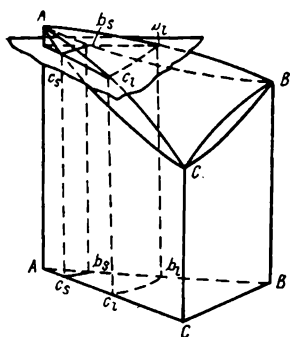


Fig. 10.6. Three-dimensional constitutional diagram of ternary alloys with their components being fully soluble in both liquid and solid state

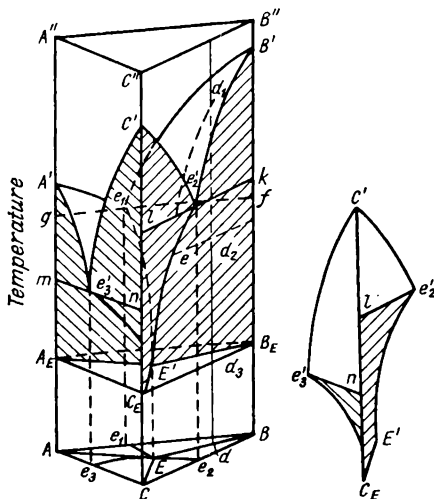


Fig. 10.7. Three-dimensional constitutional diagram of ternary alloys with their components being fully soluble in liquid state, but insoluble in solid state

Shown in Figs. 10.6 and 10.7 are examples of three-dimensional diagrams of ternary (three-component) alloys: (a) completely soluble both in liquid and solid state (Fig. 10.6); (b) completely soluble in liquid state, but insoluble in solid state (Fig. 10.7).

As with binary diagrams, the analysis of ternary alloy diagrams makes it possible to determine the phase and structural compositions, estimate qualitatively many physical, mechanical and technological properties of these alloys under conditions of equilibrium, and in some cases predict the nature of changes in the structure and properties of individual alloys on their transition to a non-equilibrium (metastable) state.

But ternary diagrams in the form of trihedral prisms (three-dimensional diagrams) are only seldom used in specialist literature because of the difficulties in representing curvilinear surfaces, the more so as these surfaces and lines of the diagrams intersect. On the other hand, extensive experimental work and studies into a large number of alloys are required to construct the complete three-dimensional model of the alloys of a ternary system.

(c) Sections Through Three-dimensional Diagrams

The analysis of ternary systems can in some cases be limited to the study of only some of the regions and concentrations which are of the highest scientific interest. Literature sources on the subject usually give only some studied sections of diagrams, rather than three-dimensional diagrams or photographs of three-dimensional models.

The following methods are used for the purpose.

Horizontal sections. These are plotted as isothermal sections or as projections of certain surfaces and lines of a three-dimensional diagram onto a horizontal plane.

Isothermal sections show the phase and structural compositions for all concentrations of ternary alloys, but at a definite temperature. These sections usually have the form of equilateral triangles, provided the prism has also been based on an equilateral triangle.

Isothermal sections are convenient for the determination of the phase and structural compositions of alloys of a given ternary system, if conodes are plotted on them. The disadvantage of this method of construction is that such a diagram cannot show how the phase and structural compositions vary with temperature. Therefore, an analysis of such a section cannot provide data on many properties of ternary alloys, in particular, on the form of the liquidus and solidus lines and the change of solubility with temperature, which determines the susceptibility of the alloys to heat treatment and their capacity to change their structure and properties.

This disadvantage can, to a large extent, be eliminated if not one, but at least two, or more horizontal sections for different temperatures are made through a three-dimensional diagram.

By comparing these sections, one can judge about the variations of the phase and structural regions and the course of the lines on the diagram, and draw conclusions as to the structure and some properties of the ternary alloy.

The advantage of using isothermal sections is that conodes can be plotted on them, i.e. straight lines connecting the conjugate points of the liquidus and solidus lines (or of the solubility lines) at the same temperature (Fig. 10.8).

Conodes are plotted on the diagrams on the basis of experimental findings. The points of intersection of a conode with the solidus or liquidus line or with the solubility lines represent respectively the composition and number of the phases (for instance, liquid and solid phases for the liquidus and solidus lines) which are in equilibrium in an alloy of the given composition at the

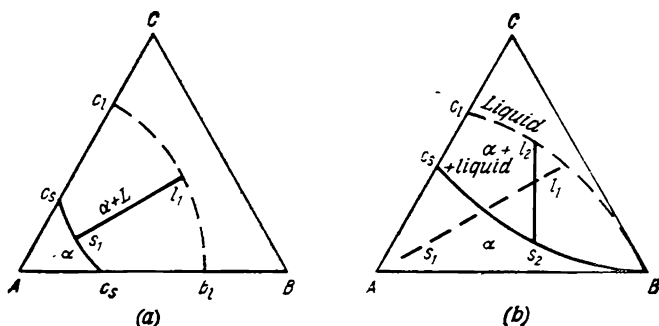


Fig. 10.8. Isothermal sections through the three-dimensional constitutional diagram of the ternary alloy shown in Fig. 10.6

(a) section made at T_1 , somewhat lower than the melting point of the most high-melting component A; (b) section made at T_2 , lower than T_1 , corresponding to the melting point of component B (l_1s_1 is a conode; its direction varies with decreasing temperature); — — — liquidus line; — solidus line

given temperature. The alloys represented by other points of the conode will have the same phase composition but different phase ratios.

The projections of the surfaces and lines of a three-dimensional diagram onto a horizontal plane usually form a concentration triangle, onto which the lines of the three-dimensional diagram can be projected, different points on these lines corresponding to different temperatures (i.e. different isothermal sections). In this way, for instance, are plotted the lines of binary eutectics for alloys forming eutectic mixtures, and the point determining the concentration of the ternary eutectic (Fig. 10.9), with the temperatures of the formation of the eutectics being indicated on

the diagram. In this case, one can judge of the course of the crystallization process.

Liquidus and solidus lines, solubility lines or lines characterizing a group of alloys having some properties in common, for instance, the same hardness, can also be projected onto the concentration triangle.

The number of lines plotted on a diagram to characterize the phase composition or certain properties of alloys must

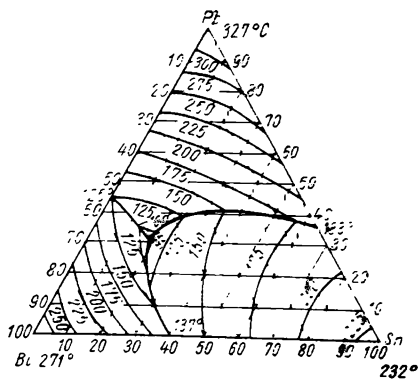


Fig. 10.9. Projection of the liquidus planes for Pb-Sn-Bi alloys

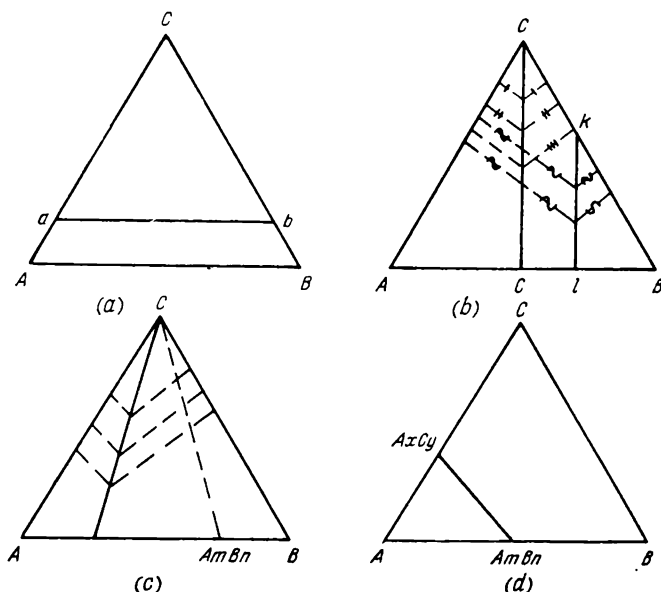


Fig. 10.10. Sections of the concentration triangle

(a) parallel to one of the sides; (b) along the altitude (Cc) and parallel to the altitude (kl); (c) along a secant (through a face of the prism); (d) through compounds formed by the alloy components

be within a reasonable limit, otherwise the diagram will be inconvenient to use.

The application of horizontal sections, however, provides no possibility for constructing the complete cooling (or heating) curve of a ternary alloy, as is possible with the diagrams of binary alloys.

Vertical sections. Such sections show qualitatively the phase and structural compositions of ternary alloys at any temperature, but only for some concentrations determined depending on how the section through the three-dimensional diagram has been made.

The following types of section are in use:

(a) a section parallel to one of the sides of the concentration triangle (i.e. parallel to one of the faces of the prism). In this case the content of one of the components (for instance, the content of component C for the section shown in Fig. 10.10a) remains constant, while those of the two other components (A and B) vary from point a to point b ;

(b) a section through one of the vertices of the concentration triangle, i.e. through an edge of the prism and along its altitude

or parallel to the latter (Fig. 10.10*b*), or else at a definite angle in a direction not coinciding with the altitude (Fig. 10.10*c*). In all such cases the ratio between the contents of two components (*A* and *B* in Fig. 10.10*b* and *c*) remains constant with variations of the component concentrations in the alloy, as shown by the perpendiculars dropped onto the sides of the triangle. Such a section is useful when it is required to show some ternary alloys characteristic of a given system or some specific features of the alloys (for instance, the effect of one component onto the properties and structure of ternary alloys with a constant ratio between the concentrations of the other two components).

If a section is made through the points corresponding to the composition of a pure component and a chemical compound formed by the other two components (for instance, $C-A_mB_n$ in Fig. 10.10*c*), it may in some cases represent the constitutional diagram of an alloy composed of two components (for instance, of a pure metal and a chemical compound). Such sections are termed *pseudo-binary*. The direction of a conode in such a section coincides with the plane of the vertical section. Conodes can be plotted on a pseudo-binary section, and phase compositions and phase ratios determined quantitatively (as on the diagrams of binary alloys);

(*c*) special sections (of the type shown in Fig. 10.10*d*), which make it possible to analyse certain ternary alloys possessing special properties, for instance, alloys formed not by pure components, but by chemical compounds, etc. In many cases such sections also represent pseudo-binary diagrams. The question of whether such a diagram can be regarded as a true binary diagram is in each case decided upon experimentally.

Depending on the structure and properties of alloys, we can select vertical sections which are most characteristic of the given system.

A diagram representing a vertical section is similar to a diagram of a binary alloy, but, on the other hand, it has certain specific features. In contrast to the diagrams of binary alloys, it is impossible to draw conodes on vertical section diagrams (except for pseudo-binary diagrams) and use them for determining the concentrations and number of the phases in equilibrium at a given temperature. A vertical section through a three-dimensional diagram usually does not coincide with the direction of a conode, since the latter changes its direction with temperature (as shown schematically in Fig. 10.8). A horizontal line drawn on a vertical section through equal-temperature points on the liquidus and solidus lines (or on solubility lines) cannot serve for de-

termining the composition and number of the phases in equilibrium, since this line is not a conode.

In addition, eutectic (and also eutectoid or peritectic and peritectoid) transformations in ternary alloys can occur not only at a fixed temperature (as in binary alloys), but also within a definite temperature range.

The nature of a transformation is determined by the phase rule. If a transformation occurs in the presence of four phases, this will correspond to a non-variant equilibrium ($C = K + 1 - P$, and therefore, $C = 3 + 1 - 4 = 0$), and will be shown by a horizontal line on a vertical section of the three-dimensional diagram, since the transformation occurs at a constant temperature. If three phases are present, the transformation occurs within a temperature interval and will be characterized by a region of transformations on the vertical section.

If a vertical section is made not through a vertex of the triangle (an edge of the prism), it often fails to include the transformations occurring in the pure components forming the ternary alloys under study. On such vertical sections the liquidus and solidus lines on ordinates (for solid solutions) do not intersect at or start from the same point. Such a course of the solidus and liquidus lines (and also of many solubility lines) is explained by the construction shown in Fig. 10.11.

Figure 10.12 shows, as an example, a vertical section through the Fe-C-W ternary diagram, which corresponds to 4 per cent W, i.e. a section parallel to the Fe-C side. As seen from the diagram, the liquidus and solidus lines do not meet in the same point on ordinates, since the ordinates correspond not to pure components, but to the binary alloys containing respectively 96 per cent Fe and 4 per cent W, and 96 per cent Fe_3C and 4 per cent W. A eutectic transformation occurs within a temperature interval, since it corresponds to the separation of a binary eutectic, but is finished (on cooling) at a fixed temperature at which a ternary eutectic is separated.

On the other hand, a eutectoid transformation begins and ends at a fixed temperature, since it proceeds in the presence of four phases: γ -phase, α -phase, $\text{Fe}_3\text{W}_3\text{C}$, and Fe_3C .

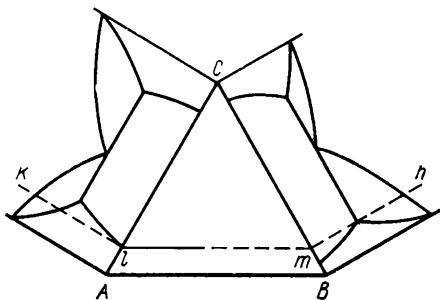


Fig. 10.11. Vertical section parallel to one of the sides of the triangle (a face of the prism)
 l_m —cutting line

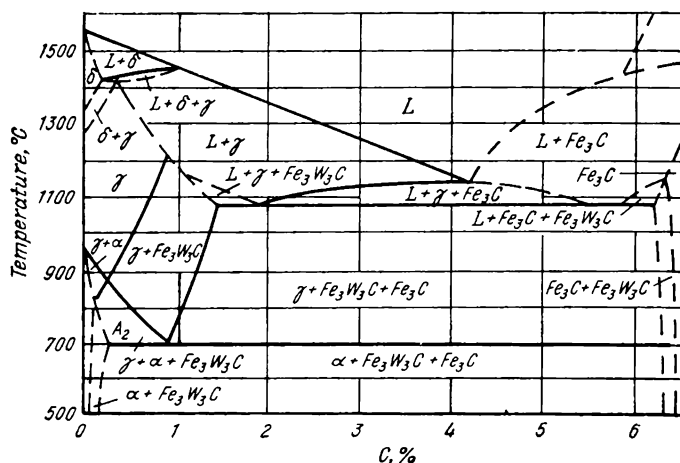


Fig. 10.12. Vertical section through the Fe-C-W three-dimensional diagram, made parallel to the Fe-C side at 4 per cent W

Vertical sections of three-dimensional diagrams are convenient for qualitative (and the pseudo-binary diagrams, also quantitative) determinations of changes in the phase and structural compositions of alloys with temperature, i.e. they characterize the processes of crystallization from liquid and transformations in the solid state. But they can describe these processes only for a small number of alloys, rather than for all alloys of the ternary system being studied.

This disadvantage can be eliminated by constructing two or more vertical sections for a given ternary system. By rationally selecting these sections, it is possible to determine quite accurately the most essential properties of the corresponding ternary alloys. For instance, by comparing a number of sections made parallel to one side of the triangle, it is in many cases possible to determine quite fully the effect of one component of a ternary alloy on its phase and structural state, as dependent on temperature, for different concentrations of the other two components.

Problems

The problems below deal mainly with various sections of three-dimensional diagrams, as such sections are the ones most often found in specialist literature. Having considered and compared the sections given in a problem, the student should give complete answers to the questions set forth.

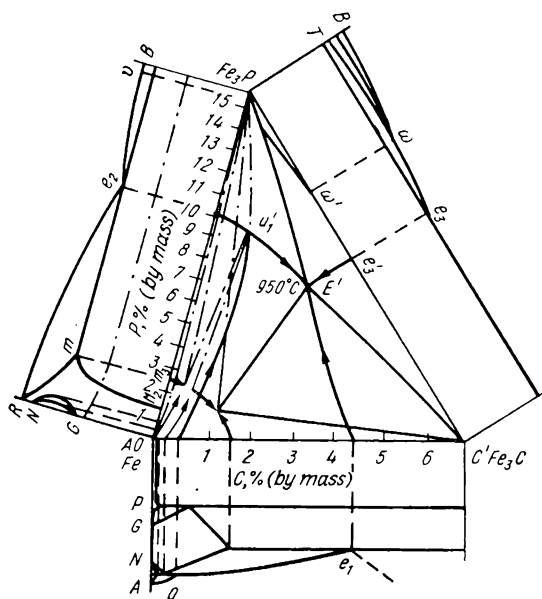


Fig. 10.13. Projection of the crystallization planes onto the concentration triangle of the Fe-C-P system, bounded by the Fe_3C - Fe_3P section

In the problems on horizontal sections, the student should indicate the positions of the given ternary alloys, using the properties of the concentration triangle.

In the problems on vertical sections, the student should construct, if required, the cooling and heating curves of the corresponding ternary alloy, following the indications given in this chapter and in the chapter on binary alloys. In ternary alloys having a eutectic (eutectoid) transformation, the binary eutectic (eutectoid) will solidify within a definite temperature range, rather than at a fixed temperature. Such cases should be shown on the cooling (heating) curve by an inclined line with bends.

No. 116. Figure 10.13 shows a projection of the crystallization surfaces onto the concentration triangle of the Fe-C-P system, the triangle being cut by a vertical section Fe_3C - Fe_3P , i.e. limited to alloys of the Fe- Fe_3C - Fe_3P system.

Describe the crystallization process of an alloy containing 4 per cent C and 1 per cent P, give its composition, and the temperature of the formation of ternary eutectic.

Compare the crystallization process of this ternary alloy with that of a binary alloy with the same carbon content (4 per cent),

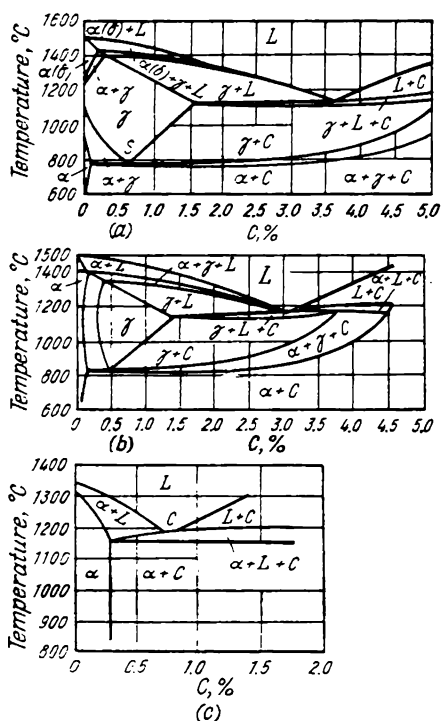


Fig. 10.14. Vertical sections through the Fe-C-Si diagram, made parallel to the Fe-C side

(a) 2% Si; (b) 3.8% Si; (c) 11% Si

transformation, the content of carbon in the eutectoid, and the solubility of carbon in α - and γ -iron.

Using the given vertical section do the following:

(a) determine the content of carbon at which the steel with 4 per cent Si can acquire a single-phase ferrite structure not subject to transformations on heating or cooling; indicate the lowest content of carbon that can be obtained in steel made in an electric or open-hearth furnace;

(b) show the effect of silicon (on dissolution in α -iron) on resistivity, noting that this characteristic determines the eddy-current loss of transformer steel.

No. 118. Figure 10.14 shows vertical sections through the iron-silicon-carbon diagram, made at 2, 3.8 and 11 per cent Si.

Compare these sections with the iron-carbon diagram and indicate the influence of silicon on (a) the carbon content in the

but without phosphorus. Explain why the casting properties of cast iron (fluidity) are improved as the phosphorus content is increased.

Show how increasing the phosphorus content affects the mechanical properties of cast iron, taking into account that its structure is thus enriched in the Fe-Fe₃C-Fe₃P phosphide eutectic which contains two compounds (Fe₃C and Fe₃P).

No. 117. Siliceous transformer steel with 4 per cent Si must possess high permeability and low eddy-current loss. For this, the structure of the steel should approximate that of a single-phase system (based on α -iron).

Figure 10.14b shows a vertical section through the iron-silicon-carbon ternary diagram, cut parallel to the iron-carbon side at 3.8 per cent Si.

Compare this section with the iron-carbon diagram. Describe the effect of silicon on the temperature of the eutectoid

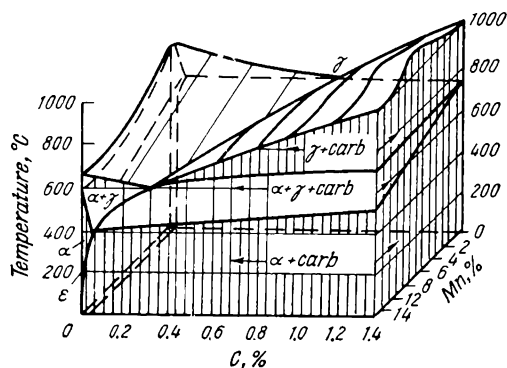


Fig. 10.15. Three-dimensional diagram of Fe-C-Mn alloys (within the region of solid-state transformations)

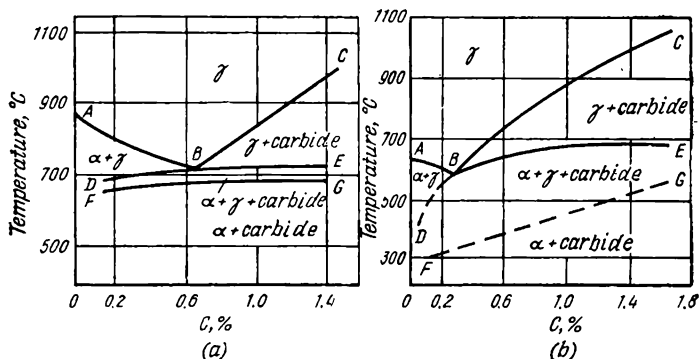


Fig. 10.16. Vertical sections through the diagram of Fe-C-Mn alloys (within the region of solid-state transformations)
 (a) 2.5% Mn; (b) 13% Mn

eutectic; (b) the carbon content in the eutectoid and the temperature of its formation from austenite; and (c) the existence region of stable austenite (as a single-phase structure).

Using the characteristic of the effect of silicon on the structure of iron-carbon alloys, obtained by this comparison, determine the structural class of an alloy with 0.6 per cent C and more than 11 per cent Si.

An alloy with 0.5-0.6 per cent C and 13-16 per cent Si has a high stability against the action of hydrochloric acid. Name the technological process (either casting or plastic working) that must be used for making articles from this alloy, in view of its structure and properties.

No. 119. Figures 10.15 and 10.16 show respectively a three-dimensional model, and vertical sections through the Fe-C-Mn diagram in the region of solid transformations, made at 2.5 and 13 per cent Mn.

Compare these sections with the Fe-C diagram and show the effect of manganese on (a) the carbon content in the eutectoid and the temperature of its formation from austenite; and (b) the region of stable austenite.

Explain (using the phase rule) why eutectoid transformations in ternary alloys occur within a temperature interval (and not at a fixed temperature, as in iron-carbon alloys).

Indicate the hardening temperature for a steel with 1.3 per cent C and 13 per cent Mn (Grade $\Gamma 13$), if a single-phase structure is required (at which the steel is paramagnetic).

No. 120. Figure 10.17a shows a vertical section through the Fe-C-Cr diagram, made at 12 per cent Cr (i.e. in a plane parallel to the iron-carbon side).

Determine the structural class of steel with 1.5 per cent C and 12 per cent Cr and describe its structure (a) in equilibrium and (b) after hardening.

Indicate the application field of this steel.

No. 121. The corrosion resistance of low carbon steels (up to 0.1 per cent C) is improved by increasing their chromium content from 12-15 per cent to 17-20 per cent. But steel containing 17-20 per cent Cr, as distinct from that with 12 per cent Cr, is unhardenable and becomes coarse-grained after heating, which impairs its ductility.

Consider the vertical sections of the Fe-C-Cr diagram, made at 12 and 20 per cent Cr (Fig. 10.17), and describe the structure of steel with 0.1 per cent C and 12 per cent Cr and that of steel with 0.1 per cent C and 20 per cent Cr at 20 and 1000°C.

Explain why the properties of these two steels are different.

No. 122. Figure 10.18 shows the structure of stainless steel with 0.05 per cent C, 20 per cent Cr, and 8 per cent Ni. The steel in this state is paramagnetic (or weakly magnetic).

Using the horizontal (isothermal) sections through the Fe-Cr-Ni diagram, made at 1100 and 400°C (Fig. 10.19), determine the structure and heat treatment conditions of this steel for the state shown in Fig. 10.18, and indicate its structure in equilibrium. When solving the problem, the effect of carbon may be disregarded.

No. 123. Permanent magnets are made of Fe-Ni-Cu alloys (60 per cent Cu, 20 per cent Ni, and 20 per cent Fe) having high magnetic properties after heat treatment and plastic deformation.

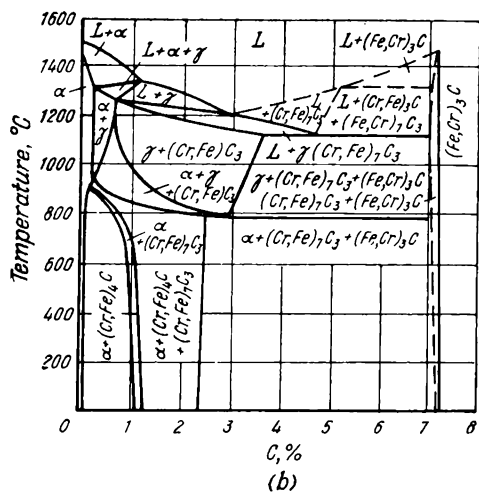
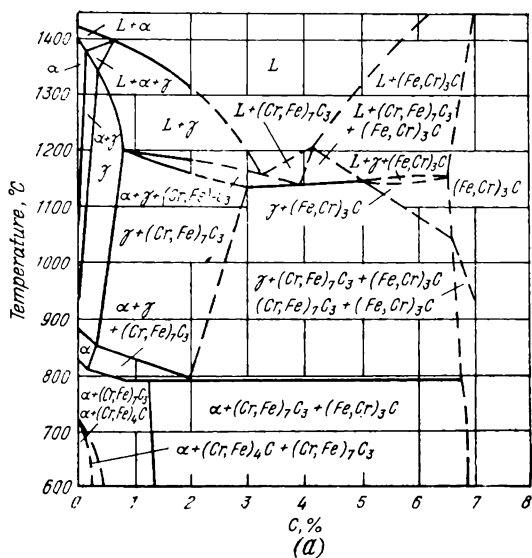


Fig. 10.17. Vertical sections through the diagram of Fe-C-Cr alloys; made parallel to the Fe-Fe₃C side
(a) 12% Cr; (b) 20% Cr



Fig. 10.18. Structure of stainless steel (0.1% C, 18% Cr, and 8.5% Ni), 500X

Figure 10.20 shows the horizontal (isothermal) sections through the Fe-Ni-Cu diagram, made at 20 and 800 °C, and Fig. 10.21, the vertical section through the same diagram corresponding to the ratio Cu : Fe = 3 : 1.

Determine by the conodes on the horizontal sections of the diagram the proportions and compositions of the phases in equilibrium at 800 and 20 °C (for the given alloy).

Plot the concentration triangle for the horizontal section made at 20 °C and draw in it a line corresponding to the vertical section shown in Fig. 10.21 (for a Cu : Fe ratio of 3 : 1).

Referring to the sections obtained, describe the heat treatment possible for the alloy with 60 per cent Cu + 20 per cent Ni + 20 per cent Fe and determine the hardening temperature which gives a single-phase structure.

No. 124. Hardening from a temperature of 1300-1400 °C followed by tempering (at 600-800 °C) can cause the precipitation hardening of many Fe-Co-W alloys due to the dissolutions of the disperse particles of $(\text{Fe, Co})_7\text{W}_6$ and Fe_3W_2 during hardening

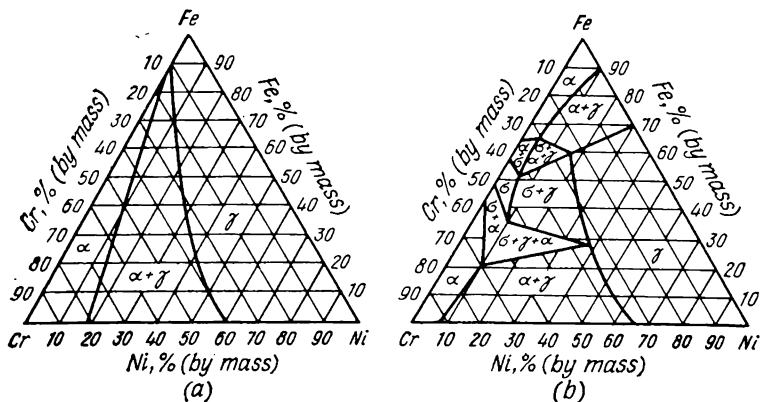


Fig. 10.19. Isothermal sections through the diagram of Fe-Cr-Ni alloys
(a) 1100 °C; (b) 400 °C

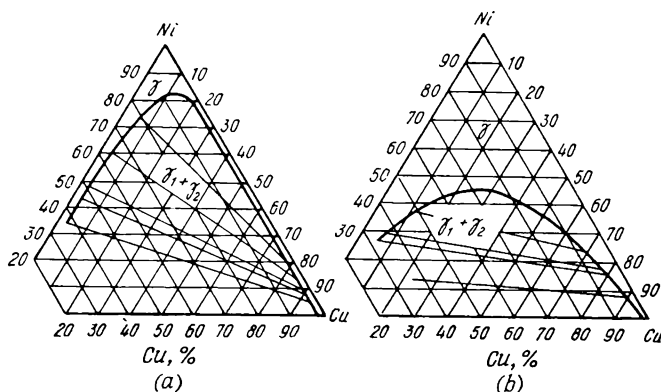


Fig. 10.20. Isothermal sections through the diagram of Fe-Cu-Ni alloys
(a) 20 °C; (b) 800 °C

and their separation during tempering, these two substances forming a solid solution (θ -phase). The hardness of these alloys then increases to 66-67 HRC and is retained even after long holding at 600-700 °C, because of which the thermal stability of these alloys exceeds that of high-speed steel.

Such alloys, however, possess high brittleness, its value being higher for alloys corresponding (by composition) to the regions of α - and γ -solid solutions of the diagram but not subject to transformations on heating or cooling, and somewhat lower for alloys undergoing $\gamma \rightarrow \alpha$ -transformation during hardening.

Figure 10.22 shows the horizontal (isothermal) sections of the Fe-Co-W diagram made at 20 and 1300 °C.

Using the diagram, do the following:

1. Exemplify the composition of the following three alloys of the same tungsten content: (a) an alloy lying within the region of α -solid solution; (b) an alloy lying within the region of γ -solid solution and undergoing no transformation; and (c) an alloy undergoing $\gamma \rightleftharpoons \alpha$ -transformations.

2. Consider the effect of high-temperature heating on the structure of these alloys and the role of the transformations occurring during passages through the critical points, and explain what the

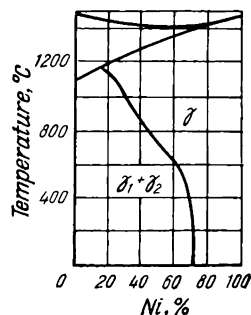


Fig. 10.21. Vertical section through the diagram of Fe-Cu-Ni alloys, made at Cu : Fe = 3 : 1

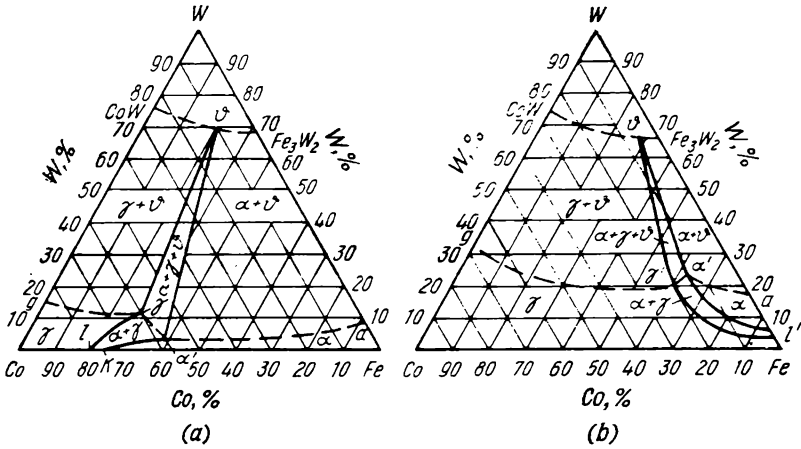


Fig. 10.22. Isothermal sections through the diagram of Fe-Co-W alloys
(a) 20 °C; (b) 1300 °C

differences are in structure between these alloys after hardening and why the alloy undergoing $\gamma \rightleftharpoons \alpha$ -transformations has a lower brittleness after hardening.

3. Decide whether the alloys lying within the region bounded by the side Fe-Co and the line $\alpha\alpha\gamma g$ are liable to precipitation hardening (line $\alpha\alpha\gamma g$ determines the solubility limit of the θ -phase).

No. 125. Figure 10.23 shows the horizontal (isothermal) sections through the Fe-Co-Mo diagram, made at 20 and 1300 °C, which indicate that many alloys of this system display the fol-

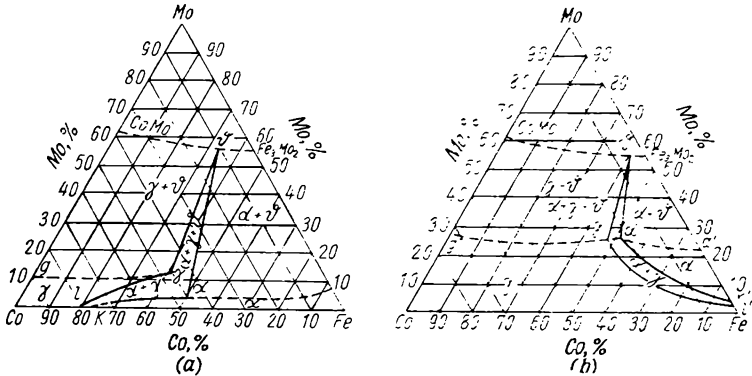


Fig. 10.23. Isothermal sections through the diagram of Fe-Co-Mo alloys
(a) 20 °C; (b) 1300 °C

lowing specific features on heating (or cooling), depending on the concentrations of their components:

(a) undergo $\alpha \rightarrow \gamma$ (and $\gamma \rightarrow \alpha$) transformations, whereas other alloys do not change their structure under these conditions;

(b) dissolve the θ -phase, the solubility of this phase being dependent on temperature [the θ -phase is a solid solution of $(\text{Fe, Co})_7\text{Mo}_6$ and Fe_3Mo_2].

Consider the alloys of the same iron content (50 per cent), having a cobalt content of 48, 30, and 10 per cent, respectively, and describe their structures at 20 and 1300 °C. Name the transformations occurring in each of these alloys during heating to 1300 °C and during subsequent cooling.

Explain why many alloys of this system, for instance, the alloys with 15 per cent Mo + 30 per cent Co + 55 per cent Fe, or those with 20 per cent Mo + 50 per cent Co + 30 per cent Fe, hardened from 1300 °C, obtain an appreciably higher hardness after tempering at 600-700 °C, their hardness values increasing from 35 HRC (as hardened) to 60-70 HRC after tempering.

Describe the structures of these two alloys after hardening and after tempering, and indicate the alloy that has a coarser grain (and therefore, greater brittleness) after hardening.

No. 126. High-strength copper-base Cunial alloys with 2-6 per cent Al and 5-15 per cent Ni have a wide industrial application. The ultimate strength of these alloys can be increased from 25-35 kgf/mm² to 80-90 kgf/mm² (with a relative elongation of 5-15 per cent) by heat treatment.

Figure 10.24 shows the horizontal (isothermal) sections through a portion (the 'copper corner') of the Cu-Ni-Al diagram, made at 1000 and 400 °C.

Determine the phase composition of the alloys with (a) 2 per cent Al and 12 per cent Ni, and (b) 4 per cent Al and 12 per cent Ni, at 1000 and 400 °C.

Indicate the kind of heat treatment suitable for these alloys.

No. 127. Figure 10.25 shows the horizontal (isothermal) sections through a portion (the 'copper corner') of the Cu-Zn-Al diagram, made at 800, 600, 475, and 410 °C, and Fig. 10.26 gives the vertical sections through this diagram, made at 2 and 4 per cent Al.

Determine the phase composition of the high-strength brass with 25 per cent Zn and 4 per cent Al at the temperatures indicated in Fig. 10.25.

Using the phase rule, explain why the $\beta \rightleftharpoons \alpha + \gamma$ eutectoid transformation in these alloys occurs within a temperature interval, rather than at a fixed temperature, as in binary alloys.

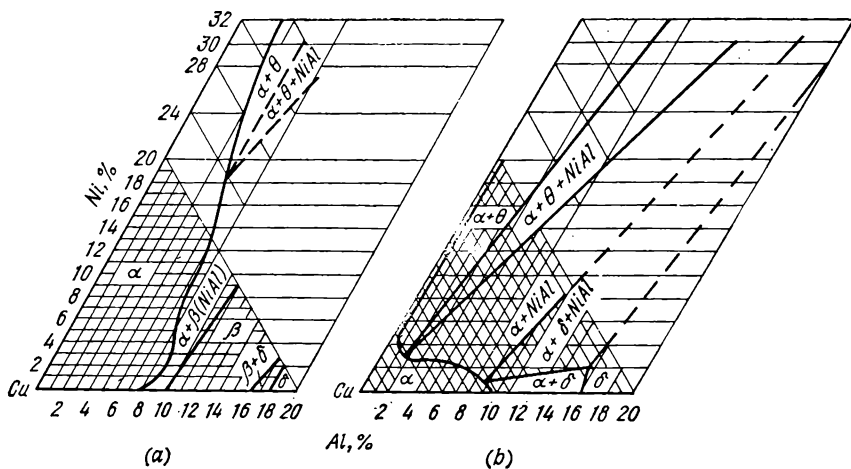


Fig. 10.24. Isothermal sections through a portion ('copper corner') of the diagram of Cu-Ni-Al alloys
(a) 1000 °C; (b) 400 °C

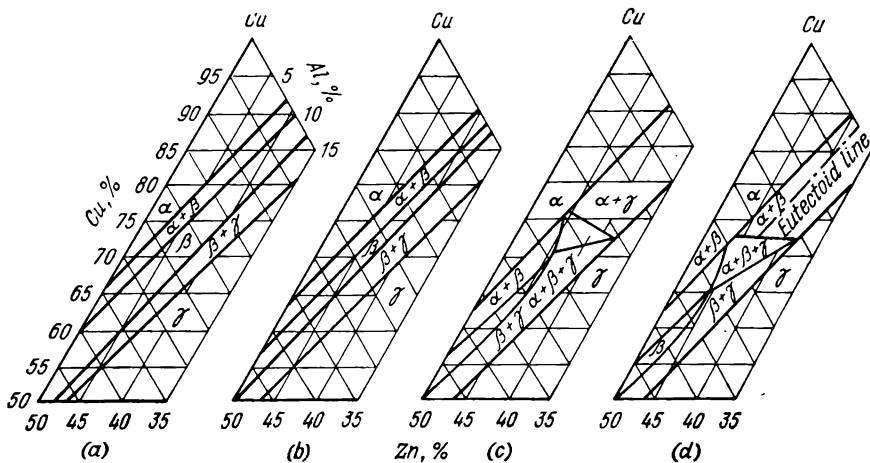


Fig. 10.25. Isothermal sections through a portion ('copper corner') of the diagram of Cu-Zn-Al alloys
(a) 800 °C; (b) 600 °C; (c) 475 °C; (d) 410 °C

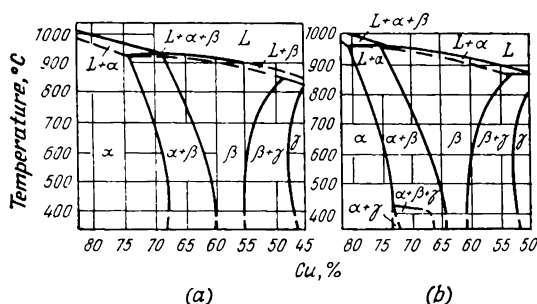


Fig. 10.26. Vertical sections through the diagram of Cu-Zn-Al alloys
(a) 2% Al; (b) 4% Al

Show the effect of aluminium on the existence of the α - and β -phases in the Cu-Zn system (see Fig. 9.16).

No. 128. Figure 10.27 shows the horizontal (isothermal) sections through the Cu-Sn-Zn diagram, made at 800, 600, and 400 °C.

The formation of a second β' -phase in Cu-Zn alloys causes a reduction of their ductility. Using the sections given in the Figure, describe the effect of an addition of tin in an amount of 1 and 5 per cent on the existence region of α - and $\alpha + \beta'(\alpha + \beta)$ -phases in brass.

Determine the maximum amount of tin to be added to brass with 70 per cent Cu to increase its corrosion stability, if it is required to retain the high cold ductility of the alloy, and hence to obtain a single-phase structure.

Explain what deviations (as compared with the equilibrium diagram) are possible in the structure of brass with 5 per cent Sn and 32 per cent Zn under conditions of rapid cooling from 800 °C.

No. 129. The strength and corrosion resistance of brasses can be increased by addition of manganese.

Figure 10.28 shows the horizontal (isothermal) sections of a portion (the 'copper corner') of the Cu-Zn-Mn diagram, made at 800, 400, and 360 °C. The ξ -phase that is formed is brittle.

Using these diagrams, show the effect of manganese on the existence region of the α -phase and explain why the manganese content in special brasses with 55 per cent Cu must not exceed 2.3 per cent.

No. 130. The group of light alloys includes aluminium-base high-strength alloys containing about 2 per cent Mg and 6 per cent Zn.

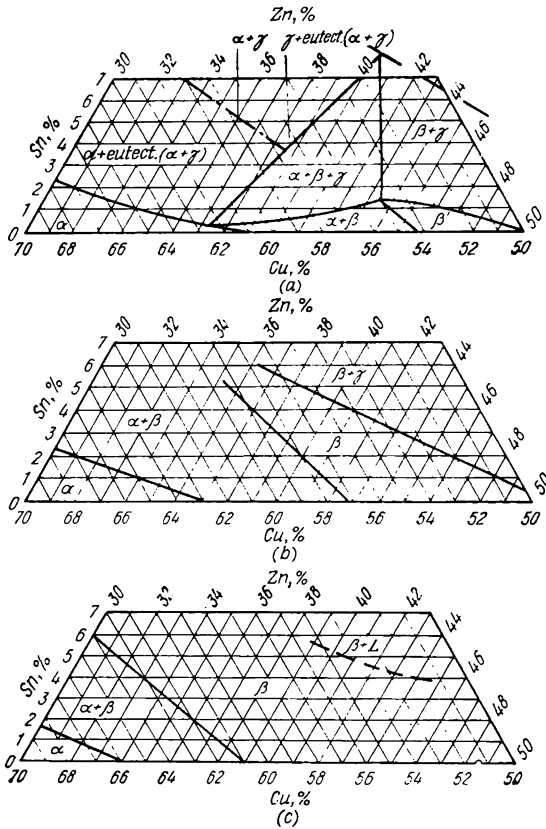


Fig. 10.27. Isothermal sections through a portion (coppe corner') of the diagram of Cu-Zn-Sn alloys
(a) 400 °C; (b) 600 °C; (c) 890 °C

Figure 10.29 shows the horizontal (isothermal) sections of a portion of the Al-Mg-Zn diagram made at 400 and 200 °C.

Determine the phase composition of the given alloy at 400 and 200 °C. Indicate the direction the solubility of the excessive phases in aluminium will change with decreasing temperature. Name the kind of heat treatment this alloy can be subjected to, and describe the effect of this treatment.

Indicate the concentration regions for the alloys of this system, which can be subjected to heat treatment, and determine the strengthening phases corresponding to these regions, i.e. the phases that cause strengthening during heat treatment.

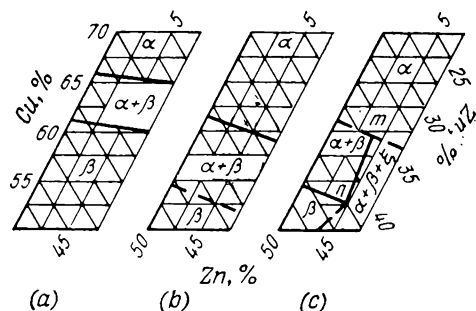


Fig. 10.28. Isothermal sections through a portion ('aluminium corner') of the diagram of Cu-Zn-Mn alloys
(a) 800 °C; (b) 400 °C; (c) 360 °C

No. 131. High-strength aluminium alloys (duralumins) are based on alloys with 3-5 per cent Cu, whose mechanical properties improve appreciably after heat treatment. Magnesium, silicon and manganese each in an amount of 0.5-1 per cent, are additionally introduced into the composition of these alloys to obtain better properties.

Using the constitutional diagram of the Al-Cu system (see Fig. 9.24), name the kind of heat treatment which can be used in order to increase the strength of the alloy with 4 per cent Cu.

Analyse the horizontal (isothermal) sections through a portion (the 'aluminium corner') of the Al-Cu-Mg diagram, shown in Fig. 10.30, and determine the phase composition of the alloys with (a) 4 per cent Cu + 0.5 per cent Mg, and (b) 4 per cent

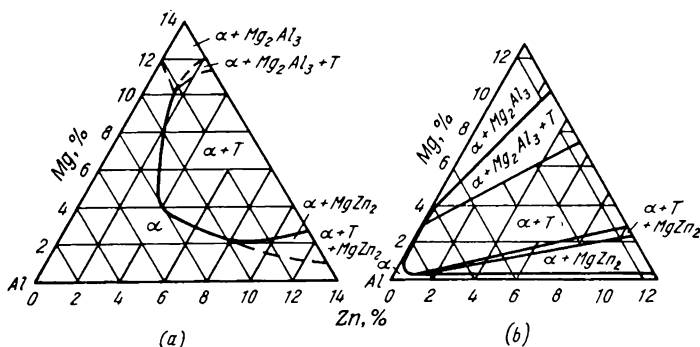


Fig. 10.29. Isothermal sections through a portion ('aluminium corner') of the diagram Al-Mg-Zn alloys
(a) 400 °C; (b) 200 °C

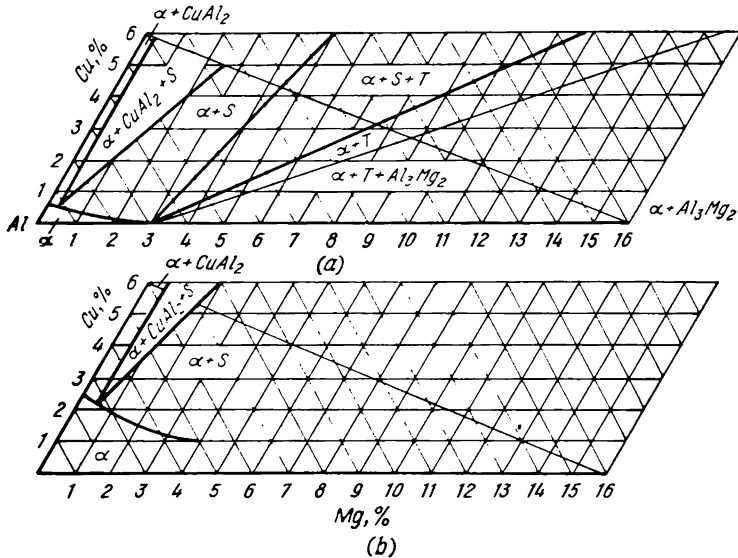


Fig. 10.30. Isothermal sections through a portion ('aluminium corner') of the diagram of Al-Cu-Mg alloys
(a) 450 °C; (b) 200 °C

Cu + 2.2 per cent Mg, at 450 and 200 °C. Determine the changes in the phase state and strengthening phases, caused by the addition of magnesium in an amount of up to 2.2 per cent.

Indicate the direction of the solubility of the excessive phases (which serve as the strengthening ones) in aluminium will change with decrease in temperature and explain why these alloys can be subjected to heat treatment to improve their mechanical properties.

No. 132. Aluminium-silicon alloys (silumins) have found application as low-density alloys with good casting properties. An undesirable impurity in them is usually iron.

Mechanical properties of silumins are impaired if iron is present in such an amount as causes the segregation of the initial crystals of the brittle β -phase in the course of solidification, these crystals being needle-shaped and representing a ternary compound. If crystals of the β -phase are present only in the ternary eutectic, their effect on the mechanical properties of silumins will be less pronounced.

Figure 10.31 shows the projection of the liquidus planes onto a portion (the 'aluminium corner') of the concentration triangle of Al-Si-Fe alloys.

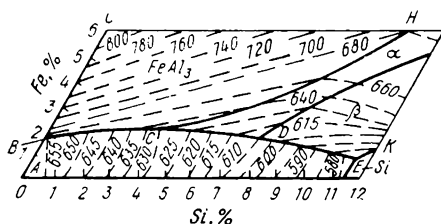


Fig. 10.31. Projection of liquidus planes onto a portion ('aluminium corner') of the diagram of Al-Si-Fe alloys

In this diagram, the phase denoted as Al is a solid solution of silicon and iron in aluminium, and the α - and β -phases are ternary compounds of a variable composition. The points *C* and *D* indicate the concentrations of the peritectic points, and point *E*, the concentration of the ternary eutectic.

Describe the solidification process of the alloys with (a) 7 per cent Si and 0.5 or 1.0 per cent Fe; and (b) 11 per cent Si and 0.5 or 1.5 per cent Fe.

Besides, indicate the silicon content (7 or 11 per cent) at which the alloy will have lower melting points and the maximum iron content admissible in such an alloy.

Determine the phases in equilibrium at points *D* and *E* of the diagram.

When solving the problem, one may disregard the fact that the introduction of a fourth component (Mn, C, or Co) reduces the harmful effect of iron; with this more complicated composition of the alloy, the needle-shaped brittle crystals of β -phase change to spherical ones.

No. 133. Figure 10.32 shows the constitutional diagram of the Pb-Sb-Sn system which includes bearing alloys (babbitts).

Tin-base alloys (with 8.3 per cent Sn¹) possess good antifric-tion properties.

Since sliding bearings heat during operation, the melting point of these alloys must not be low.

According to the USSR State Standards (GOST), the lead content in tin-base bearing alloys must not exceed a specified value.

Using as an example the alloy denoted by the point *A* in the diagram (83 per cent Sn), explain why an addition of lead is harmful to its properties.

Describe the solidification process of this alloy and compare it with that of the binary alloy with 83 per cent Sn and 17 per cent Sb.

¹ These alloys also contain about 8 per cent Cu introduced in place of a corresponding amount of antimony to lessen gravity segregation.

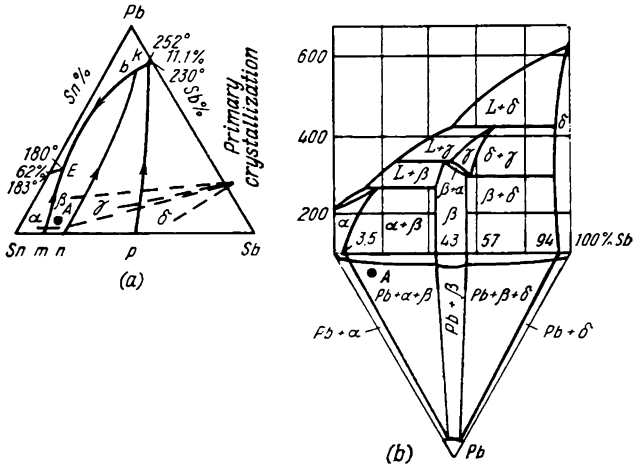


Fig. 10.32. Constitutional diagram of Pb-Sb-Sn alloys; projection of phase regions during
(a) primary crystallization; (b) secondary crystallization (20 °C)

No. 134. Apart from tin-base alloys (with approximately 83 per cent Sn), cheaper lead-base alloys (with approximately 70 per cent Pb) are used as bearing alloys; they additionally contain antimony and tin and possess good anti-friction properties.

According to the USSR State Standards (GOST), the tin content in lead-base alloys is limited to a definite tin-antimony ratio in order not to lower their melting point.

Referring to the constitutional diagram of the Sn-Sb-Pb system (see Fig. 10.32), compare the solidification process of the following two alloys having the same lead content (70 per cent), but differing in their ratio between the tin and antimony contents: (a) $\text{Sn/Sb} = 1$; (b) $\text{Sn/Sb} = 4$.

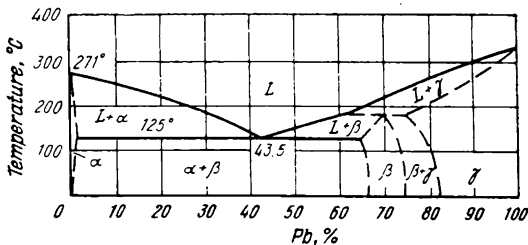


Fig. 10.33. Diagram of Bi-Pb alloys

In view of the operational requirements for sliding bearings, indicate which of these two ratios is more suitable for lead-base bearing alloys; substantiate your decision.

No. 135. Figure 10.9 shows the projections of the liquidus planes onto the concentration triangle of the Pb-Bi-Sn system.

Describe the solidification process of the alloy with 45 per cent Sn + 30 per cent Pb + 25 per cent Bi; indicate the approximate temperature at which crystallization from the liquid begins, the temperature interval of the binary eutectic precipitation, and the temperature at the end of solidification.

Characterize the phase and structural states of the alloy. Note that in binary alloys (Fig. 10.33) the components of the ternary system considered form with one another binary eutectics of solid-solution phases.

Give the composition and structure of the ternary alloy having the lowest melting point.

Part Three

PLASTIC DEFORMATION AND RECRYSTALLIZATION

Chapter Eleven

PLASTIC DEFORMATION AND RECRYSTALLIZATION OF METALS AND ALLOYS

Plastic deformation of metals in the cold state, i.e. at a temperature below that of their recrystallization, appreciably changes their structure and improves strength properties, but reduces their plasticity and ductility. Work-hardening is characteristic of metals only and is not observed in non-metallic materials.

Under practical conditions this method of strengthening and deformation is applicable to plastic pure metals and low-carbon steels. It is also suitable for medium- and high-carbon steels and copper, titanium and aluminium alloys in the equilibrium (annealed) state. The structures of these materials, which must be considered in the problems below, will be discussed in Chapters 12 and 19.

Work-hardening resulting from cold deformation may be done away with by subsequent heating above the recrystallization temperature. The structure and properties of the metal then approach their initial state.

The recrystallization temperature in the problems below may be determined by the formula proposed by A. A. Bochvar:

$$T_{rec} = aT_{m.p} \text{ } ^\circ\text{K}$$

The coefficient a is approximately 0.4 for commercially pure metals and mechanical mixtures and 0.5-0.6 for solid solutions.

For the temperatures measured in degrees Centigrade, the formula is as follows:

$$t_{rec} = a(t_{m.p} + 273 \text{ } ^\circ\text{C}) - 273 \text{ } (^\circ\text{C})$$

The object of the laboratory exercises below is to show the effect of plastic deformation and recrystallization on the structure (mainly the grain size) and mechanical properties (hardness) of materials. High-plastic metals (copper, brass, low-carbon steel) should be preferred for the tests, since this effect is more pronounced in them.

Specimens 10 mm in diameter and 15 mm high are recommended. The upsetting of specimens may be done in a press. Copper and brass specimens may also be upset manually; for this, a specimen is placed into a steel die and upset by striking the upper die with a hammer. When upsetting in a press, the degree of deformation can be increased by approximately 50-60 per cent above that given in the problems. The height of specimens before and after upsetting is measured by means of a vernier calliper to an accuracy of up to 0.1 mm. The hardness of steel specimens should be measured by the Rockwell ball test (B scale), and that of copper and brass samples, according to Brinell (with a ball 2.5 mm in diameter indented with a force of 62.5 kgf). The microstructure of specimens should be studied before and after deformation (with low and high degree of upsetting) and after recrystallization.

The layers of the metal at the end faces of a specimen are subjected to lower deformations than those on its cylindrical surfaces. For this reason, microscopic examinations at a magnification of from 200X to 300X and hardness measurements should be done on the side surfaces of deformed specimens. When preparing the area on a specimen for hardness measurement, metal may be removed to a depth of 1-2 mm.

For students studying a concise course in the science of materials, and also for correspondence-course students, the laboratory exercises below may be replaced by the following:

1. Examination, sketching, and description of microstructures of low-carbon steel: (a) after annealing; (b) after cold plastic deformation (upsetting of a cylindrical specimen by 30-50 per cent); and (c) after recrystallization of the deformed specimen; ready-made microsections can then be used by the students.

2. Solving Problems Nos. 145-163.¹

11.1. LABORATORY EXERCISES

No. 136. Subject two cylindrical specimens of single-phase brass to cold deformation by upsetting them by 10 and 30 per cent, respectively. Measure their hardness. Sketch and characterize their microstructure before and after deformation.

Plot a diagram to show how the hardness of brass depends on the degree of deformation. Explain the causes of the variation of hardness, and indicate in which direction the plasticity will vary.

No. 137. Subject two cylindrical copper specimens to cold deformation by upsetting them by 10 and 30 per cent, respectively.

¹ Problems Nos. 145-157 and 162 have been compiled by D. M. Nakhimov.

Measure their hardness before and after deformation; sketch and characterize their microstructure.

Plot a hardness *versus* degree of deformation diagram. Explain the causes of the variation of hardness. Additionally indicate in which direction the strength and relative elongation will vary.

No. 138. Take a number of specimens of cold-deformed copper (reduction of not less than 50 per cent) and heat them to 200, 250, 300, 350, and 500 °C, with each specimen being held at heat for 60 minutes.

Measure their hardness. Sketch and characterize their microstructure after deforming and after heating to 200 and 500 °C.

Plot a diagram to show how the hardness of copper varies with heating temperature. Using the results of the experiments indicate approximately the temperature at which recrystallization begins. Compare this temperature with that calculated by the formula proposed by A. A. Bochvar.

Note. Specimens upset by 30 per cent are recommended for this work.

No. 139. Carry out a microscopic examination and measure the hardness of copper specimens: (a) upset by 30 per cent; (b) upset as above and then heated to 200, 300, 500 °C and held for 60 minutes at the temperature indicated.

Sketch and characterize the microstructure of the specimens. Using the examination results, indicate roughly the temperature of the beginning of recrystallization and compare it with the temperature found by Bochvar's formula.

No. 140. Carry out a microscopic examination and measure the hardness of brass specimens: (a) not subjected to cold deformation; (b) subjected to cold deformation by upsetting by 10 per cent; (c) upset by 35 per cent; (d) after upsetting by 10 per cent and recrystallization at 600 °C (for 60 minutes); (e) after upsetting by 35 per cent and recrystallization at 600 °C (for 60 minutes).

Sketch their microstructure and explain the effect of deformation and subsequent heating on the size and shape of grains and the properties of brass. Explain why the 10-per cent upset gave a coarser grain after recrystallization than the 35-per cent upset.

No. 141. Measure the hardness of two low-carbon steel specimens upset in the cold state by 10 and 30 per cent, respectively. In addition, measure the hardness of a non-deformed specimen of the same steel.

Sketch and characterize the microstructure before and after deformation.

Plot a diagram to show the effect of the degree of deformation on hardness and explain the causes of its variation; also in-

indicate the direction in which other mechanical properties of the material will vary.

No. 142. Take specimens of cold-deformed commercial iron (upset by 30 per cent) and heat them to 200, 400, 600, and 800°C, with each specimen being held for 60 minutes at the temperature specified. Measure their hardness before and after heating.

Sketch and characterize their microstructure before deforming and after heating.

Plot a diagram to show how the hardness of cold-deformed steel varies with the heating temperature. Using the results of the experiment, indicate approximately the temperature of the beginning of recrystallization, and compare it with that found by Bochvar's formula.

No. 143. Carry out a microscopic examination and measure the hardness of low-carbon steel specimens upset by 30 per cent and then heated respectively to 100, 600, and 800°C. Study their microstructure before and after cold deformation.

Indicate approximately the temperature of the beginning of recrystallization of low-carbon steel: (a) according to the results of the microscopic examination and hardness tests; (b) according to Bochvar's formula.

No. 144. Brass specimens were subjected to cold deformation and then heated to 500°C and held at this temperature for 10, 30, and 60 minutes, respectively.

Carry out a microscopic examination of the specimens and measure their hardness (before and after heating). Sketch and characterize their microstructure. Using the results of the examination and hardness tests, explain why holding at heat is required for the recrystallization process to proceed deeper.

Note. Specimens upset by 30 per cent are recommended.

Problems

No. 145. Figure 11.1 shows the tensile test diagram of a steel specimen.

Indicate the changes in the microstructure of steel occurring when the specimen is stressed to the state corresponding to points 1, 2 and 3, respectively.

No. 146. When a specimen cut out from a zinc monocrystal is subjected to a tensile test, its relative elongation in one of the directions may be much greater than that of a specimen cut out from the common polycrystalline zinc. What is the reason for this difference?

No. 147. Parts made from copper rods 20 mm in diameter must

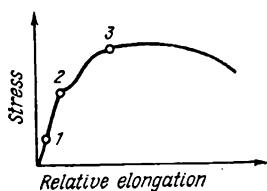


Fig. 11.1. Tension diagram of a low-carbon steel specimen

have an ultimate strength of not less than 30 kgf/mm². The copper rods available at the works are of a larger diameter, but with an ultimate strength of 22-25 kgf/mm².

How can the ultimate strength of copper be increased?

No. 148. Parts made by cold die-forging from low-carbon steel have been found to have different hardness (from 100 HB to 200 HB) in their different sections.

The hardness of steel before the die-forging was 100 HB. Explain the cause of these hardness variations.

No. 149. Is it possible to distinguish between the microstructure of cold-deformed metal and that of hot-deformed metal? What is the difference?

No. 150. Three low-carbon steel specimens were cold deformed by 5, 15, and 30 per cent, respectively, and then heated to 700 °C.

Which of the specimens obtained the coarsest grain after the heating? How can the grain growth affect the properties of steel?

No. 151. In hot plastic working of metals, the last operation should not be carried out with a small reduction. Why? How can this deformation affect the grain size and properties of the metal?

No. 152. Is it possible to obtain an appreciable work-hardening of lead by deforming it at room temperature?

No. 153. Can the deforming of tin at 20 °C cause work-hardening?

No. 154. How will the hardness value obtained, for instance, by Brinell ball test, be affected if another test is made in the same section (i.e. in the same indent or very close to it)?

No. 155. Wire drawing is done in a number of passes. If the drawing is done without intermediate operations, the wire in the last passes is often subject to breakage.

Explain the cause of this breakage and suggest measures to prevent it.

No. 156. A cold-bent brass rod is subjected to recrystallization to get rid of work-hardening.

Will the grain size of the metal be the same over the whole cross section of the rod after recrystallization?

No. 157. Decide which kind of deformation (hot or cold) is effected when (a) tin is rolled at room temperature; (b) steel is deformed at 400 °C.

No. 158. Is it possible to distinguish between the microstruc-

ture of copper deformed at room temperature and that of copper deformed in a hot state (at 600 °C)?

No. 159. Parts made of copper by cold die-forging had a reduced plasticity.

Is it possible to increase the relative elongation of this copper? Recommend the mode of processing and explain how the mechanical properties (strength, hardness and ductility) will then be affected.

No. 160. Brass rods after cold deforming were heated to (a) 200 °C and (b) 500 °C, and held at these temperatures for 60 minutes.

Say how the structure and properties of the metal were affected in each case.

No. 161. Recommend the processing conditions (the heating temperature) to partially relieve cold-deformed brass of the residual stresses without materially affecting its increased strength produced as a result of the cold deformation.

No. 162. The metal in boiler plants is often observed to suffer stronger corrosion in places near rivets.

What are the causes of this phenomenon?

No. 163. Studies of the microstructure of a forged steel shaft (100 mm in diameter) revealed a fine structure in subsurface layers and coarser structure in the core.

Name the probable causes of this phenomenon.

Part Four

LABORATORY EXERCISES AND PROBLEMS ON STEELS AND CAST IRONS

Chapter Twelve

STRUCTURE OF STEELS AND CAST IRONS IN EQUILIBRIUM

Before attempting the laboratory exercises (Problems Nos. 164-174), the students should examine microsections of typical equilibrium structures of carbon steels and cast irons.

12.1. THE STRUCTURE OF STEEL

The structure of steel in equilibrium (i.e. after annealing or, for low-carbon steels, after normalizing and high-temperature tempering) is determined by the content of carbon, as can be seen in the constitutional diagram of iron-carbon alloys (Fig. 12.1). As the carbon content is increased, the structure of steel changes as outlined below.

With the minimum content of carbon the structure of steel is ferritic (commercially pure iron) (Fig. 12.2). In a correctly deformed and normalized (annealed) steel, ferrite has a polyhedral granular structure. Lamellar ferrite inclusions may be observed (Fig. 12.3) in cast or overheated steel (in the hot worked or welded conditions).

Ferrite has a lower hardness (appr. 80 HB) than the other structural components of steel and a high plasticity ($\delta \leq 25$ per cent).

A slight increase in the carbon content, even by a few hundredths of a per cent, causes the formation of a second phase, cementite, since carbon is only poorly soluble in α -iron (up to 0.006 per cent at 20 °C). With a content of carbon of approximately up to 0.025 per cent, it is usually present in the structure of steel as relatively small amounts of ternary cementite which precipitates from ferrite on cooling because of a reduction in the solubility of carbon in α -iron. Ternary cementite is located mainly at the boundaries of ferrite grains, thus reducing the plasticity and ductility of steel.

An increase in carbon content above 0.025 per cent causes the formation of pearlite, i.e. a two-phase structure (eutectoid), which

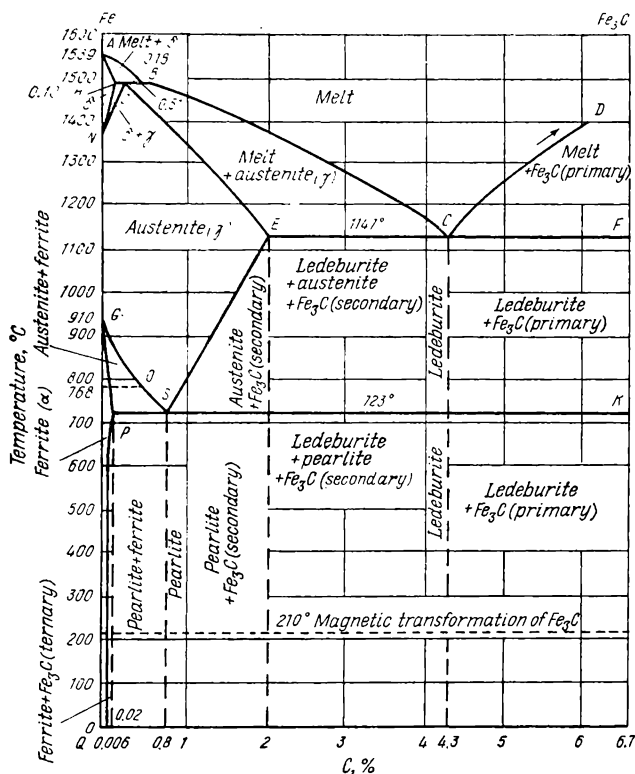


Fig. 12.1. Iron-carbon constitutional (structural) diagram

is a mechanical mixture of ferrite and pearlite with the total carbon content of 0.8 per cent. Inclusions of ternary cementite still remain in the steel (Fig. 12.2) if its carbon content does not exceed 0.1-0.15 per cent.

The amount of pearlite increases proportionally with the carbon content (Fig. 12.2*b* and *c*) while the amount of precipitated ferrite reduces accordingly.

As a two-phase structure, pearlite is more susceptible to etching (by a solution of nitric acid, for instance), than ferrite. Under a microscope, pearlite is observed as dark inclusions of non-uniform structure. Because of its appreciable dispersity, the structure of pearlite can be clearly seen only at large magnifications, 500X or more (Fig. 12.4). The pattern of pearlite structure is clearly resolvable in the electron microscopy.

In hypoeutectoid steels, pearlite usually has a lamellar structure; dark plates seen in pearlite are actually shadows of the

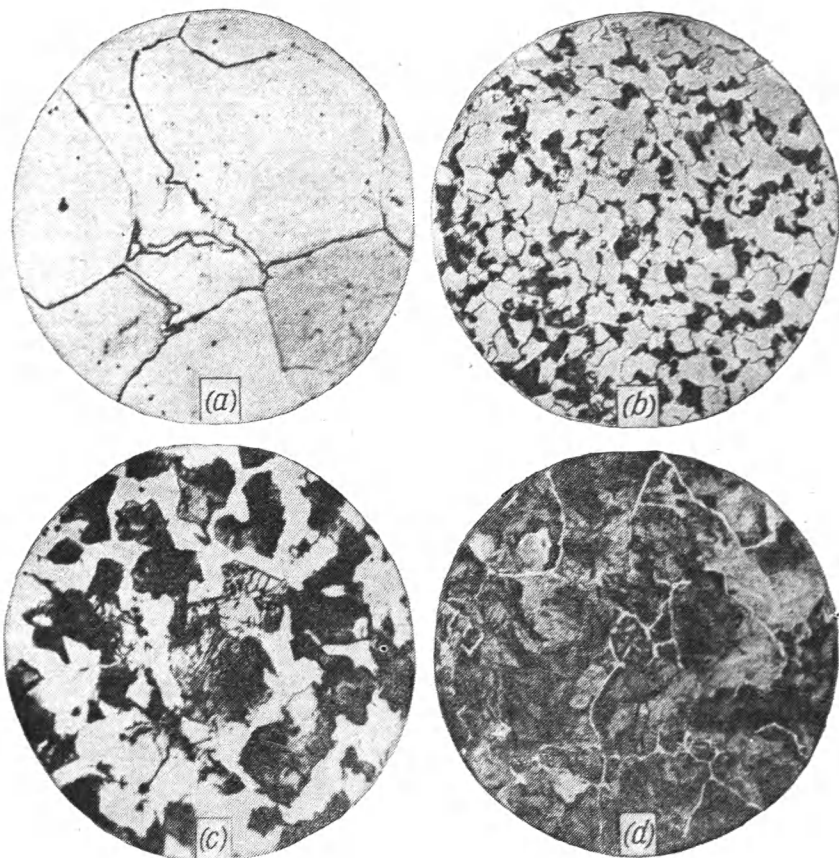


Fig. 12.2. Equilibrium structures of steels with various carbon contents
 (a) 0.05–0.1% C; (b) 0.2–0.3% C; (c) 0.4–0.5% C; (d) 0.65–0.7% C, 500X

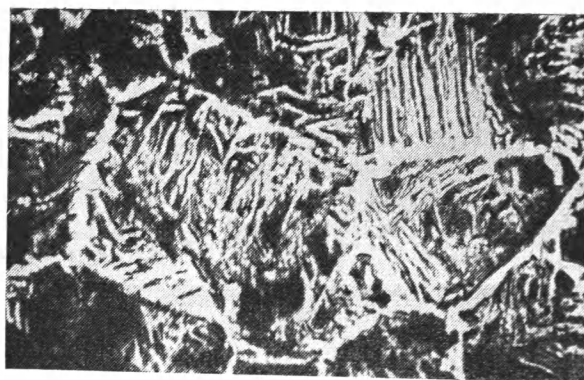


Fig. 12.3. Structure of superheated hypoeutectoid steel (Widmanstätten structure), 250X

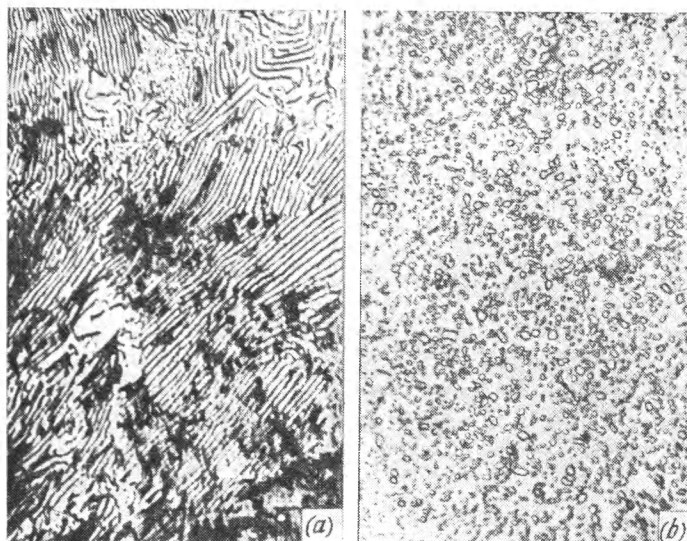


Fig. 12.4. Eutectoid steel (0.8% C), 600X
(a) lamellar pearlite; (b) granular pearlite

adjacent sections (plates) of cementite that have raised after etching. The hardness of laminar pearlite is approximately 200 HB.

The hardness of hypoeutectoid steel (composed of ferrite and pearlite) increases proportionally with the carbon content, i.e. with an increase in the amount of pearlite. Knowing this relationship, one can easily determine the hardness, and therefore, strength of a steel for a known carbon content (or a corresponding amount of pearlite).

Pearlite is the principal structural constituent in hypereutectoid steels. The shape of pearlite is determined by the annealing conditions. More often as not owing to annealing with an accelerated heating and at a low temperature, pearlite acquires a granular shape and a lower hardness (160-170 HB) than lamellar pearlite.

Apart from pearlite, the structure of hypereutectoid steels contains secondary cementite which precipitates from austenite on cooling due to a reduction in the solubility of carbon in γ -iron, as shown by line *ES* in the diagram (Fig. 12.1). With proper prior processing (rolling, forging, and annealing) the secondary cementite is present in the form of small grains distributed quite uniformly in the mass of pearlite (see Fig. 3.10).

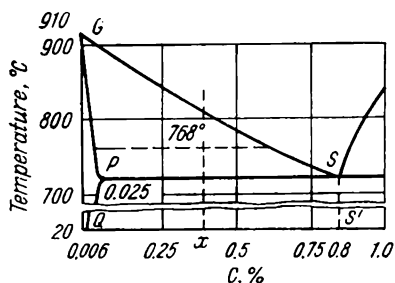


Fig. 12.5. Diagram to determine carbon content in annealed hypoeutectoid steel by the section rule

Secondary cementite can also precipitate as a network at the boundaries of pearlite grains (see Fig. 3.10). This can occur if hot working is finished at an excessively high temperature or if annealing is done with the metal being heated above point A_{cm} (instead of being heated 50-70 °C above point A_1) and is revealed as an appreciable defect of hypereutectoid steels, impairing their strength and ductility.

In some, though rare, cases, usually due to strong overheating, cementite can segregate in the form of needles (see Fig. 3.10), which also strongly impair the mechanical properties of the steel.

The microstructure of hypoeutectoid carbon steel in the equilibrium (annealed) state can be used to determine the carbon content as follows. The structure of such a steel is composed of ferrite and pearlite. Ferrite contains minute amounts of carbon (0.006 per cent). Therefore we may assume that all the carbon is contained in pearlite. As is known, pearlite contains 0.80 per cent C. Since the density of ferrite is very close to that of pearlite, we can determine the content of carbon in the steel by multiplying the relative area (in per cent) occupied by pearlite in the observed field of a microsection by a factor of 0.8.

This calculation can also be done on the basis of the rule of sections (Fig. 12.5). The ratio of the amount of pearlite Q_p to the total amount Q_t of the alloy of composition X is

$$Q_p/Q_t = Q_x/Q_s$$

whence

$$Q_x = \frac{Q_p}{Q_t} Q_s$$

where Q_s is a constant equal to 0.80 per cent (more precisely, 0.80-0.006 per cent), found in the iron-carbon diagram.

The ratio Q_p/Q_t is determined by a planimeter or by visual examination of the microsection.

The content of carbon is then found by multiplying Q_p/Q_t (as percentage) by 0.80 per cent.

For hypereutectoid steels, the rule of sections is used less frequently because of the difficulties in an accurate determining of the area of the secondary cementite (see Fig. 3.24).

For carbon steels in the non-equilibrium state, in particular, after hardening and tempering, their carbon content cannot be determined by studying the microstructure, since the structure of such steels is not reflected in the iron-carbon diagram.

The rule of sections is also inapplicable to alloy steels, since their phase composition and structure cannot be determined from the binary iron-carbon diagram.

12.2. THE STRUCTURE OF CAST IRON

The chemical composition and, in particular, the content of carbon in cast iron cannot be reliable characteristics of its properties, since its structure and principal properties are determined not only by the composition, but also by the process of smelting, the cooling conditions during casting, and the conditions of heat treatment. The properties of cast iron are determined by its structure.

White cast iron. The structure of hypoeutectic cast irons contains, apart from pearlite and secondary cementite, a certain amount of brittle eutectic (ledeburite) whose amount may reach 100 per cent in eutectic cast iron. The structure of hypereutectic cast iron consists of the eutectic and primary cementite, which precipitates as large laminae during crystallization of the liquid. White iron has a high hardness, 350 HB or more.

The metallic base of other kinds of cast iron (grey, high-strength, and malleable) is ferrite plus pearlite. Carbon is present in their structure partially or completely in the form of graphite; this is a soft and brittle component. Graphite is only weakly bonded with the metallic base and plays the part of internal cuts. Graphitized cast irons have a low hardness (130-220 HB), lower strength and plasticity than steels.

The specific volume of graphite is $0.454 \text{ cm}^3/\text{g}$, i.e. much higher than that of the metallic base and cementite ($0.128\text{-}0.130 \text{ cm}^3/\text{g}$) and the sequel of this is that the volume of cast iron decreases less during the solidification and graphite formation than that of steel, which results in improved casting properties of cast iron, and reduced shrinkage.

The dependence of the mechanical properties of cast irons on their structure is more complicated than that for steels, since it is determined by the shape, size, and number of graphite inclusions, as well as by the structure of the metallic base.

Inspection of graphite inclusions should be preferably made on unetched microsections. When a microsection is being prepared, these brittle inclusions crumble out during grinding and polishing of the surface. This gives its reason why graphite in-



Fig. 12.6. Grey iron (unetched section), 100X. Determination of graphite inclusions by the USSR State Standard GOST 3443-57

(a) class F14 (18-15% graphite), distribution of graphite F2 (as less isolated colonies);
 (b) class F05 (3-5% graphite), distribution of graphite F4 (appreciably isolated colonies)

clusions (more precisely the places where graphite was present) are seen dark under a microscope.

The metallic base of cast irons (like that of steels) is examined on etched microsections.

Grey cast iron. Under the microscope, the structure of grey cast iron reveals lamellar inclusions of graphite.

The effect of graphite inclusions on the mechanical properties of grey iron can be estimated qualitatively. If graphite inclusions are low in number, fine or largely isolated from each other, a higher strength of the cast iron will result for the same metallic base.

Graphite inclusions in cast irons are graded in accordance with the USSR State Standard GOST 3443-57 (Fig. 12.6).

The metallic base of grey cast iron is composed of ferrite and pearlite, with the ratio of these components varying widely. With the same type of graphite inclusions, pearlite iron (i.e. the one in which the pearlite component predominates) has better mechanical properties than ferrite iron (i.e. having the prevailing proportion of ferrite).

Typical structures of grey irons with various compositions of the metallic base are shown in Fig. 12.7. Their microstructure also reveals sections of phosphide eutectic, which affects not only their mechanical properties, but also their casting properties. These inclusions somewhat improve the wear resistance and fluidity of cast iron.

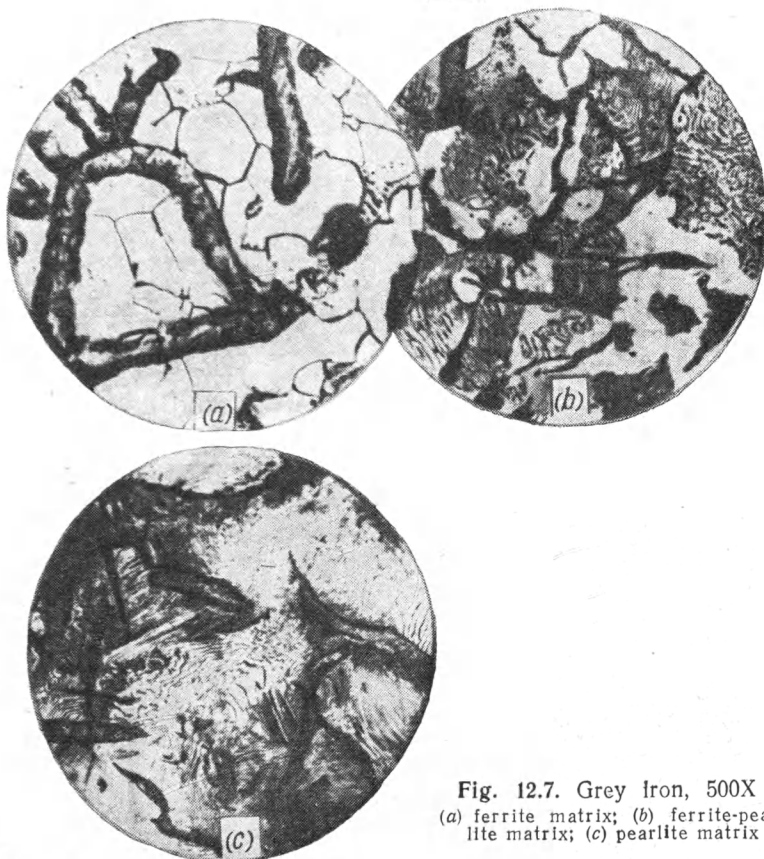


Fig. 12.7. Grey Iron, 500X
(a) ferrite matrix; (b) ferrite-pearlite matrix; (c) pearlite matrix

High-strength cast iron. This kind of cast iron is inoculated with magnesium. It has inclusions of spherical graphite (Fig. 12.8), unlike grey cast iron where graphite is present in lamellar form. The mechanical properties of this kind of cast iron are much better than those of other kinds.

The structure of high-strength cast iron is examined on unetched microsections (to reveal graphite inclusions), and then on etched ones to characterize the metallic base (this is composed of ferrite and pearlite).

Malleable cast iron. This kind of cast iron is produced by annealing white cast iron. It contains graphite (annealed carbon) in the form of flaky inclusions (Fig. 12.9a and b). There are two kinds of malleable cast iron — graphitized cast iron and decarbonized cast iron, depending on the method of producing and the structure.

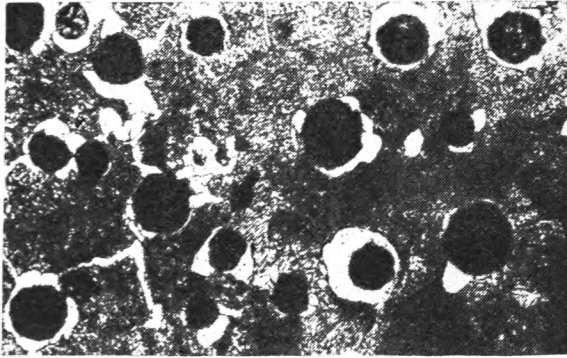


Fig. 12.8. High-strength iron having pearlite matrix, 200X

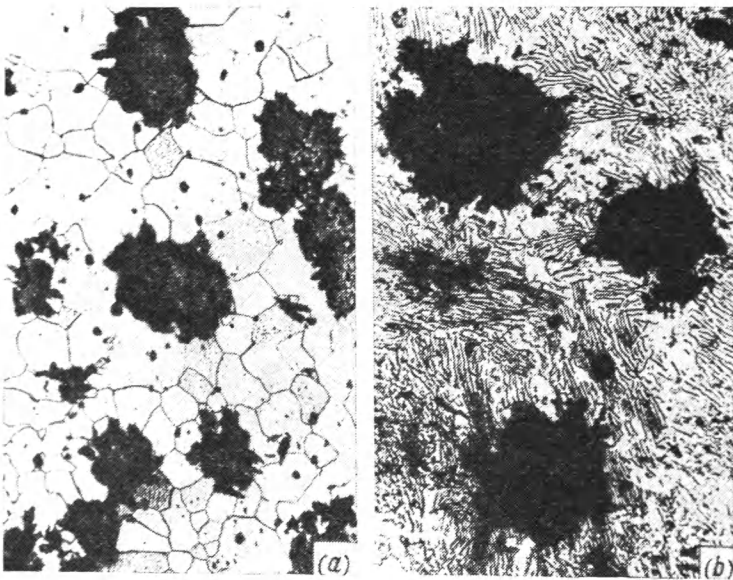


Fig. 12.9. Malleable iron, 200X

(a) ferrite matrix (graphitized iron); (b) ferrite and pearlite in the surface layer and pearlite in the core (decarbonized iron)

Graphitized cast iron has a ferritic structure the metallic base of which is comparatively uniform over the cross section of a casting. More seldom its structure may be ferrite-pearlitic or pearlitic (Fig. 12.9b).

Decarbonized iron has a pearlitic or pearlite-ferritic structure which varies considerably from the core to the surface layers

because of specific manufacturing features. The core of a casting usually contains more pearlite than the surface layers; the structure near the surface may sometimes be purely ferritic. The amount of annealed carbon varies from the core to the surface in the same manner.

12.3. LABORATORY EXERCISES

Each student must attempt two problems: one on the structure of steel (Nos. 164-174) and the other on the structure of cast iron (Nos. 175-179). Microstructures should be examined at a magnification of 200X to 300X. Solve a problem in the following sequence:

(a) select (and substantiate) the magnification of the microscope for studying the microstructures;

(b) select (and substantiate) the reagent to etch microsections;

(c) sketch the microstructures seen under the microscope;

(d) characterize the microstructure; its description should contain not only the structural components, but also data on their shape, ratios of these components, and the colour they acquire through etching;

(e) answer in detail the questions set forth in the problem.

No. 164. Carry out a microscopic examination (microanalysis) of annealed low-carbon and medium-carbon steel specimens having hardness of 120 HB and 150 HB, respectively.

Sketch the microstructure seen under the microscope and determine roughly the content of carbon in the steel and the ratio of the structural components. Indicate the fields of industrial application of these steels.

No. 165. Carry out microanalysis of annealed low-carbon structural steel and hypoeutectoid tool steel specimens. Sketch the microstructures seen under the microscope and determine roughly the content of carbon and the ratio of the structural components.

Describe the transformation processes occurring in these steels during slow cooling and name their critical points.

No. 166. Carry out microanalysis of annealed medium-carbon and high-carbon (hypereutectoid) steel specimens.

Sketch their microstructures and determine approximately the carbon content and the ratio of the structural phases existing in the medium-carbon steel. Describe the properties of the phases and structural components of the steels considered and the probable fields of their industrial application.

No. 167. Carry out microanalysis of two high-carbon steel specimens with the same carbon content, but with the different pear-

lite forms and hardness of 160-170 HB and 200-220 HB, respectively.

Sketch the microstructure. Describe the structural components and their effect on hardness.

Describe the essence of the process of eutectoid crystallization of steel and specify the conditions necessary for producing various pearlite forms.

No. 168. Carry out microanalysis of hypereutectoid carbon steel. The specimen was cut from a forged blank processed under improper conditions, i.e. the forging process was finished at an excessively high temperature (1000 degrees C) and with insufficient upsetting.

Characterize the structure. Name the variations that occurred owing to the abnormal forging conditions and explain their effect on the properties of the steel.

Recommend the conditions of thermal treatment to remedy these structural defects.

No. 169. Carry out microanalysis of two carbon steel specimens cut out from a shaped casting, one of them being cut after casting, and the other, after heat treatment.

Characterize their structures. Indicate the approximate content of carbon (according to the structure of the second specimen) and the heat treatment process conducted after casting. Explain the purpose of this treatment and say how it affected the structure and mechanical properties of the metal.

No. 170. Carry out microanalysis of two annealed carbon steel specimens with different carbon content, one of the specimens having hardness of 120 HB, and the other, 155-160 HB.

Characterize their structures. Determine the approximate carbon content in each specimen. Describe the mechanical properties of the annealed steel.

No. 171. Carry out microanalysis of two annealed carbon steel specimens with different carbon content (the hardness of the specimens being 130 HB and 170 HB, respectively).

Characterize their structures and determine roughly the concentration of carbon in each specimen. Which of these steels is better for making machine parts (for instance, gear wheels) and certain tools (for instance, hammers and chisels)?

No. 172. Carry out microanalysis and sketch the microstructure of two annealed carbon steel specimens with different carbon contents, one of the specimens having hardness of 125 HB, and the other, 165-170 HB.

Characterize their structures and determine their carbon contents.

Which of these steels should be preferred for making shafts that (after cementation and heat treatment) must possess a high wear resistance and operate under high dynamic loads?

No. 173. Carry out microanalysis of two annealed steel specimens, one of the specimens being subjected to cementation to increase the carbon content in the surface layer.

Sketch the microstructure seen under the microscope. Determine the thickness of the layer¹ having a higher carbon content as compared with that of the core. Determine the carbon content in the surface layer for each one-tenth of a millimetre of its depth and also that in the core.

Indicate the purpose of cementation and the carbon content a steel must have to be suitable for cementation.

No. 174. Carry out microanalysis of annealed hypereutectoid carbon steel and hypereutectic white cast iron.

Sketch their structures. Characterize the phase and structural state of the two alloys and explain why their mechanical properties are different.

No. 175. Carry out microanalysis of two cast-iron specimens with hardness of 150 HB and 350 HB, respectively.

Characterize their structures, the conditions for obtaining these kinds of iron, and the probable fields of their application.

No. 176. Carry out microanalysis of grey iron specimens with hardness of 140 HB and 220 HB, respectively.

Characterize their structures according to the form of precipitated graphite and the form of the metallic base. Name the conditions for obtaining these structures, the approximate mechanical properties, and the fields of industrial application.

No. 177. Carry out microanalysis of two cast iron specimens of the same hardness (140-150 HB), but with a different plasticity index, the relative elongation of one of them being 8-10 per cent, and that of the other, not more than 0.5 per cent.

Sketch and characterize their structures and explain why, with approximately the same metallic base and equal hardness, they differ in the form of precipitated carbon.

Which of these forms of carbon (graphite) precipitation produces higher plasticity?

Give examples of industrial application of these two kinds of cast iron.

No. 178. Carry out microanalysis of two cast iron specimens, one of them having an ultimate tensile strength of 20 kgf/mm² and relative elongation not more than 1 per cent, and the other, 50 kgf/mm² and 4-percent elongation, respectively.

¹ From the surface to the depth where structurally free ferrite appears.

Name the difference in the form of precipitated graphite and indicate the method of producing cast iron with better mechanical properties.

No. 179. Carry out microanalysis of two cast iron specimens with approximately the same mechanical properties ($\sigma_t = 40 \text{ kgf/mm}^2$ and $\delta = 3\text{-}4$ per cent), but with different forms of precipitated graphite: flaky in one of the specimen and spheroidal in the other.

What methods can be used for producing these kinds of cast iron?

Chapter Thirteen

TRANSFORMATIONS IN STEEL DURING HEATING. DETERMINATION OF CRITICAL POINTS

13.1. DETERMINATION OF CRITICAL POINTS

The knowledge of critical points is necessary not only for characterizing the transformations in steel, but also for determining the proper heat treatment conditions, in particular, the temperatures of heating for annealing, normalizing, hardening, and tempering.

In the iron-carbon diagram (see Fig. 12.1), the line *PSK* corresponds to the critical point A_{c1} , and the line *GS*, to the critical point A_{c3} (for hypoeutectoid steel).

The temperatures of hardening and annealing are usually chosen 20-40 degrees C above A_{c3} for hypoeutectoid steels and 50-70 degrees C above A_{c1} , for hypereutectoid steels.

The iron-carbon diagram, however, characterizes only the state of binary iron-carbon alloys. Industrial alloys additionally contain manganese, silicon, phosphorus, sulphur, and small amounts of chromium, nickel, etc. The effect of these impurities on the position of the critical points for carbon steels is not very significant, therefore the heat treatment temperature can be determined accurately enough from iron-carbon diagram.

With an increased content of manganese (above 0.7-0.8 per cent) or silicon (above 0.5-0.6 per cent) or with other alloying elements (nickel, chromium, etc.) present in appreciable amounts in a steel, the position of the critical points¹ changes considerably, so that for steels containing a number of alloying elements it then becomes impossible to determine those points from the iron-carbon diagram or from a ternary 'iron-carbon-alloying element' diagram.

Since the diagrams of a number of multi-component systems are not available, the conditions for their heat treatment should be assigned by determining experimentally the critical points,

¹ The critical points of ternary and multi-component alloys lie within a certain interval of transformation temperatures whose positions depend on the alloy composition.

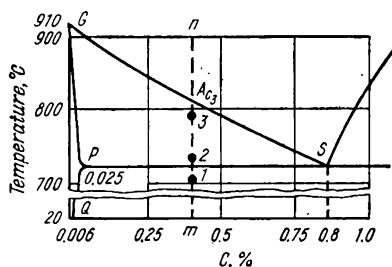


Fig. 13.1. 'Steel corner' of the iron-carbon diagram (the region of solid-state transformations)

or the regions of transformations.¹ The critical points for commonly used grades of steel have been determined and may be found in the specialist literature and reference books. But the critical points may somewhat differ for various melts of the same grade of steel, especially for complex alloyed steels with the content of individual elements deviating from the specification.

For that reason, the heat treatment conditions for alloyed steels of various melts are usually selected by prior determining their critical points. This is especially needed for steels of novel grades and compositions.

The following methods serve the purpose: (a) trial hardening; (b) dilatometric method; (c) differential thermal method,² and (d) electrical resistance measurement.

The dilatometric and differential methods were discussed in Ch. 4, and the electrical resistance method, in Ch. 5. These methods ensure high accuracy.

The method of trial hardening is simpler, but less accurate. It comprises the following procedure. Cylindrical specimens 15-20 mm in diameter and 12-15 mm high are cut from the steel to be tested (in the state as supplied by steelmaking works). One of the specimens is heated to a lower temperature than the proposed A_{c1} temperature, quickly quenched in water and its hardness measured. The second specimen is heated to a temperature 10-15 degrees C higher than that of the first specimen, quenched, and tested for hardness. These operations are performed for all the specimens, with each next specimen being heated to a higher temperature than the previous one. Suppose we have to determine the critical points A_{c1} and A_{c3} of a carbon steel containing 0.4 per cent C. The position of this steel in the iron-carbon diagram (neglecting the effect of impurities) is shown by the vertical dotted line in Fig. 13.1. It is clear that heating to a temperature below the point A_{c1} , i.e. for instance, to the point 1 in the Figure, will not alter the structure of the steel or increase its

¹ With a high rate of heating, the position of the critical points can shift towards higher temperatures; this shift can be as large as a few tens of degrees with very quick heating (for instance, by high-frequency currents).

² Determination of critical points by thermal analysis during rapid heating and cooling is performed with the use of an oscillograph (see Sec. 4.1b).

hardness. Its hardness may even drop somewhat if the steel has not been properly annealed or tempered.

The hardness will increase if the steel is heated above the point Ac_1 , for instance, to a temperature corresponding to point 2 (see Fig. 13.1) and then quenched in water. The structure of steel will then change to ferrite + austenite. After quick cooling, the steel will acquire a ferrite + martensite structure, since austenite is transformed into martensite through cooling. The ferrite, which has remained unchanged after heating to point 2, will retain its structure after cooling. The formation of a harder component, martensite, increases the hardness of the steel.

After heating to a higher temperature, for instance, to point 3 (see Fig. 13.1), the hardness of the steel will increase even more. Since the proportion of austenite increases as temperature rises within the interval from Ac_1 to Ac_3 , whereas that of ferrite correspondingly reduces, the proportion of the hard component, martensite,¹ in the steel should then increase.

Hardness will increase until the temperature Ac_3 is attained. On further heating, the steel then shows fully austenitic structure while quenching results in fully martensitic structure. Any further increase of the quenching temperature, evidently, will not alter the structure and hardness of the steel.²

The results of hardness tests are tabulated and used to plot a hardness-heating temperature diagram. Such a diagram for hypoeutectoid steel is shown in Fig. 13.2; the temperature from which the hardness begins to rise corresponds to the point Ac_1 , and the temperature after which no gain in hardness is possible, to the point Ac_3 .

Curves for eutectoid and hypereutectoid steels are of different shape; with heating below the point Ac_1 , the structure of these steels is not changed, as in the case of hypoeutectoid steels; with heating above the point Ac_1 , however, eutectoid steel acquires austenitic structure, and hypereutectoid steel shows a structure

¹ Heating within the interval Ac_1 - Ac_3 changes the composition of the austenite of hypoeutectoid steel, and therefore, the composition of the martensite which is formed on cooling. The hardness of martensite will be slightly higher if quenching has been done from the lowest temperature within the interval indicated.

² Hardened steel (with more than 0.5 per cent C) contains a small amount of residual austenite. An appreciably higher heating, by 70-100 degrees C above Ac_3 , can result in the growth of austenite grains, the formation of coarse-grained martensite, and a high amount of residual austenite remaining in the structure of steel; these variations have insignificant effect on the hardness of hypoeutectoid carbon and low-alloyed steels; with high-alloyed steels, however, and also with hypereutectoid carbon steels, hardening from high temperatures can result in a high amount of residual austenite, and therefore, in a reduced hardness.

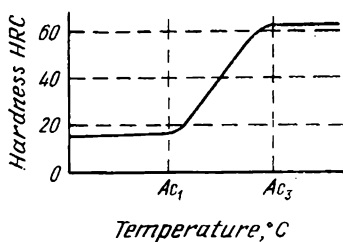


Fig. 13.2. Diagram to determine the critical points of hypoeutectoid steel by the method of trial hardening

composed of austenite and cementite. Therefore after quenching, the eutectoid steel will have the martensitic structure, and the hypereutectoid one, the structure composed of martensite and cementite; these structural states provide high hardness (over 60 HRC). Heating to a higher temperature will increase hardness only insignificantly because the curve of hardness in the diagram has a sharp bend corresponding to the Ac_1 temperature.

The accuracy of the method of trial hardening depends upon the extent of the interval in which the temperature is raised. An interval of 10 degrees C is quite sufficient for industrial determinations of hardening temperatures, with two or three specimens being heated to each temperature stage. The accuracy of determining the critical points is then approximately ± 5 degrees C.

This accuracy is, however, insufficient for studies of constitutional diagrams and for many research works. On the other hand, the method of trial hardening is unsuitable for determining the temperature and process of dissolution of cementite (points A_{cm} in hypereutectoid steel) and complex carbides in many alloyed steels. Other, more intricate methods are required for studying this type of transformation.

13.2. LABORATORY EXERCISES

In the following laboratory exercises the temperature intervals for heating specimens are taken relatively large, about 30 degrees C, in order to reduce the number of monotonously repeated operations that are of no value to educational process.

Specimens may be in the form of cylindrical discs (for instance, 10-12 mm in diameter and 15 mm high), parallelepipeds, etc. For convenience, the test specimens must be of different size and shape. All specimens must be marked.

Before putting the specimens into a hardening furnace, the hardness of one or two of them must be measured by the Rockwell ball test at a load of 100 kgf (HRB scale). The values obtained are recalculated to the HB scale.

To reduce the heating time all the specimens to be heated to various temperatures should be simultaneously put into the furnace which has been heated to the lowest temperature speci-

fied in the problem. The specimens should be held at this temperature for 5-10 minutes, until their temperature colour coincides with that of the furnace walls. Then one of the specimens is taken from the furnace and quickly quenched in water. Specimens must be vigorously stirred in the water for 2-3 seconds in order to remove the vapour jacket that is formed, since this might slow down the cooling process. The temperature of the furnace is then raised to the next step specified in the problem and the specimens are held at this temperature for 3-5 minutes. The next specimen is then hardened as previously described. The temperature of the furnace is raised further and the procedure is repeated until the last specimen is heated to its temperature and quenched.

Such hardening from five different temperatures can be accomplished within an hour. In addition, this method ensures high accuracy, since specimens are heated in the same furnace and the heating temperature is measured by the same instrument. Specimens for two or three problems may be put into the furnace simultaneously, if they are to be heated with equal temperature steps. It is advisable to use specimens of different shape and size in this case.

When placing specimens into the furnace, one has to consider that the temperature near the furnace door may be lower than that measured by the galvanometer because of the inflow of cold air. Specimens must therefore be placed in the middle of the furnace, as close as possible to the thermocouple.

Before measuring hardness, specimens must be carefully ground by an emery disc in order to remove scale and the decarburized layer. Their hardness must be measured by the Rockwell test and the results of the measurements should then be converted into the HB scale. The 'heating temperature-hardness' curve is then plotted and the critical points are found.

Next examine the microsections at a magnification of 400 to 500X and sketch their microstructure.

The record of a test must contain the following:

(a) characteristics (hardness and microstructure) of the steel in the initial state;

(b) a table of heating temperatures and the corresponding hardness values;

(c) a temperature-hardness curve;

(d) description of the transformations causing hardness variations and microstructure sketches;

(e) answers to all questions set forth in a problem, and evaluations of the accuracy of the obtained results by referring to technical literature and the iron-carbon diagram.

No. 180. Using the trial hardening method, determine the critical points Ac_1 and Ac_3 of a structural medium-carbon steel of melt I.

Heat the specimens to 710, 740, 770, 800, and 830 °C. Determine the approximate composition of the steel (on the iron-carbon diagram) and its hardening temperature from the position of the critical points.

No. 181. Using the trial hardening method, determine the critical points Ac_1 and Ac_3 of structural carbon steel of melt II.

Heat the specimens to 700, 730, 760, 790, and 820 °C. Determine the approximate composition of the steel (on the iron-carbon diagram) and its temperature of normalization from the position of the critical points.

No. 182. Using the trial hardening method, determine the critical points Ac_1 and Ac_3 of structural carbon steel of melt III.

Heat the specimens to 690, 720, 750, 780, and 810 °C.

Determine the composition of the steel (on the iron-carbon diagram) and its temperature of normalization from the position of the critical points.

No. 183.¹ Using the trial hardening method, determine the critical points Ac_1 and Ac_3 of alloyed manganese steel 45Г2.

Heat the specimens to 690, 710, 730, 750, 770, and 790 °C.

Compare the critical points of this steel (as found in the test) with those of carbon steel 45 (by reference to the iron-carbon diagram).

No. 184.¹ Using the trial hardening method, determine the critical points Ac_1 and Ac_3 of alloyed manganese steel 45Г2.

Heat the specimens to 700, 730, 760, 790, and 800 °C.

Compare the critical points of this steel (as found in the test) with those of carbon steel 35 (by reference to the iron-carbon diagram).

No. 185.¹ Using the trial hardening method, determine the critical points Ac_1 and Ac_3 of alloyed Cr-Si-Mn steel 35ХГС.

Heat the specimens to 720, 750, 780, 810, 840, 870, and 900 °C.

Compare the critical points of this steel (as found in the test) with those of a carbon steel having the same content of carbon.

No. 186.¹ Using the trial hardening method, determine the critical points Ac_1 and Ac_3 of alloyed Cr-Si-Mn steel 35ХГС.

Heat the specimens to 730, 770, 800, 830, 860, and 890 °C.

Compare the critical points of this steel (as found in the test) with those of manganese steel 45Г2 (according to the data from Problems Nos. 190 and 191).

¹ Other grades of alloyed steels, with either lower or higher temperatures of their critical points, can also be used in the problem.

No. 187. As is known, steels of various compositions must be hardened from different temperatures.

Harden specimens of steel 45 and steel Y12 from 700, 770 and 830 °C.

Explain why the specimens of steel 45, after being heated to 770°C and quenched from that temperature, have acquired a lower hardness than the specimens of steel Y12. Indicate the differences in the structures of these steels after hardening.

No. 188. Steels of various composition are heated to different temperatures before hardening.

Harden specimens of steel 50 and steel Y8 after heating them to 710, 780, and 850 °C.

Explain why the specimens of steel 50, after being hardened from 770 °C, have got a lower hardness than those of steel Y8.

Chapter Fourteen

THE STRUCTURE OF CARBON STEEL IN NON-EQUILIBRIUM (CAUSED BY HEAT TREATMENT)

14.1. THE STRUCTURE OF HARDENED STEEL

The structure of hardened steel depends on the steel composition and hardening conditions (heating temperature and quenching procedure).

Hardening of steel with a very low content of carbon (up to 0.025-0.03 per cent) by heating it only slightly above the PQ line retards the precipitation of ternary cementite at grain boundaries. The basic ferritic structure of the steel is then not changed. This hardening increases the plasticity of steel without altering its other strength characteristics. However, the subsequent structure appearing after heating to 300-400 °C or cold deformation promotes precipitation of ternary cementite particles and reduces the plasticity.

Hardening a low-carbon steel with 0.08-0.15 per cent C (heating above the point Ac_3 and water quenching) increases somewhat its hardness and plasticity; the structure of such a steel is composed of martensite and residual ferrite (Fig. 14.1).

The effect of hardening is more pronounced in steels having a higher carbon content (0.15-0.25 per cent). Their yield strength can thus be increased by 30-50 per cent, and their hardness increases from 110-130 HB to 140-150 HB.

Carbon steels with more than 0.25-0.30 per cent C sharply vary their properties upon being hardened.

Hypoeutectoid steel with more than 0.25-0.30 per cent C acquires a martensitic structure through hardening.¹ Martensite crystals are seen as characteristic needles or flakes under a microscope. If the temperature of heating is not too high (not higher than 30-70 degrees C above Ac_3), this causes no appreciable growth of austenite grains; for this reason the crystals of

¹ In carbon steels with more than 0.5-0.6 per cent C martensitic transformations are not finished on cooling down to the room temperature and the steel retains a certain amount of residual austenite. In hypoeutectoid steel with 0.5-0.6 per cent C the amount of this austenite is insignificant (2-3 per cent).



Fig. 14.1. Structure of hardened low-carbon steel (0.2% C). Martensite and inclusions of ferrite, 200X

martensite formed within an austenite grain on cooling are small and hardly discernible at small or medium magnifications (200-600X), see Fig. 14.2.

Raising the hardening temperature by 100-150 degrees C above A_{c3} causes a noticeable growth of austenite grains (Fig. 14.3), and therefore, of martensite crystals formed on cooling (see Fig. 14.2). This mode of heating reduces the plasticity of steel (either hardened or tempered) and is not used in practice.

Hardening of hypereutectoid steel is carried out by heating into the two-phase region (austenite + secondary cementite), i.e. by 50-80 degrees C above A_{c1} . The structure of the steel (Fig. 14.4) is then composed of martensite, grains of secondary cementite (not dissolved through heating), and residual austenite. Crystals (needles) of martensite are very small. The temperature of the end of martensitic transformation of a steel with an increased carbon content then drops below -50°C . The amount of residual austenite does not exceed 5-10 per cent and still cannot be detected by microanalysis.

Raising the hardening temperature above A_{cm} causes the dissolution of secondary cementite and promotes the growth of grains. Such a steel after hardening has easily discernible large crystals (needles) of martensite and some residual austenite, whose content increases to 20-30 per cent or more. These structures are formed owing to a quick quenching of carbon steel in water.

With a slower cooling, for instance in oil or air, it is impossible to prevent the decomposition of the austenite of the carbon steel into a ferrite-cementite mixture. The coagulation processes

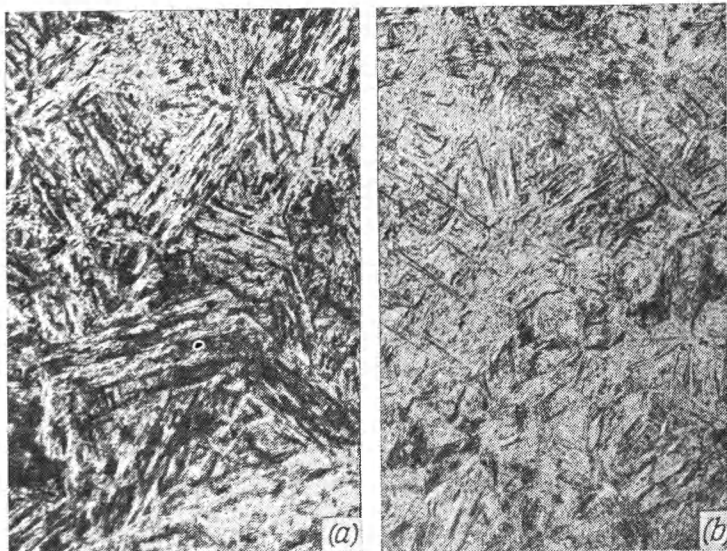


Fig. 14.2. Structure of hardened medium-carbon steel (0.5% C), 600X
 (a) hardening from 830 °C without overheating, martensite crystals are small and hardly visible; (b) hardening from 925 °C (overheating); larger crystals of martensite

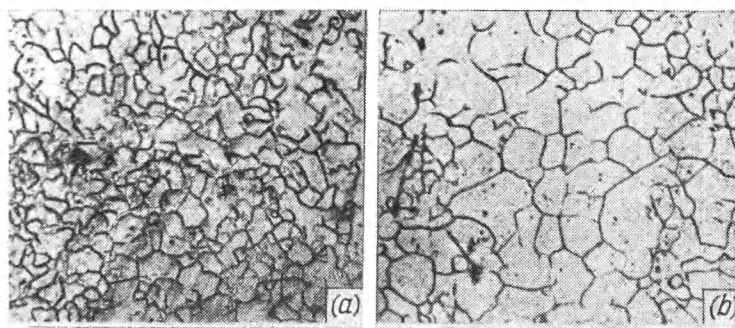


Fig. 14.3. Hypoeutectoid steel (0.5% C) after hardening. Austenite grains revealed by the oxidation method (grain boundaries were oxidized during heating of polished section in an open furnace), 100X
 (a) hardening from 820 °C. (b) hardening from 925 °C

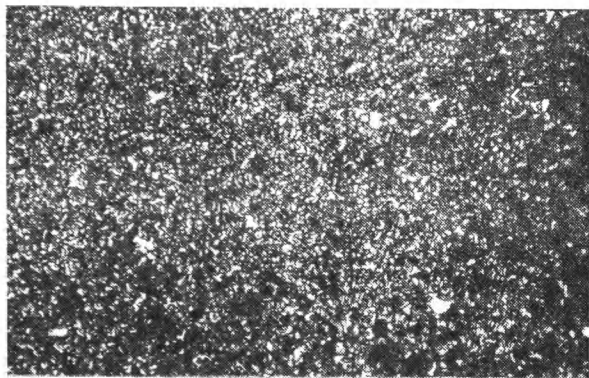


Fig. 14.4 Hypereutectoid steel (1.2% C) after hardening from 800 °C. Martensite and secondary cementite, 500X

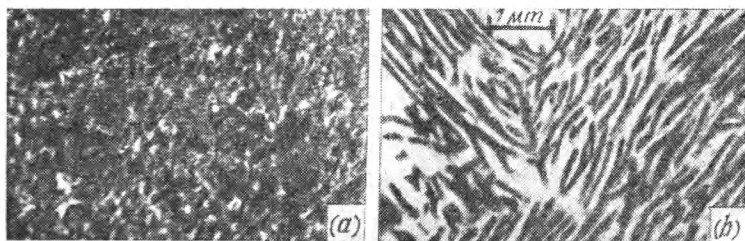


Fig. 14.5. Steel with 0.5% C after hardening from 840 °C with oil quenching.
The structure is hardened troostite
(a) optical microphotograph, 500X; (b) electron microphotograph, 7000X

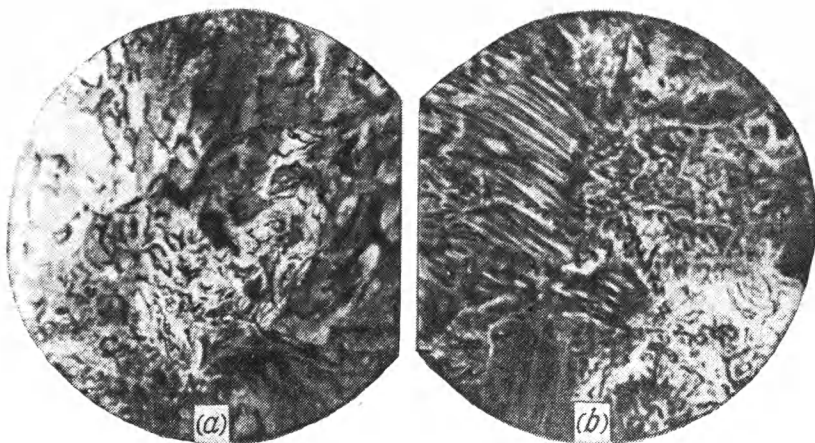


Fig. 14.6. Steel with 0.7% C, hardened sorbite
(a) 200X; (b) 1000X

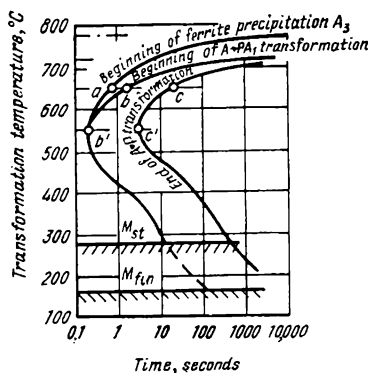


Fig. 14.7. Diagram of isothermal transformation of supercooled austenite in carbon steel (0.5% C)

cannot proceed to their end, as is the case when cooling occurs still more slowly (e.g. when steel specimens are left to cool in the furnace). Therefore the transformation products that are formed, i.e. troostite and sorbite, differ from the equilibrium pearlitic structure in being more disperse: flakes of ferrite and cementite and the distances between them are smaller compared with those observed in pearlite.

Similar structures are also formed in larger specimens (workpieces) of carbon steel after quenching in water, since the rate of

cooling of inner sections is lower than that of surface layers (see Ch. 17 on hardenability of steel).

Sorbite and troostite formed through hardening have a lamellar structure, as distinct from temper sorbite and troostite, which have the granular structure of cementite.

The structure of troostite is almost unresolvable under microscope because of the large dispersity of cementite and ferrite particles. Troostite is a very disperse two-phase structure and is more susceptible to etching than other structures. It is seen as dark formations in etched microsections (Fig. 14.5a). Electron-microscope studies have revealed the lamellar structure of hardened troostite (Fig. 14.5b).

Hardened sorbite is more readily resolvable under an optical microscope (Fig. 14.6) than hardened troostite.

As distinct from pearlite, the composition of troostite and sorbite is not constant, their carbon content varying appreciably depending on the composition of the initial austenite and the temperature of its transformation. For this reason hypoeutectoid steels with more than 0.35-0.40 per cent C, in which the structure of troostite or sorbite has been formed through heat treatment, show no regions with separate grains of structurally isolated ferrite.

The structure formed in a steel on decomposition of supercooled austenite at temperatures below the critical point under isothermic conditions may be characterized by a diagram of isothermic transformation (Fig. 14.7), called a C-shaped diagram. This diagram makes it possible to determine approximately the structure obtained after cooling with various rates.

14.2. THE STRUCTURE OF TEMPERED STEEL

Low tempering of hardened steel (with heating to 200-250 °C) causes no noticeable changes in its structure (as seen under a microscope). Only X-ray analysis can reveal the lower tetragonality of the martensite lattice and the precipitation of minute particles of carbide (cementite), which are due to the sharp reduction of the carbon concentration in martensite caused by low tempering. Steel microsections after low tempering become only more susceptible to etching, so that crystals (needles) of martensite of tempered steel are darker than in hardened steel not subjected to tempering (see Fig. 14.8a),

Tempering with higher heating (to 350-400 °C) intensifies the processes of diffusion and coagulation and thus causes decomposition of martensite and formation of troostite. Tempering at 400-500 °C results in the formation of troostite-sorbite, and at 500-600 °C, in the formation of sorbite.¹

Carbide crystals in temper troostite and sorbite are of a granular shape.

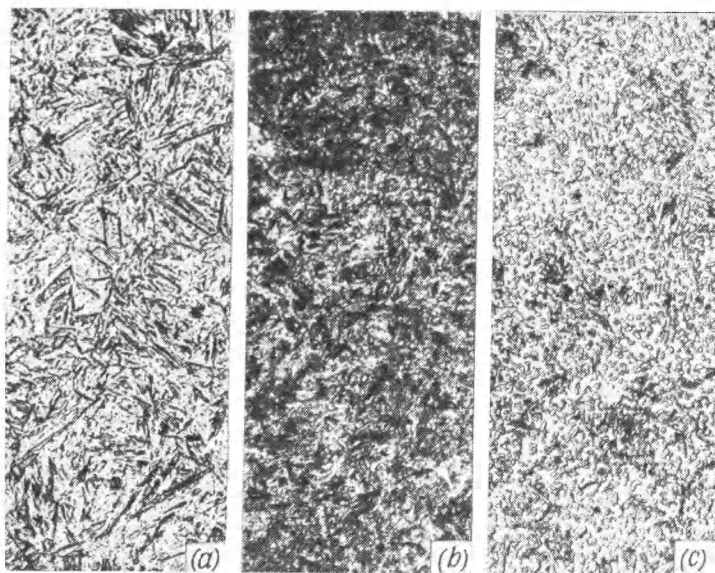


Fig. 14.8. Structure of tempered steel (0.6% C), 500X

(a) temper martensite; (b) troostite; (c) sorbite

¹ In a high-temperature hardened steel in which large needles of martensite have been formed, temper troostite and sorbite may retain the needle orientation.

The structure of temper troostite (Fig. 14.8*b*), like that of hardened troostite, is hardly detected by microanalysis, because of an appreciable dispersity of the formed particles of ferrite and cementite; troostite is seen as deep-etched dark formations.

Temper sorbite is more distinct on microsections (Fig. 14.8*c*).

A higher tempering (with heating from 650 °C to A_{c1}) causes the structure of steel to approach the equilibrium state, with the formation of pearlite and precipitation of ferrite (in hypoeutectoid steel). The structure of pearlite then becomes less and less disperse and is similar to that of granular pearlite in annealed steel.

14.3. LABORATORY EXERCISES

In these laboratory exercises, the student must carry out a microscopic examination of typical structures of steel after hardening and tempering at a magnification of 500-600X. Microsections should be prepared in the laboratory. Use the following procedure:

(a) study and sketch the microstructure as seen under microscope;

(b) characterize the structure and phase composition of the specimen;

(c) finally describe the conditions of heat treatment (or the properties of steel in non-equilibrium).

No. 189. Carry out a microscopic examination and sketch the structure of two specimens of structural carbon steel of a hardness of 150 HB (annealed steel) and 60 HRC.

Characterize the microstructure of each of the specimens, determine the carbon content, and indicate the field of industrial application of these steels.

Give the conditions of heat treatment to ensure a hardness number of 60 HRC and say whether this heat treatment is the final one or additional heat treatment should be advised and if so, what type.

No. 190. Carry out a microscopic examination and sketch the microstructures of two specimens of carbon steel 45. The first specimen has a hardness number of 50 HRC, and the second, 30 HRC.

Characterize the microstructure of these steel specimens; recommend the heat treatment necessary to obtain the corresponding microstructure and hardness, and indicate the sections of a part (cylindrical specimen) of steel 45 in which this structure is likely to form.

No. 191. Carry out a microscopic examination and sketch the structure of two carbon steel specimens of the similar composi-

tion, the first specimen having a hardness number of 30 HRC, and the second, 150 HB (annealed).

Characterize the microstructure of these steel specimens, indicate their approximate composition, recommend the conditions of heat treatment to obtain a hardness number of 30 HRC, describe the mechanical properties corresponding to this hardness, and name the industrial applications of this steel.

No. 192. Carry out a microscopic examination of two specimens of medium-carbon steel (0.5 per cent C) after hardening, one of the specimens being hardened from 820 °C and the other, from 920 °C.

Sketch their microstructure and indicate the specimen having a higher brittleness. Recommend the hardening conditions and the temperature of tempering for shafts made of this steel.

No. 193. Carry out a microscopic examination of two specimens of hypoeutectoid carbon steel with 0.4 per cent C hardened respectively from 770 and 830 °C.

Sketch their microstructure, characterize the structural components observed, and by using the iron-carbon diagram, describe the differences in the structures of these two specimens. Indicate the specimen having a higher hardness.

No. 194. Carry out a microscopic examination of specimens of carbon steel (25 mm in diameter) after hardening with water quenching and of an alloy steel (for instance, Cr-Ni, Cr-Mn or Cr-Mn-Si steel) with the same carbon content after oil quenching. Determine the variations in their microstructures and measure hardness across the section of the specimens.¹

Indicate the specimen in which the properties across its section have changed more due to hardening.

No. 195. Carry out a microscopic examination and measure the hardness of two carbon steel specimens and two alloy steel specimens with the same carbon content, after water quenching and oil quenching.

Recommend quenching conditions for these steels and explain why the alloy steel can be quenched in oil.

No. 196. Carry out a microscopic examination of two specimens of hardened carbon steel with 0.8-0.9 per cent C, one of the specimens being tempered at 200 °C after hardening.

Sketch their microstructures and explain the differences observed.

Explain the aim of low tempering of this steel and indicate the field of its industrial application.

¹ Specimens 25 mm in diameter and 50 mm long after hardening are cut in half by an emery disc.

No. 197. Carry out a microscopic examination and sketch the structure of two specimens (microsections) of carbon steel 65, the hardness number of one specimen being 170 HB, and that of the other, 64 HRC.

Characterize the steel structure of each specimen, recommend the conditions of heat treatment to obtain a hardness number of 45-48 HRC. Describe the properties of steel 65 having hardness number around 45 HRC and indicate the aim of such treatment for industrial purposes.

Chapter Fifteen

HEAT TREATMENT OF STRUCTURAL STEELS

Many properties of steel, especially its mechanical properties, may be changed substantially by a heat treatment which forms a non-equilibrium structure. In the following laboratory exercises, the student is to study the effect of heat treatment on the strength and ductility of steel, which largely determine the behaviour of steel parts during operation.

15.1. LABORATORY EXERCISES ON HARDENING AND TEMPERING OF STEEL

The effect of heat treatment on the mechanical properties of steel can be studied by tensile tests of standard specimens or by testing notched test bars in pendulum impact testing machines (see Ch. 6 and Fig. 6.11).

The majority of laboratory exercises below are based on impact tests of notched specimens, which are simple in their shape and manufacture. Tensile tests are employed only in more extensive studies.

Structural carbon steel with 0.4-0.5 per cent C and alloy steel with 0.30-0.50 per cent C are recommended for making test specimens, since their mechanical properties are strongly affected by hardening and tempering. These steels acquire high strength and low impact strength on hardening and high impact strength, after tempering at 500-650 °C.

Steel parts of large cross sections can have poor mechanical properties if the steel has a low hardenability.

The laboratory exercises are divided into individual tasks with specified conditions of hardening and tempering. Each student is to make one test on hardening and one on tempering and compile a record of the work done, which should include (a) the results obtained by the student on his individual task and (b) the

results obtained by other students in accomplishing the same laboratory exercise. Thus, the record should contain the following:

(a) a diagram showing the effect of hardening temperature and quenching conditions (in tasks on hardening) and the effect of tempering temperature (in tasks on tempering) on the mechanical properties of steel, including its hardness;

(b) a description of the changes in the structure and the fracture of the steel depending on the same factors;

(c) answers to additional questions.

The work is to be done in the following sequence:

(a) the initial hardness of one or two specimens assigned for these laboratory exercises is determined by the Rockwell ball test (scale B), the results obtained being converted to the Brinell hardness numbers;

(b) the specimens are heated in a furnace¹ in the order indicated in Sec. 13.1; quenching is done in accordance with the conditions specified in the individual task; temper cooling is done in air;

(c) cooled specimens are slightly cleaned by means of sand paper (to reveal metallic lustre);

(d) their hardness is measured by the Rockwell test (scale C); the values obtained are recalculated to the Brinell hardness numbers; hardness tests are to be performed on sections near the ends of a specimen, but not near the notch;

(e) notched specimens are subjected to impact tests in a pendulum impact testing machine, and their impact strength is determined as indicated in Ch. 6;

(f) fractures of specimens are examined visually.

Many specific features of the structure and treatment of metal may be judged upon by the appearance, form, and colour of a metal fracture (see Ch. 2). Typical fractures of steel are shown in Fig. 15.1.

Annealed hypoeutectoid carbon steel with large inclusions of precipitated ferrite has a coarse-grained fracture with comparatively smooth edges. A fracture of alloy steel has finer grains and is less smooth in its shape.

Properly hardened martensitic steel has low ductility and a smooth bright fibrous fracture. Upon superheating, its fracture becomes granular.

The fracture of hardened low-tempered steel (after heating to 300-350 °C) is almost similar to that of hardened steel, and

¹ Heat the specimens in a molten salt bath to prevent their oxidation. Temper heating of specimens can be done in a furnace, since temper temperature does not exceed 650 °C. Notches in specimens should be packed tightly with asbestos.

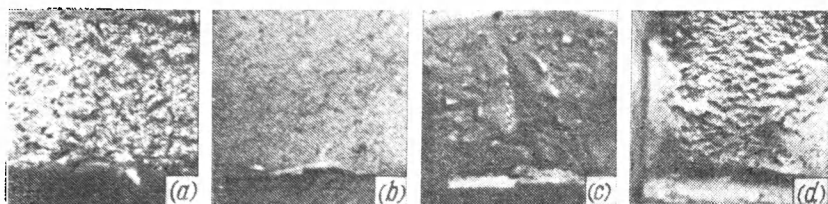


Fig. 15.1. Fractures of heat-treated carbon steel (0.5% C), 3X
(a) annealed; (b) hardened; (c) hardened and tempered at 450 °C; (d) hardened and tempered at 550 °C

the ductility of the steel increases only slightly. After higher tempering, which increases ductility, the fracture becomes uneven (with cup-shaped edges) and acquires a dull grey colour.

No. 198. Hardening of steel. Determine the effect of the temperature of heating and of the rate of cooling on the structure, hardness, and impact strength of structural carbon steel.

Determine the hardness, impact strength and the form of fracture of the steel both in the initial (annealed) state and after heat treatment.

Plot (schematically) the C-shaped diagram of carbon steel. Show the lines which correspond to the possible cooling rates of surface layers or small specimens (up to 10 mm) in various cooling media (water, oil, air) and, using the obtained data on the changing of hardness, determine the structure of steel in the surface layers of the specimen.

Using these data and the diagram, decide which of the two factors (either the cooling rate or the temperature of heating above the point A_{c3}) is more effective in providing a martensitic structure and high hardness in the steel.

The specimens should be heated to the temperatures A_{c3} , $A_{c3} + 30^\circ$, $A_{c3} + 90^\circ$, and $A_{c3} - 30^\circ$ °C and cooled from these temperatures in water, oil, and air.

No. 199. Tempering of steel. Determine the effect of temperature and time of tempering on the structure, hardness, and impact strength of hardened carbon steel.

Using the results of experiments, plot diagrams showing the effect of tempering temperature on the property being studied (hardness or impact strength). Show on the diagram how (qualitatively) the ultimate strength and relative elongation are changed on tempering.

Characterize the microstructure formed and the fracture of steel after tempering in accordance with the specified conditions.

Explain why the properties and structure of the steel depend not only on the tempering temperature, but also on the time of holding during tempering, if this time is increased from 20 to 60 minutes.

Tempering should be carried out by heating to a temperature of 200, 300, 400, 500, 600, and 650 °C with holding for 20, 30, and 60 minutes.

No. 200. Isothermic hardening. Compare the effect of hardening with oil quenching and that of step-wise hardening on the mechanical properties of structural alloyed steel.

Specimens of alloyed steel 30XTCa should be heat treated under the following conditions:

- (a) oil hardening from 800-900 °C;
- (b) hardening from 860-900 °C in a saltpetre bath¹ at a temperature of 280-310 °C for 30 minutes, followed by air cooling;
- (c) oil hardening from 880-900 °C, tempering at 280-310 °C for an hour.

Determine σ_t , σ_y , δ , ψ , hardness, and impact strength of the specimens after heat treatment according to the specified conditions.

Describe the conditions ensuring the highest mechanical properties of the metal, i.e. a high strength in combination with a high impact strength.

15.2. LABORATORY EXERCISES ON STEEL HARDENING WITH INDUCTION HEATING

These exercises should be carried out in high-frequency hardening furnaces. Specimens should be heated by the method of simultaneous hardening, i.e. by heating their whole surface at once.

Specimens may be made of structural steel 45 (or 50 or 55) which acquires high hardness on hardening, or of tool steel Y11 (or Y12, 9XC).

Cylindrical specimens 8-10 mm in diameter and 50 mm long are recommended for the purpose. Specimens of square or rectangular cross section are less suitable, since their corners are heated to a higher temperature than their faces. The shape and size of the heating inductor should match the shape and size of the specimens.

The properties acquired by steel through induction heating (with a constant frequency of the electric current) depend on the temperature and rate of heating in the region of phase transfor-

¹ The composition of the bath: 45 per cent KNO_3 + 55 per cent NaNO_2 .

mations, as can be seen from the diagrams for determining the conditions of high-frequency hardening (Fig. 15.2).

Heating to very high temperatures, even for a short time, appreciably increases the grain size of the metal and impairs its properties, as happens when the metal is heated in a furnace or in a salt bath.

Determination of the high-frequency hardening conditions on the basis of the heating time is not quite correct as at temperatures below the Curie point heating is caused by the thermal effect of the induced current and hysteresis losses, whereas at temperatures above that point, heating is caused only by the thermal effect of the current.

The transformation of steel from ferromagnetic to paramagnetic state and the growth of the electrical resistance of its surface layers cause the penetration of the induced current and heat generation in less heated deeper layers. For this reason the specific current power and the rate of heating decrease after passing through the Curie point; at the same time the depth of current penetration and the thickness of the heated layer increase (8 to 20 times for carbon steel). Thus, the time of heating to the Curie point differs from the time of heating above that point.

For proper high-frequency hardening the heating temperature and the duration of heating depending on the rate of heating in the phase transformation region (above the Curie point) and below that point must be determined accurately, which may be done by using special measuring instruments (and by calculating the rate of heating).

The heating conditions also depend on the power and frequency of the current supplied and the width of insulating gap between the inductor and the workpiece being heated. These factors must be kept constant when performing the work. The gap between the inductor and the workpiece may be taken equal to 1 mm.

No. 201. Quench specimens of steel 45 after induction heating for 2, 4, 6, and 8 seconds.

Measure the hardness of the surface of cooled specimens and plot the hardness-heating time curve; examine the fractures of

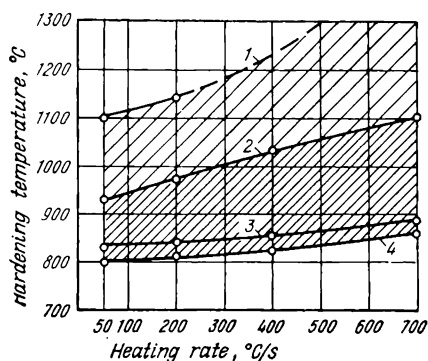


Fig. 15.2. Diagram to determine the conditions of high-frequency hardening of steel 45 (after I. N. Kidin)

1, 2 and 4—61-63 HRC; 3—64 HRC

the specimens and decide by their appearance how the time of induction heating affects the thickness of the hardened layer.

Notes. 1. Hardness measurements should be done on flat areas prepared on sides of cylindrical specimens; the thickness of the removed layer of metal should not be more than 1 mm.

2. To obtain fractures of hardened specimens, these must be cut in the middle to a depth of 2 to 3 mm by means of grinding wheel and then broken.

Characterize the appearance and thickness of the fractures, as indicated on page 316.

No. 202. Quench specimens of steel V11 after induction heating for 2, 4, 6, and 8 seconds.

Measure the surface hardness of the cooled specimens (as in Problem No. 201) and plot the curve of hardness variation depending on the time of heating.

Explain the shape of the plotted curves.

Chapter Sixteen

HEAT TREATMENT OF TOOL STEELS

16.1. DETERMINATION OF PROPERTIES OF TOOL STEEL

The laboratory exercises in this chapter relate to steels employed for making cutting tools, as these are the ones most representative of the large group of tool steels. The principal grades of steels and alloys used in cutting tools are given in Table 27.14.

Carbon and alloy tool steels differ only slightly in their hardness, wear resistance and cutting properties, all having high hardness (60-64 HRC) after hardening and low tempering at 150-200 °C.

Carbon steels (in tools more than 10 mm in cross-section) should be quenched in water to form martensitic structure and high hardness, but such a sharp cooling tends to cause increased stresses and strains.

Alloy steels can be hardened in oil or molten salts (by the method of interrupted hardening) and have lower values of stress and strain when hardened. Besides, alloy steels have a better hardenability than carbon steels, and that is why they are used for making tools of complicated shape and large dimensions.

Carbon and alloy steels retain their martensitic structure until being heated to approximately 200 °C. At higher temperatures, their hardness and wear resistance can reduce appreciably owing to the strong coagulation of carbide particles precipitating from the martensite and to decomposition of the latter. These grades are employed for cutting at relatively low speeds, i.e. so as not to heat up the cutting edge exceedingly much.

High-speed steels after hardening and tempering (at 550-600 °C) acquire high hardness as well (63-65 HRC), and they have a better heat resistance and can retain the martensitic structure and high values of hardness and wear resistance up to temperatures of 600-625 °C. This is why high-speed steels have appreciably better cutting properties and are employed for cutting at high speeds or cutting metals of high hardness (strength).

The cutting properties of a high-speed steel are, as a rule, the better, the higher is its heat resistance, i.e. the temperature

to which the steel can be heated without impairing its hardness.

The high thermal stability of high-speed steel is due to its alloying elements: tungsten, molybdenum, vanadium, and chromium, which are transferred into the solid solution through hardening. These elements only slightly precipitate from the martensite even at high temperatures (500-600 °C) and the carbides formed by them are less liable to coagulation at these temperatures.

The precipitated carbides are very dispersed and increase the hardness of a high-speed steel compared with that obtained through hardening and tempering at lower temperatures. This phenomenon, which is called precipitation hardening, is responsible for what is termed the secondary hardness of high-speed steels.

In annealed high-speed steels, the alloying elements are present mainly as carbides. In order to obtain high thermal stability of the steel, as much as possible of the tungsten, molybdenum, chromium, and vanadium must be transferred to the solid solution. This is achieved by dissolution of the complex tungsten (molybdenum) carbides, which is only possible at a high temperature of hardening (1150-1300 °C). With a higher temperature, the amount of dissolved carbides increases, as also does the thermal stability of the steel.

Even with a very high heating, part of the carbides remain undissolved (mainly initial carbides which have precipitated from the liquid during solidification of the ingot). These precipitated (residual) carbides hamper the growth of austenite grains, which enables a very high hardness to be obtained in high-speed steels.

Hard alloys, whose composition includes tungsten and cobalt carbides or tungsten, titanium and cobalt carbides, excel high-speed steels in hardness, wear resistance, and thermal stability, while their hardness reaches 88-90 HRA (72-74 HRC).¹ They retain high hardness after being heated up to 900-1000 °C and can be employed for cutting at high speeds and cutting hard materials. The hardness of hard alloys cannot be reduced by heat treatment, because of which they are only limitedly applicable for making cutting tools of complicated shape (for instance, milling cutters). In addition, hard alloys have a higher brittleness as compared with that of high-speed steels.

¹ Hardness of hard alloys is measured by indenting a diamond cone with a force of 60 kgf (instead of the usual load of 150 kgf), in order not to crumble the diamond.

By determining the thermal stability of tool steels, combined with studies of their microstructure, it is possible to establish the effect of alloying elements on their most characteristic properties. At the same time, such tests can be easily made in a laboratory.¹

16.2. LABORATORY EXERCISES

In each of the works below, the students should perform heat-treatment of two different grades of steel or two specimens of the same grade, but with different conditions of hardening and tempering, and compare the properties obtained. The hardening and normal tempering of specimens is done by the laboratory staff.

The narrowest side thickness of carbon steel specimens should not exceed 10-12 mm, for all the metal to be hardened through.

Two specimens of each grade of steel should be heated to one of the temperature values indicated in the problem (better to the mean values), and one specimen of each grade (or for each specified mode of heat treatment), to the other temperature values given.

Heating is to be done in either an electric furnace or molten-salt bath. The time of holding (40-60 min) should be the same for all the specimens. Specimens to be used in various problems, if they are to be heated to the same temperature, may be charged together into the furnace.

Proceed with laboratory work in the following order:

(a) measure the hardness of at least one specimen of each grade (or batch) in the initial state, i.e. after hardening or after hardening and tempering. After completing the treatment specified in a problem, again measure the hardness of each specimen. Use the Rockwell C scale for steel specimens and the A scale (i.e. with a load of 60 kgf) for hard alloys and recalculate the A scale values to C scale ones (see Sec. 7.3);

(b) examine the specimens of the two grades specified after hardening and tempering under a microscope at a magnification of 300-500 and sketch their microstructure. The microsections must be prepared by the laboratory staff.

The work record should include:

(a) the characteristics of the metal studied in the initial state: grade of steel (or alloy), composition, hardness, microstructure (a sketch and description), state of the metal (after annealing, hardening, etc.);

¹ In industry, thermal stability is determined by heating specimens to a high temperature (575-650 °C) for 4 hours. In laboratory exercises on determining thermal stability, the time of heating may be reduced to 1-2 hours.

(b) a hardness-heating temperature curve plotted on the basis of the test results;

(c) conclusion; if tempering modes have been studied, the conclusion must recommend the optimal tempering temperature; if thermal stability of two grades of steel has been checked, their thermal stability indices must be compared and the field of application of each of the steel grades tested recommended, etc.

Students studying an extended course of metallurgy should in addition measure the saturation magnetization and determine the amount of residual austenite in the structure of high-speed steel (after hardening and after tempering).

The additional tasks are given in problems No. 203 and Nos. 214-16. Before attempting these tasks the students should refer to the material of Chapter 5, Sec. 2.

Problems

No. 203. Determine the effect of the hardening temperature on the thermal stability of high-speed steel P18.

Materials for the study: specimens of steel P18 hardened from 1300 and 1200 °C (oil quenched); all specimens after hardening were tempered twice at 560 °C (for 1 hour).

Heat the specimens to 560, 600, and 650 °C.

Additional task. Measure the saturation magnetization of the specimens: (a) immediately after hardening; (b) after tempering twice at 560 °C and after further tempering at 600 °C. Using the results obtained, determine the amount of residual austenite in the steel after hardening and after tempering twice at 560 °C. Reference specimens are those tempered at 560 °C (twice) and then additionally tempered at 600 °C.

Use the ballistic method (see Sec. 5.2) to measure the saturation magnetization.

No. 204. Compare the heating stability (thermal stability) of high-speed steel P12 and that of alloy steel X, which have the same high hardness (63-64 HRC) after heat treatment.

Materials for the study: specimens of steel P12 and steel X heat treated under the optimum conditions (hardening from 1240 °C and tempering thrice at 560 °C for steel P12; hardening from 850 °C and tempering at 150 °C for steel X).

The specimens should be heated to 300, 500, and 600 °C.

No. 205. Many cutting tools are made of less expensive high-speed steel P12 (containing 12 per cent tungsten), instead of steel P18 which contains 18 per cent tungsten.

Compare the thermal stability of these two steels.

Materials for the study: specimens of steels P12 and P18 hardened from the optimum temperatures (1250 °C for steel P12 and 1280 °C for steel P18) and tempered three times at 560 °C.

The specimens should be heated to 580, 600, and 620 °C.

No. 206. Tungsten-molybdenum high-speed steels, which have better mechanical properties than tungsten steels, are widely employed for making cutting tools.

Compare the thermal stability of tungsten-molybdenum steel P6M5 with that of tungsten steel P12 (the compositions and applications of the steels are given in Table 27.17).

Materials for the study: specimens of steels P6M5 and P12 hardened from their optimal temperatures (1225 °C for steel P6M5 and 1240 °C for steel P12) and tempered three times at 550-560 °C.

The specimens should be heated to 580, 600, and 620 °C.

No. 207. High-speed steels of an increased thermal stability are employed for cutting hard materials; for this, the steel is additionally alloyed with cobalt.

Compare the thermal stability of steel P12 with that of steel P12Φ4K5 (the compositions and applications of the steels are given in Table 27.17).

Materials for the study: specimens of steels P12 and P12Φ4K5 hardened from their optimal temperature (1240 °C) and tempered three times at 560 °C.

The specimens should be heated to 600, 620, and 640 °C.

No. 208. Materials of a relatively high hardness, in particular, high-hardness structural steels (35-45 HRC) and heat-resistant alloys, are cut by tools made of novel grades of high-speed steel having increased hardness (up to 69-70 HRC) and a higher thermal stability.

Compare the thermal stability of tungsten-molybdenum steel P6M5 with that of cobalt steel P8M3K6C (the compositions and applications of the steels are given in Table 27.17).

Materials for the study: specimens of steel P6M5 and steel P8M3K6C hardened from their optimal temperatures (1225 °C and 1235 °C, respectively) and tempered three times at 550 °C.

The specimens should be heated to 600, 625, and 650 °C.

No. 209. Compare the thermal stability of high-speed steel P8M3K6C (which has the highest hardness and highest thermal stability in its group) with that of a hard alloy, such as BK8. For compositions and applications of these materials see Tables 27.17 and 28.1.

Materials for the study: specimens of steel P8M3K6C hardened from the optimum temperature (1235 °C) and tempered three times at 550 °C and specimens of the hard alloy made by sintering.

The specimens should be heated to 650, 700, and 750 °C. Hardness of the hard alloy should be measured by the Rockwell A scale (with the load of 60 kgf).

No. 210. Determine the effect of hardening temperature on the thermal stability of high-speed steel P12.

Material for the study: specimens of steel P12 heated to 1240 °C and 1150 °C before hardening. After hardening, all specimens were tempered twice at 560 °C.

The specimens should be heated to 560, 600, and 650 °C.

No. 211. Compare the tempering stability (thermal stability) of high-speed steel P12 and carbon steel Y10.

Material for the study: specimens of steel P12 after hardening (from 1240 °C), and tempering (twice) at 560 °C; specimens of steel Y10 after hardening (from 800 °C) and tempering at 150 °C.

The specimens should be heated to 300, 500, and 600 °C.

No. 212. Determine which of the alloying elements [whether tungsten (with additions of chromium and vanadium) or chromium] is more effective in increasing the thermal stability of steel. For this, compare the thermal stability of high-speed steel P12 with that of high-chromium steel X12Φ1.

Material for the study: specimens of steel P12 after hardening (from 1240 °C) and tempering twice at 560 °C; specimens of steel X12Φ1 after hardening (from 1125 °C) and tempering twice at 475 °C.

The specimens should be heated to 300, 500, and 600 °C.

No. 213. Compare the thermal stability of high-speed steel P12 with that of a hard alloy (for instance, BK8 containing 92 per cent WC and 8 per cent Co).

Materials for the study: specimens of steel P12 after hardening from 1240 °C and tempering twice at 560 °C; specimens of the hard alloy as delivered (sintered).

The specimens should be heated to 600, 700, and 775 °C. Measure the hardness of the hard alloy by the Rockwell A scale with the load of 60 kgf.

No. 214. Determine the optimum tempering temperature for high-speed steel P18.

Material for the study: specimens of steel P18 hardened from 1280 °C.

The specimens should be heated to 300, 500, 560, and 600 °C and held twice for 40 minutes at the temperature selected.

Additional task. Measure the saturation magnetization of specimens after hardening and after tempering, using the ballistic method (see Sec. 5.2). Using the results obtained, plot a saturation-tempering temperature curve and determine the amount of residual austenite in the steel after hardening and after tempering at 550 °C. One specimen tempered at 600 °C should be used as a reference specimen.

No. 215. Determine the optimum tempering temperature for high-speed steel P12.

Material for the study: specimens of steel P12 hardened from 1240 °C.

The specimens should be heated to 300, 500, 560, 600, or 650 °C twice for 40 minutes.

Additional task. Measure the saturation magnetization of the specimens after hardening and after tempering, using the ballistic method (see Sec. 5.2). Using the results obtained, plot a saturation-tempering temperature curve and determine the amount of residual austenite in the steel after hardening and after tempering at 560 °C. A specimen tempered twice at 560 °C and then at 600 °C should be used as a reference specimen.

No. 216. Determine when a high-speed steel and a carbon tool steel have a higher hardness: whether after normal hardening or after tempering.

Materials for the study: specimens of steel P18 hardened from 1300 °C; specimens of steel Y12 hardened from 780 °C.

Measure the hardness of the specimens after hardening and then heat them to 200, 300, 500, or 600 °C and again measure the hardness.

Additional task. Measure by the ballistic method the saturation magnetization of the specimens of high-speed steel before tempering and after tempering (see Sec. 5.2). On the basis of the results obtained, plot a saturation-tempering temperature curve and determine the amount of residual austenite in steel P18 after hardening and after tempering at 560 °C. One specimen tempered at 560 °C twice and then at 600 °C should be used as the reference specimen.

Chapter Seventeen

DETERMINATION OF HARDENABILITY OF STEELS

17.1. METHODS FOR DETERMINING HARDENABILITY

Hardenability is the capability of steel to get hardened to a certain depth across the cross section of a part or specimen, so that its structure changes to martensitic or troostite-martensitic, and therefore, acquires a higher hardness.

The thickness of the hardened surface layer is most conveniently determined by measuring the hardness of the metal, rather than by the microscopic examination. These determinations are somewhat different for structural steels and for the harder tool steels.

In structural steels the basic martensitic structure includes a definite amount of troostite (up to 10-20 per cent), so that their hardness can be varied only slightly through hardening, and therefore, the thickness of the layer having purely martensitic structure is difficult to be determined. Hardenability can be conveniently determined by the thickness of a layer having a martensitic or semi-martensitic structure (i.e. composed of 50 per cent martensite and 50 per cent troostite). A sharp reduction of hardness may occur when the content of martensite drops down below 50 per cent. In addition, a semimartensitic structure is easily determined by microscopic examination.

The hardness of martensite and troostite is mainly dependent on the content of carbon and, to a lesser extent, on the presence of alloying elements. Therefore, the hardness of a semi-martensitic layer can be known in advance if we know the content of carbon in the steel being studied (see Table 17.1).

In hypereutectoid tool steels, the hardness of the hardened semi-martensitic region has no relation to carbon content. In high-carbon steels, the hardened structure may contain residual austenite in addition to martensite, its amount being largely variable depending on the composition of the steel and the conditions of hardening. The presence of the soft austenite, even together with a slight amount of troostite, can diminish hardness noticeably (often below the limits tolerated in many cutting

Table 17.1. Hardness of Layers Composed of 50 per cent Martensite and 50 per cent Troostite

Carbon content, %	HRC number		Carbon content, %	HRC number	
	carbon steel	alloy steel		carbon steel	alloy steel
0.08-0.17	—	25	0.33-0.42	40	45
0.18-0.22	25	30	0.43-0.52	45	50
0.23-0.27	30	35	0.53-0.62	50	55
0.28-0.32	35	40			

tools). Besides, the carbon content of the martensite (austenite) in steels retaining residual carbides is always lower than its total content in the steel. Finally, the semimartensitic region is poorly visible under a microscope if the structure contains residual martensite or is highly disperse, which is characteristic of steels containing residual carbides. For this reason the hardenability of tool steels is characterized by the thickness of the hardened layer of martensitic structure, which has a high hardness number, usually more than 60 HRC.

Hardenability depends both on the composition of steel, i.e. the content of alloying elements and the concentration and size of austenite grains, and on the cross-sectional area of the hardened part and the hardening conditions.

Hardenability can be increased by increasing the temperature of hardening, which causes the growth of austenite grains and, in hypereutectoid steels, also a deeper dissolution of the carbides and saturation of the austenite with carbon and alloying elements. Higher quenching rates also increase hardness.

The properties of parts are in many respects decided by their hardenability. Steels of a higher hardenability should be used in parts for operation under high stresses and appreciable dynamic loads. This ensures a greater depth of the layer having martensitic structure upon hardening and sorbitic structure without ferrite zones, after high tempering.

With the hardening from the commonly adopted temperatures, which causes no noticeable growth of the grain, carbon steels are hardened through in parts up to 12-15 mm in cross section (with water quenching), whereas alloy steels can be hardened to depths of 50-100 mm or even 200-300 mm (with oil quenching), depending on their composition. Steels with a high content of alloying elements can acquire high hardness over the whole cross section even with still slower cooling, for instance, air cooling.

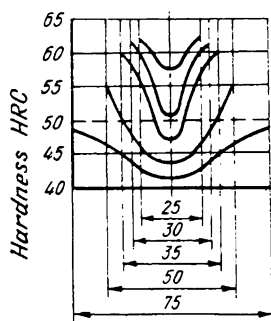


Fig. 17.1. Hardness curves in cross sections of hardened cylindrical specimens of carbon steel (0.7% C) of various diameters, mm (after A. P. Gulyaev)

In many cases hardenability must be determined experimentally by a certain method according to the expected hardenability of the steels being tested and the cross-sectional area of specimens (parts). These methods are as follows:

1. For carbon steels, mainly tool steels whose hardenability is determined on specimens of a narrow cross section, up to 25-30 mm, the following simple method is applicable. A specimen of a circular or square cross section (its length should exceed 2.5-3 times its diameter or side) is heated to the hardening temperature, held at that temperature to heat it fully over the whole cross section, and then quenched in water or other medium whose effect on the hardenability is to be studied. The cooled specimen is broken at

its centre (it can hardly be cut by a cutting tool because of the high hardness of the metal, while cutting by an emery disc can heat it appreciably and reduce the hardness of the steel¹), its fracture surface is then ground and the hardness is measured across its width or diameter at intervals of 2 mm. A 'hardness-distance from the centre' curve is plotted from the measured results (such as that shown in Fig. 17.1), which characterizes the hardness of the steel in specimens of the given diameter only. In order to characterize the hardness more thoroughly, specimens of various diameters and quenched in various media should be tested. Hardenability can be assessed in numbers from a special scale compiled for 20-mm square specimens.

2. For alloy steels which can be hardened more deeply by oil quenching, the method of end quenching is employed (according to the USSR State Standard GOST 5657-69), using specimens 25 mm in diameter and 100 mm long (Fig. 17.2). The specimen has a shoulder at one of its ends to suspend it vertically during hardening. No decarbonized layer or scale must be on its surface.

Specimens are heated in a furnace or molten-salt bath. If the heating is performed in a furnace with non-controllable atmosphere, the specimen is placed into a cylindrical steel box with its lower end placed on a graphite or carbon plate (Fig. 17.3).

¹ The hardened specimen is first notched at its centre by an emery disc in order to ensure a smoother fracture.

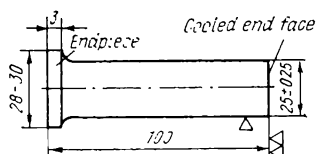


Fig. 17.2. Specimen for determining the hardenability by the end-quench test (GOST 5657-69)

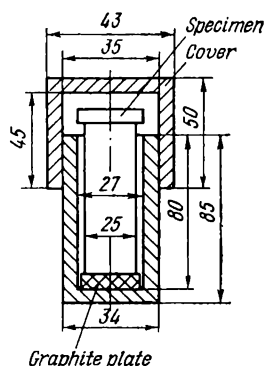


Fig. 17.3. Arrangement of a non-controlled atmosphere furnace for the end-quench test

After temperature curing, the specimens are quenched in an installation placed at such a distance from the furnace that the time of transfer of specimens may be not more than 5 s. A design of such an installation is shown in Fig. 17.4. The heated specimen

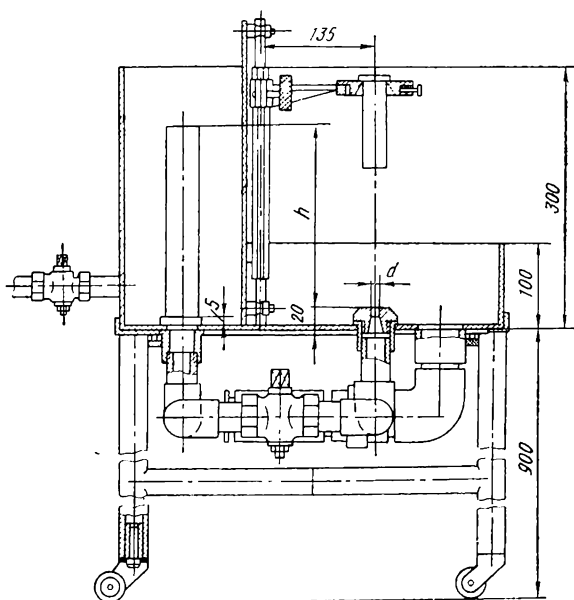


Fig. 17.4. Apparatus for end quenching (designed at NAMI)

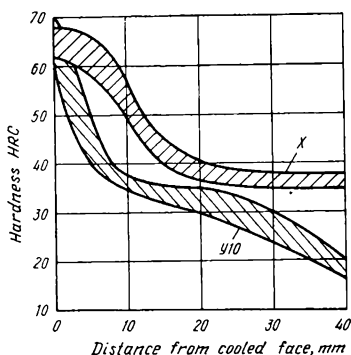


Fig. 17.5. Hardenability bands of steel Y10 and steel X (ШХ15); grain size number 9-10, hardening from 840 °C with oil quenching (steel X) and from 800 °C with water quenching (steel Y10)

is mounted in the arrangement and immediately cooled by a jet of water ejected from a nozzle.

The pressure of water is controlled so that the height of the free jet be 65 mm (for cooling specimens 25 mm in diameter). The distance from the nozzle to the lower end face of the specimen must be 12.5 mm and the jet must impinge the end face only. The specimen is held in the arrangement until cooled completely (at least 10 minutes). The temperature of water must lie within 10-25 °C.

Under such conditions the rate of cooling of the lower end face will correspond to the rate of cooling of a specimen in water (1000 °C/s), and that of the upper end face, to the rate of cooling in air (3-4 °C/s), with the intermediate rate of cooling distribution along the length of the specimen.

The hardened specimen is ground on two diametrically opposite sides along its whole length to a depth of 0.5 mm, with intensive cooling.

Hardness measurements are then made on the ground planes; the first point of measurement is 3 mm from the lower end face. The first 10 measurements are made at 3-mm intervals, and further measurements at 1.5 mm intervals. Hardness numbers (Rockwell or Vickers) are determined for each pair of points on both ground planes at the same distance from the end face, and their arithmetic mean values are then calculated.

The results of the tests are expressed graphically or as hardenability numbers. The resultant diagram is plotted in the coordinates: hardness against the distance from the quenched end face and is called the hardenability curve. To characterize the hardenability of a steel grade in various melts, hardenability curves are plotted for each of the melts, these curves forming a hardenability band (Fig. 17.5). Using these data and a special nomogram (see Figs. 17.8 and 17.9), the hardenability of specimens (parts) of various cross sections can be determined.

The hardenability number according to GOST is defined as l_c , where l is the distance from the quenched face to the point having

the hardness of a semimartensitic structure layer and c is the corresponding HRC number.

The hardness of the layer of semi-martensitic structure is given in Table 17.1, and the distance from the end face to the point having this hardness number is found on the hardenability curve plotted from the results of end quenching. For instance, for steel 40X (whose hardenability band is shown in Fig. 17.5), the value of c , i.e. the hardness of the semi-martensitic layer, is 45 HRC, and the distance $l = 10.5$ mm. Therefore, its hardenability number is 10.5₄₅.

This procedure is, however, inapplicable for determining hardness in various sections of a hardened specimen. First of all, for practical considerations, it is important to know the hardness in the zones next to the surface of a hardened part which are subjected to appreciable loads, as the core of the part is practically subjected to neither bending nor torsional stresses.

The end-quench method is inapplicable for air-hardenable steels (mainly high-alloyed steels) since it gives martensitic structure and high hardness along the whole length of a specimen. This also relates to steels for which the distance from the water-quenched face to sections of semi-martensitic structure turns out to be larger than 50 mm.

3. To determine the hardenability of air-hardenable steels, i.e. those fully hardenable in very large sections (a diameter or side larger than 100 mm), a method based on thermal simulation is employed, in which the mass of a metal is simulated by a thermo-insulative layer, for instance, asbestos. The layer of insulation must ensure that heat is given up by the specimen through its end faces only. Therefore, the rate of cooling of the insulation must not differ from that of the specimen and there must be no heat exchange between the specimen and insulation. For this reason the thickness of the insulation is selected according to the thickness of the specimen (Fig. 17.6).

To determine the maximum thickness or diameter of a part that can be hardened fully, specimens 20 mm square or 20 mm in diameter are used, their length being equal to the thickness or diameter of the corresponding part; both end faces of the specimen are left open.

The insulation (asbestos sheets) is placed layerwise into a box made of scale-resistant steel sheets 1 mm thick. The box, in the form of two opened halves (without a specimen, Fig. 17.7) is placed into a furnace heated to the hardening temperature of the given steel, and is held there for 1.5-2 hours. The specimen is then heated to the same temperature and placed into the heated box, and the whole arrangement is left to cool in the air.

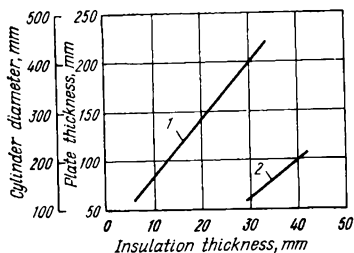


Fig. 17.6. Thickness of the insulation layer depending on the thickness (diameter) of a simulated specimen and conditions of cooling during hardening (after A. E. Pavaras)

1—oil quenching; 2—air cooling

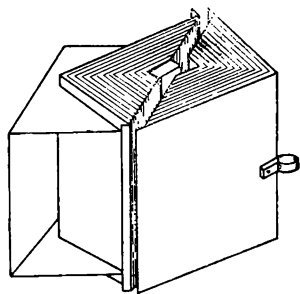


Fig. 17.7. Arrangement for determining the hardenability of air-hardening steel (after A. E. Pavaras)

After cooling, hardness is measured on one of the edges of the specimen. The distribution of hardness along the length of the specimen thus corresponds to the distribution of hardness across the cross section of a larger article.

This method is also suitable for determining the hardenability of parts of greater thickness with oil or water quenching. In this case a different insulation thickness is used (see Fig. 17.6) and nozzles for supplying oil or water are pressed against the end faces of the specimen.

17.2. LABORATORY EXERCISES

The problems given below are of two types: (a) on experimental determination of hardenability and (b) calculation matters.

(a) Experimental Determination of Hardenability

Perform experiments: (a) on hardened specimens of low-hardenable carbon steels, cut in the middle of their length; (b) on specimens of alloy steels oil-hardened by the end-quench test (as used most commonly for alloy steels). The end-quench tests should be made by groups of two students.

No. 217. Plot the hardenability curve and characterize the effect of chromium on the hardenability of hypereutectoid tool steel.

Materials for the study: cylindrical specimens 25 mm in diameter, made of carbon steel Y11A and low-alloyed steel 11X.

After fine-grain hardening (790-800 °C for steel Y11A and 820-830 °C for steel 11X) with water quenching, break the specimens at their centre section and grind the fracture plane carefully. Measure the hardness over the diameter at intervals of 1.5-2 mm.

No. 218. Plot the hardenability curve and indicate the effect of manganese on the hardenability of structural steel.

Materials for the study: cylindrical specimens of carbon steel 40 and alloy steel 40Г2 25 mm in diameter. After fine-grain hardening (840-850 °C for steel 40 and 830-840 °C for steel 40Г2), break the specimens in their centre section and carefully grind the fracture plane. Measure the hardness along the diameter at 1.5-2-mm intervals.

No. 219. Characterize the effect of hardening temperature on the hardenability of carbon steel Y12. Plot the hardenability curve and explain why hardenability is changed on changing the hardening temperature.

Materials for the study: cylindrical specimens 25 mm in diameter hardened from 790-800 °C (the first specimen) and from 830-840 °C (the second specimen) with water quenching. After hardening, break the specimens in the middle of their length and carefully grind the fracture plane. Measure the hardness along the diameter at intervals of 1.5-2.0 mm.

No. 220. Characterize the hardenability of carbon tool steel depending on the cross-sectional area of a specimen. Plot the hardenability curve and indicate approximately the critical diameter for the steel studied.

Materials for the study: specimens of steel Grade Y12A 12 mm and 25 mm in diameter, hardened from 790-800 °C (fine-grain hardening) and quenched in water. After water quenching, break the specimens in their centre sections and carefully grind the fracture plane. Measure the hardness along the diameter at intervals of 1.5-2.0 mm.

No. 221. Determine by the end-quench test the effect of the quenching when hardening steel Grade 45X to obtain a martensitic and semi-martensitic structure (50 per cent martensite plus 50 per cent troostite) at a distance of 30 mm from the surface.

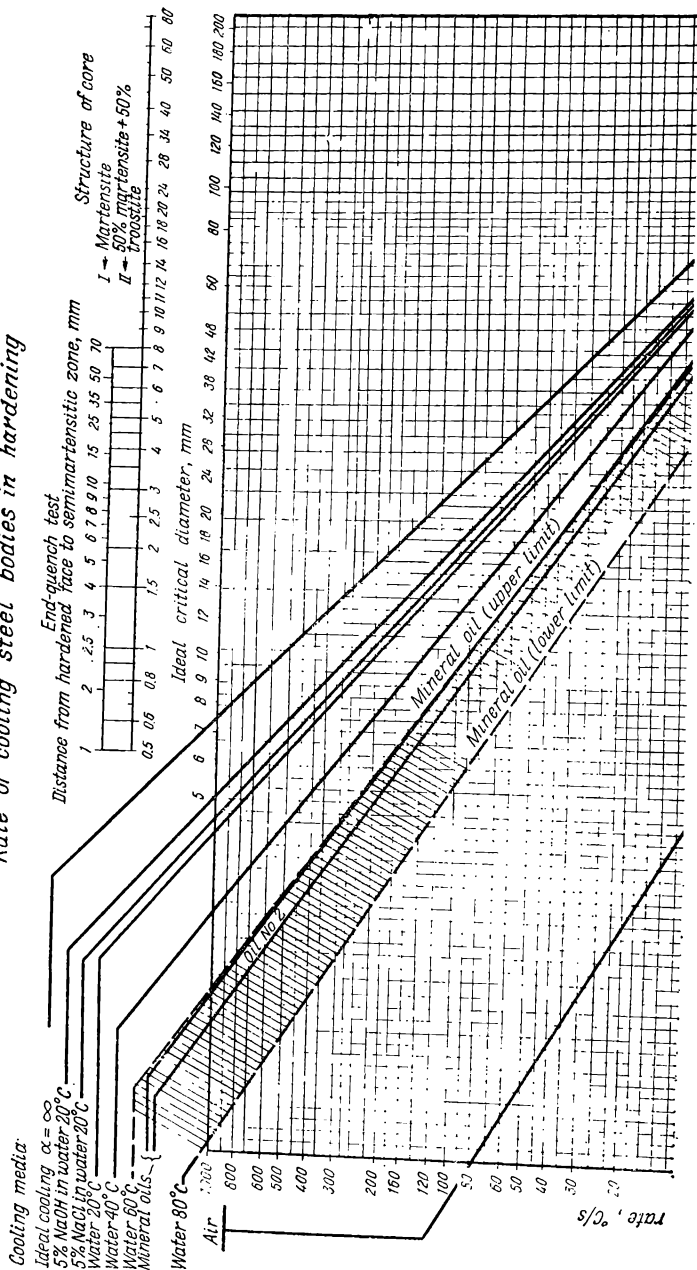
Heat the specimens to 840-850 °C and quench: (a) in oil; (b) in water.

Calculate by the nomogram (Figs. 17.8 and 17.9) for a cylindrical specimen with the $L : D$ ratio = 10 (a long specimen) and $L : D = 0.25$ (a washer).

No. 222. Determine by the end-quench test the hardening temperature for steel Grade 65Г (with water quenching) to obtain martensitic or semi-martensitic structure 20 mm from the surface.

Heat the specimens: (a) to 820-830 °C and (b) to 860-870 °C.

Rate of cooling steel bodies in hardening



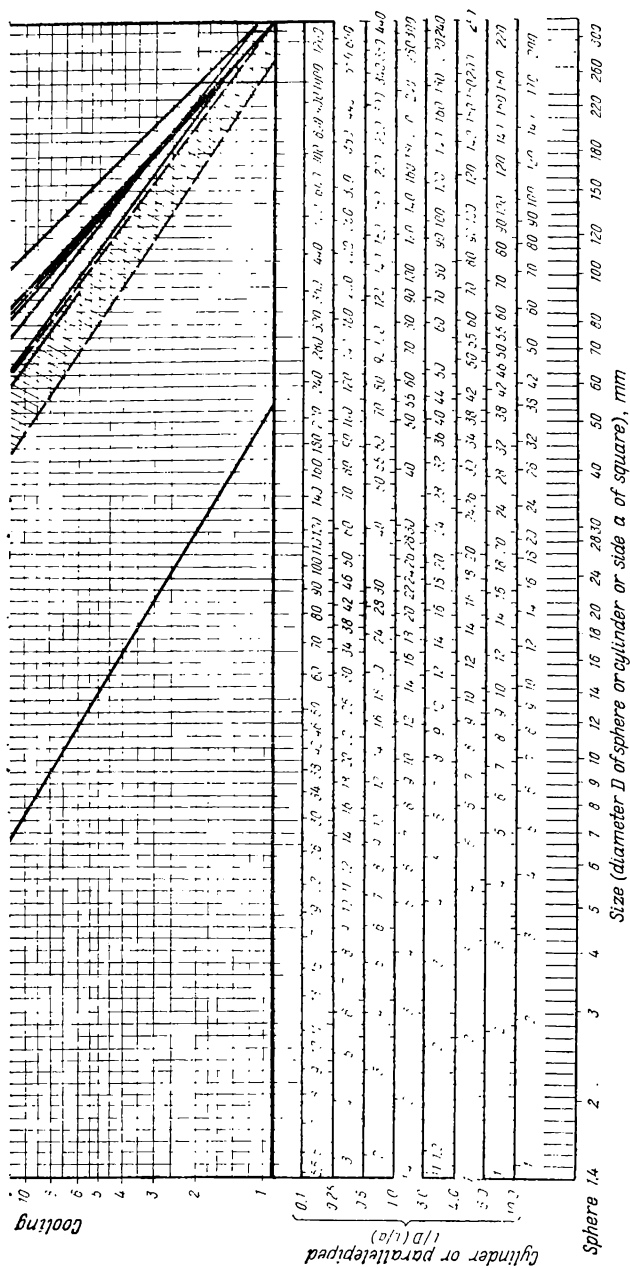


Fig. 17.8. Nomogram for calculation of hardenability (after M. E. Blanter)

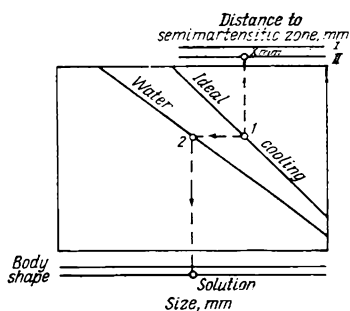


Fig. 17.9 Scheme of using the nomogram in Fig. 17.8

Explain why the critical diameters of these steels are different.

No. 224. Determine by the end-quench test the effect of temperature on the critical diameter for steel X (with oil quenching). Heat the specimens to 845-855 °C and to 880-890 °C.

Calculate the values for a cylindrical specimen ($L:D = 3$) using the nomogram in Figs. 17.8 and 17.9.

Explain why the critical diameter for steel X increases with hardening temperature.

(b) Problems on Calculating Hardenability

In these problems the students calculate the critical diameter for cylindrical parts (with various height-to-diameter ratios), spheres or parallelepipeds, with various quenching conditions, using the data on the thickness of martensitic and semimartensitic zones specified in the problems below or determined experimentally by the end-quench test.

To solve the problems, use the nomogram¹ in Fig. 17.8. The two scales I and II in its upper portion characterize the distance from the quenched end face of a specimen. Use scale II to determine the maximum diameter (critical diameter) of an article or specimen to be hardened fully across its cross section with the formation of a martensitic structure, and scale I to determine the maximum diameter (thickness) of the semimartensitic zone (50 per cent martensite plus 50 per cent troostite). The way to use this nomogram is shown in Fig. 17.9. The distance from the end face to the end of martensitic or semimartensitic zone determined experimentally for the given grade of steel, is laid along

Calculate the values for a cylindrical specimen with $L:D = 4$ (using the nomogram in Figs. 17.8 and 17.9). Explain why hardenability can be changed by varying the hardening temperature.

No. 223. Determine by end-quench test the critical diameters of the martensitic and semi-martensitic zones of steel Grade 40X and Steel Grade 40XH after oil quenching. Heat the specimens to 850-860 °C.

Calculate the values for a cylindrical specimen ($L:D = 3$) using the nomogram in Fig. 17.8 or 17.9.

¹ Blanter M. E. in: *Zavodskaya laboratoriya*, 1949, No. 5, pp. 557-61.

scale *H* or *I*, respectively. A perpendicular is dropped from the point found to the line on the nomogram which determines the ideal quenching conditions (ideal quenching medium, i.e. the one ensuring high and uniform rate of cooling from the hardening temperature down to $+20^{\circ}\text{C}$), which gives point *I* (see Fig. 17.9). A horizontal line is drawn to the left from that point to intersect a line indicating the particular quenching medium being used (water, oil, or air). A vertical line is then drawn from point 2 just found to intersect with the scale 'size, mm' in the lower portion of the diagram. This gives the maximum diameter (thickness) of a specimen that can be hardened fully in the given quenching medium.

No. 225. In an experimental determination of the hardenability of a melt of steel 40X by the end-quench test, the distance to the zone of semimartensitic structure was found to be 12 mm.

Using the nomogram, determine the critical diameter for a specimen of this melt of steel for (a) oil quenching and (b) water quenching.

Calculate for a cylindrical specimen with $L:D = 10$.

No. 226. When determining experimentally the hardenability of a melt of hypereutectoid steel Grade XBГ, the length of the zone of martensitic structure was found to be 25 mm.

Find on the nomogram the critical diameter for this melt of steel for cylindrical specimens with $L:D = 10$ (long bars) and $L:D = 0.5$ (flat washers).

Assume that the specimens were quenched in oil.

No. 227. In an experimental determination of the hardenability of two melts of steel Grade 40XH, with heating to the same temperature, the distance to the semimartensitic zone was found to be 18 mm for the specimen of one melt and 20 mm for that of the other melt.

Find on the nomogram the critical diameters for these two melts for oil quenching and indicate the possible causes of unequal hardenability of steel in these melts.

Calculate for a cylindrical specimen with $L:D = 10$.

No. 228. In an experimental determination of the hardenability of a melt of hypereutectoid steel Grade XBГ, the length of the martensitic zone was found to increase from 25 to 28 mm because of the elevation of the hardening temperature from 860° to 900°C .

Find on the nomogram the critical diameter for these two hardening procedures for a cylindrical specimen with $L:D = 5$.

Explain why a higher temperature increases hardenability.

No. 229. In determination of the hardenability of hypereutectoid steel Grade X, the length of the martensitic zone was found

to be 8 mm for oil quenching and 10 mm for water quenching.

Find on the nomogram the critical diameter for these two hardening procedures for a cylindrical specimen with $L : D = 5$.

No. 230. In the determination of the hardenability of steel Grades 35Г2 and 35ХГС, the distance to the zone of semimartensitic structure was found to be 6 mm for the first grade of steel and 9 mm for the second.

Explain why steel Grade 35ХГС has a higher hardenability.

Find on the nomogram the critical diameter for these two steels for a cylindrical specimen with $L : D = 3$.

Chapter Eighteen

PROBLEMS ON THE ANALYSIS OF MICROSTRUCTURE OF STEELS AND CAST IRONS

Before attempting the problems below, recapitulate the material on typical structures of cast iron and steel in the equilibrium and non-equilibrium states (Chapters 12 and 14). Solve and make a record of one or two problems.

No. 231. Figure 18.1 shows the well-known Chernov's dendrite, and Fig. 18.2, macrostructure of a steel ingot (in cross section).

Describe the macrostructure of the ingot in its individual zones and explain why crystals of different size and shape have formed over its cross section.

Indicate the portion of the ingot and describe the conditions under which Chernov's dendrites are likely to be formed.

No. 232. Figure 18.3 shows the macrostructure of an ingot of low-carbon silicon steel (0.1 per cent C and 4 per cent Si); as can be seen, the shape and position of crystals are different but typical of various zones of the ingot.

Describe the macrostructure and properties in particular zones of the ingot and explain why crystals of different structure have formed over the cross section.

No. 233. Figure 18.4 shows the microstructure of a shaped steel casting (steel with 0.3 per cent C): (a) after casting and (b) after heat treatment.

Indicate the structure which characterizes the steel in the cast state and describe the structures shown. Explain how and for what purpose the heat treatment of the casting was made and how it has changed the mechanical properties of the metal.

No. 234. Figure 18.5*a* shows the macrostructure of a bolt, and Fig. 18.5*b*, the microstructure of the steel the bolt is made of.

By examining the microstructure indicate the approximate content of carbon in the steel, and by examining the macrostructure the process by which the bolt has been manufactured.

Describe the method revealing the macrostructure.

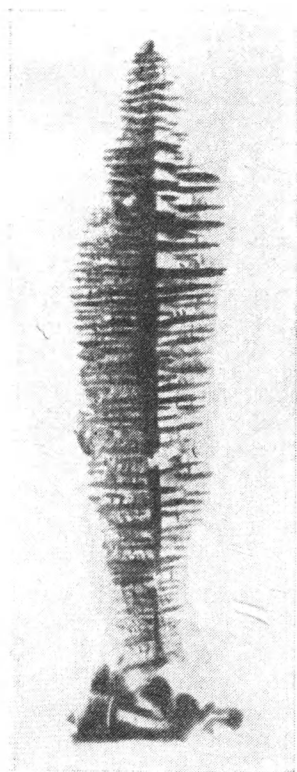


Fig. 18.1. Chernov's dendrite



Fig. 18.2. Macrostructure of steel ingot (full size) in a cross section

No. 235. Figure 18.6*b* shows the microstructure of the steel bolt illustrated in Fig. 18.6*a*.

Characterize the microstructure and indicate the content of carbon in the steel. Using the results of the macroanalysis describe the process by which the bolt was manufactured (Fig. 18.6*b*).

What would be the difference in the macrostructure of the bolt if this were machined from a rolled rod?

No. 236. The properties of steel depend largely on the size of grain. Fig. 18.7*a* and *b* shows austenite grains in carbon steel of two melts.

Using the scale of numbers (see Fig. 3.24), determine the number for each grade of steel and indicate the method by which the grain size can be determined.

Describe the effect of grain size on the properties of steel.

No. 237. Figure 18.8 shows the microstructures of carbon steel (0.3 per cent C) after forging and slow cooling. Microscopic examination indicates that one of the steels was forged under improper temperature conditions.

Characterize the structure of the steel in each forging and indicate:

(a) which of them has been forged improperly;

(b) what kind of structural defect it has and how this defect influences the properties of the steel;

(c) what has caused this defect and how it could be prevented.

No. 238. Figure 18.9 shows the microstructure of low-carbon steel in two melts, *A* and *B*, the carbon content being roughly 0.06 per cent. One of the steels has shown a lower plasticity in cold deforming (die-forming).

Indicate which of these steels has the lower plasticity; explain this by using the data of microscopic examination.

What characteristic features of the structure of low-carbon steel, apart from those shown in the photograph, determine the plasticity and cold drawability of the steel?

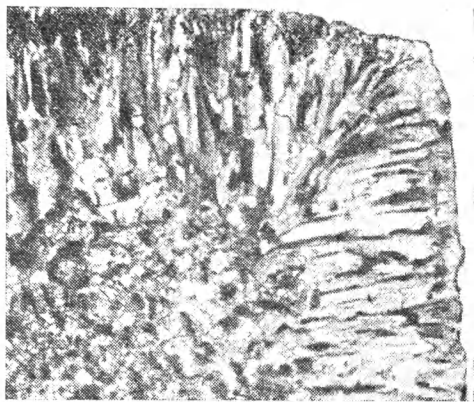


Fig. 18.3. Macrostructure of an ingot of low-carbon silicon steel (0.1% C, 4% Si) in a cross section

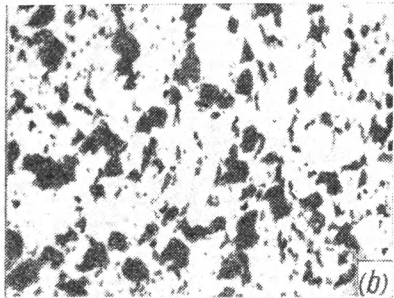


Fig. 18.4. Microstructure of carbon steel (0.3% C) in a complex-shape casting, 200X

(a) after casting; (b) after heat treatment

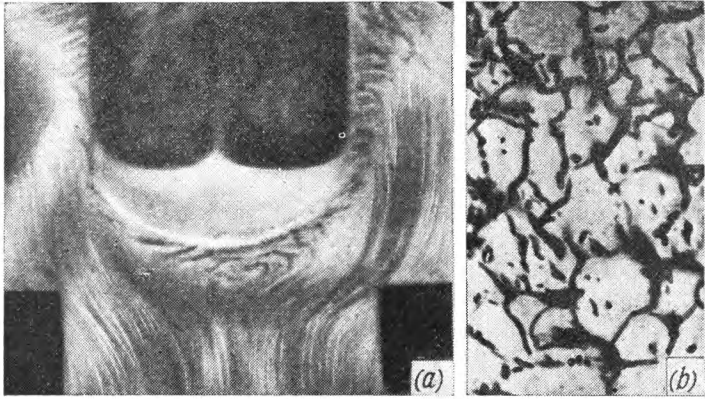


Fig. 18.5. Forged steel bolt
 (a) macrostructure (full size); (b) microstructure, 350X

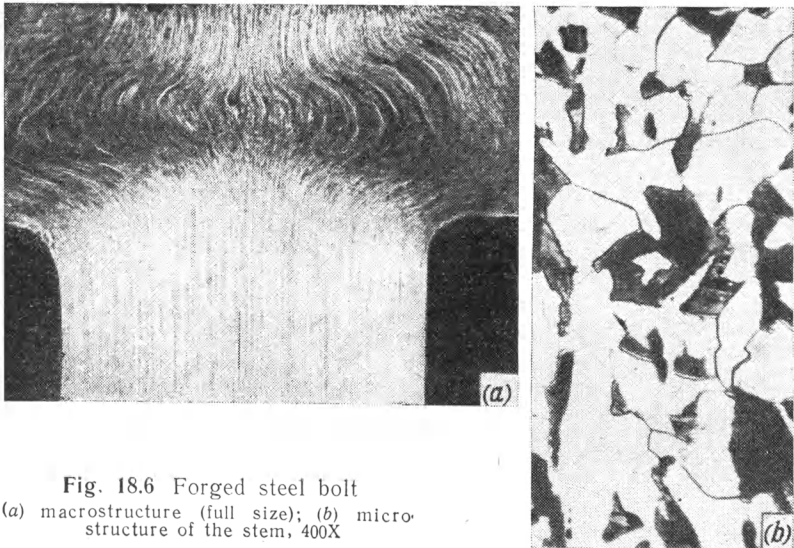


Fig. 18.6 Forged steel bolt
 (a) macrostructure (full size); (b) microstructure of the stem, 400X

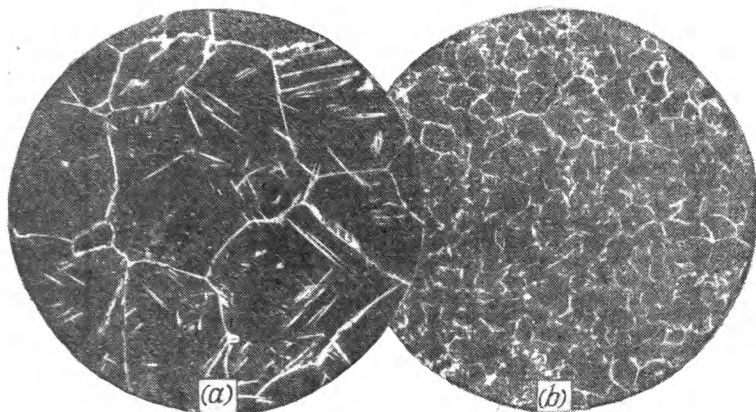


Fig. 18.7. Grains in carbon steel, 100X
(a) melt A; (b) melt B

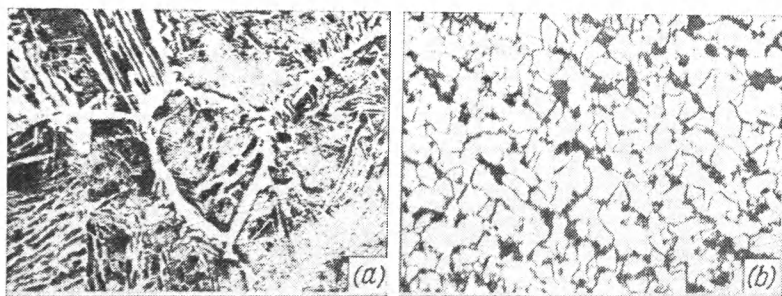


Fig. 18.8. Microstructure of carbon steel (0.3% C) after forging, 200X

No. 239. Figure 18.10 shows the microstructures of low-carbon steel after cold deforming and subsequent heating to various temperatures.

Give the composition of the steel and characterize the variations of its structure caused by cold deforming and heating.

Also indicate how this affects the mechanical properties (ultimate strength and relative elongation) of the steel.

Using the microstructures shown, determine the temperature of the recrystallization on set and compare the result obtained with that calculated by Bochvar's formula.

No. 240. A strip of fine-grained low-carbon steel was subjected to slight local deformation (local bending) and then heated.

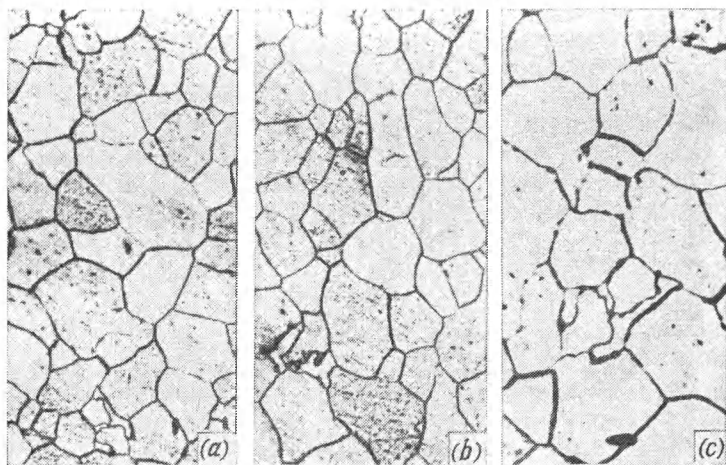


Fig. 18.9. Microstructure of low-carbon steel
 (a) steel A, 100X; (b) steel B, 100X; (c) steel B, 400X

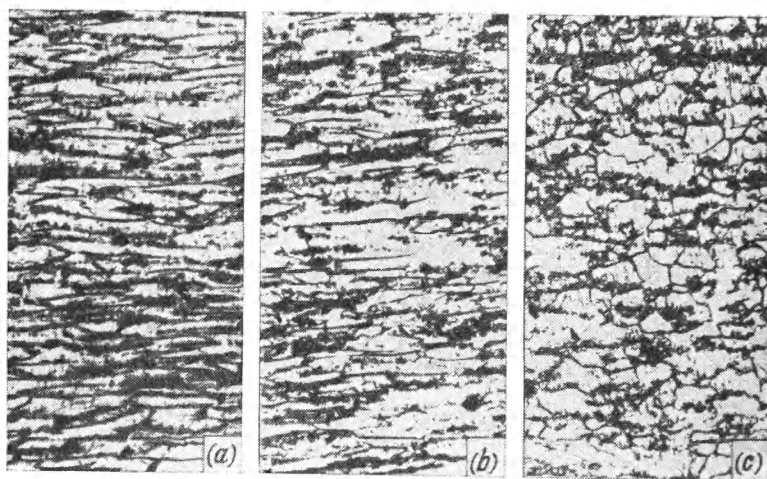


Fig. 18.10. Microstructure of steel after cold deforming and after recrystallization, 100X
 (a) heated to 250 °C; (b) heated to 350 °C; (c) heated to 650 °C

Figure 18.11 shows the microstructure of the steel (after heating) at the boundary of the deformed zone.

Indicate the differences in the size of grains in the deformed section and the section not deformed. Describe the structure shown, give the content of carbon in the steel, and explain the causes of the appreciable grain growth and the ways this affects the mechanical properties of the steel.

No. 241. Figure 18.12 shows the microstructure of annealed carbon steel.

Describe the structure and determine the content of carbon; using the Fe-Fe₃C diagram, find the critical point for this steel.

Decide whether it is possible to subject this steel to heat treatment in order to improve its mechanical properties. Indicate possible applications of this steel.

No. 242. Microscopic examination of a ship's anchor made in the last century revealed the microstructure shown in Fig. 18.13.

Describe this structure and determine from it the approximate carbon content; indicate the method by which the steel of this type can be manufactured. Explain why it is not produced in our times and why its mechanical properties are inferior to those of a modern steel of the same carbon content.

No. 243. Figure 18.14 shows the microstructure of annealed carbon steel.

Describe this structure, determine the carbon content and indicate on the Fe-C diagram the critical points and hardening conditions (heating temperature), in addition, specify the quenching conditions for this steel.

Indicate the class (as regards industrial application) to which this steel should be referred.

No. 244. Figure 18.15 shows the microstructure of a steel in equilibrium.

Describe this structure, determine carbon content and show on the Fe-C diagram the critical points for this steel.

Compare the steel structures shown in Figs. 18.14 and 18.15; decide which of them has the better plasticity; recommend where each of these steels may be employed.

No. 245. Figure 18.16*a, b* shows the microstructures of annealed carbon steel with different carbon content.

Describe these structures and roughly indicate the carbon content in each steel.

Specify the heat treatment conditions needed to ensure martensitic structure, high hardness and high wear resistance of the surface layer in each steel, with retention of the initial structure, and therefore high toughness in the core.

Indicate industrial applications of these steels.

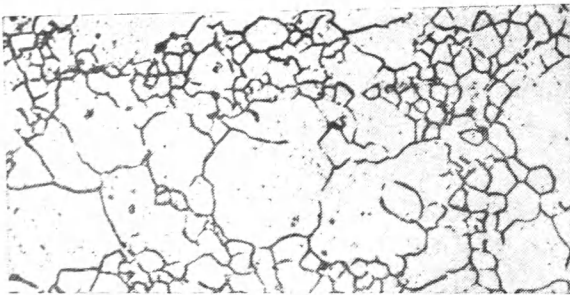


Fig. 18.11. Microstructure of fine-grained low-carbon steel after local deforming and heating, 100X

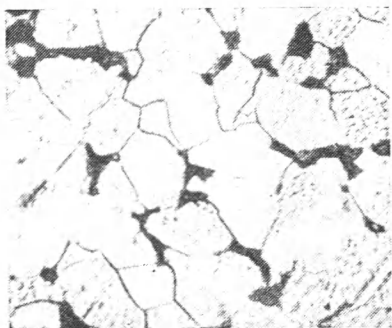


Fig. 18.12 Microstructure of carbon steel, 200X



Fig. 18.13. Microstructure of carbon steel, 300X



Fig. 18.14. Microstructure of carbon steel after annealing, 250X



Fig. 18.15. Microstructure of carbon steel after annealing, 250X

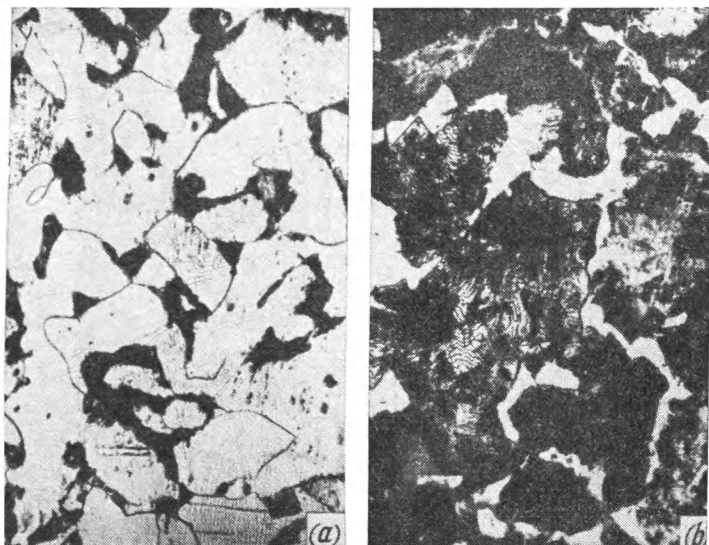


Fig. 18.16. Microstructures of annealed carbon steels with various carbon contents, 300X

No. 246. Determine the approximate carbon content and characteristic features of the steel structure shown in Fig. 18.17.

Explain what factors caused the formation of this structure and how this structure can affect the mechanical properties of the steel.

What may cause such a defect in the steelmaking process?

No. 247. During quality control of annealed carbon steel forgings delivered to the shop, the surface defect shown in Fig. 18.18 was found.

Indicate the structure of the steel and the carbon content in the surface layer and deeper layers and characterize in detail the steel defect determined by microscopic examination; what may cause it and how it could be prevented.

How would the mechanical properties of the steel change if a similar defect remained in the surface layer of finished part?

No. 248. Figure 18.19a, b shows the microstructure of hardened steel containing 0.4 per cent C after correct and incorrect hardening, respectively.

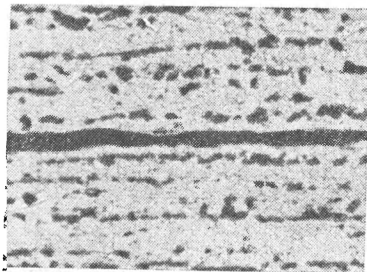


Fig. 18.17. Microstructure of carbon steel after annealing, 100X

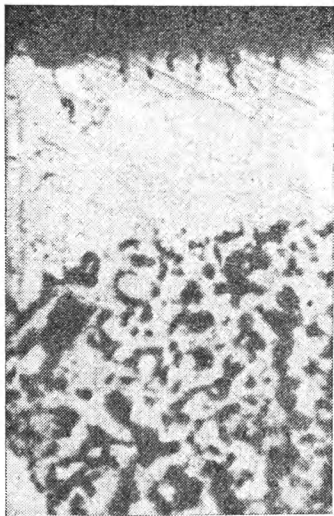


Fig. 18.18. Microstructure of carbon steel after annealing, 200X

Describe the microstructures and explain which of them characterizes truly the structure of hardened steel.

Recommend the hardening temperature for a steel with 0.4 per cent C. Explain in what respect the hardening conditions were disturbed and the effect this could have on the steel after final heat treatment.

No. 249. Figure 18.20*a, b* shows the microstructures of a steel containing 0.45 per cent C in specimens 10 mm in diameter after hardening from 750 and 825 °C with water quenching.

Describe these structures, indicate the differences between them and the difference in the hardness of the specimens.

Recommend the hardening temperature for this grade of steel so as to form a homogeneous structure of sorbite through tempering (specify the tempering temperature).

No. 250. Taps made of carbon steel containing 1.1 per cent C broke long before the normal bluntness was attained. Microscopic examination of the steel (Fig. 18.21) revealed the cause of the defect.

Explain the defects in the structure of this steel and decide whether it is possible to amend the structure in a batch of taps delivered for heat treatment, and how it can be done.

No. 251. Figure 18.22*a, b* shows the microstructure of a carbon steel (in a cylindrical specimen 15 mm in diameter) after annealing and after improving heat treatment.

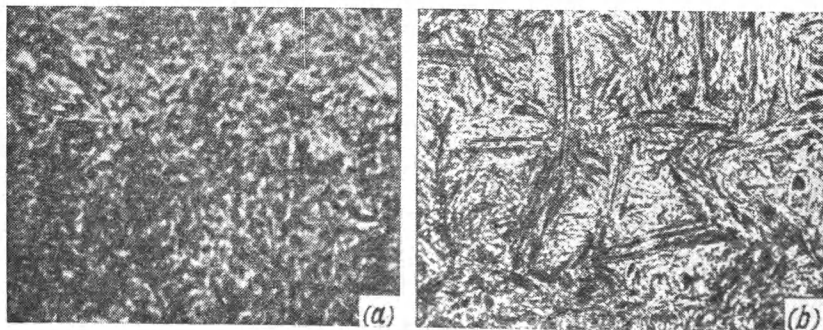


Fig. 18.19. Microstructure of carbon steel (0.4% C) after hardening, 400X

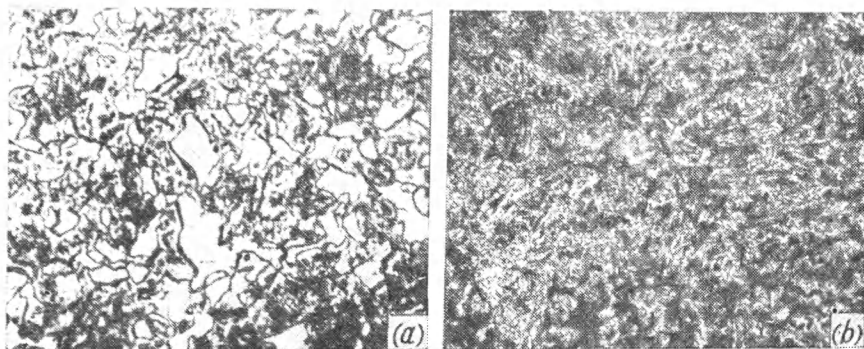


Fig. 18.20. Microstructure of carbon steel (0.45% C) after hardening from various temperatures, 300X
(a) 750 °C; (b) 825 °C

Which of the photographs shows the structure of the annealed steel. Indicate the approximate content of carbon in the steel and characterize the structures shown.

Give the conditions of heat treatment required to form these structures. Name industrial applications of steels of the given composition.

No. 252. Figure 18.23 shows the microstructure and hardness of carbon steel (0.45 per cent C) after being heat treated by different methods.

Describe these structures and decide on the heat treatment the steel must be subjected to to form the structures shown.

No. 253. The structure and hardness of carbon steel can be varied by varying the quenching conditions.

Figure 18.24a shows the microstructure of a eutectoid steel after water quenching, and Fig. 18.24b, its structure after oil quenching.

Describe these structures, indicate the hardness number, and explain why water quenching gives a different structure than oil quenching does.

No. 254. Figure 18.25 shows the microstructures of carbon steel after improving heat treatment (hardening and tempering) of a

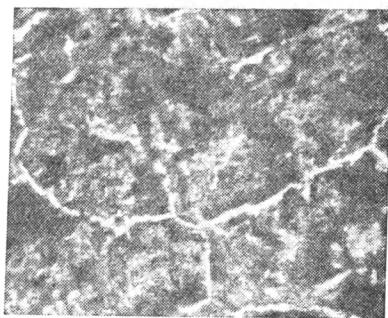


Fig. 18.21. Microstructure of carbon steel (1.1% C) after annealing, 200X

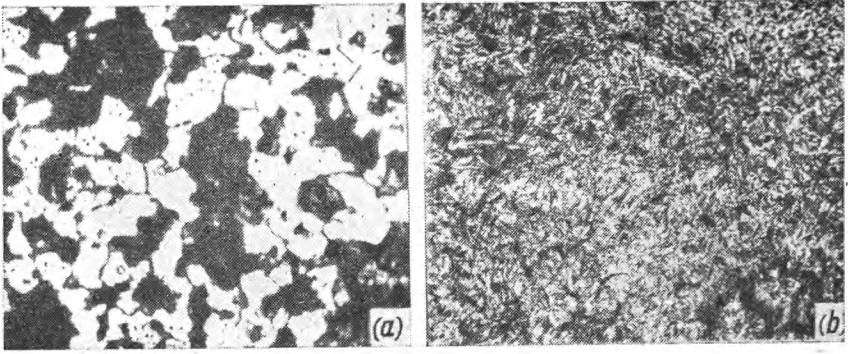


Fig. 18.22. Microstructure of carbon steel after heat treatment, 300X

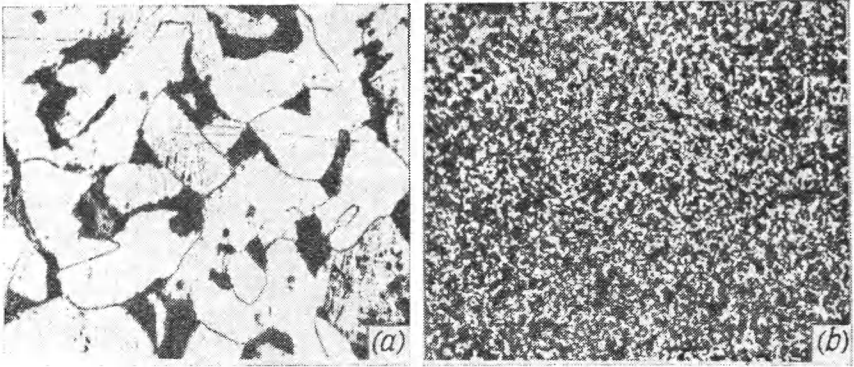


Fig. 18.23. Microstructure of carbon steel, 200X
(a) 160-170 HB; (b) 240-260 HB

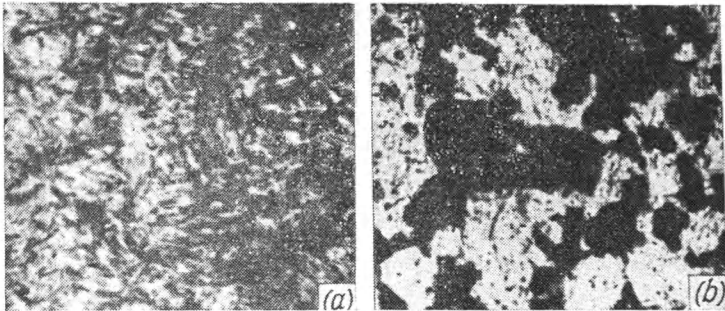


Fig. 18.24. Microstructures of hardened carbon steel (0.85% C), quenched with different rates, 400X
(a) water quenched; (b) oil quenched

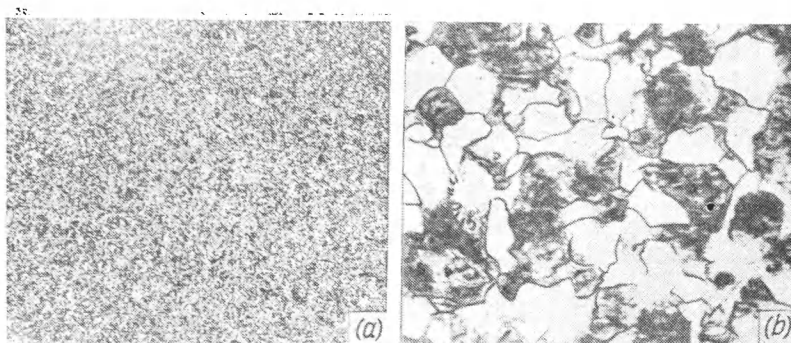


Fig. 18.25. Microstructure of carbon steel (0.45% C) in a specimen 40 mm in diameter after hardening and tempering, 200X
(a) surface layer, 35 HRC; (b) core, 180 HB

specimen 40 mm in diameter, the structure in the surface layer being given at *a*, and that in the core, at *b*.

Describe these structures, indicate the carbon content of the steel and the conditions of improving heat treatment and explain why the structure and hardness of the steel are different over the cross section and whether this is linked with the conditions of heat treatment or the properties of carbon steels.

No. 255. Carbon steel parts can be given a high hardness in surface layers (and retain a tough core) by treating by various methods: chemical heat treatment (cementation); hardening with heating by high-frequency currents; common hardening (the last method being only applicable for hardening parts above 20 mm in diameter, since carbon steel has low hardenability).

Figure 18.26*a*, *b* and *c*, shows photographs of microsections and hardness numbers of the surface layers and core of gear wheels 60 mm wide which have been hardened by the methods mentioned above.

Compare the nature of the distribution of the hardened surface layers and the hardness in the metal of the gear wheels, taking into consideration the heating conditions and the effect of carbon content on the properties of carbon steel; name the method used for treating each of the wheels.

Explain what grade of steel (as regards to the carbon content) should be used for hardening by each of the methods indicated and recommend the conditions of tempering after each hardening process.

No. 256. The fracture of a steel specimen, as well as the structure and mechanical properties, can characterize the state and

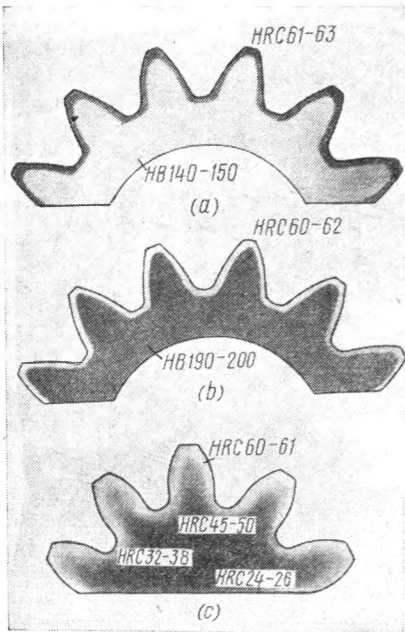


Fig. 18.26. Variations of hardness over the cross sections of three hardened gear wheels; the wheels were made of carbon steels with various carbon contents and subjected to different modes of heat treatment (full size)

(a) macrosection of a gear wheel after etching by an alcohol solution of cupric chloride; (b) and (c) macrosections of gear wheels after etching by an alcohol solution of nitric acid

properties of the steel it is made of.

Figure 18.27 shows the types of fracture of structural steel specimens obtained in impact tests: after annealing, after hardening, and after hardening and tempering, and gives impact strength values.

Describe the peculiarities of the fractures shown and name the state of steel in each of them.

No. 257. Some steels, for instance, chrome-nickel grades, sometimes show typical defects which sharply reduce their mechanical properties and are the cause of manufacturing failure (Fig. 18.28). These defects can be seen in steel fractures as characteristic white spots, and after acid etching, as more or less numerous fissures, as can be seen from Fig. 18.29.

Explain the nature of these defects, their origin, and name the methods that can prevent them.

No. 258. Figure 18.30a and b shows the microstructures of cast irons most commonly used in machine-building.

Describe these structures, methods of manufacture and treatment of these cast iron grades.

Name the differences in the mechanical properties of these grades of cast iron and the field of application of each grade.

No. 259. Figure 18.31 shows the microstructure of cast irons of two different grades.

Describe their structures, name the differences in the structures and properties and in the methods of manufacture of these grades of cast iron.

No. 260. Mechanical properties of cast iron depend on the nature of the metallic matrix, and also on the amount and form of graphite.

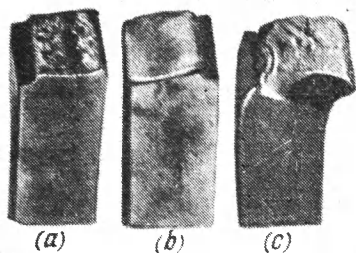


Fig. 18.27. Fractures of notched carbon steel specimens (0.4% C) after different modes of heat treatment (full size)
 (a) 5-6 kgf m/cm²; (b) 1 kgf m/cm²;
 (c) 8-10 kgf m/cm²

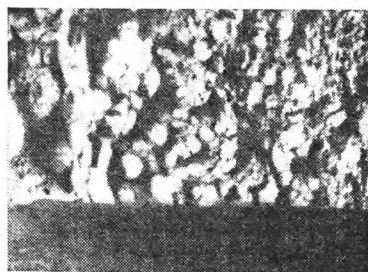


Fig. 18.28. Fracture of a specimen of rejected melt of Cr-Ni steel (full size); after V. M. Doronin

Decide which of the two grades of cast iron, whose microstructures are illustrated in Fig. 18.32*a* and *b*, has better mechanical properties.

No. 261. Figure 18.33 shows the microstructure of a cemented low-carbon steel.

Describe the variations of the structure from the surface to the core caused by cementation and hardening and indicate the thickness of the surface layer formed through chemical heat treatment. Determine approximately the time of cementation if the diffusion rate is approximately 0.1 mm/hour (in solid carburizer cementation).

No. 262. Figure 18.34 shows the microstructure of the surface layer of steel after nitration at 600 °C.

Determine the thickness of the nitrated layer and describe tentatively, by referring to the Fe-N constitutional diagram (see Fig. 9.10), how the structure varies in the direction from the surface to the core, if the concentration of nitrogen at the surface reaches 9 per cent.

No. 263. Figure 18.35 shows the microstructures and hard-

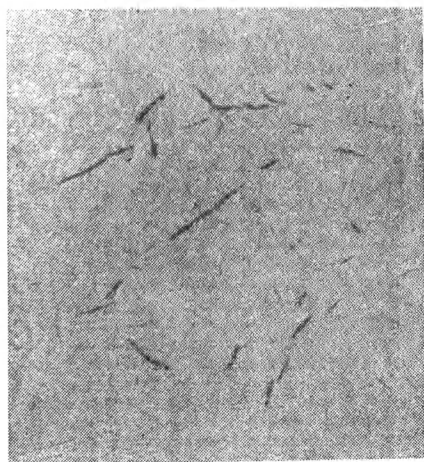


Fig. 18.29 Macrosection of a specimen of rejected melt of Cr-Ni steel (full size)

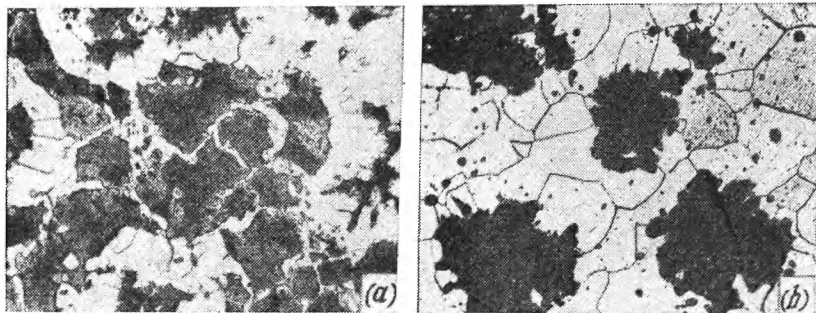


Fig. 18.30. Microstructures of cast irons employed for making machine elements, 100X

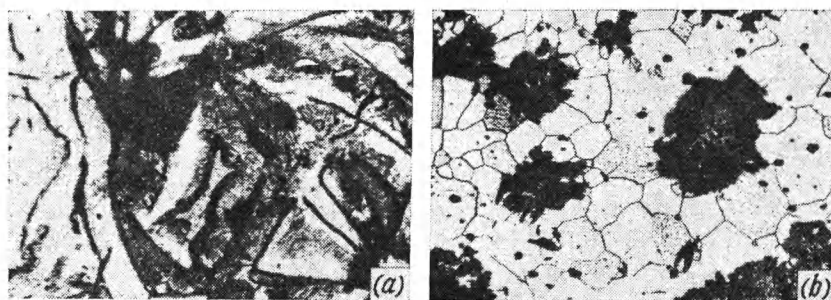


Fig. 18.31. Microstructure of cast irons employed for making machine elements, 200X

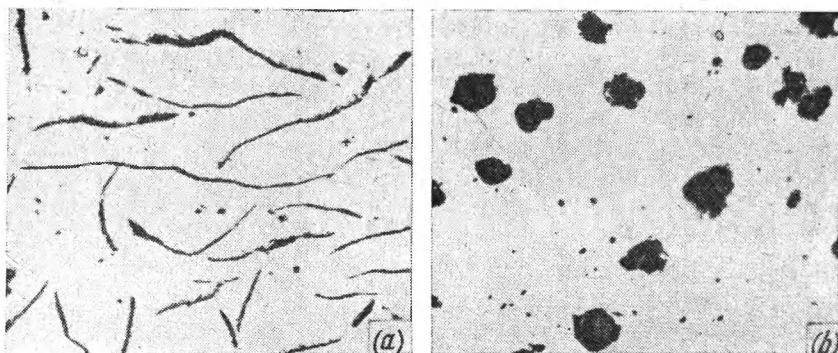


Fig. 18.32. Unetched sections of cast irons of two different structural classes, 100X



Fig. 18.33. Microstructure of low-carbon steel after cementation, 100X

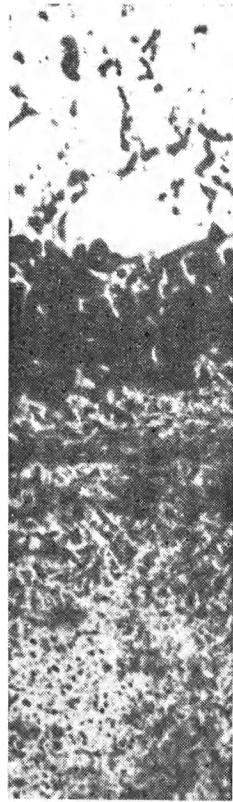


Fig. 18.34. Microstructure of surface layer of steel Grade 38XM10A, 500X

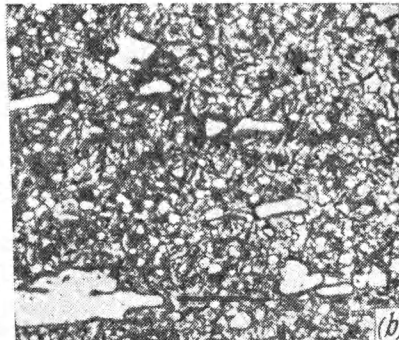
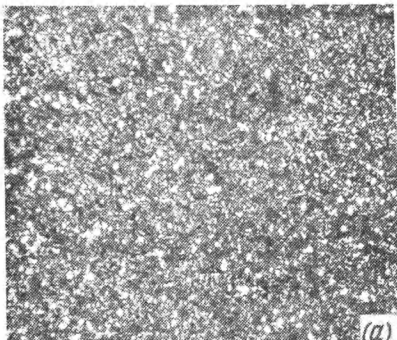


Fig. 18.35. Microstructure of high-carbon chromium steel after hardening and tempering, 500X
 (a) 1.0% C and 1.5% Cr (62 HRC); (b) 1.5% C and 12% Cr (62 HRC)

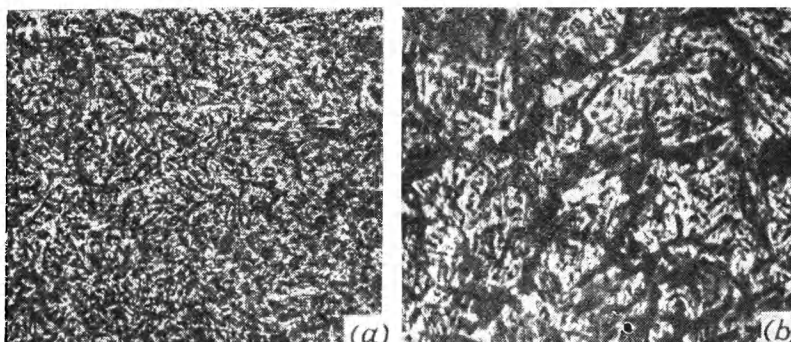


Fig. 18.36. Microstructure of chromium steel (0.4% C and 1% Cr) in the core of a specimen after hardening, 500X

(a) specimen 25 mm in diameter; (b) specimen 50 mm in diameter

ness numbers of high-carbon chromium steels after hardening and tempering.

Describe these structures and explain, by using the Fe-Cr-C diagram (see Fig. 10.17), which structural class each of these steels (after annealing) should be referred to.

No. 264. Figure 18.36*a* and *b* shows the microstructure and hardness numbers in the core of two specimens of chromium alloy steel with 0.4 per cent C and 1 per cent Cr after hardening; one of the specimens was 25 mm in diameter, and the other, 50 mm.

Characterize the structures illustrated and explain why similar hardening conditions (heating to 850°C, oil quenching) have produced different structures and different hardness in the core of the specimens.

No. 265. Figure 18.37*a* shows the structure of austenitic stainless steel with 0.1 per cent C, 18 per cent Cr, and 8 per cent Ni after air cooling. But after welding the structure of the steel next to the weld seam has changed to that shown in Fig. 18.37*b*.

Characterize the structure of the steel before and after welding. Explain how this structure change can affect the corrosion resistance of the steel and indicate the alloying element which should be additionally introduced into the composition of stainless steels of this structural grade to give it good weldability.

No. 266. The manufacturing shop has got a batch of sheets of stainless steel with 0.1 per cent C, 18 per cent Cr, and 8 per cent Ni, to manufacture parts by deep drawing, but the steel, as delivered, has a reduced plasticity and cannot be used for the pur-

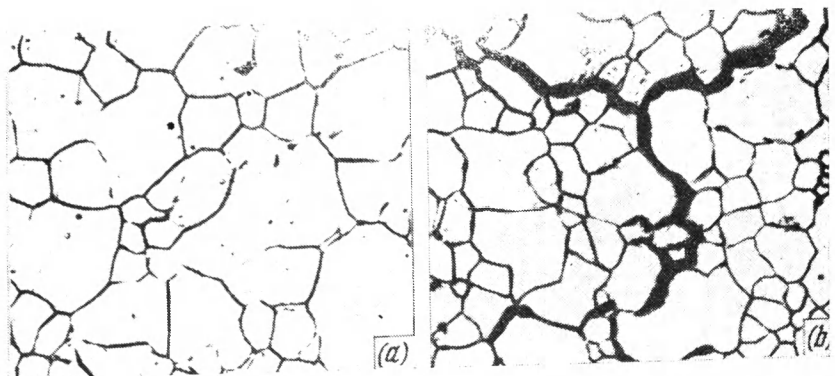


Fig. 18.37. Microstructures of stainless steel (0.10% C, 18% Cr, and 9% Ni), 500X

(a) after rolling and heat treatment; (b) after welding (near weld seam)

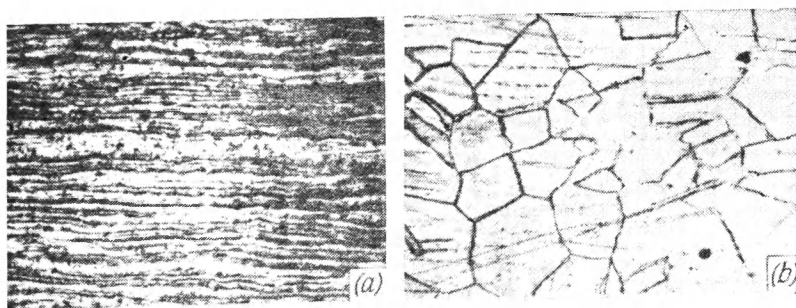


Fig. 18.38. Microstructures of stainless steel (0.1% C, 18% Cr, 9% Ni)
(a) 100X; (b) 600X

pose. Microscopic analysis of the steel of this melt showed the structure to be as illustrated in Fig. 18.38a.

After heat treatment, the steel acquired high plasticity. Its structure is shown in Fig. 18.38b.

Describe the structures shown in Fig. 18.38a and b, indicate the process in which they can be formed, and name the approximate mechanical properties corresponding to each of these structures of stainless steel.

No. 267. Figure 18.39a shows the microstructure of a high-manganese steel (1.2 per cent C and 12 per cent Mn) after casting and slow cooling, and Fig. 18.39b, the structure of the same steel after hardening (from 1050 °C) with water quenching.

Describe these structures and name the one having greater plasticity and greater toughness.

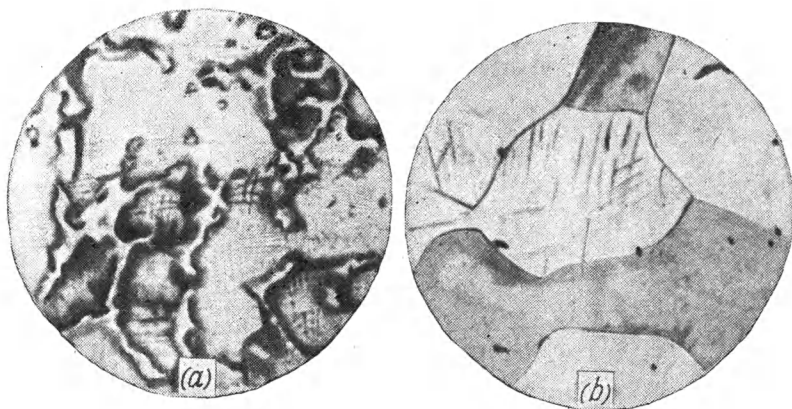


Fig. 18.39. Microstructures of high-carbon high-manganese steel (1.2% C, 12% Mn), 300X
(a) after casting; (b) after high-temperature hardening

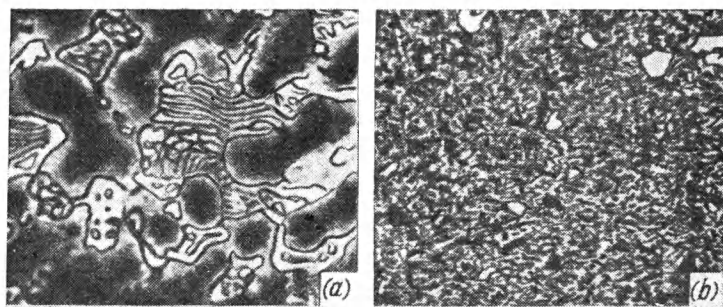


Fig. 18.40. Microstructures of high-speed steel (0.75% C, 18% W, 4% Cr, and 1% V), 500X
(a) after casting; (b) after forging and annealing

Give examples of industrial application of this grade of steel.

No. 268. Figure 18.40 shows the microstructures of high-speed steel (0.75 per cent C, 18 per cent W, 4 per cent Cr, and 1 per cent V) at various stages of its manufacture and processing at the steelmaking works.

Describe the structures illustrated and explain the effect of forging on them.

Name the state of the steel ensuring the highest strength and toughness.

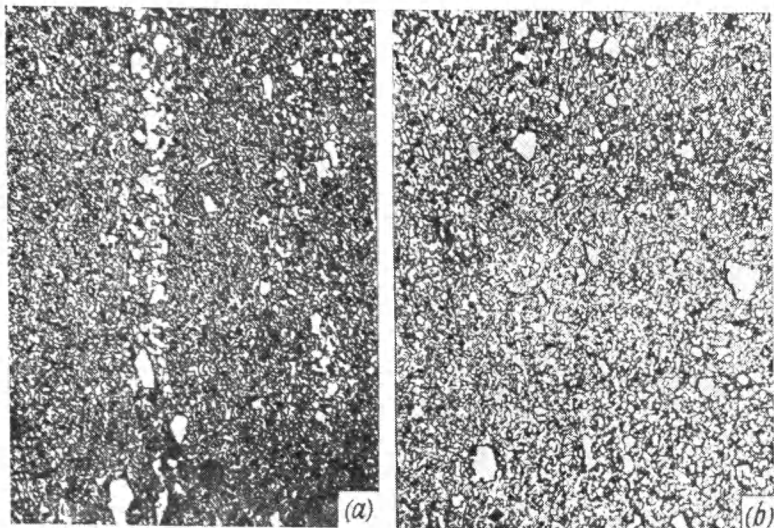


Fig. 18.41. Microstructures of high-speed steel Grade P18 after rolling with different degrees of deformation, 500X
 (a) from rolled stock 60 mm in diameter; (b) from rolled stock 10 mm in diameter

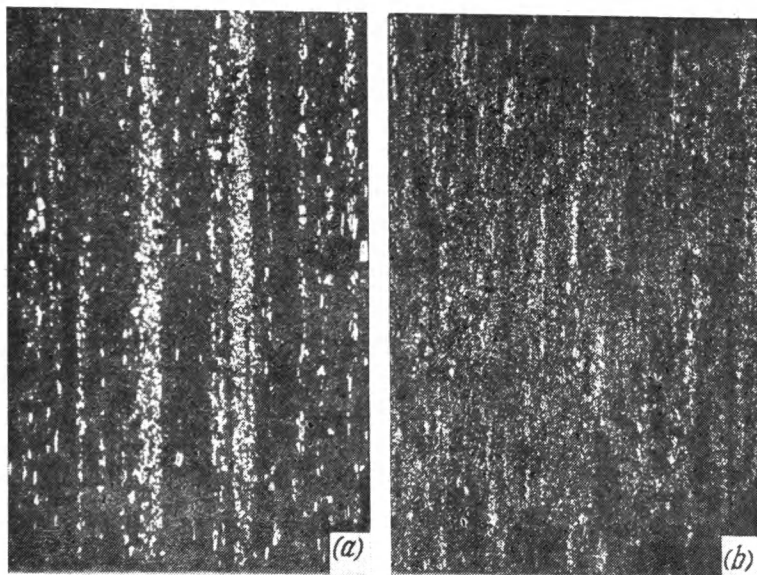


Fig. 18.42. Effect of the composition of high-speed steel on the structure obtained after rolling and annealing. Both specimens made from rolled stock 25 mm in diameter, 100X
 (a) steel Grade P18; (b) steel Grade P6M5

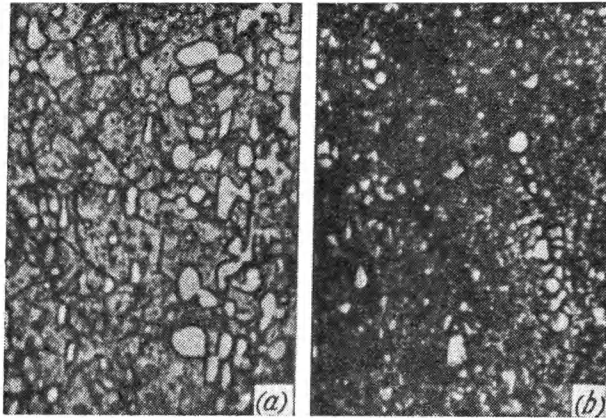


Fig. 18.43. Microstructures of high-speed steel Grade P12, 500X
(a) after hardening; (b) after hardening and tempering thrice at 560 °C

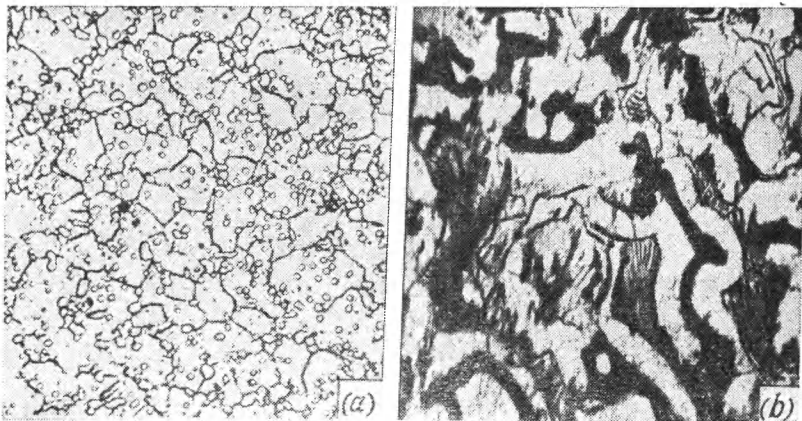


Fig. 18.44. Microstructures of high-speed steel depending on hardening temperature, 500X

No. 269. Figure 18.41 shows the microstructure of high-speed steel P18 from the same melt but rolled with different degrees of deformation.

Characterize the effect of plastic deformation on the distribution of carbides and name the state in which the steel has the highest strength and toughness.

No. 270. Figure 18.42 shows the microstructures of two grades of high-speed steel of different compositions: high-tungsten steel

Grade P18 and tungsten-molybdenum steel Grade P6M5 in rolled stock of the same cross section.

Characterize the differences in the structures of these steels caused by the effect of tungsten and explain how these differences can affect the strength and toughness of high-speed steels.

No. 271. Figure 18.43 shows the microstructure of high-speed steel Grade P12 (0.9 per cent C, 12 per cent W, 4 per cent Cr, and 1.7 per cent V) after hardening and after tempering.

Characterize the structures of this steel in these states and name the state providing a higher hardness.

No. 272. Figure 18.44 shows the microstructure of high-speed tungsten-molybdenum steel Grade P6M5 after correct and incorrect hardening (oil-quenched in both cases).

Decide in which case the steel attains a larger grain size and how this can influence its mechanical properties.

Part Five

LABORATORY EXERCISES AND PROBLEMS ON NON-FERROUS METALS AND ALLOYS

Chapter Nineteen

LABORATORY EXERCISES ON MICROANALYSIS OF NON-FERROUS ALLOYS

Before attempting the exercises given below (Nos. 270-283), study the typical structures of non-ferrous metals and alloys.

19.1. THE STRUCTURES OF NON-FERROUS METALS AND ALLOYS

High-purity copper in the cast and annealed state has a polyhedral structure typical of all pure metals (see Fig. 19.1). Copper subjected to deformation and annealing is additionally characterized by the presence of twins in its structure (see Fig. 3.4), i.e. grain portions in which the atomic planes neighbouring the remaining portion of a grain are shifted to distances which are not multiple of the whole period and increase in the direction from the twin boundary (or twinning plane). This portion of a crystal, as regards to the position of atomic planes, may be arbitrarily considered as a mirror image of the remaining part of the crystal.

Commercial copper may contain various harmful impurities, such as lead, bismuth, oxygen, sulphur, and the like. The most dangerous among them are lead and bismuth, the former causing red shortness, and the latter, also cold brittleness. These kinds of brittleness are due to the fact that the lead and bismuth inclusions are usually located at grain boundaries in the metal (see Fig. 21.9).

Oxygen, sometimes left in copper owing to insufficient deoxidation, forms portions of the Cu-Cu₂O eutectic (Fig. 19.2) seen only in castings. In the course of metal deforming, these eutectics are destroyed and the structure has then only isolated Cu₂O inclusions of a light-grey or bluish colour. Oxygen impurities in copper reduce electric conductivity and plasticity at normal temperature.

Sulphur (usually as Cu₂S) may be present as separate inclusions and can be reliably distinguished from the Cu₂O inclusions

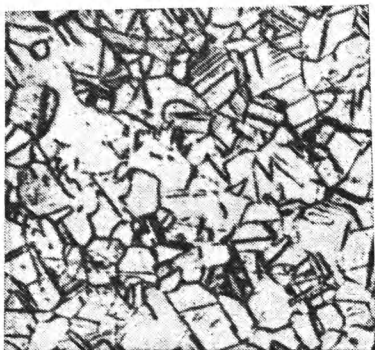


Fig. 19.1. Microstructure of deformed and annealed copper, 200X

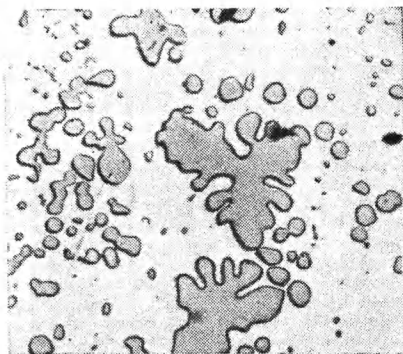


Fig. 19.2. Microstructure of cast copper containing oxygen, 250X

only by the polarized-light microscopic technique in which sulphur inclusions become reddish.

Brasses. The structure of single-phase α -brass (see the constitutional diagram in Fig. 9.16) contains grains of α -solid solution (Fig. 19.3a). In the structure of $\alpha + \beta$ -brass, darker inclusions of the β -phase (revealed by etching, see Fig. 19.3b) may be present in addition to grains of α -solid solution.

Lead impurities may be present in single-phase brass in the form of continuous interlayers at grain boundaries, causing a noticeable unfavourable effect on the mechanical properties of the metal. In $\alpha + \beta$ -brass, they may be present as separate isolated formations inside the grains and thus cannot cause red shortness.

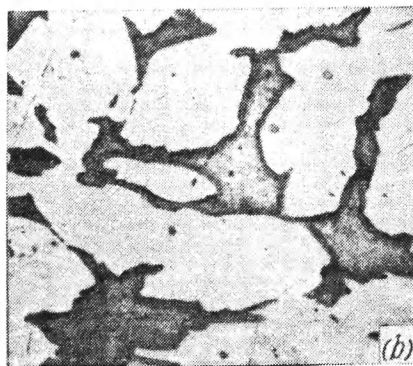


Fig. 19.3. Microstructures of brass, 250X
(a) single-phase brass (30% Zn); (b) two-phase brass (40% Zn)

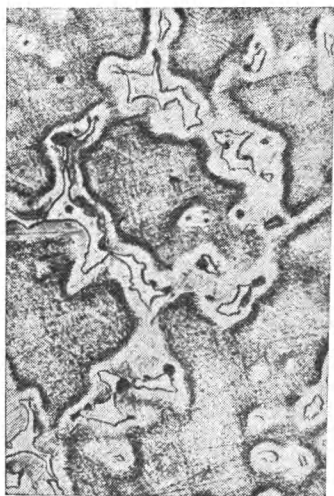


Fig. 19.4. Microstructure of cast tin bronze (6% Sn), 250X

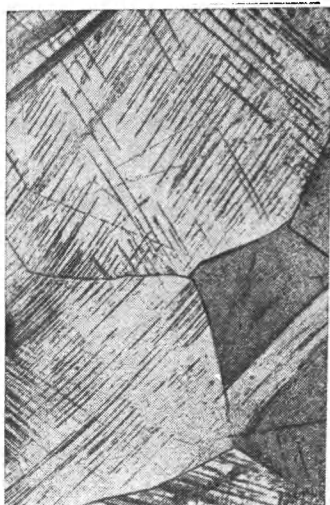


Fig. 19.5. Microstructure of deformed and annealed tin bronze (6% Sn), 250X

Alloying elements: silicon, aluminium, and manganese may be present in the solid solution in the α - and β -phase and shift the region of existence of these phases towards a lower concentration of zinc than that indicated in the diagram (see Fig. 9.16).

Tin bronzes. Their structure upon casting differs from that shown in the Cu-Sn constitutional diagram (Fig. 9.17). In bronzes with 4-6 per cent Sn there may be regions of the eutectoid ($\alpha + \text{Cu}_3\text{Sn}_8$) or ($\alpha + \text{Cu}_3\text{Sn}$) (Fig. 19.4), in addition to the grains of α -solid solution (or α -solid solution and secondary precipitates of Cu_3Sn). They are formed due to the strong segregation and low rate of the diffusion processes.

Alternating processes of annealing and deforming may equalize the composition of bronze and its structure becomes the single-phase one even in alloys with 6-7 per cent Sn. This is seen in the form of polyhedral grains of α -solid solution (Fig. 19.5).

The structure of alloys with 7-10 per cent Sn in the cast state is composed of grains of α -solid solution and regions of the ($\alpha + \text{Cu}_3\text{Sn}$) eutectoid. The presence of the eutectoid makes these alloys non-deformable. The content of the eutectoid in alloy increases with the rise in the concentrations of tin and alloying elements: i.e. zinc, nickel, and phosphorus which form no new phases and are dissolved in the α -solution. Lead, which is so-

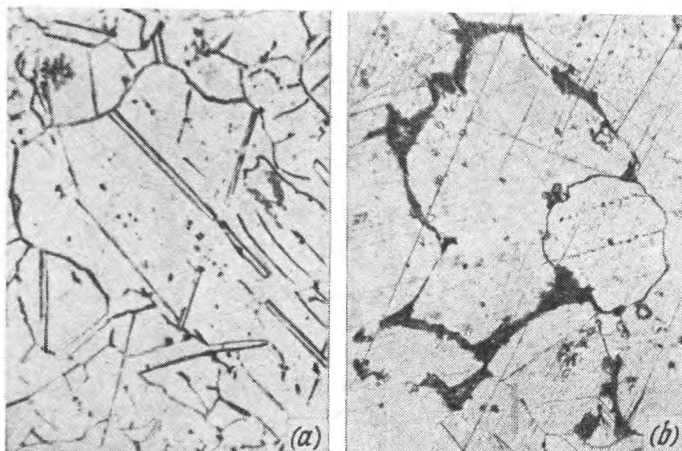


Fig. 19.6. Aluminium bronze
(a) single-phase (5% Al); (b) two-phase (10% Al), 250X

metimes added into tin bronze, may be present as individual inclusions of a more or less rounded shape.

Aluminium bronzes. The structure of a bronze containing up to 9.8 per cent aluminium after deforming and annealing is composed of grains of α -solid solution (Fig. 19.6a).

With an aluminium content of from 9.8 to 15.2 per cent, the structure can also contain regions of the $(\alpha + \beta)$ eutectoid (Fig. 19.6b). After hardening these bronzes from a temperature corresponding to the region of β -solid solution, their structure is made up of needle-shaped crystals of the martensitic β' -phase (Fig. 19.7). Addition of alloying elements (nickel and manganese) to the bronze causes no formation of new phases; only the concentration of aluminium is shifted, which corresponds to the transition from the single-phase to the double-phase region (see Fig. 19.15). Addition of iron can form inclusions of the iron phase.

Aluminium and aluminium alloys. Aluminium after deforming and annealing has a homogeneous granular structure (Fig. 19.8). Microscopic examination reveals harmful impurities: iron as dark FeAl_3 inclusions and silicon as greyish inclusions. With both silicon and iron present in aluminium, the structure may contain ternary compounds of aluminium, silicon and iron denoted by α and β (see Fig. 10.31) and present as dendritic inclusions; they can reduce the plasticity of both aluminium and aluminium-base alloys.



Fig. 19.7. Microstructure of hardened aluminium bronze (10.5% Al), 500X

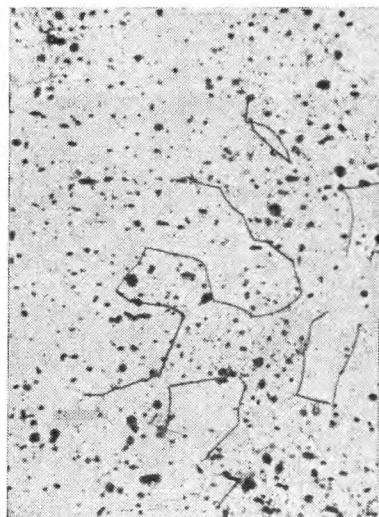


Fig. 19.8. Microstructure of annealed aluminium, 300X (after N. P. Dronova)

The structure of (annealed) duralumin in equilibrium contains grains of α -solid solution, which includes copper, manganese and magnesium, and also disperse phase inclusions of W or S (seen light-grey when etched by NaOH or HF solutions) and Mg_2Si , as well as some phases (compounds of the Cu_2FeAl type) as dark formations (Fig. 19.9). After hardening or hardening and ageing, the structure of duralumin shows grains of α -solid solution and inclusions of aluminium-iron and aluminium-silicon compounds.

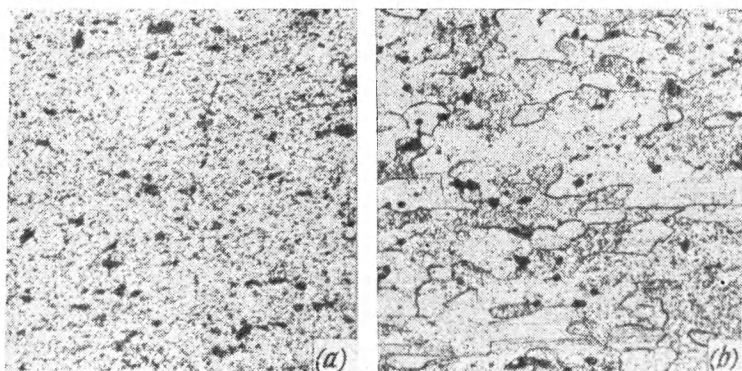


Fig. 19.9. Microstructures of duralumin Grade Д16, 250X
(a) after annealing; (b) after hardening (after N. P. Dronova)

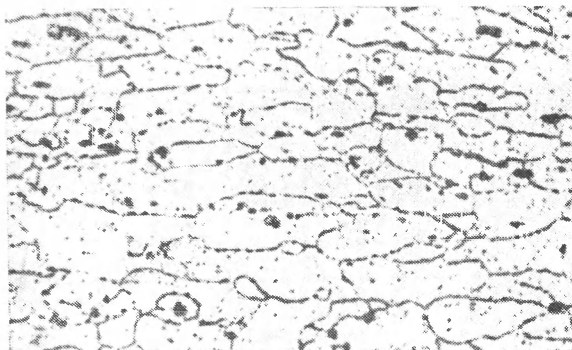


Fig. 19.10. Microstructure of AMr6 alloy after annealing, 300X (after N. P. Dro-nova)

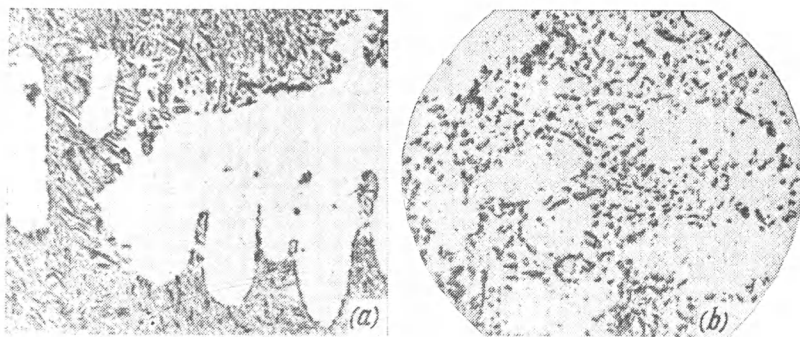


Fig. 19.11. Microstructures of silumin (12% Si)
(a) before modifying, 250X; (b) after modifying, 250X

The structure of a deformation-strengthenable alloy AMr6 after annealing (Fig. 19.10) shows grains of α -solid solution of magnesium in aluminium and particles of ferruginous inclusions.

Silumins are casting alloys with 5-14 per cent Si. Their structure with the Si content up to 11.3 per cent (hypoeutectic alloys) is composed of primary crystals of α -solid solution (silicon in aluminium) and ($\alpha + \text{Si}$) eutectic (Fig. 19.11a). With a higher concentration of silicon (hypereutectic alloys) the structure also contains lamellar silicon crystals.

After modification of silumins the structure of the eutectic becomes more disperse and the eutectic concentration of silicon higher. For this reason the content of primary crystals of α -solid solution increases in hypoeutectic alloys after modification (Fig. 19.11b).

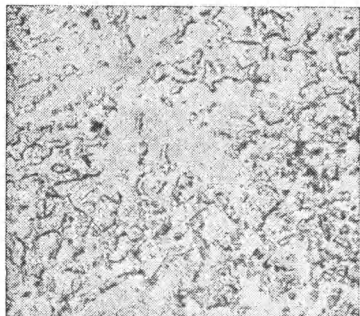


Fig. 19.12. Microstructure of magnesium alloy, (7% Al), 250X

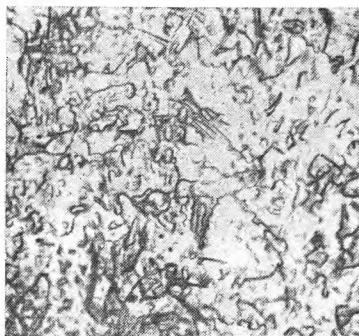


Fig. 19.13. Microstructure of annealed titanium Grade BT1-1, 600X

In special silumins alloyed with copper or magnesium, particles of CuAl_2 or respectively Mg_2Si may be present. Particles of the (Al_2CuMg) phase may be formed in the presence of copper and magnesium. These phases are dissolved in the course of hardening and precipitate in a disperse form after ageing, thus strengthening the alloy.

Iron impurities in silumins can additionally cause the formation of precipitated brittle α - and β -phases (see Fig. 10.31).

Magnesium and magnesium alloys. The structure of technical magnesium after deforming and annealing is composed of polyhedral grains.

Castable or deformable magnesium alloys have the structure of α -solid solution plus a precipitated phase of the Mg_3Al_2 type (Fig. 19.12).

Titanium and titanium alloys. Figure 19.13 shows the structure of deformed and annealed technical sheet titanium BT1-1. As can be seen, the structure is fine-grained, some grains showing recrystallization twins.

The structure of most titanium alloys may be either single-phase α -solid solution (alloys Grades BT5, OT4, AT3, etc.) or two-phase, composed of $\alpha + \beta$ -solid solutions (alloys Grades BT3-1, BT6, BT8, etc.), see Fig. 19.14. Some alloys of the BT15 type have the single-phase structure of β -solid solution.

Alloys having a two-phase structure ($\alpha + \beta$) in the equilibrium state can be strengthened by heat treatment—hardening and ageing. After hardening from the temperatures of the single-phase β -region they have a structure composed of two metastable phases: needle-shaped martensitic α' -phase and β -phase; with a

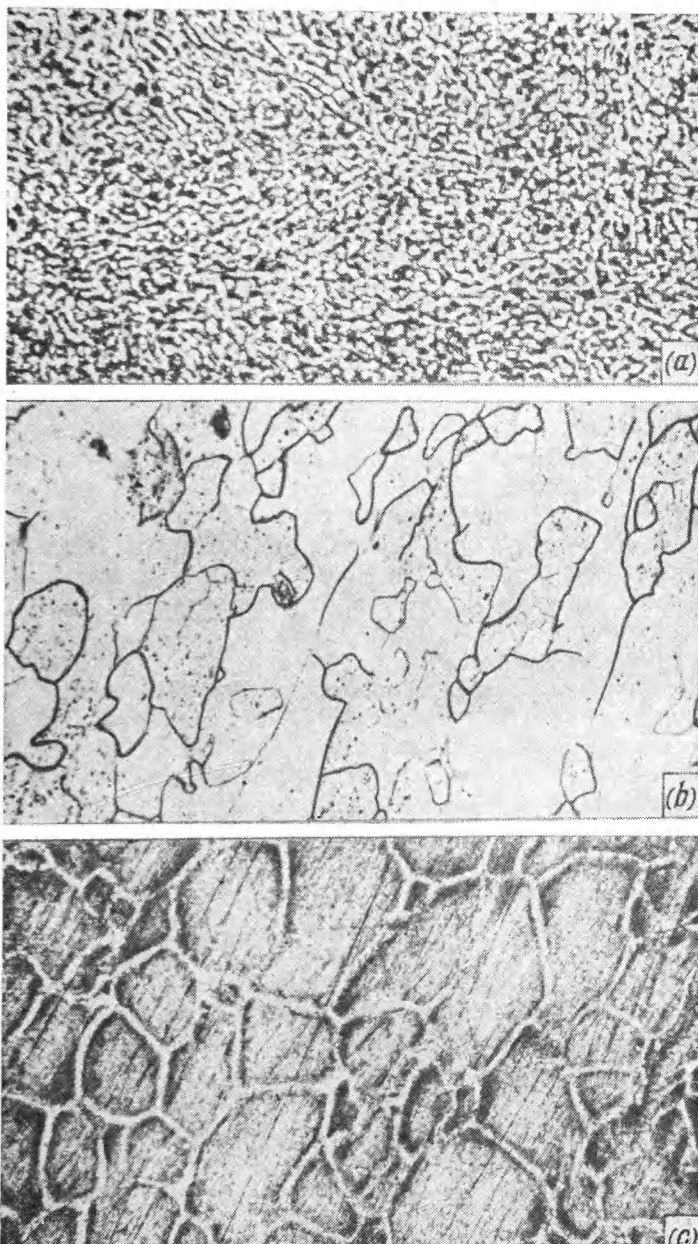


Fig. 19.14. Microstructures of BT3-1 alloy, 500X
(a) after annealing; (b) after hardening from 800 °C; (c) after ageing at 483 °C

higher content of stabilizing β -elements it consists solely of the metastable β -phase (Fig. 19.14).

If the hardening of single-phase alloys is carried out (as usual) from temperatures not above the boundary of the two-phase region, their structure will be composed of the metastable phases (α' and β) and the α -phase.

In the course of ageing at the optimum temperature (450–550°C) which is selected according to the composition of an alloy and the required properties to be obtained, the metastable α' - and β -phases decompose with the formation of disperse particles of α -phase. In alloys showing eutectoid transformations, particles of chemical compounds may also precipitate. Such ageing treatment improves the strength properties of an alloy, but reduces its plasticity and toughness. The latter decreases sharply owing to low-temperature ageing (below 450°C), when the formation of the metastable ω -phase of martensitic type becomes possible.

Tin, lead and antimony alloys. These are mostly bearing alloys (babbitts). Their structure is composed of a relatively plastic eutectic and harder and, therefore, more wear-resistant primary crystals of antimony.

The structure of other widely used bearing alloys based on the Sn-Sb or Sn-Sb-Cu system consists of a plastic α -solid solution of antimony and tin (see the dark regions in Fig. 21.24), and relatively hard precipitated crystals of SnSb compound having more or less regular shape (see the bright cubes in Fig. 21.24).

In the structure of copper-containing alloys, dendritic star-like formations of Cu_3Sn compound can be additionally present; their formation reduces density segregation in an alloy.

19.2. LABORATORY EXERCISES

Deal with the problems given below in the following sequence:

- sketch the microstructures observed under a microscope;
- describe in detail the microstructures observed, the structural components detected and the form of their precipitation (granular, needle-shaped, along grain boundaries), and indicate the approximate proportions of the components and how they are tinted through etching;
- answer in detail any additional questions set.

Problems

No. 273. Carry out microscopic examination of cast copper with a low and somewhat higher (up to 0.1–0.3 per cent) oxygen content.

Indicate: the structure that is formed in the cast copper in the presence of oxygen. Using the section rule find on the Cu-Cu₂O diagram the approximate content of oxygen in each of the specimens; name the possible defects of the oxygen-containing copper when it is heated in a reducing atmosphere; what measures should be taken to reduce the concentration of oxygen in the process of copper manufacture.

No. 274. Carry out microscopic examination of three copper specimens: before deforming, in the deformed state, and annealed after deforming.

Determine: (a) the approximate recrystallization temperature of copper (by Bochvar's rule) and explain the mechanism of this process and its effect on the properties of copper; (b) the degree of grain drawing in the deformed copper; for this, compare the length (i.e. along the direction of flow) and width of grains.

No. 275. Carry out microscopic examination of brass with 32 per cent Zn: after casting, deforming, and annealing.

Indicate: (a) the specific features of the structure of the brass in the cast state; (b) the cause of the formation of the heterogeneous structure after casting; (c) the processes occurring during deforming and subsequent annealing, which change the structure of the brass as compared with the cast metal.

No. 276. Carry out microscopic examination of specimens of brasses with a Zn content of 20, 30, and 42 per cent respectively. Indicate: (a) changes in the structure of brass caused by increasing zinc content and the phases present in the alloys (see also the Cu-Zn constitutional diagram in Fig. 9.16) as well as their structure; (b) industrial applications of brasses of the given compositions.

No. 277. Carry out microscopic examination of two specimens of brasses having respectively the structure of α -phase and of $\alpha + \beta'$ -phase. Indicate: (a) the properties (qualitatively) the α - and β' -phases possess in Cu-Zn alloys; (b) the temperature range within which single-phase and two-phase brasses can undergo appreciable plastic deformation (see also the Cu-Zn constitutional diagram in Fig. 9.16); (c) industrial applications of these brasses.

No. 278. Carry out microscopic examination of two specimens of brasses: with 30 per cent Zn; with 40 per cent Zn and 1 per cent Pb (JIC59-1).

(a) Analyse the Cu-Zn and Cu-Pb constitutional diagrams (Figs. 9.16 and 9.18) and describe the structural pattern when lead is present; (b) using the results of microscopic examination of an unetched specimen, indicate the nature of the location of lead inclusions in JIC59-1 brass; and using the results of micro-

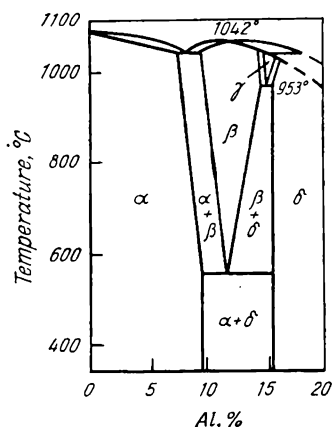


Fig. 19.15. Constitutional diagram of Cu-Al alloys

forming and annealing; (c) industrial applications of bronzes containing 4-6 per cent Sn.

No. 280. Carry out microscopic examination of aluminium bronze containing 5 per cent Al after deforming and annealing. Indicate: (a) the peculiarities of the cast structure of the bronze containing 4-6% Sn; by referring to the Cu-Al constitutional diagram (Fig. 19.15) explain the causes of the heterogeneous structure observed in the microsections; (b) the peculiarities of the structure of that bronze after deforming and annealing; explain why it differs from cast bronze; (c) the nature of the variation (in equilibrium) of the structure and mechanical properties of aluminium bronze with an increase of the aluminium content in it up to 9.5 per cent.

No. 281. Carry out microscopic examination of annealed aluminium bronze with 5 per cent Al (Бр. А5) and with 10 per cent Al (Бр. А10). Determine: (a) the structure and phases present in these bronzes; (b) the composition of a hardenable bronze (among the grades considered, see the Cu-Al constitutional diagram in Fig. 19.15).

No. 282. Carry out microscopic examination of duralumin specimens: (a) cast; (b) plastically deformed and annealed; (c) hardened.

scopic examination of etched specimens, describe the structure of both bronzes; (c) explain for what purpose the ЛС59-1 brass is alloyed with a small amount of lead¹.

No. 279. Carry out microscopic examination of tin bronze containing 4-6 per cent Sn after casting, deforming and annealing.

Indicate: (a) the peculiarities of the structure of cast bronze of the specified composition and, referring to the Cu-Sn constitutional diagram (see Fig. 9.17), explain the cause of the formation of the heterogeneous structure detected by the microscopic examination; (b) causes of the variation of the structure of this bronze after de-

¹ To solve the problem one may possibly refer to the book: Mal'tsev M. V., Barsukova T. A., Borin F. A., *Metallografiya tsvetnykh metallov i splavov* (Physical Metallurgy of Non-ferrous Metals and Alloys). Moscow, Metallurgiya Publishers, 1960, 372 pp., ill.

Assuming the duralumin to be an alloy of the Al-Cu system (see Fig. 9.24)¹ indicate: (a) its structure with copper content of 5 per cent (refer to the Al-Cu or Al-Cu-Mg constitutional diagram, Figs. 9.24 and 10.30); (b) the cause of the formation of eutectic in the cast duralumin; (c) the structure of hardened duralumin, and show that heat treatment of this duralumin is feasible.

No. 283. Carry out microscopic examination of silumin (12 per cent Si) before special (modification) treatment and after the modification. Indicate: (a) the differences in the structures of the modified and non-modified silumin; (b) the processes occurring during modification and their effect on the mechanical properties of silumin.

No. 284. Carry out microscopic examination of duralumin and an aluminium-copper alloy with 8-10 per cent Cu. Describe: (a) the peculiarities of the structures of these alloys, regarding them arbitrarily as alloys based on the Al-Cu system (see Fig. 9.24); (b) the casting properties of these alloys and their susceptibility to plastic deformation, taking into consideration the position of these alloys in the Al-Cu constitutional diagram.

No. 285. Carry out microscopic examination of titanium alloys BT5 (5 per cent Al) and BT3-1 (5 per cent Al, 2 per cent Cr, and 2.5 per cent Mo).

Indicate: (a) the structure of these alloys; referring to the Ti-Al constitutional diagram, describe the transformations occurring in the BT5 alloy during heating; (b) the effect of chromium and molybdenum on the regions of existence of α - and β -modifications of titanium (by comparing the structures of BTK and BT3-1 alloys); (c) the possibility of hardening the BT3-1 type alloy and the nature of the transformations which then take place (refer conditionally to the Ti-Cr constitutional diagram in Fig. 9.22).

No. 286. Carry out microscopic examination of tin-base bearing alloys (type B83) and lead-base bearing alloys (type BC). Describe: (a) the principal peculiarities of their structures; (b) typical transformations in these alloys during solidification.

To accomplish the prescribed work, refer to the Sn-Sb constitutional diagram (see Fig. 4.22) and Pb-Sb constitutional diagram (see Fig. 4.18).

¹ Duralumin also contains magnesium, silicon, manganese, and iron.

Chapter Twenty

LABORATORY EXERCISES ON HEAT TREATMENT OF DURALUMIN

20.1. METHODICAL INSTRUCTIONS

Duralumins are a large group of aluminium-base alloys (see Table 27.32), which can be deformed (by forging, rolling, pressing or drawing) and strengthened by heat treatment.

The structure of duralumin after annealing includes the following phases: α -solid solution (matrix) and compounds Mg_2Si , $W(Al_xCu_yMg_zSi_u)$ or $S(Al_2CuMg)$ and an iron-containing phase $N(Cu_2AlFe)$. The phases Mg_2Si , W and S dissolve at the hardening temperature (400-500 °C) and precipitate during ageing, causing strengthening of the alloy.

The structure of duralumin is essentially a supersaturated single-phase α -solid solution (and also the N -phase which is insoluble through heating).

The transformations occurring in duralumin during its heat treatment can be approximately examined on the Al-Cu constitutional diagram (Fig. 9.24), since copper is the principal alloying element in this alloy. As can be seen from the diagram, the $CuAl_2$ compound can be dissolved in the α -phase only through heating above the line of limited solubility of copper in aluminium. With a rapid cooling from that temperature, the solid solution cannot decompose and will remain supersaturated at 20 °C relative to the equilibrium (annealed) state of the alloy. The solution is metastable and changes its state towards equilibrium upon long holding at normal temperatures (natural ageing) or through a comparatively short heating (artificial ageing). Ageing generally increases the strength and hardness but reduces the plasticity (Table 20.1).

Table 20.1

Process of treatment (Д16 alloy)	σ_t , kgf/mm ²	HB	δ , %
Hardening	26	70	25
Natural ageing	47	105	17

The structural transformations occurring during ageing cannot be observed under an optical microscope (because of a low resolution of the latter); they are determined by electron microscopy or X-ray structure analysis. According to the results obtained by these methods, natural ageing forms groups of atoms of alloying elements (copper, magnesium or silicon) in the lattice of α -solid solution, the composition of these groups at the stage of the maximum strengthening being close to that of the corresponding precipitated phases (Mg_2S , W, or S). These groups are termed Guinier — Preston zones (G.P.2).

With artificial ageing, groups of atoms are formed in the lattice of solid solution, their composition and structure being close to the intermediate states of the precipitated phases mentioned above. The G.P.2 zones or regions of the type of intermediate phases being thus formed in the lattice of solid solution, which are linked coherently with the lattice, offer an appreciable resistance to dislocations. For dislocations to move further, they have either to cut through or to skirt these zones (or regions) or portions of the phases being formed which requires high stresses to be applied and is the actual cause of the strengthening of the alloys.

Natural ageing is more often employed in industry, though it takes much more time than artificial ageing. This can be explained not only by a simpler technique needed for natural ageing, but also by the fact that the metal acquires a higher corrosion resistance and a higher fracture toughness (see Sec. 6.5), i.e. becomes less susceptible to brittle fracture.

A method also used in industry may be called 'recovery heat treatment.' It essentially consists in short heating of duralumin to 250°C after natural ageing, followed by quick quenching. This method causes dissolution of Guinier — Preston zones, so that the state of the alloy after cooling is close to that it has after common hardening. 'Recovered' duralumins have a lower strength and hardness, but a high ductility and can be subjected to the same operations of plastic working (die-forming, bending, etc.) as a just hardened alloy, in which natural ageing has not yet initiated. After 'recovery treatment', as after common hardening, duralumin can be strengthened through natural or artificial ageing.

The problems given below are aimed at studying the effect of heat treatment (hardening, ageing, and recovery) on mechanical properties of duralumin,¹ any grade of the alloy (see Table 27.32) being suitable for the purpose.

¹ For students studying a concise course in the science of materials, the problems below may be reduced to hardness measurements only.

Hardness measurements may be done on plates or discs, and determinations of the strength, yield limit and relative elongation, on standard round or rectangular tension test specimens (Sec. 6.2a).

The time of holding of specimens 20 mm in diameter and 5 mm long before hardening should be at least 15 minutes for heating in a saltpetre bath or 30 minutes for electric-furnace heating. The heated specimens must be quenched in water.

For natural ageing, specimens are held at room temperature for four to seven days. Their hardness is measured by the Rockwell ball test under a load of 100 kgf,¹ first in 60- and 120-minute intervals and then every 24 hours from the beginning of holding.

Ageing at 100 °C is to be done in boiling water and that at 150 ° or 175 °C, in an oil bath (or a furnace); if higher temperatures are specified, ageing is done in a furnace or a bath of fusible salts with subsequent water quenching.

To study the recovery process, the specimens should be preliminarily hardened and subjected to natural ageing. Recovery is effected by heating them to 250 °C for 3 minutes (for specimens 20 mm in diameter and 5 mm long) and quenching in water.

20.2. LABORATORY EXERCISES

No. 287. Determine the effect of the ageing (tempering) temperature on the hardness of hardened duralumin.

For ageing, specimens should be kept for 15, 30, 45, or 60 minutes at 100 °C; for 5, 15, 30, 45, or 60 minutes at 150 °C; for 3, 5, 10, 15, 30, or 45 minutes at 200 °C; for 1, 3, 5, 10, 15, or 30 minutes at 250 °C; and for 1, 3, 5, 10, and 15 minutes at 300 °C.

Hardness should be measured on one or two specimens from a series after hardening and on each specimen, after ageing.

Every student has to perform ageing at one temperature and one holding time and, then using also the results obtained by other students of the group plot a hardness-ageing time curve. For each specified ageing temperature, an individual curve should be plotted.

Explain what transformations in the structure could cause the pattern of hardness variation represented by the plotted curves.

No. 288. Harden duralumin specimens from 500 °C and then perform artificial ageing at 150 °C with holding times of 15, 30, 45, 60, and 120 minutes.

¹ The hardness of larger specimens is better to be measured by the Brinell ball test with a ball of 2.5-mm diameter under a load of 62.5 kgf.

Plot a curve of the hardness variations during artificial ageing, explain the mechanism of the hardness growth (and of the strength growth) and indicate how the ductility of the alloy is changed by ageing.

No. 289. Harden duralumin specimens from 500 °C and subject them to artificial ageing at 175 °C for 15, 30, 45, and 60 minutes.

Plot a curve showing how the properties of the metal change with the ageing time.

Explain the artificial ageing process and describe the precipitated phases.

No. 290. Harden duralumin specimens from 500 °C and carry out their artificial ageing at 200 °C for 15, 30, 45, or 60 minutes. Plot a curve showing variations of the properties of the metal during natural and artificial ageing.

Consider duralumin conditionally as a binary alloy based on the Al-Cu system and characterize its structure with 5 per cent Cu after hardening and artificial ageing.

Explain the coalescence process and its effect on the properties of the alloy.

Chapter Twenty-one

PROBLEMS ON ANALYSIS OF MICROSTRUCTURES OF NON-FERROUS METALS AND ALLOYS

Before attempting the problems below, the students should examine the typical structures given in Chapter 19. Every student attempts one or two problems (either at the laboratory or as a home work).

No. 291. Two copper specimens were heated to 600-800 °C in a reducing atmosphere. One of them was found to have the surface defects as shown in Fig. 21.1*a* and the other was free of such defects. Defects were also discovered in an unetched microsection of the first specimen (Fig. 21.1*b*).

The microstructure of the specimens before heating is shown in Fig. 21.2.

Describe the peculiarities of the structure and, using the results of microanalysis of the specimens before heating, explain why the first specimen had the surface defects shown in Fig. 21.1*a*.

No. 292. Figure 21.3*a* shows the microstructure of brass after cold deforming, and Fig. 21.3*b*, *c* and *d* the same microstructure after annealing to 300, 500, and 700 °C, respectively.

Determine the point of recrystallization and indicate the properties of the metal after cold deforming and after recrystallization. Explain how the properties of the brass will be changed by annealing at a temperature substantially above the recrystallization point (700 °C).

No. 293. Figure 21.4*a*, *b* shows the microstructure of two widely used grades of brass with different contents of zinc.

By referring to the Cu-Zn diagram (see Fig. 9.16), describe the microstructures shown and give their phase composition.

Using the general principles of the effect of the phase composition and structure on the properties of metals, indicate how the brasses illustrated in Fig. 21.4 should differ in their mechanical properties.

No. 294. Single-phase copper-zinc alloys (α -brasses) after casting have the microstructure shown in Fig. 21.5*a*. Subsequent heat treatment can change appreciably the initial structure of cast

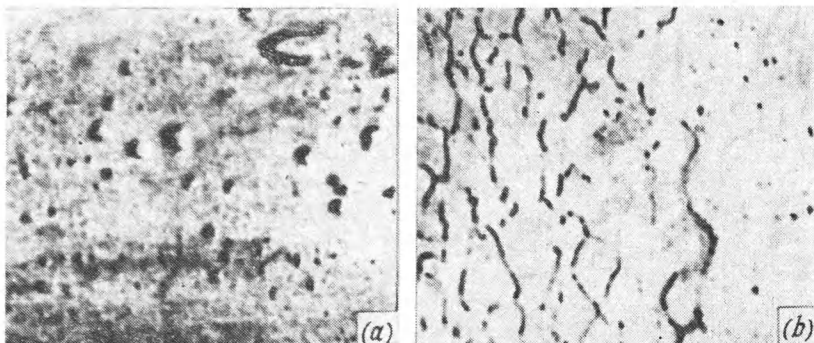


Fig. 21.1. Copper after heating in a reducing atmosphere (600-800 °C), after V. V. Zholobov and N. I. Zedin, 130X
(a) surface of metal, full size; (b) microstructure of unetched section

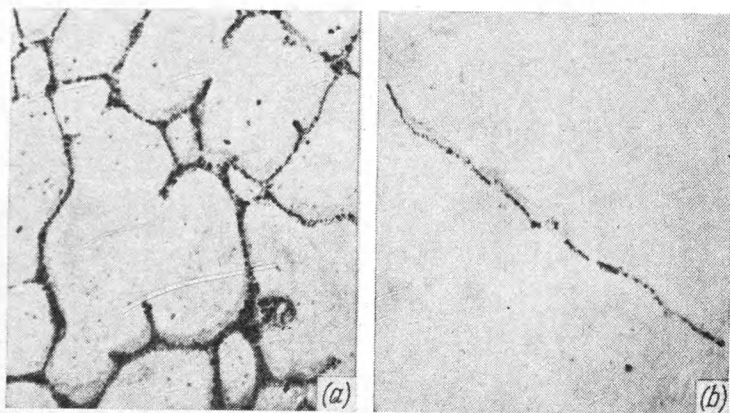


Fig. 21.2. Microstructures of copper specimens before heating in a reducing atmosphere, 130X (after V. V. Zholobov and N. I. Zedin)
(a) specimen with the defects shown in Fig. 21.1; (b) specimen without defects

single-phase brass, as, for instance, is illustrated by the microstructure in Fig. 21.5b, where twin grains are clearly seen.

Describe the structure of the brass shown in Fig. 21.5a and b and suggest a method of treatment to change its structure. Indicate in what direction the mechanical properties of the metal will be changed through this treatment.

No. 295. Two microstructures of α -brass after cold deforming and annealing are shown in Fig. 21.6.

What were the differences in the conditions of heat treatment of these two specimens that caused the change in their grain

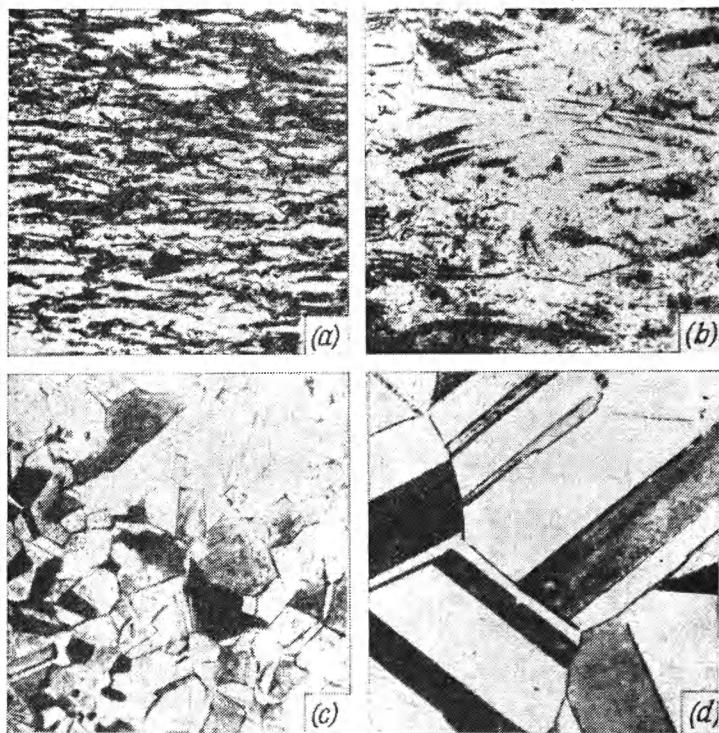


Fig. 21.3. Microstructures of brass, 130X

(a) after cold plastic working; (b), (c), (d) ditto, after annealing at 300, 500, and 700 °C, respectively

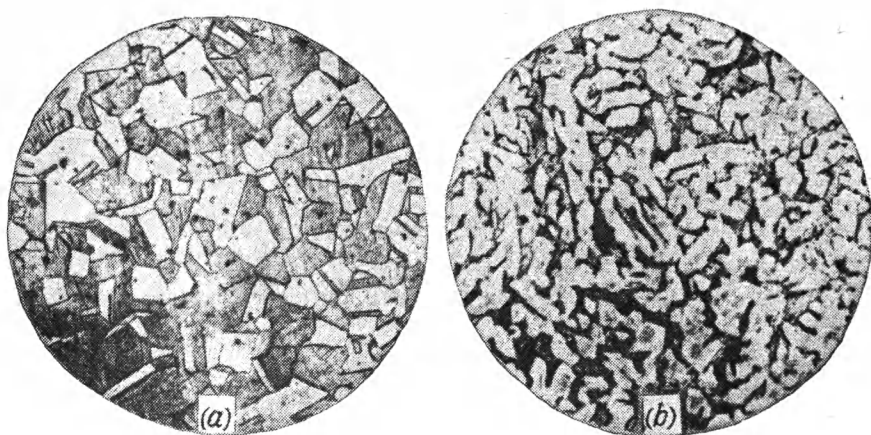


Fig. 21.4. Microstructures of brasses with various contents of zinc, after plastic working and annealing, 200X

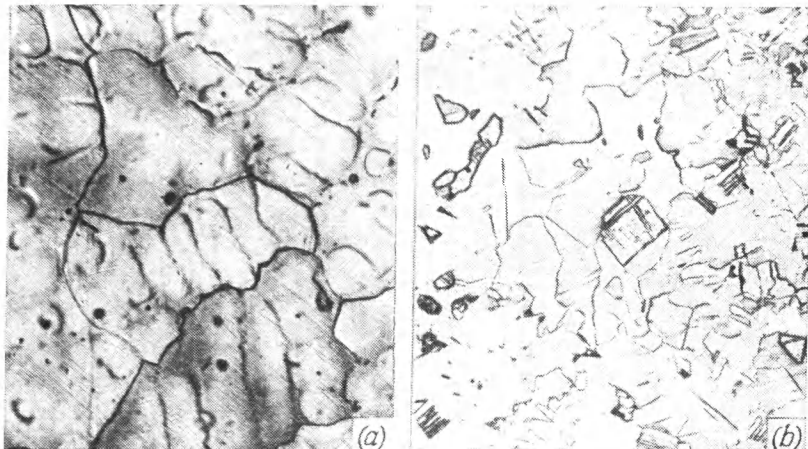


Fig. 21.5. Microstructures of single-phase brass, 100X

(a) after casting; (b) after casting and heat treatment

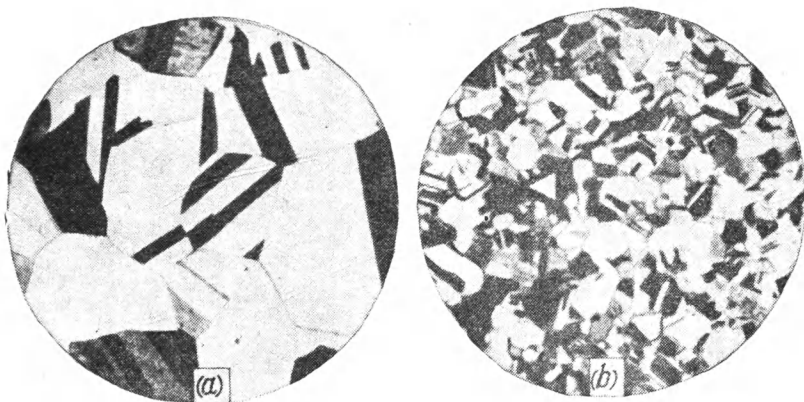


Fig. 21.6. Microstructures of brass after cold deforming and annealing, 125X

size, which is clearly visible in the photographs, and how were the mechanical properties of the metal affected?

No. 296. Ship-building widely uses brass containing 1.5 per cent Sn and 37 per cent Zn (naval brass). Slow cooling after heat treatment makes the metal brittle. On the other hand, quickly quenched naval brass is sufficiently tough.

The microstructures of naval brass after slow cooling and quick quenching are shown in Fig. 21.7*a* and *b*. Using the Cu-Zn-Sn constitutional diagram (see Fig. 10.27), determine the

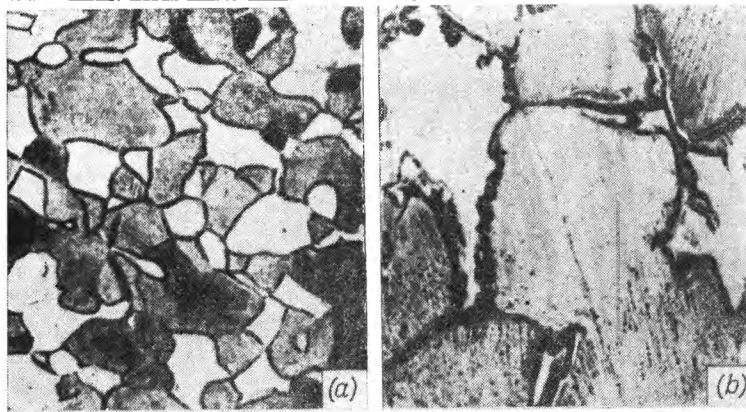


Fig. 21.7. Microstructures of brass with 1.5% Sn and 37% Zn (after V. V. Zholobov and N. I. Zedin)
(a) after rapid cooling; (b) after slow cooling, 300X

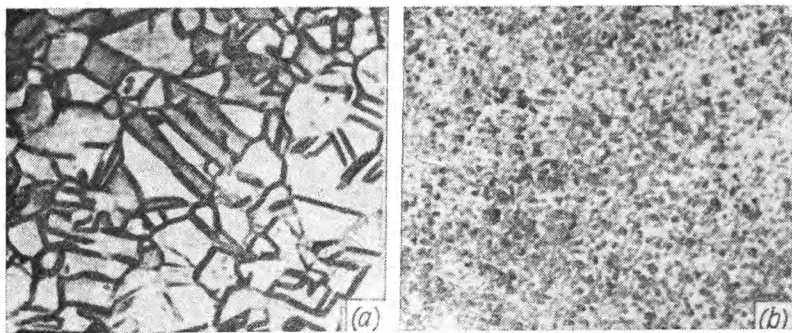


Fig. 21.8. Microstructures of brass with 70% Cu and 2% Al, 100X (after V. V. Zholobov and N. I. Zedin)
(a) without addition of iron; (b) with 1 per cent iron

phase composition of this brass and explain from the results of microanalysis the cause of brittleness.

No. 297. Brasses with 1-3 per cent Al have a higher strength and better corrosion resistance than common brasses. Besides, the strength of these brasses can be increased by alloying with 1 per cent Fe.

The microstructure of a brass containing 70 per cent Cu and 2 per cent Al is shown in Fig. 21.8*a*, and that of a brass having the same contents of copper and aluminium and 1 per cent Fe

in Fig. 21.8*b* (the microstructures obtained after deforming and recrystallization are illustrated in the photographs).

Explain what changes in the structure of the brass occurred owing to the introduction of iron and why these changes increased the strength of the metal.

No. 298. Figure 21.9 shows the microstructure of copper with a slight percentage of bismuth.

Using the Cu-Bi constitutional diagram indicate the structural form of the precipitates seen in the microphotograph.

Taking into consideration the mechanical properties and melting point of bismuth characterize its effect on the ductility of copper at low and high temperatures.

Name the ranges of tolerable bismuth content specified by GOST for high-purity grades of copper and the measures employed in copper-making to reduce the content of bismuth.

No. 299. Fig. 21.10*a* illustrates the microstructure of aluminium bronze with 5 per cent Al.

Describe the conditions of heat treatment of the bronze to form the structure shown in Fig. 21.10*b*.

Explain what effect a change of the microstructure may have on the properties of the bronze.

No. 300. Aluminium bronze containing 8.1 per cent Al after cold deforming was heated to 700 or 900 °C for two hours with subsequent rapid cooling (in air).

The microstructures of the bronze formed through this treatment are shown in Fig. 21.11*a* and *b*.

Describe the processes occurring in the metal during heating to 700° and 900 °C. Using the Cu-Al constitutional diagram and the photographs shown, determine the phase composition of the bronze after heating to the temperatures mentioned and subsequent rapid cooling.

No. 301. Figure 21.12*a*, *b* and *c* shows the microstructures of aluminium bronze with 10.2 per cent Al after plastic working, hardening, and tempering.

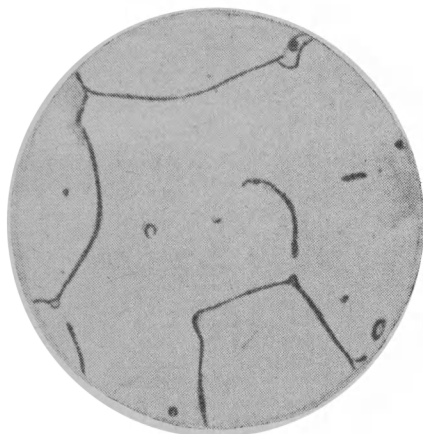


Fig. 21.9. Microstructure of cast copper with a slight addition of bismuth, 130X (after V. D. Turkin and M. V. Rumyantsev)

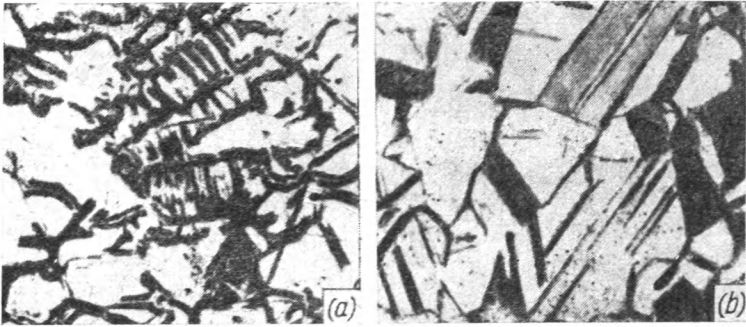


Fig. 21.10. Microstructures of aluminium bronze (5% Al), after V. V. Zholobov and N. I. Zedin
(a) in the initial state, 50X; (b) after heat treatment, 230X

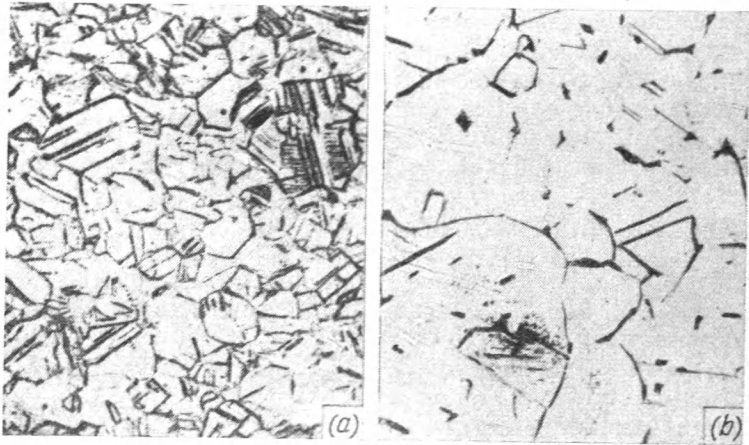


Fig. 21.11. Microstructures of aluminium bronze (8.1% Al) after cold deforming and heating (after V. V. Zholobov and N. I. Zedin)
(a) 700 °C; (b) 900 °C

Describe these structures and the mechanism of the transformations in the bronze during hardening.

Describe the processes occurring in the hardened bronze during tempering at 500 °C.

Indicate how the properties of the bronze change upon hardening and tempering.

No. 302. Figure 21.13 shows the microstructures of aluminium bronze containing 10 per cent Al (a) as cast, (b) after plastic working and annealing, and (c) after hardening.

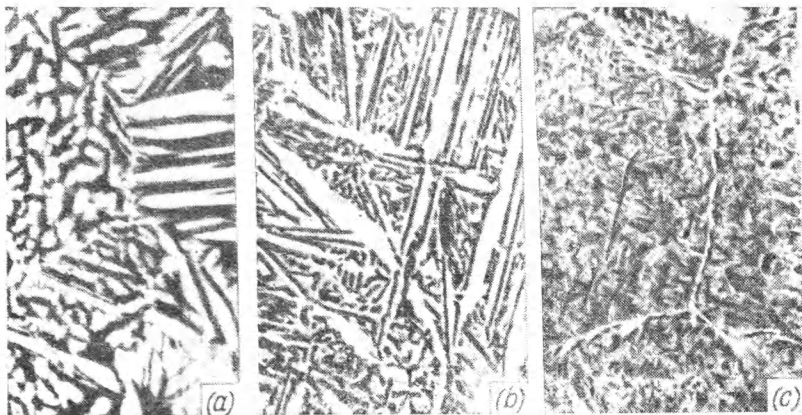


Fig. 21.12 Microstructures of aluminium bronze with 10.2% Al after pressing and heat treatment (after V. V. Zholobov and N. I. Zedin)

(a) after pressing, 150X; (b) after hardening, 150X; (c) after tempering, 520X

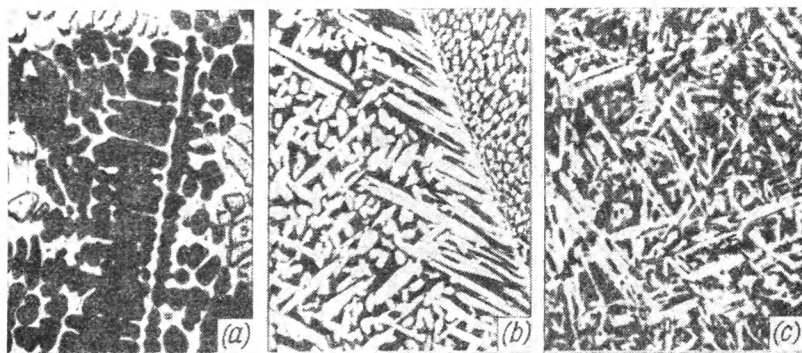


Fig. 21.13. Microstructures of aluminium bronze with 10% Al

(a) after casting, 100X; (b) after pressing, 200X; (c) after hardening, 200X

Describe these structures, and, using the Cu-Al constitutional diagram, determine the phase and structural composition of the metal.

Explain why aluminium bronze with 10 per cent Al is hardenable and indicate the changes in the structure and properties occurring during hardening.

No. 303. Tin bronzes with about 5-6 per cent Sn after casting have the structure shown in Fig. 21.14, i.e. with eutectoid regions.

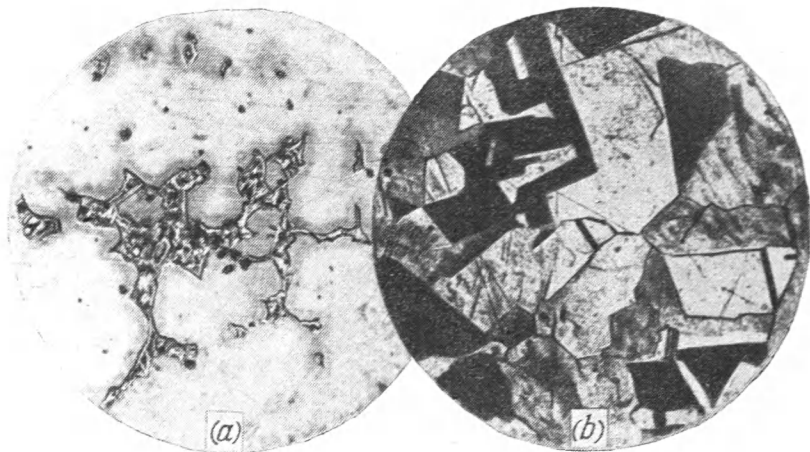


Fig. 21.14. Microstructures of tin bronze with 5-6% Sn, 200X
(a) after casting; (b) in a state near equilibrium

Under conditions approaching the equilibrium (for instance, after long annealing) the same bronze has the structure shown in Fig. 21.14b.

Referring to the Cu-Sn constitutional diagram (see Fig. 9.17), show the possibility of formation of the eutectoid in the structure of cast bronze and determine the phase and structural composition in the equilibrium and non-equilibrium states.

Describe the heat treatment necessary to bring the bronze to the equilibrium state and show how this will change the structure and properties of the metal.



Fig. 21.15. Microstructure of lead bronze with 30% Pb, 130X

No. 304. Figure 21.15 shows the microstructure of lead bronze containing 30 per cent Pb.

To describe the structure of this bronze refer to the Cu-Pb constitutional diagram (see Fig. 9.18).

Noting the difference in the densities of copper and lead, determine how much the metal is liable to segregation and recommend measures to diminish density segregation in lead bronze.

Considering the nature of distribution of lead in copper in this alloy and the wear characteristics

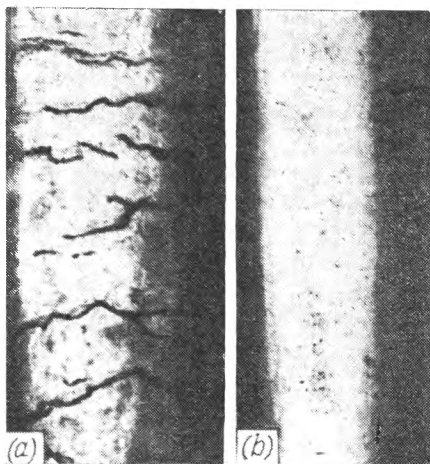


Fig. 21.16. Appearance of brass specimens after work-hardening and air curing for 75 days (after V. V. Zholobov and N. I. Zedin)

(a) 57% Cu (balance zinc); (b) 57% Cu, 3% Pb (balance zinc)

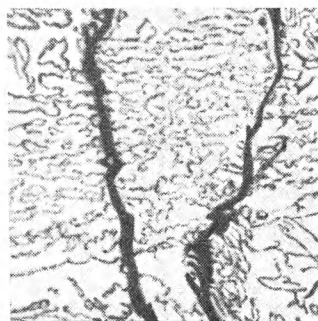


Fig. 21.17. Microstructure of the brass shown in Fig. 21.7, 130X (after V. V. Zholobov and N. I. Zedin)

of copper and lead recommend the field of industrial application of lead bronze.

No. 305. Figure 21.16 shows photographs of two specimens of brass respectively with 57 per cent Cu (the balance — zinc) and 57 per cent Cu and 3 per cent Pb (the balance — zinc) after deforming by 15 per cent and air curing for 75 days.

The specimen in Fig. 21.16a has cracks; its microstructure is shown in Fig. 21.17.

Explain why cracks can develop in brass during storage with time.

No. 306. Macrostructure of many alloys cast into ingots depends on the temperature of tapping and teeming of molten metal. Figure 21.18 shows the macrostructure of three aluminium ingots cast in different conditions.

Describe the macrostructure of each of the ingots and indicate the differences in their casting conditions.

No. 307. The composition of aluminium alloys is selected in accordance with the methods of manufacture of articles (either shaping or casting).

Describe the structures of widely used aluminium alloys shown in Fig. 21.19a and b and indicate which of them was formed and which was cast.

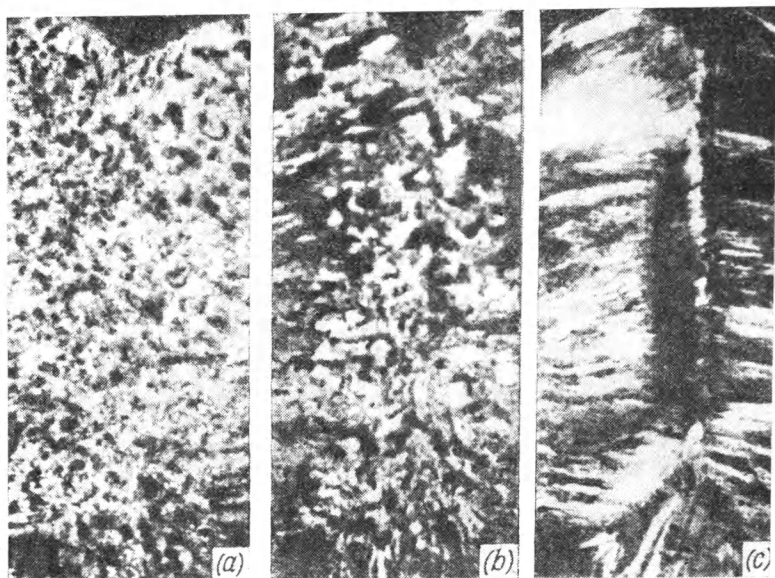


Fig. 21.18. Macrostructures of three aluminium ingots (longitudinal sections) cast at different temperatures of molten metal

No. 308. In order to improve the mechanical properties of castings made of aluminium alloys (silumins) the molten metal is specially treated. Figure 21.20*a* and *b* shows the microstructures of silumin with 12 per cent Si smelted respectively without and with such treatment.

Describe the differences in the structures and methods of treatment of the molten metal and explain how this affected the properties of silumin.

No. 309. Alloys of the duralumin type can be given good mechanical properties by hardening and ageing. When hardening close control of the heating temperature is of special importance.

Figure 21.21 shows the microstructure of duralumin after hardening from a normal and a higher temperature.

Describe these structures and indicate the overheated specimen.

No. 310. Figure 21.22 shows the structures of aluminium alloys based on the aluminium-copper system.

Indicate which of the alloys shown is deformable (and has been shaped) and which is suitable for casting only.

Describe their structures, give approximate compositions of the two alloys and indicate the field of their industrial application.

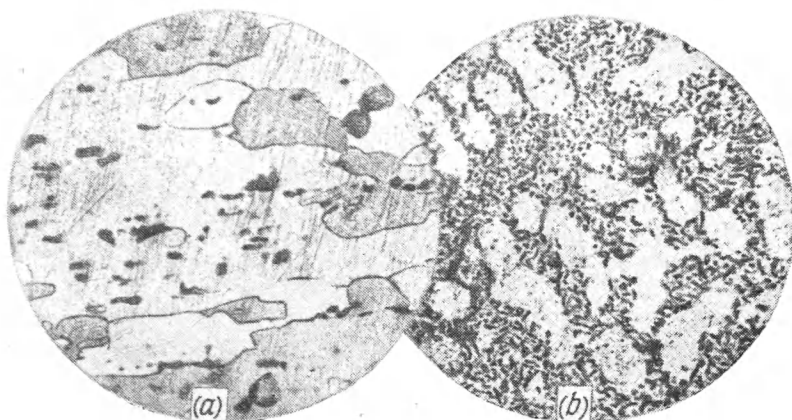


Fig. 21.19 Microstructures of aluminium alloys
(a) deformed, 500X; (b) cast, 200X

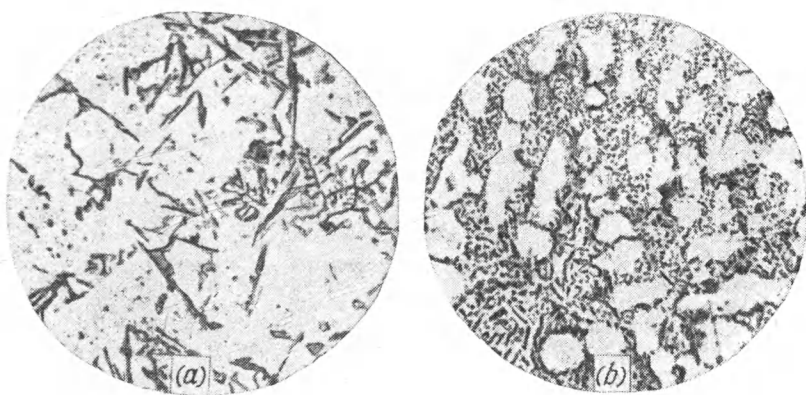


Fig. 21.20. Silumin, 200X
(a) after casting without any additions made to the molten metal; (b) after casting with special additions

No. 311. Aluminium- and magnesium-base alloys of the Al-Mg system are widely employed in industry.

Figure 21.23a and b shows the microstructures of Al-Mg alloys with 10 per cent Mg and with 8 per cent Al respectively.

Determine from the Al-Mg constitutional diagram (see Fig. 9.26) the phase composition and structure of these alloys and recommend the fields of their industrial application.

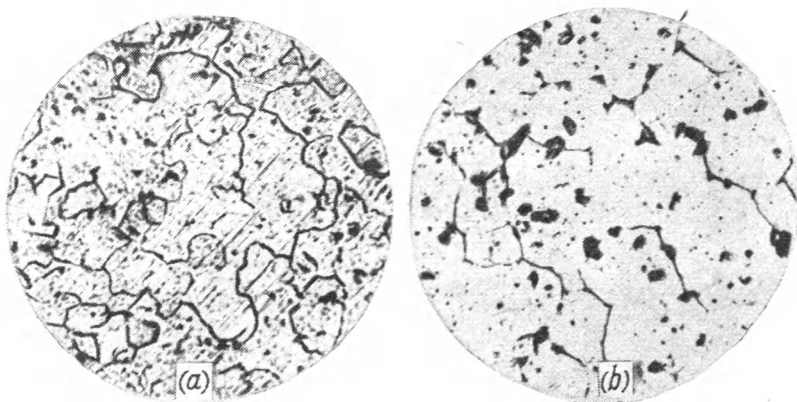


Fig. 21.21. Duralumin after hardening
(a) 100X; (b) 200X

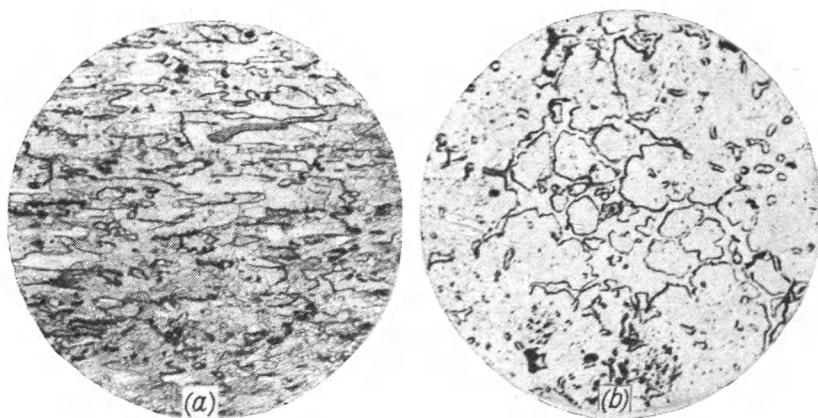


Fig. 21.22. Microstructures of aluminium alloys of different composition, 200X

No. 312. Figure 21.24a and b shows the microstructures of two bearing alloys (babbits), one of them based on the lead-antimony system, and the other, on the tin-antimony system.

Referring to the Pb-Sb and Sn-Sb constitutional diagrams (see Figs. 4.18 and 9.27), describe these structures and determine which of the two alloys relates to each of these structures.

No. 313. Figure 21.25a and b shows the microstructures of a tin-base bearing alloy (babbitt) with 11 per cent Sb and 6 per cent Cu; the specimens were cast under different cooling conditions.

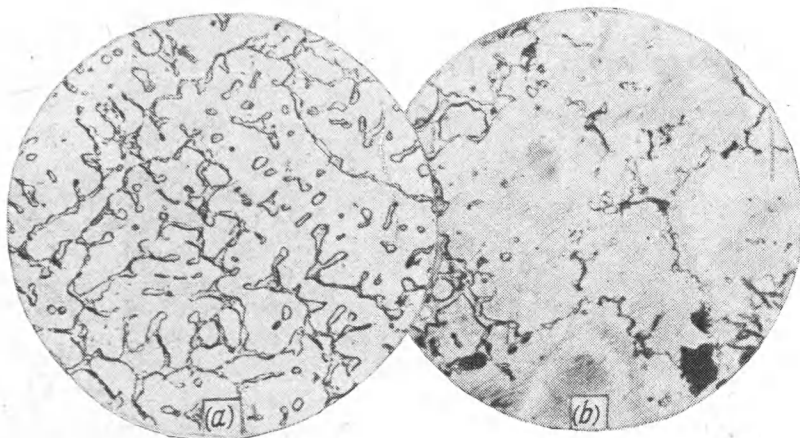


Fig. 21.23. Microstructures of aluminium-magnesium alloys, 200X
(a) aluminium alloy with 10% Mg; (b) magnesium alloy with 8% Al

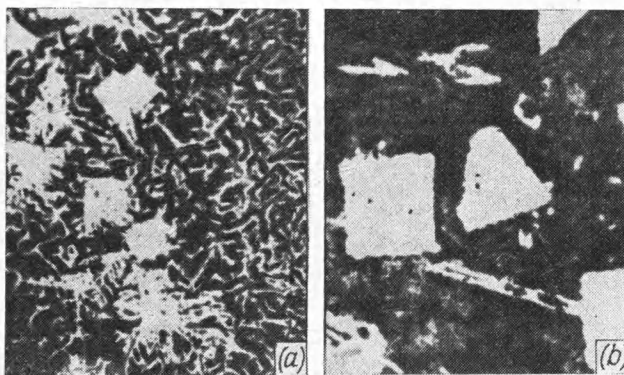


Fig. 21.24. Microstructures of bearing alloys (babbitts), 150X
(a) tin-base alloy; (b) lead-base alloy (after V. D. Turkin and M. V. Rumyantsev)

What are the differences in the microstructures illustrated in the photographs and in which case was cooling done at the greater rate?

Indicate how precipitates of the copper-antimony compound (which are seen as needle-shaped formations in the photographs) can influence the conditions of density segregation in these alloys.

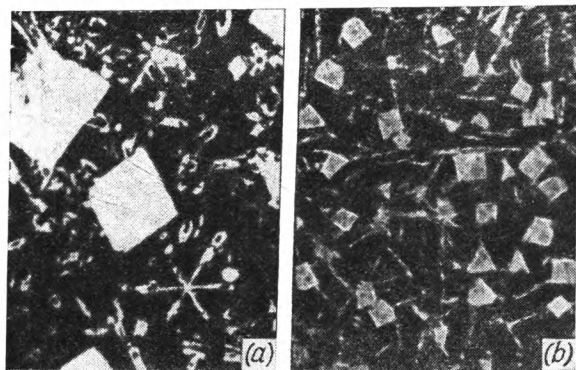


Fig. 21.25. Microstructure of tin-base bearing alloy (babbitt) the specimens shown at (a) and (b) were cast under different conditions. 130X

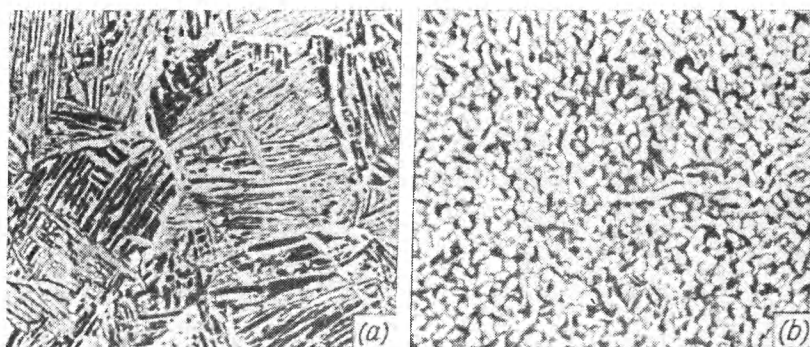


Fig. 21.26. Microstructure of BT3-1 alloy after deformation in the $(\alpha + \beta)$ - and β -region and isothermal annealing; heating to 870 °C for 1 h, holding at 650 °C for 2 h, air cooling, 500X (after N. A. Vorobyev and A. G. Pronin)

No. 314. Figure 21.26 shows the structures of BT3-1 alloy after deforming in the two-phase $(\alpha + \beta)$ -region and in single-phase (α) -region and slow cooling.

Compare these structures and indicate in which case the thermal conditions of deforming are better as providing better properties to the alloy.

Part Six

PROBLEMS ON SELECTION AND HEAT TREATMENT OF ALLOYS IN ACCORDANCE WITH OPERATING CONDITIONS OF ELEMENTS AND STRUCTURES

Chapter Twenty-two

METHODICAL INSTRUCTIONS

When solving the problems given below, the student should substantiate his selection of an alloy and its heat-treatment conditions necessary to ensure the maximum reliability and durability of machine components under the specified operating conditions. The problems, as a rule, are based on the most typical operating conditions of the components in various branches of industry. In addition, the problems formulate the characteristic properties the alloy used for making the given components should possess.

To solve a problem, the student should, in the first place, select a suitable group of alloys (for instance, common structural steels, cast irons, heat-resistant steels and alloys, tool steels, etc.) whose properties approach most closely those specified in the problem. For this purpose the student is advised to acquaint himself with the classification, compositions and application of basic materials used in engineering (see Chapter 27).

Then, when finally selecting the most suitable alloy from a group and the conditions of its heat treatment, the student should, as a general rule, consider the possibility of using a cheaper material, for instance, a common carbon steel or grey iron.

If it turns out that the alloy selected does not satisfy the conditions of the problem in certain respects, for instance, as regards its strength or toughness, the possibility of improving these properties by heat treatment or chemical heat treatment should be considered. Expensive alloy steels containing nickel, tungsten, molybdenum, as also expensive non-ferrous alloys should only be selected when cheaper materials cannot satisfy the requirements of the problem. The selection of an alloy should be properly substantiated.

When heat treatment or chemical heat treatment is needed to improve the properties of the selected material, the student should specify the treatment and the structure and properties obtained through it. Again, the most economic and efficient me-

thods of treatment, for instance, induction heating, gas cementation, etc., should be preferred, especially for mass-produced machine parts. For components operating under varying loads, such as shafts, gears and the like, the student should recommend a process of treatment to increase their durability (for instance, cementation, cyaniding, nitration, induction hardening, shot blasting, or some other process suitable for the steel or alloy selected).

To help the student select the right type of material for the given problem and substantiate his recommendations, the following chapters give exemplary solutions to three types of problem: on common structural steels (No. 315), tool steels (No. 381), and on non-ferrous alloys (No. 413).

Chapter Twenty-three

PROBLEMS ON STRUCTURAL STEELS AND CAST IRONS

No. 315. A shop is to manufacture a shaft 70 mm in diameter for heavy-duty operation. The steel for the shaft should possess a yield strength of at least 75 kgf/mm², fatigue strength, at least 40 kgf/mm², and impact strength at least 9 kgf m/cm.²

Three grades of steel: Ст. 4, 45, and 20XH3A are available.

Which of these should be used for making the shaft? What kind of heat treatment will be needed, if any? Describe the structure and mechanical properties of the steel after the final heat treatment.

Solution. The compositions of steel Grades Ст. 4, 45 and 20XH3A are as given in Table 23.1 below.

Table 23.1. Composition of Steels, Per Cent

Grade	Standard (GOST)	C	Mn	Si
Ст. 4	380-71	0.18-0.27	0.40-0.70	0.12-0.30
45	1050-60	0.42-0.50	0.50-0.80	0.17-0.37
20XH3A	4543-71	0.17-0.23	0.30-0.60	0.17-0.37

Table 23.1 (continued)

Grade	Standard (GOST)	Cr	Ni	S	P
Ст. 4	380-71	≤ 0.3	≤ 0.3	≤ 0.050	≤ 0.040
45	1050-60	≤ 0.25	≤ 0.25	≤ 0.045	≤ 0.040
20XH3A	4543-71	0.60-0.90	2.75-3.15	≤ 0.025	≤ 0.025

Steel Grade Ст. 4, according to USSR State Standards (GOST), has the following characteristics in the commercial state of deli-

very (after rolling or forging): $\sigma_t = 42\text{--}54 \text{ kgf/mm}^2$, $\sigma_y \geq 24\text{--}26 \text{ kgf/mm}^2$, $\delta \geq 21$ per cent.

Steel Grade 45, according to standards (GOST), has a hardness number not above 207 HB after rolling and annealing. Its ultimate strength σ_t is not more than $60\text{--}62 \text{ kgf/mm}^2$ at a hardness number of 190-200 HB, or not more than $55\text{--}60 \text{ kgf/mm}^2$ at a hardness below 180 HB. The σ_y/σ_t ratio for annealed carbon steel is approximately 0.5. Therefore, the yield strength of steel Grade 45 in this state does not exceed $27\text{--}32 \text{ kgf/mm}^2$.

According to standards (GOST), steel Grade 20XH3A after rolling and annealing has a hardness number not above 250 HB. Its ultimate strength at a hardness of 230-250 HB cannot therefore exceed $67\text{--}75 \text{ kgf/mm}^2$ and can even be below 60 kgf/mm^2 for melts of a lower hardness. The yield strength will then be $35\text{--}40 \text{ kgf/mm}^2$, since the σ_y/σ_t ratio for annealed alloy steel is 0.5-0.6.

Thus, the shaft must be heat treated to obtain the specified yield strength.

For the low-carbon steel Grade Cr. 4, heat treatment can only insignificantly improve its properties. Besides, steel Grade Cr. 4 relates to the group of common steels, and therefore, is high in sulphur and phosphorus (see Table 23.1) which impair its mechanical properties, especially its resistance to impact loads.

Thus, it would be irrational to use the cheaper common steel for making the shaft which is a critical part whose breakage would stop the operation of the machine.

Steel Grade 45 relates to the class of quality carbon steels, while steel Grade 20XH3A, to that of high-quality alloy steels, their carbon contents being 0.42-0.50 per cent and 0.17-0.23 per cent, respectively. Both are hardenable.

Their strength can be increased by either normalizing or hardening followed by high tempering.

The latter version of heat treatment is more complicated, but it can ensure higher toughness, as well as higher strength. The minimum impact strength (a_n) for steel Grade 45 after normalizing is $2\text{--}3 \text{ kgf m/cm}^2$ and can be increased to $6\text{--}7 \text{ kgf m/cm}^2$ through hardening and tempering with heating to 550°C .

Since the shaft will be subjected to appreciable dynamic loads and vibration, hardening followed by tempering is preferable.

The structure of steel Grade 45 after hardening in water is martensitic. In components with a diameter of more than 20-25 mm, however, this structure can only be formed in a relatively thin surface layer up to 2-4 mm thick, due to the poor hardenability of carbon steel.

Subsequent tempering will transform the martensite and troostite into sorbite only in a thin surface layer without affecting the structure and properties of pearlite and ferrite in the main core of the metal.

Temper sorbite has higher mechanical properties than those of ferrite or pearlite.

The highest stresses due to bending, torsion and alternating loads are taken up by the outer layers of the shaft and these must therefore possess improved mechanical properties. Dynamic loads, however, act on both superficial and deeper layers of the metal of the shaft. Thus, carbon steel cannot ensure the required properties for the shaft 70 mm in diameter (Fig. 23.1).

Steel Grade 20XH3A is alloyed with nickel and chromium to increase its hardenability. After hardening, its structure and mechanical properties are sufficiently uniform over a cross section of up to 75 mm in diameter.

The following heat treatment can be recommended for steel Grade 20XH3A:

1. Oil hardening at 820-835 °C.

Hardening with oil quenching (but not with water quenching, as required for carbon steels) causes lower stresses, and therefore, lower strains. The steel after hardening has a martensitic structure and a hardness number not less than 50 HRC.

2. Tempering at 520-530 °C. The shaft after temper heating should be cooled in oil to prevent temper brittleness which chromium (and manganese) steels are liable to.

The mechanical properties of steel Grade 20XH3A in a component with a diameter of up to 75 mm after heat treatment will be as follows:

ultimate strength σ_t , kgf/mm ²	90-100
yield strength σ_y , kgf/mm ²	75-80
fatigue strength σ_{-1} , kgf/mm ²	40-43
relative elongation δ , %	8-10
relative reduction ψ , %	45-50
impact strength a_n , kgf m/cm ²	9

Thus, these properties meet the requirements of the problem (for a shaft 70 mm in diameter).

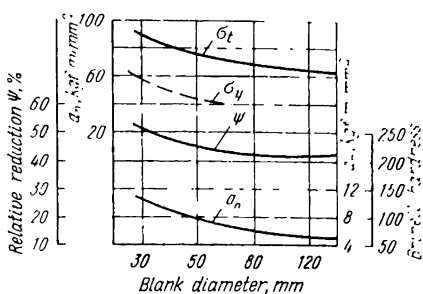


Fig. 23.1. Mechanical properties of carbon steel with 0.45% C after hardening and tempering, depending on blank diameter

No. 316. Gears may be made of common steel, quality carbon steel, or alloyed steels with various contents of alloying elements, the choice depending upon the operating conditions and the stresses developing in the gears.

Gears 50 mm in diameter and 30 mm wide should be made of a metal having an ultimate strength of at least 36-38 kgf/mm². Select a steel grade most suitable for the purpose from the engineering and economical standpoints.

Decide on the heat treatment of the gears. Name the mechanical properties and structure of the steel in finished components and compare them with those of steel Grades 45 and 40XH after heat treatment.

No. 317. Select a steel for making shafts 50 mm in diameter for two reducer gears. The design yield limit of the metal must be at least 35 kgf/mm² in one shaft and at least 50 kgf/mm² in the other.

Indicate: (a) the composition and grade of the selected steels; (b) the recommended heat treatment; (c) the structure after each heat-treatment operation; and (d) the mechanical properties of the metal in the finished components.

Is it possible to use common-quality carbon steel for these shafts?

No. 318. Crankshafts 80 mm in diameter for heavy-duty operation are made of quality carbon steel at one works and of alloy steel at another.

What type of steel must be used for the purpose? Indicate its grade and composition.

Recommend the hardening and tempering conditions and compare the mechanical properties which can be provided by the selected quality carbon and alloy steels in a shaft of the given diameter.

No. 319. Select a steel for making heavy-duty crankshafts 60 mm in diameter; the ultimate strength of the metal must be at least 75 kgf/mm².

Recommend the composition and grade of steel, and heat-treatment conditions and name the structure and mechanical properties of the metal after hardening and after tempering.

Figure 23.2 shows the macrostructure of two shafts, that shown at (a) being made correctly, and that at (b), incorrectly. How do their mechanical properties compare, if both are of the same diameter, made of the same steel and heat treated similarly?

Indicate a method of manufacture of a crankshaft from a blank to ensure the optimum mechanical properties and a method of study which will reveal the macrostructure.

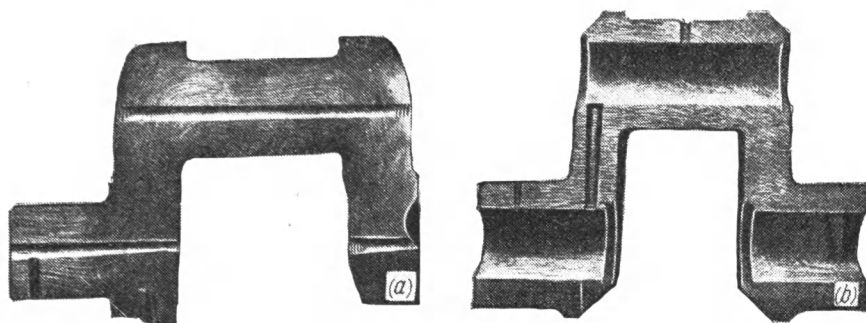


Fig. 23.2. Macrostructure of a crankshaft (after N. V. Geveling), 1/3 full size
(a) correct location of fibres; (b) incorrect

No. 320. Car bodies are manufactured by the cold drawing of sheet steel.

Select a steel for the sheets. Indicate its composition and the specifics of the steelmaking process to ensure increased drawability.

No. 321. A batch of hooks for railway cars was rejected, since the works laboratory found that the steel had the macrostructure shown in Fig. 23.3a.

The results of the macroscopic examination were confirmed by subsequent mechanical tests in which the hooks broke, 67 per cent of the breakages being in the nose portion, 19 per cent at the tail, and 14 per cent across the eye.

The hooks were made from rimming steel Grade Cr. 3.

Hooks in other batches withstood the tests and were accepted by the works. Their macrostructure is shown in Fig. 23.3b.

Explain: (a) the test method employed to reveal the macrostructure shown in Fig. 23.3; and (b) the manufacturing methods used to make the rejected hooks and the good ones.

Indicate the composition and grade of steel suitable for making the hooks, its macrostructure, and heat-treatment conditions for the ultimate strength of the metal to be at least 40 kgf/mm².

No. 322. The driving axle of the carriage of an overhead travelling crane is 70 mm in diameter. Formerly it was made of steel Grade

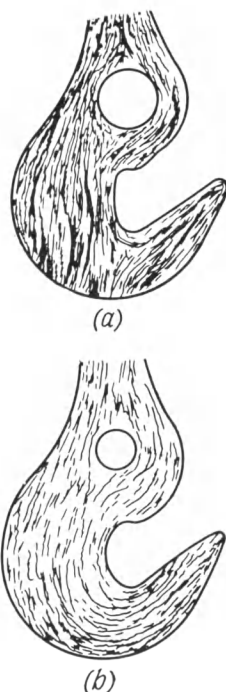


Fig. 23.3. Macrostructure of a hook (1/10 full size)

(a) incorrectly manufactured; (b) correctly manufactured

Ст. 5. During the reconstruction of the crane to increase its load-carrying capacity, the constructor did not change the diameter of the axle, but used a different grade of steel having a higher yield strength (by a factor of 1.5).

Indicate quality carbon and alloy steel grades suitable for making the axle; recommend the heat-treatment conditions and compare the mechanical properties of the selected steels with those of steel Grade Ст. 5.

No. 323. A works has to manufacture three engine shafts, the specified ultimate strength of the shaft metal being at least 75 kgf/mm². The diameters of the shafts are 35 mm, 50 mm, and 120 mm, respectively.

Select steel for making the shafts, substantiate your selection, recommend the heat-treatment conditions, and indicate the structure of the metal in the finished shafts.

No. 324. A works was manufacturing internal combustion engine shafts 60 mm in diameter from steel having a yield limit of 20-23 kgf/mm² and relative elongation of 20-22 per cent.

Later on, an order was made to manufacture shafts of the same diameter for more powerful engines. The works had to guarantee the yield limit of at least 60 kgf/mm² and impact strength of at least 6 kgf m/cm² in shafts of one type and, respectively, 80 kgf/mm² and 8 kgf m/cm² in those of another type.

Indicate the grades of steel, their heat-treatment conditions, structure, and mechanical properties after the final treatment.

How will the σ_y/σ_t ratio of the selected steels be changed through the heat treatment?

No. 325. Gears are subjected to alternating and impact loads and should possess maximally uniform properties in both the longitudinal and transverse directions. They are manufactured of steel having an ultimate strength of either 70-75 kgf/mm² or 90-95 kgf/mm², depending on the type of the engine they are used for. The impact strength must be at least 7-8 kgf m/cm² in both cases.

Select steel for the gears of both types, give its composition, grade and heat treatment, and describe the microstructure and mechanical properties of the finished components.

By analysing the macrostructure of a gear forging (see Fig. 23.4), give the sequence of the manufacturing operations, beginning from the steel delivery to the gear manufacturer. Recommend a process that will ensure a uniform structure in the steel, and hence, uniform properties in both the longitudinal and transverse directions.

No. 326. A works manufactures two types of gear, 60 mm in diameter and 80 mm wide, for operation under similar conditions.

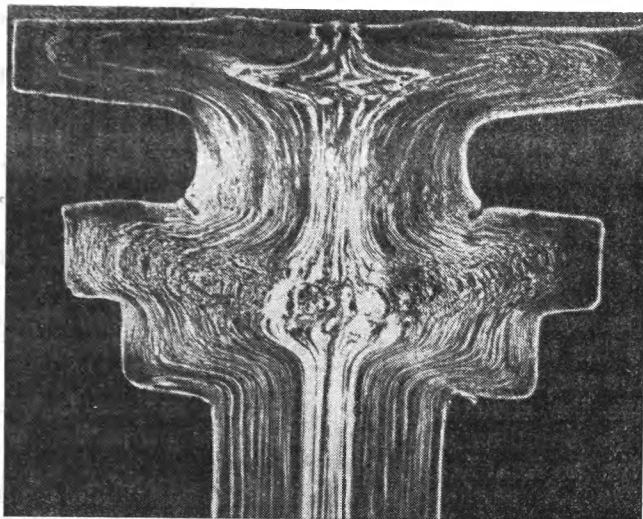


Fig. 23.4. Macrostructure of a gear forging (1/4 of full scale)

The yield strength of the metal must be at least 54-55 kgf/mm². Gears of the second type have a more complicated shape than those of the first.

Select steel for making the gears; name its grade and composition in view of the specifics of heat treatment and the necessity to prevent deformation and cracking during hardening. Substantiate your selection and recommend the heat treatment. Indicate the mechanical properties of the metal in the finished components.

No. 327. The worm of a reducer gear, 35 mm in diameter, may be manufactured of either cementable or non-cementable steel. Explain, in which cases the cementable steel is more preferable, and where the other type suits more.

The ultimate strength in the core of the component must be 60-70 kgf/mm².

Select the grades of the cementable and non-cementable steels. Indicate their compositions, recommend the heat treatment, and compare the mechanical properties of the two steels in the finished products.

No. 328. A shop manufactures gears 50 mm in diameter from cementable steel. Select steel suitable for gears to operate under conditions of wear, impacts, and high stresses.

Indicate the compositions of the selected steels and recommend their heat treatment. Describe the purpose of each heat-treatment

operation and its effect on the structure and properties of the steels.

Recommend the thickness of the cemented layer for the given component.

No. 329. A machine-tool works manufactures lathe spindles to operate under conditions of high speeds and increased wear, because of which the hardness number of the surface layer must be at least 58-62 HRC.

Select steel to make lathe spindles 40 mm and 75 mm in diameter.

Give the composition and grade of the selected steels and recommend the heat treatment which will give the specified hardness to the surface layer.

Describe the structure of steel in the surface layers and the core of the spindles and the mechanical properties of the core metal after the final heat treatment.

No. 330. A works has to manufacture lathe spindles for operation under conditions of severe wear and also spindles for grinding machines which, in addition, must ensure a high machining accuracy. For this reason the spindles for the grinding machines must have the lowest possible deformation after heat treatment and, besides, possess an increased wear resistance.

Select steels for both types of spindle and recommend their heat treatment.

Describe the structure of steel and the hardness of the surface layer and core after the final heat treatment.

No. 331. Machine-tool beds are cast. The ultimate strength of their metal must be not less than 20-25 kgf/mm².

Select the grade of an alloy suitable for manufacturing a stand whose thickness is different in different cross sections, and indicate the heat-treatment conditions and the final structure of the metal.

When solving the problem, take into consideration the fact that stresses in cast components should be minimized and that the heat treatment should be such as to prevent the deformation (buckling) of the stand when in use.

No. 332. The crankshaft of passenger car engines is most economical to be made of cast iron which, in addition, is almost insensitive to notching. High-quality grades of cast iron are used for this purpose.

Select the class and grade of cast iron to have an ultimate strength of not less than 40 kgf/mm² and relative elongation of 2-3 per cent.

Describe the structure of the selected cast iron and the type of graphite precipitation in it and explain how the iron-making process should be changed in such a case.

No. 333. Cylinder blocks of tractor engines are made of cast iron having a hardness number of 170-241 HIB and increased strength and wear resistance.

Select the grade of cast iron, describe its structure and mechanical properties, and give its composition to ensure the specified properties.

What will the requirements to the composition and structure of the cast iron be if the cylinders are to operate at temperatures up to 500-600 °C?

No. 334. Bevel gears of an electrical carriage, 50 mm in diameter, operate under conditions of high dynamic loads and wear. This stipulates a high toughness in the steel core.

Select a cementable carbon steel, indicate its composition, recommend the heat treatment to obtain maximum toughness in the core, if the cementation is to be done in a solid carburizer. For comparison, give the heat-treatment conditions for gas cementation.

Describe the mechanical properties of steel in the core of the component and the surface hardness after the final heat treatment. Decide whether it is advisable to use a common-quality steel for the purpose.

No. 335. A joint pin, 30 mm in diameter, is subjected to bending and shear; its surface must possess high wear resistance and the core must be tough.

Select carbon steel, give its composition and grade, recommend the chemical heat-treatment conditions, and describe the structure and mechanical properties of the core and the hardness of the surface layer after the final treatment. What is the most desirable thickness for the hard surface layer?

Explain when an alloy steel must be preferred and what mechanical properties can be guaranteed in steels of the two types indicated.

No. 336. A works has to make gears of a complicated shape 50 mm in diameter and 100 mm wide. The surface hardness must be at least 58-60 HRC, and the core must have an ultimate strength of at least 40 kgf/mm² and impact strength of at least 5-6 kgf m/cm². The works made the first batch of the gears from cementable carbon steel, but some gears deformed during hardening.

Select suitable steel and recommend the heat treatment after cementation to ensure the required mechanical properties and prevent spoilage through deformation.

Indicate the structure of steel in the core and surface layer after the final treatment and the causes of deformation during hardening.

No. 337. Cylinder sleeves of powerful engines must possess an especially high wear resistance and high hardness (950-1000 HV) of their working surface, be combined with good mechanical properties of the core (a yield limit of at least 75 kgf/mm²). Indicate a suitable steel grade, and recommend conditions of heat treatment and chemical heat treatment.

Compare the sequence of the thermal operations employed, the duration of the chemical heat treatment, and the thickness, structure and hardness of the surface layer for the two types of treatment. Compare the composition and heat treatment mode of the selected steel with those of another steel suitable for cementation or cyaniding.

No. 338. A works is manufacturing crankshafts 35 mm in diameter; the steel in the finished component must have a yield strength of not less than 30 kgf/mm² and impact strength of not less than 5 kgf m/cm². Besides, the shaft must have an increased wear resistance in the necks only, i.e. in places subject to wear by bearings.

Select steel suitable for the purpose; recommend the heat treatment for the shaft to obtain the specified properties, and a highly productive mode of subsequent heat treatment to increase hardness only in certain portions of the shaft; name the equipment to be used for this treatment.

Indicate the structure and hardness of the metal in the surface layer of the shaft necks and also the structure and mechanical properties in the remaining portions of the shaft.

No. 339. Many large parts for railway transport vehicles, such as automatic couplers, are cast. The castings are then heat treated to improve their mechanical properties.

Select a suitable grade of steel and recommend the heat-treatment conditions to obtain an ultimate strength of not less than 35 kgf/mm².

Indicate the structure and mechanical properties of steel after casting and after heat treatment.

No. 340. Some automobile parts (brake shoes, wheel hubs, etc.) which have a relatively complex shape and are subjected to dynamic loads, may be made of cast iron instead of steel, which provides an appreciable economy in manufacture. The cast iron used for the purpose must, however, possess high mechanical properties.

Recommend a method for making cast iron with an ultimate strength of not less than 35 kgf/mm² and relative elongation of

at least 8-10 per cent, and indicate its microstructure and the field of application.

Indicate the grade, composition and mechanical properties of steel suitable for the manufacture of similar components.

No. 341. A works was manufacturing worm wheels, 150 mm in diameter and 40 mm wide, from grey iron. Later, it became necessary to make the wheels of cast iron having a higher ultimate strength (by a factor of 1.5) and a relative elongation of at least 2-3 per cent.

Indicate the structure and ultimate strength of grey iron possessing the best mechanical properties that can be obtained in a casting of the given thickness.

Give a method for making cast iron having a strength 1.5 times greater than that of the grey iron indicated, and characterize its structure.

No. 342. A works is manufacturing cast iron components of two types: (a) solid components of a complex shape (without internal holes) and (b) thin-walled ones. All will be subjected to dynamic loads during operation, because of which the metal in both cases must have good mechanical properties, including a relative elongation of at least 2 per cent.

Select the type and grade of cast iron suitable for making each component type and substantiate your selection.

No. 343. In the manufacture of bearing bushings for certain types of mechanism the expensive non-ferrous metals (brasses and bronzes) can be replaced with a cheaper antifriction grey iron.

Indicate the structure of the metallic matrix of grey iron and the type of graphite precipitation most suitable for the bushings to have high wear resistance. Give approximate mechanical properties for the selected iron, if the minimum thickness of the bushing is 15-20 mm.

No. 344. As has been found in practice, some thin-walled grey cast-iron components obtain a very hard surface layer, causing machining difficulties.

Indicate the causes of this higher hardness, and the structure of the surface layer. What kind of heat treatment can be used to reduce the hardness? When is a high-hardness surface layer advantageous in cast components? What casting methods can produce such a hard layer?

No. 345. The hulls of modern sea-going ships and river boats are excessively large and heavy when made of common-quality structural carbon steel.

Select a grade of structural steel having approximately the same low carbon content, but with the yield strength 1.5 times higher than that of steel Grade Cr. 3 and good weldability.

Explain how these properties can be improved.

No. 346. Leaf springs for lorries, up to 10 mm thick, are made of quality alloy steel.

The metal in the finished spring must have high ultimate strength, fatigue strength, and elastic limit.

Recommend the heat-treatment conditions and name the structure and mechanical properties that can be obtained with properly selected steel composition and heat treatment for the springs. Explain how the surface condition of the springs can affect their quality and indicate a method for treating the surface layer to increase fatigue strength.

No. 347. The leaf springs of a 3-ton lorry are made from 10-mm thick sheets of steel Grade 60C2, which after hardening and tempering must have high strength over the whole cross section. For a heavier automobile, the springs must be 20 mm thick, and if steel Grade 60C2 is used it becomes impossible to ensure uniform strengthening over the whole cross section.

Recommend another grade of steel suitable for making the springs and the heat-treatment conditions ensuring high strength over the whole cross section.

No. 348. Complex mechanisms use gears of several types; they are made of different materials and heat treated in different ways. A works manufactures gears of the following types: (a) of cemented steel, having an ultimate strength of 65-70 kgf/mm² in the core and an impact strength of at least 8 kgf m/cm²; (b) of nitrated steel, having an ultimate strength of the core of at least 95-100 kgf/mm² and an impact strength of at least 9 kgf m/cm²; (c) of thermally improved steel with an ultimate strength of 90-100 kgf/mm² and impact strength of at least 6 kgf m/cm²; and (d) of aluminium-iron bronze with a hardness of 220-230 HB.

Select the grades of alloys, give their compositions, heat treatment and structures required to obtain the mechanical properties indicated. Compare the conditions of their heat treatment and, taking into consideration the properties obtained in the finished components, determine the operating conditions in which the gears of each of the above types are most advantageous.

It may be assumed in the solution that all the gears are of the same diameter (50 mm) and width (80 mm).

No. 349. A works heat treats large batches of gears 50 mm in diameter made of steel Grade 20. The gears were being delivered to the heat-treatment department from a machine shop and then returned to the latter for the final machining.

To increase productivity and shorten the production cycle, the works changed over to another grade of steel and introduced in-

duction hardening. This made it possible to carry out the heat treatment directly in the production flow of the machine shop.

Name the grade of steel suitable for making induction-hardened gears.

Indicate the technological conditions of the two heat-treatment processes and compare them as regards the time required for their individual operations.

No. 350. Piston pins 30 mm in diameter and 50 mm long must have a tough core and a hard surface (58-62 HRC) offering a high resistance to wear.

Select the heat-treatment conditions to ensure the specified characteristics, if large batches of the pins are to be manufactured of steel Grades 20 and 45.

Give the composition of steel Grades 20 and 45, and compare the holding time of the components made of steel Grade 20 during cementation with that of the components made of steel Grade 45 in other methods of heat treatment to produce a hard surface layer 0.8-1.0 mm thick. Describe the whole cycle of the heat-treatment operations for the piston pins made of these grades of steel and the mechanical properties obtained in the core.

No. 351. A shop heat treats gears 30 mm in diameter made of steel Grade 20X. The shop is to abandon solid-carburizer cementation method and introduce the more productive liquid cyaniding process.

Compare the conditions of the whole cycle of the chemical heat treatment with those of the heat treatment of the gears for the cases of solid-carburizer cementation and liquid cyaniding. The specified thickness of the hard surface layer is 0.4-0.6 mm.

Indicate the microstructure and hardness number of the surface and the mechanical properties in the core of the metal after the final heat treatment.

No. 352. Cylinder sleeves of internal combustion engines, having a wall thickness of 40 mm, must possess high wear resistance of the surface. A shop makes these components of steel Grade 20, and subjects them to cementation and heat treatment. Now the shop has to make cylinder sleeves for a more critical service, a higher wear resistance and a surface hardness of not less than 950-1000 HV being required of them. The metal must retain this hardness when heated to 300-400 °C.

Select steel suitable for the purpose and name the changes that must be made in the heat treatment and chemical heat-treatment processes.

Compare the two processes as regards the sequence and duration of the individual operations, and also the mechanical properties and hardness of superficial and deeper layers of the metal

obtained through changing the composition of the steel and the application of each of these processes.

No. 353. Cylinder sleeves of powerful internal combustion engines are nitrated to increase their wear resistance.

Select steel suitable for nitration, give its composition, recommend the heat treatment and nitration conditions and indicate the hardness of the surface layer and the mechanical properties of deeper layers in the finished product.

Compare (a) the hardness numbers obtained by nitration and cementation; (b) the maximum temperatures at which the hardness of the nitrated or cemented layers can be retained; and (c) the deformations of products caused by these processes (name the process causing a lower deformation).

Chapter Twenty-four

PROBLEMS ON SPECIAL STEELS AND ALLOYS AND PLASTICS

No. 354. Select the grade of steel for the manufacture of bolts on high-speed automatic machine tools so as to ensure the highest machining rate and a high class of surface finish; the bolts will not be subjected to high operating loads.

Indicate the grade, composition, mechanical properties and purpose of the selected steel.

Explain the effect of various alloying elements in this grade of steel.

For comparison, give the composition, structure and mechanical properties of a non-ferrous alloy of high machinability employed for the same purpose.

No. 355. Vessels, tanks and pipelines for the storage and transportation of liquid products in agriculture are recommended to be manufactured from light-weight materials (with a density not more than 1.5 g/cm^3) which are not liable to corrosion and can be easily cleaned.

Recommend the composition of the material (according to Table 29.1) and compare its mechanical properties with those of steel Grade Cr. 3.

No. 356. Some gears for machine-tool gearboxes, which are not subjected to critical pressures, are manufactured of plastics in order to reduce noise.

Using Table 29.1, select the type of material and compare its structure and properties with those of the working layer of the cementable steel Grade 12XH3A which is used for making heavy-duty gears.

No. 357. Pipes for supplying cooling liquids in machine tools and some other mechanisms must be made of easily washable transparent materials.

Select the type of material and compare its properties with those of stainless steel Grade 10X13 used for making pipes.

No. 358. Gearbox covers, handles and like parts not subjected to high mechanical loads are recommended to be made of light-weight materials (with a density of not higher than 1.5 g/cm^3).

Recommend the composition of such a material and compare its properties with those of steel grade Cr. 3, formerly widely used for the purpose.

No. 359. Lips and scoops of earth-digging machines, made of carbon steel, are subject to rapid wear due to intensive friction work in soil. The durability of the lips and scoops can be increased several times by making them of austenitic alloy steel possessing an increased wear resistance at impact loads.

Name the composition of such a steel, its heat-treatment conditions, structure and properties, and explain why this steel has a high wear resistance under the given operating conditions.

For comparison, name the type of steel that should be used for the manufacture of machine parts operating under conditions of impact-free rolling friction on metal.

No. 360. Jaws and balls of ore and rock grinding mills operate under heavy wear and impact conditions.

Select the grade of steel for their manufacture and name its composition and properties, including machinability.

Recommend the most effective technological process for the manufacture and heat treatment of the jaws and balls. What is the structure of steel in the finished components?

No. 361. Medium-module spur gears are being manufactured of steel Grade 45 and strengthened by induction hardening with surface heating. But with this method the tooth spaces remain unhardened, so that the manufactured gears have a low durability.

Recommend the grade of steel and the method of its treatment to ensure the hardening of the gears over their whole contour, and hence, their strengthening over the whole surface. Name for comparison the composition of carbon or low-alloy steel suitable for the manufacture of the gears with subsequent strengthening by chemical heat treatment.

No. 362. Gears made of steel Grade 40X and hardened to 40-42 HRC, when operated under high loads, including dynamic ones, have been found to develop cracks at low ambient temperatures.

Explain the causes of this defect and recommend a better grade of steel whose toughness will decrease only slightly with the temperature changing from $+20$ to -60°C .

No. 363. Recommend the composition (grade) of steel and the method of its metallurgical conversion for the manufacture of critical gears intended to operate at temperatures between -60°C and $+60^{\circ}\text{C}$.

The yield strength of steel must be at least $75\text{-}80\text{ kgf/mm}^2$.

Name the factors that are favourable for reducing the limit of cold shortness of the metal, and the heat-treatment conditions and mechanical properties of the finished components.

No. 364. To prevent brittle fracture, the elements of refrigerating machines are manufactured of steels or alloys having a low limit of cold shortness and correspondingly high toughness at low temperatures.

Recommend the composition of steel for the refrigerator elements operating at a temperature of: (a) -70°C ; (b) -259°C (in liquid hydrogen).

Explain the differences in the structure, and hence, in the composition of these two steels.

No. 365. Instrument springs are being manufactured of steel Grade 70C2XA hardened to 40-44 HRC. However, the characteristics of these springs often change when heated even to a low temperature, as their elasticity modulus changes. This reduces the accuracy of the instruments.

Recommend an alloy for making springs whose elasticity modulus will be almost constant at temperatures between -50 and $+100^{\circ}\text{C}$.

Compare the hardening conditions for steel Grade 70C2XA and the alloy selected.

No. 366. Parts of hydraulic pumps, in particular valves, were being manufactured of steel Grade 40X. In more powerful pumps with appreciably higher flow speeds the surface of such valves was found to erode rapidly.

Explain why these changes in the pump operating conditions resulted in wear of the valves, and describe the phenomena responsible for this.

Recommend the composition of steel having appropriate durability (a) at high water flow speeds and (b) in sea-water pumps.

No. 367. Recommend two types of material ensuring the lowest possible coefficient of friction for the manufacture of gears of mechanisms intended for use in the tropics:

(a) with the least density, to be used at relatively low stresses;

(b) with a high density, to operate at high stresses.

No. 368. Many steam boilers of power stations operate at a pressure of 500 at and temperature of 600°C . The steel for the manufacture of such boilers must have a high creep resistance.

Name the composition, grade and structure of steel suitable for operation under such conditions.

Compare the characteristics of the selected steel with those of another grade of steel usually used in boilers operating at temperatures of $300-400^{\circ}\text{C}$.

No. 369. Steel for the manufacture of superheaters of high-pressure boilers must retain its good mechanical properties under long-term loads and temperatures of the order of 500 °C, and have sufficient ductility to allow for cold deforming processes (bending, beading, etc.) to be carried out during the boiler assembly.

Name the composition, microstructure and mechanical properties of the steel at room temperature and at a high temperature (400-500 °C).

What are the principal differences between this steel and boiler carbon steel?

No. 370. Many elements of petroleum cracking plants, in particular cracker pipes, are subjected to high temperatures.

Select the composition of steel for pipes not subjected to high loads, but heated to 450-500 °C and 600 °C.

Specify the heat-treatment conditions and name the microstructure obtained; explain the role of alloying elements which make the steel suitable for long operation at high temperatures.

No. 371. Many steam turbine components, such as turbine blades, operate at high temperatures (400-500 °C) and are acted upon by steam and moisture. Steel for making such components must possess high creep and corrosion resistance.

Select the grade of steel for the blades, name its composition, heat-treatment conditions and microstructure in the finished component.

What are the mechanical properties of this steel at 20 and 500 °C? Compare them with those of quality carbon steel of the same carbon content.

In what direction must the composition and microstructure of this steel be changed to make it suitable for operation at temperature up to 600-650 °C?

No. 372. The blades of jet and turbojet engines operate at high temperatures (up to 800-900 °C) in an oxidizing medium. Alloys for making them must possess high corrosion resistance (scale resistance), high creep resistance, and high long-term strength at these temperatures.

Select the composition of an alloy and methods of its heat treatment. How will the properties and structure of the alloy change in the course of this treatment?

No. 373. Blades and other parts of high-power jet engines for short-term operation are subjected to strong oxidation at high temperatures (1000-1500 °C). The metal for their manufacture must possess high corrosion resistance and high short-term strength at the temperatures indicated. Select a metal or alloy for the manufacture of these components, name its composition and properties and a method providing protection against oxidation.

No. 374. Many elements of instruments and mechanisms employed on sea-going ships must be stable against the action of water, water vapours and atmospheric air and be additionally resistant against the stronger corroding action of sea water.

Select the composition of steels which will be suitable for this purpose. Describe their grades, composition, heat-treatment conditions, microstructure, and mechanical properties.

At the same time indicate the composition and grade of a non-ferrous alloy which is stable against the action of sea water. Compare the structure, mechanical and physical properties of the selected steels and non-ferrous alloy.

No. 375. Many elements of seaplanes are made of high-strength steel (σ_t at least 120 kgf/mm²); these elements should be additionally stable against sea-water corrosion.

Select the grade of steel and describe its composition, structure, and mechanical properties after hardening.

Select a method of treatment for the selected steel, which will increase its ultimate strength to 120 kgf/mm², and indicate how other mechanical properties of the steel will be changed through this treatment.

No. 376. Cables of marine aircraft must have high ultimate strength (80-100 kgf/mm²) and high resistance to sea-water corrosion.

Indicate the composition and structure of steel stable against the corrosive action of sea water (without protective coatings) and the process used for the manufacture of cables to ensure their high mechanical properties.

Compare the structure, corrosion resistance and welding properties of the selected steel with those of chromium steel containing 14 per cent Cr and 0.1 per cent C.

For further comparison, give the mechanical properties, conditions of treatment and structure of steel suitable for the manufacture of cables which are not subjected to sea-water corrosion.

No. 377. Some grades of chromium stainless steel possess high resistance to a number of aggressive media, but after welding they become sensitive to intercrystalline corrosion in the zones near the welds.

Name the composition, heat-treatment conditions and macrostructure of stainless steel stable against the action of organic acids. What component must be present in steel to make it resistant against intercrystalline corrosion after welding?

Explain the causes of intercrystalline corrosion.

Compare the composition, structure, heat-treatment conditions and field of application of the selected steel with similar cha-

racteristics of a chromium stainless steel having the same carbon content.

No. 378. Magnetic cores of radioengineering devices are made of magnetically soft metallic alloys possessing high magnetic permeability and low remagnetization and eddy-current losses. But these alloys become unsuitable with a sharp increase of the field frequency up to 50 MHz, because of very high eddy-current losses.

Indicate: (a) a suitable material and the method for the core manufacture; (b) the composition of metallic alloys suitable for cores operating at medium frequencies.

No. 379. A works produced vibration-frequency sensors for instruments used for controlling the pressure and flow rate of gases, liquids, etc. Elastic elements of the sensors were made of low-alloy spring steel Grade 50XΦA hardened to 42-45 HRC.

Now the works has to manufacture sensors for the pressure and flow rate control of aggressive oxidizing media, which necessitates the use of corrosion-resistant ferromagnetic steel for the sensors.

Indicate the composition of a suitable steel with the minimum content of expensive alloying elements and recommend the heat-treatment conditions to ensure a hardness of 42-45 HRC.

Compare these heat-treatment conditions with those employed for spring steel Grade 50XΦA.

No. 380. A works produced precision moving-coil instruments (oscillographs, galvanometers, millivoltmeters, etc.) whose operating principle is based on the interaction of the magnetic field formed by the measuring system with that of a permanent magnet. Alloy Grade ЮНДК 24 (see Table 27.24) was used for making these instruments. Now it has been decided to employ an alloy of a higher magnetic energy in order to improve the sensitivity and reduce the dimensions of the magnets, and hence, of the instruments.

Describe the composition, heat-treatment conditions and properties of a new alloy that will meet these requirements.

Compare the properties and heat-treatment conditions of this alloy with the same characteristics of alloy Grade ЮНДК 24, and explain why the new alloy has a higher magnetic energy.

Chapter Twenty-five

PROBLEMS ON TOOL STEELS AND ALLOYS

No. 381. The durability of drills and milling cutters made of high-speed steel Grade P12 of a moderate heat resistance was satisfactory for cutting structural steels with a hardness number of 180-200 HB, but became very much less when cutting heat-resistant austenitic steel.

Recommend a grade of high-speed steel having a higher heat resistance to efficiently cut heat-resistant steels, and describe its composition, heat treatment, and microstructure in the finished tool.

Compare the heat resistance of steel Grade P12 with that of the chosen steel.

Solution. Cutting tools for highly productive machining are made of high-speed steels as these have a high heat resistance; at high temperatures (up to 500-650 °C) developing at the cutting edge they retain their martensitic structure and high hardness.

However, the durability of cutting tools made of high-speed steel and subjected to optimum heat treatment depends not only on their composition, structure, and cutting conditions, but, to a large measure, on the properties of the metal being machined.

When cutting steels and alloys of austenitic structure (stainless steels, refractory steels, etc.), which are finding an ever wider use in industry, the durability of tools and the maximum cutting speed can reduce appreciably compared with those when cutting common structural steels and cast irons having a relatively low hardness (up to 220-250 HB). This is explained mainly by the fact that austenitic alloys have a lower thermal conductivity, because of which the heat evolved during cutting is only poorly absorbed by the chips and component being machined and is mainly transferred to the cutting edge. In addition, these alloys are strongly liable to work-hardening under the cutting edge in the course of cutting, because of which the cutting force increases substantially.

Such materials, which are classed as poorly machinable, are not suitable for machining with high-speed steels of moderate heat resistance which retain a high hardness (60 HRC) and their martensitic structure only at temperatures below 615-620 °C. High-speed steels of a higher heat resistance, in particular, cobalt steels, should be selected for machining austenitic steels and alloys. In tempering, cobalt promotes the precipitation of intermetallide particles together with carbides, these intermetallides being more stable against coagulation, and impedes the diffusion processes occurring at the temperatures of the cutting edge heating. Cobalt steels can retain their high hardness (60 HRC) when heated to higher temperatures (640-645 °C). Besides, cobalt increases noticeably (by 30-40 per cent) the thermal conductivity of steel, and therefore, favours a temperature reduction at the cutting edge owing to a better heat transfer into the tool body. Finally, cobalt-containing steels have a higher hardness (up to 68 HRC in steel Grade P8M3K6C).

Cobalt steel Grades P12Φ4K5 and P8M3K6C are recommended for drills and milling cutters used for machining austenitic alloys. Their heat treatment does not differ from that of other high-speed steels and is basically as follows.

Tools are hardened from very high temperatures (1240-1250 °C for steel Grade P12Φ4K5 and 1210-1220 °C for steel Grade P8M3K6C), which is needed for the dissolution of a major portion of carbides and saturation of austenite (or martensite) with the alloying elements — tungsten, molybdenum, vanadium, and chromium. A higher temperature, which might accelerate the passage of carbides into the solution, is inadmissible, since it can cause the growth of grains, and therefore, reduce strength and toughness. The structure of the steel after hardening is martensite, residual austenite (15-30 per cent) and precipitated carbides which are insoluble on heating and retard the growth of grains. The hardness of the hardened steel is 60-62 HRC.

The tools are then tempered at 550-560 °C (three times of 60 minutes each), these tempering operations causing (a) precipitation of disperse carbides and intermetallides from the martensite (precipitation hardening), which increases the hardness number to 66-69 HRC; (b) transformation of the soft component (residual austenite) into martensite; and (c) removal of the stresses caused by the martensitic transformation.

After tempering, the tools are ground and then subjected to cyaniding, most often in a liquid mixture of NaCN (50 per cent) and Na₂CO₃ (50 per cent), with a holding time of 15-30 minutes (depending on the cross-sectional area of the tool).

The hardness of the cyanidized layer (0.02-0.03 mm thick) rises to 69-70 HRC and the heat resistance of the metal also increases slightly (approximately by 10 degrees C). The heating before cyaniding also removes the stresses formed during grinding. Cyaniding can increase the durability of tools by as much as 50-80 per cent.

After cyaniding, it is advisable to steam-heat the tools to 450-500 °C and cool them in oil; their surface then becomes blue and obtains a slightly better resistance against air corrosion.

No. 382. Select a steel for hob cutters to be used for milling structural steels with a hardness of 220-240 HB.

Explain why carbon tool steel Grade Y12 which has a high hardness (63-64 HRC) is unsuitable for this purpose.

Recommend the heat-treatment conditions for the cutters from the selected high-speed steel, assuming that they are made of rolled rods 40 mm in diameter.

No. 383. A shop is to manufacture gear cutters to machine structural steels with a hardness of 200-230 HB under dynamic load conditions.

Choose the grade of high-speed steel most suitable for the purpose, recommend its heat-treatment conditions, and describe its structure and properties (for the cutters with an outside diameter of 60 mm).

No. 384. A shop manufactured broaches of high-tungsten steel Grade P18. Decide whether it is possible to use a less alloyed, and hence cheaper steel for the same purpose.

Select the grade of steel suitable for making broaches to machine structural steels with a hardness of up to 250 HB, describe the heat-treatment conditions, structure and properties for the cases when the broaches are to be made from rolled rods 40 and 85 mm in diameter.

No. 385. A shop manufactures hob cutters of two sizes — 30 and 80 mm in the outside diameter — the material being high-speed steel rolled stock of the corresponding cross section.

Select the grade of high-speed steel of a moderate heat resistance and recommend the heat-treatment conditions.

Name a method of chemical heat treatment which can additionally increase the durability of the cutters.

Explain what the differences are in the structure and properties of high-speed steel in rolled rods 30-32 mm and 80-82 mm in diameter.

No. 386. Tools made of high-speed steels have an insufficient durability when cutting at increased speeds (above 80-100 m/min).

Select tool alloy grades suitable for the high-speed cutting of (a) steels and (b) cast irons.

Describe the composition, structure and properties of the selected alloys and compare them with similar characteristics of high-speed steels. Explain why alloys of different compositions must be used for machining steel and iron.

No. 387. Two grades of high-speed steel are available: (a) tungsten-molybdenum steel Grade P6M5 and (b) cobalt steel Grade P12Φ4K5.

Explain the differences in the basic properties of these steels and recommend the optimum use for each.

Describe the heat-treatment conditions for these steels and their structure and properties in the finished tools 20 and 60 mm in diameter.

No. 388. A machine shop lathe-turns cast-iron and steel components at high cutting speeds.

Select alloys for making cutting tools ensuring high productivity when machining (a) steel and (b) cast iron.

Describe the composition, structure, hardness, strength, and heat resistance of these alloys and the method of tool manufacture, and compare them with similar characteristics of high-speed steel.

No. 389. Cutting tools made of high-speed steel have a poor durability when machining steels with a hardness of more than 280-300 HB.

Indicate the composition of an alloy possessing better cutting properties.

Since this alloy is expensive and highly brittle, indicate the method of the manufacture of inserted cutter tools and name a metal for making the cutter holders.

Compare the structure, hardness, heat resistance and method of manufacture of the selected alloy with similar characteristics of high-speed steel.

No. 390. A machine-building works manufactures machine parts under various cutting conditions: alloy steels with a hardness of 300-350 HB are machined at high speeds with cutting tools; steels having a hardness of 200-220 HB, with thread milling cutters at moderate cutting speeds; and steels of a hardness of 120-140 HB, with threading dies 60 mm in diameter at low cutting speeds.

Select the grade of alloy (steel) for each of the above tools, substantiate your choice, and compare the microstructure and basic properties of the selected materials.

No. 391. Select the grade of alloyed tool steel for making round threading dies to cut soft low-alloy steel.

Name the heat-treatment conditions and methods for protecting against decarbonization and oxidation during hardening.

Compare the composition, microstructure, basic properties, and the field of application of the selected steel with those of high-speed steel.

No. 392. Measuring instruments (limit gauges, gauge blocks, etc.) should possess not only high hardness and wear resistance, but also the property of retaining their dimensions with time. On the other hand, articles after hardening and low tempering sometimes show slight changes in their dimensions during operation, a fact inadmissible for high-precision instruments.

Indicate the causes of these changes (ageing), and name the grade of steel and the heat-treatment conditions for the measuring instruments, which can appreciably reduce the ageing effect.

No. 393. Many measuring instruments of a plane shape (templates, rules, sliding calipers, etc.) are made from sheet steel; their working edges must possess high wear resistance.

Indicate the heat-treatment conditions to ensure these properties, if the instruments are to be made in large batches from steel Grades 15 and 20.

No. 394. A machine-building works manufactures gears from steel rods (steel Grade 40X) supplied by a steelmaking works, the hardness of the steel being 160-180 HB. The steel in one batch supplied by the steelmaking works turned out to have a hardness of 230-250 HB. Because of the higher hardness of the steel in this batch its machining would have made it necessary to lower the cutting speeds adopted at the works.

Indicate the method and heat-treatment conditions which will enable the machinability of the steel in this batch to be improved.

Name the composition, structure and heat-treatment conditions of steel suitable for making milling cutters to machine steel Grade 40X.

No. 395. Producing billets by hot deforming is an efficient method of metal processing.

Select the grade of steel for making a large forging die ($500 \times 400 \times 400$ mm), recommend its heat-treatment conditions, and indicate the microstructure and mechanical properties of the metal after tempering.

Explain why such dies should not be made of carbon steel.

No. 396. Cylinder sleeves of internal combustion engines are made of steel by hot die-forging. The internal cavity is formed by piercing, i.e. by pressing the piercing punch into the heated metal held in a counter die. The punch operates under the conditions of alternating heating (during piercing) and cooling (after piercing).

Indicate the temperature of the die-forging (piercing) of billets, if these are to be made of steel Grade 50.

Select the grade of steel for making piercing punches 40 mm in diameter, substantiate your selection; indicate the conditions of heat treatment and the structure of steel in the finished punch.

No. 397. Upper dies for hot pressing must be made of heat-resistant die steel, since they must for a long time be in contact with the hot metal being deformed.

Select the grade of steel for hot pressing refractory alloys; the die steel for these processing conditions should retain its high strength at temperatures up to 700-720 °C.

Recommend the heat-treatment conditions of the upper dies and the structure of the steel in the finished die.

No. 398. Dies of a complicated shape, especially those with internal holes, can deform strongly upon hardening.

Recommend the temperature for hardening dies made of high-chromium steel Grade X12M so as to appreciably reduce their deformation.

What is the structure of the steel after hardening and what is the cause of the reduced deformation?

No. 399. Dies for cold stamping steel sheets should have high wear resistance and as high a toughness as possible.

Select steel for this purpose and recommend heat treatment for it. Indicate the hardness number obtained and the structure of the steel.

In which die (with the shorter side of 50 mm or 90 mm) will the steel have a higher strength and toughness? What causes this difference?

No. 400. Dies for cold embossing of copper alloys and soft steels must combine high hardness and resistance to plastic deformation (to prevent premature crushing of the die impression) with appropriate toughness.

Select steel for making embossing dies and their heat-treatment conditions, and indicate the structure of the metal in the finished die.

Explain why high-carbon steels (appr. 1 per cent C) are not suitable for this purpose.

No. 401. Plastic articles are made by pressing after a low heating (appr. to 150 °C). The material of the pressing mould should possess high wear resistance.

Select steel for the purpose and the heat-treatment conditions for the moulds: (a) of a simple shape and small dimensions and (b) of a complex shape (take into consideration that the steel must possess high machinability and, in addition, the deformation of the mould during heat treatment should be at its minimum).

No. 402. Pneumatic drilling bits used in mining must have a relatively high hardness (55-58 HRC) and a high wear resistance, but, on the other hand, must possess an appropriate toughness to withstand impact loads.

Indicate the composition and grade of carbon steel (for bits of a simple shape) and of alloy steel (for large bits of a complex shape) and the heat-treatment conditions ensuring the required structure and hardness.

No. 403. Select steel for making carpenter's axes. The edge of the axe should neither crush nor crumble when in use; for this reason it must have a hardness within 50-55 HRC to a distance of not more than 30-40 mm, the remaining part of the axe being left unhardened to have a lower hardness.

Indicate the composition of the steel, the heat-treatment conditions ensuring the required hardness of 50-55 HRC and the method of hardening in which only the cutting edge is hardened to this value.

No. 404. Select steel for making rip saws and their heat-treatment conditions. Name the structure and hardness number of the finished saw.

The heat-treatment conditions should be selected so as to prevent the deformation of a saw during hardening and tempering, and also to impart high elastic properties to the steel after tempering (the saw must be springy).

No. 405. The working sections of the casting moulds for pressure-die casting are heated to a high temperature and at each pouring of liquid metal are alternatively subjected to heating and cooling, and also to erosion.

Select steel suitable for making casting moulds to die-cast aluminium alloys and characterize its stability against fire cracking. Recommend the heat-treatment conditions and describe the structure and properties of steel in the finished mould.

Chapter Twenty-six

PROBLEMS ON NON-FERROUS METALS AND ALLOYS

No. 406. The worm of a reducer gear is often made of steel and the rim of the worm wheel, of a copper-base alloy in order to minimize friction.

Select the composition and grade of an alloy to make the wheel rim for it to have good anti-friction properties and an ultimate strength σ_t of not less than 25 kgf/mm².

Explain how the mechanical properties of the alloy will change depending on its casting conditions (i.e. either sand casting or chill casting).

For comparison, give the composition, heat treatment, structure and mechanical properties of steel suitable for making the reducer worm 30 mm in diameter, if its ultimate strength should be not less than 70 kgf/mm².

No. 407. Many articles are manufactured of sheet metal by deep drawing.

Select the composition of a non-ferrous alloy possessing high plasticity and good drawability; describe its structure.

Indicate purpose and the conditions of the heat treatment employed between individual drawing operations to increase the metal's plasticity; describe the mechanical properties of the metal after drawing and after heat treatment.

Give the composition of steel suitable for deep drawing and compare the mechanical properties of the non-ferrous alloy selected with similar characteristics of the steel.

No. 408. Certain types of bolts, screws, nuts, etc. are made of brass on high-speed automatic machine tools, but the surface of the machined components is rough, if the brass employed has high toughness and plasticity.

Select brass which will provide a clean machined surface with high productivity of the machining. Compare its properties and structure with similar characteristics of brass of high toughness and plasticity.

No. 409. Fittings (cocks, valves, etc.) of boilers operating on fresh water and steam at a pressure of up to 25 at, as also connecting pipes and housings of measuring instruments (such as pressure gauges) operating under similar conditions, are made of non-ferrous alloys having high corrosion resistance.

Indicate the composition, structure, mechanical properties, and method of manufacture of (a) an alloy for making fittings, which must possess good castability and machinability; (b) an alloy for making pipes and housings of instruments, which must have high plasticity in the cold state.

No. 410. Some mass-produced cast elements of fittings for turbines, boilers, hydraulic pumps, etc. have a rather complex shape, and are intended for operation in a moist atmosphere. In the casting process, the maximum accuracy of their dimensions must be ensured.

Name the composition of a non-ferrous alloy suitable for the purpose, and also its structure and mechanical properties. What casting method can ensure the required high dimensional accuracy with the minimum subsequent machining?

Name the composition of steel suitable for making moulds for casting the said alloy and indicate the heat-treatment conditions and the final structure of the steel in the mould.

No. 411. Many elements of instruments and devices subjected to the action of sea water are manufactured by cold deforming non-ferrous alloys in a number of operations.

Select an alloy which will be stable against the action of sea water and name its composition.

Indicate the conditions of intermediate heat-treatment operations for the selected alloy and its mechanical properties after deforming and after heat treatment.

For comparison, give the composition, mechanical properties and structure of steel stable against sea water, and indicate the conditions of its heat treatment.

No. 412. Pipes of steam power plants must be corrosion-resistant.

Select the grade of a copper-base alloy suitable for making pipes, but containing no expensive elements; name the composition of the chosen alloy.

Indicate a method for the manufacture of pipes and compare the mechanical properties of the selected alloy after its final heat treatment with the mechanical properties of steel which is corrosion-resistant in the same media.

No. 413. Many articles are made by cold drawing brass sheets. Cracks may form in some articles without any external load ap-

plied (what is called 'season cracking'). Figure 26.1 shows a deep-drawn article which cracked during storage.

Explain this phenomenon and name methods to prevent it.

Select a grade of brass not liable to season cracking. In addition, describe the structure, mechanical and technological properties of α - and $\alpha + \beta'$ -brasses.

Solution. Brasses can be classed into the following three groups according to their zinc content and structure:

1. α -brasses up to 39.5 per cent Zn
2. $\alpha + \beta'$ -brasses . . from 39.5 to 45.7 per cent Zn
3. β' -brasses from 45.7 to 51 per cent Zn

Thus, the structure and properties of brass vary with its zinc content (Fig. 26.2).

Increasing the zinc content to a definite limit increases the plasticity and strength of the metal. Plasticity reaches the maximum value at 30-32 per cent Zn, and strength, at 40 per cent. A further increase of the zinc content causes the reduction of both the strength and plasticity.

These changes are determined by the properties of the respective phases being formed with the addition of zinc.

The α -phase is a solid solution of the substitutional type and its plasticity and strength increase with the zinc content.

The β' -phase is a solid solution on the basis of an electron compound with a cubic lattice and ordered location of atoms. This phase has high brittleness and hardness, and hence reduces toughness and increases hardness.

On heating above 450 °C, β' -phase is transformed into a disordered β -solid solution whose plasticity is greater than that of the β' -phase. As can be seen from the constitutional diagram, $\alpha + \beta'$ -brasses after such heating obtain a homogeneous structure of β -solid solution, and therefore, a higher plasticity (see Fig. 9.16).

These properties of the phases suggest the technological process for the manufacture of articles from various types of brass and also determine their purpose. Articles of α -brass are manufactured mostly by cold or hot deforming; machining cannot provide the appropriate surface finish. Articles of $\alpha + \beta'$ -brass can be made by hot deforming (pressure moulding, die-forging), cold deforming (but without drawing), or machining.

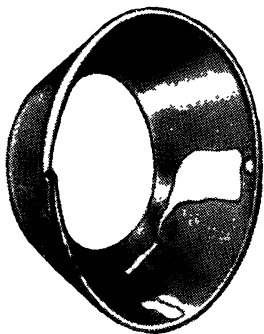


Fig. 26.1. Cracking of a brass article after deep drawing and storage

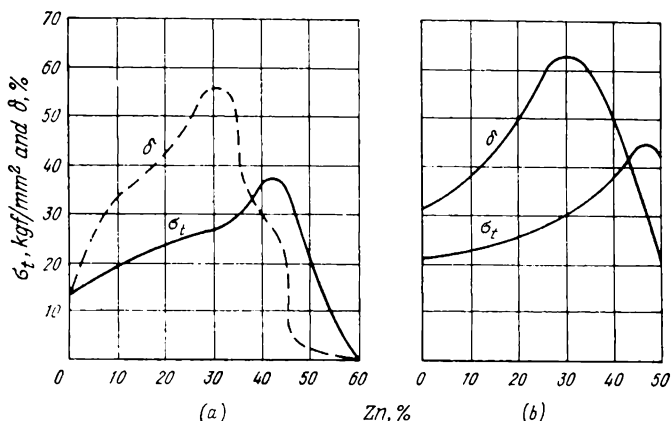


Fig. 26.2. Mechanical properties of brass, depending on zinc content
(a) cast brass; (b) rolled and annealed brass

Articles of α - and $\alpha + \beta'$ -brasses are employed in the annealed or work-hardened state, since their heat treatment (hardening and tempering) cannot produce a noticeable effect. Work-hardened brass (i.e. after cold deforming) has high strength and reduced toughness (see Fig. 26.2).

Subsequent annealing reduces the strength and increases the plasticity of the alloy (Fig. 26.3).

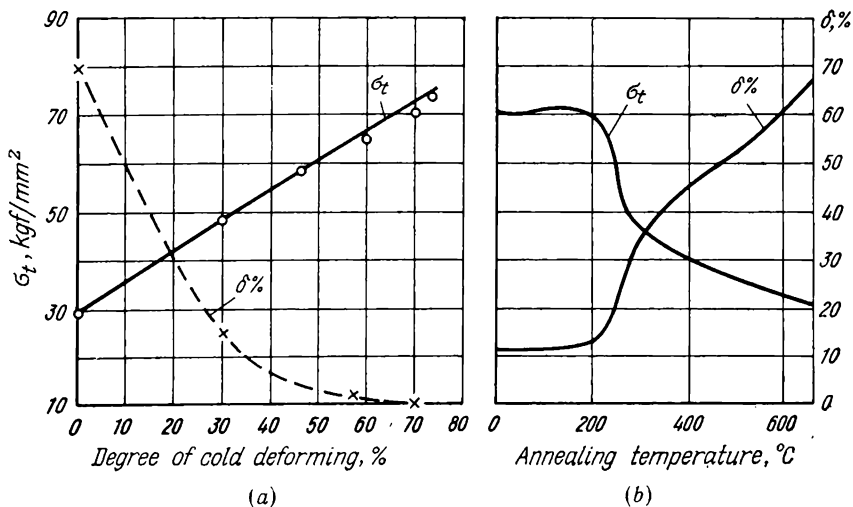


Fig. 26.3. Mechanical properties of brass Л68 depending on
(a) degree of deformation; (b) annealing temperature

The cold deforming of brass causes residual stresses in the articles, as also does local cold deforming (during bending, embossing, beading, etc.). Cracks sometimes form in brass articles during storage or operation. Season cracking is mainly observed in brasses containing more than 20 per cent Zn, especially in hollow articles, rods, and the like. Season cracking is enhanced in chemically active media, especially in ammonia vapours, mercury salts, mercury, soapy water, etc. These cracks result from the combined action of the residual stresses formed in cold deforming (tensile stresses being most dangerous) and chemically active media.

To prevent season cracking, brass articles must be annealed at 200-300 °C; this removes the majority of the residual stresses and has only a slight effect on strength.

However, during the manufacture and assembly of structures, involving flaring, bending, etc., it is not always possible to avoid local, let them be small, deformations, and therefore, season cracking. In such cases use is made of more expensive brass Grades Л196 and Л190 which have a lower strength, but are not liable to season cracking.

The mechanical properties and composition of these brasses, of brass Grade Л170 which is widely used in industry, and of the typical $\alpha + \beta'$ -brass Grade ЛС59-1 are given in Table 26.1.

Table 26.1. Composition and Mechanical Properties of Brasses

Structural class of alloy	Grade	Composition, %				Mechanical properties	
		copper		Impurities	zinc	σ_t , kgf/mm ²	δ , %
		average	allowance			at least (after rolling and annealing)	
α -brass	Л1-96	96	± 1	≤ 0.30	balance	23	35
	Л1-90	90	± 1	≤ 0.30		27	38
	Л1-80	80	± 1	≤ 0.30		28	45
	Л1-70	70	$+2$	≤ 0.30		30	55
$\alpha + \beta'$ -brass	ЛС59-1	59 Pb	$+1-2$ 0.8-1.9	0.75	balance	35 40 *	30 15 *

* For annealed strips and sheets and pressed rods.

Л196 and Л190 brasses possess a high thermal conductivity.

Brasses can be replaced by an aluminium bronze, provided this is not liable to season cracking and has commensurate strength and plasticity.

No. 414. Screw propellers of sea-going ships usually have a complex shape and very large mass; for instance, the mass of the screw propeller of a modern large ocean-liner may be as large as 30-50 tons.

Design a technological scheme for the manufacture of such a propeller, taking into consideration its shape. On the basis of this scheme and the operating conditions of the propeller (in sea water), select a suitable alloy, and describe its composition, structure and mechanical properties.

For comparison, give the composition, structure and mechanical properties of stainless steel which is stable against sea water corrosion; explain why stainless steels are not recommended for making screw propellers of ships.

No. 415. Special brasses are used in the chemical engineering industry to cast heavy-loaded corrosion-resistant elements.

Select the grade of a suitable alloy having an ultimate strength of not less than 45 kgf/mm^2 , give its composition, mechanical properties and structure; and indicate the media in which the alloy will be stable.

Compare the mechanical properties of the brass of the selected composition with similar characteristics of the brass Grade JIC59-1 and indicate the field of application of the latter.

No. 416. Gears are to be made of an alloy having appropriate stability in water and steam and providing for low friction. The ultimate strength of the alloy must be not less than 35 kgf/mm^2 .

Explain why stainless steel, which is corrosion-resistant in water and steam, is inapplicable in such cases.

Indicate the composition and structure of a non-ferrous alloy containing no expensive elements, which is suitable for making these gears.

No. 417. Crankshaft and crankpin bearing bushings of internal combustion engines are made of bronze containing no especially expensive elements and possessing high anti-friction properties.

Select the composition of a suitable alloy, name its structure and mechanical properties; indicate a method for the manufacture of components from this alloy; explain why the selected alloy has high wear resistance.

For comparison, give the composition and structure of other anti-friction materials having a lower melting point and used for bearing lining.

No. 418. The frames of subsonic aircraft are subjected to appreciable loads and are often made of a light alloy having an ultimate strength of not less than 40 kgf/mm^2 .

Select the composition of a suitable alloy and give its density, structure and heat-treatment conditions. Indicate the mechanical

properties of the alloy after each heat-treatment operation and explain which transformations in the alloy are favourable for increasing its strength.

Compare the mechanical properties of the alloy with those of chrome-nickel stainless steel. Consider in this comparison that the specific strength of the elements at a given temperature must be not less than a certain tolerable limit.

No. 419. Some elements of aircraft, for instance, control rods are made of light alloys with an ultimate strength of not less than 40-45 kgf/mm², in order to make them capable of withstanding high-operating loads.

Give the composition and density of a suitable alloy, describe the heat-treatment conditions, and indicate the structure and mechanical properties obtained after each heat-treatment stage. Which methods can be recommended to increase the corrosion resistance of the components made of this alloy?

Some of these heavy-duty elements may alternatively be made of an alloy having a density of 4.5 g/cm³ and yield limit of 75 kgf/mm², and possessing high corrosion resistance (in particular, in sea water). Name an alloy to suit these more rigorous requirements.

No. 420. With an appreciable increase of the speed (above the sonic speed) of aircraft and other flying vehicles, their shells and other structural elements are heated substantially, so that commonly used aluminium alloys turn out to be inapplicable under such conditions.

Recommend an alloy having improved mechanical properties and high specific strength at temperatures up to 400-500 °C, based on a metal with a density of 4.5 g/cm³.

Give the composition of the alloy and its properties at normal and increased temperatures.

No. 421. Pipes and other elements operating in hot nitric acid and solutions of chlorides must be made of an alloy having a corrosion resistance higher than that of stainless steel.

Select from Table 27.19 an alloy grade and characterize its corrosion resistance as compared with that of steel Grade 12X18H10T.

No. 422. Rotating elements of many jet engines, which are heated to 500-600 °C, must be made of alloys with a density (appr. 4.5 g/cm³) lower than that of steel.

Select an alloy grade and compare its heat resistance (long-term strength after 1000 hours) at 500 °C with similar characteristics of (a) duralumin and (b) heat-resistant steel Grade 12X18H10T.

No. 423. Seamless pipes of distilling plants to supply sea water heated to 80-120 °C are recommended, for better durability, to be made of an alloy having an appreciably greater corrosion resistance than stainless steel.

Select an alloy and compare its properties with those of stainless steel Grade 12X18H10T.

No. 424. Stainless steels, including high-alloyed steels of the austenitic class, are poorly resistant to hydrochloric acid.

Select a metal with a density of approximately 4.5 g/cm³ to make tanks and pipelines which will possess high stability under the given conditions. Compare its mechanical properties with similar characteristics of stainless steel Grade 12X18H10T.

No. 425. The elements of aircraft wheels, units, instruments, etc., which have a complex shape and are not subjected to high mechanical loads, are cast from light alloys (with a density of 2.7 g/cm³) possessing good castability.

Select an alloy, give its microstructure and methods of treatment for improving its mechanical properties (in the course of melting). How does the structure of the alloy change during this treatment?

Name iron-base casting alloys for which similar methods of improving their structure and mechanical properties are employed.

No. 426. Aircraft components of a relatively complex shape (pedals, levers, pedal supports, etc.) are made of alloys having good casting properties and, in addition, good machinability. The ultimate strength of the alloy should be not less than 22 kgf/mm².

Recommend the composition of an alloy and the conditions of its heat treatment. Give the structure and mechanical properties of the metal in the finished components.

Compare the mechanical properties and heat-treatment conditions of the alloy with similar characteristics of a plastically deformable aluminium-base alloy.

No. 427. Cylinder heads of aircraft piston engines which operate at high temperatures are cast in light alloys.

Give the composition of an alloy suitable for the purpose. Indicate the effect of the individual elements in its composition, and also its structure and mechanical properties.

No. 428. Pistons of many internal combustion engines are made of a deformable aluminium-base alloy with additions of certain alloying elements which make for the alloy to retain its high mechanical properties when heated to 250-300 °C.

Give the composition and properties of a suitable aluminium-base alloy, and also, recommend the composition of a titanium-base alloy having an increased strength at temperatures up to

400-500 °C and therefore, suitable for making engine pistons operating at temperatures higher than those indicated above.

No. 429. Petroleum and oil tanks of aircraft, whose material is not subjected to high mechanical loads, are welded from sheets of light alloys possessing high corrosion resistance, high plasticity, and good weldability.

Recommend an alloy suitable for the purpose and indicate its structure and mechanical properties.

For comparison, give the composition, heat treatment, and structure of steel having the same corrosion resistance.

No. 430. The power of internal combustion engines can be increased by reducing the mass of their pistons.

Recommend an alloy of a minimum density to suit this purpose. Indicate its composition, mechanical properties and heat-treatment conditions.

Compare the density and mechanical properties of the selected alloy with similar characteristics of the aluminium-base alloys employed for making pistons.

No. 431. Fuel and oil tanks and some other components of aircraft are made of an alloy with a density of 1.7 g/cm³, which has high plasticity when heated, high corrosion resistance, and good weldability (permits long welds).

Indicate the composition, structure and mechanical properties of this alloy.

Compare its composition, structure, mechanical properties and density with similar characteristics of materials (an aluminium alloy and an alloy steel) which are stable against sea water and moisture.

No. 432. Many instruments and devices of automatic control systems use elastic elements which, apart from having high strength ($\sigma_t \geq 100$ kgf/mm²), should possess high electric conductivity and high corrosion resistance.

Recommend an alloy for making these elastic elements to suit the above requirements and give the conditions of heat treatment to improve its strength characteristics.

No. 433. Chemical engineering widely uses chrome-nickel stainless steels, but some especially critical elements are made of a nickel-base alloy possessing high plasticity and high stability against the action of moisture, acids, and alkalis.

Give the composition of the alloy, its structure and conditions of application in structures (as regards its contact with other metals).

Compare its structure, mechanical properties and corrosion resistance in the indicated media with similar characteristics of chromium and chrome-nickel stainless steels.

No. 434. Many parts of modern mechanisms and machines are subjected to wear, but the conditions and nature of their wear may be different. For this reason use is made of wear-resistant materials which differ in their composition and properties.

Indicate and substantiate the cases of and the reasons for the application of (a) high-manganese austenitic steel; (b) hyper-eutectoid chromium steel (bearing steel); (c) brasses or bronzes; and (d) bearing alloys (babbits).

Indicate the composition and heat-treatment conditions of these alloys.

No. 435. The composition of an alloy for lining the bushings of crankshaft bearings is selected according to the engine power. Give the composition of a bearing alloy to be used for lining the bushings of turbocompressors and turbopumps of 500 HP or more.

Indicate the structure of the alloy and the principle of its composing, and the effect of its individual alloying elements. Compare the composition, properties and fields of application of this alloy with similar characteristics of a copper-base bearing alloy.

Part Seven

CLASSIFICATION AND INDUSTRIAL APPLICATIONS OF MATERIALS

Chapter Twenty-seven

CLASSIFICATION AND APPLICATIONS OF METALS AND ALLOYS

The number of metallic alloys employed industrially is very high (many thousand grades) and is continually increasing to meet the new and diversified demands of many industries. A unified classification of all metals and alloys by a single feature common for all of them is impossible, since their properties and applications differ greatly.

The classification of alloys by their composition based on indicating the principal component of an alloy (iron, copper, aluminium, etc.) is only suitable for dividing the alloys into a small number of large principal classes, but cannot be used for a more detailed classification of numerous alloys within a class.

It is also impossible to classify alloys within each of the classes mentioned by one or more characteristic properties possessed by all the alloys in a class. Some properties which are critical for some alloys (for instance, mechanical properties and hardenability for structural steels) are of secondary importance for other alloys in a class (for instance, for many steels with special physical or chemical properties, some tool steels, etc.).

It is therefore expedient to divide metals of a class into smaller groups and classify them by the characteristics that are most representative of all the alloys in a group.

These considerations are taken into account below in order to give a systematic description of all grades of alloys widely employed in industry, whose compositions are standardized and may be found in the specialist literature^{1, 2} and textbooks on the sub-

¹ *Materialy v mashinostroenii* (Machine-building Materials). A reference book. Volumes 1-5. Moscow, Mashinostroenie Publishers, 1969-70; *Metallovedenie i termicheskaya obrabotka* (Physical Metallurgy and Heat Treatment of Metals). A reference book. Volumes 1-2. Moscow, Metallurgizdat Publishers, 1961-62.

² The data given in this chapter are far from being exhaustive; they do not include some alloys whose compositions and industrial applications are still indeterminate.

ject. All alloys¹ are classed, according to their common division, into: (A) steels, (B) cast irons, (C) copper alloys, (D) aluminum alloys, (E) magnesium alloys, (F) titanium alloys, and (G) tin and lead bearing alloys (babbitts).

All alloys in a class are divided into groups, and the most numerous groups, as those of steels, into smaller subgroups. The distribution in a group or subgroup is most often done by the features of application of alloys in industry, and in some cases, by their composition or properties. This classification, which, on the face of it, may seem to lack uniformity, is based on the principal approach to classify all metals and alloys in each of the groups so as to characterize their most typical properties or applications.

A. STEELS. PRINCIPLES OF CLASSIFICATION AND DESIGNATION

Steels are the materials most widely employed in industry and represented in modern engineering by the largest number of grades. Their classifications which may follow different principles are discussed below.

Composition classification. This type of classification is mainly used for structural steels which are divided by this feature into carbon steels, chromium steels, etc., and more complex (quaternary) steels, such as chrome-nickel, chrome-silicon and some more complex grades. It is less common with other steels, such as tool steels, heat-resistant steels, or steels with special physical or chemical properties, since some of them are alloyed with three, four, or even five or six elements. Therefore, they should be divided into a great number of subgroups according to their composition. This would make this classification very cumbersome.

Besides, classification of these steels by their composition would be insufficiently representative. Many of these steels may differ largely in their compositions, but possess similar properties and are employed for similar purposes in industry, whereas composition classification would separate them into different groups.

Classification by manufacturing method. This classification defines the conditions of metallurgical manufacture and control of steels, and, in the first place, the content of harmful impurities in

¹ The metals and alloys which have found only a limited application (e.g. nickel-, molybdenum- and chromium-base alloys, sintered oxides, and alloys of metals with oxides and nitrides) are not classed into separate groups, but only quoted in the corresponding groups of steels to indicate that they may substitute these steels under heavier operating conditions.

them. According to this classification, all steels are divided into: (A) common (or plain) steels; (B) quality steels; (C) high-quality steels; and (D) superhigh-quality steels.

A. *Common steels* are steels with up to 0.6 per cent carbon, manufactured in either Bessemer converters (mostly oxygen-blown) or large open-hearth furnaces and cast into large ingots (or by continuous casting); for these reasons they are the cheapest in the group. They may have a higher content of sulphur and phosphorus than is tolerated in other quality groups: up to 0.055 per cent or even 0.060 per cent sulphur and up to 0.050-0.070 per cent phosphorus. Also more segregation is allowed in the common steels.

Besides, common steels may have a higher content of non-metallic inclusions than other quality grades. When rolled, they often may display banding along metal fibres; this defect is readily detected by macroscopic or microscopic examination, as has been shown in Chapters 2 and 3. Common steels are inferior to other steels in their mechanical properties.

The principal element determining the mechanical properties of common-quality steels is carbon. With increasing carbon content, the strength properties (ultimate tensile strength and yield limit) of steel increase, while its ductility reduces (see Table 27.1).

According to the purpose and characteristics specified by the manufacturer these steels are in turn divided by their mechanical properties (converter or open-hearth steel), composition [converter (more definitely, oxygen-converter) or open-hearth steel], and both composition and mechanical properties (improved-quality open-hearth steel).

Common steels delivered according to their mechanical properties are graded as given in the State Standard GOST 380-71 (see Table 27.1); those designated by a greater numeral having a higher carbon content and higher strength properties, but lower impact strength and ductility.

Besides, common steels are divided by the method of manufacture into killed, semi-killed and rimming grades.

Killed steels are those deoxidized not only by manganese, but also by silicon (ferro-silicon) that is a more active deoxidant, because of which they have a reduced content of oxygen and various oxides. The content of silicon in killed steels should be not less than 0.15-0.20 per cent (usually 0.15-0.35 per cent). The presence of silicon, even in such relatively small amounts, increases the yield limit and reduces ductility.

Rimming steels are not deoxidized with silicon and contain this element only as an impurity (≤ 0.1 per cent). Partial removal of the oxygen dissolved in the steel occurs during solidifi-

cation through interaction of the oxygen with the carbon of steel. Some bubbles of CO formed in this process float up into the top portion of an ingot (thus increasing the volume of the metal and causing 'boiling') and some remain in the bulk of solidified metal, thus forming what are called blowholes; these may be filled up in subsequent heat treatment of the metal.

Rimming steels have a lower yield limit than killed steels, with roughly the same ultimate strength and because of this are more suitable for cold rolling and then for deep drawing, in particular for making steel sheets for automobile industry and the like. They are, however, more prone to brittle fracture, especially at low temperatures, and operate at lower stresses and dynamic loads.

The content of carbon tolerated in rimming steels is 0.2-0.25 per cent, since the ductility of steel increases with lowering carbon content. Besides, a low carbon content is more favourable for filling in blowholes.

Semi-killed steels may contain up to 0.17 per cent Si, and their properties are somewhere between those of killed steel and rimming steel. They excel rimming steels as regards the yield limit and have a lower brittleness point. Semi-killed steels are employed, in particular, for cold extrusion of bolts and like articles.

B. *Quality steels* are carbon or alloy steels made most often in basic open-hearth furnaces with a more rigid control of the composition of the charge and the conditions of melting and teeming. Their sulphur and phosphorus contents should not exceed 0.035 per cent each. Besides, they have a lower content of non-metallic inclusions than common steels. Variations in carbon content of the same grade of quality steel must not exceed 0.08 per cent.

Quality steels for making sheets intended for deep drawing are melted as rimming steels, and as semi-killed if intended for cold upsetting.

C. *High-quality steels* are mainly alloy steels manufactured in acid open-hearth or electric furnaces. They have a still lower content of sulphur and phosphorus, below 0.025 per cent, and are less contaminated with non-metallic inclusions. Variations in carbon content of the same grade of high-quality steel must not exceed 0.07 per cent, i.e. within narrower limits than for quality steels.

D. *Superhigh-quality steels* are made in electric furnaces by the method of electroslog melting (or other advanced methods) and have the lowest content of sulphur (up to 0.015 per cent). The content of carbon and alloying elements is the same as in corresponding grades of high-quality steels. Steels made by the

electroslag melting have a lower content of gases. All this increases the impact strength, especially at low temperatures, lowers the point of brittleness (see Ch. 6), and increases ductility and contact endurance. Because of this superhigh-quality steels may have a higher strength and, at the same time, a higher hardness than is possible in steels made by the common technique.

All quality grades of steel are designated as follows: the first numeral gives the average content of carbon, as hundredths of a per cent for steels containing up to 0.7 per cent C (structural steels) or tenths of a per cent for those with a higher carbon content (mainly tool steels). For example, a steel having 0.07-0.14 per cent carbon is designated steel 10, that with 0.42-0.50 per cent C, steel 45, etc. while that containing 0.95-1.05 per cent will be designated Y10, etc.

Rimming steels are denoted with the letters 'кп' and semi-killed steels, with 'пк' at the end of designation.

Alloying elements are designated, according to the USSR State Standards, by the Russian letters as follows: H (nickel), K (cobalt), Г (manganese), X (chromium), B (tungsten), M (molybdenum), Ю (aluminium), С (silicon), Ф (vanadium) and P (boron), the latter being placed after the numeral indicating the carbon content. When the content of an alloying element is within 1-1.5 per cent, no numeral is written after the letter designation, the exceptions being molybdenum and vanadium whose content in most steels is 0.2-0.3 per cent.

With an alloying element contained in an amount more than 1.5 per cent, the numeral after the corresponding letter gives its percentage. For instance, 15X denotes a steel containing, on the average, 0.15 per cent C and 1.0-1.5 per cent Cr; 35Г2 is a steel with 0.35 per cent C and 2 per cent Mn.

High-quality steels are distinguished from quality grades by a capital 'A' at the end of their designation. For instance, 40XHM is quality steel and 40XHMA is a high-quality grade. Similarly, superhigh-quality grades are designated by 'Ш'.

Steel grades intended for casting (casting steels) are designated with 'Л' at the end.

There are some exceptions to these rules, mostly for high-quality steels. They are as follows:

1. All tool steels, alloy steels, steels and alloys with special physical properties, stainless steels and heat-resistant steels are always high-quality (or super-high quality) grades, therefore, the letter 'A' is omitted in their designations.

2. The designation of some grades of steel for special purposes may include a symbol indicating where the steel is employed.

For example, ball bearing chromium steels are designated with

'III' in the beginning of their designation, then follows a numeral showing the content of chromium in tens of a per cent; their carbon content is usually not indicated; therefore, a steel of this type containing 1 per cent C and 1.5 per cent Cr will be designated as IIIX15.

High-speed (complex-alloyed) steels are designated by the letter 'P' in the beginning; the following numeral gives the percentage of tungsten which is the principal alloying element in this group of steels. Other alloying elements are designated in the usual manner, if present in an amount of more than 1 per cent (or more than 4 per cent for chromium).

Electric (transformer) steels have the letter 'Э' in the beginning of their designation, the numeral that follows giving the percentage of silicon.

Other non-standard designations of steels may be found in the tables given later.

3. New grades of steel, not covered by State Standards or manufactured according to technical specifications, are denoted by certain abbreviations indicating the name of the manufacturing works (for instance, ЭП or ЭИ for the Elektrostal' works, ДИ for Dnepropetsstal' works, etc.) and a serial number given by the works. Some non-standardized steels which are in wide use are given in the tables below.

According to the SAE code (USA), structural steels (carbon grades and those alloyed with one or two elements) are designated by four numerals, the first numeral indicating the main alloying element, the second, its percentage concentration, and the third and the fourth, the content of carbon in hundredths of a per cent. The first numerals designating alloying elements are as follows: 1 for carbon steels (the second numeral is then zero), 2 for nickel steels, 3 for nickel-chrome steels, 4 for molybdenum steels, 5 for chromium steels, 6 for chrome-vanadium steels, 7 for tungsten steels, 8 for vanadium steels, and 9 for silicon-manganese steels.

For instance, the designation 1045 corresponds to steel 45 according to the Soviet Standard GOST, 5140 to steel 40X, etc. Steels alloyed with a greater number of elements have a more complicated designation.

The classification by the method of manufacture gives the necessary but only preliminary evaluation of steels. A large class of steels manufactured by the same metallurgical technique may include steel grades of different purpose and very diverse properties. For instance, the class of high-quality steels includes such different grades as the majority of structural steels, magnet steels, tool steels, stainless steels, etc.

Classification by application. This type of classification characterizes steels most fully. The following classes of steel are distinguished here: (1) constructional steels; (2) structural steels; (3) special structural steels; (4) tool steels; (5) steels with special physical properties; (6) steels with special chemical properties (corrosion-resistant steels).

27.1. CONSTRUCTIONAL STEELS

This category includes carbon steels and some low-alloy grades having a low carbon content.

Constructional carbon steels are mostly of common-quality grades discussed earlier.

Steels with a relatively low carbon content (up to 0.25 per cent), when being cooled with different rates from the tempera-

Table 27.1. Common-quality Constructional Carbon Steels Supplied According to Their Mechanical Properties (GOST 380-71)

Grade	Mechanical properties *			Approximate composition, %			Applications
	σ_t , kgf/mm ²	σ_y , kgf/mm ²	δ , % (at least)	C	Mn	Si	
Cr0	≥ 31	—	20	≤ 0.23	—	—	Sheets and sectional rolled stock for structures; reinforcement bars
Cr1	32-42	—	31	0.06-0.12	0.25-0.50	0.12-0.30	Anchor bolts, rigid ties, rivets
Cr2	34-44	20-23	29	0.09-0.15	0.25-0.50	0.12-0.30	Rivets, sheets, tubes, non-critical furnaces
Cr3	38-49	21-25	23	0.14-0.22	0.40-0.65	0.12-0.30	Sheets and sectional rolled stock for structures, bridges, etc.; bolts, hooks
Cr3 (rimming)	37-47	20-24	24	0.14-0.22	0.30-0.60	≤ 0.07	Sheets and sectional rolled stock for structures; bolts

* The values of ultimate strength and yield limit in large-section rolled stock must be not less than those specified here.

tures of hot deforming (such as in possible heat treatment), vary only slightly their ultimate strength, hardness and ductility. For this reason, the mechanical properties of these grades remain almost constant across their cross section and in melts of the similar carbon content. The most characteristic of these carbon steels are open-hearth steels supplied according to their mechanical properties. Their characteristics and applications are given in Table 27.1.

Constructional alloy steels are produced in ever increasing quantities; they are alloyed with less expensive elements. The purpose of their alloying is to increase the hardening capacity and thus obtain better mechanical properties (mainly the yield limit). In order that the ductility, impact strength and weldability were not impaired by this strengthening, the content of carbon and alloying elements in these steels is limited as given in Table 27.2. Mechanical properties of some of these steels are indicated in Table 27.3.

Table 27.2. Low-alloy Constructional Steels (GOST 5058-65)

Grade	Composition, %				Applications and properties
	C	Si	Mn	Cr	
Steels for Building Structures					
14Г	0.12-0.18	0.17-0.37	0.7-1.0	≤ 0.3	Angle and beam sections Good weldability; no cold brittleness down to -70 °C; for high-pressure pipes
14Г2	0.12-0.18	0.17-0.37	1.2-1.6	≤ 0.3	
18Г2	0.14-0.20	0.25-0.55	1.2-1.6	≤ 0.3	Resists well atmospheric corrosion
16ГC	0.12-0.18	0.4-0.7	0.9-1.2	≤ 0.3	Housings of chemical apparatus, bottoms of boilers and pressure vessels (from -40° to +450 °C)
10Г2C1	up to 0.12	0.9-1.2	1.3-1.65	≤ 0.3	
14ХГC	0.11-0.16	0.4-0.7	0.9-1.3	0.5-0.8	
15ХЧД *	0.12-0.18	0.4-0.7	0.4-0.7	0.6-0.9	Trusses, bridges, axles, ties; resists well atmospheric corrosion
Steels for Reinforcement Bars					
18Г2C	0.14-0.23	0.6-0.9	1.2-1.6	≤ 0.3	Reinforcement bars of various profile and cross section; σ _{0.2} is from 30 kgf/mm ² (18Г2C) to 40 kgf/mm ² (35ГC)
25Г2C	0.20-0.29	0.6-0.9	1.2-1.6	≤ 0.3	
35ГC	0.30-0.37	0.6-0.9	0.8-1.2	≤ 0.3	

* Additionally alloyed with 0.3-0.6 per cent Ni and 0.2-0.4 per cent Cu.

Table 27.3. Mechanical Properties of Low-alloy Constructional Steels (Lowest Values), GOST 5958-65

Grade	Rolled thickness, mm	σ_f , kgf/mm ²	σ_y , kgf/mm ²	δ , %	a_n , kgf m/mm ² at		
					+20 °C	-40 °C	-70 °C
Steels for Building Structures							
As supplied							
14Г	4-10	46	29	21		3.5	
14Г2	4-10	47	34	21		3.5	
	11-32	46	33	21		4	
18Г2	8-10	52	36	21		4	
16ГC	4-10	50	33	21		4	3
	11-20	49	32	21	6	3	2.5
	21-32	48	30	21	6	3	2.5
	33-60	47	29	21	6	3	2.5
	61-160	46	28	21	6	3	2.5
10Г2C1	4-10	52	38	21		4	3
	11-20	51	36	21	6	3	2.5
	21-32	47	31	21	6	3.5	3
	33-60	46	29	21	6	3.5	3
	61-80	45	28	21	6	3.5	3
	81-160	44	27	21	6	3.5	3
14ГC	4-10	50	35	22		4	
15XCHД	4-32	50	35	21		3	3
After improving heat treatment (hardening and tempering)							
14Г2	10-32	54	40	19		5	3
16ГC	10-32	52	40	18		4	3
10Г2C1	10-40	54	40	19		5	3
15XCHД	10-32	60	50	17		4	3
Steels for Reinforcement Bars (as Supplied)							
18Г2C	6-9	50	40	14			
	40-90	60	30	14			
25Г2C	6-40	60	40	14			
35ГC	6-40	60	40	14			

27.2. GENERAL-PURPOSE STRUCTURAL STEELS (TABLE 27.4)

The steels of this group are used widely for the manufacture of diverse machine elements (shafts, axles, worm wheels, etc.) in all branches of machine-building: automotive industry, tractor building, machine-tool industry, etc. Since machine elements can vary much in shape, size, operating conditions, and stressed states, a large diversity of steel grades with various contents of

carbon and alloying elements are needed to meet all these conditions.

The most critical characteristic by which these steels are selected are the mechanical properties and the pattern of their distribution over the cross section.

The mechanical properties and hardenability of these grades of steel are determined by their carbon content, which may vary between 0.05 and 0.65 per cent.

Alloying elements principally determine the hardenability and hardening capacity and, to a lesser extent, the mechanical properties (except for nickel and molybdenum which improve impact strength).

The mechanical properties of typical steels depending on the heat-treatment are given in Table 27.5.

In order to characterize better their properties and applications, structural steels may be divided into (a) those used without heat treatment, (b) those hardenable in the surface layer, and (c) improvable steels hardenable through the whole cross section.

(a) Steels Used Without Heat Treatment

These are mainly manufactured as sheets for subsequent stamping, drawing, or extrusion, as tubes, etc.

By their composition they relate to carbon steels with a reduced silicon content (produced as rimming or semi-killed grades) or low-alloy steels. They have a lowered content of carbon (see Table 27.3).

These steels are delivered normalized after rolling. The alloy steels in this group have higher strength properties than the carbon grades, and are strengthened more owing to cooling from the temperatures of rolling.

(b) Steels Hardenable in the Surface Layer

These steels are suitable for articles subjected to strong wear and high dynamic loads, but without high stresses. With a high hardness of the surface layer, formed by heat treatment or chemical heat treatment, they retain an appreciably tough core.

The following subgroups are distinguished in this group of steels.

Cementable steels. These have a low carbon content (up to 0.3 per cent). After cementation and hardening they have high hardness in the surface layer only, usually 1-1.5 mm deep, and a comparatively low hardness of the tough core. Their surface hardness (60-62 HRC) and wear resistance are rather high, because

Table 27.4. Structural Carbon Steels (GOST 1050-60) and Alloy Steels (GOST 4543-71)

Grade	Composition, %					Applications and properties
	C	Mn	Si	Cr	Ni	
Steels Used Without Heat Treatment						
08Ю	0.05-0.11	0.25-0.50	≤ 0.03	≤ 0.1	≤ 0.2	Sheets for cold stamping with deep drawing Same; higher strength For complex bending; good weldability Same, for less critical applications
08кп (1008) *	0.05-0.11	0.25-0.50	≤ 0.03	≤ 0.1	≤ 0.2	
10кп (1010)	0.07-0.14	0.25-0.50	≤ 0.07	≤ 0.15	≤ 0.2	
15кп (1015)	0.12-0.19	0.25-0.50	≤ 0.07	≤ 0.25	≤ 0.2	
08	0.05-0.12	0.35-0.65	0.17-0.37	≤ 0.1	≤ 0.2	
Cr3	0.14-0.22	0.40-0.65	0.12-0.30	Not determined		
Steels Hardened in Surface Layer						
Cementable Steels						
15 (1016)	0.12-0.19	0.35-0.65	0.17-0.37	≤ 0.25	≤ 0.25	For cementation and cyaniding when high strength of the core is not critical Same, with higher strength of the core Same, for articles of complicated shape Same, insensitive to overheating in cementation For cementation when high strength and ductility of the core are required; for articles of larger size Same, for smaller cross sections Same, for lower ductility
20 (1020)	0.17-0.24	0.35-0.65	0.17-0.37	≤ 0.25	≤ 0.25	
15Х (5015)	0.12-0.18	0.40-0.70	0.17-0.37	≤ 0.30	≤ 0.30	
15ХА	0.12-0.17	0.40-0.70	0.17-0.37	≤ 0.30	≤ 0.30	
15ХФ (6117)	0.12-0.18	0.40-0.70	0.17-0.37	≤ 0.30	≤ 0.30	
12ХН3А	0.09-0.16	0.3-0.6	0.17-0.37	0.6-0.9	2.75-3.15	
12Х2Н4А (3310)	0.09-0.15	0.3-0.6	0.17-0.37	1.25-1.65	3.25-3.65	
20ХГНП	0.16-0.23	0.7-1.0	0.17-0.37	0.7-1.1	0.8-1.1	0.001-0.005 B
18ХГТ	0.17-0.23	0.8-1.1	0.17-0.37	1.0-1.3	—	0.03-0.09 Ti

45 (1045)	0.42-0.50	0.5-0.8	0.17-0.37	≤ 0.25	≤ 0.25	} Shafts, axles, gear wheels, etc. Same, for higher strength of the core Same, for large articles of complicated shape
55 (1055)	0.52-0.60	0.5-0.8	0.17-0.37	≤ 0.2	≤ 0.25	
60 (1060)	0.57-0.65	0.5-0.8	0.17-0.37	≤ 0.2	≤ 0.25	
45X (5045)	0.41-0.49	0.5-0.8	0.17-0.37	0.8-1.1	≤ 0.30	} Same, for large articles of complicated shape
50X (5050)	0.46-0.54	0.5-0.8	0.17-0.37	0.8-1.1	≤ 0.30	

Steels of Reduced Hardenability for Surface Hardening with Deep Induction Heating (Not Standardized)						
55ΠΠ	0.55-0.63	0.1-0.3	≤ 0.2	≤ 0.15	≤ 0.25	} Same, for operation at high stresses
58ΠΠ	0.54-0.62	≤ 0.3	≤ 0.2	≤ 0.15	≤ 0.2	

Steels of Specified Hardenability						
47ТТ	0.44-0.51	≤ 0.17	1.0-1.2	≤ 0.25	≤ 0.25	} Same, for larger articles and operation at still higher stresses
					0.06-0.12 Ti	

Steels for Nitration						
38ХМЮА	0.35-0.42	0.3-0.6	0.2-0.45	1.35-1.65	0.7-1.1 Al	} Spindles of high-speed machine tools, cylinder sleeves Same, for quicker nitration Gear wheels and bolts for critical operation
30ХТ2М	0.28-0.36	0.3-0.6	0.8-0.45	1.3-1.6	≤ 0.2	
40ХНМА	0.37-0.44	0.5-0.8	0.17-0.37	0.6-0.9	1.25-1.65 Ni	

Improbable Steels						
Steels for Through-hardening Articles Up to 12-15 mm in Dia						
35 (1035)	0.32-0.40	0.5-0.8	0.17-0.37	≤ 0.25	≤ 0.25	} Axles, shafts, rotors not subjected to high stresses Axles, shafts, rods, gear wheels
40 (1040)	0.37-0.45	0.5-0.8	0.17-0.37	≤ 0.25	≤ 0.25	
45 (1045)	0.42-0.50	0.5-0.8	0.17-0.37	≤ 0.25	≤ 0.25	} Same, also spindles, gear wheels and bolts for heavy-duty operation
50 (1050)	0.47-0.55	0.5-0.8	0.17-0.37	≤ 0.25	≤ 0.25	
55 (1055)	0.52-0.60	0.5-0.8	0.17-0.37	≤ 0.25	≤ 0.25	} Axles, shafts; usually employed normalized

Table 27.4 (continued)

Grade	Composition, %					Applications and properties	
	C	Mn	Si	Cr	Ni		other alloying elements
Steels for Through-hardening Articles Up to 25-35 mm in Dia							
Manganese steels							
35Г2 (1141)	0.31-0.39	1.4-1.8	0.17-0.37	≤ 0.30	≤ 0.30	Crankshafts, axles, pins Propeller shafts, connecting rods, railway-car axles	
45Г2 (1144)	0.41-0.49	1.4-1.8	0.17-0.37	≤ 0.30	≤ 0.30		
Chromium steels							
35X	0.31-0.39	0.5-0.8	0.17-0.37	0.8-1.1	≤ 0.30	Axles, shafts, gear wheels Same, for higher strength Same, for higher loads	
40X	0.36-0.44	0.5-0.8	0.17-0.37	0.8-1.1	≤ 0.30		
45X (5045)	0.41-0.49	0.5-0.8	0.17-0.37	0.8-1.1	≤ 0.30		
Chromium-silicon steels							
33XC	0.29-0.37	0.3-0.6	1.0-1.4	1.3-1.6	≤ 0.30	Thin-walled tubes, shafts, axles Gear wheels, high-strength shafts	
40XC	0.37-0.45	0.3-0.6	1.2-1.6	1.3-1.6	≤ 0.30		
Chromium-vanadium steel							
40XΦA (6145)	0.37-0.44	0.5-0.8	0.17-0.37	0.8-1.1	≤ 0.30	0.10-0.18 V	Same, also crankshafts; insensitive to over-heating during hardening

Steels for Through-hardening Articles Up to 50-75 mm in Dia

25XTCA	0.22-0.28	0.8-1.1	0.9-1.2	0.8-1.1	≤ 0.30	—	Units and frames for critical service; rods, thin-walled tubes
30XTC	0.28-0.35	0.8-1.1	0.9-1.2	0.8-1.1	≤ 0.30	—	Same, for higher strength
35XTCA	0.32-0.39	0.8-1.1	1.1-1.4	1.1-1.4	≤ 0.30	—	Axles, gear wheels of high strength and large dimensions when toughness is not critical
Chrome-molybdenum steel							
35XM	0.32-0.40	0.4-0.7	0.17-0.37	0.8-1.1	≤ 0.30	0.15-0.25 Mo	Rotors, shafts, gear wheels, engine cylinders
Steels for Through-hardening Articles Up to 75-120 mm in Dia							
Chrome-nickel steel							
30XH3A	0.27-0.33	0.3-0.6	0.17-0.37	0.6-0.9	2.75-3.15	—	Shafts, rods, crankshafts of high strength
Chrome-nickel-molybdenum steels							
40XHMA (4340)	0.37-0.44	0.5-0.8	0.17-0.37	0.6-0.9	1.25-1.65	0.15-0.25 Mo	Heavy-duty shafts, axles, gear wheels

* Numbers in brackets are corresponding SAE designations.

Table 27.5. Mechanical Properties of Typical Structural Steels Used in Machine-building *

Heat treatment	Diameter (thickness), mm	σ_t , kgf/mm ²	$\sigma_{y'}$, kgf/mm ²	δ , %	ψ , %	a_n , kgf m/cm ²
<i>Carbon Steel 15 (Cementable) **</i>						
Normalizing (or high tempering)	up to 30	37	22	27	55	6
Cementation at 950 °C, hardening from 800-820 °C and tempering at 180-200 °C	up to 30	45	25	20	50	—
<i>Alloy Steel 15X (Cementable)**</i>						
Normalizing (or high tempering)	up to 40	40	25	25	50	7
Cementation at 950 °C, hardening from 810-830 °C and tempering at 180-200 °C	up to 40	65	43	10	45	6
<i>Alloy Steel 12XH3A (Cementable) **</i>						
Cementation at 950 °C, hardening from 800-820 °C and tempering at 180-200 °C	up to 60	100	85	12	55	12
<i>Carbon Steel 45 (Improveable)</i>						
Normalizing (or high tempering)	up to 60	60	34	16	40	3
Hardening from 820-840 °C and tempering at 550-600 °C	up to 60	70	45	17	35	5
Hardening from 820-840 °C and tempering at 520-530 °C	60	85	58	13	30	4
<i>Alloy Steel 40X (Improveable)</i>						
Annealing	60	65	36	14	38	4
Hardening from 830-850 °C and tempering at 570-620 °C	30	78	56	15	50	6
Same	50	75	52	15	48	5
<i>Alloy Steel 40XHMA (Improveable)</i>						
Annealing	80	70	38	15	40	5
Hardening from 830-850 °C and tempering at 600-620 °C	80	110	90	12	55	8

Table 27.5 (continued)

Heat treatment	Diameter (thick- ness), mm	σ_t , kgf/mm ²	σ_y , kgf/mm ²	δ , %	ψ , %	a_n , kgf m/cm ²
<i>Alloy Steel 35XFGA (Improvable)</i>						
Annealing	80	75	42	12	35	3
Hardening from 870-890 °C and tempering at 540-560 °C	80	110	90	10	45	6
<i>Alloy Steel 38XMIOA (Nitridable) **</i>						
Hardening from 930-950 °C, tempering at 630-650 °C, and nitration at 520-540 °C	60	105	90	18	52	8

* Minimum values are given.

** The properties are indicated for the core.

the content of carbon in the surface layer increases through cementation to approximately 0.8 per cent. But their resistance to local loads is reduced owing to the low thickness of the hard surface layer and especially because of the comparatively high difference in the hardness of the surface and core, this difference being especially large in the carbon steels of the group (these are used for light loads only), and less sharp in the alloy steels which also have a higher strength and hardness in the core after hardening.

Cementable carbon steels are usually quality and high-quality steels or, less frequently, common-quality Grades Ст. 2 and Ст. 3; the use of the last two grades is gradually being abandoned because of their low toughness.

Cementable alloy steels are employed for making articles of larger dimensions and complicated shape, because they have higher hardenability and higher strength in the core. In addition, they can be hardened with quenching in less sharp coolants, which reduces the risk of deforming and cracking.

Steels hardenable by induction heating. These grades have a higher carbon content, 0.5-0.65 per cent, and therefore, are more suitable for induction hardening than the cementable steels, since they acquire higher hardness in the core. The wear resistance of these steels is slightly less than that of the cementable grades (which have a higher carbon content in the surface layer); their toughness is lower as well because more carbon is present in the core. Induction-hardened steels resist static and fatigue loads

better than the cementable grades because of the lower hardness gradient across the cross section.

Steels of reduced hardenability. These are relatively new grades of steel finding ever wider application in industry. They contain 0.5-0.6 per cent C and can be hardened. They differ from the improvable carbon steels of the same carbon content (discussed later in this section) in having an appreciably lower content of manganese, silicon (see Table 27.3) and other alloying elements (chromium, nickel, copper). Articles made of these steels are subjected to the usual through-hardening, but acquire high hardness in the surface layer only, their hardness being the same as in common steels of the same carbon content after induction hardening. It is essential that the hardened surface layer follows exactly the contour of an article, which forms useful compressive stresses.

Another advantage of steels of reduced hardenability is that the layers just below the hardened surface layer are partially hardened, and their structure is thus improved. The hardness of the metal varies smoothly from the surface to the core, which makes these steels suitable for operation at higher pressures.

Nitridable steels. Steels alloyed with chromium, titanium or aluminium are most suitable for this purpose, because of the peculiarities of the interaction of the surface layers of the metal with the nitrogen that diffuses during nitration. In addition, the carbon content in these steels should be not less than 0.35-0.5 per cent, and therefore they can be hardened before nitration (when the latter is to be the final process of the treatment).

The highest hardness (up to 69-71 HRC, i.e. higher than with cementable steels) and highest wear resistance are exhibited by aluminium-alloyed steels (such as 38XM10A). Besides, the high hardness of the nitrated layer remains upon heating to 400-420 °C. Because of the sharp drop of hardness across the cross section (the hardness of deeper layers is about 35 HRC) and the small thickness of the hard nitrated layer (up to 0.5 mm), these steels can be used under severe wear and heating conditions, but without large pressures.

Other grades of nitridable steels (containing no aluminium) have a lower surface hardness (appr. 50 HRC), but a higher fatigue strength and higher wear resistance.

(c) Steels Hardenable Through the Whole Cross Section

This group includes steels having a high hardenability to suit the purpose, in particular, carbon and low-alloy steels with a carbon content of more than 0.35 per cent and medium- and

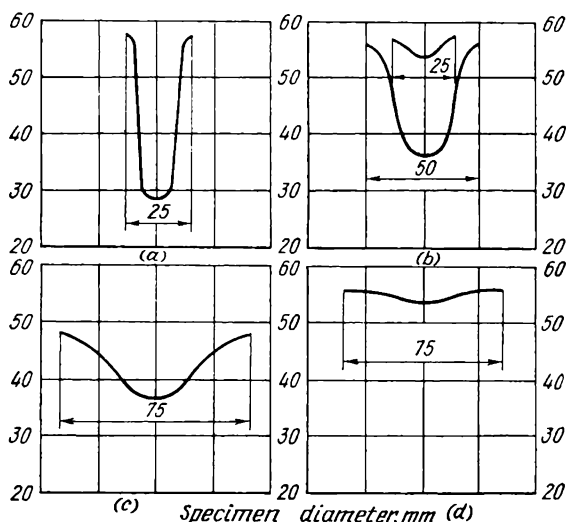


Fig. 27.1. Hardenability of steels with 0.4% C

(a) carbon steel; (b) chromium steel (0.8-1.1% Cr); (c) chrome-nickel steel (1.0% Cr and 1.8% Ni); (d) chrome-nickel-molybdenum steel (1.5% Cr, 2% Ni, and 0.2% Mo)

high-alloy steels with more than 0.2-0.3 per cent C. The hardenability of the steels of this group may vary and is determined by the effect of the alloying elements.

The lowest hardenability is exhibited by carbon steels; these acquire a high hardness (more than 55-57 HRC) only in articles of diameter or thickness of up to 12-15 mm. Hardenability becomes higher with increase in the alloying degree and attains 90-100 mm in high-alloy steels, such as Grade 37XH3A (Fig. 27.1).

Improvable steels of the same carbon content but with various content of alloying elements may have similar strength properties in articles of small cross section. Their properties will, however, differ appreciably in larger articles being lower with carbon and low-alloy steels. Thus the selection of a particular grade of improvable steel should be decided by the properties required in the article and its thickness.

In this connection improvable steels can be conveniently divided into groups as follows (see Table 27.4):

steels of a low hardenability (hardenable fully in sections up to 12-15 mm);

steels of medium hardenability (hardenable fully in sections up to 25-35 mm);

steels of high hardenability (hardenable in sections up to 50-75 mm); and

steels of very high hardenability (hardenable in sections up to 75-125 mm). These steels are alloyed with nickel and molybdenum in order to increase their hardenability (and also to prevent temper brittleness); hence, they have a higher toughness than the steels in the other indicated groups.

27.3. SPECIAL STRUCTURAL STEELS AND ALLOYS

These steels are evaluated not only by their mechanical properties at 20 °C (as for general-purpose steels), but also by a number of other properties: mechanical (at low and high temperatures) and physical, chemical and technological. This is linked with the fact that steels of this group are used in various branches of industry only under strictly defined conditions, such as very high pressures, low or high (sometimes very high) temperatures, dynamic wear or wear by hydro-abrasive loads or for a very narrow utilization in machines and instruments, for instance, in springs, contacts, etc., in radioengineering and electrical engineering, or for obtaining a high cleanliness of machined surfaces.

(a) Steels with a Very High Strength and Toughness (Maraging Steels)

Maraging steels undergo martensitic transformations owing to precipitation hardening and tempering (martensitic ageing, whence the name).

As distinct from the general-purpose structural steels, maraging steels contain almost no carbon, but are usually highly alloyed with nickel, cobalt, molybdenum, and, in smaller amounts, with titanium or sometimes beryllium.

Maraging steels have very high strength ($\sigma_t = 180-200 \text{ kgf/mm}^2$) and at the same time retain high toughness ($\delta \geq 10$ per cent and $\psi \geq 40$ per cent) and high impact strength at +20 °C ($a_n \geq 8-10 \text{ kgf m/cm}^2$) and low temperatures ($a_n \geq 4-5 \text{ kgf m/cm}^2$ at -196 °C).¹

When additionally alloyed with chromium (approx. 12 per cent), maraging steels can be made corrosion-resistant, even to very aggressive media (sea water, acids, etc.).

¹ For comparison, structural steel Grade 40XHM of the same impact strength ($a_n \approx 8-10 \text{ kgf m/cm}^2$ at +20 °C) has an ultimate strength of approx. 100-110 kgf/mm².

The technological properties of these steels are rather high: good weldability, machinability, and toughness in the hardened state, insignificant deformation of machined articles after tempering (which increases the mechanical properties of the steel).

Maraging steels relate to superhigh-quality steels and are manufactured exclusively by vacuum-arc or vacuum-induction methods.

Because of their high cost, maraging steels find application in most critical articles only.

Maraging steels are very diverse in their composition and may be divided into the following groups:

- (a) steels of high strength and toughness;
- (b) steels of high strength, toughness and corrosion-resistance; and
- (c) steels that are stable to heating (heat-resistant).

Typical maraging steels are given in Table 27.6.

Table 27.6. Steels with Very High Strength and Toughness (Maraging Steels)

Grade	Composition, %						Applications
	C	Ni	Co	Mo	Cr	Ti	
<i>Steels with Very High Strength and Toughness</i>							
H18K9M5T	≤ 0.03	18	9	5	≤ 0.1	0.5	Gear wheels, shafts, rocket bodies
<i>Same, Plus Corrosion-resistant</i>							
H10X12Д2T	≤ 0.03	10	2 Cu	—	12	0.4	Chemical processing equipment; springs
<i>Same, Plus Heat-resistant</i>							
H4X12K15M4T	≤ 0.03	4	15	4	12	0.4	Chemical processing equipment; heat-power units for temperatures up to 500 °C; hot-pressing dies

(b) High-temperature (Refractory and Heat-resistant) Steels and Alloys

The diverse grades of steels and alloys in this group are divided into (a) refractory and (b) heat-resistant according to their composition and the principal properties.

Refractory steels. These are resistant against gas corrosion in air, furnace gases (including sulphur-containing gases), combustion products (including those causing carburizing effect) at temperatures up to 900-1200 °C, but cannot withstand high loads, i.e. elements and structures made of them are not calculated for creep resistance.

Their high stability against gas corrosion is due, in the first place, to alloying with chromium which forms a protective oxide film on the surface of metal. Their resistance depends on temperature and increases with increasing chromium content. Resistance to carburizing agents is ensured by additionally alloying with nickel.

The properties of these steels can be conveniently characterized by the temperature at which intensive oxidation begins (Table 27.7).

Table 27.7. Refractory Steels (GOST 5632-72)

Grade	Composition, %				Temperature of intense oxidation beginning, °C	Applications
	C	Si	Cr	Ni		
<i>Steels Stable in Oxidizing Media (including sulphur-containing gases)</i>						
15X5	≤ 0.15	≤ 0.5	4.5-6.0	—	600-650	Tubes, sheets
40X9C2	0.35-0.45	2.0-3.0	8.0-10.0	—	850	Discharge valves of automobile and tractor engines
30X13H7C2	0.25-0.34	2.0-3.0	12.0-14.0	6.0-7.5	950	Discharge valves of piston engines
12X17	≤ 0.12	≤ 0.8	16.0-18.0	—	900	Heat exchangers
15X28	≤ 0.15	≤ 1	27-30.0	—	1100-1150	Tubes for pyrolysis plants
<i>Steels Stable in Oxidizing and Carburizing Media</i>						
20X20H14C2	≤ 0.20	2.0-3.0	19.0-22.0	12.0-15.0	1000-1050	Tubes, sheets, furnace conveyers, cementation boxes

Heat-resistant steels and alloys. These materials are used in elements and structures operating under loads at temperatures above 400-450 °C, i.e. under the conditions where creep should be counteracted.

As distinct from the refractory grades, heat-resistant steels and alloys should retain their high strength when heated. At the same

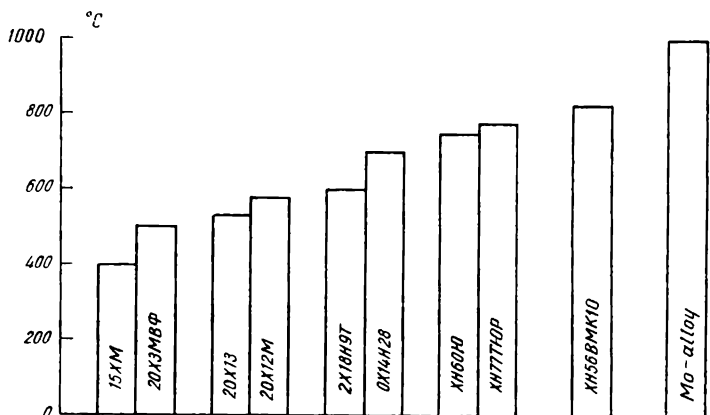


Fig. 27.2. Maximum service temperatures of refractory and heat-resistant steels and alloys

15XM, 20X3MBΦ—refractory ferrite-carbide steels; 20X13, 20X12M—high-refractory ferrite-carbide steels; 2X18H9T, OX14H28—heat-resistant austenitic steels; XH60Ю, XH77TЮP—heat-resistant austenitic nickel base alloys; XH56BMKЮ—ditto, additionally alloyed with cobalt; Mo-alloy—molybdenum alloy with 0.1% Ti

time they should possess high corrosion resistance (like the refractory alloys which they can substitute).

Heat resistance of these alloys, under the same conditions of long heating, depends on the heating temperature. For this reason the composition, structure and properties of alloys employed in articles of similar purpose and shape may differ substantially if the articles are intended for operation at different temperatures.

With a very high heating, heat-resistant steels, even those high-alloyed, lose their heat resistance and in such cases must be replaced with heat-resistant alloys based on nickel (sometimes in combination with cobalt), chromium or, more often, molybdenum and niobium.

The numerous heat-resistant alloys are classified by their principal parameters, i.e. the operating temperature.

Individual alloys are compared below (Table 27.8) by their long-term strength which is determined by loading specimens for 10,000 h at the specified temperature (Fig. 27.2).

Steels for long-term operation at 400-550 °C (ferrite-pearlitic steels). In operation at the lower temperature limit creep can only develop after a very long time. However long heating of carbon steels can cause coagulation of the strengthening carbide phase (cementite in pearlite) or even its graphitization, which strongly reduces yield limit.

Table 27.8. Heat-resistant Steels and Alloys (GOST 5632-72)

Grade	Composition (average), %						Applications
	C	Si	Cr	Ni	Mo	other elements	
Steels Stable at 400-550 °C (Ferrite-Pearlitic, GOST 10500-63)							
15XM	0.11-0.18	0.17-0.37	0.8-1.1	≤ 0.2	0.4-0.55	—	Superheater pipes, boiler fittings
12X1M1Φ	0.08-0.15	0.17-0.37	0.9-1.2	≤ 0.25	0.25-0.35	0.15-0.35 V	Rotors, discs, fastenings
25X2MΦ	0.22-0.29	0.17-0.37	2.1-2.6	≤ 0.25	0.9-1.1	0.3-0.5 V	Pipes of hydrogenation
20X3MBΦ	0.16-0.24	0.17-0.37	2.8-3.3	≤ 0.25	0.35-0.55	0.6-0.85 V	and petroleum-processing plants where resistance against hydrogen corrosion is needed
Steels Stable at 500-600 °C (High-chromium Ferrite-carbide)							
15X5M	≤ 0.15	≤ 0.5	4.5-6.0	≤ 0.2	0.45-0.60	—	Fittings of petroleum-processing plants, pump elements
40X10C2M	0.35-0.45	1.9-2.6	9.0-10.5	≤ 0.2	0.7-0.9	—	Engine valves, fastenings
20X13	0.16-0.25	≤ 0.8	12.0-14.0	≤ 0.2	—	—	Steam-turbine blades, pipes (for 500-520 °C)
18X11MHΦБ	0.15-0.21	≤ 0.6	10.0-11.5	0.5-1.0	0.8-1.1	0.20-0.45 Nb 0.20-0.40 V	Rotors, discs, blades (for 550-580 °C)
Steels Stable at 600-650 °C (Austenitic)							
12X18H9T	≤ 0.12	≤ 0.8	17.0-19.0	8.0-9.5	—	≤ 2.0 Mn % Ti = (%C-0.02) × 5 ≤ 0.7	

Carbide-strengthened austenitic

45X14H14B2M	0.40-0.50	≤ 0.8	13.0-15.0	13.0-15.0	0.25-0.40	2.0-2.8 W	Pipes, valves (for 600-650 °C)
-------------	-----------	-------	-----------	-----------	-----------	-----------	--------------------------------

Intermetallide-strengthened austenitic

10X11H23T3MP	≤ 0.1	≤ 0.6	10.0-12.5	21.0-25.0	1.0-1.6	2.6-3.2 Ti ≤ 0.8 Al ≤ 0.02 B	Turbine blades and discs (for 670-720 °C)
--------------	-------	-------	-----------	-----------	---------	------------------------------------	--

Nickel-base Alloys (Austenitic)

XH160H	≤ 0.10	≤ 0.8	15-18	Base	—	2.6-3.5 Al ≤ 0.003 Ce	Sheet elements of turbines (for 750-800 °C)
XH70Ю	≤ 0.1	≤ 0.8	26-29	Base	—	≤ 0.1 Ba 2.8-3.5 Al ≤ 0.003 Ce	Same, gas pipelines
XH77TЮP	≤ 0.07	≤ 0.6	19-22	Base	—	≤ 0.1 Ba 0.6-1.0 Al 2.3-2.7 Ti ≤ 0.01 B ≤ 0.01 Ce	Turbine discs and blades (for 720-750 °C)

Nickel-base Alloys with Cobalt (Austenitic)

XH56BMKЮ	≤ 0.1	≤ 0.6	8.5-10.5	Base	6.5-8.0	6.0-7.5 W 5.4-6.2 Al 11-13 Co ≤ 0.02 B ≤ 0.02 Ce	Turbocompressor blades (for 800-850 °C)
XH62MBKЮ	≤ 0.1	≤ 0.6	8.5-10.5	Base	9.0-11.5	4.3-6.0 W 4.0-6.0 Co 4.2-4.9 Al	Same

Note. For characteristics of alloys based on other high-melting metals see in the text.

Chromium-alloy steels are suitable for long-term operation at 400-450 °C only if their chromium content is relatively low, one to three per cent. This retards coagulation and graphitization of cementite. With increasing the working temperature to 450-550 °C (especially under conditions of hydrogen corrosion) the content of chromium should be increased to 3-3.5 per cent and, additionally, strong carbide-forming agents should be introduced into the steel, such as molybdenum, tungsten, or vanadium as shown in Table 27.8. These high-alloy steels can also be used in boiler plants at heating up to 550 °C.

With such alloying, the steel retains its ferrite-pearlitic structure and high values of ductility and weldability, which are needed in pipes, boilers, etc.

Steels for long-term operation at 500-600 °C. These are of ferrite-carbide type. To have a higher temperature of the beginning of recrystallization and development of creep, they should contain alloyed ferrite with a high concentration of chromium and carbides Me_{23}C_6 which are more stable against coagulation than cementite. These steels contain 5-15 per cent Cr.

Steels for operation at the upper temperature limit indicated above are additionally alloyed with molybdenum, tungsten, vanadium, or niobium. Steels alloyed with 12 per cent Cr only retain their long-term strength (for 10,000 hours of loading) within 20 kgf/mm² at temperatures up to 500 °C; for a more highly alloyed steel (18X12BMBΦP) this limit is 550 °C.

Steels for long-term operation at 600-650 °C (austenitic and austenitic with strengthening phases — carbides and intermetallics). A high resistance to creep at these temperatures is achieved if the steel has an austenitic structure which is characterized by a high temperature of the beginning of recrystallization. These steels are alloyed with nickel in an amount of not less than 9-12 per cent.

The heat resistance of these types of steel can be additionally increased by forming the strengthening phases in the austenitic matrix structure, which inhibit metal creep under load. Such phases may be carbides or intermetallides of the type $\text{Ni}_3(\text{Ti}, \text{Al})$, which are still more stable against coagulation. In the former case the steel is additionally alloyed with tungsten, and in the latter, with titanium and aluminium. The long-term strength of 20 kgf/mm² (for 10,000 hours of loading) is retained in austenitic steels (1X18H9T) on heating up to 600 °C, in carbide-strengthened steels, to 620-630 °C, and in steels with intermetallide strengthening, to 640-650 °C.

Alloys for long-term operation at 650-700 °C (nickel-base alloys). The nickel-base γ -solid solution has a high temperature of

development of recrystallization processes. Disperse particles of compounds: intermetallides $\text{Ni}_3(\text{Ti}, \text{Al})$, nitrides (TiN) and carbides TiC and Me_{23}C_6 are formed in the structure of nickel-base alloys in order to increase the absolute values of strength. For this, an alloy is alloyed with aluminium and titanium (in addition to chromium).

At temperatures of 650-700 °C these alloys retain well their long-term strength (45-50 kgf/mm² and 25-28 kgf/mm², respectively).

Alloys for long-term operation at 750-800 °C (nickel-base alloys additionally alloyed with cobalt). Cobalt retards the processes of coagulation of the strengthening phases and weakening of the matrix metal; this increases the working temperature limit by 30-50 °C compared with nickel-base alloys containing no cobalt.

Alloys based on high-melting metals. Use is made of alloys based on chromium, niobium or molybdenum as components having high melting points: 1900 °C for chromium, 2450 °C for niobium, and 2625 °C for molybdenum.

Chromium-base alloys usually contain 25 per cent molybdenum and 15 per cent iron. They remain heat-resistant up to 1000-1100 °C, their long-term strength (100 h) at 1000 °C being 15.4 kgf/mm².

A drawback of these alloys is their high brittleness, that is why they can only be used in articles not subjected to dynamic loads.

Niobium-base alloys have a long-term strength of 25 kgf/mm² (100-h loading) at 1000 °C and can withstand lower loads up to 1200 °C. The best properties are shown by niobium-base alloys containing 15 per cent W, 3 per cent Ti and 1 per cent Zr or 10 per cent Mo, 3 per cent Ti and 1 per cent Zr (according to D. A. Prokoshkin).

Niobium-base alloys have a higher ductility than molybdenum alloys and can be plastic-worked either hot or cold with high pressures and welded by electric-arc and argon-arc welding. Their drawback is strong oxidation on heating, but this can be removed by siliconizing. The main application is for blades of jet engines.

Molybdenum-base alloys contain around 0.5 per cent Ti and 0.5 per cent Zr (or 0.3 per cent Ti and 0.07 per cent Zr). Their long-term strength (100 h) is roughly 35 kgf/mm² at 1100 °C; lower loads can be withstood at temperatures up to 1300 °C. These alloys can be plastic-worked and welded by argon-arc welding. They are produced as sheets, tubes or rods and are used mainly for making blades of jet engines.

The strong oxidation at temperatures above 600-700 °C inherent in these alloys can be prevented by chemical heat treatment: siliconizing or chrome-siliconizing.

(c) Steels for Operation at Low (Cryogenic) Temperatures

The plasticity and toughness of steels of this group should vary only insignificantly at low temperatures, and without a sharp drop of toughness, which is characteristic of the cold brittleness limit. The steels used for this purpose are as follows:

(a) steels of the ferritic (martensitic) class, mainly, down to temperatures of -196°C ; they have a low carbon content and a high content of nickel, which largely lowers the cold brittleness limit and increases toughness;

(b) austenitic steels — chrome-nickel, chrome-manganese-nickel, etc., which can retain their face-centred lattice on cooling down to hydrogen-boiling (-253°C) or helium-boiling (-269°C) temperatures (Table 27.9).

In the latter group, chrome-manganese-nickel and chrome-manganese steels are less expensive and have a higher strength than chrome-nickel grades. But some of them, for instance steel Grade X21Г7H5, require heat treatment after welding (which is not always possible).

Maraging steels with 18-20 per cent Ni may be promising in this group since they possess a much higher strength.

When certain additional properties are required, the following materials are used:

precipitation-hardening austenitic alloys, such as Grade 36HXTiO, which exceed in their strength the austenitic steels mentioned above;

invar 36H alloy, having face-centred lattice and a low coefficient of expansion;

copper alloys, in particular, aluminium bronze Grade Бр.АЖ9-4 or beryllium bronze Grade Бр.Б2 (see Table 27.31), having a low coefficient of friction; low-density aluminium alloys Grades АМр, Д16 (see Table 27.32) can also be employed, but they have a lower strength than the austenitic steels.

(d) Wear-resistant Steels (Table 27.10)

The highest resistance of articles to cavitation erosion and mechanical wear with strong impacts can be achieved (despite certain differences in the stressed state) by forming an austenitic

Table 27.9. Low-temperature Alloys

Grade	Composition, %					Applications and properties
	C	Cr	Ni	Mn	other elements	
<i>Ferritic (Martensitic) Steels</i>						
06HA *	≤ 0.06	—	6.0-7.0	0.45-0.60	—	Low-temperature equipment, liquefied-gas vessels; refrigerators, liquefied-gas generators, etc. Operating temperature down to -196 °C
09HA **	≤ 0.06	—	8.5-9.5	0.45-0.60	—	
<i>Austenitic Steels</i>						
Chrome-nickel steels (GOST 5632-72)						
08X18H10	≤ 0.08	17.0-19.0	9.0-11	1.0-2.0	—	Same; also fittings, pipes, valves and other cryogenic equipment; rocket shells, vessels for rocket fuels, etc. Operating temperature down to -253 °C
08X18H10T	≤ 0.08	17.0-19.0	9.0-11	1.0-2.0	% Ti = 5% C-0.7%	
Chrome-nickel-manganese steels (GOST 5632-72)						
10X14Г14Н4Т	≤ 0.10	13.0-15.0	2.8-4.5	13.0-15.0	% Ti = (% C-0.02 %) × 5 ≤ 0.6	For unloaded structures; no heat treatment is needed after welding. Operating temperature down to -196 °C
10X14Г14Н3	0.09-0.4	12.5-14.0	2.8-3.5	13.0-15.0	0.15-0.25 N	
07X21Г7АН5	≤ 0.07	19.5-21.0	5.0-6.0	6.0-7.5		

* According to ГОСТ 14174-70.

** According to ГОСТ-14174-70.

* According to ЧМТУ ЦНІІЦМ 1-854-70.

** According to ЧМТУ ЦНІІЦМ 1-181-70.

Table 27.10. Wear-resistant Steels to Withstand Cavitation Erosion and Dynamic Loads

Grade	Composition, %						Applications
	C	Si	Mn	Cr	Ni	other alloying elements	
<i>Wear-resistant Steels under Conditions of Cavitation Erosion</i>							
Stable in water at medium flow rates *							
12X18H9T	≤ 0.12	≤ 0.8	≤ 2.0	17.0-19.0	8.0-9.5	Ti = = (%C - 0.02) × × 5 ≤ 0.7%	Blades of hydraulic turbines
Stable at high flow rates							
30X10Γ10	0.3-0.4	0.5-0.6	9.0-11	9-11	—	—	Blades of hydraulic turbines and pumps
Steels of increased cavitation, corrosion and abrasion resistance							
10X14AΓ12	≤ 0.1	≤ 0.3	10-15	13-17	—	0.1-0.3 N	Blades of hydraulic turbines and pumps, including those for sea water operation
10X14AΓ12M	≤ 0.1	≤ 0.3	10-15	13-17	—	0.1-0.3 N	
						≤ 0.3 Mo	
<i>Wear-resistant Steels to Withstand Dynamic Loads</i>							
Γ 13	1.1-1.3	≤ 0.5	12-14	—	—	—	Rail cross-pieces, crushing mill jaws, scoops of earth-digging machines, caterpillar track shoes

* For low flow rates, structural steels can be used, in particular, for making cast blades of hydraulic turbines and elements of hydraulic pumps (Grades 35Л and 20ГЦЛ (0.6-0.9% Si and 1.0-1.3% Mn)).

structure and partial transformation of the latter in operation, i.e. in steels containing unstable austenite.

These steels are most often employed in the cast or forged (rolled) state with subsequent hardening. Their inherent feature is poor machinability, the worst in the steels of the second group

(Grade F13) having a high carbon content (see Table 27.10). Steels resisting cavitation erosion and having a low carbon content can be machined by tools made of high-speed steel of high heat resistance (see Table 27.17).

Wear-resistant steels to withstand cavitation erosion. These steels are employed in elements and structures (propeller screws, blades of hydraulic turbines, cylinders of hydraulic pumps, etc.) that must be stable when interacting with liquid flows, i.e. resist cavitation erosion. Cavitation erosion is caused by discontinuities, voids, steam and gas bubbles, etc. forming in a moving liquid flow, which through their growth and contraction produce multiple microimpacts. A complex stressed state then forms in the surface layer of the metal, and conditions are created for the initiation and growth of cracks. At the initial stage, cavitation erosion is of local nature, but can gradually expand over the whole surface of an article and penetrate a great depth. It can also be accelerated by corrosion.

Partial martensitic transformation during the microimpacts reduces the impact energy (since part of the energy is spent for the transformation proper and for accelerating the stress relaxation at the moment of transformation). Upon the formation of martensite the strength of the metal increases, and therefore, its resistance to crack development also increases.

High cavitation resistance is also shown by maraging steels (see Table 27.6), but these are more expensive.

Copper-base alloys (see Tables 27.27-27.29) can be employed for the same purpose, when high corrosion resistance and a low coefficient of friction are needed.

Wear-resistant steels to withstand dynamic loads. Elements to operate under conditions of sliding friction and high mechanical pressures and impacts are made of high-carbon austenitic steels. A typical example is high-manganese steel having a low yield limit (approximately 30 per cent of the ultimate strength). The metal is strengthened much by pressure and impacts owing to the formation of martensite in the surface layer. In the absence of high pressures, for instance, with abrasion wear, the wear resistance of this steel is not high.

(e) Spring Steels and Alloys

These steels and alloys are employed at various stresses and temperatures and in various media (including corrosive ones). They are very diverse in composition and properties, but may be conveniently divided into two groups as follows:

(a) steels in which only high mechanical properties are essential; and

(b) steels and alloys additionally having some special chemical or physical properties: non-magnetic, corrosion-resistant, with a low constant temperature coefficient of the modulus, with a high electric conductivity, etc.

Spring steels and alloys can be used in both relatively large and very small cross sections, such as wire or strips, sometimes of diameter or thickness less than 0.1-0.2 mm. The mechanical properties of spring alloys, especially of those liable to work-hardening, depend strongly on the size of cross section, as can be seen from Table 27.11.

Table 27.11. Effect of Cross-sectional Area on Mechanical Properties of Spring Wire (GOST 9389-60)

Wire diameter, mm	V8-V10 steels (class I)		65Г steel (class II)	
	σ_t , kgf/mm ²	number of twists, at least	σ_t , kgf/mm ²	number of twists, at least
0.15	270-310	34	225-270	34
0.25	270-310	27	225-270	27
0.50	265-305	16	220-265	19
1.0	250-285	16	206-250	20
3.0	170-195	10	165-195	13
5.0	150-175	4	140-165	9

Spring steels with high mechanical properties (Table 27.12). These are carbon or alloy steels which, in the first place, should have a high resistance to low plastic deformations (elastic limit and proportionality limit), a high endurance limit, and an increased relaxation stability, with appropriate values of toughness and plasticity. High levels of these parameters can be achieved:

(a) by cold plastic deformation (after patenting), which is preferably employed for carbon steels and some alloy steels (50XΦA and 70C2XA). The strengthening effect will be the higher, the higher the carbon content and the greater the degree of compression. Manufactured springs (after coiling, bending or die-forming without drawing) are tempered at 150-250 °C;

(b) by martensite hardening or isothermal hardening to form lower bainite, and by tempering. A higher carbon content of steel then provides a higher elastic limit (Fig. 27.3). Martensite hardening (with either water or oil quenching, depending on the hardening capacity and hardenability of the steel) of springs is followed by tempering them at 350-500 °C. After isothermal har-

Table 27.12. Spring Steels with High Mechanical Properties (GOST 14959-69)

Grade	Composition, %						Applications and properties
	C	Mn	Si	Cr	Ni	other alloying elements	
<i>Carbon steels * (see also GOST 9389-60)</i>							
65Г	0.62-0.70	0.90-1.20	0.17-0.37	≤ 0.25	≤ 0.25	—	} Springs for various machines and mechanisms. With higher carbon content they have higher strength but lower plasticity
70 (1070) **	0.67-0.75	0.50-0.80	0.17-0.37	≤ 0.25	≤ 0.25	—	
75 (1074)	0.72-0.80	0.50-0.80	0.17-0.37	≤ 0.25	≤ 0.25	—	
<i>Alloy steels</i>							
50ХГ *** (5150)	0.46-0.54	0.70-1.00	0.17-0.37	0.90-1.2	≤ 0.25	—	} Automobile springs, Railway vehicle springs. Springs of large presses and machine-tools. Higher alloy steels are for larger springs for especially critical applications.
55ХГР (51В60)	0.52-0.60	0.9-1.2	0.17-0.37	0.90-1.2	≤ 0.25	0.002-0.005 B	
55С2 *** (9255)	0.52-0.60	0.60-0.90	1.50-2.00	≤ 0.30	≤ 0.25	—	
60С2 *** (9260)	0.58-0.63	0.60-0.90	1.50-2.00	≤ 0.30	≤ 0.25	—	
50ХΦА (6150)	0.46-0.54	0.50-0.80	0.17-0.37	0.8-1.1	≤ 0.25	0.10-0.20 V	} Car springs Springs of machine tools and presses Same, for temperature up to 200-250 °C Large valve springs, torsion shafts Clock and watch springs
55ХГСΦ (ЭП464)	0.56-0.64	0.55-0.85	0.6-0.9	0.8-1.2	≤ 0.25	0.1-0.2 V	
60С2ХΦА	0.56-0.64	0.40-0.70	1.40-1.80	0.90-1.2	≤ 0.25	0.1-0.2 V	
65С2ВА	0.61-0.69	0.70-1.00	1.50-2.00	0.30	≤ 0.25	0.80-1.20 W	}
45ХНМΦА	0.42-0.50	0.50-0.80	0.17-0.37	0.80-1.10	1.30-1.80	0.20-0.30 V	
70С2ХА	0.65-0.75	0.40-0.60	1.40-1.70	0.20-0.4	≤ 0.2	0.10-0.20 Mo	

* Carbon tool steels 99A-V12A (see Table 27.17) are also used for making springs, in particular instrument springs.
** Numbers in brackets are SAE designations.
*** Also manufactured as high-quality grades.

* Carbon tool steels Y9A, Y12A (see Table 27.17) are also used for making springs, in particular instrument springs.

** Numbers in brackets are SAE designations.

*** Also manufactured as high-quality grades.

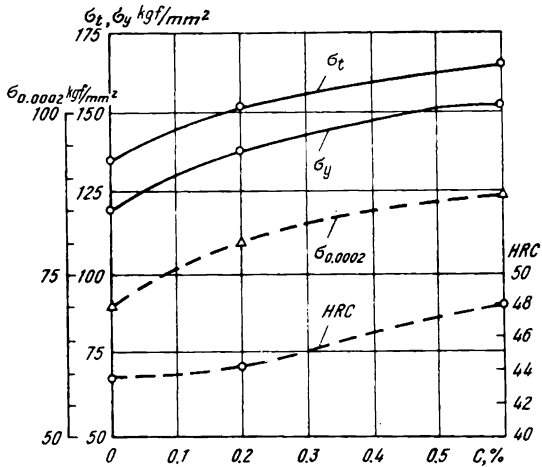


Fig. 27.3. Effect of carbon content on strength properties and elastic limit of carbon steels after hardening and tempering for the maximum elastic limit

dening which gives a higher fatigue strength, the steel is tempered at the same temperature as that of isothermal holding (150 °C). Heat treatment conditions and mechanical properties of spring steels are given in Table 27.13;

Table 27.13. Heat Treatment and Mechanical Properties of Spring Steels

Grade	Hardening conditions		Temper temperature, °C	Mechanical properties (minimum values)			
	heating temperature, °C	quenching		yield limit, kgf/mm ²	ultimate strength, kgf/mm ²	relative elongation, %	relative reduction, %
65Г	830	Oil	480	80	100	8	30
70	830	Same	480	85	105	9	30
75	820	Same	480	90	110	9	30
50ХГ	840	Same	440	110	130	7	35
55ХГР	830	Same	450	125	140	5	30
55С2	870	Oil or water	460	120	130	6	30
60С2	870	Oil	460	120	130	6	25
50ХΦА	830	Same	450	125	140	5	30
60С2ХΦА	852	Same	410	170	190	5	20
65С2ВА	850	Same	420	170	190	5	20

(c) by thermomechanical strengthening (high- or low-temperature) and deformation strengthening of martensite, which ensures the optimum combination of high mechanical properties.

In order to increase the fatigue strength and durability of springs, their surface is improved by removing the decarbonized layer and oxides and reducing their roughness; shot-blasting of the surface is also employed.

Springs made of these steels can operate only in atmospheric air; for better corrosion protection they are cadmium-plated or painted with special lacquers or resins.

The highest working temperature for springs made of carbon steels and most alloy steels is 100-150 °C, and for alloy steels Grades 50XΦA, 60C2XΦA, 65C2BA, and 70C3XMBA, 200-250 °C.

Spring steels and alloys with special chemical and physical properties. 1. Corrosion-resistant steels and alloys (Table 27.14).

Table 27.14. Corrosion-resistant Spring Steels and Alloys (GOST 5632-74)

Grade	Composition, %				Applications
	C	Cr	Ni	other elements	
<i>Martensitic Steels</i>					
30X13	0.26-0.35	12.0-14.0	≤ 0.2	—	} For operation in water and steam
40X13	0.36-0.45	12.0-14.0	≤ 0.2	—	
<i>Austenitic Steels</i>					
08X18H10T	≤ 0.08	17.0-19.0	9.0-11.0	% Ti = 5. % C-0.7%	For operation in corrosive media
<i>Austenite-martensitic Steels</i>					
09X15H8Ю	≤ 0.09	14.0-16.0	7.0-9.4	0.7-1.3 Al	} For operation in aggressive corrosive media
09X17H7Ю	≤ 0.09	16.0-17.5	7.0-8.0	0.5-0.8 Al	
<i>Austenitic Alloys (GOST 10994-64)</i>					
36HXTЮ	≤ 0.05	11.5-13.0	35-37	2.8-3.2 Ti, 0.9-1.2 Al	} Springs, membranes, silphons. Maximum working temperature 200 °C Same, up to 300 °C
36HXTЮM5	≤ 0.05	12.5-13.5	35-37	2.8-3.2 Ti, 0.9-1.2 Al, 4.5-6.5 Mo	
40KHXM	0.07-0.12	19.0-21.0	15.0-17.0	39.0-41.0 Co, 6.4-7.4 Mo	Mainsprings of clocks and like mechanisms

These include:

(a) ferrite-carbide steels with 0.2-0.4 per cent C and 12-14 per cent Cr; they are stable in water and steam and can be strengthened by hardening and tempering;

(b) austenitic steels stable in sea water and nitric and other acids; they can be strengthened by cold plastic deforming with subsequent tempering at 400-500 °C, after which their elastic limit ($\sigma_{0.002}$) is 100-110 kgf/mm² (when cold worked);

(c) austenite-martensitic steels; with the same corrosion resistance as in the previous group, they have better elastic properties ($\sigma_{0.002} = 100$ kgf/mm² without cold working); these steels are strengthened owing to the martensite transformation during hardening (which is stronger if the metal is then subjected to low-temperature treatment) and precipitation hardening during tempering; still greater strengthening effect can be attained by cold deforming after hardening, and by ageing at 450-550 °C;

(d) precipitation-hardening iron-nickel-chrome-base austenitic alloys for long-term operation under corrosion and at temperatures up to 250-350 °C; these alloys can be strengthened ($\sigma_{0.002} = 70-80$ kgf/mm²) by hardening and tempering (ageing); a higher strengthening ($\sigma_{0.002} = 90-100$ kgf/mm²) is obtained by an appreciable plastic deforming after hardening;

(e) high-strength alloys of the cobalt-nickel-chrome-iron system with additions of molybdenum and/or tungsten, and sometimes of titanium, beryllium, etc. ($\sigma_{0.002} = 150$ kgf/mm²).

2. Spring steels having a low constant temperature coefficient of elastic modulus, or elinvar alloys (Table 27.15). These are

Table 27.15. Spring Alloys with Temperature-Independent Elastic Modulus (GOST 10994-64)

Grade	Composition, %							Applications
	C	Si	Mn	Cr	Ni	Al	Ti	
42HXTIO	≤ 0.05	0.50-0.80	0.50-0.80	5.3-5.9	41.5-43.5	0.4-0.8	2.4-3.0	For various elastic elements. Retains a low coefficient of elastic modulus up to +200 °C
42HXTIOA	≤ 0.05	0.50-0.80	0.50-0.80	4.9-5.7	41.5-43.5	0.5-1.0	2.2-3.0	Same, up to +100 °C. For hair springs of timepieces
44HXTIO	≤ 0.05	0.50-0.80	0.50-0.80	5.2-5.8	43.5-45.5	0.5-1.0	2.2-2.7	Same, up to 180-200 °C

nickel-base alloys with an increased content of chromium. A low temperature coefficient of elastic modulus is ensured due to the

ferromagnetic anomaly.¹ To improve the strength properties, the metal is alloyed additionally with 2-3 per cent Ti and 0.5-1 per cent Al; this produces the effect of precipitation hardening owing to solid-solution hardening and subsequent tempering ($\sigma_{0.002} = 60-70$ kgf/mm²). Still greater strengthening is obtained through hardening, cold plastic deforming, and tempering ($\sigma_{0.002} = 80-90$ kgf/mm²).

3. Corrosion-resistant copper-base spring alloys possessing high electric conductivity. These include:

(a) brasses and bronzes which can be strengthened in sheets or wire owing to a high cold deformation and low-temperature (pre-recrystallization) tempering;

(b) beryllium bronzes which can be strengthened by hardening and ageing at 320-340 °C or (for greater effect) by cold plastic deforming (after hardening) and ageing. Beryllium bronzes excel other copper alloys in electric conductivity and elastic limit ($\sigma_{0.002} = 60$ kgf/mm² in beryllium bronzes and up to 40 kgf/mm² in other copper alloys used in springs). Beryllium bronzes are also characterized by low values of elastic hysteresis.

The compositions and applications of copper-base spring alloys are given in Tables 27.27-27.31.

(f) Free-cutting Steels (Table 27.16)

These steels are employed for not very critical purposes, in particular, for machining screws, nuts, bolts, gear wheels, etc. not subjected to dynamic loads.

To reduce friction in such elements, a smooth surface must be formed by machining. This is achieved by reducing the toughness of the steel to be machined, in particular by:

(a) increasing the sulphur and phosphorus content of steel; to make the metal suitable for hot deforming and prevent red shortness, it is simultaneously alloyed with manganese; or

(b) by alloying the steel with lead (0.15-0.30 per cent); this increases the productivity of machining. The mechanical properties of steels alloyed with lead are better than those of steels containing much sulphur and phosphorus.

Free-cutting steels are designated by the letters A (steels with sulphur and phosphorus) or AC (lead-alloyed steels) before the numerals indicating the content of carbon.

¹ Significant paraprocess magnetostriction is observed in these alloys, which is accompanied with a volume effect compensating the resulting elastic deformation of the alloy.

Table 27.16. Free-cutting Steels

Grade	Composition, %					Applications
	C	Mn	Si	Cr	Mo	
<i>Steels with Increased Content of Sulphur (0.08-0.15% S) and Phosphorus (up to 0.06% P), GOST 1414-54</i>						
A15	0.1-0.2	0.6-0.9	0.15-0.35	≤ 0.2	—	Screws, bolts, nuts Same, for higher stresses
A15Г	0.1-0.2	1.0-1.4	0.15-0.35	≤ 0.2	—	
A20	0.15-0.25	0.6-0.9	0.15-0.35	≤ 0.2	—	Same, lead screws; A35 steel had higher strength and wear resistance, but lower ductility
A35	0.30-0.39	0.8-1.2	0.15-0.35	≤ 0.2	—	
<i>Lead-alloy Steels * (0.15-0.25% P)</i>						
AC11	0.07-0.15	0.8-1.1	0.15-0.30	≤ 0.2	—	Screws. nuts bolts
ACV10	0.95-1.04	0.15-0.3	0.15-0.30	≤ 0.2	—	Elements of time-pieces and like instruments
AC35Г2	0.32-0.39	1.35-1.65	0.17-0.30	≤ 0.2	—	Gear wheels and the like
AC45Г2	0.40-0.48	1.35-1.65	0.15-0.30	≤ 0.2	—	
AC30XMA	0.27-0.34	0.35-0.65	0.17-0.37	0.8-1.1	0.15-0.25	

* Specified sulphur content: ACV10 and AC30XMA, up to 0.03%; AC11, 0.15-0.25%; AC35Г2, 0.08-0.13%; and 45Г2, 0.24-0.33%; phosphorus content: up to 0.1% in AC11 steel and up to 0.03% in other grades.

27.4. TOOL STEELS

Tool steels are produced in diverse grades for the manufacture of various cutting tools, hot- and cold-deforming dies, measuring instruments, etc. Accordingly, their properties may be very diverse, but the principal one, indispensable in all tool steels, is their thermostability (or red hardness), i.e. their capability of retaining high values of hardness, strength and wear resistance at working temperatures which may be as high as 500-700 °C with cutting tools and even 800 °C with dies. Red hardness of tool steels is ensured by special alloying and heat treatment.

Many cutting tools are subjected to dynamic loads in service. Then, the steel they are made of should have an increased toughness; in most cases this is achieved by selecting a tool steel with a lower carbon content and by tempering it to a lower hardness

(50-40 HRC). For this reason tool steels are additionally classed by their mechanical properties into (a) steels with high values of hardness and wear resistance (with a lower toughness) and (b) steels with a high toughness with the inevitably lower values of hardness and wear resistance. The following groups of tool steel are distinguished (Fig. 27.4):

1. *Non-thermostable steels* which retain their high hardness (60 HRC) on heating not above 190-225°C. They are used for cutting or deforming relatively soft materials at low speeds. The carbide phase in them is cementite (appr. 950 HV) which coagulates at relatively low temperatures.

These include:

(a) high hardness steels (60-65 HRC); hypereutectoid carbon and alloy steels with a relatively low content of alloying elements; their ultimate strength in bending is 200-250 kgf/mm²;

(b) steels with increased toughness, mainly of the eutectoid type.

2. *Semi-thermostable steels* (mostly die steels) which retain their hardness on heating up to 400-500°C:

(a) steels with high hardness (58-62 HRC), used for making cold-deforming dies; they contain a large amount of hard carbides $M_{23}C_6$ and M_7C_3 (up to 1500 HV) and their structure is ledeburitic or hypereutectoid;

(b) steels with increased toughness, used mainly in dies of forging presses, i.e. at large impacts; in their structure they are close to eutectoid steels but some are hypoeutectoid.

3. *Thermostable steels*:

(a) steels with high hardness (62-65 HRC in most grades and even 69-70 HRC in Grades P8M3K6C and B11M7K23, see Table 27.17). These are typical high-speed tool steels used for cutting at high speeds. They can retain their high hardness (60 HRC) after heating for 4 hours to 620-625°C (steels of medium red hardness), 635-650°C (steels of improved red hardness) or 700-720°C (steels of high red hardness). The structure of high-

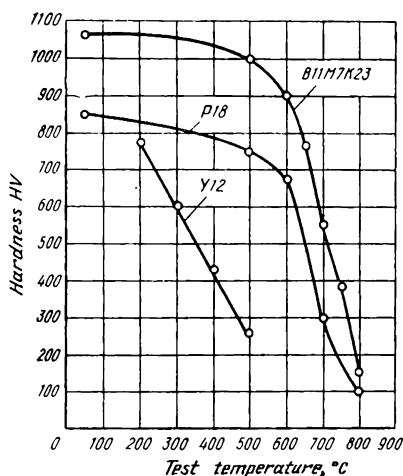


Fig. 27.4 Hardness of tool steels on heating

Y12—common carbon steel; P18—heat-resistant high-speed steel (of a moderate performance); B11M7K23—heat-resistant high-speed steel with intermetallide strengthening

Table 27.17. Tool Steels *

Grade	Composition (average), %							Applications
	C	Mn	Si	Cr	W	Mo	V	
Non-thermostable Steels								
High-hardness steels								
Y10A, Y10	1.0	0.2	≤ 0.3	≤ 0.2	—	—	—	—
Y11A, Y11	1.1	0.2	≤ 0.3	≤ 0.2	—	—	—	—
Y12A, Y12	1.2	0.2	≤ 0.3	≤ 0.2	—	—	—	—
Y13A, Y13	1.3	0.2	≤ 0.3	≤ 0.2	—	—	—	—
13X	1.3	0.2	≤ 0.3	≤ 0.6	—	—	—	—
X (11X15)	1.0	0.3	≤ 0.35	1.5	—	—	—	—
XBCГ	0.95	0.7	≤ 0.8	0.8	0.8	—	—	—
9XΦ	0.9	0.35	≤ 0.2	0.6	—	—	—	—
7XГ2BM	0.7	2	≤ 0.3	1.6	0.6	0.6	0.2	—
Drawing and piercing dies, files, taps for soft materials								
Files, razor blades								
Files, drawing dies								
Screw dies								
Wood saws								
Large and complex piercing dies								
Steels of improved ductility								
Y7, Y7A	0.7	0.2	≤ 0.35	≤ 0.2	—	—	—	—
7XΦ	0.7	0.5	≤ 0.35	0.55	—	—	0.2	—
6XC	0.65	0.4	0.8	1.1	—	—	—	—
6X3ΦC	0.58	0.3	0.5	3.0	—	—	0.3	—
Wood-cutting instruments								
Wood-cutting knives								
Embossing dies								
Semi-thermostable Steels								
High-hardness steels								
X12M	1.6	0.3	0.3	12	—	0.5	0.2	—
X6Φ4M	1.7	0.3	0.3	6	—	0.8	3.8	—
X18MΦ	1.2	0.3	0.3	18	—	0.7	0.1	—
X6B3MΦC	0.55	0.5	0.8	6	3	0.8	0.8	—
Drawing, piercing and pressing dies								
Same, with better wear resistance								
Corrosion-resistant tools								
Knurling rollers								
Steels of improved ductility								
Ni								

Thermostable Steels

High-speed steels of medium red hardness

P12	0.85	0.3	0.3	3.6	12.5	≤ 1	1.7	—	Broachers, milling cutters, counterbores, drills
P6M5	0.8	0.3	0.3	4.0	6.5	5	1.8	—	Taps, broachers, milling cutters, drills
P18	0.75	0.3	0.3	4.0	18	≤ 1	1.2	—	Taps, thread cutters of small diameters

High-speed steels of increased red hardness

P12Φ3 (ЭП597)	1.0	0.3	0.3	3.8	12.5	1	2.7	—	Reamers, broachers, counterbores of increased stability for cutting structural steels
------------------	-----	-----	-----	-----	------	---	-----	---	---

C₀

P12Φ4K5 (ЭП600)	1.3	0.3	0.3	3.8	12.5	1	3.5	5.5	For cutting heat-resistant stainless steels
P8M3K6C	1.1	0.9	0.3	3.8	8	3.6	1.7	6	Same, for structural steels with 35-45 HRC

High-speed steels of high red hardness

B11M7K23	0.1	≤ 0.1	≤ 0.1	≤ 0.2	11	7	0.1	23	For cutting titanium and heat-resistant alloys
----------	-----	-------	-------	-------	----	---	-----	----	--

Die steels (of improved ductility) of medium red hardness

4X5MΦC	0.35	0.3	1.0	5	—	1.5	0.8	—	Dies, pressure-casting moulds
4X5B2ΦC	0.4	0.3	1.0	5	2	—	0.5	—	
4X4M2BΦC	0.4	0.4	0.8	3.5	1	1.5	0.8	—	

Die steels of increased red hardness

5X3B3MΦC	0.48	0.3	0.7	2.8	3.3	0.9	1.6	—	Drawing and piercing upper dies
----------	------	-----	-----	-----	-----	-----	-----	---	---------------------------------

Die steels of high red hardness

2X8B8M2K8	0.2	0.3	0.3	8	8	2	0.1	8	Drawing upper dies, rings, deforming rollers for operation at 650-750 °C
-----------	-----	-----	-----	---	---	---	-----	---	--

* Carbon tool steels according to GOST 1435-74; alloy steels according to GOST 5950-73; high-speed steels according to GOST 19265-73; ЭП steels are not standardized.

speed steels is ledeburitic, the main strengthening phase being M_6C (tungsten or molybdenum carbide with hardness of 1300 HV) or intermetallides $(Fe, CO)_7$, $(W, Mo)_6$ and Fe_3W_2 in steel Grade B11M7K23. The bending strength of these steels is 250-350 kgf/mm²;

(b) steels with increased toughness for hot-pressing dies which can retain their high values of hardness (45 HRC) and yield limit (100 kgf/mm²) upon being heated up to 550 °C (steels of medium red hardness), 580-620 °C (steels of improved red hard-

Table 27.18. Heat Treatment of Typical Tool Steels

Grade	Hardening *		Tempering	
	Heating temperature, °C	HRC	Heating temperature, °C	HRC
<i>Non-thermostable Steels</i>				
Steels of high hardness				
Y12A, Y12	780-800	62-65	150-180	61-63
XBCΓ	855-870	62-64	160-190	61-62
7XΓ2BM	850-870	59-61	170-200	59-60
Steels of improved ductility				
7XΦ	810-830	62-64	250-260	53-55
6X3ΦC	950-970	60-62	300-350 (150-160)	53-55 (58-59)
<i>Semi-thermostable Steels</i>				
Steels of high hardness				
X12M	990-1010	61-63	180-220	59-61
6X6B3MΦC	1060-1075	60-62	525-550	59-61
Steels of improved ductility				
5XHM	820-860	55-58	580-640	33-37
<i>Thermostable Steels</i>				
Steels of high hardness				
P6M5	1220-1240	63-64	550-560 **	63-64
P18	1270-1290	63-64	560-570 **	63-64
Steels of improved ductility				
4X5MC	1050-1070	56-58	600-610	45-46
2X6B8M2K8	1180-1200	56-58	640-680	48-50

* Quenching in oil (20-40 °C) or in salt bath at 150-160 °C for non-thermostable and semi-thermostable steels and at 250-400 °C for thermostable steels; steel Y12A (Y12) is water quenched (15-30 °C).

** Steel P6M5 is tempered twice and P18, three times.

ness) or 700-720 °C (steels of high red hardness). These are eutectoid or hypereutectoid steels with the carbide $M_{23}C_6$ phase (and M_6C in steel Grade 2X6B8M2K8).

The grades and applications of the most typical tool steels are given in Table 27.17.

High-speed steels are designated by the letter 'P'; the following numeral denotes the percentage of tungsten which is the principal alloying element in them. Other tool steels are designated as shown on p. 438; if there is no numeral before the designation letters, the content of carbon is approximately 1 per cent.

Heat treatment of typical tool steels is given in Table 27.18.

27.5. STEELS AND ALLOYS WITH SPECIAL CHEMICAL PROPERTIES (CORROSION-RESISTANT)

Corrosion resistance is determined by (a) the composition of an alloy and its structure (which may be changed, when needed, by heat treatment) and (b) the properties of the aggressive medium in which the alloy is to be used. For this reason an alloy can show different corrosion resistance to various media. Iron alloys, including high-alloy steels, have an appropriate corrosion resistance only to certain media. For instance, many stainless steels which are stable to oxidizing acids (diluted or concentrated nitric acid) have a poor resistance to hydrochloric acid and some other reagents.

In order to ensure corrosion resistance to a wider range of corrosive media, non-ferrous metals and alloys are extensively used.

For these reasons, corrosion-resistant alloys can be characterized and selected for some or other application only by considering the medium in which they will be employed.

The most typical corrosion-resistant alloys are presented in Table 27.19. They may be divided into the groups as follows.

Alloys stable in weak aggressive media (air, water, steam). These are mainly steels with 13 per cent Cr and also aluminium and copper alloys.

Steels become corrosion-resistant when their content of chromium is increased to not less than 12.5-13 per cent (Fig. 27.5). In this case the metal is protected by a rather dense film of passive chromium oxides formed on the surface of the metal.

The content of carbon in the majority of steels of this type (12X13, 20X13) should be low in order to reduce the possibility of the chromium passing into carbides ($M_{23}C_6$), which would inevitably reduce its concentration in the protective oxide film below the required 12 per cent (Fig. 27.6). These steels have only

Table 27.19. Corrosion-resistant (Stainless) Steels and Alloys (GOST 5632-72)

Grade	Composition, %					Applications and properties
	C	Mn	Cr	Ni	other elements	
<i>Steels and Alloys with Ferrite-carbide or Martensitic Structure, Stable in Weak Aggressive Media (Air, Water, Steam), GOST 5632-72</i>						
12X13	0.09-0.15	≤ 0.8	12.0-14.0	—	—	Turbine blades, cracking-plant fittings (up to 500 °C)
20X13	0.16-0.25	≤ 0.8	12.0-14.0	—	—	Same; higher strength
20X17H2	0.17-0.25	≤ 0.8	16.0-18.0	1.5-2.5	—	Articles of increased wear resistance and strength
30X13	0.26-0.35	≤ 0.8	12.0-14.0	—	—	Surgical instruments, springs, needles (50-52 HRC)
40X13	0.36-0.45	≤ 0.8	12.0-14.0	—	—	Same; 56 HRC and more
95X18	0.9-1.0	≤ 0.8	17.0-19.0	—	—	Ball bearings, valves subject to high wear, tools
<i>Copper alloys (see Tables 27.27-27.30)</i>						
<i>Steels and Alloys of Increased Corrosion Resistance (GOST 5632-72)</i>						
15X28	≤ 0.15	≤ 0.8	27.0-30.0	—	—	Apparatus for nitric and phosphoric acid solutions
12X18H10T	≤ 0.12	≤ 2.0	17.0-19.0	9.0-11.0	$\% \text{ Ti} = \left(\frac{\% \text{ C} - 0.02}{5} \right) \times 5 \leq 0.7\%$	Tanks, pipes; good weldability and high resistance to intercrystalline corrosion in sea water, lacquers, nitric and organic acids, and weak alkalis

Maraging Steels (see Table 27.4)

10X17H13M3T	≤ 0.1	≤ 2.0	16.0-18.0	12.0-14.0	0.3-0.6 Ti 3.0-4.0 Mo	Same; greater resistance to phosphoric, acetic and lactic acids
09X15H8Ю	≤ 0.09	≤ 0.8	14.0-16.0	7.0-9.4	0.7-1.3 Al	Disks, shafts (in zinc chloride solutions and phosphorous fertilizers)

Complex brasses, aluminium and tin bronzes, titanium alloys
(see Tables 27.27-27.29, 27.34)

Steels and Alloys of High Corrosion Resistance (GOST 5632-72)

06XH28MДT	≤ 0.06	≤ 0.8	22.0-25.0	26.0-29.0	0.5-0.9 Ti 2.5-3.0 Mo 2.5-3.5 Cu	Welded structures in contact with hot phosphoric or sulphuric acid (20-per cent) at temperatures up to 60°C
H70MΦ	≤ 0.05	≤ 0.5	0.3	Base	25.0-29.0 Mo 1.4-1.7 V	Same; in hydrochloric and phosphoric acids, and also in diluted (60-per cent) sulphuric acid
Lead	—	—	—	—	—	Sulphuric acid in any concentration

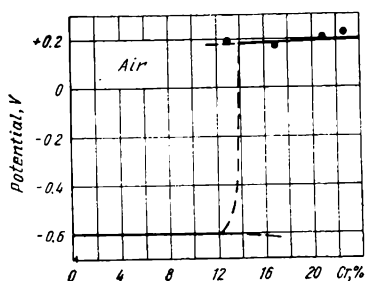


Fig. 27.5. Potential of iron in air depending on chromium content

fair values of strength (below 70 kgf/mm²), hardness and wear resistance. Their structure is usually ferrite plus carbides.

With a higher carbon content (0.3-0.4 per cent or more), heat treatment becomes indispensable: hardening from 1000-1100 °C (to remove chromium carbides into the solid solution) and low tempering (150-200 °C). Steels of this type are employed in cutting tools (particularly medical and domestic ones) and springs in

the state when they have a martensitic structure (chromium being present in the α -phase) and a high hardness: 52-55 HRC for Grades 30X13 and 40X13 and up to 58-59 HRC in steel 9X18. The metal, however, has reduced toughness.

More expensive copper alloys — brasses and bronzes, whose compositions are given in Tables 27.27-27.30, are used instead of steels mostly in elements and units where a low coefficient of friction is needed.

Aluminium is used in structures where its low density (2.74 g/cm³) is of merit.

Alloys stable in more aggressive media (sea water, organic acids, etc.). These are mostly austenitic steels high in chromium and nickel, and also special brasses and bronzes (tin- and aluminium-alloyed) and titanium alloys. Their compositions may be found in Tables 27.27-27.31, 27.32, and 27.34.

Alloys stable in high aggressive media (hot or concentrated acids). These compositions may be very diverse, depending on the medium, as shown in Table 27.19.

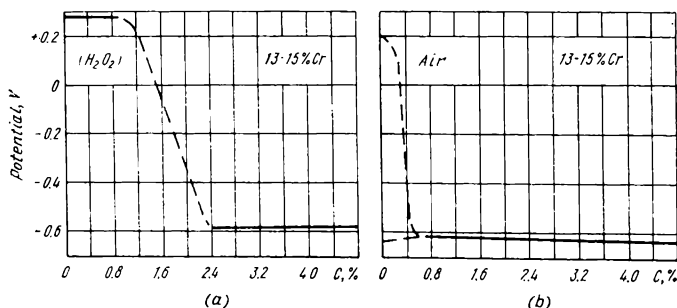


Fig. 27.6. Potential of steel with 13-15% Cr depending on carbon content (a) in hydrogen peroxide; (b) in air

27.6. STEELS AND ALLOYS WITH SPECIAL PHYSICAL PROPERTIES

These materials are needed in the instrument-making, electrical engineering, radioengineering and electronic industries. A required physical property is formed in a metal by special alloying and heat treatment. The following groups may be distinguished according to the principal property required.

(a) Alloys with a Low Specified Coefficient of Expansion (Table 27.20)

These are alloyed with nickel, cobalt, chromium, and copper (GOST 10994-64), the coefficient of expansion being varied by changing the proportions of these elements. The lowest expansion is shown by an alloy with 36 per cent Ni: it is only $1.5 \times 10^{-6} \text{ } 1/^{\circ}\text{C}$ at $20\text{--}200^{\circ}\text{C}$ against $12 \times 10^{-6} \text{ } 1/^{\circ}\text{C}$ for iron. These alloys are used for articles to be soldered in into inorganic dielectrics: glass, ceramics, mica, etc.

(b) Alloys with Temperature-independent Elastic Modulus

These alloys are used in springs of measuring instruments (GOST 10994-64); the composition was given earlier (Table 27.15).

(c) Alloys of High Magnetic Permeability (Magnetically Soft Alloys, Fig. 27.7)

These alloys usually combine this property with a low coercive force and a high resistivity (which reduces eddy-current losses). Two groups may be distinguished here according to the method of manufacture, structure, and some properties.

The first group includes:

(a) *transformer and dynamo silicon steels* produced as thin sheets by hot or cold rolling (Table 27.21); cold-rolled steel is characterized by anisotropy, which increases magnetic properties in the direction of rolling and reduces remagnetization losses;

(b) *iron-nickel alloys (permalloy)* manufactured as thin sheets

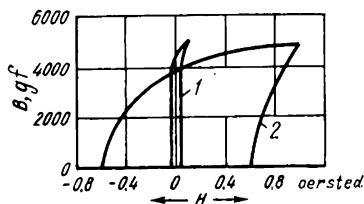


Fig. 27.7. Magnetic hysteresis loops

1—magnetically soft alloys; Armco iron and alloys of the permalloy type; 2—magnetically hard alloy; Alnico

Table 27.20. Alloys with Low Specified Expansion Coefficient (GOST 10994-64)

Grade	Composition, %						Expansion coefficient ($\times 10^{-6}$ 1/°C), properties, and applications
	C	Si	Mn	Ni	Co	Cu	other elements
36H	≤ 0.05	≤ 0.30	0.30-0.60	35.0-37.0	—	—	0.15 Cr
32HKД 29HK	≤ 0.05 ≤ 0.03	≤ 0.20 ≤ 0.30	0.40 0.40	31.5-33.0 28.5-29.5	3.2-4.2 17.0-18.0	0.6-0.8 —	— —
30HKД	≤ 0.05	≤ 0.30	0.40	29.5-30.5	13.0-14.2	0.3-0.5	—
47HX	≤ 0.05	≤ 0.30	0.40-0.70	46.0-47.5	—	0.20	0.7-1.0 Cr
47HД	≤ 0.05	≤ 0.30	0.40	46.0-48.0	—	4.5-5.4	—
47HXP	≤ 0.05	≤ 0.30	0.40	46.0-48.0	—	—	4.5-6.0 Cr B ≤ 0.02
18ХМТФ	≤ 0.07	≤ 0.65	≤ 0.60	≤ 0.60	—	—	17-19 Cr 0.25-0.45 V 0.25-0.45 Mo 0.4-0.8 Ti

Instruments where dimensions must be constant within the range of climatic temperatures 1.0; same
4.5-5.5 at -70 to $+420^\circ\text{C}$. Vacuum-tight junctions of radio-electronic devices; can be welded with glasses C-49-1, C-49-2, C-48-1, etc.
3.8-4.6 at $20-400^\circ\text{C}$. Vacuum-tight junctions with refractory glass C-38-1 and C-40-1
8.0-9.0 up to 450°C . Vacuum-tight junctions with thermometric glass
8.0-11.0 at -70 to $+460^\circ\text{C}$. For welding together with soft glasses, mica, and ceramics
8.0-11.0 at -70 to $+360^\circ\text{C}$. Vacuum-tight junctions of radio-electronic devices with glasses C-87-1, C-89-1, C-88-1, etc.
10-11.4 at -70 to $+550^\circ\text{C}$. Vacuum-tight junctions with glass C-87-1, B-9-1 for television tubes

Table 27.21. Steels and Alloys of High Magnetic Permeability (Magnetically Soft), GOST 802-58

Grade	Minimum induction, gauss · 10 ⁴ at field intensity		Total specific loss, W/kg, at most	Resistivity, ohm mm ² / m	Applications
	25 A/cm	50 A/cm			
<i>Hot-rolled Low-alloy Steel (0.8-1.8% Si)</i>					
Э-11	1.53	1.64	3.3	0.25	Rotors and stators of low-power asynchronous motors; armatures of low-power d. c. motors
Э-12	1.50	1.62	3.2	0.25	
<i>Cold-rolled Low-texture Low-alloy Steel (1.0-1.8% Si)</i>					
Э-1100	1.53	1.64	3.3	0.25	Same
Э-1200	1.53	1.64	2.8	0.25	Same
<i>Hot-rolled Medium-alloy Steel (1.8-2.8% Si)</i>					
Э-21	1.48	1.59	2.5	0.40	Armatures of medium-power d. c. motors
Э-22	1.48	1.59	2.2	0.40	
<i>Hot-rolled High-alloy Steel (2.8-3.8% Si)</i>					
Э-31	1.46	1.57	2.0	0.50	Stators and rotors of high-power asynchronous motors
Э-32	1.46	1.57	1.8	0.50	
<i>Cold-rolled Textured High-alloy Steel (2.8-3.8% Si)</i>					
Э-3100	1.50	1.60	1.7	0.50	Same
Э-3200	1.48	1.58	1.5	0.50	
<i>Cold-rolled Low-texture High-alloy Steel (2.8-3.5% Si)</i>					
Э-310	1.75	1.83	1.1	0.50	Power transformers and stators of large hydro- and turbogenerators
Э-320	1.80	1.87	0.95	0.50	
Э-330	1.85	1.90	0.8	0.50	
<i>Hot-rolled Very High-alloy Steel (3.8-4.8% Si)</i>					
Э-41	1.46	1.57	1.55	0.60	Power transformers and stators of large electric machines
Э-42	1.45	1.56	1.4	0.60	
Э-43	1.44	1.55	1.25	0.60	

- Notes. 1. All the grades have a low carbon content ($\leq 0.05\%$).
2. The first numeral in the designation indicates the degree of alloying (silicon content), the second, the guaranteed electrical and magnetic properties; the larger the second numeral, the smaller the unit losses (1 — normal unit losses; 2 — reduced losses; and 3 — low losses); a zero (0) after the second numeral implies a cold-rolled textured steel, and two zeros (00), a cold-rolled low-texture steel. The properties are given for steel sheets 0.50 mm thick; with smaller thickness the total unit losses reduce.

Table 27.22. Alloys of Especially High Magnetic Permeability
(Magnetically Soft Alloys; Permalloys), GOST 10994-64 and 10160-62

Grade	Composition*, %				Magnetic permeability, ** gauss/oersted		Applications
	Si	Ni	Cr	Mo	Initial	maximum	
Technical Saturation ≥ 15,000 gauss							
50H	0.15-0.30	49.0-50.5	≤ 0.2	—	1 800	18,000	Cores, chokes, relays, small-size power transformers, etc. Possesses crystalline structure and rectangular hysteresis loop
50HП	0.15-0.30	49.0-50.5	≤ 0.2	—	500-1 000	35,000	
Technical Saturation ≥ 13,000 gauss							
65HП	0.15-0.30	64.5-66.0	≤ 0.2	—	300-1 500	35,000	Same
Technical Saturation ≥ 10,000 gauss with Higher Electrical Resistance							
50HXC	1.10-1.40	49.5-51.0	≤ 3.8-4.2	—	1 500	12,000	Cores of pulse transformers; audio- and high-frequency communication means
Technical Saturation 6500-7500 gauss; High Magnetic Permeability							
79HM	0.30-0.50	78.5-80.0	≤ 0.2	3.8-4.1	16,000	60,000	Cores of small-size transformers, chokes of magnetic screens (mainly for weak fields)
80HXC	1.10-1.50	79.0-81.0	2.6-3.0	—	18,000	70,000	

* The content of carbon is ≤ 0.03 per cent and that of manganese, 0.3-0.1 per cent.

** The properties indicated are for cold-rolled strip 0.02-0.04 mm thick.

and strips for magnetic circuits operating in variable magnetic fields (GOST 109994-64 and 10160-62). The grades and composition of these alloys are given in Table 27.22.

The maximum magnetic permeability of silicon steels (around 17,000 gauss/oersted in steel Э330) is higher by a factor of ten than in carbon steel 10 (1700 gauss/oersted) and is still higher (around 150,000 gauss/oersted) in permalloys.

The second important group are non-metallic ferromagnetic compounds (ferrites) which possess the properties of semiconductors. They have an appreciably higher (by six orders of magnitude) electrical resistance and a lower saturation magnetization than in silicon steels and permalloys. This reduces eddy-current losses and makes the ferrites suitable for making cores and coil chokes of radioengineering and electrical devices.

**Table 27.23. Alloys of High Magnetic Permeability
(Magnetically Soft Alloys, Ferrites)**

(A) Alloys for High-frequency Devices

Grade	Magnetic permeability, gauss/oersted		ρ , ohm mm ² / m	Curie point, °C	Applications
	initial	maximum			
6000HM	6 000	10,000	1×10^{-2}	110	Transformer cores of magnetic amplifiers Same; induction coils, radio communications devices Same, chokes and transformers
1000HM	1 000	2 000	5×10^{-2}	200	
2000HH	2 000	7 000	1×10^{-3}	70	

(B) Alloys for Superhigh-frequency Devices

Grade	B_s , gauss	B_r , gauss	H_c , A/m	ρ , ohm mm ² / m	Curie point, °C	Applications
4C44 (magnesium-base)	1130	780	300	4.8×10^5	310	Switches, phase shifters
10C412 (nickel-base)	890	590	625	5.2×10^4	350	Resonance devices
30C4 (magnesium-base ferrochromate)	600	300	170	3.3×10^5	180	Waveguide circulators, coaxial valves

The majority of ferrites — spinels — have a structure of $\text{MeO Fe}_2\text{O}_3$ where Me is the ion of bivalent iron (or nickel, chromium or magnesium) with a complex cubic lattice. The frame of the lattice is formed by 32 oxygen anions, with the voids between them being filled with metal cations. The magnetic vectors of cations are different in various voids; they are directed anti-parallel, which ensures a low saturation magnetization. The grades and properties of ferrites are given in Table 27.23.

(d) Alloys of High Coercive Force (Magnetically Hard Alloys)

These steels and alloys may be characterized by a high coercive force and remanence and correspondingly high magnetic energy. The coercive force of these alloys is 10-20 times higher than that of hypereutectoid steel Grade X(ШХ15) with 1 per cent C and 1.5 per cent Cr, which is used in less powerful magnets.

Table 27.24. Steels and Alloys of High Coercive Force (Magnetically Hard Alloys for Permanent Magnets), GOST 4402-48 and 9575-60

Grade	Composition, %					Applications
	Ni	Al	Co	Cu	Ti	
Steels of Low Magnetic Energy, (HB) _{max} ≥ 1.5 Mgauss oersted						
AH1	22	11	—	—	—	Electric machines and devices
AH2	24.5	13.5	—	3.5	—	
Steels of Medium Magnetic Energy, (HB) _{max} = 1.5-2.5 Mgauss oersted						
AHK01	18	10	12	6	—	Electric machines and devices
ЮНДК15	20	9	15	4	—	
Steels of High Magnetic Energy, (HB) _{max} = 2.5-5.5 Mgauss oersted						
ЮНДК18	19	10	18	—	—	High-capacity electric machines and devices
ЮНДК24	14	9	24	4	0.3	
ЮНДК24Т2	14	9	24	4	2	
ЮНДК24Б	14	9	24	4	0.8	
Steels of Especially High Magnetic Energy, (HB) _{max} = 5.5-12 Mgauss oersted						
ЮНДК35Т5	15	8	35	4	5	Very high-capacity electrical machines and devices
ЮНДК35Т5А	14	7.2-7.6	35	4	5-6	
ЮНДК42Т8	—	7.2-7.5	42	4	8	

Notes. 1. Classification is given according to Dovgalevsky, Ya. M., *Legirovanie i termicheskaya obrabotka magnitnotverdykh splavov* (Alloying and Heat Treatment of Magnetically Hard Alloys). Moscow, Metallurgiya Publishers, 1971.

2. The capacity factor of a machine increases with increasing magnetic energy.

The composition of these alloys is essentially Fe-Ni-Al, some grades being additionally alloyed with copper or with copper, cobalt, and titanium (Table 27.24), which increases the coercive force even more. Because of their low plasticity, the alloys are employed only in castings.

Hardening with a definite rate (for alloys having ≥ 18 per cent Co, also with application of a magnetic field) and tempering can form a heterogeneous structure in which fine (single-domain) anisotropic inclusions of the ferro-magnetic phase are distributed within the paramagnetic matrix; this ensures a high coercive force.

(e) Alloys with High Electrical Resistance

These alloys should combine a high electrical resistance with a high refractoriness. Their electrical resistance is usually ten times that of low-carbon steel (0.1 ohm m), while refractoriness may be as high as 1000-1200 °C (Table 27.25). In addition, they have a low temperature coefficient of electrical resistance and plasticity sufficiently high to form them into rods, strips, wire, etc., including small-size sections.

The composition of these alloys may be Fe-Cr-Al, Fe-Ni-Cr or Ni-Cr, and their structure is usually the solid solution with a high concentration of alloying elements: chromium in nickel-base alloys and chromium and aluminium in iron-base alloys.

B. CAST IRONS

Among all metals, cast irons are used most widely for casting articles to operate at relatively low stresses and low dynamic loads. Their advantages are good castability and low cost (compared with steel).

The melting points of cast irons are appreciably lower (by 300-400 degrees C) than for steels, which facilitates the casting process. Besides, they are less liable to segregation.

Furthermore, cast irons in whose structure much graphite is formed upon solidification (this phase has a higher unit volume than the iron matrix) have a low shrinkage ratio approaching that of tin bronze.

Cast irons containing much graphite are machined well (with the formation of brittle chips) owing to the presence of this soft and brittle component, and the machined surface is cleaner than with most steels (except for free-cutting grades).

Cast irons have a high content of carbon (2.2-4 per cent) and silicon (0.8-2 per cent), the latter element favouring graphitization. Usually the composition of cast iron grades is not given,

Table 27.25. Alloys with High Electrical Resistance (GOST 12766-67)

Grade	Composition, %					Resistivity, $\frac{\text{ohm} \cdot \text{mm}^2}{\text{m}}$ at 20 °C	Optimum working temperature, °C	Applications
	C	Mn	Si	Cr	Ni	Al		
X13Ю4	≤ 0.15	≤ 0.7	≤ 1.0	12.0-15.0	≤ 0.6	3.5-5.5	1.18-1.34 *	900 Rheostats, heating elements of domestic appliances
0X23Ю5	≤ 0.06	≤ 0.5	≤ 0.7	21.5-24.5	≤ 0.6	4.5-5.5	1.29-1.45 *	1150 Same; for industrial and laboratory furnaces
0X23Ю5A	≤ 0.05	≤ 0.3	≤ 0.6	21.5-23.5	≤ 0.6	4.6-5.3	1.3-1.4 *	1175 Same; higher refractoriness
0X27Ю5A	≤ 0.05	≤ 0.3	≤ 0.6	26.0-28.0	≤ 0.6	5.0-5.8	1.37-1.47 *	1250 Heating elements of industrial and laboratory furnaces
X25H20 X20H80	≤ 0.15 ≤ 0.15	≤ 2.0 ≤ 0.7	≤ 1.0 0.4-1.5	24.0-27.0 20.0-23.0	17.0-20.0 Base	— ≤ 0.2	0.83-0.96 * 1.03-1.13 **	900 Heating elements of electric furnaces and other electric devices

* For rods and wire 0.2 to 10.1 mm in diameter.

** For wire and strips 0.1 to 0.5 mm thick.

since (as distinct from the majority of other metallic alloys) it cannot characterize their properties sufficiently, and therefore, the field of application. The structure and properties of cast irons are strongly dependent on the conditions of casting (the temperature of molten metal, introduction of modifiers) and especially on cooling conditions after casting. Therefore, with the same composition, cast irons may have strongly differing structures and properties (for instance, white and grey irons).

The mechanical properties of cast iron, which determine its use, can be more or less fully characterized by its structure, i.e. by (a) the shape and size of graphite inclusions and (b) the structure of the metallic matrix.

Graphitized cast irons are less sensible to notching than steels. For this reason the mechanical properties of cast irons and steels differ more in articles of simple shape without notches or sharp changes of cross section and are less different in notched articles.

By their structure, cast irons are classified as shown in Table 27.26. The mechanical properties are given for unnotched specimens.

Grey iron. Grey irons are mainly used for casting articles in sand or in metallic (iron) moulds. Graphite is present in lamellar form in their structure (see Fig. 12.7). With a higher thickness of casting (i.e. with slower cooling) and with higher silicon content, more graphite is formed in the metal and its lamellae are larger, while the content of ferrite in the iron matrix increases. In smaller castings or with a lower content of silicon (or a higher content of manganese),¹ less graphite is formed and the metallic matrix is ferrite-pearlite or pearlite, which increases the strength.

Because of the relative ease of the casting process, grey irons have long been the most widely used variety of cast irons. But their mechanical properties are inferior to those of other graphite irons (Table 27.26). In particular, they have poor plasticity and cannot withstand dynamic loads and for this reason are only employed for less critical applications.

Malleable iron. The structure of malleable iron contains flaky graphite (see Fig. 12.9). Because of this, malleable irons have better mechanical properties, in particular plasticity, but their manufacture is more complicated. High-quality grades of malleable iron are melted in electric furnaces, which makes it possible to reduce their carbon content and remove sulphur and

¹ Or chromium in alloy irons.

Table 27.26. Cast Irons (Structure, Properties and Applications)

Grade	Ultimate strength, kgf/mm ² , in		Relative elongation, %	Applications
	tension	bending		
Grey Irons				
Ferritic				
C412-28 *	12	28	1	Non-critical articles (co- vers, pulleys, etc.)
C415-32	15	32	1	
Ferrite-pearlitic				
C418-36	18	36	1	Stands of machine tools and mechanisms; pis- tons, cylinders
C421-40	21	40	1	
Pearlitic				
C424-44	24	44	1	Wear-resistant elements: brake drums, cylinders, gear wheels
C428-48	28	48	1	
C432-52	32	52	1	
Malleable Irons				
Ferritic				
K435-10 **	35	—	10	Flanges, couplings
K437-12	37	—	12	
Ferrite-pearlitic				
K445-6	45	—	6	Automobile rear axles, crankcases, wheel bos- ses
High-strength (Magnesium-modified) Irons				
Ferritic				
B445-5 ***	45	—	5	Press traverses, flanges, cylinders, gear wheels
Pearlitic				
B450-2	50	—	2	Cylinders, pistons, crank- shafts
Chilled Iron				
	—	—	—	Rolling-mill rolls, work- ing parts of crushing mills, non critical wheels

* GOST 1412-70.
** GOST 1215-59.
*** GOST 7293-70.

phosphorus more deeply. Besides, all grades of malleable iron are low in silicon.

As cast, they form the structure of white hypoeutectic iron. Small-size thin-walled castings are preferable, since they can be cooled rapidly to interrupt graphitization.

Subsequent graphitization of castings to form the final structure of flaky graphite and high mechanical properties is done by heating to 950-980 °C, i.e. in the solid state, the heating being followed by slow cooling, which takes much time, up to 100-120 hours.¹

High-strength iron. This contains spheroidal (globular) graphite (see Fig. 12.8) in the structure, which is less harmful for the continuity of the iron matrix (especially as compared with lamellar graphite). The strength properties of high-strength iron are the highest among cast irons and comparable with structural carbon steels after heat treatment; only their plasticity is lower than that of steel or malleable iron.

High-strength irons are modified by adding magnesium (or cerium) into the ladle after tapping the molten metal from a cupola furnace. Casting is done in sand or metallic moulds, as with grey iron. Because of their better mechanical properties high-strength irons are gradually displacing grey irons for casting large parts.

Chilled cast iron. Articles made of chilled iron have the structure of grey or high-strength iron in the core and ledeburitic or pearlitic structure in the surface layer which thus has a high hardness (450-550 HB). This provides high wear resistance, but sharply impairs machinability of castings. Chilled iron finds a limited application for casting simple-shape articles when a clean surface of castings is essential. The casting is usually done in metallic moulds in order to accelerate cooling of surface layers.

White iron. This has the structure of pearlite plus cementite over the whole cross section or to an appreciable depth and is usually of hypoeutectic type. Despite its high wear resistance and hardness, white iron finds almost no use because of poor machinability and low mechanical properties.

C. COPPER ALLOYS

Copper alloys with zinc, tin, aluminium, silicon, etc. have higher strength than the pure metal (30-60 kgf/mm² against 25-29 kgf/mm² in commercially pure copper) and are widely em-

¹ In some advanced processes for treating liquid metal, the graphitization time has been reduced by 20-30 per cent.

ployed for making various machine elements (see Tables 27.27-27.31).

Copper alloys cannot be heat treated (except for beryllium bronze and some aluminium bronzes) and their mechanical properties and wear resistance are fully determined by their composition and structure. The elastic modulus of copper alloys (9000-12,000 kgf/mm²) is lower than that of steel.

The main merit of copper alloys is their low coefficient of friction (making advantageous their use in sliding pairs), which in many alloys is combined with high plasticity, high corrosion resistance to various aggressive media, and high electric conductivity.

The coefficient of friction is almost the same in all copper alloys, whereas their mechanical properties, wear resistance, and corrosion resistance depend on the composition, and therefore, on the structure. Higher values of strength are usually exhibited by two-phase alloys, while single-phase alloys are more plastic.

Grades of copper alloys. Designation of copper alloys in the USSR is as follows.

The first letter in the designation may be either Л (for brass) or Бр. (for bronze). The letter that follows may denote: А — aluminium, Б — beryllium, Ж — iron, К — silicon, Мн — manganese, Н — nickel, О — tin, С — lead, Ц — zinc, and Ф — phosphorus.

The numerals after the letters indicate the average percentage of alloying elements, the order to those numerals adopted for brasses being different from that for bronzes.

For brass grades, the first two numerals after the letters give the content of the main element — copper. Other numerals, separated by a dash, indicate average percentages of alloying elements, these numerals being written in the same order as the letters. Therefore, the content of zinc is not given in the designation and may be found by subtraction. For instance, Л68 is brass with 68 per cent Cu (on the average) and no alloying elements, except zinc; the latter's content is therefore 32 per cent. ЛАЖ60-1-1 denotes brass with 60 per cent Cu, alloyed with 1 per cent aluminium and 1 per cent iron, the content of zinc being found as the balance, i.e. 100 per cent minus the percentages of copper, aluminium and iron.

For bronzes (as for steels), the content of the main component (copper) is not indicated, but determined as the balance. Alloying elements are denoted by numerals separated by dashes, the order of numerals being the same as that of the letters denoting the alloying elements. For instance Бр.ОЦ10-2 denotes bronze with 10 per cent tin (О) and 2 per cent zinc (Ц), the balance being copper. Бр.АЖН10-4-4 is bronze with 10 per cent Al, 4 per

Table 27.27. Brasses (GOST 15527-70)

Grade	Composition, %					Applications
	Cu *	Al	Pb	Sn	other elements	
<i>Ordinary Brasses</i>						
Single-phase plastic brasses for hot and cold deforming						
J196 (tombac)	95.0-97.0	—	—	—	—	Radiator pipes, sheets, strips
J180 (semitombac)	79.0-81.0	—	—	—	—	Pipes, strips, wire
J168	67.0-70.0	—	—	—	—	Sheets and strips for deep drawing
Two-phase brasses of lower plasticity for hot deforming and casting						
J1C59-1	57.0-60.0	—	0.8-1.9	—	—	Sheets, pipes, castings; high machinability
<i>Complex Brasses with Increased Corrosion Resistance</i>						
Single-phase brasses for plastic working						
J1A77-2	76.0-79.0	1.7-2.5	—	—	—	Pipes for the ship-building and machine-building industries
J1O70-1	69.0-71.0	—	—	1-1.5	—	Heat-exchanger pipes
Two-phase casting brasses (GOST 17711-72)						
J1A67-2.5	66-68	2-3	≤ 1.0	—	—	Machine-building and ship-building castings
<i>Complex Brasses with Increased Strength and Corrosion Resistance</i>						
Single-phase brasses for plastic working						
J1A159-3-2	57.0-60.0	2.5-3.5	—	—	2-3 Ni	Pipes, heavy-duty elements for engine-building and ship-building industries
J1A160-1-1	58.0-61.0	0.75-1.5	≤ 0.4	—	0.8-1.5 Fe	
Two-phase casting brasses (GOST 17711-72)						
J1M111K55-3-1	53-58	—	≤ 0.5	1.3-4.5	0.5-1.5 Fe 4-3 Mn	Large ship-building castings
J1M111OC58-2-2-2	57-60	—	0.5-2.5	1.5-2.5	1.5-2.5 Mn	Pinions and gear wheels

* Balance is zinc.

* Balance is zinc.

cent Fe, and 4 per cent Ni (and 82 per cent Cu). Бр.КМц3-1 is bronze with 3 per cent Si and 1 per cent Mn (and 96 per cent Cu).

Copper-zinc alloys. Brasses (Table 27.27). The composition of brasses may be either ordinary or complex and their structure, single- or two-phase.

Ordinary brasses are those alloyed with a single element — zinc.

Single-phase ordinary brasses have high plasticity, the highest values being exhibited by brasses with 30-32 per cent Zn (Grades Л170 and Л167). Brasses with a lower content of zinc (tombacs and semitombacs) are less plastic but have higher values of electric and thermal conductivity. They can be manufactured rolled or forged.

Two-phase ordinary brasses are malleable (mainly upon heating) and have improved castability. They are manufactured rolled or cast. They are less plastic than single-phase grades, but have better values of strength and wear resistance owing to the effect of hard particles in the second phase.

The strength of ordinary brasses is 30-35 kgf/mm² in single-phase structures and 40-45 kgf/mm² in two-phase structures. Single-phase grades can be strengthened appreciably by cold plastic deforming. They possess appropriate corrosion resistance to water and steam (provided that the stresses formed through cold deforming have been released).

Complex-alloy brasses have higher strength (up to 50-55 kgf/mm²) and are stable in sea water.

Tin bronzes (Table 27.28). Single- and two-phase tin bronzes excel brasses in their strength and corrosion resistance (especially in sea water).

The strength and elastic properties of single-phase tin bronzes can be improved (with $\sigma_t \geq 40$ kgf/mm²) by rolling, especially by strong cold plastic deforming.

A feature characteristic of two-phase bronzes is their higher wear resistance. Another merit inherent in them is good castability: the shrinkage of castings is smaller than with all other metals, including cast irons. Tin bronzes are used for casting articles of complicated shape. They can be employed for making boiler fittings and like articles, but only for low operating pressures. A disadvantage of tin bronze castings is their high micro-porosity, that is why they are replaced more and more with aluminium bronzes, especially in articles which are to operate at high steam pressures.

Because of the high cost of tin, in some grades of tin bronze it is often partially replaced with zinc (or lead).

Table 27.28. Tin Bronzes

Grade	Composition, %					Applications
	Sn	P	Zn	Ni	Pb	
<i>Single-phase Bronzes for Plastic Working (GOST 5017-49)</i>						
Бр.ОФ6.5-0.15	6-7	0.1-0.25	—	—	—	Strips and nets for chemical and paper-making industries. Membranes, springs, friction parts
Бр.ОЦ4-3	3.5-4	—	2.7-3.3	—	—	Springs, membranes, contacts
<i>Two-phase Casting Bronzes (Not Standardized)</i>						
Бр.ОЦ10-2	9-11	—	2-4	—	—	Pinions, sleeves, bearings
Бр.ОФ10-1	9-11	0.8-1.2	—	—	—	Same, higher plasticity
Бр.ОЦ11-4-3	—	—	—	4	3	Same, for higher temperatures; valve sleeves

Aluminium bronzes (Table 27.29). These bronzes (single- and two-phase) find ever wider application to replace brasses and tin bronzes.

Table 27.29. Aluminium Bronzes (GOST 18175-72)

Grade	Composition, %			Applications
	Al	Fe	Ni	
<i>Single-phase High Plasticity Bronzes</i>				
Bp.A5	4-6	—	—	Strips, springs
<i>Two-phase High-Strength Bronzes</i>				
Bp.AЖ9-4	8-10	2-4	—	Pinions, sleeves, fittings, including sea-water applications (rolled or cast)
Bp.AЖН10-4-4	9.5-11	3.5-5.5	3.5-5.5	Same, for higher pressure and friction

Single-phase aluminium bronzes have the highest plasticity of all copper alloys (δ up to 60 per cent). They are used for manufacture of sheets (including thin sheets) and for die-forming with appreciable deformations. Strong cold plastic deformation may increase their strength and elasticity.

Two-phase aluminium bronzes can be hot deformed or cast. They have poorer castability (fluidity) and higher shrinkage than tin bronzes, but form no pores in castings. Their casting properties can be improved by adding small amounts of phosphorus. Aluminium bronzes are used in particular for casting boiler fittings of relatively simple shape but for operation at high stresses.

In addition, two-phase aluminium bronzes have higher strength than brasses and tin bronzes. In complex-alloy aluminium bronzes containing nickel and iron, the ultimate strength is as high as 55-60 kgf/mm².

All aluminium bronzes, like tin bronzes, resist well corrosion in sea water and moist tropical atmosphere.

Aluminium bronzes are employed in ship-building, aviation and other industries as strips, sheets, wire, etc. for manufacture of elastic elements, in particular current-conducting springs.

Silicon bronzes (Table 27.30). Silicon bronzes find only a limited application, single-phase grades being used more as they are more plastic. They excel aluminium bronzes and brasses in their strength and stability in alkaline media (including sewage waters). They are used, in particular, for making pipes and fittings to operate in these media.

Table 27.30. Silicon Bronzes (GOST 18175-72)

Grade	Composition, %			Applications
	Si	Mn	Ni	
Бр.КМц3-1	2.75-3.5	1-1.5	—	Springs, sleeves, pipes for ship-building, aviation and chemical industries
Бр.КН 1-3	0.6-1.1	0.1-0.4	2.4-3.4	Sleeves, valves, bolts and other elements for operation in sea and sewage waters

Silicon bronzes additionally alloyed with manganese acquire a high strength and a high elasticity through strong cold deforming and are used as sheets and wire or for making various elastic elements.

Beryllium bronzes (Table 27.31). Beryllium bronzes combine a very high strength (up to 120 kgf/mm²) with corrosion resistance and high electric conductivity. These properties are formed in

Table 27.31. Beryllium Bronzes (GOST 18175-72)

Grade	Composition, %				Applications
	Be *	Ni	Ti	Mg	
Бр.Б2	1.8-2.1	0.2-0.5	—	—	High-strength and current-conducting springs; membranes, bellows
Бр.БНТ1,7	1.6-1.85	0.2-0.4	0.1-0.25	—	
Бр.БНТ1,9	1.85-2.1	0.2-0.4	0.1-0.25	—	
Бр.БНТ1,9Мг **	1.85-2.1	0.2-0.4	0.1-0.25	0.07-0.13	

* Elastic properties can be improved by increasing beryllium content or adding magnesium.

** Not standardized.

them through heat treatment or thermomechanical treatment. In the former case bronze is hardened from 770-780 °C and aged at 320-340 °C for 2-4 hours, and in the latter, subjected to cold plastic deforming after hardening (by rolling or drawing) and then to ageing, which provides a higher strength, but lower plasticity and toughness. Beryllium bronzes are rather expensive and, despite their excellent physico-mechanical properties, are only employed for very critical applications in articles of small cross section in the form of strips or wire for making springs, membranes, silphons, and electric contacts.

D. ALUMINIUM ALLOYS

The principal advantage of aluminium alloys, which determines the field of their application is their low density (2.7-3.0 g/cm³) combined with appropriate mechanical characteristics. They have, however, a lower elastic modulus than iron-base alloys, which is 7×10^3 kgf/mm² in aluminium and 20×10^3 kgf/mm² in steel and cast iron. Besides, aluminium alloys are not suitable for surface hardening by chemical heat treatment, and their hardness and wear resistance are lower than in steel. Some of them, especially duralumin, are not corrosion-resistant in the usual atmosphere and have only poor weldability.

Aluminium alloys (like steels and cast irons) may be classed into: (a) pressure-deformable alloys (by rolling, pressing or die-forming); (b) casting alloys; and (c) those produced by powder metallurgy technique.

The most widely used grades of aluminium alloys and their applications are given in Table 27.32.

Table 27.32. Aluminium Alloys

Grade	Composition, %				Applications
	Cu	Mg	Si	other elements	

Deformable Alloys (GOST 4784-65)

High-strength alloys (duralumins)

Д1	3.8-4.8	0.4-0.8	≤ 0.7	0.4-0.8 Mn	Pipes, rods, rivets for medium-strength structures
Д16	3.8-4.9	1.2-1.8	≤ 0.5	0.3-0.9 Mn	Same, for higher strength
В95	1.4-2.0	1.8-2.8	≤ 0.5	0.2-0.6 Mn 5-7 Zn	Aircraft wing spars, propeller blades, frames; for very high strength

Heat-stable alloys

AK2	3.5-4.5	0.4-0.8	0.5-1.0	1.8-2.3 Ni	Engine pistons
AK4	1.9-2.5	1.4-1.8	0.5-1.2	0.8-1.3 Ni	Discs and rings of turbojet engines, compressor blades, pistons

High-plasticity alloys

AB * (Avial)	0.1-0.5	0.45-0.9	0.5-1.2	0.2-0.4 Mn	Pipelines and articles made by deep drawing
AMr2	—	1.8-2.8	≤ 0.4	0.2-0.6 Mn	Welded tanks, pipelines, window frames. Good weldability

High-plasticity corrosion-resistant weldable alloys

AMц	—	—	≤ 0.6	1.0-1.6 Mn	Petroleum and oil pipelines, welded tanks, rivets
AMr6	—	5.6-6.8	≤ 0.4	0.02-0.1 Ti	

Casting Alloys (GOST 2685-63)

Alloys with improved casting properties and corrosion resistance to moist atmosphere (aluminium-silicon silumins) *

АЛ2	—	—	10-13	—	Elements of wheels, units and instruments for low-load application
АЛ4	—	0.17-0.3	8-10.5	—	Large heavy-loaded parts of engines (cylinder heads, crankcases, etc.)

Table 27.32 (continued)

Grade	Composition, %				Applications
	Cu	Mg	Si	other elements	
AJ19	—	0.2-0.4	6-8	—	Thin-walled parts of complex shape for low and medium loads. Welded articles
AJ13	1.5-3.0	0.35-0.6	4.5-5.5	0.6-0.9 Mn	Housings and elements of instruments

Alloys with Improved Mechanical Properties

Aluminium-magnesium alloys (magnaliums)

AJ18 **	—	9.5-11.5	—	—	Critical parts of simple shape for operation at dynamic loads and in moist atmosphere
---------	---	----------	---	---	---

Aluminium-copper alloys

AJ17	4.0-5.0	—	—	—	Articles for medium loads; pedals, levers, fittings; poorer castability than for magnalium
------	---------	---	---	---	--

Heat-resistant alloys

AJ11	3.75-4.5	1.25-1.75	—	1.7-2.2 Ni	Cylinder heads, pistons and other parts of I. C. engines heated up to 275°C
AJ20	3.5-4.5	0.7-1.2	1.5-2	1.2-1.7 Fe 0.15-0.3 Mn 0.15-0.25 Cr 0.05-0.1 Ti	Same, better castability

Sintered Alloys

CAП	Aluminium + 20-22% Al ₂ O ₃				Sheets and sections heated up to 300-325 °C in operation
-----	---	--	--	--	--

* No heat treatment is employed.

** Employed after hardening.

Plastic-worked aluminium alloys. These alloys are strengthened by heat treatment: hardening, which forms the structure of super-saturated solid solution, and ageing (precipitation hardening), either natural or artificial. Besides, they may be subjected to thermomechanical treatment which comprises the stages of hardening, cold plastic working, and ageing.

Some alloys, mainly duralumins, are corrosion-protected by plating, i.e. covered by a protective layer of aluminium. (This, however, reduces somewhat their strength and wear resistance.)

The alloys of this group are employed under various operating conditions and therefore are very diverse in composition and properties. They may be classed into:

(a) high-strength alloys (duralumins); the ultimate strength σ_t is 40-50 kgf/mm² in most duralumins and up to 60 kgf/mm² in the Grade B95. Their composition is rather complex, the principal alloying elements being copper and magnesium (and zinc in B95);

(b) heat-resistant alloys (duralumins), retaining their strength on heating up to 300-350 °C (lower than with heat-resistant steels and titanium alloys). Duralumins of this subgroup have a still more complex composition, most of them being additionally alloyed with nickel (to replace part of copper);

(c) high-plastic alloys for deep drawing and welding; the content of copper in them is limited to 0.5 per cent, because of which their strength is not higher than 25 kgf/mm², but the plasticity is higher than that of duralumins;

(d) high-plastic alloys with good weldability and corrosion resistance. These are alloyed with manganese, and less frequently with magnesium and, unlike duralumins, contain almost no copper, i.e. the component which could form strengthening phases and make the alloys multi-phase and poorly resisting corrosion. These alloys are stable against oils, petroleum, etc. Besides, they suit cold drawing well and have fair weldability.

Casting aluminium alloys. (a) The best casting properties are exhibited by aluminium alloys containing silicon; these are called silumins. They have a low casting temperature and high fluidity and are not liable to forming porosity in castings, but their mechanical properties are not high: σ_t up to 22-25 kgf/mm² and relative elongation of 2-3 per cent (in modified grades). Silumins are used for casting articles of complicated shape not to be subjected to high loads.

(b) Alloys with improved mechanical properties, alloyed with magnesium and copper for the purpose; they are inferior to silumins in castability.

(c) Heat-resistant alloys; they are similar to the corresponding group of plastic-worked alloys and can withstand temperatures up to 300-350 °C.

Sintered aluminium alloys. These alloys (designated САП) are made by sintering aluminium powder containing aluminium oxide (Al_2O_3) in surface layers.

In the sintered state, aluminium forms a cellular matrix in which disperse particles of Al_2O_3 form inclusions in the strengthening phase. The optimum concentration of aluminium oxide is 20-22 per cent.

Al_2O_3 particles do not react with the metallic matrix nor coagulate during heating, because of which the strength properties of the alloy vary only slightly with increasing temperature. Their strength at 20 °C is lower than that of duralumins, but at 200-300 °C is, on the contrary, higher and, in addition, their corrosion resistance is also high.

The metallic matrix provides fair plasticity to the alloy. After sintering, the alloys are rolled into sheets or sections or die-formed.

The САП alloys are predominantly used as heat-resistant alloys for operation at temperatures 30-50 degrees C higher than the maximum temperatures of plastic-worked and casting aluminium alloys.

E. MAGNESIUM ALLOYS

Machine-building uses magnesium alloys, predominantly with aluminium, manganese and zinc and less frequently with zirconium and niobium. (The strength of pure magnesium is appreciably lower than in its alloys.)

The principal advantage of magnesium alloys over other industrial metals is their low density, 1.7-1.8 g/cm³. But they have a low elastic modulus: only 4300 kgf/mm², because of which they can withstand only light loads. Another feature characteristic of magnesium alloys is a high damping level (i.e. their capacity of damping vibrations), which reduces the risk of forming resonant stress peaks.

Magnesium alloys, like aluminium and iron alloys, may be classed into:

- (a) plastic-worked alloys and
- (b) casting alloys.

The compositions of typical magnesium alloys are given in Table 27.33.

Plastic-worked magnesium alloys. These are used as rolled stock (sheets, strips, tubes) and forgings.

Table 27.33. Magnesium Alloys

Grade	Composition, %					Properties and applications
	Al	Mn	Zn	Zr	rare-earth metals	
Plastic-Worked Alloys (GOST 14957-69)						
High-strength alloys						
MA2-1	3.8-5	0.3-0.7	0.8-1.5	—	—	Good weldability; sheets, pipes for oil and petroleum Less weldable, one-piece articles
MA14	—	—	5-6	0.3-0.9	—	
Heat-stable alloys						
MA1	—	1.3-2.5	—	—	0.15-0.30 Ce	For temperatures up to 150 °C; $\sigma_{0.2}$ up to 10 kgf/mm ² Same, up to 200 °C
MA2	3-4	0.15-0.5	0.2-0.8	—		
MA8	—	1.3-2.2	—	—		
Casting Alloys (GOST 2856-68)						
Alloys for normal temperatures						
MJ3	2.5-3.5	0.15-0.5	0.5-1.5	—	—	Fittings, pump elements, handles, pedals of simple shape
MJ5	7.5-9	0.15-0.5	0.2-0.8	—	—	Same; articles of more intricate shape; corrosion resistant to moist air
Heat-stable alloys						
MJ10	—	—	0.1-0.7	0.4-1.0	2.2-2.8 Nd	For temperatures up to 250 °C
MJ15	—	—	4.0-5.0	0.7-1.0	0.6-1.2 La	For temperatures up to 300-400 °C

With increasing aluminium content their structure becomes richer in the Mg_4Al_3 phase (see Fig. 9.26), which increases strength. The yield limit of alloys Grade MA1 (containing no aluminium) is 9-10 kgf/mm², and that of MA2-1 alloy (with 3.8-5 per cent Al), 14-15 kgf/mm².

However, the presence of the second phase Mg_4Al_3 (or of a phase formed by zinc) reduces corrosion resistance, both in air and water.

On the contrary, manganese, which forms no precipitated phase, increases corrosion resistance of the alloy on heating in the atmospheric air. Magnesium alloys, in particular those containing manganese, can therefore be employed as heat-stable alloys, but at lower temperatures (see Table 27.33) than aluminium and titanium alloys.

Casting magnesium alloys. The mechanical properties of casting magnesium alloys are poorer than those of plastic-worked grades but can be improved by modifying and heat treatment. The yield limit can then be raised to 8-10 kgf/mm² (alloys Grades MJ13, MJ15) or 14-15 kgf/mm² (MJ115).

The thermal stability of casting and plastic-worked magnesium alloys is roughly the same.

F. TITANIUM ALLOYS

The principal advantages of titanium alloys which determine the applications of this relatively novel structural material are a low density (approx. 4.5 g/cm³), a high corrosion resistance, and high strength properties. Besides, titanium alloys are not liable to cold brittleness, even at very low temperatures. In addition, some titanium alloys exhibit high heat resistance (which however is lower than with steels).

Titanium alloys practically excel stainless steels and copper and nickel alloys as regards corrosion resistance in sea water, particularly in long-term operation, and also in such aggressive media as moist chlorine, hot nitric acid of high concentration, and others. Corrosion resistance of titanium alloys can be increased even more by alloying with very small quantities of palladium.

The strength properties of titanium alloys may be different depending on their composition and the structure formed through heat treatment. Some alloys, though having a low density, after heat treatment become comparable in strength with alloy structural steels. The grades of titanium alloys are given in Table 27.34, and the conditions of heat treatment and the mechanical properties obtained, in Table 27.35.

Table 27.34. Titanium Alloys

Grade	Composition, %					Properties
	Al	Mn	V	Mo	Cr	
Single-phase α -structure Alloys						
BT5	5	—	—	—	—	Good weldability, high plasticity and strength at low temperatures
Two-phase ($\alpha + \beta$) Alloys						
OT4-1	2	1.5	—	—	—	Same, higher plasticity at 20 °C (can be used in sheets), ultimate strength 30-70 kgf/mm ²
OT4	3	1.5	—	—	—	
BT6	6	—	4	—	—	Same, ultimate strength 80-90 kgf/mm ²
AT3 *	3	—	—	—	1.5 *	High corrosion resistance; heat-resistant alloy
BT8 **	6.5			3.5		
Single-phase β -structure Alloys						
BT15	3			8	11	High plasticity at 20 °C, strength 100-120 kgf/mm ²

* (Fe + Cr + Si + B).

** Additionally 0.2 per cent Si.

Titanium alloys containing chromium have higher strength properties, in particular on heating to 550-600 °C, which, combined with their density lower than that of steels, makes them very attractive for making articles subjected to high centrifugal forces.

On the other hand, titanium alloys are inferior to carbon steels in hardness and wear resistance, which restricts their use in articles subjected to appreciable wear.

G. BEARING ALLOYS (BABBITS)

These are used for filling in bushings of sliding bearings. Their principal types (Table 27.36) are as follows:

1. Tin babbits (in particular, Grade B83); they fit well the surface of shafts and have a high wear resistance. Their structure is the soft matrix (α -solid solution of antimony in tin) with uniformly dispersed hard particles of SnSb compound.

Table 27.35. Heat Treatment and Properties of Titanium Alloys in Die-formed Articles
(According to B.K. Wulf)

Grade	Heat treatment	Mechanical properties				
		ultimate strength σ_u , kgf/mm ²	relative elongation δ , %	relative reduction ψ , %	Impact strength α_H , kgf m/cm ²	Brinell hardness
BT5	Annealing at 800-850 °C	75-80	10-14	25-40	3-6	229-321
OT4-1	Annealing at 640-660 °C	60-75	15-25	35-40	5-12	197-255
OT4	Annealing at 740-760 °C	70-90	10-20	34-55	3.5-10	207-285
BT6	Annealing at 750-800 °C	95-110	10-13	35-60	4-8	269-363
	Hardening from 900-950 °C, water quenching; ageing at 450-550 °C for 4-2 h	115-123	10-12	32-48	—	302-415
AT3	Annealing at 800-850 °C	60-75				
BT8	Annealing at 530-620 °C	105-125	10-20	25-40	4-10	300
	Hardening from 920-940 °C; water quenching; ageing at 500-600 °C for 6-1 h	~ 120	10-18	32-55	3-5	330
			~ 6	~ 20	—	—
BT15 *	Hardening from 700-800 °C; water quenching; ageing at 450-500 °C for 25-15 h or at 550-570 °C for 15 min	135-150	—	4-8	2.5	341-444

Table 27.36. Bearing Alloys (Babbits), GOST 1209-73 and 1320-55

Grade	Composition, %					Applications
	Sb	Pb	Sn	Cu	other elements	
B83	10-12	—	Base	5.5-6.5	—	Heavy-duty bushings (turbines, etc.)
BH *	13-15	Base	9-11	1.5-2	1.25-1.75 Cd	Bushings for moderate loads (automobile engines, etc.)
B16	15-17	Same	15-17	1.5-2	—	
BKA **	≤ 0.25	Same	—	—	0.95-1.15 Ca, 0.7-0.9 Na	Railway vehicle bearings

* Additionally 0.75-1.25 per cent Ni and 0.5-0.9 per cent As.

** Additionally 0.05-0.2 per cent Al.

2. Lead-base babbits have a somewhat lower wear resistance (at high pressures); their structure is a soft eutectic with dispersed (less uniformly than in the first group) particles of the harder antimony. These alloys are used for lighter bearing loads.

Copper is added to these grades in order to prevent density segregation of the main components: heavy tin and lead and much lighter antimony.

3. Tin-free lead-base babbits (with additions of calcium, aluminium or sodium); these are less expensive.

Chapter Twenty-eight

HARD MATERIALS

This group includes materials of diverse composition and properties, which are used to cut, form or grind other materials. According to their hardness numbers they may be divided into (a) hard (1500-2000 HV), (b) very hard (2000-2500 HV), and (c) extra-hard (8000-10,000 HV).

28.1. HARD ALLOYS (1500-2000 HV)

Hard alloys (Table 28.1) appreciably excel high-speed steels in hardness¹ (the respective numbers are 73-75 HRC in the former and 65-69 HRC in the latter), wear resistance, heat resistance (900-1000 °C and 620-720 °C), and elastic modulus E (approx. 50,000 kgf/mm²). They, however, have lower strength values (ultimate bending strength 90-200 kgf/mm² against 220-350 kgf/mm² in high-speed steels). They are employed for cutting the materials of increased hardness at high speeds, and also for die-forming without high mechanical loads. Because of their high rigidity the machined surfaces are cleaner than those cut by high-speed steel tools.

Hard alloys are manufactured by pressing and sintering a powdered mixture and are used as plates, which are soldered to or fastened in cutting tool holders or dies, and also separately as simple-shape cutting tools (for instance, short drills). A disadvantage inherent in them is that they cannot be machined, since their high hardness cannot be modified by heat treatment.

The properties and applications of hard alloys are determined by their composition and structure.

Their structure is usually hard particles of titanium and tungsten carbides (and additionally of tantalum carbide in some grades) bonded in a soft cobalt-base eutectic. An increase in the

¹ Hardness of hard alloys is measured by Rockwell A scale (60-kgf load). HRA values can be reduced to HRC values by the formula $HRC = 2HRA - 104$.

Table 28.1. Hard Alloys (1500-2000 HV), GOST 3882-74

Grade	Composition, %				HRA number *	Ultimate strength, kgf/mm ²	Applications
	WC	TiC	TaC	Co			
<i>Titanium-Tungsten Alloys for Machining Carbon and Alloy Steels</i>							
T30K4	66	30	—	4	92	95	Finish turning with small feeds; threading and reaming
T15K6	79	15	—	6	90	115	Semi-rough continuous turning; interrupted finish turning; threading
T15K12	83	5	—	12	87	165	Rough turning (including castings with sand crust, pits, etc.); planing, threading
<i>Titanium-tantalum-tungsten Alloys for Machining Carbon and Alloy Steels</i>							
T17K12	81	4	3	12	87	165	Same, rough milling
<i>Tungsten Alloys for Machining Cast Iron, Non-ferrous Metals, Austenitic Steels and Alloys, Titanium, Non-metals; Hot Drawing and Shaping</i>							
BK3	97	—	—	3	90	110	Finish turning with small feeds; threading, reaming. Also for cutting glass and glass-reinforced plastics
BK6	94	—	—	6	88.5	150	Rough and semi-rough turning; semi-finish milling, reaming and broaching; wire drawing; rock drilling
BK6-M	94	—	—	6	90	135	Semi-finish machining (including austenitic alloys and hardened steels)
BK6-B	94	—	—	6	87.5	155	Rough and semi-rough turning, milling, boring and reaming
BK8	92	—	—	8	87.5	160	Rough turning of rough surfaces, planing, milling, drawing and pressing
BK8-B	92	—	—	8	86.5	175	Turning of austenitic alloys, planing, hard rock drilling

Table 28.1 (continued)

Grade	Composition, %				HRA number *	Ultimate strength, kgf/mm ²	Applications
	WC	TiC	TaC	Co			
BK15	85	—	—	15	86	180	Wood cutting, drawing, pressing, die forming, upsetting, trimming
<i>Tungsten Alloys for Cold Plastic Working and for Measuring Instruments</i>							
BK20	80	—	—	20	84	195	Die-forming, upsetting, trimming with impact loads of moderate intensity
BK25	75	—	—	25	82	200	Same, for higher impact loads

* HRC numbers: 78 for the hardest alloy Grade T30K4, 74-75 for Grade T15K6, and 62-64 for the softest alloy Grade BK25.

content of cobalt reduces hardness and wear resistance but improves strength.

The presence of titanium carbides increases the temperature point at which metal chips might weld to the cutting edge and quickly damage it.

Alloys with tungsten and titanium carbides are used for machining steels, i.e. materials having a high liability to chip welding. Addition of tantalum carbide, besides, improves somewhat the toughness of the alloy.

Alloys with tungsten carbide only are employed for machining cast irons and in dies.

The designation of hard alloys is as follows:

When the first letter is 'B', this implies that the alloy contains tungsten carbide (WC) and no other carbides; when it is 'T', the alloy contains titanium carbide TiC (in addition to tungsten carbide), and the following numeral gives the percentage of TiC. When another 'T' follows the first 'T' (instead of a numeral), this implies that the alloy additionally contains tantalum carbide (TaC), and the next numeral is the total content of TaC and TiC. Cobalt-containing alloys are designated by 'K' and a numeral of its percentage content.

Thus, the content of the basic tungsten carbide WC is determined as the balance (except for alloys containing three carbide phases: WC, TiC, and TaC).

A letter 'B' written at the end of a designation (after 'K') may imply that carbide particles in the alloy are unusually large; such alloys have a higher toughness, but lower hardness.

An 'M' at the end of a designation denotes a fine-grain alloy, which has a higher hardness and wear resistance and a lower strength.

28.2. HARD MATERIALS (2000-2500 HV)

These are used as abrasive materials in the form of grains (monocrystals) bonded in the matrix material of grinding discs for grinding steels, cast irons, and the like. These materials are brittle, their bending strength being not higher than 30-40 kgf/mm². In this case brittleness is a valuable property: hard grains of the material are crushed in the grinding process instead of being deformed, and thus remain sharp and capable of further grinding.

The most common materials of this group are:

(a) electrocorundum used in discs for grinding steels; its hardness is 2200-2500 HV, bending strength approximately 8 kgf/mm², and softening point around 1800 °C;

(b) silicon carbide employed mainly in discs for grinding non-ferrous metals.

These materials are less suitable for grinding high-hardness steels which may contain very hard strengthening phases in their structure, mainly vanadium carbide whose hardness is 1800-2000 HV. The disc rapidly clogs with fine particles of the ground material, becomes overheated and thus loses hardness in some places.

28.3. EXTRA-HARD MATERIALS (8000-10,000 HV)

Natural and artificial diamonds have the highest hardness (10,000 HV) and elastic modulus (80,000 kgf/mm²) among all materials, but a low bending strength (30 kgf/mm²). They are heat-stable at temperatures up to 800 °C, but charring can occur at higher temperatures. Besides, diamonds can interact with steel if machining is done with high speeds causing overheating above 800 °C.

Diamonds are mainly used for cutting very hard and wear-resistant materials, such as glass, porcelain, and for making abrasive discs for grinding steels and other metals.

Cubical boron nitride (borazon) is a novel promising material manufactured by special techniques (under high pressures).¹ It

¹ Boron nitride is produced as fine monocrystals or polycrystalline materials with particles 5-6 mm in size.

has a somewhat lower hardness (8500-9000 HV) than that of diamond, with almost the same values of elastic modulus and strength, but fortunately is oxidation-resistant even at very high temperatures (up to 1400 °C) and does not react with the materials being processed (including steel) when being heated appreciably during cutting or grinding.

Cubical boron nitride is employed for grinding high-hardness steels with appreciably thick layers of metal being removed. As distinct from the other materials discussed, it is not overheated in the process, and therefore, the surface being ground is not affected and the roughness value obtained is 1-3 classes better. Apart from steel, it is also suitable for grinding some other materials.

Chapter Twenty-nine

PLASTICS

Plastics possess some useful physical properties and are finding ever wider application in various branches of industry, such as electrical engineering, chemical and civil engineering, and also in machine-building, where they are used for making machine elements and structures not subjected to high loads.

When selecting plastics for making machine elements, the following peculiarities of their properties should be considered.

Plastics are advantageous in having a low density (1.5 g/cm^3 , i.e. much lower than with metals), a low coefficient of friction, and high chemical stability to many reagents (oil, petroleum, moisture, etc.). At the same time they are easier to machine than metals.

The principal drawbacks of plastics to be considered in machine-building are: a low modulus of elasticity ranging from 20 to 2000 kgf/mm^2 (against 7000, 11,000, and $20,000 \text{ kgf/mm}^2$ in aluminium, titanium and steel, respectively), insufficient heat stability and form stability even at moderate temperatures (not above $70\text{--}80^\circ\text{C}$ for most plastics), high sensitivity to impacts, and low wear resistance. The ultimate tensile strength of most plastics is only $5\text{--}10 \text{ kgf/mm}^2$ and only few of them have a value of $25\text{--}30 \text{ kgf/mm}^2$.

For the reasons indicated, plastics are most suitable for articles operating at low stresses when a low coefficient of friction is required (some types of bearing, noiseless gears, etc.) or when a low mass (covers, etc.) or corrosion resistance and transparency of the material (some tanks and pipelines) are essential. The most typical plastics employed in machine-building are tabulated in Table 29.1.

Table 29.1. Typical Plastics Used In Machine-building

Name	Ultimate strength, kgf/mm ²	Elastic modulus, kgf/cm ²	Density, g/cm ³	Other properties	Applications
Polyethylene	4	2000	0.9	Acid-resistant (except nitric acid and peroxides)	Tubes, tanks, valves
Polypropylene	3	6000	0.9	Stable in acid and alkaline solutions	Tubes, valves, elements of pumps
Polytrifluorochloroethylene	2-3	5000	2	Creep-stable at low temperatures; withstands temperatures not above +70 °C	Same
Polycarbonates	6-7	22,000-2500	1.17-1.22	Stable in lubricants; not resistant to alkalis and benzene	Threaded joints
Polyamides	6-7		1.1	Low friction coefficient (0.055, i.e. only half that of steel); stable in oils, petroleum, alkalis	Bearings, gears, sleeves, spacers
<i>Laminated Plastics</i>					
Textolites	6-10	3800	1.7-1.9	Low friction coefficient; manufactured in plates	Pinions, bearings, bushings
Wood-laminated plastics	25-30	—	1.5	Same, stable in oils; low friction coefficient: 0.09-1.1 with steel and 0.13-0.14 with cast iron	Same, elements of aircraft structures

Table 29.1 (continued)

Name	Ultimate strength, kgf/mm ²	Elastic modulus, kgf/cm ²	Density, g/cm ³	Other properties	Applications
Glass-cloth reinforced plastics	22-24.5	130,000	1.6-1.9	Relatively high thermal stability (up to 300 °C); anisotropic properties determined by the structure of glass cloth	Large structures for long-term operation at 200 °C and short-term operation at 300 °C
<i>Thermosetting Composite Plastics</i>					
Phenolaldehyde resin-based (Grades K-18-56 and K-8-56) composite plastics (GOST 5689-66)	2-8		1.75	Stable in water, moist air, acids, and at temperatures from -40° to +120 °C	Threaded joints
Phenolxyleneformaldehyde resin-based (Grades K-17-82, K-18-82) composite plastics	3.0		1.5	High antifriction properties	Sliding bearings
Phenolformaldehyde resin-based (Grades KΦ-3, KΦ-3Г) composite plastics	2.7		1.7-1.85	High mechanical properties; heat stable up to +150 °C	Brake shoes of railway vehicles, cranes, clutch plates

Appendix 1. Brinell Hardness Numbers

Indent diameter, mm: d_{10} or $2d_5$	HB number at load P of		Indent diameter, mm: d_{10} or $2d_5$	HB number at load P of	
	30 kgf	10 kgf		30 kgf	10 kgf
2.90	444	—	4.5	179	59.5
2.95	430	—	4.55	174	58.1
3.0	418	—	4.60	170	56.8
3.05	402	—	4.65	166	55.5
3.10	387	129	4.70	163	54.3
3.15	375	125	4.75	159	53.0
3.20	364	121	4.80	156	51.9
3.25	351	117	4.85	153	50.7
3.30	340	114	4.90	149	49.6
3.35	322	110	4.95	146	48.6
3.40	321	107	5.0	143	47.5
3.45	311	104	5.05	140	46.5
3.50	302	101	5.10	137	45.5
3.55	293	98.7	5.15	134	44.6
3.60	286	95	5.20	131	43.7
3.65	277	92.3	5.25	128	42.8
3.70	269	89.7	5.30	126	41.9
3.75	262	87.2	5.35	124	41.0
3.80	255	84.9	5.40	121	40.2
3.85	248	82.6	5.45	118	39.4
3.90	241	80.4	5.50	116	38.6
3.95	235	78.9	5.55	114	37.9
4.0	228	76.3	5.60	112	37.1
4.05	223	74.3	5.65	109	36.4
4.10	217	72.4	5.70	107	35.7
4.15	212	70.6	5.75	105	35.0
4.20	207	68.8	5.80	103	34.3
4.25	202	67.1	5.85	101	33.7
4.30	196	65.5	5.90	99	33.1
4.35	192	63.9	5.95	97	32.4
4.40	187	62.4	6.0	95	31.8
4.45	183	60.9			

Appendix II. Brinell, Rockwell and Vickers Equivalent Hardness Numbers

Brinell hardness numbers			Rockwell hardness numbers			Vickers hardness number, load 1-120 kgf, HV
HB	indent diameter d, mm		load 150 kgf (cone), HRC	load 60 kgf (cone), HRA	load 100 kgf (ball), HRB	
	10-mm ball, 3000-kgf load	5-mm ball, 750-kgf load				
782	2.2	1.1	72	89	—	1220
—	—	—	71	88	—	—
—	—	—	70	87	—	—
744	2.25	—	69	87	—	1114
—	—	—	68	86	—	—
713	2.3	1.15	67	85	—	1021
—	—	—	66	—	—	—
683	2.35	—	65	84	—	940
—	—	—	64	—	—	—
652	2.40	1.20	63	83	—	867
—	—	—	62	—	—	—
627	2.45	—	61	82	—	803
—	—	—	60	—	—	—
600	2.5	1.25	59	81	—	746
578	2.55	—	58	80	—	694
—	—	—	57	—	—	—
555	2.60	1.30	56	79	—	649
—	—	—	55	—	—	—
532	2.65	—	54	78	—	606
—	—	—	53	—	—	—
512	2.70	1.35	52	77	—	587
495	2.75	—	51	76	—	551
—	—	—	50	—	—	—
477	2.80	1.40	49	76	—	534
460	2.85	—	48	75	—	502
444	2.90	1.45	47	74	—	474
—	—	—	46	—	—	—
430	2.95	—	45	73	—	460
418	3.0	1.50	44	73	—	435
402	3.05	—	43	72	—	423
—	—	—	42	—	—	—
387	3.10	1.55	41	71	—	401
375	3.15	—	40	71	—	390
364	3.20	1.60	39	70	—	380
351	3.25	—	38	69	—	361
340	3.30	1.65	37	69	—	344
332	3.35	—	36	68	—	333
321	3.40	1.70	35	68	—	320
311	3.45	—	34	67	—	312
302	3.50	1.75	33	67	—	305

Appendix II (continued)

Brinell hardness numbers			Rockwell hardness numbers			Vickers hardness number, load 1-120 kgf, HV
HB	indent diameter d , mm		load 150 kgf (cone), HRC	load 60 kgf (cone), HRA	load 100 kgf (ball), HRB	
	10-mm ball, 3000 kgf load	5-mm ball, 750-kgf load				
293	3.55	—	31	66	—	291
286	3.60	1.80	30	66	—	285
277	3.65	—	29	65	—	278
269	3.70	1.85	28	65	—	272
262	3.75	—	27	64	—	261
255	3.80	1.90	26	64	—	255
248	3.85	—	25	63	—	250
241	3.90	1.95	24	63	100	240
235	3.95	—	23	62	99	235
228	4.0	2.0	22	62	98	226
223	4.05	—	21	61	97	221
217	4.10	2.05	20	61	97	217
212	4.15	—	19	60	96	213
207	4.20	2.10	18	60	95	209
202	4.25	—	—	59	94	201
196	4.30	2.15	—	58	93	197
192	4.35	—	—	58	92	190
187	4.40	2.20	—	57	91	186
183	4.45	—	—	56	89	183
179	4.50	2.25	—	56	88	177
174	4.55	—	—	55	87	174
170	4.60	2.30	—	55	86	171
166	4.65	—	—	54	85	165
163	4.70	2.35	—	53	84	162
159	4.75	—	—	53	83	159
156	4.80	2.40	—	52	82	154
153	4.85	—	—	52	81	152
149	4.90	2.45	—	51	80	149
146	4.95	—	—	50	78	147
143	5.0	2.50	—	—	77	144
140	5.05	—	—	—	76	—
137	5.10	2.55	—	—	75	—
134	5.15	—	—	—	74	—
131	5.20	2.60	—	—	72	—
128	5.25	—	—	—	71	—
126	5.30	2.65	—	—	70	—
124	5.35	—	—	—	69	—
121	5.40	2.70	—	—	67	—
118	5.45	—	—	—	66	—
116	5.50	2.75	—	—	65	—

INDEX

- Absolute elongation 163
- Actual stresses 163
- Aggressive media for corrosion tests 221
- Air-hardenable steels 333
- Akulov N. S. 147
- Akulov's anisometer 147
- Alloying elements, designations 438
- Alloys,
 - classification 434 *ff.*
 - invar 460
 - of low magnetic permeability 479
 - magnetically hard 484
 - magnetically soft 479
 - molybdenum-base 459
 - nickel-base 458
 - niobium-base 459
 - phase composition of, 135
 - in equilibrium 36
 - with special physical properties 479
 - structure in equilibrium 36
- Aluminium, structure of 367
- Aluminium alloys, 495
 - structure of 367
- Aluminium bronzes, 493
 - structures of 367
- Ammeter — voltmeter method 141
- Amplifying ocular 72
- Anosov P. P. 33
- Antimony alloys 372
- Aplanatic focus 72
- Apochromats 71
- Aqua regia 66
- Artificial ageing,
 - of duralumins 376
- Artificial diamonds 508
- Austenometer 217

- Babbitts 372, 502
- Ballistic constant 146
- Ballistic method,
 - for determining saturation magnetization 145
- Banding 27
- Barsukova T. A. 374
- Bearing alloys 372, 502
- Bending tests 170
- Berkovich E. S. 206
- Beryllium bronzes 494
- Binary alloys,
 - constitutional diagrams of 224
- Bismuth,
 - in copper 364
- B'anter M. E. 337, 338
- Blowholes in steel 437
- Bochvar A. A. 280
- Bogdanov N. A. 209
- Borazon 508
- Borin F. A. 374
- Brasses, 490
 - structures of 365
- Bright-etching reagent 68
- Bright-field technique 76
- Brinell hardness numbers 513
- Brinell hardness test 195
- Bronzes 490

- Calibration of thermocouples 110
- Carbon,
 - effect on mechanical properties of steel 436
- Carbon replicas 94
- Carbon segregation 26
- Carbon steel,
 - structure in non-equilibrium 306
- Cast iron, 485
 - structure of 291
- Cavitation erosion 463
- Cementable steels 443
- Cementation 47
- Cementite networks 49
- Chemical properties of metals,
 - determination 218
- Chernov's dendrite 341
- Chevenard's dilatometer 119
- Chilled cast iron 489
- Chromatic aberration 71
- Chromium,
 - in high-speed steels 322
- Classification of metals 434 *f*
- Cobalt steels 418
- Coercive force,
 - measurement of 149
- Cold brittleness,
 - of copper 364
- Common steels 436
- Compensating eyepiece 72
- Compensation wires for thermocouples 103
- Compression tests 165
- Concentrational segregation 135
- Concentration triangle 251
- Conditional creep limit 190
- Conditional stresses 162
- Constructional steels 440
- Contactless methods 142
- Copper,
 - in duralumin 376
 - structure of 364
- Copper alloys, 489
 - designations 490
- Correction lenses 70
- Corrosion cracking,
 - tests for 220
- Corrosion-resistant steels 475
- Creep tests 189
- Critical points,
 - of metals 104
 - of steel, determination 299
- Crystalline fracture 19
- Cubical boron nitride 508
- Cyaniding 418

- Dark-field technique 76
- Decarbonized cast iron 293
- Decomposition of solid solution 229
- Deep etching reagents 20
- Dendritic segregation 25
- Dendritic structure 24
- Differential dilatometers 119
- Differential thermal analysis 115
- Differential thermocouple 117
- Diffraction contrast method 91
- Diffusion coating 47
- Dilatometric analysis 15, 117
- Dilatometric pyrometers 118
- Dislocations, 91
 - in single-phase alloys 37
- Distribution curves 56
- Doronin V. M. 22, 355
- Double-bridge method 138
- Dovgalevsky Ya. M. 484
- Dronova N. P. 368, 369

- Dry objectives 73
 Duralumin,
 heat treatment 376 *ff.*
 structure 368, 376
 Dynamic hardness test 192
 Dynamic tests 176
- Eddy-current method 142
 Edge dislocations 91
 Elastic limit 160
 Electric steels,
 designation 439
 Electro-chemical polishing 61
 Electrocorundum 508
 Electromagnetic lens 88
 Electron-beam oscillograph 113
 Electron microscopy 85
 End quench test 331
 Endurance limit 173
 Epi-objective 76
 Equilibrium structure of alloys 36
 Etching reagents 66 *ff.*
 Etch patterns 36
 Eutectics,
 structure of 37
 Extra-hard materials 508
 Eyepiece micrometer 74
- Fatigue strength 173
 Fatigue-testing machines 174
 Fatigue tests 172
 Ferrite networks 49
 Ferrite-pearlitic steels 455
 Ferrites 483
 Fibrous fracture 19, 180
 First-order transition 104
 Flakes 19
 Forman — Kobayashi correction for fracture toughness 185
 Fractures,
 macroanalysis of 18
 Fracture toughness 181
 Free-cutting steels 469
 Fridman Ya. B. 193
- Geller Yu. A. 144, 254
 Geveling N. V. 401
 Glass-reinforced plastics 512
 Gordezian I. A. G. 96
 Gorlenko N. P. 96
 Grain size in metals,
 determination 47
 Granular fracture 19
 Graphite,
 in cast iron 292
 Graphite segregation 63
 Graphitized cast iron 293
 Grey cast iron 292, 487
 Guinier — Preston zones 377
 Gulyaev A. P. 330
- Hard alloys 322, 505
 Hard materials 508
 Hardenability, 328
 nomogram for calculation of 337
 Hardened steel,
 structure of 306
 Hardness 192
 Hardness numbers,
 conversion table 514 *ff.*
- Heat-resistant steels 435, 454
 Heat treatment,
 of alloys 395 *ff.*
 of duralumins 376
 High-quality steels 437
 High-speed steels 321
 High-strength cast iron 293, 489
 High-temperature steels 453
 High-temperature tests 187
 Histograms 56
 Hot hardness testing 209
 Huygenian eyepiece 72
 Hypereutectic alloys 225
- Illuminating system of microscope 75
 Immersion objectives 73
 Impact strength 177
 Impact-testing machines 178
 Indentation test 192
 Infra-red microscopes 84
 Initial banding 27
 Inter-crystalline corrosion 219
 Interphase transformations 135
 Invar alloy 460
 Iron, in aluminium 367
 Irwin correction for fracture toughness 185
 Izhevsky's reagent 66
- Khrushchov M. M. 206
 Killed steel 436
 Kurnakov N. S. 136, 143
 Kurnakov's pyrometer 116
- Lacquer replicas 93
 Lead, in brass 365
 in copper 364
 Lead alloys 372
 Local elongation 163
 Long-term strength 191
 Long-term tests at high temperatures 189
 Low-alloy constructional steels 441
 Low-cycle endurance 173
 Low-temperature tests 186
 Lozinsky M. G. 70, 209, 210
 Lustreless fracture 19
 Lyapina A. Ya. 48
- Macroanalysis, 18
 of non-ferrous metals 23
 of steel 20
 Macrohardness test 194
 Macroscopic examination 15, 18
 Macrosection 18
 Magnesium 370
 Magnesium alloys 370, 499
 Magnetic analysis 143
 Magnetic flaw detection 217
 Magnetic transformations 135
 Magnetically hard alloys 484
 Magnetically soft alloys 479
 Magnification of microscope 74
 Malleable cast iron 293, 487
 Mal'tsev M. V. 374
 Manganese, in bronzes 367
 Maraging steels 452
 Marble's reagent 67
 Markovets M. P. 199
 Martensitic structure of hardened steel 41
 Mechanical properties of materials,
 determination of 156 *ff.*

- Mechanical system of microscope 77
 Metallurgical microscope, 70
 types of 79
 Method of parallels 252
 Method of perpendiculars 251
 Microanalysis 33
 Microhardness tests 195, 206
 Microporosity 63
 Microscopic examination 15, 33
 Microsections, 58
 preparation of 59
 Microstructures, 33
 of non-ferrous metals and alloys 380 *ff.*
 Millivoltmeters 108
 Minkevich N. A. 198
 Mirror galvanometers 108
 Modification of silumins 369
 Modulus of elasticity 160
 Molybdenum,
 in high-speed steels 322
 Molybdenum-base alloys 459

 Nakhimov D. M. 281
 Natural ageing of duralumins 376
 Natural diamonds 508
 Natural tests of materials 157
 Naval brass 383
 Nickel in bronzes 367
 Nickel-base alloys 458
 Niobium-base alloys 459
 Nitration 47
 Nitridable steels 450
 Non-equilibrium structures 41
 Non-ferrous metals,
 microstructures of 380 *ff.*
 structures of 364 *ff.*
 Non-thermostable tool steels 471
 Numerical aperture 73

 Ordering, 135
 of solid solution 229
 Ordinary-bridge method 138
 Oxidation etching 65
 Oxygen, in copper 364

 Packing defects 91
 Paravas A. E. 334
 Pearlite 286
 Permalloy 479
 Permanent-magnet oscillographs 113
 Phase composition of alloys 135
 Phase transformations 104
 Phosphorus segregation 26
 Physical properties of metals 216
 Plastic deformation of metals 280
 Plastics 510
 Pogodin-Alekseev G. I. 192
 Polarized-light microscopes 77
 Polarized-light technique 77
 Polishing of microsections 60
 Polyamides 511
 Polycarbonates 511
 Polyethylene 511
 Polymorphous transformations 229
 Polypropylene 511
 Polytrifluorochloroethylene 311
 Precipitation hardening 322
 Precipitation-hardening austenitic alloys 460
 Primary crystallization 226
 Projection eyepiece 72

 Prokoshkin D. A. 459
 Pronin A. G. 394
 Proportionality limit 159
 Pseudo-binary sections 260
 Pyros alloy 119

 Quality steels 437
 Quantimet 57
 Quantitative metallography 47
 Quartz replicas 94
 Quaternary steels 435

 Rebound test 192
 Recovery heat treatment 377
 Recrystallization 280
 Recrystallization temperature 280
 Recrystallization twins in titanium 370
 Red shortness of copper 364
 Refractory steels 453
 Relative elongation 163
 Relative expansion 165
 Relative reduction 164
 Relative shortening 165
 Relative torsional shear 169
 Replicas for electron microscopy 92
 Resistometric analysis 135
 Rimming steel 436
 Rockwell hardness test 199
 Rotating magnetic field method 142
 Rule of three sections 254
 Rumyantsev M. V. 385, 393
 Rzheshotarsky's reagent 66

 Sagadeeva T. G. 96
 Saturation magnetization,
 measurement of 143
 Scanning electron microscope 95
 Schlieren method 91
 Scratch hardness test 192
 Screw dislocations 91
 Season cracking in brasses 428
 Secondary banding 27
 Secondary cementite 289
 Secondary crystallization 229
 Secondary hardness in high-speed steels 322
 Second-order transition 104
 Segregation of alloys 25
 Semi-killed steel 436
 Semi-thermostable tool steels 471
 Shear modulus 167
 Short-term tests at high temperatures 188
 Silicon, in aluminium 367
 Silicon bronzes 494
 Silicon carbide 508
 Silumins 369
 Sintered oxides 435
 Slipping 186
 Solidus line 226
 Sorbite 310
 Special structural steels 452
 Spherical aberration 71
 Spring steels 463
 Stage micrometer 74
 Stainless steels 476
 Standard specimens for tensile tests 159
 Static tests 158
 Steel(s),
 air-hardenable 333
 classification of 435

- Steel(s),
 corrosion-resistant 475
 ferrite-pearlitic 455
 free-cutting 469
 hardenability of 328
 hardenable by induction heating 449
 heat-resistant 454
 high-speed 321
 high temperature 453
 macroanalysis of 20
 maraging 452
 nitridable 450
 of reduced hardenability 450
 refractory 454
 with special chemical properties 475
 with special physical properties 479
 special structural 452
 spring 463
 stainless 476
 structure of 286
 tool 470
 transformations in 299
 wear-resistant 460
- Structural methods 15
 Structural steels, 435, 442
 heat treatment of 315
 Structure of steel 286
 Substances for calibration of thermocouples 110
 Sulphur in copper 364
 Sulphur segregation 25
 Superhigh-quality steels 437
 Surface-etching reagents 21
- Temperature,
 methods of measuring 105
- Tempered steel,
 structure of 311
- Tempering of steel 311
 Temper sorbite 311, 399
 Temper troostite 311
 Tensile tests 158
 Ternary alloys, constitutional diagrams of 251
 Tests for total corrosion 218
 Textolites 511
 Thermal analysis 15, 104
 Thermal stability 323
 Thermocouples 105
 Thermosetting plastics 512
 Thermostable tool steels 471
 Three-dimensional diagrams 255
 Tin alloys 372
 Tin bronzes 366, 492
 Titanium, structure of 370
 Titanium alloys 501
 Titanium-tantalum-tungsten alloys 506
 Titanium-tungsten alloys 506
 Tool steels, 417 *ff.*, 435, 470
 heat treatment of 321
 non-thermostable 471
 semi-thermostable 471
 thermostable 471
 Torsional tests 166
 Transformations in duralumin during heat treatment 376
 Transformations in steel 299
 Transformer steels 439
 Transmission microscope 68
 Troostite 310
 Troostite network 49
 Troost-sorbite 311
 Tungsten, in high-speed steels 322
 Tungsten alloys 506, 507
 Tungsten-rhenium alloys 106
 Turkin V. D. 385, 393
 Twinning 186
 Twinning plane 364
 Twins, in copper 364
 in titanium 370
- Ultimate tensile stress 162
 Uniform elongation 163
 Utevsky L. M. 94
- Vacuum metallography 70
 Vanadium,
 in high-speed steels 322
 Vickers hardness test 204
 Vorobyev N. A. 394
- Wear-resistant steels 460
 White cast iron 291, 489
 Widmanstätten structure 288
 Wood-laminated plastics 511
 Wulf B. K. 503
- X-ray examination 15
 X-ray spectrum microscopy 98
- Yield limit 161
- Zedin N. I. 381, 384, 386, 387, 389
 Zholobov V. V. 381, 384, 386, 387, 389
 Zonal segregation 25
 Zone of fatigue fracture 172

TO THE READER

Mir Publishers welcome your comments on the content, translation, and design of the book.

We would also be pleased to receive any suggestions you to make about our future publications.

Our address is:

USSR, 129820,
Moscow, I-110, GSP,
Pervy Rizhsky Pereulok, 2,
Mir Publishers

The first Russian edition of the book was published in 1955 and since then it has been widely used in the USSR as a fundamental study aid on the science of materials for students specializing in machine-building, iron- and steel-making, instrument-making, etc.

The book discusses modern techniques for examining the structure and properties of engineering materials, and contains numerous laboratory exercises and practical problems.

A separate part gives a systematic classification of a wide range of metallic alloys and non-metallic materials employed in industry, and teaches the students how to make a rational choice of materials for particular structures, machine elements and instruments.

This English translation has been made from the fourth Russian edition (1975) thoroughly revised by the authors. The book was also translated into German.

Mir Publishers of Moscow publish Soviet scientific and technical literature in eleven languages — English, German, French, Italian, Spanish, Czech, Serbo-Croat, Slovak, Hungarian, Mongolian, and Arabic. Titles include textbooks for universities, technical schools and vocational training, literature on the natural sciences and medicine, including textbooks for medical schools and schools for nurses, popular science, and science fiction. The contributors to Mir Publishers' list are leading Soviet scientists and engineers in all fields of science and technology and include more than 40 Members and Corresponding Members of the USSR Academy of Sciences. Skilled translators provide a high standard of translation from the original Russian.

Many of the titles already issued by Mir Publishers have been adopted as textbooks and manuals at educational establishments in France, Cuba, Egypt, India and other countries.

Mir Publishers' books in foreign languages are exported by V/O "Mezhdunarodnaya Kniga" and can be purchased or ordered through booksellers in your country dealing with V/O "Mezhdunarodnaya Kniga".